IAEA-TECDOC-457

NUCLEAR DATA

FOR

FUSION REACTOR TECHNOLOGY

PROCEEDINGS OF AN ADVISORY GROUP MEETING
ORGANIZED BY THE
INTERNATIONAL ATOMIC ENERGY AGENCY
AND HELD IN GAUSSIG, GERMAN DEMOCRATIC REPUBLIC
1–5 DECEMBER 1986

FOREWORD

Following recommendations by the International Nuclear Data Committee (INDC) and the International Fusion Research Council, the Nuclear Data Section has organised the Advisory Group Meeting on Nuclear Data for Fusion Reactor Technology in co-operation with the Technical University Dresden, German Democratic Republic, 1-5 December 1986, with the general aim to review changes in the requirements and status of nuclear data for fusion reactor technology since the first meeting on the same topic which the Agency held in 1987.

The meeting dealt with the following topics:

- assessment of changes (since the last AGM on the topic in 1978) in specific nuclear data requirements, including required accuracies and priorities, on the basis of benchmark testing of currently available nuclear data files, and comparisons of the required with the presently achieved data accuracies;

- review of recent measurements, evaluations and theoretical calculations of fusion relevant nuclear data;

- identification and discussion of measurements, compilations, evaluations and theoretical calculations required to satisfy the current and foreseeable nuclear data needs for fusion reactor technology;

- formulation of specific recommendations and measures for future activities and their coordination;

One of the most essential outcome from the meeting was the investigation of the possibility and work out concrete ideas for the creation of an international nuclear library for use in fusion reactor neutronics calculations on the basis of international co-operation of the countries expected to participate in the International Test Engineering Reactor (ITER) project. In fact a working scientific programme for creation of a joint file specifically for the design of the ITER was composed.

The International Organizing Committee advised on topics and selection speakers. It included: Prof. D. Seeliger (Technical University Dresden, GDR), Dr. F. Mann (Hanford, USA), Dr. D. Dudziak (LANL, USA), Dr. B.H. Patrick (Harwell, UK), Dr. Y. Seki (JAERI, Japan), Dr. H. Küsters (Kfk, FRG) and Dr. V.D. Markovskij (IAE, Moscow).

The meeting was organized in four sessions and four working groups. The major credit for the success of the meeting goes to all speakers for their excellent talks, to the chairmen of scientific sessions and the working groups for their stimulating of discussions, to attendees for their active participation in the discussions.

On behalf of the IAEA we would like to express our deep appreciation to the Staatlisches Amt für Atomsicherheit und Strahlenschutz der DDR as well as to the managment of the Technical University Dresden, in

particular to Prof. Gross, Prodekan of the University, for the generous
support of the meeting, to the Local Organizing Committee: Prof. D.
Seeliger, Dr. Seidel, Dr. Helfer, Ms. Keiser for their help and
assistance throughout the meeting.

All participants in this meeting most gratefully acknowledged the
excellent help and the outstanding hospitality during the meeting. This
warm reception contributed a lot to the success of the meeting and helped
to create an active and co-operative atmosphere for all the participants.

EDITORIAL NOTE

CONTENTS

REQUIREMENTS OF NUCLEAR DATA FOR FUSION REACTOR TECHNOLOGY (Session A)

STATUS OF EXPERIMENTAL AND THEORETICAL INVESTIGATIONS OF MICROSCOPIC NUCLEAR DATA (Session B)

STATUS OF EXISTING LIBRARIES FOR FUSION NEUTRONIC CALCULATIONS (Session C)

STATUS OF INTEGRAL EXPERIMENTS AND BENCHMARK TESTS (Session D)

REPORT OF WORKING GROUP I

NUCLEAR DATA REQUIREMENTS AND STATUS OF AVAILABLE NUCLEAR DATA FOR INTEGRAL CALCULATIONS FOR BLANKET, SHIELDING, AND ACTIVATION PROBLEMS

Chairman: F.M. Mann, Westinghouse Hanford Co., U.S.A.

Secretary: M. Scott, University of Birmingham, U.K.

List of
participants: Cheng E.T., Goulo V., Gruppelaar H., Ilieva K., Jones R.,
              Maekawa H., Markovskij D.V., Mehta M.K., Rado V., Schmidt
              J.J., Seeliger D. and Vonach H.K.

1) Introduction

This workshop dealt with the needs and status of evaluated nuclear data
for fusion reactor technology. Nuclear data requirements for fusion
applications were determined by investigating neutronic functional areas
(Table 1) and the most important elements in the reactor components
(Table 2). These tables are primarily based on the input from the United
States (see paper by E. Cheng, "Nuclear Data Requirements for Fusion
Reactor Transport Calculations and Testing of ENDF/B-V and VI
Libraries"); however, input from Europe, Japan, and the U.S.S.R. was also
considered.

The requirements and status stated below are from the viewpoint of a
designer of fusion devices or a modeler of fusion processes. Thus the
data are effectively averaged over energy (usually over 1/4 lethargy bin:
i.e. about 2.2. MeV at 10 MeV) and over angle (usually about 20-30
degrees for elastic scattering).

2) Requirements and Status

It must be emphasized that the requirements and status that the workshop
determined were for the reactor components and not for each material in
the component. Thus the major constituents of a component may need to be
known to the accuracy stated for the component, but a minor constituent
would need to be known to a much lower extent. Tables 3, 4, 5 and 6

TABLE 1

Fusion Functional Needs for Nuclear Data

Application	Nuclear Data Required
Flux Determination	total cross section neutron emission cross section double differential neutron emission cross sections neutron multiplication cross sections dosimetry cross sections (see table 3) diagnostic reactions [e.g. Si(n,p) - see text]
Fuel Production	Li-6(n,alpha)t and Li-7(n,n'alpha)t corss sections
Radiation Hazards	Activation cross sections (see table 4), Decay Data
Material Behavious	dpa: recoil spectra and charged particle production cross sections and their covariances gas: hydrogen and helium production cross sections, transmutation cross sections
Power Generation	Kerma: recoil spectra and charged particle spectra and production cross sections
Fuel Burnup	d+d and d+t

TABLE 2

Fusion Materials

Component (Zone)	Major Elements
Structure	Fe, Cr, Ni, V, Ti, Al, W, Mn, Si
Breeder/Coolant	Li, H, O, Pb, F, He, Be, Al + structure
Multiplier	Be, Pb
Magnet	Cu, N, Nb, Al + structure
First Wall/Divertor/Limiter	C, Cu, W + structure
Magnet Shield	C, Cu, W, H, O + structure
Biological Shield	Ca, Si, Ba + structure
Hybrid Blanket	Th, U, Pu

present the workshop's conclusions for transport, dosimetry, activation and other reactions respectively.

For transport data, the highest accuracy data are needed for the breeder/coolant (including a hybrid blanket), multiplier, and shields. Although total cross sections are not needed to 3% for direct use by fusion designers, such accuracy is needed for the determination of optical potential parameters and providing other data for nuclear model codes. Neutron emission data requirements, although less restrictive, have been met less often because of the difficulty of the experiments. In particular, the workshop believes that the need for emission cross sections known to 3% in the shield region is unlikely to be met with current experimental techniques; rather a 5% uncertainty is likely the limit. The need for detailed angular information is greatest for elastic scattering. However, nonelastic scattering angular distributions should not be simply entered as isotopic unless they really are.

Heat production needs to be known to 20% locally and 10% globally. The workshop is uncertain how such requirements translate into nuclear data requirements. However, evaluations must insure energy conservation for heating calculations to make any sense.

In general, dosimetry cross section needs have not been met. Few data are known to 3% over the relevant energy range and needed covariance data is often missing. Evaluations are also many years behind the experimental information, making the gap between requirement and status more serious. Besides the dosimetry data listed in Table 4, the proton emission spectra from Si+n must be known for diagnostic purposes.

There are a tremendous number of activation cross sections to be determined, although only the most critical ones need experimental effort. Many, particularly those involving unstable targets or long-lived products, are very difficult to measure.

Nuclear data for material behavior is at a much more satisfactory state than the data for other applications, mainly because the connections between nuclear data and the damage parameters are much better known than the connection between the damage parameters and the change in material behavior. However, inclusion of such nuclear data in evaluations still must be done.

The main charged particle cross sections (d+d and d+t) are experimentally well enough known at the present. However, a standardized equation is needed to represent the experimental data.

3) Other notes

a) If d+Li reactions are used to produce neutron fields to test material properties, then a new energy range of nuclear data will be needed.

b) There is a continual need for reevaluation to incorporate new experimental data and to incorporate the changing needs of designers of fusion devices.

c) The workshop recognizes the need for horizontal evaluations (i.e. evaluations of a particular reaction or property as a function of isotope). Examples of such horizontal evaluations are neutron emission at 14 MeV and isomeric ratios at 14 MeV.

d) The need for covariance information is stressed, particularly in the area of dosimetry reactions. Sensitivity analyses which lead to data requirements need covariance data as a necessary input.

Table 3

Needs and Status for Transport Cross Sections

	Component					
Nuclear Data	Breeder/Coolant % Met	Multi-plier % Met	Magnet % Met	First Wall + % Met	Shield % Met	Hybrid % Met
Total sigma:						
E-n < 10 MeV	3 P	3 Y	3 Y	3 Y	3 Y	1 P
E-n > 10 MeV	1 N	1 N	3 Y	3 Y	1 N	1 P
Neutron Emission	10 N	10 N(Y for Pb)	20 P	- -	3 N	10 Y(N for Pu,Th)
Neutron Multiplication	- -	3 N	- -	- -	- -	- -
Elastic Angular Distribution	10 N	10 N	20 P	- -	3 N	10 Y
Non-Elastic Angular Distribution	not very important					

Y -> experimental data exist and evaluations may incorporate such data
P -> partially met
N -> experimental data do not exist or do not satisfy requested accuracy

13

Table 4a

Needs and Status for Dosimetry Reactions
(Complete Covariance Data is Needed
for all Reactions and Between Reactions)
(Comment from U.S. DOE/BES Experimenters)

Short-Lived Product

No.	Material and Reaction	Energy Threshold	Reaction Product Half Life	Review/ Comment
1.	$^{16}O(n,\alpha)^{13}C$	~14 MeV		Measured
2.	$^{24}Mg(n,p)^{24}Na$	~ 6 MeV	15.0 h	Measured
3.*	$^{27}Al(n,p)^{27}Mg$	~ 2.3 MeV	9.5 min	Measured
4.*	$^{27}Al(n,\alpha)^{24}Na$	~ 8 MeV	15.0 h	Met
5.	$^{28}Si(n,p)^{28}Al$	~ 5 MeV	2.25 min	Met @ 14 MeV
6.	$^{31}P(n,p)^{31}Si$	~ 1.5 MeV	2.6 h	Consider Replacing
7.	$^{34}Cl(n,2n)^{34m}Cl$	~13.1 MeV	32 min	Review Needed
8.	$^{39}K(n,2n)^{38}K$	~13.5 MeV	7.6 min	Review Needed
9.*	$^{47}Ti(n,p)^{47}Sc$	~ 3 MeV	3.4 d	Met @ E < 10 MeV
10.*	$^{48}Ti(n,p)^{48}Sc$	~ 6.8 MeV	43.7 h	Met
11.*	$^{56}Fe(n,p)^{56}Mn$	~ 1.5 MeV	2.6 h	Met
12.*	$^{58}Ni(n,2n)^{57}Ni$	~12.5 MeV	36 h	Met
13.*	$^{59}Co(n,\alpha)^{56}Mn$	~ 5 MeV	2.6 h	Met, Measurement in Progress
14.*	$^{63}Cu(n,\gamma)^{64}Cu$	0	12.7 h	Consider Replacing[2]
15.*	$^{63}Cu(n,2n)^{62}Cu$	~10.9 MeV	9.7 min	Review Needed
16.*	$^{64}Zn(n,P)^{64}Cu$	~ 2 MeV	12.7 h	Met, Measurement in Progress
17.	$^{64}Zn(n,2n)^{63}Zn$	~12 MeV	38 min	Review Needed
18.	$^{85}Rb(n,2n)^{84m}Rb$	~10.7 MeV	20.5 min	Replace with ^{93}Nb[1]
19.	$^{90}Zr(n,p)^{90m}Y$	~ 4 MeV	3.2 min	Consider Replacing
20.	$^{90}Zr(n,2n)^{89m}Zr$	~13 MeV	4.2 min	Evaluation Needed
21.*	$^{103}Rh(n,n')^{103}Rh$	~ 0.04 MeV	46 min	Consider Replacing[3]
22.*	$^{115}In(n,\gamma)^{116}In$	0	54 min	Consider Replacing[2]
23.*	$^{115}In(n,n')^{115m}$	~ 0.8 MeV	4.5 h	Met
24.*	$^{197}Au(n,\gamma)^{198}Au$	0	2.69 d	Standard at Low[2]
25.	$^{197}Au(n,2n)^{196}Au$	~10 MeV	6.2 d	Review Evaluation
26.	$^{199}Hg(n,n')^{199m}Hg$	~ 0.5 MeV	43 min	Work in Progress
27.*	$^{235}U(n,f)$	0	Varied	Met, Standard
28.	$^{237}Np(n,f)$	~ 0.5 MeV	Varied	Evaluation Needed
29.*	$^{238}U(n,f)$	~ 1.5 MeV	Varied	Met

*These cross sections will be available in the ENDF/B-VI dosimetry files.

1. Other possible dosimetry cross sections and their status are $^{93}Nb(n,2n)92mNb$ (~8.9 MeV threshold energy; 10.2 d half-life; Status: met), and $^{58}Ni(n,p)^{58}Co$ (~1 MeV; 70.9 d; status: met).
2. Capture reactions on dosimeters need to be justified in fusion reactors.
3. A suitable dosimetry cross section, $^{93}Nb(n,n')^{93m}Nb$ (0.04 MeV threshold energy; 13.6 Y half life), can be considered.

14

Table 4b

Long-Lived Products Dosimetry

Important Activation Cross-Sections for Integral Experiments

Required Accuracy: ~3%

$$^{27}Al(n,\alpha)^{24}Na$$

$$^{197}Au(n,2n)^{196}Au$$

$$^{197}Au(n,\gamma)^{198}Au$$

$$^{54}Fe(n,p)^{54}Mn$$

$$^{115}In(n,n')^{115m}In$$

$$^{115}In(n,p)^{116}In$$

$$^{93}Nb(n,2n)^{92m}Nb$$

$$^{58}Ni(n,2n)^{57}Ni$$

$$^{58}Ni(n,p)^{58}Co$$

$$^{90}Zr(n,2n)^{89}Zr$$
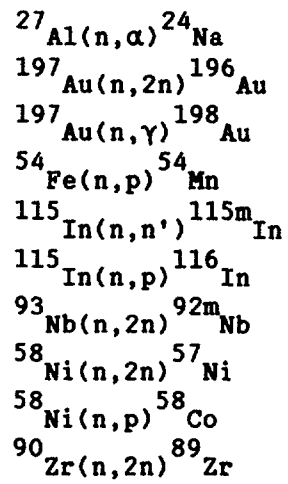
Table 5
Needs and Status for Activation Reactions
(Data from E. Cheng, Evaluation from U.S. DOE/BES Experimenters)

Isotope	Quantity	Radionuclide	Half Life	Review Comment
Ag				
^{109}Ag	n,2n	^{108m}Ag	127 y	(L).[1] Model calculation.[2]
^{107}Ag	n,γ	^{108m}Ag	127 y	(L). Measured.[3]
Al				
^{27}Al	n,α	^{24}Na	15.0 h	Met.
^{27}Al	n,2n	^{26}Al	7.2×10^5 y	(L). Measured.
Ar				
^{40}Ar	n,2n	^{39}Ar	269 y	(L). Model calculation.
Ba				
^{134}Ba	n,2n	^{133}Ba	10.7 y	(L). Measured.
^{137}Ba	n,p	^{137}Cs	30.2 y	(L). Model calculation.
^{138}Ba	n,np	^{137}Cs	30.2 y	(L). Model calculation.
Bi				
^{208}Bi(*)	n,2n	^{207}Bi	32.2 y	(L). Model calculation.
^{209}Bi	n,2n	^{208}Bi	3.7×10^5 y	(L). Met.
^{209}Bi	n,γ	^{210m}Bi	3.0×10^6 y	(L). Met.
Cl				
^{35}Cl	n,γ	^{36}Cl	3.01×10^5 y	(L). Measured.
^{37}Cl	n,2n	^{36}Cl	3.01×10^5 y	(L). Measured.
Ca				
^{40}Ca	n,2p	^{39}Ar	269 y	(L). Model calculation.
^{43}Ca	n,2p	^{42}Ar	32.9 y	(L). Model calculation.
^{44}Ca	n,^{3}He	^{42}Ar	32.9 y	(L). Model calculation.
^{40}Ca	n,γ	^{41}Ca	1.03×10^5 y	(L). Met.
^{42}Ca	n,2n	^{41}Ca	1.03×10^5 y	(L). Model calculation.
^{45}Ca	n,α	^{42}Ar	32.9 y	(L). Model calculation.
^{42}Ca	n,α	^{39}Ar	269 y	(L). Model calculation.
^{43}Ca	n,nα	^{39}Ar	269 y	(L). Model calculation.
^{44}Ca	n,γ	^{45}Ca	164 d	Measured.
^{40}Ca	n,α	^{37}Ar	35.0 d	Met.

Table 5 (continued)

Isotope	Quantity	Radionuclide	Half Life	Review Comment
Co				
^{59}Co	n,γ	^{60}Co	5.27 y	Met.
^{59}Co	n,2n	^{58}Co	70.9 d	Met.
^{59}Co	n,p	^{59}Fe	44.5 d	Met.
^{60}Co(*)	n,p	^{60}Fe	1.49×10^6 y	(L). Model calculation.
Cr				
^{50}Cr	n,γ	^{51}Cr	27.7 d	Measured.
^{50}Cr	n,np	^{49}V	330 d	Measured.
^{50}Cr	n,d	^{49}V	330 d	Measured.
^{52}Cr	n,2n	^{51}Cr	27.7 d	Met.
Cu				
^{63}Cu	n,p	^{63}Ni	100 y	(L). Met.
^{65}Cu	n,t	^{63}Ni	100 y	(L). Model calculation.
^{63}Cu	n,γ	^{64}Cu	12.7 h	Measured.
^{63}Cu	n,α	^{60}Co	5.27 y	Met.
^{65}Cu	n,2n	^{64}Cu	12.7 h	Met.
^{65}Cu	n,γ	^{66}Cu	5.10 min	Measured.
F				
^{19}F	n,γ	^{20}F	11.0 s	Model calculation. (M)[4]
^{19}F	n,2n	^{18}F	110 min	Measured.
Fe				
^{54}Fe	n,np	^{53}Mn	3.7×10^6 y	(L). Measured.
^{54}Fe	n,d	^{53}Mn	3.7×10^6 y	(L). Measured.
^{59}Fe(*)	n,γ	^{60}Fe	1.49×10^6 y	(L). Model calculation.
^{54}Fe	n,γ	^{55}Fe	2.68 y	Measured.
^{54}Fe	n,α	^{51}Cr	27.7 d	Being measured.
^{54}Fe	n,p	^{54}Mn	313 d	Met.
^{56}Fe	n,2n	^{55}Fe	2.68 y	Met.
^{56}Fe	n,p	^{56}Mn	2.58 h	Met.
^{58}Fe	n,γ	^{59}Fe	44.5 d	Measured.

Table 5 (continued)

Isotope	Quantity	Radionuclide	Half Life	Review Comment
K				
^{39}K	n,α	^{36}Cl	3.01×10^5 y	(L). Model calculation.
^{39}K	n,p	^{39}Ar	269 y	(L). Measured.
^{39}K	n,t	^{37}Ar	35.0 d	Model calculation.
^{41}K	n,γ	^{42}K	12.4 h	Model calculation(M).
^{41}K	n,p	^{41}Ar	1.83 h	Measured.
Kr				
^{82}Kr	n,2n	^{81}Kr	2.1×10^5 y	(L). Model calculation.
^{82}Kr	n,α	^{79}Se	65000 y	(L). Model calculation.
^{83}Kr	n,nα	^{79}Se	65000 y	(L). Model calculation.
^{86}Kr	n,2n	^{85}Kr	10.7 y	(L). Model calculation.
Mg				
^{24}Mg	n,p	^{24}Na	15.0 h	Met.
Mn				
^{55}Mn	n,γ	^{56}Mn	2.58 h	Met.
^{55}Mn	n,2n	^{54}Mn	313 d	Met.
Mo				
^{92}Mo	n,p	^{92}Nb	3.5×10^7 y	(L). Measured.
^{92}Mo	n,γ	^{93}Mo	3.5×10^3 y	(L). Measured.
^{94}Mo	n,2n	^{93}Mo	3.5×10^3 y	(L). Measured.
^{94}Mo	n,p	^{94}Nb	2.03×10^4 y	(L). Model calculation.
^{95}Mo	n,np	^{94}Nb	2.03×10^4 y	(L). Measured.
^{95}Mo	n,d	^{94}Nb	2.03×10^4 y	(L). Measured.
^{96}Mo	n,α	^{93}Zr	1.53×10^5 y	(L). Model calculation.
^{97}Mo	n,nα	^{93}Zr	1.53×10^5 y	(L). Measured.
N				
^{14}N	n,p	^{14}C	5730 y	(L). Measured.

18

Table 5 (continued)

Isotope	Quantity	Radionuclide	Half Life	Review Comment
Na				
^{23}Na	n,γ	^{24}Na	15.0 h	Measured.
^{23}Na	n,2n	^{22}Na	2.60 y	Measured.
Nb				
^{93}Nb	γ	^{94}Nb	2.03×10^4 y	(L). Measured.
^{93}Nb	n,2n	^{92}Nb	3.5×10^7 y	(L). Met.
^{93}Nb	n,α	^{90}Y	64.1 h	Met.
^{93}Nb	n,^{3}He	^{91}Y	58.5 h	Measured.
^{93}Nb	n,p	^{93}Zr	1.53×10^6 y	(L). Measured.
Ni				
^{62}Ni	n,γ	^{63}Ni	100 y	(L). Measured.
^{60}Ni	n,2n	^{59}Ni	7.5×10^4 y	(L). Being measured.
^{64}Ni	n,2n	^{63}Ni	100 y	(L). Being measured.
^{58}Ni	n,γ	^{59}Ni	7.5×10^4 y	(L). Met.
^{61}Ni	n,2p	^{60}Fe	1.49×10^6 y	(L). Model calculation.
^{60}Ni	n,p	^{60}Co	5.27 y	Met.
^{58}Ni	n,p	^{58}Co	70.9 d	Met.
^{58}Ni	n,2n	^{57}Ni	36.1 h	Met.
^{58}Ni	n,np	^{57}Co	271 d	Measured.
^{58}Ni	n,d	^{57}Co	271 d	Measured.
^{58}Ni	n,α	^{55}Fe	2.68 y	Met.
^{63}Ni(*)	n,α	^{60}Fe	1.49×10^6 y	(L). Model calculation.
Pb				
^{204}Pb	n,γ	^{205}Pb	1.52×10^7 y	(L). Measured.
^{206}Pb	n,2n	^{205}Pb	1.52×10^7 y	(L). Measured.
^{206}Pb	n,α	^{203}Hg	46.6 d	Measured.
^{206}Pb	n,nd	^{204}Tl	3.78 y	Model calculation.
^{206}Pb	n,t	^{204}Tl	3.78 y	Model calculation.
^{204}Pb	n,p	^{204}Tl	3.78 y	Model calculation.
^{204}Pb	n,2n	^{203}Pb	51.9 h	Model calculation.

Table 5 (continued)

Isotope	Quantity	Radionuclide	Half Life	Review Comment
Si				
^{30}Si	n,γ	^{31}Si	2.62 h	Model calculation.
^{29}Si	n,2p	^{28}Mg	20.9 h	Model calculation.
Sr				
^{89}Sr	n,γ	^{90}Sr	28.6 y	(L). Model calculation.
Ti				
^{46}Ti	n,p	^{46}Sc	83.8 d	Met.
^{46}Ti	n,2p	^{45}Ca	164 d	Model calculation.
^{47}Ti	n,p	^{47}Sc	3.35 d	Met.
^{47}Ti	n,np	^{46}Sc	83.8 d	Measured.
^{47}Ti	n,d	^{46}Sc	83.8 d	Measured.
^{48}Ti	n,p	^{48}Sc	43.7 h	Met.
^{48}Ti	n,np	^{47}Sc	3.35 d	Measured.
^{48}Ti	n,2p	^{47}Ca	4.54 d	Model calculation.
^{48}Ti	n,α	^{45}Ca	164 d	Measured.
^{49}Ti	n,d	^{48}Sc	43.7 h	Measured.
^{50}Ti	n,α	^{47}Ca	4.54 d	Measured.
V				
^{51}V	n,nα	^{47}Sc	3.35 d	Measured.
^{51}V	n,α	^{48}Sc	43.7 h	Met.
^{51}V	n,γ	^{52}V	3.75 min	Measured.
^{51}V	n,p	^{51}Ti	5.76 min	Met.
^{50}V	n,2n	^{49}V	330 d	Model calculation.
W				
^{186}W	n,nα	^{182}Hf	9×10^6 y	(L). Model calculation.
^{182}W	n,nα	^{178}Hf	31 y	(L). Model calculation.
^{186}W	n,γ	^{187}W	23.9 h	Measured.
^{186}W	n,2n	^{185}W	75.1 d	Measured.
^{184}W	n,γ	^{185}W	75.1 d	Measured.
^{182}W	n,2n	^{181}W	121 d	Measured.
^{180}W	n,γ	^{181}W	121 d	Model calculation.
^{180}W	n,np	^{179}Ta	665 d	Model calculation.
^{180}W	n,d	^{179}Ta	665 d	Model calculation.

Table 5 (continued)

Isotope	Quantity	Radionuclide	Half Life	Review Comment
Zn				
^{64}Zn	n,2p	^{63}Ni	100 y	(L). Model calculation.
^{66}Zn	n,α	^{63}Ni	100 y	(L). Model calculation.
^{64}Zn	n,p	^{64}Cu	12.7 h	Met.
^{64}Zn	n,γ	^{65}Zn	244 d	Measured.
^{64}Zn	n,2n	^{63}Zn	38.1 min	Measured.
^{66}Zn	n,2n	^{65}Zn	244 d	Measured.
Zr				
^{93}Zr	n,α	^{90}Sr	28.6 y	(L). Model calculation.
^{94}Zr	n,nα	^{90}Sr	28.6 y	(L). Model calculation.
^{94}Zr	n,2n	^{93}Zr	1.53×10^6 y	(L). Model calculation.
^{90}Zr	n,2n	^{89}Zr	78.4 h	Measured.
^{90}Zr	n,p	^{90}Y	64.1 h	Measured.
^{94}Zr	n,γ	^{95}Zr	64.0 d	Measured.
^{96}Zr	n,2n	^{95}Zr	64.0 d	Measured.

[1] (L) indicates long-lived daughter radionuclide.

[2] Model calculation could be made or already available. Measurement appears difficult.

[3] Measured data available.

[4] (M) indicates that the data could be measured.

Table 6

Needs and Status of Other Reactions

Material Behavior:

Energy dependence of dpa and gas production cross sections is needed to better than 20%. Using experimental data and nuclear model codes this is probably met.

Transmutation cross sections are needed to roughly 30%. When evaluated, this will be met.

Local heating needs to be known to 20% and global heating to 10%. The workshop is unsure how this translates into uncertainties in nuclear data as the problem is non-local.

Fuel production cross sections:

Li-6 (n, alpha)t needs to be known to 20% and is known to that level
Li-7 (n,n alpha)t needs to be known to 3% and is probably known that well but a new evaluation is needed.

Fuel Burnup cross sections:

Known t desired accuracy bu a standardized equation is needed for plasma codes.

REPORT OF WORKING GROUP II

STATUS OF DIFFERENTIAL DATA, THEORY AND POSSIBILITIES TO MEET DATA NEEDS

Chairman: Prof. H. Vonach
Secretary: Dr. H. Conde

List of   Cheng E.T., Elfruth O., Goulo V., Gruppelaar H., Kanda Y.,
participants: Liskien H., Mehta M.K., Oblozinsky P., Schmidt J.J., Seeliger
                D., Seidel K.

1) Status of differential data

The working group agrees with results of working group I concerning the extent
to which present differential data meet the requirements of fusion reactor
designers and to the conclusions of the review talk of Prof. Seeliger on the
status of double-differential neutron-emission data. The working group
especially wants to point out that the requirements for double-differential
neutron-emission cross-sections to 3-10% and activation cross-sections
(dosimetry) to 3% are not met at present.

2) Possibilities of satisfying the data needs

The working group agrees that the data needs established in working group I
can be met with present techniques except for the demand to determine
double-differential neutron-emission cross-sections to 3% for some breeding
and shielding materials. With reasonable effort it seems possible to
determine energy-differential neutron-emission cross-sections to 5% and
activation cross-sections for dosimetry applications to 2-3% accuracy.

There was a general agreement that the data requests can only be fullfilled by
a combination of experimental and theoretical efforts.

The role of experiment and theory is rather different for different mass
ranges and was discussed in some detail:
a) Light nuclei (Li, Be, C, N, O):
   It was concluded that theory does not provide reliable predictions except
   for R-matrix calculations on ^{6}Li in the low-energy region. Measurements
   are therefore needed at many energies to fulfill the requests.

b) Medium-light nuclei (Al, Si, Mg, Ca):

Cross-sections in this mass-range can be calculated more reliably than for the light nuclei, using coupled-channels, DWBA and Hauser-Feshbach models. Measurements are therefore only needed at some selected energies in order to determine the model parameters. Measurements which confirm this claim have been done at the Technische Universität Dresden for incident energies between 6.8 and 14 MeV.

c) Medium and heavy nuclei (A = 50-209):

A number of double-differential neutron-emission cross-sections (DDX) exists at 14 MeV and at low energies, but very few at intermediate energies. It is not clear at present whether this gap can be filled by model calculations. The 14 MeV data can be explained by the assumption of contributions from direct, precompound and compound nucleus reactions,however,different theoretical approaches for the direct and precompound parts are possible. Therefore the working group recommended that accurate measurements should be made for one nucleus at different incident neutron energies to check the theoretical models. Because of the large amount of data already existing Nb is suggested for this purpose. Measurement of DDX at one energy below 14 MeV (e.g. 10 MeV) is recommended for all requested elements, need for more incident energies should be decided according to the result of the Nb exercise.

d) Hybrid fuel elements (Th, U, Pu):

The DDX values for the actinides were reported to be very badly known. Likewise the fission spectra were described by the Watt formula which is not scientifically justified.Therefore the working group recommended that measurements at E_n = 6, 10 and 14 MeV should be made and the complex evaporation model should be used for the fission neutron spectra analysis.

3) Specific recommendations concerning procedures to be followed in new measurements

The working group agrees that the guide-lines for activation measurements worked out by Prof. Csikai for activation measurements and by Prof. Seeliger for double-differential neutron-emission cross-section measurements are very valuable and should be made available especially to new experiments.

24

In addition two points were made:

a) It was recommended that the neutron-emission spectra from natural lead should be used as reference continuum spectrum by all groups.

b) Impurities of the neutron field are one of the most important sources of systematic error in the measurement of activation cross-sections. Careful minimization of the contribution from neutrons of wrong energies and correction for the unavoidable remainder of this effect is therefore necessary for any precision measurement.

4) Coordinated research programme on fusion related nuclear data measurements

The working group was informed that the IAEA had approved a new CRP on fusion-related nuclear data measurements as a result of a recommendation from the last meeting of the 14 MeV CRP at Dubrovnik.

The working group recommends that the program for the new CRP be strictly limited to double-differential neutron-emission cross section measurements for elements of special importance in fusion reactor technology.

The following elements were selected for this purpose: V, Cr, Fe, Nb, Ta and ^{238}U. Furthermore the working group recommends a double-differential cross-section measurement on ^{208}Pb for checks of model calculations. The working group asks the IAEA to investigate the possibilities to provide the CRP with enough material of ^{208}Pb ($\sim$ 100 g).

The energy resolution of the measurments should be better than 4nsec/m and the accuracy better than 10%.

5) Scope of a possible CRP on activation cross-sections

The working group agrees that such a CRP could also be very useful but it was felt that its scope should be defined only after a thorough review of the present situation. This review should make use of the contributions to this meeting (Cheng, Gruppelaar, Forest, Vonach) and especially look into the problems of isomer ratios and long-lived activities. It is suggested that Dr. Gruppelaar and Prof. Vonach look into these questions and produce some recommendations to the next INDC meeting in October 1987.

REPORT OF WORKING GROUP III

INTERNATIONAL FUSION NUCLEAR DATA FILE

Chairman: Dr. H. Gruppelaar

Secretary: Dr. R.A. Forrest

List of
participants: Borisov A.A., Cheng E.T., Elfruth O., Goulo V., Ilieva K.,
              Kanda Y., Liskien H., Mann F.M., Markovskij D.V., Pelloni S.,
              Schmidt J.J., Sumita K., Vonach H.K.

1. Introduction

The main task of WG3 was to investigate the possibility for creating an
international nuclear data file for use in fusion-reactor technology and
to indicate how such a file could be organised. The current evaluations
for nuclear data for fusion reactors are connected to the fission-reactor
programmes of the various countries or regions. The newest versions of
these evaluations will be completed in the period 1987 to 1989. At present
some of these regional evaluations are still restricted with respect to
their distribution, but it is expected that these restrictions will disap-
pear in the near future, certainly for the materials important in
fusion-reactor design. After about two years further evaluation work
could perhaps be organised with world-wide participation. However, there
is already now a need for one joint file, specifically for the design of
the planned international Engineering Test Reactor (ETR). The presently
available INTOR file (INDL-F) is not adequate for this purpose and
therefore this file should be updated to form an international ETR-file
consisting of the best evaluations that could be obtained within one or
at most two years. This short-term goal could also be the start of a
fully international cooperation in the field of nuclear data evaluation,
certainly after the completion of the current regional data files.

2. Availability of current evaluations

The availability of the current evaluations is shown in Table 1. Some
comments are added in the last column.

Table 1. Availability of current evaluations

Library	Availability	Remarks
ENDF/B-IV	Available	Not adequate for fusion applications
ENDF/B-V	Only parts available	Fusion material evls. less restricted
ENDF/B-VI	Expected to become available	Completed mid 1989; released element by element
EFF-1,2	Largely unavailable at present	Part of JEF 2, except for Li, Al, Si, Pb
JENDL-2	Available	Not adequate for fusion applications
JENDL-3	Available by March'88	Preliminary evaluations are JENDL-3-PR1,2
BROND	Available by Jan.'87	USSR + Dresden (56 nuclides)
ENDL	Available	Not strictly ENDF-V format; large number of materials
CENDL	Available (INDL-V)	China, 14 materials
IRDF	Available	International Reactor Dosimetry File (ENDF/B-V + 10 evaluations from IRK, Vienna and other sources)

The completion date of ENDF/B-VI, EFF-2, JEF-2 and JENDL-3 is in the period 1988 to 1989. Until that time most of the evaluators are involved in these regional evaluations. However, there are already at present a number of recent evaluations for individual fusion materials that have been released or could be made available for the purpose of an international fusion file.

3. Status of the present international (INDL-F) fusion file

The International Nuclear Data Library for Fusion (INDL-F) was completed in 1983. It is a collection of evaluations mainly from ENDF/B-IV with parts of ENDF/B-V (some standards and some dosimetry cross sections) and ENDL. The format is ENDF-5.

This data file is not adequate for the design calculations for ETR. However, it could be used as a "starter file" for the ETR-project. The first step would be to translate this file into ENDF-VI format (there should also be an option to translate files in ENDF-VI format into ENDF-V format

to serve users with version-V processing codes). As information becomes available the data on this starter file could be replaced material by material.

4. Need for an international fusion file

At the ETR-related meeting in Kyoto, Japan, in November 1986 it was stated that a joint numerical file with atomic and nuclear data is wanted for the ETR-project. The Nuclear Data Section of IAEA could play a role in the nuclear data part of this file.

A pre-condition for the success of setting up an ETR file is that both users and evaluators agree on this initiative. Therefore the proposal for a joint nuclear data file for fusion needs to be discussed with the ETR-team. This team should support the project of setting up an international nuclear data file.

5. Requirements for an international fusion file

The detailed requirements for the ETR nuclear data file should be specified by the ETR-team. The working group has made the following comments. First of all, the format of the file should be ENDF-VI. The file should be made to facilitate neutron and photon transport calculations, e.g. to obtain the tritium breeding ratio and the (magnet) shielding properties. For activation and dosimetry calculations a separate file is needed (see also section 7).

The file should be specific for fusion applications, with no information on fissile materials. The materials listed in EFF are used as a basis, and these are shown in Table 2 with two addional materials. If possible the evaluations should be isotopic rather than elemental where the elements are not mono-isotopic. Only about a few of these materials are design-dependent.

Table 2. Materials in ETR file

H, D, T, ^{6}Li, ^{7}Li, Be, ^{10}B, ^{11}B, C, O, N
Al, Si, Ti, V, Cr, Mn, Fe, Ni, Co, Cu, Zr
Nb, Mo, Ba, W, Pb, Bi.

To develop this file an "evaluation of the existing evaluations"could be carried out. It is hoped and expected that for this purpose some new evaluations (as yet not widely distributed) will be made available. By mid 1988 the starter file should have had each material examined and the preferred evaluation should be selected. This library will require testing and checking prior to distribution, and this is expected to take about one year to be completed. Therefore by mid 1989 a useful version of the file could perhaps be distributed. A further phase where new evaluations (where required) can be carried out can then follow.

6. Organization to create and maintain an international fusion file

A similar method of organisation to that used for JEF-1 could also be employed for the ETR file. The details will need to be specified by IAEA but the following ideas may be useful. An "expert committee" comprising evaluators, users and experimentalists would oversee the project. This will need technical support of approximately 1 to 2 MY/Y, e.g. to cover the production of "review kits" in the initial phase. Once the library exists it will require a similar level of support to cover maintenance etc. The details of where the technical support will be based (at IAEA or at one of the data centres) will need further study. A small subcommittee of evaluators for each material (or a set of materials) should be formed by the expert committee. A typical example is: Pb evaluation - Oak Ridge, Japan, ECN and TUD. The subcommittee would act as a group of referees on the existing evaluations and would be supplied with a "review kit" with possible contents shown in Table 3.

Table 3. Contents of review kit to be produced by IAEA

Numerical data for each evaluation

Graphs of data for individual evaluations

Comparative graphs

Documentation

Summary of integral quantities

14 MeV data points

Multigroup Data (3 groups per decade)

Results of runs of checker codes (both format & physical)

30

The referee reports from the subcommittee should also contain recommenda-
tions about parts of the chosen evaluation that need revisions in the
second phase of the project.

Data arising from several of the new Coordinated Research Programmes
(e.g. on 14 MeV Double Differential Cross Sections and on Methods of
Calculations for Structural Material Fast Neutron Cross Sections) should
be used by the subcommittees. Also new CRPs could be suggested.

The first meeting of the expert committee should be held early in 1987.
This could be linked with the first ETR project meeting and should contain
members of the ETR design team so as to facilitate a two-way flow of
information. Following meetings should be held every six months.

7. Other evaluated data

A new activation file (from Dr. F. Mann) is freely available. This con-
tains approximately 6000 reactions and is already being used for activa-
tion calculations. Improvements are being made by Hanford, Petten and
Harwell. A slight change in format will be agreed by January 1987 before a
copy is sent to IAEA.

For dosimetry there is already an international file (IRDF) that could be
further extended and updated to satisfy the data needs for ETR.

REPORT OF WORKING GROUP IV

IAEA SPONSORED INTERNATIONAL COMPARISON
OF BENCHMARK MEASUREMENTS AND CALCULATIONS

Chairman: Dr. P.K. Sumita

Secretary: Dr. R. Jones

List of   Borisov A.A., Cheng E.T., Conde H., Elfruth O., Goulo V.,
participants: Gruppelaar H., Ilieva K., Liskien H., Maekawa H., Mann F.M.,
               Markovskij D.V., Pelloni S., Schmidt J.J., Seeliger D.,
               M.C. Scott, Seidel K.

Introduction

The role of the working group was to decide what benchmarks should be
included in the intercomparison and what the responsibilities of the IAEA
should be. Two types of benchmark were discussed: a calculational
benchmark intended to intercompare and validate different neutron
transport codes, and an experimental benchmark that would allow comparison
of the experimental techniques used in different laboratories. The role
of the IAEA was expected to be in the publication of the specifications,
assisting with the provision and exchange of data files, and in sponsoring
a meeting for the discussion of results.

Calculational Benchmark

It was proposed that this should be a fairly simple benchmark to
begin with and that it could be expanded later. It is proposed that the
calculations be for single material (Pb) in a simple geometry (sphere).
The size of the sphere should be the same as that used in measurements by
the Dresden group which are to be published early in 1987 in Atomkern-
energie. The data for the calculation should be the ECN file for lead
(from Gruppelaar). The proposed geometry and the parameters to be
calculated are summarized below.

(1)   Size of sphere: Outer diameter 50 cm
                        Thickness 22.5 cm

(2)   Source spectrum: As given in Dresden report

(3) Parameters to calculate:

    a) Leakage spectrum per source neutron
       (energy group structure to be defined)

    b) Spatial distribution of reaction rates, at least of
       U-238, Cu-65 and Al-27 (using ENDF/B-V for dosimetry file)

    c) Neutron multiplication as a function of energy

This is a minimum set of parameters, the calculation of others and the use of other data files would be welcomed.

Experimental Benchmark

The intention here is to provide the specifications of a benchmark assembly that can be set up in any laboratory so that measurements made on it can be compared with the same set-up elsewhere. It was decided to propose the same size lead sphere as that described in the calculational bencmark.

It was felt that the most useful measurements that could be made would be of the low energy part of the neutron spectrum ($\leq$ 1 MeV) inside the sphere (scalar flux), normalized to the source strength.

Role of the IAEA

This should be as follows:

1) Publish the benchmark specifications and invite participation.

2) Provide participants in the calculational benchmark with the ECN Pb file and a suitable processing code to enable group averaged data to be produced.

3) It is recommended to arrange a Specialists' Meeting in 1988 (fall) for communication and discussion of the results obtained.

34

REQUIREMENTS OF NUCLEAR DATA
FOR FUSION REACTOR TECHNOLOGY

(Session A)

Chairman

K. SUMITA
Japan

NUCLEAR DATA REQUIREMENTS FOR FUSION REACTOR TRANSPORT CALCULATIONS AND TESTING OF ENDF/B-V AND VI LIBRARIES

E.T. CHENG
GA Technologies Inc.,
San Diego, California,
United States of America

Abstract

We have reviewed recent fusion reactor and blanket design studies in which promising blanket concepts were identified for future development, based on the D-T fuel cycle. We have developed a list of elements whose nuclear data are needed for fusion reactor transport calculations and reviewed the status of their neutron emission data. We found that most of these data are available to 15 MeV, both in experiment and evaluation, although some discrepancies exist between the experimental and evaluated data. We have identified some elements lacking experimental data at energies below 14 MeV. We also briefly discuss the nuclear data requirements in the areas other than those for fusion reactor transport calculations.

1. INTRODUCTION

The quest for inexhaustible energy sources for future generations of humankind has been a major international activity since the 1950's. Fusion energy has been considered a promising candidate ever since that time. Because of the necessary integration of sciences and technologies, many of which are still in the early development stage, the maturity of fusion energy seems slow. We are now approaching the demonstration of scientific breakeven. The first fusion energy applications are necessarily conceived with the deuterium-tritium fuel cycle

$$D + T \rightarrow \alpha(3.5 \text{ MeV}) + n(14.1 \text{ MeV}) \quad ,$$

because of its high reaction cross section resulting in lower plasma confinement requirements and ignition temperatures, and more importantly, its economical feasibility for electricity generation. One of the reacting hydrogen isotopes, tritium, is radioactive with a half-life of 12 years, and hence does not exist in nature. Fusion reactors based on the D-T fuel cycle will need to breed their own tritium via the following reactions, with the 14 MeV energetic neutrons and subsequently slowed down neutrons in the blanket surrounding the plasma:

$$^7Li + n \rightarrow n' + T + \alpha - 2.8 \text{ MeV}, \text{ and}$$

$$^6Li + n \rightarrow T + \alpha + 4.8 \text{ MeV}.$$
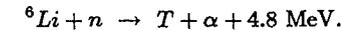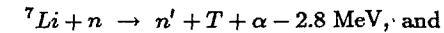
Because of the need to breed tritium, the element lithium inevitably becomes an important constituent of the reactor blanket in various forms, such as liquid lithium, lithium lead eutectic, LiF-BeF Salt, and the solid lithium compounds, Li_2O and $LiAlO_2$, just to mention those more often considered in recent reactor studies. The D-T fuel cycle cannot assure a truly inexhaustible energy source, but the earth can supply enough lithium to provide energy for approximately 1000 years.

The deuterium-deuterium based fuel cycles, namely the following D-D reactions,

$$D + D \rightarrow T + n(2.5 \text{ MeV}), \text{and}$$

$$D + D \rightarrow P + {}^3He$$
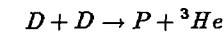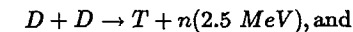
and subsequent burning of the reacting products, T and ^{3}He, via the following reactions,

$$D + T \rightarrow {}^4He + n, \text{and}$$

$$D + {}^3He \rightarrow P + {}^4He$$
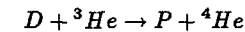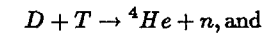
will be able to promise an inexhaustible energy source because of the large percentage of deuterium in the element hydrogen (15 atoms of deuterium in every thousand atoms of hydrogen isotopes), which is the most abundant element on earth. A long-term goal of fusion energy research must be making the D-D based fusion reactor economically more attractive, since its reaction cross section is about two orders of magnitude less than the D-T reaction.[1]

Fuel cycles beyond the D-D cycles are more difficult because of still smaller reaction cross sections and higher required plasma temperatures. A recent study revealed that from the magnetically confined physics viewpoint, these cycles are not feasible energetically.[2]

A common characteristic of the D-T and D-D fueled fusion reactors is that a large portion of nuclear energy is obtained from one of their reaction products, the neutron. The neutrons should be intercepted in the material medium, or blanket, surrounding the reacting plasma, in order to extract the kinetic and additional nuclear energy in the form of thermal energy. The blanket is thus cooled by selected coolant and the extracted thermal heat is converted into electricity through the necessary power conversion systems. The process of tritium breeding, which is essential in a D-T fueled fusion reactor, must also be done in the blanket. Additional material capable of neutron slowing-down and absorbing, is needed behind the blanket to further reduce the neutron intensity and nuclear heating (from both neutron and gamma-ray) to an acceptable level for the operation of the magnets

that produce the magnetic field needed to confine the plasma. Neutron and gamma-ray transport in the blanket and shield material is normally calculated following the integral-differential Boltzman transport equation,[3]

$$\vec{\Omega} \cdot \vec{\nabla} \; \phi \; (\vec{r}, \vec{\Omega}, E) + \sigma_t(\vec{r}, \; E) \; \phi \; (\vec{r}, \; \vec{\Omega}, \; E) = \int \; \sigma_e(\vec{r}, \; \vec{\Omega}' \rightarrow \vec{\Omega}, E' \; \rightarrow E)$$

$$\phi(\vec{r}, \vec{\Omega},' E') \text{d} \; \vec{\Omega}' \; \text{d} \; E' \; + Q(\vec{r}, \vec{\Omega}, E) \quad ,$$

where $\phi(\vec{r}, \; \vec{\Omega}, \; E)$ is the neutron/gamma-ray flux at location $\vec{r}$, angle $\vec{\Omega}$, and energy E; $\sigma_t(\vec{r}, \; E)$ is the total cross section at location $\vec{r}$ and energy E; $\sigma_e(\vec{r}, \; \vec{\Omega}' \rightarrow \; \vec{\Omega}, \; E' \rightarrow E)$ is the neutron emission cross section at location $\vec{r}$, incident angle and energy, $\vec{\Omega}'$ and E', and emitting angle and energy, $\vec{\Omega}$ and E; and $Q(\vec{r}, \; \vec{\Omega}, E)$ is the external neutron source at location $\vec{r}$, angle $\vec{\Omega}$, and energy E. Once the neutron/gamma-ray fluxes are solved, the neutron reaction rates, such as tritium breeding, and the nuclear heating rate can be obtained by multiplying the neutron and gamma-ray fluxes with the corresponding reaction cross section and kerma (kinetic energy release per material atom) factors.

To solve the above transport equation and relevant nuclear reaction rates, nuclear data are essential. The general nuclear data needs and their availability and validity have been the subjects of many investigations, since the beginning of fusion energy research.[4-17] The types of nuclear data needed for fusion energy development are given as follows: (1) Charged particle nuclear and physics data for plasma transport and fusion reaction calculations. These data determine the source term for the subsequent transport calculations. (2) Total neutron and secondary neutron and gamma-ray emission data for neutron and gamma-ray transport and nuclear heating calculations. (3) Tritium production reaction data for D-T fueled reactors. (4) Neutron activation and dosimetry data. (5) Helium production data important to materials radiation damage studies.

In this paper we briefly discuss the needs for and status of nuclear data for the above areas. The focus of the review will be in the area of total neutron and gamma-ray emission data, which are essential for fusion reactor transport calculations. The organization of this paper is as follows. Section 2 is devoted to the review of recent fusion reactor blanket/shield concepts and reactor study activities in the U.S. The nuclear data requirements for these blanket/shield concepts are presented. Section 3 discusses the status of the required nuclear data for transport calculations. The status of ENDF/B-VI files and testing of ENDF/B-V data are also given in this section. Section 4 briefly discusses the need and reviews the status of nuclear data in the areas other than those needed for reactor transport calculations. Finally, a summary of this paper is given in Section 5.

2. RECENT REACTOR STUDIES AND BLANKET/SHIELD CONCEPTS

The major commercial application of D-T fueled fusion reactors, anticipated early in the 21st century, is to provide electricity. An important effort for magnetically confined fusion is the development of feasible reactor components. Among the reactor components, the fusion blanket, which intercepts the fusion neutrons and converts the kinetic energy into heat for power conversion and breeds tritium, is one of the most important. All the power conversion and tritium breeding functions in the blanket depend on the interaction of fusion neutrons with the blanket materials, and hence calculations of these functions are critically dependent on nuclear data associated with these materials. In this section, we summarize recent reactor and blanket design studies in which the most promising blanket concepts and attendant blanket materials have been identified. We then review the status of important nuclear data pertaining to the blanket materials of these promising concepts, and other reactor materials for shielding and magnets applications.

Many reactor studies have been performed in the U.S. since the beginning of fusion energy research in the late 1950s. Most of these early studies were encouraged to identify engineering problem areas and critical issues through integral conceptual reactor designs. These design studies are an important part of fusion energy development. They address the feasibility issues relevant to confinement concepts and reactor engineering. A list of the studies and blanket descriptions associated with these reactor designs was compiled and analyzed in detail as part of the Blanket Comparison and Selection Study (BCSS).[18]

The recent BCSS study was a multilaboratory effort led by Argonne National Laboratory and completed in 1984. This study focused on:

- the development of reference guidelines, evaluation criteria, and a methodology for evaluating and ranking candidate blanket concepts,

- the compilation of the required data base and development of a uniform systems analysis for comparison,

- the development of conceptual designs for comparative evaluation,

- the evaluation of leading concepts for engineering feasibility, economic performance, and safety,

- the identification and prioritization of R&D requirements for the leading blanket concepts.

The BCSS project identified 16 leading candidate blanket concepts for tokamak and tandem mirror reactors.[19] These leading blanket concepts were evaluated in detail. The conclusion was that based on the overall evaluation, four blanket concepts should be selected for the blanket research and development program. These blanket concepts (breeder/coolant/structure) are given as follows:

- lithium/lithium/vanadium alloy,
- Li_2O/helium/ferritic steel,
- LiPb alloy/LiPb alloy/vanadium alloy,
- lithium/lithium/ferritic steel.

In addition to the above four blanket concepts, several other promising concepts were identified in the MINIMARS program led by the Lawrence Livermore National Laboratory.[20] These are:

- FLiBe/FLiBe/vanadium alloy,
- FLiBe+Be/helium/vanadium alloy
- Li+Be/helium/vanadium alloy
- LiPb+Be/helium/ferritic steel

From the above promising blanket concepts, we have concluded that the following elements are most important for fusion blanket development:

- Structure: V, Fe, Cr, and Ti,
- Breeder/coolant: Li, O, Pb, F and Be.

Among these elements, vanadium and iron are the major constituent elements for the structural alloys, ferritic steel, and vanadium alloys. Lithium (particularly ^7Li), Be, and Pb are the dominant neutron multipliers in these blanket systems. The shield concepts conceived of in early reactor studies are still promising, since the need for an efficient neutron slowing down and absorbing material combination remains the goal of the shield design. The promising materials for shielding are stainless steel (304 SS or 316 SS) and manganese steel (Fe 1422) for high-energy neutron moderating; boron carbide for neutron moderation and absorption; and lead for gamma-ray attenuation.[20, 21] Water (boronated or pure) and helium are proposed for shielding coolants. In the magnet area, copper appears to be the major conducting material, although aluminum is proposed as an alternate material in some designs because of low activation considerations. The coil case and structural materials are mainly stainless steel and aluminum alloy. There are also insulation materials, helium and superconductors such as NbTi and Nb_3Sn proposed for the superconducting magnet. However, relatively small quantities are involved, hence they are less important than the major conductor and structural materials. A summary of the natural elements constituting the materials promising for the construction of near-term D-T fusion reactors is given in Table 1.

3. STATUS OF NUCLEAR DATA FOR FUSION REACTOR TRANSPORT CALCULATIONS

Table 1 lists the elements whose total neutron cross section and secondary neutron and gamma-ray emission spectra data are needed for neutron transport calculations as a function of angle and energy for fusion engineering feasibility demonstrations. The accuracy required is in general ±10% for most nuclear cross sections of the above materials. However, it is important to point out that the specific required accuracy for each nuclear cross section not only depends upon the degree of importance of the associated reaction product but also upon the quantity of the related material, which may affect the resultant neutron and gamma-ray spectra and flux in the reactor components. The required accuracy must be determined by detailed sensitivity and uncertainty analysis and may be design-dependent.

TABLE 1
ELEMENTS WHOSE TOTAL AND SECONDARY NEUTRON AND GAMMA-RAY
EMISSION CROSS SECTION DATA ARE NEEDED
FOR FUSION FEASIBILITY DEMONSTRATIONS

Element	Use
Fe	First wall, structure, shield
V	First wall, structure
Cr	First wall, structure, shield
Mn	First wall, structure, shield
Ti	First wall, structure, shield
Be	Neutron multiplier
Pb	Neutron multiplier, gamma shield
^7Li	Tritium breeding
^6Li	Tritium breeding
O	Coolant, shield, insulation
F	Breeder compound material (FLiBe)
H	Coolant, insulation, shield
Cu	Electrical conductor
Al	Electrical conductor, insulation, structure
C	Reflector, shield, insulation
W	Shield
B	Shield

Because neutron transport nuclear data up to 9 MeV are relatively well known, and because sensitivity studies indicate that the 11 to 15 MeV range is the most important for defining neutron transport in a fusion reactor, these data are needed particularly in the 9 to 16 MeV range. Sixteen MeV was chosen as the upper limit to ensure that the range

covers the most energetic neutron from a D-T reactor, since the contribution at energies above 16 MeV drops off to less than 0.1% of the total. Note that there are exceptions in which more accurate data may be needed in energy ranges below 9 MeV, due to specific design requirements of the fusion reactor.

We have reviewed the status of the neutron emission data as follows:

Hydrogen. There is little dispute about cross sections for this element at energies from thermal to 15 MeV. There are abundant, precise total cross-sections and ^{1}H(p,p) measurements that, when used in phase-shift or R-matrix analyses, allow determination of neutron emission from ^{1}H+n reactions to better than ±5% of the fusion energy range. The differential cross section is isotropic in the center of mass to a very high order to 10 to 14 MeV. Certainly the readily available accuracy conservatively meets fusion needs.[23]

Lithium. Neutron emission data are available experimentally for ^{6}Li and ^{7}Li from about 6 to 10 MeV, and 5 to 15 MeV, respectively, for the evaluation of the ENDF/B-V file. More measured data have become available recently.[24-27] Particularly noted is the measurement extending the neutron energy to 14 MeV for ^{6}Li neutron emission data.[24] These experimental data should be incorporated into the evaluation of the ENDF/B-VI file.

Beryllium. The neutron emission data from 5.9 to 14 MeV were measured by Drake (LANL) in 1977.[28] A number of 14 to 15 MeV measurements have been made since the Drake measurement. A recent experiment was performed by Takahashi using the OKTAVIAN facility at Osaka University.[29]

Recent LLNL experiments and re-evaluation indicate that beryllium evaluation is in good shape with n,2n cross section accuracy within about 5%.[30, 31] The new evaluation will be adopted as version VI of the ENDF/B file, after the data testing procedure is completed.

Oxygen. The neutron emission data are available only at 14 MeV in a recent OKTAVIAN experiment.[29] The elastic differential data at a number of energies from 9.21 to 14.93 MeV were recently measured.[32] There also appears to be a persistent discrepancy between calculation and experiment in and near the low-lying scattering resonances at 450 keV and the MeV energy range.

Aluminum. The neutron emission data are available from 1 to 20 MeV. Recent experiments also gave the differential data at 14 MeV.[29] Some elastic and inelastic differential data were obtained from the Triangle University Nuclear Laboratory (TUNL) at energies from 11 to 14 MeV.

The ENDF/B-V status reviewed by Hetrick, Larson, and Fu indicate that there is a discrepancy between evaluation and experiment in the neutron emission data at 14 MeV,

with the evaluation overestimating the outgoing neutron cross section at energies above about 9 MeV.[34]

Vanadium. Vanadium alloy is a promising high-temperature (~750°C for liquid lithium systems) structural material for fusion power reactor applications. However, there are no experimental neutron emission data available for vanadium at energies between 5 and 14 MeV. Some elastic and inelastic differential data were measured at ANL in the energy range from 1.8 to 4 MeV for ^{51}V (>99% abundance) and total cross sections were measured from 1.5 to 5.5 MeV.[35] A new evaluation is under way at ANL.[36]

Iron. The neutron emission data for iron are available from 1 to 20 MeV. Recent OKTAVIAN experiments also gave the differential data at 14.6 MeV.[29] There are some elastic and inelastic differential data for ^{54}Fe and ^{56}Fe available from Ohio University and TUNL at various energies between 8 and 26 MeV. An updated evaluation was recently made available at ORNL, however, in ENDF/B-V format. This evaluation should be converted into ENDF/B-VI format.

Copper. The neutron emission data for copper were measured at ORNL from 1 to 20 MeV. The recent OKTAVIAN measurements also included copper at 14 MeV.[29] Elastic and inelastic differential cross sections were obtained isotopically at a few energies between 8 and 17 MeV at TUNL. It was indicated [34] that the ENDF/B-V evaluation may not be adequate for fusion applications. A new evaluation was recently completed at ORNL for adoption as ENDF/B-VI file, and the results should be tested against the experimental values.[37]

Lead. No neutron emission data are available from CINDA83 except Hermsdorf (1975), Clayeux (1972) and the recent OKTAVIAN experiment,[29] all at 14 MeV. There are some isotopic elastic/inelastic differential data at 7 and 10 MeV energies available at Ohio University, University of Kentucky, and TUNL.

The ORNL review concluded that the ENDF/B-V evaluation and experiment at 14 MeV agree very well as far as the neutron emission data are concerned.[34] However, recent data testing of ENDF/B-V evaluation against OKTAVIAN experiments revealed that the measured and evaluated neutron emission cross sections do not agree with each other, particularly at energies above 10 MeV.[38]

Chromium. Cr is an alloying element for vanadium alloy (V15Cr5Ti) and ferritic steel (HT-9). The measured neutron emission data were available only at energies of about 14 MeV.[29] Experimental data are needed at energies other than 14 MeV. The ENDF/B-V file will most likely be carried over for the new version VI of the ENDF/B file.

Fluorine. F is an important element for the salt, FliBe, as a promising blanket material. The neutron emission data are available only at 14 MeV.[29] No work is planned to update the ENDF/B-V file. More experimental data are needed at energies other than 14 MeV.

Manganese. Mn is considered to be an energy-enhancing element in manganese steel, Fe 1422, for use as a reflector or hot shield component in the blanket. Experimental differential data are available only at 14.6 MeV.[29] Data other than 14 MeV are needed. A new ORNL/JAERI evaluation is underway.

Titanium. Ti is an alloying element in vanadium alloy, V15Cr5Ti. The neutron emission data were measured from 1 to 20 MeV at ORNL. Other measured data at 14.6 MeV were also made available.[29] A new evaluation is planned at ANL.

Tungsten. W is the most efficient 14 MeV neutron shield for fusion reactor design consideration. An extensive isotope evaluation was made recently at LANL[39, 40] to resolve the nuclear heating calculation problem. However, the neutron emission data were only available at 14.6 MeV.[41] A new evaluation is not planned at the present time.

Boron. The neutron emission cross section data for boron were measured from 6 to 14 MeV at LANL.[26, 42] The version V of ENDF/B file for ^{11}B and ^{10}B were evaluated in 1974 and 1977, respectively. An updated evaluation is underway at LANL.

Carbon. The neutron emission data for carbon are available from 1 to 20 MeV at ORNL.[42] New measured data have recently become available.[29] These newly available data should be considered when the ENDF/B-VI evaluation is performed.

Status of ENDF/B-VI Files

The upcoming ENDF/B-VI evaluations, scheduled to be completed and released in October 1989,[43] are expected to eliminate the nuclear data discrepancies, particularly in the double-differential data areas discussed above for those elements important to fusion reactor development. However, the personnel resources currently available are simply not enough to accomplish the evaluation of all materials. An extended schedule for the release of ENDF/B-VI and a reduction of the number of materials to be evaluated will be required. In order to alleviate these problems, international effort is needed. Some initiatives in the collaboration of this nature have taken place as a result of a meeting at the May 1985 international nuclear data conference held in Santa Fe, New Mexico, USA.[44] We should also expect international collaboration in the effort of data testing for ENDF/B-VI files.

4. OTHER NUCLEAR DATA NEEDS

In this section we briefly review the nuclear data areas other than those needed for the fusion reactor transport calculations. These are: charged-particle cross sections, tritium breeding related cross sections, dosimetry data, activation data, and helium production cross sections.

Charged Particle Cross Sections

The following D-D and D-T based charged-particle cross section data are needed to support operation of experimental devices, or for design studies of later experiments. Advanced fuel cycles beyond the D-D cycle were found not to be viable energetically. Data compilations are needed for σ versus energy and $\langle \sigma v \rangle$ versus temperature. The desired accuracies for the main reaction data, T(D,α)n, D(D,^{3}He)n, and D(D,p)T, are less than 5%. All other scattering data and other minor reaction data are needed to 10%. Most cross section data, except D+α and T+α scattering cross sections, were reviewed recently and were found to be satisfactory.[45] The status of these cross sections is summarized below:

T(D,α)n. A state-of-the-art experiment from 8 to 80 keV with absolute errors about 1.4% has been completed at LANL. Improved accuracy is not feasible at present.

T(T,α)2n and T(T,n)nα. Measurements are complete for 30 to 115 keV at LANL. Accuracies for the (T,α) and (T,n) reactions are anticipated to be ±5% and improvement will be difficult.

D(D,^{3}He)n and D(D,p)T. Measurements of both reactions are complete for the energy range 20 to 117 keV with absolute errors ranging from 1.6% to 2%.

D(^{3}He,p)α. Measured data available. Absolute cross section values should be good to 5–10%.

D(α,α)D and T(α,α)T. Facilities exist at LANL to obtain these data but direct measurements are not planned at present. Existing data and R-matrix analysis results are available to 2–4%.

Tritium Breeding Related Cross Sections

Tritium breeding calculations could be strongly influenced by the neutron multiplication reaction cross sections, namely ^{7}Li(n,n'α)t, Be(n,2n), and Pb(n,2n), since these cross sections determine the total neutron population available in the blanket for subsequent tritium production reaction with ^{6}Li. The status of each of these cross sections is briefly reviewed below.

^{7}**Li(n,n'α)t.** ^{7}Li(n,n'α)t is the principal nuclear reaction that provides excess neutrons for adequate tritium breeding in both lithium and Li$_2$O blanket concepts. It also helps the FLiBe blanket concept to breed tritium. If the tritium breeding ratio in a lithium or Li$_2$O blanket is to be predicted within 1%, the ^{7}Li(n,n'α)t cross section must be known to within 3%. This is because the contribution to total tritium breeding from the ^{7}Li(n,n'α)t reaction is, in general, 25–30%. Recently, several measurements of this cross section around 14 MeV were reported.[46−51] All these measured cross sections are subject to experimental errors of ±5–6%. The recently evaluated data, ENDF/B-V, also gives an uncertainty of about

±4% at energies near 15 MeV.[52] The accuracies of these measurements and evaluation still do not meet the required ±3% goal for tritium breeding prediction, although they are close to it. It is recommended that more experiments or new evaluations be performed so that either the experimental results themselves or the evaluations derived from them can meet the accuracy requirement.

The measured data are not satisfactory either. The lowest experimental values at 14–15 MeV were obtained by Swinhoe and Uttley, 235 mb (±4.7%) at 14.1 MeV.[46] The most recent two measurements performed in the U.S., Goldberg et al. at LLNL[50] and Smith et al. at ANL,[51] showed consistent results: 302 mb (±5%) at 14.94 MeV and 301 mb (±5.3%) at 14.7 MeV, respectively. These values are higher than those measured by Swinhoe and Uttley by about 29%. Moreover, they are within the experimental error with the ENDF/B-V evaluation which is 298 mb at 14.9 MeV. The measured values by Liskien et al. [47] and Maekawa et al. [48] are close to each other and are lower than the experimental values given by Goldberg et al. and Smith et al. by about 13%. Recent measured cross sections by Takahashi et al. [49] were found to lie between the values measured by the U.S. experimenters and those by Liskien et al. and Maekawa et al. Further work, either experiment or evaluation, particularly on the ENDF/B-VI file, is necessary to resolve the discrepancies among the measured values.

^{9}Be(n,2n). To obtain a 1% accuracy in tritium breeding ratio calculation, the required 14 MeV Be(n,2n) cross section accuracy is about 8% for a FLiBe/FLiBe/V blanket concept. However, if the beryllium material is employed primarily for neutron multiplication, as in blanket concepts with an explicit beryllium multiplier, the required data accuracy should be around 3%. Recently, measurements of 14 MeV neutron multiplication leakage spectra were performed in the U.S. at LLNL by Wong et al. [30] and in Switzerland at the LOTUS facility by Haldy et al.[53] A new evaluation was also completed recently at LLNL by Perkins et al.[31] The measured results at LLNL were compared with calculations using the new evaluation. It was found that the new evaluation is able to reproduce the experimental results within about 10%. This new evaluation is probably satisfactory as far as the self-cooled FLiBe blanket development is concerned. A test with the new evaluation should also be performed against the Swiss LOTUS experiments as well as the OKTAVIAN experiments in Japan.[29]

Pb(n,2n). The required accuracy for a Pb(n,2n) reaction cross section in a lithium-lead system is about 3%, if the needed tritium breeding prediction accuracy is to be within 1%. The current ENDF/B-V evaluation is an updated version of the previous ENDF/B-IV evaluation by Fu, with improved model calculations.[54] The current ENDF/B-V Pb(n,2n) reaction cross sections are in good agreement with the experimental values measured in 1975 by Frehaut and Mosinsky.[55] However, the uncertainties estimated for the ENDF/B-V evaluation are in the range of 10–30%.[54] A comparison between ENDF/B-V and

recent Frehaut et al. (1980) values[56] revealed that the ENDF/B-V values are probably higher than the experimental results. The theoretical calculation performed by Iwasaki et al. [57] using the multistep Hauser Frebach model with precompound effect also confirmed this observation at energies less than about 14.5 MeV. However, at energies about 14.5 MeV, the calculated values by Iwasaki et al. are higher than the ENDF/B-V values. Note that the experimental errors quoted by Frehaut et al. (1980) for their measurements around 14 MeV are about ±7%.

From the above discussions, we believe that more experiments should be performed for Pb(n,2n) at energies between 13 and 16 MeV to resolve the discrepancies observed in physics model calculations and in existing measurements. In order to meet the 3% accuracy goal, it is mandatory that careful experiments be carried out.

Dosimetry Data

The fusion program needs neutron dosimetry to: (1) measure the neutron fields in materials testing devices; (2) measure the neutron flux distributions in fusion blankets; and (3) study the thermonuclear processes in hot plasmas. The comments that follow pertain to the multiple foil analyses (MFA) technique in which a small package of foils is exposed to a neutron field for a specified time, after which the individual foils are examined for their induced activities. In the MFA method, each foil response is the product of a nuclear cross section $\sigma(E)$ and a neutron flux energy spectrum $\phi(E)$. The foils are selected to provide a range of reaction threshold energies spanning the energy spectrum of interest. From the measured foil responses, it is possible to "unfold" the neutron energy spectrum by means of an iterative calculation starting with an assumed trial spectrum. The success of the unfolding process depends upon the availability of accurate and complete reaction cross section data for suitable foil materials.

Criteria for the selection of foil materials include: (1) The half-life of the reaction product should be reasonably long compared with the exposure time; the exposure time could be a short as one minute for plasma diagnostics or as long as one year for materials damage studies; (2) activities should be easily detected without large self-shielding corrections; gamma decay is generally preferred; and (3) materials should be readily available in a physically convenient form and should not significantly modify the neutron spectrum by neutron moderation, etc. The list of higher priority fusion dosimetry cross sections compiled previously was expanded to the 29 reactions given in Ref. 16. The accuracies needed for these cross sections are about 5%. A recent review shows that all these dosimetry cross sections have been measured. Measurement work is needed only for those requested recently by PPPL for TFTR D-T operation: ^{104}Ru(n,p) (4.7–15 MeV); ^{109}Ag(n,p) (0.4–15 MeV); and ^{183}W(n,p) (0.3–15 MeV). Evaluations of these cross sections for ENDF/B-VI files are needed.

Activation Data

The deuterium-tritium (D-T) fusion reaction, which is the most promising fuel cycle for near-term fusion reactors, produces only helium and a neutron; radioactive products are not produced. About 80% of the D-T fusion energy, about 14.1 MeV, is carried by the neutron. The large neutron flux resulting from the 14 MeV neutrons, however, can activate the materials surrounding the plasma chamber, producing radioactive by-products of fusion. The fusion neutron-induced radioactivity is a consideration for three reactor design problems areas:

1. **Safety and Biological Hazard.** Fusion reactor safety is concerned with the release of radioactive materials into the environment during abnormal operating conditions. The radioactive decay heat plays a very important role as the source energy that triggers the release mechanism. The quantity and quality of radioactive material inventory stored in the fusion reactor impose a serious concern about the biological hazard.

2. **Reactor Maintenance.** In an activated area, the maintenance of reactor components during scheduled and unscheduled shutdowns will be complicated by the level of biological dose rate from the radioactive decay gamma-rays.

3. **Waste Disposal and Materials Recycle.** The disposal and/or recycling of the decommissioned reactor component materials should be handled according to the activity level and radioactive half-life of radionuclides involved in the component materials, and according to federal regulations.

A very important possibility for fusion energy is to establish a relatively clean energy source compared to conventional nuclear fission-based energy, which produces radioactive fission products as a result of fission reaction. Waste disposal and materials recycling were recently explored by the U.S. DOE Low Activation Fusion Materials Panel[58] and by the UKAEA.[59] The consensus of these investigations was that the goal of employing cheaper shallow land burial waste disposal schemes and eventual materials recycling within a reasonable time after irradiation is achievable if the materials for the fusion reactor first wall, blanket, and shield are carefully selected to minimize the long-term-induced radioactivity. This implies that at the early stages of fusion energy development, the activation cross sections for long-lived (half-life greater than five years) activation products should be investigated and made known either experimentally or by nuclear model calculations. For this reason, we believe a higher priority should be assigned to the long-lived activation cross sections.

A list of high priority activation cross sections, activation products, and their half-lives in each element for Ag, Al, B, Be, Bi, C, Ca, Co, Cr, Cu, F, Fe, K, Mg, Mn, Mo, N, Na, Nb,

H. P, Pb, S. Si, Sn, Ti, V, W, Zn, and Zr can also be found in Ref. 16. These were identified from activation calculations of a lithium/lithium/vanadium blanket spectrum, considering the above radioactivity-related problem areas. The activation calculation code and cross section library used are those developed by Mann.[60] While most of these activation cross sections were measured, we found that 54 of them lack experimental data. New or updated evaluations are needed for all activation cross sections to be included in ENDF/B-VI activation files.

Helium Production Data

The assessment of radiation damage to the structural materials in a fusion reactor is one of the crucial feasibility issues for the successful development of fusion energy. The helium production rate in an intense 14 MeV neutron environment at the first wall of a fusion reactor is particularly needed for the radiation damage assessment of the potential first wall and structural materials. Most helium production cross sections for the important elements identified for potential fusion structural alloys such as vanadium, iron, chromium, manganese, and titanium were recently measured at 14 MeV under the joint support of the Offices of Basic Energy Sciences and Fusion Energy of the U.S. Department of Energy.[61] Evaluations of these data for ENDF/B-VI files are needed.

5. SUMMARY

We have reviewed recent fusion reactor and blanket design studies in which promising blanket concepts for future development were identified based on the near-term D-T fuel cycle. A list of elements for which nuclear data up to 15 MeV are needed for fusion reactor transport calculations was made available, and the status of their neutron emission data reviewed. We found that most of the data needed are available both in experiment and evaluation, although some discrepancies exist between the experimental and evaluative data. We hope that the upcoming ENDF/B-VI files will be able to resolve these discrepancies with the help of more recent experimental data. Some elements still lack experimental double-differential data at energies below 14 MeV and above 6 MeV, and we recommend that work be done for these elements: O, F, V, Cr, Mn, W and Pb.

The nuclear data requirements in the areas other than those needed for fusion reactor transport calculations were also identified and briefly discussed. The charged particle cross sections appear to be in good shape, both experimentally and evaluatively, for D-T and D-D based fuel cycles. Most dosimetry cross sections, activation cross sections, and helium production cross sections needed for fusion energy development have been measured, although 3 dosimetry cross sections and 54 activation cross sections lack experimental data and should be measured. Evaluations of all these cross sections are needed for ENDF/B-VI files. Better measurements of cross sections for $^9Be(n,2n)$ and $Pb(n,2n)$

reactions are needed. New or updated evaluations of ^{7}Li(n,n'α)t, ^{9}Be(n,2n) and Pb(n,2n) cross sections are needed for ENDF/B-VI files.

Acknowledgements

REFERENCES

[1] GEORGE H. MILEY, "Fusion Energy Conversion," Chapter 2, *Fuel Cycles and Energy Balances*, **American Nuclear Society** (1976).

[2] J.D. GORDON, *et al.*, "Viability of the ^{11}B(p,α)2α Cycle," **Nucl. Technology/Fusion 4**, 348 (1983).

[3] G.I. BELL, S. GLASSTONE, "Nuclear Reactor Theory," Van Nostrand Reinhold, New York, 1970, Chap. 1.

[4] M.A. ABDOU, "Nuclear Data Requirements for Fusion Reactor Shielding," Proc. Advisory Group Meeting on Nuclear Data for Fusion Reactor Technology, IAEA-TECDOC-223, p. 91, IAEA, Vienna (1979).

[5] G. CONSTANTINE, "Nuclear Data Requirements for Fusion Reactor Design, Neutronics Design, Blanket Neutronics and Tritium Breeding," *ibid*, p. 11.

[6] C.R. HEAD, "Nuclear Data Requirements of the Magnetic Fusion Power Program of the United States of America," *ibid*, p. 1.

[7] O.N. JARVIS, "Nuclear Data Requirements for Transmutation and Activation of Reactor Wall and Structural Materials," *ibid*, p. 47.

[8] S.M. QAIM, "Nuclear Data Needs for Radiation Damage Studies Relevant to Fusion Reactor Technology," *ibid*, p. 75.

[9] Y. SEKI, "Review of Nuclear Heating in Fusion Reactors," *ibid*, p. 31.

[10] D.J. DUDZIAK, "An Assessment of Nucleonic Methods and Data for Fusion Reactors," Proc. Second Topical Meeting on the Technology of Controlled Nuclear Fusion, CONF-760935, p. 819, U.S. ERDA (1976).

[11] M.R. BHAT and M.A. ABDOU, "Nuclear Data Requirements for Fusion Reactor Nucleonics," Proc. Fourth Topical Meeting on the Technology of Controlled Nuclear Fusion, CONF-801011, p. 405, U.S. DOE (1980).

[12] D.J. DUDZIAK and P.G. YOUNG, "Review of New Developments in Fusion Reactor Nucleonics," *ibid*, p. 419.

[13] E.T. CHENG, D.R. MATHEWS, and K.R. SCHULTZ, "Magnetic Fusion Energy Program Nuclear Data Needs," GA Technologies Report GA-A16889 (1982), GA-A17324 (1983), GA-A17754 (1984), and GA-A18152 (1985).

[14] C.R. WEISBIN, *et al.*, "Meeting Cross Section Requirements for Nuclear Energy Design," ORNL/RM-8220, Oak Ridge National Laboratory, July 1982.

[15] M.A. ABDOU, "Nuclear Data Requirements for Fusion Reactors," **Trans. Am. Nucl. Soc., 44**, 186 (1983).

[16] E.T. CHENG, "Nuclear Data Needs for Fusion Energy Development," Fusion Technology **8**, 1423 (1985).

[17] J. JUNG, *et al.*, "Neutronic Data-Base Assessment for U.S. INTOR," **Fusion Technology 10**, 382 (1986).

[18] M. ABDOU, *et al.*, "Blanket Comparison and Selection Study, Interim Report," ANL/FPP/TM-177, Argonne National Laboratory, September 1983, Chapter X.

[19] D. L. SMITH, *et al.*, "Overview of the Blanket Comparison and Selection Study," **Fusion Technology 8**, 10 (1985).

[20] L.J. PERKINS, *et al.*, "MINIMARS: An Attractive Small Tandem Mirror Fusion Reactor," Proc. 11th Symp. on Fusion Engineering, Austin, Texas, Nov. 18-22, 1985.

[21] C.C. BAKER, *et al.*, "STARFIRE - A Commercial Tokamak Fusion Power Plant Study," ANL/FPP-80-1, Argonne National Laboratory (1980), Chap. 11.

[22] D.L. SMITH, *et al.*, "Blanket Comparison and Selection Study, Final Report," ANL/FPP-84-1, Argonne National Laboratory, Sept. 1984, Sec. 6.11.

[23] A.B. SMITH, Argonne National Laboratory, private communication, June 1984.

[24] S. CHIBA, *et al.*, "Interaction of Fast Neutrons with ^{6,7}Li," Proc. of the International Conf. on Nuclear Data for Basic and Applied Science, Santa Fe, New Mexico, USA, May 13-17, 1986, p. 227.

[25] E. DEKEMPENEER, *et al.*, "Double-Differential Neutron-Emission Cross Section for the ^{7}Li(n,xn) Reaction Between 1.6-16 MeV," *ibid*, p. 133.

[26] M. DROSG, *et al.*, "Double-Differential Neutron-Emission Cross Sections of ^{10}B and ^{11}B at 6, 10 and 14 and of ^{6}Li, ^{7}Li and ^{12}C at 14 MeV," *ibid*, p. 145.

[27] J.H. DAVE and C.R. GOULD, "Optical Model Analysis of Scattering of 7 to 15 MeV Neutrons from 1-p Shell Nuclei," Phys. Rev. C, 28, 2212 (1983).

[28] D.M. DRAKE, et al., "Double-Differential Beryllium Neutron Cross Sections at Incident Neutron Energies of 5.9, 10.1 and 14.2 MeV," Nucl. Sci. Eng., 63, 401 (1977)

[29] A. TAKAHASHI, et al., "Measurement of Double-Differential Neutron-Emission Cross Sections with 14 MeV Source for D, Li, Be, C, O, Al, Cr, Fe, Ni, Mo, Cu, Nb, and Pb," Proc. Int. Conf. Nuclear Data for Science and Technology, Antwerp, Belgium, Sept. 6–10, 1984, EUR-8355, p. 360.

[30] C. WONG, et al., "Measurements and Calculations of the Leakage Multiplication from Hollow Core Beryllium Spheres," Fusion Technology 8, 1165 (1985).

[31] S.T. PERKINS, et al., "A Reevaluation of the ^{9}Be(n,2n) Reaction and its Effect on Neutron Multiplication in Fusion Blanket Applications," Nucl. Sci. Eng. 90, 83 (1985).

[32] S.G. GLENDINNING, et al., "Neutron Elastic Scattering Cross Sections for ^{16}O Between 9 and 15 MeV," Nucl. Sci. Eng. 82, 393 (1982).

[33] K. GUL, et al., "Measurements of Neutron Emission Cross Sections for Al, Cu, and Pb at 14.6 MeV Neutron Energy," Proc. of Int. Conf. Nuclear Data for Basic and Applied Science, Santa Fe, New Mexico, May 13–17, 1985, p. 187.

[34] D.M. HETRICK, D.C. LARSON and C.Y. FU, "Status of ENDF/B-V Neutron Emission Spectra Induced by 14 MeV Neutrons," ORNL/TM-6637, ENF-280, Oak Ridge National Laboratory, April 1979.

[35] P. GUENTHER, et al., "Fast Neutron Cross Sections of Vanadium and an Evaluated Neutron File," ANL/NDM-24, Argonne National Laboratory, May 1977.

[36] A.B. SMITH, ANL, private communication.

[37] D.M. HETRICK, C.M. FU, and D.C. LARSON, "Calculated Neutron Induced Cross Sections for ^{63}Cu, ^{65}Cu from 1 to 20 MeV and Comparison with Experiments," ORNL/TM-9083, ENDF-337, Oak Ridge National Laboratory, August 1984.

[38] E.T. CHENG, D.R. MATHEWS, and K.R. SCHULTZ, "Magnetic Fusion Energy Program Nuclear Data Needs," GA-A18152, UC-20, GA Technologies report, October 1985.

[39] E.D. ARTHUR, et al., "New Tungsten Isotope Evaluations for Neutron Energies Between 0.1 and 20 MeV," Trans. Am. Nucl. Soc., 39, 793 (1981)

[40] G.D. ESTES, "Calculations Using New Tungsten Isotope Evaluation," ibid., p. 794.

[41] CINDA 85 (1982–1985), IAEA, Vienna, 1985.

[42] CINDA 83 (1977–1983), IAEA, Vienna, 1983.

[43] S. PERLSTEIN and C.L. DUNFORD, "Plans for ENDF/B-VI," Proc. Int. Seminar on Nuclear Data, Cross Section Libraries and Their Applications in Nuclear Technology, Bonn, Federal Republic of Germany, 1–2 October, 1985.

[44] F. MANN, Private communication, May 1985.

[45] NELSON JARMIE, "Requirements for Charged-Particle Reaction Cross Sections in the D-T, D-D, T-T and D-^{3}He Fuel Cycles," Proc. Advisory Group Meeting on Nuclear Data for Fusion Reactor Technology, Gaussig/Dresden, GDR, 1–5 December, 1986.

[46] M.T. SWINHOE and C.A. UTTLEY, "An Absolute Measurement of the ^{7}Li(n,n'α)t Reaction Cross Section Between 5 and 15 MeV by Tritium Assaying," Nucl. Sci. Eng., 89, 261 (1985).

[47] H. LISKIEN, et al., "Determination of ^{7}Li(n,n't) ^{4}He Cross Sections," Proc. Int. Conf. Nuclear Data for Science and Technology, Antwerp, Belgium, September 6–10, 1982, EUR-8355, p. 349.

[48] H. MAEKAWA, et al., Reactor Engineering Department Annual Report, JAERI-M-83-196 (1983) and 86-125 (1986).

[49] A. TAKAHASHI, et al., "Measurements of Tritium Breeding Ratios in Lithium Slabs using Rotating Target Neutron Source," Proc. 13th Symposium on Fusion Technology, Commission of the European Communities, 1984, p. 1325.

[50] E. GOLDBERG, et al., "Measurements of ^{6}Li and ^{7}Li Neutron-Induced Tritium Production Cross Sections at 15MeV," Nucl. Sci. Eng. 91, 173 (1985).

[51] D.L. SMITH, et al., "Cross Section Measurement for the ^{7}Li(n,n't) ^{4}He Reaction at 14.74 MeV," ANL/NDM-87, Argonne National Laboratory (1984).

[52] P.G. YOUNG, "Evaluation of n+^{7}Li Reactions Using Variance-Covariance Techniques," Trans. Am. Nucl. Soc. 39 272 (1981).

[53] P.A. HALDY, et al., "Blanket Neutronics Experiments at the LOTUS Facility," Proc. Int. Conf. Nuclear Data for Basic and Applied Science, Santa Fe, New Mexico, USA, May 13–17, 1985.

[54] C.Y. FU, "Summary of ENDF/B-V Evaluations for Carbon, Calcuim, Iron, Copper, and Lead and ENDF/B-V Revision 2 for Calcium and Iron," ORNL/TM-8283 (ENDF-325), Oak Ridge National Laboratory, September 1982.

[55] J. FREHAUT and G. MOSINSKI, "Measurement of (n,2n) and (n,3n) Cross Sections for Incident Energies between 6 and 15 MeV," Proc. Int. Conf. Neutron Cross Section and Technology, Washington, D.C., March 1975, p. 897.

[56] J. FREHAUT, et al., "Status of (n,2n) Cross Section Measurements at Bruyeres-Le-Chatel," Sym. Neutron Cross Sections from 10 to 50 MeV, BNL-NCS-51245, Brookhaven National Laboratory, May 1980, p. 399.

[57] S. IWASAKI, et al., "Measurements and Analysis of Neutron Emission Spectra for Pb(n,xn) Reaction between 14 and 20 MeV," Proc. Int. Conf. Nuclear Data for Pure and Applied Science, Santa Fe, New Mexico, USA, May 13–17, 1985.

[58] R.W. CONN, et al., "Report on the DOE Panel on Low Activation for Fusion Applications," UCLA/PPG-728, Center for Plasma Physics and Fusion Engineering, University of California, Los Angeles, 1983.

[59] O.N. JARVIS, "Low-Activity Materials: Reuse and Disposal," AERE-R 10860, UKAEA Harwell Report, July 1983.

[60] F. MANN, et al., "REAC Nuclear Data Libaries," Proc. Int. Conf. Nuclear Data for Pure and Applied Science, Santa Fe, New Mexico, USA, 13–17 May, 1985, p. 207.

[61] D.W. KNEFF, et al., "Helium Production in Pure Elements, Isotopes and Alloy Steels by 14.8 MeV Neutrons," Nucl. Sci. Eng., 92, 491 (1986).

NUCLEAR DATA REQUIREMENTS FOR TRITIUM BREEDING CALCULATIONS AND TESTING OF EVALUATED NUCLEAR DATA IN JAPAN

H. MAEKAWA
Japan Atomic Energy Research Institute,
Tokai-mura, Naka-gun, Ibaraki-ken,
Japan

Abstract

A brief review of fusion blanket experiments and analyses in Japan is summarized as well as code developments for fusion neutronics. Nuclear data for important nuclei relevant to tritium breeding calculations is discussed. The status of these data is assessed through the analyses of integral and differential experiments. These experiments are very useful for the evaluation of methods and data. The obtained results will be applied to the evaluation of the JENDL-3 nuclear data file.

I. Introduction

Experimental examinations are required to verify the accuracy of both calculational methods and nuclear data which are used in nuclear design and analysis of a fusion reactor. The most suitable experiments for this type of method and data verification are clean benchmark experiments on a simple geometry with simple material compositions. Analyses of the experimental results are expected to identify the accuracy as well as the deficiencies in the currently available methods and nuclear data.

Since 1973, a series of blanket benchmark experiments was started at JAERI using the PNS-A neutron generator [1-11]. As the neutron intensity of PNS-A was not enough for measuring directly the tritium production rate (TPR) distribution in the assembly, the new intense 14 MeV neutron source, named Fusion Neutronics Source (FNS), had been planned to construct. The FNS facility was completed in April 1981 at Tokai-site of JAERI [12]. The other intense neutron source OKTAVIAN was installed at Osaka University and started operation in 1981 [13]. These two sources have accelerated the fusion neutronics activities in Japan.

Since April 1983, JENDL-2 had been distributed and widely used as the Japanese standard nuclear data library. As JENDL-2 was evaluated for applying mainly to fission reactors, the accuracy of evaluated data above 5 MeV was pointed out to be insufficient for fusion neutronics study. In order to analyze the experiments at FNS, a new evaluated nuclear data file was strongly requested to Japanese Nuclear Data Committee. Selected eight nuclei, ^6Li, ^7LI, ^9Be, ^{12}C, ^{16}O, Cr, Fe and Ni, have been evaluated as JENDL-3PR1 (JENDL-3 preliminary version one) by Dec. 1983 [14]. A revised version JENDL-3PR2 was released in March 1985. The data of ^6Li, ^7Li and ^{12}C were modified taking into account of the result of Chiba et al. [15-16]. It was used successfully for analyses not only of the integral experiments at FNS and OKTAVIAN but of the double differential neutron emission cross sections (DDX) measured in the Universities.

Many reports related to the fusion neutronics experiments and analyses were reported in the various meetings, such as Annual Meeting of Atomic Energy Society of Japan. Under this situation, a Specialists' Meeting on Nuclear Data for Fusion Neutronics was held in July 23-25, 1985 at Tokai Research Establishment of JAERI [17]. The contents of presentations and discussions in this meeting are helpful for me to make this report.

In this report, first, I summarize the fusion neutronics activities and code developments in Japan. Second, nuclear data requirements for tritium breeding assessments are presented. Next, the status of important nuclear data in JENDL-3PR1/2 and ENDF/B-IV/V for tritium breeding is discussed.

II. Survey of Integral Experiments and Code Developments in Japan

1. Integral Experiments

Various fusion blanket benchmark experiments have been carried out at JAERI and Universities in Japan. They are summarized in Table 2.1. The first blanket experiment was performed at JAERI using Li-metal blocks [1]. In the case of fusion neutronics experiment, there is no good measure such as the criticality in fission reactor physics. In order to compare measured values with calculated ones, absolute fission rates, one of the spectral indices, were measured in simulated blanket assemblies [4]. The absolute measurements were applied to most of following experiments, because such absolute comparison between measured and calculated values is very useful for the verification of the methods and data.

As designers of JAERI adopted lithium-oxide as the tritium breeding material for blanket, simulated blanket experiments on Li_2O assemblies were started at JAERI [10]. Measurements of tritium production rate (TPR) distribution in a simulated blanket assembly are necessary for evaluating the tritium breeding ratio (TBR) in a candidate blanket system. After the intense neutron generators, FNS [12] and OKTAVIAN [13] were completed, the TPR distributions were measured directly in simulated blanket assemblies [20,22-24,27,36-40,48-52]. These blanket benchmark experiments and analyses are presented separately in this meeting.

Angle and energy distributions of secondary neutrons are especially important in the fusion neutronics study in contrast with the neutron physics in fission reactors, because of following reasons:

(1) High energy D-T neutrons are dominant in the blanket.
(2) The D-T neutrons, generated only in plasma region, enter into the blanket from one side via first wall.
(3) In cases of elastic and inelastic scattering for high energy neutrons, secondary neutrons have an anisotropic distribution.

Therefore measurements and analyses of angle-dependent leakage spectrum from an assembly of candidate fusion blanket materials are useful for the examination of evaluated nuclear files. This type of studies have also been done at FNS and OKTAVIAN [28-35,43,45-47].

Neutron spectra in an assembly are also useful for fusion neutronics study as well as the spectral indices such as fission rates and foil activation rates. Measurements of in-system neutron spectra were performed in various assemblies using a miniature NE213 spectrometer [24-26,50,60-62].

Table 2.1 Integral Experiments in Japan

(1) Japan Atomic Energy Research Institute

Neutron Source	Assembly	Measured Item	Reference
PNS-A	Sphere •Li •U-Li •Li-C •U-Li-C	•Fission Rates (^{235}U, ^{238}U, ^{237}Np, ^{232}Th)	[1] ∿ [7]
	Sphere •Li •Li-C	•TLD Response (^6LiF, ^7LiF)	[8]
	Sphere •Li-C	•Angle-Dependent Leakage Spectra	[9]
	Sphere •Li$_2$O-C	•Fission Rates (^{235}U, ^{238}U, ^{237}Np, ^{232}Th)	[10],[11]
FNS[12]	Sphere •Li$_2$O-C	•Fission Rate •TPR(T_6) •Induced Activity (SS316)	[18] ∿ [21]
	Cylindrical Slab •Li$_2$O •Graphite •Li$_2$O-C	•TPR(T_6, T_7) •Fission Rates (^{235}U, ^{238}U, ^{237}Np, ^{232}Th) •Reaction Rate [$^{27}Al(n,\alpha)^{24}Na$, $^{58}Ni(n,2n)^{57}Ni$, etc.] •TLD Response •In-System Spectra	[22] ∿ [27]
	Slab •Li$_2$O •Li •Graphite •Be	•Angle-Dependent Leakage spectrum	[28] ∿ [35]
	Engineering Benchmark Assemblies •Reference (Li$_2$O) •First Wall (SS304, PE + Reference) •Neutron Multiplier (Be + Reference)	•TPR(T_6,T_7,T_N) •Reaction Rates [$^{27}Al(n,\alpha)^{24}Ni$, $^{58}Ni(n,2n)^{27}Ni$, etc.] •In-System Spectra	[36] ∿ [40]
	Concrete	•Induced Activity	[41]

Table 2.1 (Continued)

(2) Osaka University

Neutron Source	Assembly	Measured Item	Reference
150 keV Cockcroft-Walton accelerator	Slab •Graphite •Pb •Lithium •UO$_2$	•Angular Flux Spectra	[42] $\sim$ [44]
OKTAVIAN[13]	Slab •Li •Graphite •SS316 •Concrete •Water •Polyethylene	•Angular Flux Spectra	[45] $\sim$ [47]
	Sphere •Pb	•Leakage spectra	[45], [48]
	Slab •Li-C	•TPR (T$_6$, T$_7$)	[49]
	Sphere •Li •Pb-Li	•Leakage Spectra •TLD reponse •TPR (T$_6$, T$_7$)	[50] $\sim$ [53]

(3) Tohoku University

Neutron Source	Assembly	Measured Item	Reference
DYNAMITRON	Rectangular •Li	•Time-Dependent Neutron Spectra	[54]
Cyclotron	•Graphite	Neutron spectra	[55]

(4) The University of Tokyo

Neutron Source	Assembly	Measured Item	Reference
Cockcroft-Walton Accelerator (KAMAN,A-1254)	Slab •LiF	•Neutron Spectra •TPR •Radiation heating-rate •Fast Neutron Fluence	[56] $\sim$ [57]
OKTAVIAN	Sphere •Fe •Ni	•Leakage Spectra	[58] $\sim$ [59]

(5) Tokyo Institute of Technology

Neutron Source	Assembly	Measured Item	Reference
Philips PW-5310	Rectangular •Water •Graphite •LiF •LiF-C	•Neutron Spectra	[60] $\sim$ [62]

Another type of experiment, time-dependent leakage spectra were measured at Tohoku University [53]. To evaluate the nuclear data for the components of stainless steel that is hopefull candidate for structural material, leakage neutron spectra from Fe and Ni spherical assemblies were measured by the time-of-flight method [58-59].

Integral experiments on various materials have been performed at Research Reactor Institute, Kyoto University using a γ-n neutron source LINAC. These experiments and analyses are omitted in this report because non-D-T source was used. It can be emphasized that these results are also useful for the verification of methods and data.

2. Code developments in Japan

There are many activities in the code development for fusion neutronics in Japan. Thy are summarized in Table 2.2. It is noticeable that most of the developed transport codes, not only determinastic codes but a Monte Carlo code are using the double-differential form cross section (DDX) [63-72]. Many Japanese researchers have thought that the DDX form cross section is useful for interpretation of neutron behavior in fusion blankets. This is also reflected in JENDL-3, i.e., JENDL-3 has DDXs as the file-6.

Two types of processing codes have been developed at JAERI to generate the DDX-type cross section set [74-75]. The PROF-GROUCH-G/B code might be only one code to be able to process the file-6 in the world.

A new code SUSD was developed at the University of Tokyo to perform the sensitivity and uncertainty analyses for secondary angular or energy distributions [76-77].

The THIDA-2 code [78] is a revised version of THIDA, and is a system for calculation of transmutation, activation, decay heat and dose rate. The code system has a transport calculation routine for a three-dimensional model.

III. Nuclear Data Requirement for Tritium Breeding Calculations

A good review of the requirements for nuclear data relating to tritium breeding ratio (TBR) was presented at the Specialists Meeting mentioned above [79]. It can be summarized as follows.

1. Nuclear Data Relating to TBR

Following reactions give large effect on TBR during each process.

* Neutron through first wall to the multiplier
    slowing down cross sections such as (n,n) & (n,n')
    charged-particle production cross-sections such as (n,p) & (n,α)
* Neutrons in the multiplier before (n,2n) reaction
    slowing down cross sections
    charged-particle production cross section
    neutron multiplying cross sections such as (n,2n)
* Neutrons in the multiplier after (n,2n) reaction
    absorption cross sections in the energy range from several hundred keV to thermal
* Neutrons from the multiplier to breeder
    absorption cross sections such as (n,γ) & (n,p) of structural material
    ^{6}Li(n,α)^{3}T, ^{7}Li(n,n'α)^{3}T

Table 2.2 Code Development in Japan

(1) Deterministic transport codes using DDX

Name	Remarks	Method	Reference
BERMUDA-series	1D/2D/3D, Neutron/gamma/adjoint	direct integration	[63] ∿ [65]
NITRAN-1 -2	1-D 2-D	SN	[66] ∿ [67]
ANISN-DD DOT-DD	1-D 2-D	SN	[68]
AIDA	2-D(troidal geometry)	direct integration	[69]
DIAC	1-D	SN	[70]

(2) Monte Carlo transport codes

Name	Remarks	Reference
MORSE-DD	using DDX	[71] ∿ [72]
MORSE-I	toroidal geometry	[73]

(3) Group constants processing codes

Name	Remarks	Reference
PROF-GROUCH-G/B	for BERMUDA, ANISN, DOT etc.	[74]
PROF-DD	for MORSE-DD	[75]

(4) Sensitivity and uncertainty analysis code

Name	Remarks	Reference
SUSD	SAD, SED	[76] ∿ [77]

(5) Induced activation calculation code system

Name	Remarks	Reference
THIDA-2	revised version of THIDA	[78]

2. Requirements for Nuclear Data

Many types of fusion power and/or experimental reactors have been proposed. Candidate materials/elements used in their designs were summarized by reviewers [80-84]. These elements are almost same among the reviewers. The candidated elements for tritium breeder, neutron multiplier, coolant and so on are summarized in Table 3.1. The status of priority for data needs, that were pointed out by Abdou [81], is seemed to be unchanged at this time.

Table 3.1 A list of the elements of interest in fusion reactor technology.

Tritium Breeder	^{3}He, ^{6}Li, ^{7}Li, ^{9}Be, ^{10}B, ^{11}B
Neutron Multiplier	Be, Zr, Mo, Pb, Bi
Coolant	H, D, He, Li, Be, O, F, Na, Al, Pb
Structural Material (including limiter, diverter and wall protector)	Be, C, Al, Si, Ti, V, Cr, Fe, Ni, Zr, Nb, Mo, Ta, W
Reflector	Be, C, O, Al, Cr, Fe, Ni
Shielding Material	H, ^{10}B, C, O, Si, Ca, Fe, Ta, W, Pb
Magnet	Mg, Al, Ti, V, Cu, Ga, Nb, Sn
Fission-Fusion Hybrid	Th, U, Pu

Material of stainless steel, the most commonly used material in fusion reactors as structural material, is proposed for the first wall materials and its protectors. Molybdenum and vanadium alloys are also proposed for the first wall materials. A ceramic SiC is proposed for the protectors.

For the structural materials of blanket vessels, stainless steel is adopted in most blanket designs. Molybdenum and vanadium alloys are proposed for the blanket vessels of further generation fusion reactors.

Beryllium and lead are most commonly used as the neutron multiplier. Their oxides or alloys are also proposed for the neutron multipliers.

Lithium metal, Li_2O, $LiAlO_3$, Li_2SiO_3 etc. have been proposed as the tritium breeding materials.

For the cooling channel tube, stainless steel, molybdenum alloy, vanadium alloy etc. are presented . Light water and helium gas are proposed for the coolant. In the cases of liquid breeder, lithium metal, Li-Pb alloy, flibe etc., they are usually used as the self-coolant.

For the other structural materials, stainless steel, molybdenum alloy, vandium alloy, etc. are adopted in most fusion reactor designs.

3. Comments from Sensitivity and Uncertainty Anlyses

Furuta et al., have made a cross-section sensitivity and uncertainty analysis on four types of fusion blanket concept [77]. This analysis includes the sensitivities of secondary energy and angular distributions (SED, SAD). The result of sensitivity for tritium breeding ratio (TBR) is shown in Table 3.2. Their conclusions about TBR are summarized as follows :

(1) The relative standard deviation due to uncertainties in the evaluated nuclear data available at present is 2 $\sim$ 4 % in the TBR.

(2) Neutron multiplying reactions, such as $^7Li(n,n'\alpha)T$, Fe(n,2n) or $^9Be(n,2n)$, and their competitive threshold reactions such as Fe(n,α) or Fe(n,n'), have a large impact on the TBR.

(3) Threshold reactions of iron, as well as lithium, seem to be important for an accurate TBR assessment.

(4) The direct effect of $^7Li(n,n'\alpha)T$ reaction is also significant, especially for the blankets with liquid lithium breeder.

(5) The SAD for elastic scattering of ^9Be is more sensitive to tritium breeding ratio than that of ^7Li.

(6) The SAD of $^9Be(n,2n)$ reaction has a sensitivity coefficient of the same order as the SAD of $^7Li(n,n\frac{1}{2})$ reaction.

Table 3.2 Reactions which have a large contribution to uncertainties in the tritium breeding ratio [77].

Reaction	Li/Li		Li/Li+He		Li₂0/H₂0		Li₂0/Be/H₂0	
	RSD*1 (%)	Sensitivity	RSD (%)	Sensitivity	RSD	Sensitivity	RSD	Sensitivity
$^6Li(n,n_c^1)$	0.40	-1.132-2*3	0.38	-1.066-2				
$^7Li(n,n'\alpha)^3T$*2	1.3	3.225-1	1.2	2.903-1	0.71	1.799-1	0.40	1.004-1
$^7Li(n,2n)$	0.37	1.866-2						
$^7Li(n,n_c^1)$	0.60	-6.807-2	0.56	-6.446-2				
$^7Li(n,n_c^1)$ SED	0.66	1.758-1*4	0.51	1.427-1*4				
$^9Be(n,2n)$							1.8	2.142-1
$^{16}O(n,\alpha)$					0.62	-5.360-2	0.35	-3.231-2
Fe inelastic	0.75	-5.795-2	0.70	-5.423-2	0.43	-3.300-2	0.75	-4.751-2
Fe(n,2n)	0.44	4.395-2	0.75	7.529-2	0.88	8.846-2	0.36	3.654-2
Fe(n,α)	0.63	-6.807-2	0.83	-3.151-2	0.77	-2.856-2	0.60	-2.231-2

*1 Relative standard deviations in the total breeding ratio(TBR).
*2 Direct effect only.   *3 Read as -1.132 $\times$ 10^{-2}
*4 Values listed are the total gain terms.

The value of 2 $\sim$ 4 % seems to be small, but it depends on the input conditions for sensitivity and uncertainty analysis. Uncertainties in cross-section data will cause overestimation in neutron flux at some locations and underestimations at other locations; and these two effects will compensate each other by integration over the whole system when the TBR is evaluated. The local values such as TPR are dependent on uncertainties of nuclear data rather sensitive than the volume-integrated values such as TBR.

IV. Status of Nuclear Data Relevant to Tritium Breeding in Fusion Blanket Through the Analyses of Integral and Differential Experiments

The status of JENDL-3 is presented by Kanda in this meeting. The status of JENDL-3PR1/2 was reported by Asami [85] and Chiba [86] at the Specialists Meeting mentioned above. In this section, I would like to discuss the status of nuclear data relevant to tritium breeding in fusion blanket through the analyses of integral experiments, angle-dependent leakage spectra and DDX measurements.

1. $^7Li(n,n'\alpha)^3T$

Integral experiments [20-22,49] have suggested that the calculation with ENDF/B-IV overestimates the T₇ by about 15 %. Reupke et al. reported the almost same results from their consistency analysis of $^7Li(n,xt)$ cross section [87]. In the case of JENDL-3PR1/2, the value is 286 mb at 14 MeV and is 15 % less than that in ENDF/B-IV.

Recently measurements of $^7Li(n,n'\alpha)^3T$ cross section were performed in Japan using FNS and OKTAVIAN [49,88]. The results are shown in Fig. 4.1 with evaluated curves. The groups of the University of Tokyo and Osaka University used $^7Li_2CO_3$ pellets and Dierckx method, while JAERI used $^7Li_2O$ pellets and newly developed method. Though the data of three groups were obtained independently and the data of Osaka University were not corrected for escaped recoil-triton (this correction is estimated to be about + 2 %), good agreement has been obtained among them. They agree also well with the results of Goldberg et al. [89], Smith et al. [90] and Chiba et al. [16] within experimental error. The data of Liskien et al. [91] are a little lower than Japanese data, however, the differences are still within experimental errors. The new data between 7.9 and 10.5 MeV, measured at Julich [92], support both JENDL-3PR1/2 and Young's evaluation [93].

It can be concluded for the cross section of $^7Li(n,n'\alpha)^3T$ around 14 MeV as follows [87] :

(1) The value of cross section seems to be convergent.
(2) The value measured by Swinhoe [96] is too low.
(3) It is recommended that the value in JENDL-3PR2 increase by about 7 %.

Recently, Iguchi and Nakazawa have measured the cross section avareged over fission spectrum using the fast neutron source reactor YAYOI [94]. Their results after the adjustment using NEUPAC-83 [95] suggests that the data between 5 and 9 MeV in JENDL-3PR1/2 increases by 3 $\sim$ 5 %.

2. ^6Li, ^7Li

From the measurement and analysis of tritium production rates for ^6Li and ^7Li (T₆, T₇) in a Li₂0 assembly [22-23,27], the calculation based on JENDL-3PR1 predicted the experimental values for both T₆ and T₇ very well. The calculated value based on JENDL-3PR2 was a little higher than that based on JENDL-3PR1. While the calculated T₇ based on ENDF/B-IV was higher than the measured one by about 20 %. It is noticeable that the change of $^7Li(n,n'\alpha)^3T$ cross section affects remarkably on the calculation of T₆ as well as T₇.

In the case of Li sphere assembly at OKTAVIAN [52], reasonable agreement was obtained for T₆ and T₇ distributions between the experiment and calculation based on JENDL-3PR1.

Hashikura et al. analyzed the LLNL Pulsed Sphere Program [97] by the use of MCNP [98] with ENDF/B-IV. They pointed out that the calculation for the leakage spectrum from a ^{6}Li sphere agreed well with the measurement above 8 MeV but overestimated it below 8 MeV [99]. They also indicated that the calculation for ^{7}Li sphere overestimeted the measurement below 7 MeV. These discrepancies are attributed to the secondary neutron distribution from the (n,n') continuum and (n,2n) reactions. These data have been revised in JENDL-3PR1/2. Nakagawa et al. also analyzed the same experiments by the use of MORSE-DD [72] with ENDF/B-IV and JENDL-3PR1 [100]. For ^{6}Li and ^{7}Li spheres, calculated spectrum based on JENDL-3PR1 was better than that on ENDF/B-IV, but there was still some discrepancy.

From the analysis [23,30,101] of time-of-flight experiment on lithium-oxide assemblies at FNS using DOT3.5 [102], the calculations based on ENDF/B-IV underestimate the measured spectra around 9 MeV. This discrepancy is caused by the lack of 4.63 MeV level for ^{7}Li. The calculation based on JENDL-3PR2, which has the 4.63 MeV level, shows good agreement with the measurement within almost experimental error (See Fig. 4.2). For the partial/differential comparison between measured and calculated spectra, there is, however, some discrepancy of about 10 % [101]. It is recommended to re-evaluate the data of angular and energy distributions of secondary neutrons in JENDL-3PR2. Recently Oyama has analyzed the experiment by MCNP with JENDL-3PR1/2 [103]. The agreement is better than that by DOT3.5.

From the experiment and analysis on a natural lithium sphere of 40 cm in diameter at OKTAVIAN [104], the calculated leakage spectrum based on JENDL-3PR2 agrees well with the measured one. This agreement is better than that based on ENDF/B-IV.

The analyses [105-107] of DDX measurements for ^{N}Li, ^{6}Li and ^{7}Li support the above analyses for the three measurements of leakage neutron spectra.

3. ^{9}Be

From the result of analyses [37-38] for the experiment on the beryllium sandwiched system at FNS, three calculations (DOT3.5 & JENDL-3PR2, MORSE-DD & JENDL-3PR1, MCNP & ENDF/B-V) overestimated T_6 by 5 $\sim$ 10 % except in Be and front Li$_2$O regions. A comparison of C/E value for ^{6}Li between the reference (Li$_2$O only) and Be-sandwiched systems is shown in Fig. 4.3. In the Li$_2$O region after the Be-zone, the C/E values are closer to unity than those of the reference case, while gradually increase to the same level at the rear end of the system. This fact suggests that the data of Be in the files are inadequate.

A time-of-flight experiment on Be slabs has been carried out at FNS. The measured spectra have been analyzed by the DOT3.5, MORSE-DD and MCNP codes with the JENDL-3PR1, ENDF/B-IV and LASL-SUB files [35]. A typical result is shown in Fig. 4.4. A comparison of C/E values among the nuclear data files is summarized in Table 4.1. Any calculation does not reproduce the measured spectra well. From the analysis of the Pulsed Sphere Program, Nakagawa et al. pointed out the same results for JENDL-3PR1 and ENDF/B-IV [100].

A graph of measured and evaluated DDX is shown in Fig. 4.5. The secondary neutron energy spectrum of JENDL-3PR1 is lower than that of experiment around 7.5 MeV. If the inelastic cross section of 6.8 MeV level increases by appropriate quantity, the calculated spectrum will improve not only around 7.5 MeV but below 6 MeV because of second step neutrons.
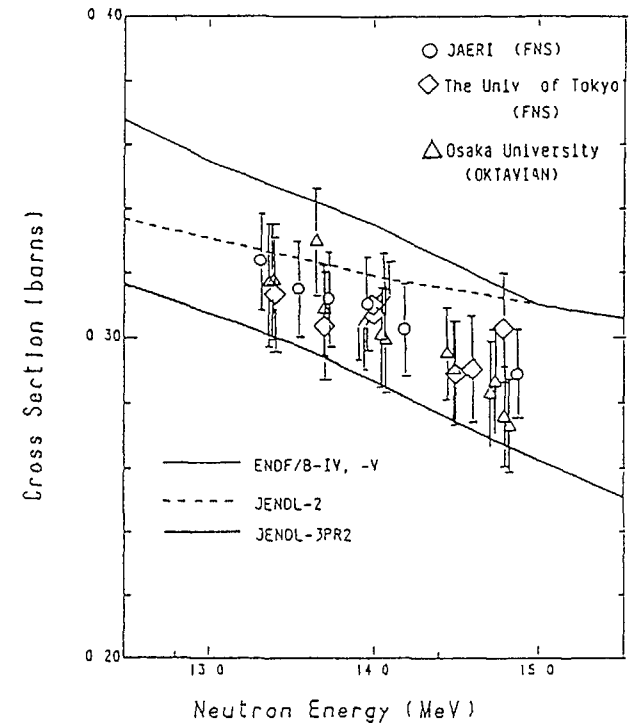
Fig 4 1 Measured cross section of ^{7}Li(n,n'α)^{3}T
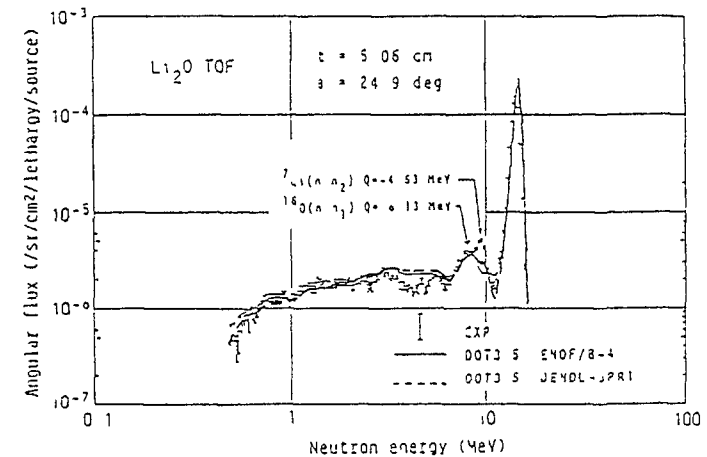
Fig 4 2 Measured and calculated neutron leakage spectra from a Li$_2$O slab
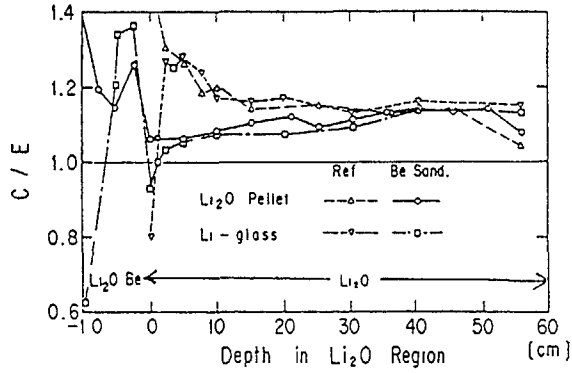
Fig. 4.3 C/E values for TPR of ^{6}Li in reference and Be-sandwiched systems.

Table 4.1 Comparison of C/E values among nuclear data files.

En [MeV] Cross section	> 10	10 ⌁ 2	2 ⌁ 0.5	0.5 ⌁ 0.1
JENDL-3PR1	△	X under	O	X under
ENDF/B-IV	△	△	X under	X under
LASL-SUB	△	△ over	over	△ under
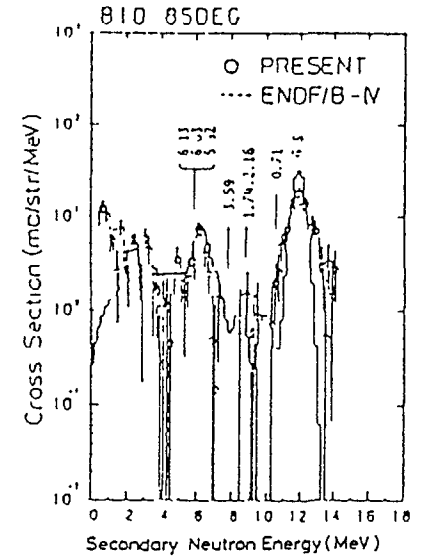
(a) ^{10}B at 85 deg.
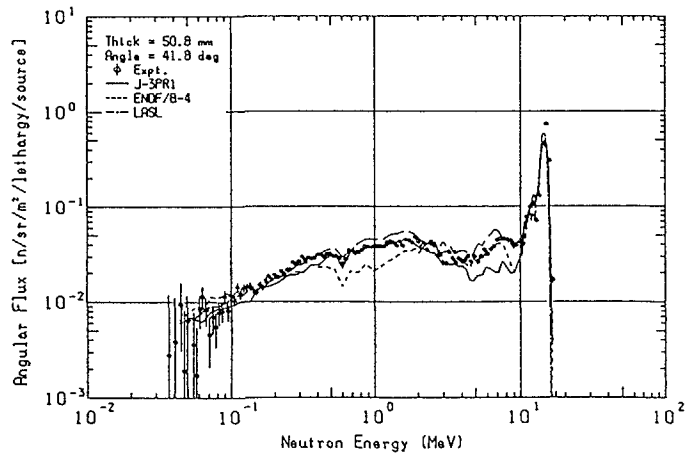
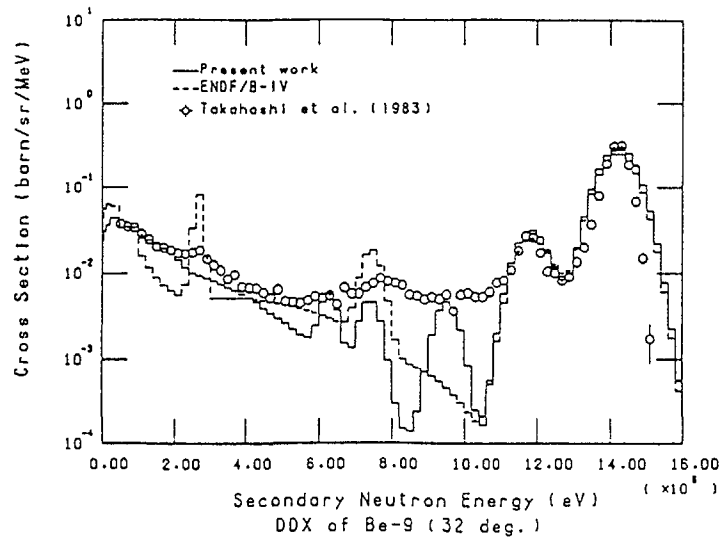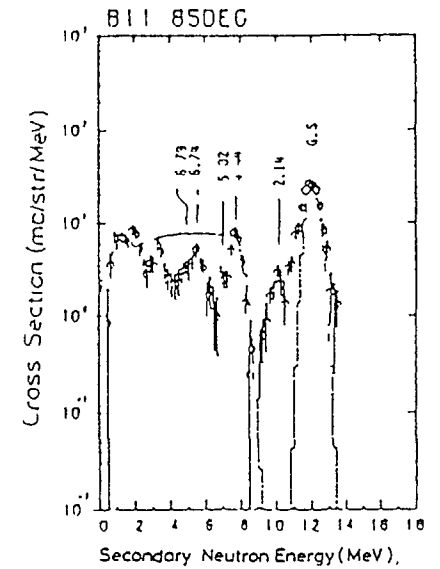Fig. 4.4 Measured and calculated neutron leakage spectra from a Be slab.

Fig. 4.5 DDX of ^{9}Be 14 MeV at 32 deg.

(b) ^{11}B at 85 deg.

Fig. 4.6 DDX of boron for 14.2 MeV.

Baba pointed out from the DDX measurement as follows [107] :

(1) The inelastic-scattering from the 1.7 MeV level was not observed in the experiment, whereas substantial cross section is given to this branching in the evaluation.
(2) The experiments indicate notable excitation of 3.0 MeV level, while it is neglected in the evaluation.
(3) The discrete inelastic peaks from levels higher than 4 MeV are greatly smeared compared with the evaluated ones.

4. ^{10}B, ^{11}B

There is no integral experiment on boron in Japan. I would like to discuss from the DDX measurements. Figure 4.6 shows neutron emission spectra of ^{10}B and ^{11}B measured at Tohoku University [108]. For ^{11}B, the present emission spectra considerably differ from ENDF/B-IV, while the agreement of ^{10}B results is fairly well. The measured elastic cross sections of ^{11}B are larger than those of ENDF/B-IV by about 50 %. For ^{10}B, the experiment indicates that there are large contributions of the low energy neutrons due to (n,2n) or multi-particle decay process. Takahashi pointed out the same result for ^{11}B from the DDX measurement on natural boron [106].

5. ^{12}C

From the analyses of integral experiments on graphite (C) and Li_2O-C cylindrical assemblies [25-26], the agreements between measured and calculated reaction rates were almost same as those of Li_2O assembly except for the fission rates of ^{235}U. The calculated distribution of ^{235}U(n,f) in the graphite regions depends on group structure and weighting function. The result does not suggest that the nuclear data of ^{12}C in any file are insufficient.

From the analysis of the time-of-flight experiment on graphite slabs at FNS [101], the calculated spectra based on JENDL-3PR1 and ENDF/B-V agree well with the measured ones (See Fig. 4.7). The energy-integrated comparison suggests that the angular distributions of secondary neutrons should be checked again in both files. Baba also pointed out the same problem from the study of DDX measurements [107]. In the case of JENDL-3PR2, the calculated spectra were almost same as those of JENDL-3PR1. Oyama has carried out the analysis for the same time-of-flight experiment by the use of MCNP [103]. The result is a little better than that by DOT3.5.

In the case of the analysis for the time-of-flight experiment on graphite slab at OKTAVIAN [104], reasonable agreement is obtained between the measured and calculated spectra based on ENDF/B-IV.

Baba pointed out from the DDX measurements that the low energy parts of emission spectra are not described satisfactorily by either JENDL-3PR1 or ENDF/B-V. He suggested that the reduction of cross sections of 2nd level (Q = -7.6 MeV), 3rd level (Q = -9.6 MeV), and the spectra and cross sections of continuum neutrons (See Fig. 4.8) [107]. JENDL-3PR2 has been revised considering these points.
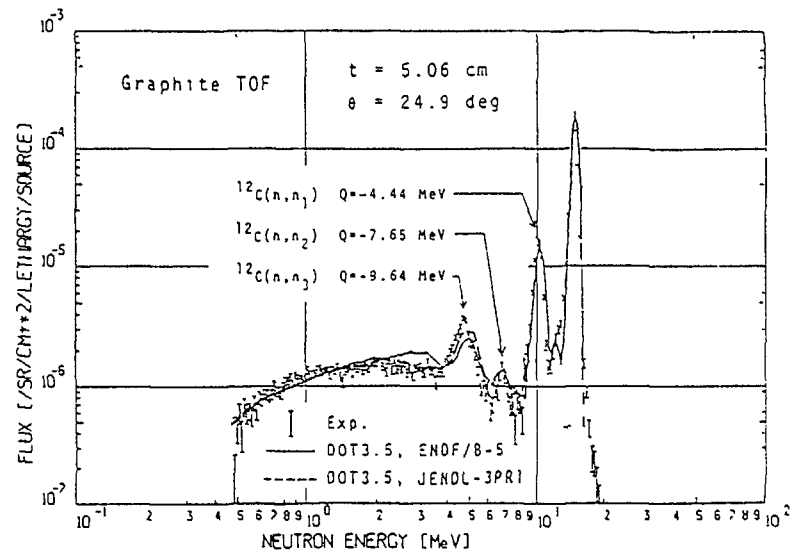
Fig. 4.7 Measured and calculated neutron leakage spectra from a graphite slab.
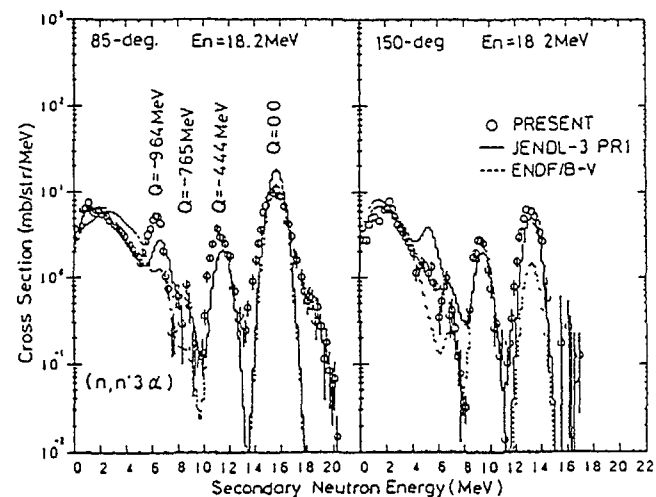
Fig. 4.8 DDX of ^{12}C for 18.2 MeV at 85 and 150 deg.

From the analyses of the Pulses Sphere Program, Nakagawa et al. and Hashikura et al. obtained the same results [99-100]. The calculated spectra based on JENDL-3PR1 were about twice higher than the measured ones between 4 and 7 MeV (See Fig. 4.9). In the case of ENDF/B-IV, the agreements fairly improved, while there were still large discrepancies around 6 MeV and below 5 MeV.

Hashikura pointed out for JENDL-3PR1 as follows [99] ·

(1) The total (n,n') cross section is too small.
(2) The distribution of (n,n') cross section for 21 levels is inadequate, i.e., Too much cross section values are assigned to the levels between 6 and 10 MeV.

7.   Cr

There is no integral experiment on Cr assembly using D-T source in Japan. Measured DDXs are shown in Fig. 4.10 with evaluated ones . In the case of 80 degree, the values of JENDL-3PR1 agree fairly well with the measured ones. While the agreement is not so good in the case of 29 degree in the region between 5 and 13 MeV. The values of ENDF/B-IV are inadequate.

8.   Fe

Hashikura et al. measured the neutron leakage spectra from iron sphere [58]. Measured spectra is shown in Fig. 4.11 with calculated one based on JENDL-3PR1 [99]. The calculated result underestimates the measured flux in the energy region between 5 and 10 MeV, and An evident peak is observed around 9 MeV. This fact indicates that the secondary neutron distribution from the (n,n') continuum is inadequate.

Measured DDXs are shown in Fig. 4.12 with evaluated ones. The values of JENDL-3PR1 and ENDF/B-IV for 37 degree are lower than the measured ones between 7 and 13 MeV. Minor change is recommended to the JENDL-3PR1 file.

9.   Ni

Hashikura et al. obtained following results from the experiment and analysis of neutron leakage spectrum from nickel sphere [59] (See Fig 4.13) :

(1) The calculated spectrum using JENDL-3PR1 generally shows closer agreement with the measured one than that using ENDF/B-IV.
(2) The calculation using JENDL-3PR1 overestimates the measured neutron flux in the energy region near 13 MeV and does not reproduce the small peak near 10 MeV. This is due to the fact that the inelastic scattering cross sections to 1.33 and 1.45 MeV levels are too large and the 3- level of ^{58}Ni is not considered in JENDL-3PR1.
(3) The calculation using ENDF/B-IV differs from the measured result in the energy range of 5 $\sim$ 12 MeV. This arises from the large value of the (n,n') continuum cross section. The present study shows that the experimental value of the total (n,n') cross section which is adopted in ENDF/B-IV is too large.

Measured and evaluated DDX of natural nickel is shown in Fig. 4.14 [106]. The status of DDX in JENDL-3PR1 is just the same as that of iron.
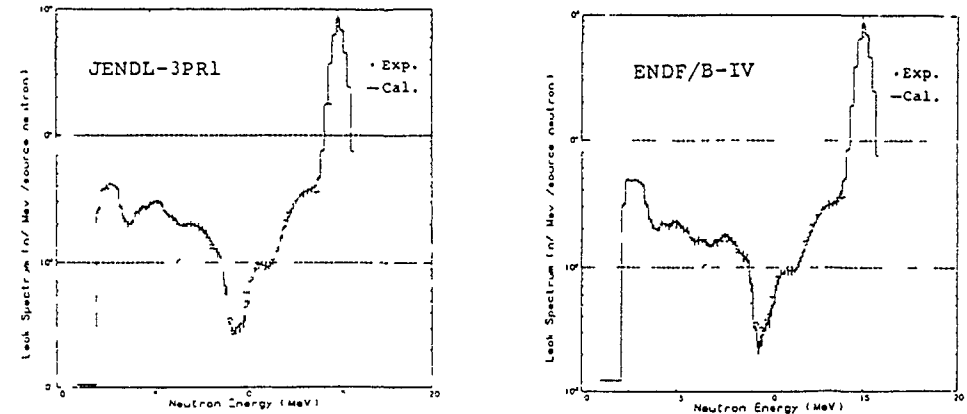
Fig 4.9 Measured and calculated spectra for oxygen.
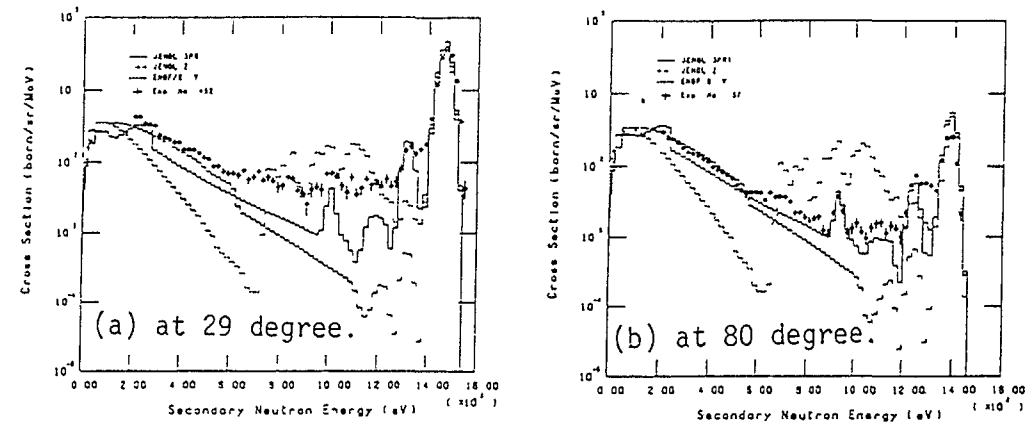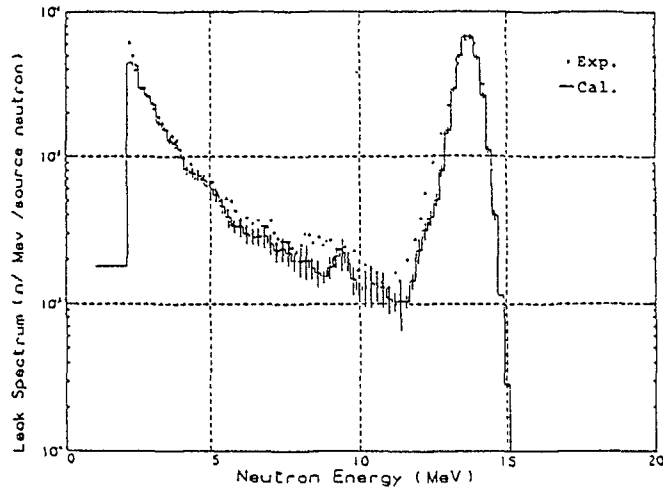

Fig. 4.10 DDX of natural chromium.

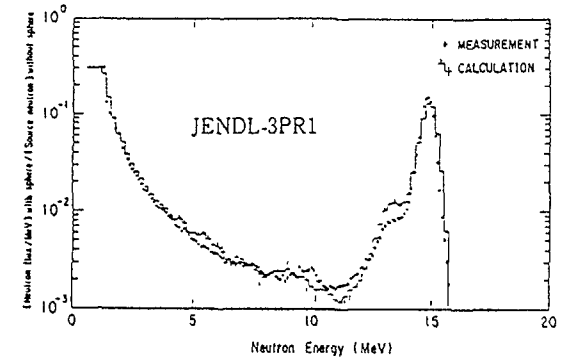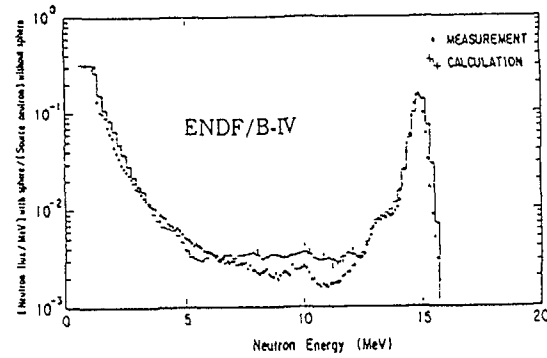Fig. 4.11 Measured and calculated spectra
from an iron sphere.

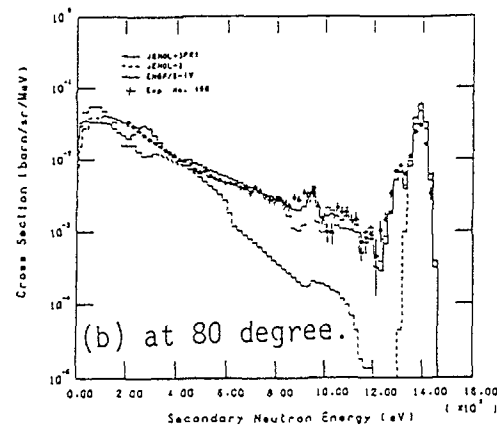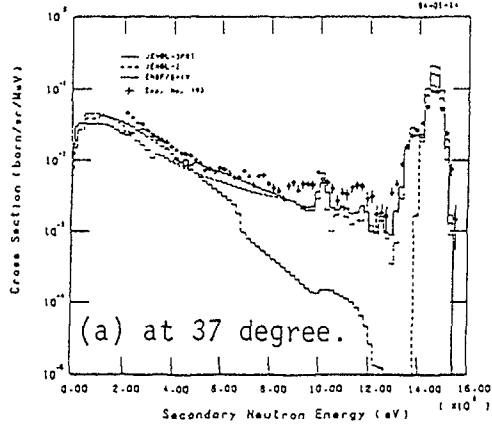Fig. 4.13 Measured and calculated spectra from a nickel sphere.

(a) at 37 degree.

(b) at 80 degree.

(a) at 32 degree.
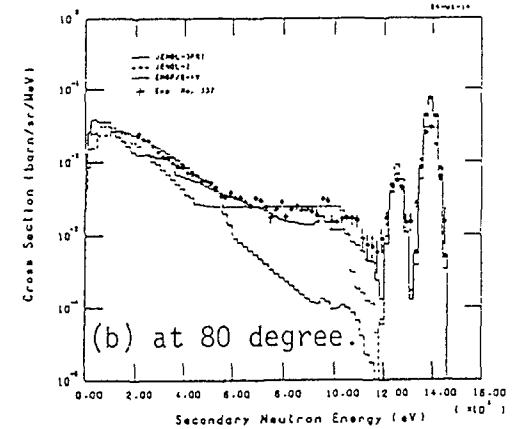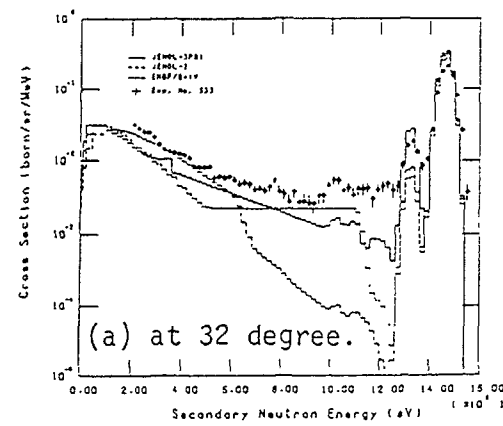
(b) at 80 degree.

Fig. 4.12 DDX of natural iron.

Fig. 4.14 DDX of natural nickel.

10. Pb

Neutron multiplication effect on lead was measured at OKTAVIAN using spherical shell assemblies [45,48]. Differential measurement was also performed as a back-up experiment. A typical measured leakage spectrum is shown in Fig. 4.15 with calculated one using ENDF/B-IV. The measured spectra are harder than the calculated ones using ENDF/B-IV. This result is consistent with the DDX measurement. The broken lines in the figure is calculated by the use of a modified nuclear temperature of Pb(n,2n) reaction which is obtained from the DDX measurement. The modified curve is much closer to the experiment. The C/E values of partial multiplication factors are shown in Fig. 4.16 for three energy range, where the eastic, the inelastic and (n,2n) neutrons contribute dominantly, respectively. For the elastic peak, the agreement is well within the experimental error. While in the region between 6.5 and 12.2 MeV, the calculated values are 20 ∿ 30 % lower than the measured ones. The discrepancy is about 40 %

in the case of the differential experiment. In the region below 6.5 MeV, the calculated values are 13 ∿ 17 % lower than the measured ones. It is recommended from a sensitivity analysis that the Pb(n,2n) cross section increases by 20 %.

Iwasaki et al. measured and analyzed the neutron emission spectra for Pb(n,xn) reaction [109]. Their conclusion supports the above results, i.e., the measured neutron spectra for Pb(n,xn) from 14 to 20 MeV are not consistent with those by ENDF/B-IV. These spectra are reproduced rather well by the multi-step Hauser-Feshbach model with precompound effect using the back shifted Fermi-gas level density formula.

Recently, the experiment of neutron multiplier effect for lead was performed at OKTAVIAN using Pb-Li spheres [53]. Measured T_6 and T_7. distributions are shown in Fig. 4.17 with the calculated ones by MCNP with ENDF/B-IV. It is concluded that the (n,n') and (n,2n) cross sections are inadequate includiding their secondary neutron emission data.
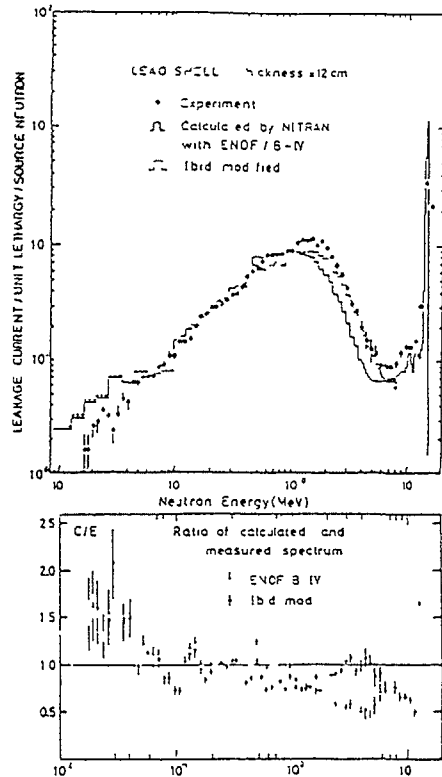

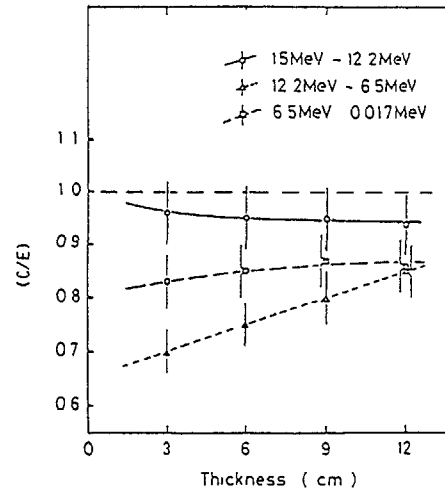Fig. 4.15 Measured and calculated leakage current from 12 cm thick lead shell and C/E values.

Fig. 4.16 Ratio (C/E) of calculated and measured partial multiplication factor for 0° experiment.
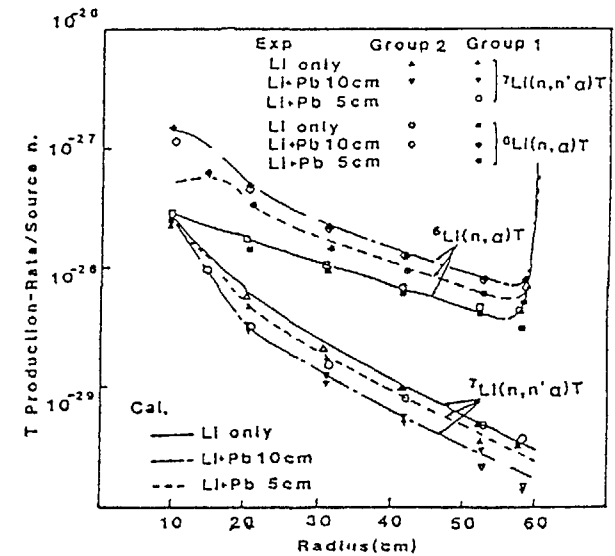
Fig. 4.17 Tritium production rate distributions in the radial direction of zero degree

V. Concluding Remarks

Many integral and differntial experiments have been carried out in Japan in order to verify the accuracy of calculational methods and nuclear data. Especially, the construction of two powerful neutron sources, FNS and OKTAVIAN, have accelerated the fusion neutronics activities. We believe these experimental results should be very useful for the evaluation and/or verification of ENDF/B-VI, JEF, EFF, and so on.

The nuclear data in JENDL-3 Preliminary Version (JENDL-3PR1/2), which includes the most interesting nuclei for fusion reactor blanket, have been examined and the problems of data are pointed out. From the tests by the integral experiments, the data in JENDL-3PR2 seem to be adequate. While from the experimental data of angle-dependent leakage spectra and double-differential cross section (DDX), the data of angular and energy distributions of secondary neutrons (SAD and SED) are inadequate for the most of nuclei in any nuclear data files.

If the calculational model is good and the nuclear data are processed by appropriate manner to obtain a cross-section set, integral values such as TPR might be estimated within 10 % using JENDL-3PR2.

Shibata and Chiba indicate for the evaluation of JENDL-3, i.e., following modification will be performed on JENDL-3PR1/2 [110] ·

^{6}Li	unchange or minor change
^{7}Li	$(n,n'\alpha)T$, (n,n')
^{9}Be	6.8 MeV level
^{12}C ·	unchange or minor change
^{16}O	(n,n), SAD, SED

Some important reactions, such as (n,2n) of Zr, Mo and Bi, are not discussed here. A series of systematic experiments on activation cross-section measurements is being carried out at FNS including these reaction [111-113]. The results including digital data will be available soon.

Additional integral and differential experiments on candidate materials for fusion reactor system are, of course, expected for the tests of methods and data.

Measurements of reaction-rate distribution in a simulated fusion blanket assembly give useful informations for the verification of methods and data. Finally, I would like to request an accurate dosimetry file including the reactions such as ^{27}Al(n,α), ^{58}Ni(n,p), ^{58}Ni(n,2n), ^{115}In(n,n')^{115m}In and so on. If the assessment of TPR/TBR is requested to be less than 5 % through integral tests, the accuracy of less than 3 % is required to the data in the dosimetry file.

References

[1] HIRAOKA T., et al., "Integral Experiments on a Spherical Lithium Metal Blanket System," Proc. Symp. Fusion Reactor Design Problems, CONF-740131, pp363-376, IAEA (1974).

[2] MAEKAWA H., et al., Nucl. Sci. Eng. 57, 335-340 (1975).

[3] SEKI Y., MAEKAWA H., J. Nucl. Sci. Technol. 13 [5] 272-275 (1976).

[4] MAEKAWA H., SEKI Y., ibid., 14 [2] 97-107 (1977).

[5] SEKI Y. MAEKAWA H., ibid., 14 [3] 210-225 (1977).

[6] SEKI Y., MUIR D. W., MAEKAWA H., ibid., 14 [9] 680-681 (1977).

[7] SEKI Y., MAEKAWA H., Nucl. Sci. Eng. 66, 243-268 (1978).

[8] MAEKAWA H., KUSANO J., SEKI Y., "Response Distributions of ^{6}LiF and ^{7}LiF Thermoluminescence Dosimeters in Lithium Blanket Assemblies," JAERI-M 6811 , NEACRP-L-165 (1976).

[9] ITOH S., SEKI Y., MAEKAWA H., "Measurement and Calculation of Fast Neutron Spectra in a Graphite-Reflected Lithium Assembly," Third Topical Meeting on the Technology of Controlled Nuclear Fusion, May 9-11, 1978, Knoxville, CONF-780508, Vol. 1, 385-393.

[10] MAEKAWA H., et al., J. Nucl. Sci. Technol., 16 [5] 377-379 (1979).

[11] SEKI Y., et al., "Calculation of Absolute Fission Rate Distributions Measured in Graphite-Reflected Lithium-Oxide Blanket Assembly," JAERI-M 83-061 (1983).

[12] NAKAMURA T., et al., "Fusion Neutronics Source (FNS)," Proc. Third Sym. on Accelerator Science and Technology, Osaka Univ., Osaka, Japan, Aug. 27-29, pp55-56 (1980).

[13] SUMITA K., et al., "Neutron Source and Its Utilizations for Fusion Studies (OKTAVIAN Program)," Proc. 12th Symp. Fusion Technology, Julich, Sep. 13-17, 1982, Vol. 1, pp675-680 (1982).

[14] SHIBATA K., KIKUCHI Y., "Evaluation of Nuclear Data for Fusion Neutronics," ibid., 1985, Vol. 2, 1585-1588.

[15] CHIBA S., et al., "Interaction of Fast Neutrons with ^{6,7}Li," Proc. Int. Conf. Nucl. Data for Basic & Applied Science, Santa Fe, May 13-17, 1985, Vol. 1, 227-230.

[16] CHIBA S., et al., J. Nucl. Sci. Technol. 22 [10] 771-787 (1985).

[17] IGARASI S., ASAMI T. (Ed.), "Proceedings of Specialists' Meeting on Nuclear Data for Fusion Neutronics," JAERI-M 86-029 (1986).

[18] NAKAMURA T., MAEKAWA H., "Integral Experiments on Lithium-Oxide Spherical Assembly with a Graphite Reflector and on Duct Streaming, Third IAEA Workshop on Fusion Reactor Design and Technology," Tokyo, Oct. 5-16, 1981, IAEA-TC-392/39.

[19] NAKAMURA T., MAEKAWA H., "Blanket and Shield Experiments in Fusion Neutronics Source (FNS)," 9th Int. Conf. on Plasma Physics and Controlled Nuclear Fusion Research, Baltimore, U.S.A., Sep. 1-8, 1982, IAEA-CN-41/O-4.

[20] MAEKAWA H., et al., "Measurements of Tritium Production-Rate Distribution in Simulated Blanket Assemblies at the FNS," JAERI-M 83-195 (1983).

[21] IKEDA Y., et al., "Measurements of Induced Activity in Type 316 Stainless Steel by Irradiation in D-T Neutron Fields," Proc. of 6th Topical Meeting on the Technology of Fusion Energy, Fusion Technology, 8 [1] 1466-1472 (1985).

[22] MAEKAWA H., et al., "Measurement of Tritium Production-Rate Distribution in a 60 cm-thick Li$_2$O Slab Assembly and Its Analysis," ibid., 1460-1465, (1985).

58

[23] MAEKAWA H., et al., "Integral Test of JENDL-3PR1 Through Benchmark Experiments on Li_2O Slab Assembly," Proc. of Int. Conf. on Nuclear Data for Basic and Applied Science, May 13-17, 1985, Santa Fe, Vol. 1 pp101-106.
[24] MAEKAWA H., et al., "Blanket Benchmark Experiments on a 60 cm-thick Lithium-Oxide Cylindrical Assembly," JAERI-M Report (In press).
[25] MAEKAWA H., et al., "Benchmark Experiments on a 60 cm-thick Graphite Cylindrical Assembly," To be published in JAERI-M Report.
[26] MAEKAWA H., et al., "Fusion Benchmark Experiments on a 40 cm-thick Lithium-Oxide and 20 cm-thick Graphite Cylindrical Assembly," To be published in JAERI-M Report.
[27] MAEKAWA H., "Clean Benchmark Experiments and Analyses at FNS," Proc. Specialists' Meeting on Nuclear Data for Fusion Neutronics, July 23-25, 1985, JAERI-M 86-029, pp171-182 (1986)
[28] MAEKAWA H., et al., "Measurements of Angular Flux on Surface of Li_2O Slab Assemblies and Their Analysis by Direct Integration Transport Code 'BERMUDA'," Proc. 5th Topical Meeting on the Technology of Fusion Energy, Knoxville, Apr. 26-28, 1983, Nucl. Technol./Fusion 4 [2] 1165-1170 (1983).
[29] OYAMA Y., MAEKAWA H., "Measurements of Angle-Dependent Neutron Spectra from Lithium-Oxide Slab Assemblies by Time-of-Flight Method," JAERI-M 83-195 (1983).
[30] OYAMA Y., YAMAGUCHI S., MAEKAWA H., "Analysis of Time-of-Flight Experiment on Lithium-Oxide Assemblies by a Two-Dimensional Transport Code Dot3.5," JAERI-M 85-031 (1985).
[31] OYAMA Y., MAEKAWA H., Nucl. Instr. Meth. A245, 173-181 (1986).
[32] OYAMA Y., YAMAGUCHI S., MAEKAWA H., "Measurements of Angle-Dependent Neutron Spectra from Graphite Slab Assemblies by Time-of-Flight Method," To be published in JAERI-M Report.
[33] OYAMA Y., YAMAGUCHI S., MAEKAWA H., "Measurements of Angle-Dependent Neutron Spectra from Lithium Metal Slab Assemblies by Time-of-Flight Method," To be published in JAERI-M Report.
[34] OYAMA Y., MAEKAWA H., "measurements of Angle-Dependent Neutron Spectra from Beryllium Slab Assemblies by Time-of-Flight Method," To be published in JAERI-M Report.
[35] OYAMA Y., MAEKAWA H., "Neutron Angular Flux from Beryllium Slab Assemblies," Proc. Fall Mtg. of Atomic Energy Soc. of Japan, A36 (1986); To be submitted to Nucl. Sci. Eng.
[36] NAKAMURA T., "Fusion Blanket Engineering Benchmark Experiments," Proc. Specialists' Meeting on Nuclear Data for Fusion Neutronics, July 23-25, 1985, JAERI-M 86-029, pp183-191 (1986).
[37] NAKAMURA T., ABDOU M. A., "Summary of Recent Results from the JAERI/U.S. Fusion Neutronics Phase-I Experiments," Seventh Topical Meeting on the Technology of Fusion Energy, Reno, Nevada, June 15-19, 1986.
[38] YOUSSEF M. Z., et al., "Analysis of Intercomparison for Phase-I Experiments at FNS," ibid. (1985).
[39] MAEKAWA H., et al., "Measured Neutron Parameters for Phase-I Experiments at the FNS," ibid.
[40] YAMAGUCHI S., NAKAMURA T., "Tritium Production Measurements by the Lithium-Glass Scintillation Method," ibid.
[41] OISHI K., et al., "Experiments and Analysis of Induced Activities in Concrete Irradiated by 14 MeV Neutrons," ibid.
[42] TAKAHASHI A., et al., J. Nucl. Sci. Technol., 14 [4], 308-311 (1977).
[43] YAMAMOTO J., et al., ibid., 17 [4], 255-268 (1980).
[44] YAMAMOTO J., et al., ibid., 19 [4], 276-288 (1982).

[45] TAKAHASHI A., et al., ibid., Vol. 1, pp687-692 (1982).
[46] YAMAMOTO J., et al., "Measurement and Analysis of Leakage Neutron Spectra from SS-316, Concrete, Water and Polyethylene Slabs with D-T Neutron Source," Proc. 6th Int. Conf. on Radiation Shielding, Tokyo, Vol. I pp464-473 (1983).
[47] YAMAMOTO J., et al., "Numerical Tables and Graphs of Leakage Neutron Spectra from Slabs of Typical Shielding Materials with D-T Neutron Source," OKTAVIAN Reort A-83-05, Osaka University (1983).
[48] YANAGI Y., TAKAHASHI A., "Differential and Integral Experiments of Neutron Multiplier Candidate Elemnts," OKTAVIAN Report A-84-02, Osaka University (1984).
[49] TAKAHASHI A., et al., "Measurements of Tritium Breeding Ratios in Lithium Slabs Using Rotating Neutron Source," Proc. of 13th Sym. Conf. on Fusion Technology, Varese, Italy, Sep. 24-28, 1984, Vol.II, 1325-1330.
[50] SUGIYAMA K., et al., "Neutronic Experiments in a 120 cm Lithium Sphere," ibid., Vol. II, 1375-1380.
[51] SUGIYAMA K., et al., "Integral Experiments in a 120-cm Lithium Sphere," Proc. 6th Topical Meeting on Technology of Fusion Energy, Fusion Technology, 8 [1] 1491-1496 (1985).
[52] IGUCHI T., et al., "Tritium Production and Foil Reaction Rates in a Large Lithium Sphere by D-T Neutrons," Proc. of Int. Conf. on Nuclear Data for Basic and Applied Science, Santa Fe, May 13-17, 1985, Vol. 1, 203-206.
[53] SUGIYAMA K., et al., "Neutronic Experiments in a Li-Pb Spherical Assembly," 14th Sym. Conf. on Fusion Technology Sep. 8-12, 1986, Avignon, France.
[54] KANDA K., HIRAKAWA N., J. Nucl. Sci. Technol., 17 [12] 888-899 (1980).
[55] TAKAHASHI H., SUGIYAMA K., "A Benchmark Experiment for Fast Neutron Transport in Graphite," Proc. Int. Conf. Nucl. Data for Science & Technology, Antwerp, Sep. 6-11, 1982, pp380-382.
[56] IGUCHI T., et al., "Neutron Spectra and Tritium Production Rate Measurements in the One-Dimensional LiF Slab Geometry as a Fusion Reactor Blanket Benchmark Experiment," Proc. 4th Topical Meeting on Technology of Controlled Nuclear Fusion, Oct. 14-17, 1980, King of Prussia, CONF-801011, Vol. I, 387-394 (1981).
[57] IGUCHI T., NAKAZAWA M., SEKIGUCHI A., "A Benchmark Experiment on Tritium Production and Rdiation Heating in the LiF Assembly," Proc. 5th Topical Meeting on Technology of Fusion Energy, Knoxville, Apr. 26-28, 1983, Nucl. Technol./Fusion 4 [2] 817-822 (1983).
[58] HASHIKURA H., et al., "Measurements of Neutron Leakage Spectra from 50.32 cm Radius Iron Sphere," OKTAVIAN Report A-83-07, Osaka University, (1983) ; UTNL-R 0159, The University of Tokyo.
[59] HASHIKURA H., et al., J. Nucl. Sci. Technol., 23 [6] 477-486 (1986).
[60] SEKIMOTO H., et al., J. Nucl. Material 133&134, 882-886 (1985).
[61] SEKIMOTO H., HOJO K., HOJO T., J. Nucl. Sci. Technol., 22 [3] 174-182 (1985).
[62] SEKIMOTO H., LEE D., ibid., 23 [5] 381-386 (1986).
[63] SUZUKI T., ISHIGURO Y., MATSUI Y., "PALLAS-TS : A One -Dimensional Neutron Transport Code for Analyzing Fusion Blanket Neutronics," JAERI-M 9492 (1981) (in Japanese), (PALLAS-TS has been remaned as BERMUDA-1DN).
[64] SUZUKI T., HASEGAWA A., MORI T., ISE T., "BERMUDA-2DN : A Two-Dimensional Neutron Transport Code," Proc. of 6th Int. Conf. on Radiation Shielding, May 16-29, 1983, Tokyo, Japan, Vol. I, 246-258.
[65] SUZUKI T., HASEGAWA A., KANEKO K., NAKASHIMA H., "BERMUDA-1DG : A One-Dimensional Photon Transport Code," JAERI-M 84-177 (1984).

[66] TAKAHASHI A., RUSCH D., "Fast Regorous Numerical Method for the Solution of the Anisotropic Neutron Transport Problem and the NITRAN System for Fusion Neutronics Application, Part I and II," KfK 2832/I and II (1979).

[67] TAKAHASHI A., et al.,J. Nucl. Sci. Technol., 19 [4] 276-288 (1982).

[68] MORI T., SASAKI M., "Development of a 2-D Sn Transport Code Using Double Differential Form Cross Section Library," JAERI-M 86-125 pp42-44 (1986).

[69] IDA T., KONDO S., TOGO Y., "Development of a Radiation Transport Code in Axisymmetric Toroidal geometry for Nuclear Design of Fusion Reactor," Proc. 6th Int. Conf. on Radiation Shielding, Tokyo, May 16-20, 1983, Vol. II, 741-759.

[70] YAMANO N., KOYAMA K., J. Nucl. Sci. Technol., 16 [12] 919-922 (1979).

[71] NAKAGAWA M., MORI T., ISHIGURO Y., "Development of Monte Carlo Code Using Multi-Group Double-Differential Cross Section Library and Its Application to Shielding Calculation for Fusion Materials," Proc. 6th Int. Conf. on Radiation Shielding, Tokyo, May 16-20, 1983, Vol. I, 171-179.

[72] NAKAGAWA M., MORI T., "MORSE-DD : A Monte Carlo Code Using Multi-Group Double Differential Form Cross Sections," JAERI-M 84-126 (1984).

[73] IIDA H., "Application of Monte Carlo Transport Code to Neutronics Design of Tokamak Fusion Reactor," JAERI-M 9717 (1981).

[74] HASEGAWA A., "Development of Processing Module for File 6: Energy-angular Distribution Data of END/F-V Format," JAERI-M 86-125 pp12-14 (1986) ; "PROF-GROUCH-G/B Code System," To be published in JAERI report.

[75] MORI T., NAKAGAWA M., ISHIGURO Y., "PROF-DD · A Code System for Generation of Multi-Group Double-Differential Form Cross Section Library," JAERI-M 86-124 (1986).

[76] FURUTA K., OKA Y., KONDO S., "SUSD : A Cross Section Sensitivity-Uncertainty Analysis Code for Secondary Angular Distribution or Secondary Energy Distribution," UTNL-R 0186, The University of Tokyo (1986).

[77] FURUTA K., OKA Y., KONDO S., Nucl. Eng. Design/Fusion 3 287-300 (1986).

[78] SEKI Y., et al., "THIDA-2 . An Advanced Code System for Calculation of Transmutation, Activation, Decay Heat and Dose Rate," JAERI 1301 (1986).

[79] MAKI K., "A High Tritium Breeding Ratio (TBR) Blanket Concept and Requirements for Nuclear Data Relating to TBR," JAERI-M 86-029, PP57-67 (1986).

[80] CONSTANTINE G., "Nuclear Data Requirements for Fusion Reactor Neutronics Design, Blanket Neutronics and Tritium Breeding," Proc. Advisory Group Meeting on Nucl. Data for Fusion Reactor Technology, Vienna, Dec. 11-15, 1978, IAEA-TECDOC-223,11-29 (1979).

[81] ABDOU M. A., "Tritium Breeding in Fusion Reactor," Proc. Int. Conf. Nucl. Data for Sci. & Technol., Sep. 6-10, 1982, Antwerp, pp293-312.

[82] CHENG E. T., "Nuclear Data Needs for Fusion Energy Development," Proc. 6th Topical Meeting on Technology of Fusion Energy, San Francisco, March 3-7, 1985, Fusion Technology 8 [1] 1423-1430 (1985).

[83] GOHAR Y., "Nuclear Data Needs for Fusion Reactors," Proc. Int. Conf. Nuclear Data for Basic & Applied Science, May 13-17, 1985, Santa Fe, Vol. 1, 15-44.

[84] KANDA Y., "Review on Nuclear Data for Fusion Reactors," Proc. of Specialists' Meeting on Nuclear Data for Fusion Neutronics, JAERI-M 86-029, pp3-14 (1986).

[85] ASAMI T., "Status of JENDL-3PR1 and -3PR2," JAERI-M 86-029, pp15-31 (1986).

[86] CHIBA S., "Revision of the Neutron Nuclear Data of Lithium," ibid. pp32-40.

[87] REUPKE W. A., et al., Nucl. Sci. Eng., 82 416-428 (1982).

[88] MAEKAWA H., et al., "Measurement of ^{7}Li(n,n'α)^{3}T Cross Section Between 13.3 and 14.9 MeV," JAERI-M 86-125, pp130-132 (1986).

[89] GOLDBERG E., et al., "Measurements of ^{6}Li and ^{7}Li Neutron-Induced Tritium Production Cross Sections at 15 MeV," Nucl. Sci. Eng., 91 173-186 (1985).

[90] SMITH D. L., et al., ibid., 78 359-369 (1981).

[91] LISKIEN H., et al., "Determination of ^{7}Li(n,nt)^{4}He Cross Sections," Proc. Int. Conf. Nuclear Data for Science and Technology, Antwerp, Sep. 6-11, 1982, pp349-352.

[92] QAIM S. M., WOLFLE R., "^{7}Li(n,n't)^{4}He Reacton Cross Section via Tritium Counting," To be submitted to Nucl. Sci. Eng.

[93] YOUNG P. G., Tansactions Amer. Nucl. Soc., 39 272-274 (1981).

[94] IGUCHI T., NAKAZAWA M., "Measurement of the Fission Spectrum Averaged Cross Section of ^{7}Li(n,n'α)T Reaction," Proc. Fall Mtg. of Atomic Energy Soc. of Japan, A49 (1986).

[95] NAKAZAWA M., et al., "A New Data Processing Technique for Reactor Neutron Dosimetry," Proc. 2nd ASTM-EURATOM Sym. Reactor Dosimetry, pp1423-1434 (1977), NEUT Research Report 83-10, Univ. of Tokyo (1983).

[96] SWINHOE M. T., UTTLEY C. A., Nucl. Sci. Eng. 89 261-272 (1985).

[97] WONG C., et al., "Livermore Pulsed Sphere Program: Program Summary Through July 1971," UCRL-51144 Rev. I (1972).

[98] Los Alamos Radiation Transport Group (X-6), "MCNP - A General Monte Carlo Code for Neutron and Photon Transport," LA-7396-M, Revised (1981).

[99] HASHIKURA H., et al., "Comparison between Measurements of the Neutron Spectra from Materials used in Fusion Reactors and Calculations using JENDL-3PR1," JAERI-M 86-029, pp160-170 (1986).

[100] NAKAGAWA M., "Benchmark Test of MORSE-DD Code Using Double-Differential Form Cross Sections," JAERI-M 85-009 (1985).

[101] YAMAGUCHI S., et al., "Analysis of the Time-of-Flight Experiment on Lithium-Oxide and Graphite Assemblies Using JENDL-3PR1," JAERI-M 85-116, pp132-134 (1985).

[102] RHOADES W. A., MYNATT F. R., "The DOT-III Two Dimensional Discrete Ordinates Transport Code," ORNL/TM-4280 (1973).

[103] OYAMA Y., Private communication (1986), To be published elsewhere.

[104] YAMAMOTO J., et al., "14 MeV Integral Experiment at OKTAVIAN to Check Differential Data of Secondary Neutrons," JAERI-M 86-029, PP149-159 (1986).

[105] TAKAHASHI A., et al., J. Nucl. Sci. Technol., 21 [8] 577-598 (1984).

[106] TAKAHASHI A., "Double Differential Neutron Emission Cross Sections at 14 MeV Measred at OKTAVIAN," JAERI-M 86-029, pp99-118 (1986).

[107] BABA M., "Measurements of Double-Differential Neutron Emission Cross Sections at Tohoku University," ibid., pp119-140.

[108] BABA M., et al., "Scattering of 14.1-MeV Neutrons from ^{10}B, ^{11}B, C, N, O, F and Si," Proc. Int. Conf. Nucl. Data for Basic & Applied Science, Santa Fe, May 13-17, 1985, Vol. 1 pp223-226.

[109] IWASAKI S., "Measurement and Analysis of Neutron Emission Spectra for Pb(n,Xn) Reaction Between 14 and 20 MeV," ibid. Vol. 1 pp191-194.

[110] SHIBATA K., CHIBA M., Private communication (1986).

[111] IKEDA Y., et al., "Measurement of High Threshold Activation Cross Sections for 13.5 to 15.0 MeV Neutrons," JAERI-M 85-116, pp106-111 (1985) ; Proc. Int. Conf. Nucl. Data for Basic and Applied Science, Santa Fe U.S.A., May 13-17 1985, Vol. 1 pp175-178.

[112] IKEDA Y., et al., "Activation Cross Section Measurement of Zr and Cr for 14 MeV Neutrons," JAERI-M 86-125, pp127-129 (1986).

[113] KONNO C., et al., "Measurements of Activation Cross Sections --- Short-Lived Nuclides ---," ibid., pp133-135 (1986).

NUCLEAR DATA REQUIREMENTS FOR DOSIMETRY AND RADIATION DAMAGE ESTIMATES

L.R. GREENWOOD
Chemical Technology Division,
Argonne National Laboratory,
Argonne, Illinois,
United States of America

Presented by F.M. Mann

Abstract

Status of neutron dosimetry measurements and radiation damage calculations for the US Fusion Materials Program is presented. Nuclear data needs for fission and fusion reactors as well as requirements for damage calculations are enumerated.

Neutron dosimetry measurements and radiation damage calculations are routinely performed for the U.S. Fusion Materials Program. These irradiations are being performed in a variety of facilities including mixed-spectrum and fast fission reactors such as the High Flux Isotopes Reactor (HFIR) at Oak Ridge National Laboratory and the Fast Flux Test Facility (FFTF) at Hanford Engineering Development Laboratory, the 14 MeV d-t Rotating Target Neutron Source II (RTNS II) at Lawrence Livermore National Laboratory, and higher-energy accelerator-based neutron sources. A subtask group has been formed to characterize these facilities and to measure neutron fluence and energy spectra as well as displacement damage, gas production, and other transmutation for each materials experiment. These measurements are generally conducted using activation measurements to adjust calculated neutron spectra with the least-squares computer code STAY'SL. Radiation damage calculations are then routinely provided by the SPECTER computer code. The following material is intended to provide an overview of current research and nuclear data requirements. Recent references are also provided. [Ref. 1-3]

Accurate nuclear data is crucial to these measurements and calculations. Consequently, we have initiated a program to test and develop neutron cross sections. Activation and helium production cross sections have been measured in fission reactors, 14 MeV sources, Be(d,n) sources, and spallation facilities. Integral and differential data are being combined to adjust discrepant data. Activation measurements were reported recently for 22 reactions at 14.8 MeV. We have previously published integral measurements in Be(d,n) fields at deuteron energies of 14, 16, 30, and 40 MeV and new measurements are in progress at 7 MeV. Spal-lation cross sections are being developed to extend our dosimetry techniques for higher-energy neutron sources. [Ref. 4-6]

The production of very long-lived isotopes is of interest to waste disposal, maintenance, and dosimetry applications. Recent effort has focussed on the measurement of these cross sections at 14 MeV and we have reported data for the production of ^{26}Al, ^{55}Fe, ^{63}Ni, ^{91}Nb, and ^{94}Nb using high fluence irradiations at RTNS II followed by radiochemical separations, gamma spectroscopy, liquid scintillation counting, and accelerator mass spectrometry. [Ref. 7-8]

Helium measurments have been completed for 26 elements, 22 separated isotopes, and 3 alloy steels at 14.8 MeV and further work is in progress at RTNS II. Integral measuremets in fission reactors have uncovered serious discrepancies in calculated gas production rates for Ti, Nb, and Cu, while data for Fe and Ni (including thermal production from ^{59}Ni) show good agreement. We have discovered a new thermal helium production effect in copper, similar to the well-known effect in nickel. The effect involves thermal capture and decay from ^{63}Cu to ^{65}Zn which has been found to have a high thermal (n,α) cross section. The effect may be useful in simulating fusion-like helium production. Integral helium measurements have also been reported in Be(d,n) fields and new monoenergetic measurements are in progress at 10 MeV. [Ref. 9-12]

The SPECTER computer code has been developed to calculate displacement damage and gas production for 38 elements for any measured neutron spectrum. We have recently developed the SPECOMP code which performs displacement calculations for compound materials such as insulators, tritium breeders, and alloys. These calculations properly integrate over all combinations of recoiling atoms and matrix atoms. By making use of the recoil energy spectra in the SPECTER master libraries, the calculations do not need to reference nuclear data and hence are quite fast and inexpensive in computer time and memory. Results show that there are significant diffenerces in calculated displacement damage (30-40%) for breeder materials; however, the dpa rates are not changed very much when all elements in the compound have similar mass values. Calculations are in progress for other compound materials and we intend to add the results to SPECTER for routine use. [Ref. 2,3,13]

Acknowledgements

References

[1]L. R. Greenwood and R. K. Smither, Proceedings of Fifth ASTM -EURATOM Symposium on Reactor Dosimetry, Reactor Dosimetry, J.P. Genthon and H. Rottger,eds.,251-261(1985).

[2]L. R. Greenwood, J. Nucl. Mater. 141 − 143(1986).

[3]L. R. Greenwood, Effects of Radiation on Materials, Thirteenth Symposium, Seattle, in press,1986.

[4]L. R. Greenwood, R. R. Heinrich, R. J. Kennerley, and R. Medrzychowski, Nucl. Technol. 41,(1978)109-128 .

[5]L. R. Greenwood, R. R. Heinrich, M. J. Saltmarsh, and C. B. Fulmer, Nucl. Sci. Eng. 72, (1979)175-190 .

[6]D. R. Davidson, L. R. Greenwood, R. C. Reedy, and W. F. Sommer, ASTM STP 870, F.A. Garner and J. S. Perrin, Eds., (1985)1199-1208.

[7]R. K. Smither and L. R. Greenwood, J. Nucl. Mater. 122, 1071-1077 (1984).

[8]L. R. Greenwood, D. G. Doran, and H. L. Heinisch, Production of ^{91}Nb, ^{94}Nb, and ^{95}Nb from Mo by 14.5-14.8 MeV Neutrons, accepted for publication in Physical Review C, June 1986.

[9]L. R. Greenwood, J. Nucl. Mater. 115, 137-142 (1983).

[10]L. R. Greenwood, D. W. Kneff, R. P. Skowronski, and F. M. Mann, J. Nucl. Mater. 122, 1002-1010 (1984).

[11]D. W. Kneff, L. R. Greenwood, B. M. Oliver, R. P. Skowronski, and E. L. Callis, Radiation Effects, 92 − 96, 553-556(1986).

[12]D. W. Kneff, B. M. Oliver, H. Farrar IV, and L. R. Greenwood, "Helium Production in Pure Elements, Isotopes, and Alloy Steels by 14.8 MeV Neutrons", Nucl. Sci. Eng.92(1986)491-524.

[13]L. R. Greenwood and R. K. Smither, SPECTER: Neutron Damage Calculations for Materials Irradiations, ANL/FPP/TM-197, January 1985.

FUSION DOSIMETRY AND RADIATION DAMAGE

- Characterization of Irradiation Facilities

  - Fission Reactors (HFIR, ORR, OWR, EBRII)

  - Accelerator Neutron Sources [(d,t),Be(d,n)]

- Cross Section Measurements

  - Fission Reactor Dosimetry

  - Fusion Reactor Dosimetry, Diagnostics, Waste

  - 14 MeV Measurements at RTNS II

  - Helium Production Cross Sections

  - Integral Testing in Be(d,n) Fields

  - Spallation Neutron Sources (IPNS,LAMPF)

- SPECTER: Radiation Damage Calculations

  - DPA, Recoil Spectra for 38 Elements

  - Gas Production, Total Dose

  - New SPECOMP for compounds

RECENT HIGHLIGHTS

- Fusion Reactor Data

  - 14.8 MeV Activation Cross Sections for 22 Reactions

  - ^{94}Nb, ^{91m}Nb from Mo and ^{94}Mo

  - ^{27}Al, ^{54}Fe(n,2n) Reactions for Plasma Diagnostics

  - Other Long-Lived Isotopes: ^{55}Fe, ^{63}Ni, ^{59}Ni

- Gas Production Measurements

  - Discovered New Thermal Effect for Cu and Zn

  - Extra Damage Effects for Ni and Cu

  - Testing of ENDF/B-V Gas File in HFIR

  - 14 MeV Data at RTNS II; 10 MeV Data at LANL

- Damage Calculations

  - SPECOMP code for insulators, breeders, alloys

  - New Models of Capture Gamma and Beta Decay

Long-lived Activities in Fusion Materials

Reaction	Half-life,y	Comment/Status
^{14}N(n,p)^{14}C	5730	RTNS - in progress
^{13}C(n,α)^{10}Be	1.6x10^6	ams
* ^{27}Al(n,2n)^{26}Al	7.2x10^5	ams,γ - done
^{40}Ar(n,2n)^{39}Ar	269	gas
* ^{54}Fe(n,2n)^{53}Fe(β)^{53}Mn	3.7x10^6	γ - done
* ^{56}Fe(n,2n)^{55}Fe	2.7	RTNS - done
* ^{60}Ni(n,2n)^{59}Ni	7.5x10^4	RTNS - in progress
* ^{64}Ni(n,2n)^{63}Ni	100.	RTNS - done
* ^{63}Cu(n,p)^{63}Ni	100.	RTNS - done
^{94}Zr(n,2n)^{93}Zr	1.5x10^6	RTNS - in progress
^{93}Nb(n,p)^{93}Zr	1.5x10^6	RTNS - in progress
^{93}Nb(n,2n)^{92}Nb	3.2x10^7	RTNS - in progress
* ^{94}Mo(n,p)^{94}Nb	2.0x10^4	RTNS - done
^{94}Mo(n,2n)^{93}Mo	3000.	RTNS - in progress

* New measurements

Measured Cross Sections (mb) for Mo

E$_n$ (MeV)	14.55	14.60	14.78	14.80	$\pm\%^a$
^{94}Mo(n,p)^{94}Nb	57.2	-	53.1	-	10
^{Nat}Mo(n,x)^{94}Nb^b	-	7.9	-	7.8	11
^{95}Mo(n,x)^{94}Nb^c	-	16.3	-	18.3	15
^{95}Mo(n,p)^{95}Nb	40.4	-	37.1	-	6
^{92}Mo(n,x)^{91m}Nb^d	157.	153.	145.	145.	7
^{98}Mo(n,α)^{95}Zr	6.56	6.56	6.24	6.21	6
^{92}Mo(n,x)^{91g}Nb^c	$\approx$300				
^{Nat}Mo(n,x)^{91g}Nb^c	$\approx$ 45				

Fusion Reactor Activation of Mo (STARFIRE 20 MW-y/m^2)

| Isotope	Half-life (y)	Activity
^{94}Nb	20,300	70 μCi/g
^{91g}Nb	700	11 mCi/g

DAMAGE CALCULATIONS FOR COMPOUNDS

- SPECOMP Computer Code

  - Sums damage for different recoil and matrix atoms

  - DPA for breeders, insulators, alloys, etc.

  - Recoils available for each species

  - Based on SPECTER pka files

  - Fast, efficient, ENDF not required

  - Li_2O, $LiAlO_2$, Al_2O_3, SiO_2 Complete

  - Files added to SPECTER for routine use

  - Other materials in progress

SPECOMP Results

Spectral-averaged dpa cross sections, b

Compound		14 MeV	Fusion	HFIR	EBR II
Li_2O	SPECOMP	1040	754	2410	939
	Sum	728	517	2321	636
$LiAlO_2$	SPECOMP	1648	978	1120	1031
	Sum	1336	777	1050	808
Al_2O_3	SPECOMP	1685	935	303	924
	Sum	1718	945	304	925
SiO_2	SPECOMP	1700	938	305	944
	Sum	1764	955	306	943
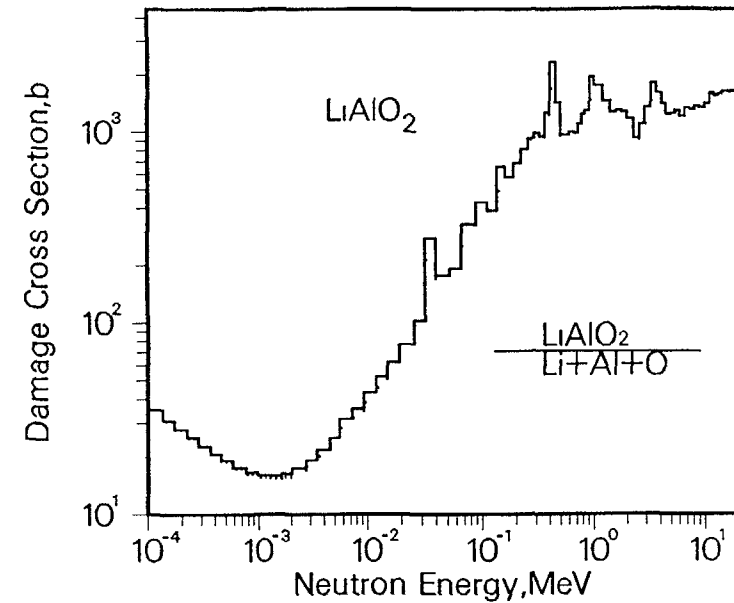
FUTURE DAMAGE CALCULATIONS

- DPA for Insulators/ Alloys

- Spallation Calculations to 1 GeV

- Gas Production, Transmutation Data

- Damage Efficiency?

- DPA Adequate for Data Correlations?

- Uncertainties/ Covariances for All Data

- International Intercomparisons/ Standardization

HELIUM PRODUCTION CROSS SECTIONS

- Correlate He Measurements with Dosimetry

  - Radiometric Dosimetry - Argonne

  - He Mass Spectrometry - Rockwell International

- Thermal Ni and Cu Effects for Fusion

  - Discovered New Effect in Cu to ^{65}Zn(n,He)

  - ^{59}Ni Calculations Agree with 45 Measurements

  - Extra dpa Effect: 1 dpa/ 567 appm He

- HFIR/ORR Tests of ENDF/B-V Gas File

- 14 MeV Measurements at RTNS II

  - Data for 25 Elements Published NSE 92,1986

  - New Experiments Initiated 7/86

- 10 MeV Measurements at LANL

  - ANL/Rockwell/LANL Irradiation 10/86

HELIUM PRODUCTION IN HFIR SUMMARY OF C/E VALUES

MATERIAL	C/E VALUE	COMMENTS
NICKEL	0.95 ± 0.07	INCL. THERMAL N
IRON	0.96 ± 0.06	FLUENCE EFFECT
CHROMIUM	1.06	1 COMPARISON
TITANIUM	2.34 ± 0.20	
NIOBIUM	0.73 ± 0.03	
COPPER	0.58 ± 0.02	RB POSITION
	0.76 ± 0.05	PTP; FAST N ONLY

^{63}Cu(n,γ)^{64}Cu(β^-)^{64}Zn(n,γ) ^{65}Zn(n,α)
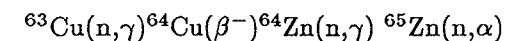
Thermal Cross Sections(b) for He Production in Cu

Reaction	Data^a	ENDF/B-V
^{64}Cu(n,γ)^{65}Cu	270±170	$\prec$6000
^{65}Zn(n,abs)^b	66±8	-
^{65}Zn(n,α)^{62}Ni	4.7±0.5	250±150

^{a}Data measured in HFIR with 7% epithermal flux
^{b}Total absorption includes (n,γ), (n,p), and (n,α)

Rate equation for HFIR - PTP:

$$He(appm) \approx 0.67 \ \Phi^{2.58}$$
$$(\Phi = \text{thermal fluence x}10^{22} \text{ n/cm}^2)$$

Extra damage from ^{62}Ni Recoil:

1 dpa / 492 appm Helium (thermal)

At a thermal fluence of 10^{23} in HFIR:

250 appm extra Helium; 0.5 extra dpa

FLUENCE, $\times 10^{22}$ n/cm^2
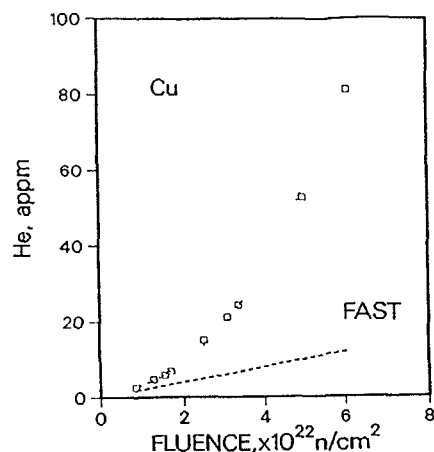
NUCLEAR DATA NEEDS

- Fission Reactors
  - Resolve Integral/ Differential Differences
  - Reactions with Low Thresholds (Nb)
  - Reactions for Long Irradiations ($T_{1/2}$,burnup)

- Fusion Reactors
  - Dosimetry/ Diagnostics
  - Long-Lived Isotopes in Waste/ Maintenance
  - Data for Shielding/ Breeding Applications

- Accelerator Neutron Sources
  - (n,xn) Reactions in 15-50 MeV Range
  - Spallation Yields above 40 MeV

- Uncertainties/ Covariances for All Data

- International Intercomparisons/ Standardization

- Specific Requests to Nuclear Data Committee

REQUIREMENTS FOR CHARGED PARTICLE LIGHT ISOTOPES REACTION DATA FOR ADVANCED FUEL CYCLES INCLUDING TWO STEP REACTION MECHANISM*

R. FELDBACHER, M. HEINDLER
Institute for Theoretical Physics,
Technical University Graz,
Graz, Austria

G. MILEY
Department of Nuclear Engineering,
University of Illinois,
Urbana, Illinois,
United States of America

Abstract

Requirements for light charged isotopes nuclear reaction data
for advanced fusion fuel cycles are identified. This is
performed in the frame of the compilation of charged particle
nuclear reaction data. Those reactions are considered which
determine the nuclear energy production, burn kinetics,
neutron- and radionuclide production among fuel and ash
isotopes. Emphasis is put on the fuel p-11B for which a
review of the status of existing data is given. Other exotic
fuel candidates (e.g. p-6Li) and some exotic reactions
occuring in D-3He based fuels are also considered, however in
less detail. We conclude that there is a lack of experimental
and evaluated data for several important reactions. It is
recommended that evaluations be performed, existing ones
reexamined, and that they are made easily accessible for the
increasing number of researchers studying advanced fuels.

1. INTRODUCTION

Fusion experiment devices of the present generation are being
prepared for injection of a deuterium-tritium mix, and the first
generation of fusion reactors is generally expected to operate
using the nuclear reaction T(d,n)α. The reason for the choice of
D-T as fuel is the high cross section of this reaction at low
collision energies. Unfortunately, this reaction uses radioactive
tritium as a primary fuel, requires a sophisticated breeding
technology, produces large amounts of energetic neutrons and thus
is associated with radioactivity of the fuel, induced activation
and the associated safety, design and technology problems.

The use of advanced fuels may offer a way to get around these disadvantages. An advanced fuel is any fusion fuel that offers less neutron yield than D-T and does not use tritium as a primary fuel component. Many fusion scientists seem to agree that neutron- and radioactivity- lean advanced fuel fusion is the ultimate goal for fusion research /MILEY 1981/. Of course, problems associated with higher temperature and confinement requirements and the lower potential for power amplification and for ignition margin impose the need for new ideas and different approaches to confinement and reactor concepts. Some proposals exist and are being explored worldwide, although at a much lower level of funding than the mainline D-T oriented research.

The investigation of the characteristics of various light isotope mixtures and their applicability and attractivity as an advanced fusion fuel requires a knowledge of cross section data for a large variety of reaction partners and channels.

The aim of this paper is to define the present status and to identify requirements for advanced fuel related nuclear reaction data. A survey of existing data is given to describe their status and availability from the user's point of view. Attention is focussed on nuclear reactions and nuclear elastic and inelastic scattering occuring among fuel isotopes, reaction products and isotopic fuel impurities (e.g. 10B in 11B). Emphasis is laid on the fuel p-11B, where the relevant nuclear reactions are discussed in detail. A less detailled treatment is given for the fuels based on lithium and beryllium isotopes. Fuels of the D-3He family are also treated shortly, the principal reactions of them being discussed in detail at this conference in a paper by N.Jarmie /JARMIE 1986/.

Charge exchange and ionization reactions as well as reactions with structural materials also play an important role in fusion research, but are not included here.

2.ADVANCED FUEL CYCLES

Table 1 displays the D-T fuel and the various isotopical mixtures which have been considered as candidates for advanced fuels, together with their principal fusion reactions.

Cycles 1.b,c,d,e (D-3He-family) are known as the so-called 'conventional' advanced fuel cycles. On the other hand, cycles 1.f-n are sometimes called the 'exotic' advanced fuel cycles. Conventional cycles are the more promising ones from the energetical point of view, since they more likely gain breakeven, ignition etc. However, they suffer from a still high level of neutron and tritium production due to the D+D reactions which always occur if there is deuterium contained or produced in the burning fuel /KERNBICHLER 1986/. This conclusion might be changed if the use of spin polarized nuclei turns out to offer the potentiality to swich off unwanted reaction channels /ERICE 1987/.

TABLE 1: ADVANCED FUEL CANDITATES AND MAIN REACTIONS

	FUEL	MAIN REACTIONS	ENERGY GAIN [MEV]
1.a	D-T	D+T -> n+α	17.589
b	D-D	D+D -> n+3He	3.269
		-> p+T	4.033
c	D-3He	D+3He -> p+α	18.353
d	CAT-D	produced T,3He burned in situ	21.622 [1]
e	SCAT-D	prod. T burned in situ 3He extracted	12.445 [1]
f	3He-3He	3He+3He -> p+p+α	12.860
g	D-6Li	D+6Li -> p+7Li	5.025
		-> α+α	22.371
		->	
h	p-6Li	p+6Li -> α+3He	4.018
		3He+6Li -> p+α+α	16.878
		-> D+7Be	0.112
		->	
i	p-7Li	p+7Li -> α+α	17.346
		-> n+7Be	- 1.644
		->	
k	p-9Be	p+9Be -> D+α+α	.651
		-> α+6Li	2.126
		-> n+9B	- 1.851
		->	
l	3He-9Be	3He+9Be -> α+α+α	19.004
		-> p+11B	10.323
		-> n+11C	7.558
		->	
m	"Compound Fuel": generalization (p-D-T-3He-Li-Be)		
n	p-11B	p+11B -> α+α+α	8.681

[1] per initial D+D reaction

From the point of view of data requirements there is little
difference between the fuel combinations D-6Li and p-6Li (g,h in
Table 1). However, the accuracy requirements are different. In
both cases the subsequent reactions produce a complicated mixture
of almost all isotopes from protons up to Boron-11. This mixture
is called, in our terms, the 'compound fuel' (m in Table 1). The
composition of this mixture depends on the operating parameters
such as the relative feed currents of the different isotopes, the
temperature, etc.

A special feature of the p-6Li fuel is a chaining effect: The 3He
ion produced in a p+6Li reaction may react during its slowing
down process with a further 6Li nucleus, thus producing again a
fast proton:

$$p + {}^6Li \longrightarrow \alpha + {}^3He$$

$$^3He + {}^6Li \longrightarrow \alpha + \alpha + p$$

It should be noted that the kinetics of this chain depends
strongly on the cross sections of the chain carrying reactions
relative to those of the competing reactions. This fact explaines
the higher accuracy requirement.

Sometimes more special modes of operating the compound fuel are
considered as advanced fuel candidates. They are: p+7Li, p+9Be,
3He+9Be taken as primary fuels, i,k,l in Table 1, respectively.
They suffer from neutronic channels in the primary reaction that
have relative low thresholds (i,k) or are even exothermic (l),
from poor energy gain in the main reactions (k), or from the use
of poisonous Beryllium in the primary fuel (k,l). Therefore they
are not treated here further.

The p-11B fuel (n in Table 1) seems very promising from a
radiological point of view, because it produces only stable
charged particles in its single dominating reaction. However, in
addition to the main reaction, nuclear cross sections of side and
progeny reactions of protons and alphas with 11B are required in
order to answer the question of the importance of residual
radioactivity such as 11C, 14C and of neutron production
reactions. Also, possible impurity isotopes D and 10B must be
taken into account. However, according to the results of our
analysis /KERNBICHLER 1984/, this fuel suffers from a poor energy
balance. This problem is compounded in magnetically confined
plasmas, where cyclotron radiation losses at the elevated
temperatures add to the problem. This is also concluded by an
evaluation of proton-based fuels performed by TRW /GORDON 1981/.

3. GENERAL REQUIREMENTS

In the present state of investigation of advanced fusion fuels,
nuclear reaction data are required for

- Studies of the energy feasibility, in particular for the
  exotic fuel compositions. They must emphasize the main
  reaction channels which provide the bulk of the fusion
  energy.

- Evaluation of the production rate of neutrons, gammas and
  radionuclides in the plasma, in particular for the exotic
  fusion fuels requires emphasizing side and progeny reactions
  which may be of considerable importance in spite of their
  relative low probabilities of occurence.

There is reason to believe that it is not a serious restriction
if the data include isotopes up to Z=5 only /MCNALLY 1982/. A
further investigation would be required, however, if this
assumption was to be verified.

Quantities required are:

fusion reaction data:
  - total cross section σ (E)
  - Maxwellian reactivity $\langle \sigma.v \rangle$ (T)
  - particular reactivities, averaged
    over the actual ion distribution;
    e.g. beam into Maxwellian plasma $\langle \sigma.v \rangle$ (E,T)

nuclear elastic and inelastic scattering data:
  - total cross section σ (E)
  - angular distribution $d\sigma/d\Omega$ (E,θ)

Nuclear elastic scattering plays an important role in two
respects. On the one hand it affects the slowing down time of
fast ions and thus their probability to undergo a "fast fusion"
event before thermalization. On the other hand scattering can
influence the background fuel ion distribution by knock-on events
and, as a consequence, it modifies the overall reaction rate.

The cross sections should cover an energy range up to 5 or 10 kT,
where T is the temperature of the background plasma. Of course,
data for interactions involving fusion products or injected fuel
ions during their slowing down must extend to their respective
birth energies.

To be on the safe side and to make evaluations compatible with
international evaluated data files (e.g./ECPL/), the recommended
energy range for measurements and evaluations is from threshold
energy to 20 MeV.

An accuracy of about 10% or better is presently thought to be
required over the energy range of principal interest for the main
reactions and for the radioactivity producing side reactions.

4. EXISTING DATA SOURCES

The earliest compilation of charged particle nuclear reaction cross sections was performed by N.Jarmie et al. /JARMIE 1956/. It contains integral and differential cross sections for reactions with isotopes up to Fluorine in graphical form. Of course, the data contained therein are now rather old; however, this compilation has been an important base for our work.

/MILEY 1974/ provides a popular source of data and gives analytical fits. Its popularity is due to its convenient form, but it is not up to date and does not cover all reactions of interest.

The EXFOR (exchange format) library /EXFOR/ contains experimental nuclear data in general and data for charged particle reactions in particular for our purpose. Its format is easily eyereadable and also computer compatible. It is optimized for a convenient exchange of data between experimentalists, evaluators and users. In our case it turned out to be the most comprehensive and convenient source for our data compilation work as it contains the data in tabulated form.

The ECPL-82 /ECPL/ is the Lawrence Livermore Evaluated Charged Particle Library. It contains evaluated data for five projectile particles (p,d,t,3He,α) reacting with targets from Hydrogen to Oxygen-16. It is optimized for computer and user application. As a consequence, many informations about original data sources, evaluation methods etc. are not contained, as opposed to the case of the EXFOR-library. The ECPL-data are given in the ENDL format which is partly compatible with ENDF/B processing codes /LEMMEL 1983/.

The work by Fowler et al. /FOWLER 1975/ containes formulae for Maxwellian reactivity parameters for astrophysical applications. The data collection by McNally et al. /MCNALLY 1979/ containes Maxwellian reactivity parameters in tabulated form. For some reactions there are rather large deviations between data from these two sources. For an example see Figure 1. A list of reactions contained in any of the evaluations /FOWLER 1975/, /MCNALLY 1979/, /ECPL/ is given in Table 2.

Shuy et al. /SHUY 1979/ and Holden et al. /HOLDEN 1980,82,84,86/ provide comprehensive bibliographies for charged particle cross section literature. They are the basis of our compilation of original data sources. However, the original literature very often contains data in a form which is not directly evaluable or gives data in graphical form on small figures. This creates difficulties and errors in extracting the data and thus turns out to be a significant inconvenience for users.

An additional comprehensive bibliography is provided by Lawrence Livermore National Lab. /PERKINS 1984/. Its inclusion in our work is on the way.
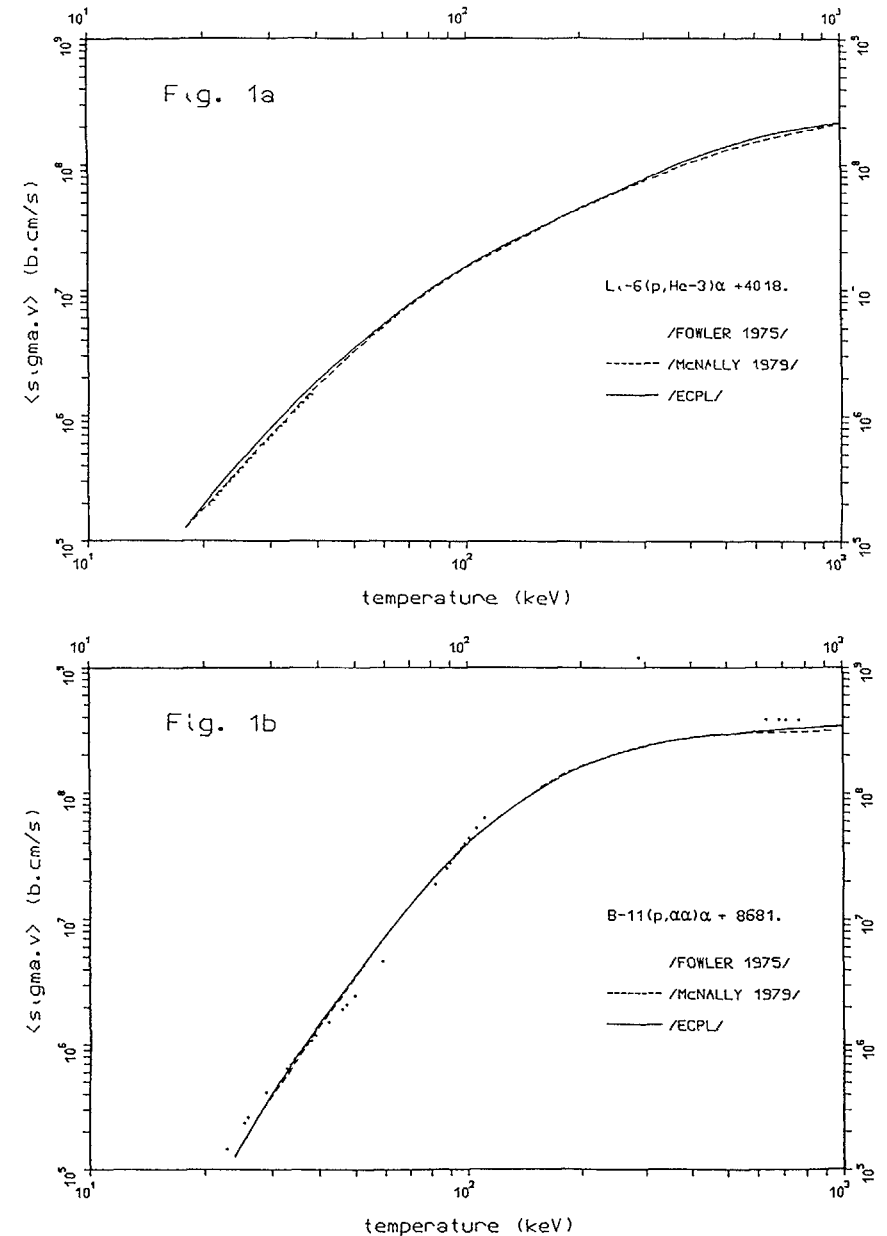

Figure 1: Maxwellian averaged reactivity vs. temperature for two different nuclear reactions, from three different references.

TABLE 2   EVALUATED DATA IN EXISTING LIBRARIES

+   data for this reaction are contained in the library
(+) included recently, data not yet available at AEP

REACTION	Q /MeV/	ECPL	McNALLY	FOWLER
D (p , γ) 3He	+ 5494 keV			+
D (p , np) P	- 2225 keV			+
D (d , n) 3He	+ 3269 keV	+	+	+
D (d , p) T	+ 4033 keV	+	+	+
T (p , γ) α	+19814 keV	+		+
T (p , n) 3He	- 764 keV	+	+	+
T (d , n) α	+17589 keV	+	+	+
T (d , np) T	- 2225 keV	+		
T (t , nn) α	+11332 keV	+	+	+
3He (d , p) α	+18353 keV	+	+	+
3He (t , np) α	+12096 keV	(+)	+	+
3He (t , d) α	+14320 keV	(+)	+	+
3He (3He, pp) α	+12860 keV		+	+
α (d , np) α	- 2225 keV	(+)		
α (t , γ) 7Li	+ 2467 keV			+
α (t , n) 6Li	- 4784 keV			+
α (3He, γ) 7Be	+ 1588 keV			+
6Li (p , γ) 7Be	+ 5606 keV			+
6Li (p , 3He) α	+ 4018 keV	+	+	+
6Li (d , n) 7Be	+ 3381 keV	+	+	
6Li (d ,n3He) α	+ 1794 keV	(+)	+	
6Li (d , p) 7Li	+ 5025 keV	+	+	
6Li (d , pt) α	+ 2557 keV	+	+	
6Li (d , α) α	+22371 keV	+	+	
6Li (t , nn) 7Be	- 2876 keV	+		
6Li (t , nα) α	+16118 keV	(+)		
6Li (t , d) 7Li	+ 994 keV	(+)		
6Li (3He, pα) α	+16878 keV	(+)	+	
6Li (3He, d) 7Be	+ 112 keV	+	+	
6Li (α , γ) 10B	+ 4460 keV			+
6Li (α , p) 9Be	- 2125 keV	(+)		
6Li (α , dα) α	- 1473 keV	(+)		
6Li (6Li, n) 11C	+ 9450 keV		+	
6Li (6Li, nα) 7Be	+ 1906 keV		+	
6Li (6Li, p) 11B	+12215 keV		+	
6Li (6Li, d) 10B	+ 2985 keV		+	
6Li (6Li, t) 9B	+ 805 keV		+	
6Li (6Li, αα) α	+20896 keV		+	

REACTION	Q /MeV/	ECPL	McNALLY	FOWLER
7Li (p , n) 7Be	- 1644 keV	+		+
7Li (p , α) α	+17346 keV	+	+	+
7Li (d , nn) 7Be	- 3869 keV	+		
7Li (d , nα) α	+15121 keV	(+)	+	+
7Li (t , n) 9Be	+10439 keV	(+)		
7Li (t , nnn) 7Be	-10126 keV	+	+	
7Li (t , nnα) α	+ 8864 keV	(+)	+	+
7Li (3He, npα) α	+ 9628 keV	(+)	+	+
7Li (3He, p) 9Be	+11203 keV	(+)		
7Li (3He, dα) α	+11852 keV	(+)		
7Li (3He, t) 7Be	- 8805 keV	+		
7Li (3He, α) 6Li	+13328 keV	(+)		
7Li (α , γ) 11B	+ 8666 keV			+
7Li (α , n) 10B	- 2790 keV			+
7Be (p , γ) 8B	+ 138 keV			+
7Be (d , pα) α	+16766 keV		+	+
7Be (t , npα) α	+10508 keV	.	+	+
7Be (3He, ppα) α	+11272 keV		+	+
7Be (α , γ) 11C	+ 7545 keV			+
9Be (p , γ) 10B	+ 6585 keV			+
9Be (p , n) 9B	- 1851 keV			+
9Be (p , dα) α	+ 651 keV		+	+
9Be (p , α) 6Li	+ 2126 keV		+	+
9Be (α , γ) X		(+)		
9Be (α , n) 12C	+ 5701 keV	(+)	+	+
9Be (α ,nαα) α	- 1574 keV	+		
10B (p , γ) 11C	+ 8690 keV			+
10B (p ,3Heα) α	- 442 keV	+	+	
10B (p , α) 7Be	+ 1146 keV	+	+	
10B (d , n) 11C	+ 6465 keV	+	+	
10B (d , p) 11B	+ 9230 keV	+	+	
10B (d , αα) α	+17911 keV	+	+	
11B (p , γ) 12C	+15956 keV			+
11B (p , n) 11C	- 2764 keV	+		+
11B (p , αα) α	+ 8681 keV	+	+	+
11B (d , n) 12C	+13732 keV	+		
11B (d , p) 12B	+ 1145 keV	+		

TABLE 3

COMPREHENSIVE LIST OF REACTIONS BETWEEN LIGHT CHARGED NUCLEI

Reaction	Q-value
P (p , p) P	
D (p , γ) 3He	+ 5494 keV
D (p , np) P	− 2225 keV
D (p , p) D	
D (d , γ) α	+ 23847 keV
D (d , n) 3He	+ 3269 keV
D (d , np) D	− 2225 keV
D (d , nnp) P	− 4449 keV
D (d , p) T	+ 4033 keV
D (d , d) D	
T (p , γ) α	+ 19814 keV
T (p , n) 3He	− 764 keV
T (p , nnp) P	− 8482 keV
T (p , p) T	
T (d , γ) 5He	+ 16700 keV
T (d , n) α	+ 17589 keV
T (d , np) T	− 2225 keV
T (d , d) T	
T (t , nn) α	+ 11332 keV
T (t , t) T	
3He (p , p) 3He	
3He (d , γ) 5Li	+ 16389 keV
3He (d , np) 3He	− 2225 keV
3He (d , p) α	+ 18353 keV
3He (d , pp) T	− 1461 keV
3He (d , d) 3He	
3He (t , np) α	+ 12096 keV
3He (t , d) α	+ 14320 keV
3He (t , x) α	
3He (t , t) 3He	
3He (3He, pp) α	+ 12860 keV
3He (3He,3He) 3He	
α (p , p) α	
α (d , γ) 6Li	+ 1475 keV
α (d , np) α	− 2225 keV
α (d , p) 5He	− 3114 keV
α (d , d) α	
α (t , γ) 7Li	+ 2467 keV
α (t , n) 6Li	− 4784 keV
α (t , t) α	
α (3He, γ) 7Be	+ 1588 keV
α (3He,3He) α	
α (α , α) α	
6Li (p , γ) 7Be	+ 5606 keV
6Li (p , p) 6Li	
6Li (p ,3He) α	+ 4018 keV
6Li (d , n) 7Be	+ 3381 keV
6Li (d ,n3He) α	+ 1794 keV
6Li (d , p) 7Li	+ 5025 keV
6Li (d , pt) α	+ 2557 keV
6Li (d , d) 6Li	
6Li (d , t) 5Li	+ 593 keV
6Li (d , α) α	+ 22371 keV
6Li (t , nn) 7Be	− 2876 keV
6Li (t , nα) α	+ 16118 keV
6Li (t , p) 8Li	+ 801 keV
6Li (t , d) 7Li	+ 994 keV
6Li (t , t) 6Li	
6Li (3He, np) 7Be	2112 keV
6Li (3He, pα) α	+ 16878 keV
6Li (3He, d) 7Be	+ 112 keV
6Li (3He,3He) 6Li	
6Li (α , γ) 10B	+ 4460 keV
6Li (α , p) 9Be	− 2125 keV
6Li (α , dα) α	− 1473 keV
6Li (α , α) α	
6Li (6Li, n) 11C	+ 9450 keV
6Li (6Li, nα) 7Be	+ 1906 keV
6Li (6Li, p) 11B	+ 12215 keV
6Li (6Li, pα) 7Li	+ 3550 keV
6Li (6Li, d) 10B	+ 2985 keV
6Li (6Li, t) B-9	+ 805 keV
6Li (6Li, αα) α	+ 20896 keV
7Li (p , n) 7Be	− 1644 keV
7Li (p , p) 7Li	
7Li (p , α) α	+ 17346 keV
7Li (d , nn) 7Be	− 3869 keV
7Li (d , nα) α	+ 15121 keV
7Li (d , p) 8Li	− 192 keV
7Li (d , d) 7Li	
7Li (d , t) 6Li	− 993 keV
7Li (d ,3He) 6He	− 4481 keV
7Li (t , n) 9Be	+ 10439 keV
7Li (t , nnn) 7Be	− 10126 keV
7Li (t , nnα) α	+ 8864 keV
7Li (t , p) 9Li	− 2386 keV
7Li (t , d) 8Li	− 4225 keV
7Li (t , t) 7Li	
7Li (t , α) 6He	+ 9839 keV
7Li (3He, npα) α	+ 9628 keV
7Li (3He, nd) 7Be	− 7138 keV
7Li (3He, p) 9Be	+ 11203 keV
7Li (3He, dα) α	+ 11852 keV
7Li (3He, t) 7Be	− 8805 keV
7Li (3He,3He) 7Li	
7Li (3He, α) 6Li	+ 13328 keV
7Li (α , γ) 11B	+ 8666 keV
7Li (α , n) 10B	− 2790 keV
7Li (α , α) 7Li	
7Be (p , γ) 8B	+ 138 keV
7Be (d , pα) α	+ 16766 keV
7Be (t , npα) α	+ 10508 keV
7Be (3He, ppα) α	+ 11272 keV
7Be (α , γ) 11C	+ 7545 keV
9Be (p , γ) 10B	+ 6585 keV
9Be (p , n) 9B	− 1851 keV
9Be (p , p) 9Be	
9Be (p , dα) α	+ 651 keV
9Be (p , t) 7Be	− 12082 keV
9Be (p , α) 6Li	+ 2126 keV
9Be (d , γ) 11B	+ 15816 keV
9Be (d , n) 10B	+ 4362 keV
9Be (d ,nnpα) α	− 3798 keV
9Be (d , p) 10Be	+ 4587 keV
9Be (d , d) 9Be	
9Be (d , tα) α	+ 4684 keV
9Be (d , α) 7Li	+ 7152 keV
9Be (t , n) 11B	+ 9559 keV
9Be (t , t) 9Be	
9Be (3He, n) 11C	+ 7558 keV
9Be (3He, nn) 10C	− 5564 keV
9Be (3He, nα) 7Be	+ 14 keV
9Be (3He, p) 11B	+ 10323 keV
9Be (3He,3He) 9Be	
9Be (3He, αα) α	+ 19004 keV
9Be (α , n) 12C	+ 5701 keV
9Be (α , n) X	
9Be (α ,nαα) α	− 1574 keV
9Be (α , α) 9Be	
10B (p , γ) 11C	+ 8690 keV
10B (p , n) 10C	− 4433 keV
10B (p , p) 10B	
10B (p , d) 9B	− 6212 keV
10B (p ,3Heα) α	− 442 keV
10B (p , α) 7Be	+ 1146 keV
10B (d , γ) 12C	+ 25186 keV
10B (d , n) 11C	+ 6465 keV
10B (d , p) 11B	+ 9230 keV
10B (d , d) 10B	
10B (d , t) 9B	− 2180 keV
10B (d ,3He) 9Be	− 1093 keV
10B (d , αα) α	+ 17911 keV
10B (t , p) 12B	+ 6342 keV
10B (t , pα) 8Li	− 3659 keV
10B (t , d) 11B	+ 5197 keV
10B (t , t) 10B	
10B (t , α) 9Be	+ 13227 keV
10B (t ,6He) 7Be	− 6361 keV
10B (3He, γ) 13N	+ 21636 keV
10B (3He, n) 12N	+ 1572 keV
10B (3He, np) 11C	+ 972 keV
10B (3He, p) 12C	+ 19692 keV
10B (3He, d) 11C	+ 3196 keV
10B (3He, t) 10C	− 3669 keV
10B (3He,3He) 10B	
10B (3He, α) 9B	+ 12141 keV
10B (3He,6Li) 7Be	− 2873 keV
10B (α , n) 13N	+ 1058 keV
10B (α , p) 13C	+ 4061 keV
10B (α , d) 12C	+ 1339 keV
10B (α , α) 10B	
11B (p , γ) 12C	+ 15956 keV
11B (p , n) 11C	− 2764 keV
11B (p , p) 11B	
11B (p , αα) α	+ 8681 keV
11B (d , γ) 13C	+ 18678 keV
11B (d , n) 12C	+ 13732 keV
11B (d , nn) 11C	− 4989 keV
11B (d , p) 12B	+ 1145 keV
11B (d , d) 11B	
11B (d , t) 10B	− 5197 keV
11B (d , α) 9Be	+ 8031 keV
11B (t , p) 13B	− 233 keV
11B (t , t) 11B	
11B (t , α) 10Be	+ 8585 keV
11B (t , αα) 6He	+ 1175 keV
11B (3He, γ) 14N	+ 20735 keV
11B (3He, n) 13N	+ 10182 keV
11B (3He, p) 13C	+ 13184 keV
11B (3He, t) 11C	− 2001 keV
11B (3He,3He) 11B	
11B (3He, α) 10B	+ 9123 keV
11B (α , γ) 15N	+ 10991 keV
11B (α , n) 14N	+ 157 keV
11B (α , p) 14C	+ 783 keV
11B (α , d) 13C	− 5169 keV
11B (α , t) 12C	− 3858 keV
11B (α , α) 11B	
11B (11B, x) X	
11B (11B,11B) 11B	

The data review described in the next chapter was done in the frame of the development of a charged particle nuclear reaction data compilation /DATLIB/. The aim of this compilation to enable data for the various reactions and from different sources to be intercompared conveniently. Also, "recommended" cross sections are identified in DATLIB for the various reactions and used in the advanced fuel burn computations performed as part of the Alternate Energy Physics Program at the Technical University of Graz. DATLIB will be made available through the IAEA-Nuclear Data Section, Vienna.

Presently, DATLIB contains 256 data sets (files) for cross sections and related quantities for 93 different reactions between charged nuclei up to Boron-11. Moreover, it refers to about 100 additional reactions between these nuclei. In Table 3, a comprehensive list of these nuclear reactions between light charged nuclei is identified. It quotes each reaction which we were able to find in the literature and thus does not reflect its respective importance for a particular fuel evaluation.

5. NUCLEAR DATA REQUIREMENTS AND STATUS

The importance of a particular reaction relative to its contribution to the energy balance and/or to the reaction kinematics ("chain carriers") and/or to the production of radionuclides and neutrons actually depends on
- the concentration of the reactants in the plasma;
- the threshold energy, the reaction energy gain and the reaction probability.

In the following we restrict our attention to those reactions that, based on present knowledge, clearly have a strong importance in the sense defined above. Also we focus our attention to p-11B as too little has been done on lithium reactions to permit the same evaluation for them.

5.1 DATA FOR THE D-T-^{3}He FUEL

The principal reactions that these conventional advanced fuel cycles are based on are discussed at this conference in a paper by N.Jarmie /JARMIE 1986/. Some additional reaction channels occuring in these fuels would have to be taken into account in a highly sophisticated investigation of these fuels. Table 4 shows a selection of these reactions occuring in a D-T-3He plasma. They are not further discussed here. Note that the cross sections for neutron and radiation production from side reactions are not large compared to those for primary reactions, i.e. in general they are not a problem here. However, energetic gamma radiation may represent a shielding problem.

TABLE 4:   SOME EXOTIC REACTIONS IN D-BASED 'CONVENTIONAL' ADVANCED FUSION FUELS

D + D -> α + γ	+ 23.847 MeV
3He + D -> γ + 5Li	+ 16.389 MeV
3He + T -> n + p + α	+ 12.096 MeV
3He + T -> D + α	+ 14.320 MeV
α + D -> γ + 6Li	+ 1.475 MeV
α + D -> n + p + α	- 2.225 MeV
α + 3He -> γ + 7Be	+ 1.588 MeV

5.2 DATA FOR THE P-^{11}B FUEL

In the following, the nuclear reactions occurring among the different isotopes in a p-11B fusion plasma are discussed in some detail. It should be noted that here only those references have been taken into account which explicitly list integral cross sections. A comprehensive list of references which contain additional information (e.g. resonance parameters, differential cross sections, cross sections in arbitrary units, etc.) is given in the cross section library /DATLIB/. This comment applies generally to all of the reactions discussed in this paper.

11B (p , $\alpha\alpha$) α :
This is the key reaction which determines the energetics of p-11B as a fuel. This reaction occurs via three different channels:

11B + p --> α + 8Be (1st excited state)	(about 90%)
11B + p --> α + 8Be (ground state)	(<10%)
11B + p --> α + α + α (direct break up)	(<10%)

Experimental integral cross sections $\sigma(E)$ are reported for both the 8Be -1st excited state and -ground state channel in /BECKMANN 1953/, /SYMONS 1963/, /SEGEL 1965/, /DAVIDSON 1979/, covering a proton energy range from 35 - 4000 keV. Measurements of the 163-keV resonance only are reported by /SEGEL 1961/ and /ANDERSON 1974/. At higher energies, two recent measurements were performed: /BUCK 1983/ for both channels (5-50 MeV) and /BOERCHERS 1983/ for the ground state channel only (4500.-7500. keV). All these data are shown in Figure 2.a.

Fig.2a

11B(p,αα)α + 8681.

via 8Be 1st.excit.state:

——— /BECKMANN 1953/

----- /SEGEL 1965/

- - - - /BOERCHERS 1983/

+ /SYMONS 1963/

▲ /BUCK 1983/

all α-channels:

——— /DAVIDSON 1979/

11B(p,αα)α + 8681.
via 8Be ground state
symbols see list at left

cross section (barn)

proton energy (keV)

Fig.2b

11B(p,αα)α + 8681.

/MILEY 1974/

----- /GORDON 1981/

——— /ECPL/

cross section (barn)

proton energy (keV)
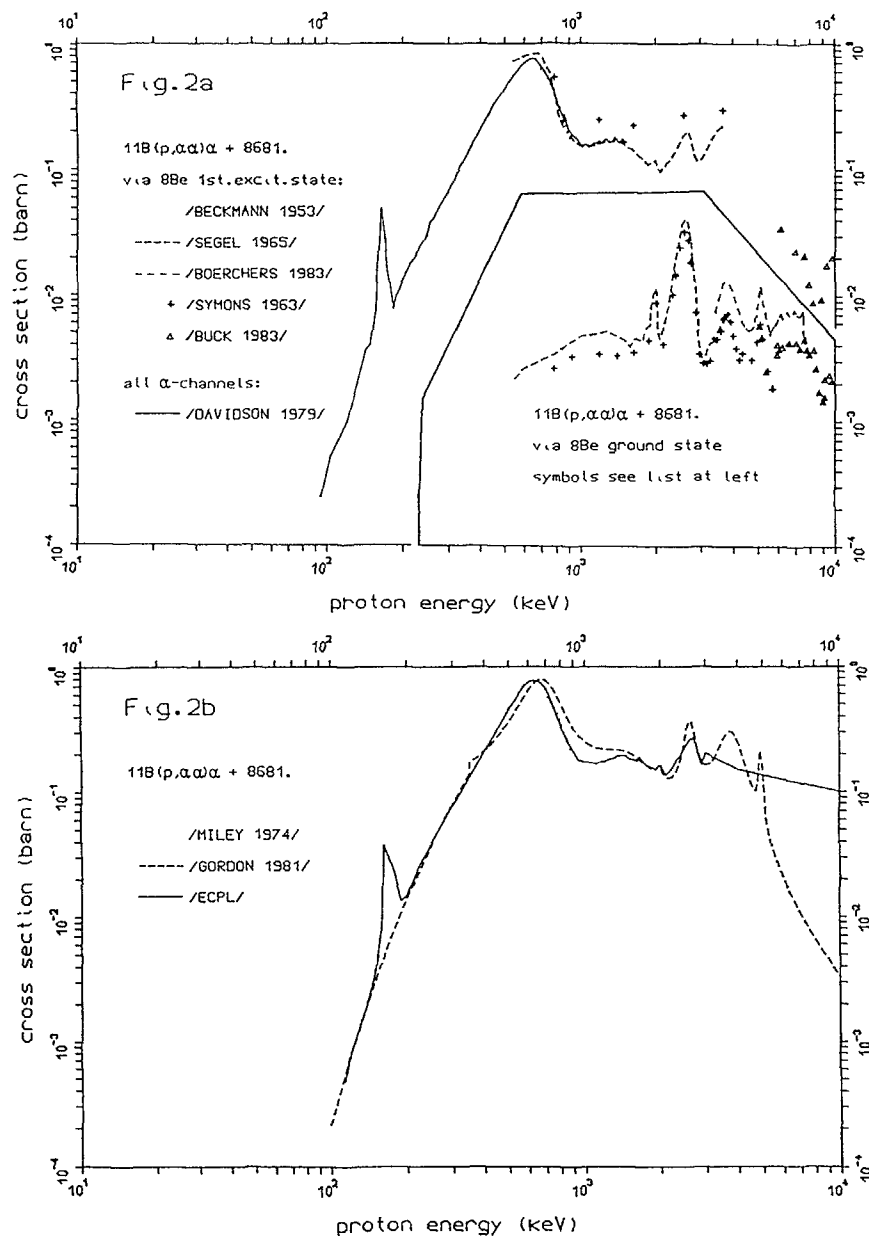
Figure 2: Experimental cross sections (Fig.2a); evaluated respectively recommended cross sections (Fig.2b) for 11B(p,α)αα.

In /GORDON 1981/ some resonance parameters are reported together with a recommended cross section based on a sum of Breit-Wigner contributons of these resonances. The most recent evaluation is given in /ECPL/. These data are shown together with a recommendation by /MILEY 1974/ in Figure 2b. Up to 3 MeV the ECPL-evaluation is good and in the region of the main resonance the data are accurate to a few percent. At higher energies /BUCK 1983/ indicates that the ECPL-data are too high by a factor of 5 to 10.

An additional measurement of the integral cross section should be done to confirm the data in that energy region, and, in view of the importance of that reaction, a new evaluation based on these data should be performed in detail. The breakup between the three channels should be determined to a higher accuracy than presently known because it affects the alpha birth energy spectrum and thus the rates of progeny reactions.

11B (p , γ) 12C :
This capture reaction produces either a 4 and a 12 MeV gamma (capture via the 4 MeV level of 12C) or one 16 MeV gamma (capture via 12C ground level). Although the cross section is in the 10 μbarn range, this reaction may result in a shielding problem. Cross section measurements for both channels are reported in /HUUS 1953/, /SEGEL 1965/ (Figure 3). /COLLINS 1982/ gives an additional measurement of the 16 MeV gamma channel for E_p=4000-14000 keV. An evaluation based on these data should be performed.

11B (p , n) 11C :
Data are given in /GIBBONS 1959/, /FURUKAWA 1960/, /ANDERSON 1964/, /SEGEL 1965/, /ANDERS 1981/, /HOEHN 1981/. The evaluation in ECPL is satisfactory for proton energies below 5 MeV. Above, measurements indicate that the cross section is actually larger by a factor of 2 to 4 than that given in the ECPL (Figure 4). This discrepancy should be investigated and resolved.

11B (α , n) 14N :
This reaction of fast fusion born alphas with 11B background ions is the main neutron source of a p-11B burn /KERNBICHLER 1984/. Measurements of the cross section are given in /WALKER 1949/ and /VAN DER ZWAN 1975/ (Figure 5). They agree fairly in the overlapping energy interval. /MANI 1966/ gives a detailed analysis of this reaction (differential cross section, Legendre coefficients) at 2500-4000 keV, but does not explicitely show the absolute integrated cross section. There exist no data above 7900 keV, and no evaluation.

11B (α , p) 14C :
This reaction produces radioactive 14C. Measurements exist for 1500-3600 keV and for 4400-6700 keV alpha energy /LEE 1959/, /DAYRAS 1976/, /HOU 1978/, (Figure 6). The gap is covered /MANI
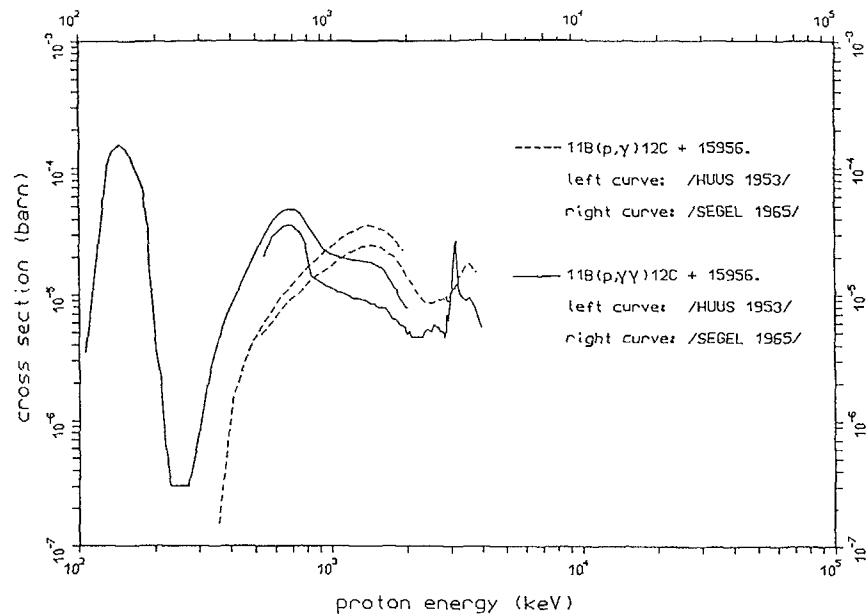
Figure 3: Experimental cross section for 11B+p capture reactions, producing either one 16 MeV gamma (dashed curve) or one 12 MeV plus one 4 MeV gamma (solid curve). The data are taken from "guide to the eye line" figures. The zigzag shape of part of the curves is more due to digitizing errors than due to the real shape of the cross section.

1963/ who performed a detailled analysis of this reaction at 2500-4500 keV, but again does not explicitely give the absolute integrated cross section. Measurements should be performed below 1500 keV and from 6700 keV up to at least 8000 keV. Again, an evaluation does not exist and should be made.

11B (11B, x) Y :
Several channels are known for 11B + 11B reactions. Some of them produce radionuclides, and in average one neutron is produced per reaction. The total cross section (sum of all channels different from scattering) was measured by /HIGH 1976/ and extrapolated using an evaluation which is based on the optical model /NORBECK 1980/, (Figure 7). No additional information is presently required for this reaction.
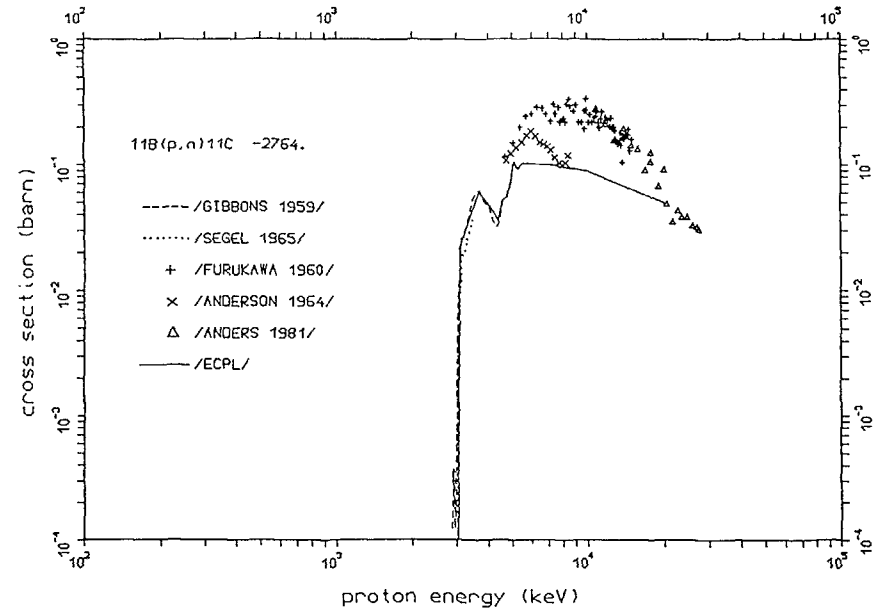
Figure 4: Cross sections for the 11B(p,n)11C reaction.
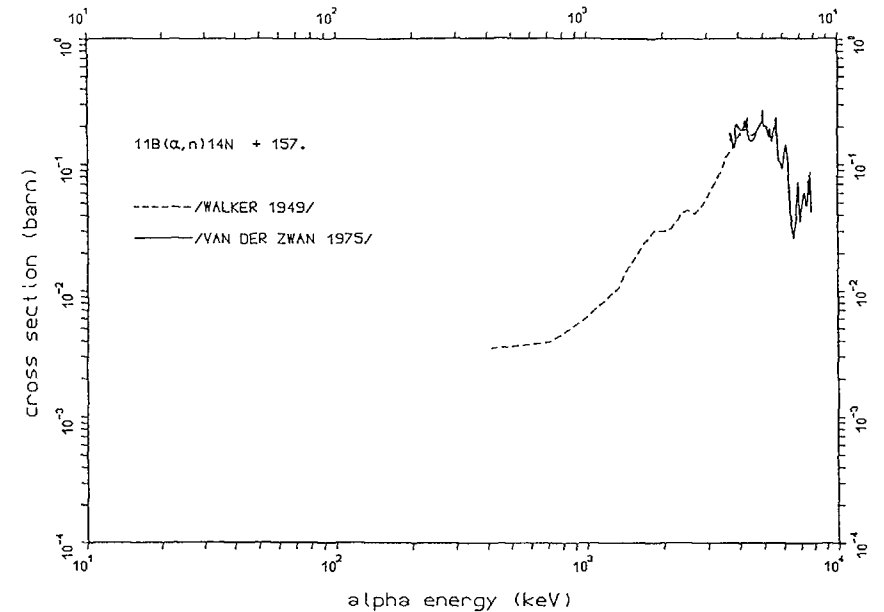
Figure 5: Cross sections for the 11B(α,n)14N reaction.
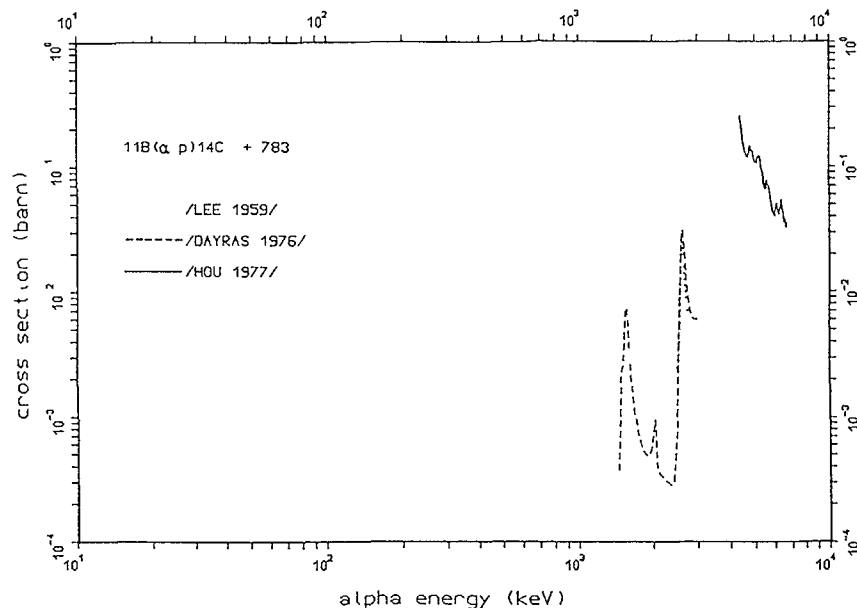
Figure 6:

Cross sections for the 11B(α,p)14C reaction. The gap between 3600 and 4400 keV is covered by a detailled analysis /MANI 1963/. Unfortunately, no integrated cross section in absolute units is given in that work.

Figure 7:

Cross section for the 11B+11B reactions. Here the sum of the cross sections for all outgoing channels except scattering is shown. 11B+11B-reactions produce one neutron per reaction in average.

11B (p , p) 11B,   11B (p , p'γ) 11B,   11B (α , α) 11B
Nuclear scattering events of fast protons and alphas on nuclei in the background plasma may play an important role, as was noted above. The scattering data among protons and alphas are well known. In contrast, scattering data of protons and alphas on Boron isotopes are scarce. In particular, some papers report systematic measurements of the differential cross sections on a dense energy-angle grid and detailled determinations of nuclear level parameters. However, in the papers only a few exemplaric data are given explicitely in graphical form. For example, see /SEGEL 1965/, /BOERCHERS 1983/ for (p,p), and /OTT 1972/, /RAMIREZ 1972/ for (α,α). Anyway, no data tables could be found.

In Table 5, an overview of data that have been found explicitely in the literature is given. The existing cross sections should be made available, gaps filled up and an evaluation should be done at least up to 10 MeV.

In the following, reactions of the isotopic impurities D and 10B are considered in order to answer the question to what extent isotope separation is required if nonnegligeable additional production of radioisotopes and neutrons is to be avoided.

11B (d , γ) 13C :
Produces 18.6 MeV gammas. No integral cross section has been found. The order of magnitude of the cross section should be determined.

11B (d , n) 12C :
There exist several measurements of differential cross sections and angular distributions for different neutron groups. However, the only integral cross section we found is that of the ECPL-evaluation (Figure 8).

TABLE 5: REFERENCES AND PARAMETER RANGES FOR SCATTERING DATA:
          11B(p,p)11B, 11B(p,p'γ)11B and 11B(α,α)11B
          dσ/dΩ (E:keV; θ:deg);   σ (E:keV)

11B(p,p)11B   elastic scattering:

/TAUTFEST 1956/   dσ/dΩ(E$_{cm}$= 600-2000; θ$_{cm}$= 152.6)

/DEARNALEY 1957/   dσ/dΩ(E$_{p}$= 300-1000; θ$_{cm}$= 90, 125.3, 140.8, 159.8)

/SYMONS 1963/   dσ/dΩ(E$_{p}$= 2400-3100; θ$_{cm}$= 157.2)

/SEGEL 1965/   dσ/dΩ(E$_{p}$= 1000-3800; θ$_{cm}$= 94.8, 163.1)

/HOEHN 1981/   dσ/dΩ(E$_{p}$= 5400-7500; θ$_{lab}$= 150)

/RAMAVATARAM 1983/   dσ/dΩ(E$_{p}$= 7000-9000; θ$_{cm}$= 140.6)

11B(p,p$_1$γ)11B   via 11B 1st excited level, E$_γ$=2130 keV

/HUUS 1953/   σ(E$_{p}$= 2500-2900)

/SEGEL 1965/   σ(E$_{p}$= 2500-4000)

/HOEHN 1981/   dσ/dΩ(E$_{p}$= 5400-7500; θ$_{lab}$= 150)

/RAMAVATARAM 1983/   σ(E$_{p}$= 4000-9500)

                     dσ/dΩ(E$_{p}$= 7000-9000; θ$_{lab}$= 137)

/BOERCHERS 1983/   σ(E$_{p}$= 4000-7500)

                     dσ/dΩ(θ$_{cm}$= 30-170; E$_{p}$= 4490-7390)

11B(p,p$_{2,3}$γ)11B   via higher excited levels:

/RAMAVATARAM 1983/   σ(E$_{p}$= 4000-9500)   (p,p$_2$)

/BOERCHERS 1983/   σ(E$_{p}$= 4000-7500)   (p,p$_2$), (p,p$_3$)

11B(α,α)11B   elastic scattering:

/OTT 1972/   dσ/dΩ(E$_{α}$= 4000-8000; θ$_{lab}$= 130, 150)

                     dσ/dΩ(E$_{α}$= 4000-5000; θ$_{lab}$= 50, 140, 150)

                     dσ/dΩ(θ$_{cm}$= 30-170; E$_{α}$= 4000, 4260, 4440, 4620)

/RAMIREZ 1972/   dσ/dΩ(E$_{α}$= 2000-4000; θ$_{cm}$= 90.4, 111.8, 161.0)

11B (d , nn) 11C :
Experimental cross section exist for Ed=7000-16000 keV /ANDERS
1981/ (Figure 8). Measurement from threshold to 7000keV and an
evaluation of these data is recommended.

10B (p , γ) 11C :
Cross section measurements exist up to 2 MeV /WIESCHER 1983/
(Figure 9). No experimental data above and no evaluation exist.

10B (p , n) 10C :
Measurements were performed from threshold to 10 MeV /EARWAKER
1963/, /MUMINOV 1980/ (Figure 10). No evaluation exists.

10B (p , α) 7Be :
Produces radioactive 7Be. Experimental cross sections /JENKIN
1964/, /SZABO 1972/, /JARMIE 1956/ are shown in Figure 10
together with the evaluated cross section from /ECPL/.
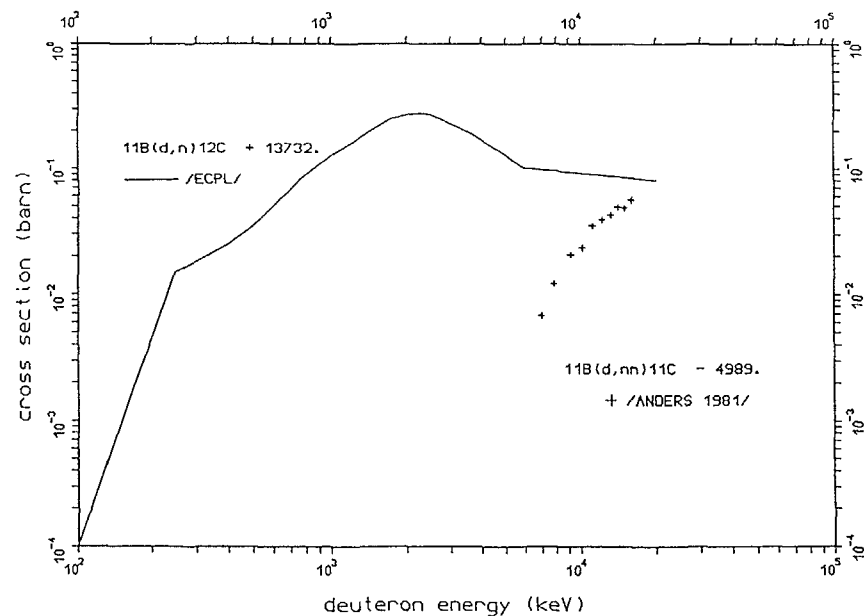
Figure 8:

Cross section for the 11B(d,n)12C and 11B(d,nn)11C reactions
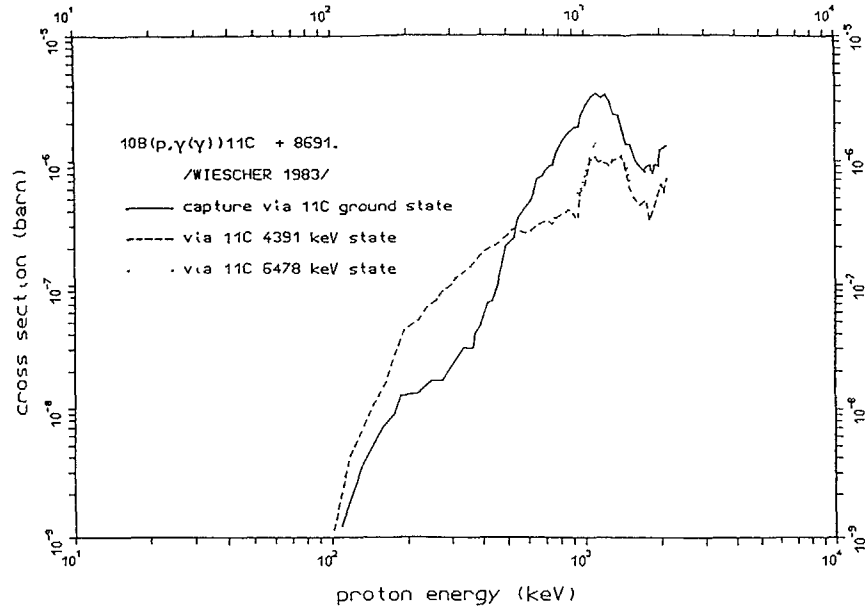
Figure 9:

Experimental cross section for the 10B+p capture reactions: directly to the 11C ground state (solid curve), to excited states of the 11C nucleus followed by subsequent gamma decay of these levels (dashed and dotted curve, resp.). The strange structure of the curves is due to errors made when digitizing curves from small figures.
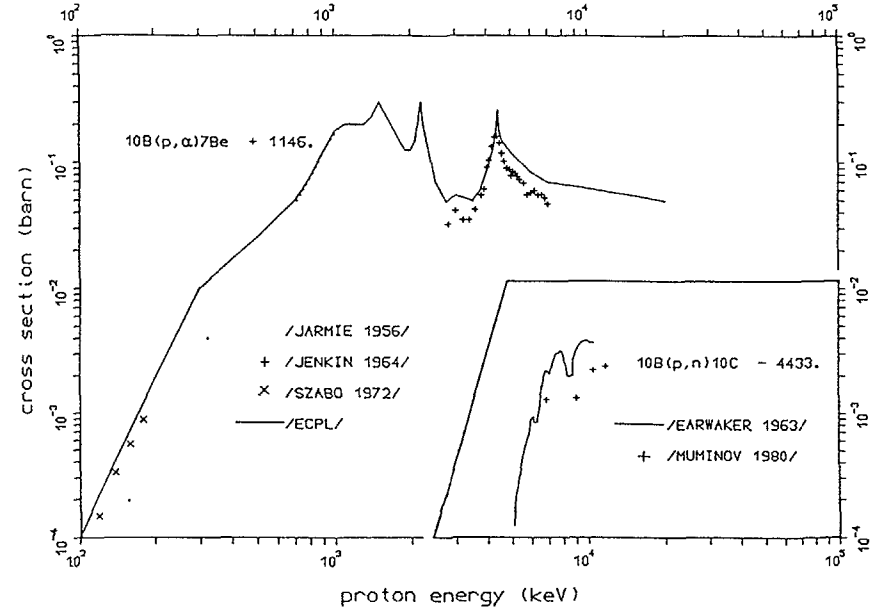
Figure 10:

Cross sections for the reactions 10B(p,α)7Be and 10B(p,n)10C.

5.3 NUCLEAR DATA FOR THE P-^{6}LI resp. D-^{6}LI FUEL

In a fusioning plasma which contains 6Li and hydrogen isotopes, a variety of reactions occur. These reactions produce further isotopes which again undergo further reactions of the next generation. After some generations almost all reactions which are listed in Table 4 occur. However, some of them (a very restricted selection) are identified as the most important ones in the sense defined at the beginning of chapter 5 (Table 6). The knowledge of the cross sections of these reactions is a minimum requirement for an evaluation of that fuel.

In Table 6, these various reactions are listed together with data libraries in which respective data are contained. Actually, a compilation and evaluation of the data which are given in the literature must be performed in order to permit statements analogous to the p-11B case.

TABLE 6: KEY REACTIONS IN A p-6Li OR A D-6Li FUSION PLASMA

REACTION	Q		IMPORTANCE	LIBRARY	
p + 6Li --> 3He + α	+	4018 keV	A	ECPL	EXFOR
3He + 6Li --> p + α + α	+	16878 keV	AB	ECPL	
3He + 6Li --> D + 7Be	+	112 keV	AC	ECPL	EXFOR
3He + 6Li --> n + p + 7Be	-	2112 keV	AC		
α + 6Li --> p + 9Be	-	2125 keV		ECPL	
α + 6Li --> D + α + α	-	1473 keV	C	ECPL	
D + 6Li --> n + 7Be	+	3381 keV	C	ECPL	EXFOR
D + 6Li --> n + 3He + α	+	1794 keV	AC	ECPL	
D + 6Li --> p + 7Li	+	5025 keV	B	ECPL	EXFOR
D + 6Li --> p + T + α	+	2557 keV	C	ECPL	EXFOR
D + 6Li --> α + α	+	22371 keV	B	ECPL	EXFOR
D + 7Li --> n + α + α	+	15121 keV	C	ECPL	EXFOR
D + 7Be --> p + α + α	+	16766 keV	B		
3He + 7Be --> p + p + α + α	+	11272 keV	AB		
6Li + 6Li --> n + 11C	+	9450 keV	C		
6Li + 6Li --> n + α + 7Be	+	1906 keV	C		EXFOR
6Li + 6Li --> p + 11B	+	12215 keV	B		
6Li + 6Li --> p + α + 7Li	+	3550 keV	B		
6Li + 6Li --> D + 10B	+	2985 keV			
6Li + 6Li --> T + 9B	+	805 keV	C		
6Li + 6Li --> α + α + α	+	20896 keV	B		

ELASTIC SCATTERING:

    6Li (p , p) 6Li
    6Li (3He,3He) 6Li
    6Li (α , α)

IMPORTANCE: A ... consumption and production of
               chain carrier 3He

           B ... production of fast protons or alphas

           C ... production of radionuclides or neutrons

6. ACKNOWLEDGMENTS

REFERENCES

/ANDERS 1981/: Anders,B., Herges,P., Scobel,W., Z.Phys.A - Atoms
and Nuclei, 301 (1981) 353

/ANDERSON 1964/: Anderson,J.D., et al., Phys.Rev.B 136 (1964) 118

/ANDERSON 1974/: Anderson,B.D., et al., Nucl.Phys.A 233 (1974)
286

/BECKMANN 1953/: Beckman,O., Huus,T., Zupancic,C., Phys.Rev.91,3
(1953) 606

/BOERCHERS 1983/: Boerchers,F., et al., Nucl.Phys.A 405 (1983)
141

/BUCK 1983/: Buck,W., et al., Nucl.Phys.A 398 (1983) 189

/COLLINS 1982/: Collins,M.T., et al., Phys.Rev.C 26, 2 (1982) 332

/DATLIB/: Feldbacher,R., The AEP Barnbook DATLIB,
AEP-report 86.007 (1986), Abteilung Energiephysik,
Inst.f.Theoret.Physics, Technical University Graz, Austria.

/DAVIDSON 1979/: Davidson,J.M., et al., Nucl.Phys.A 315 (1979)
253

/DAYRAS 1976/: Dayras,R.A., Switkowski,Z.E., Tombrello,T.A.,
Nucl.Phys.A 261 (1976) 365

/DEARNALEY 1957/: Dearnaley,G., et al., Phys.Rev.108, 3 (1957)
743

/EARWAKER 1963/: Earwaker,L.G., Jenkin,J.G., Titterton,E.W.,
Nucl.Phys.42 (1963) 521

/ECPL/: ECPL-82: The LLNL Evaluated Charged-Particle Data
Library, IAEA-NDS-56 (1983), Data received from: IAEA Nuclear
Data Section, Vienna, Austria

/ERICE 1987/: Proc. International Workshop on Muon Catalyzed
Fusion and Fusion with Polarized Nuclei, Erice, Italy, April 1987
(to be published)

/EXFOR/: Exchange Format Nuclear Data Library, Dokumentation Series IAEA-NDS-1,2,3 (1983), Data received from: IAEA Nuclear Data Section, Vienna, Austria

/FOWLER 1975/: Fowler,W.A., Caughlan,G.R., Zimmerman,B., Ann. Rev. Astron. Astrophysics 13 (1975) 69

/FURUKAWA 1960/: Furukawa,M., et al., J.Phys.Soc.Japan 15,12 (1960) 2167

/GIBBONS 1959/: Gibbons,J.H., Macklin,R.L., Phys.Rev.114, 2 (1959) 571

/GORDON 1981/: Gordon,J.D., et al., TRW-FRE-007 (1981)

/HIGH 1976/: High,M.D., Cujec,B., Phys.Rev.A 259 (1976) 513

/HOEHN 1981/: Hoehn,J., et al., J.Phys.G: Nucl.Phys. 7 (1981) 803

/HOLDEN 1980,82,84,86/: Holden,N.E., et al.,
Bibliography of integral charged particle nuclear data,
BNL-NCS-50640, Pt.1, 4th ed. (1980); see also:
BNL-NCS-50640, 4th ed., suppl.2 (1982)
BNL-NCS-51771, 1st ed., (1984)
BNL-NCS-51771, 1st ed., suppl.2 (1986)

/HOU 1978/: Hou,W-S., et al., Nucl.Sci.Eng. 66 (1978) 188

/HUUS 1953/: Huus,T., Day,R.D., Phys.Rev. 91, 3 (1953) 599

/JARMIE 1956/: Jarmie,N., Seagrave,J.D., LASL, LA-2014 (1956)

/JARMIE 1986/: Jarmie,N., LA-UR-86-3705 (also these proceedings)

/JENKIN 1964/: Jenkin,J.G., Earwaker,L.G., Titterton,E.W.,
Nucl.Phys. 50 (1964) 516

/KERNBICHLER 1984/: Kernbichler,W., Feldbacher,R., Heindler,R.,
IAEA-CN-44/I-I-6, 10th Int. Conf. Plasma Physics and Controlled
Nuclear Fusion Research, London, UK, (1984)

/KERNBICHLER 1986/: Kernbichler,W., et al., IAEA-CN-47/H-III-9,
11th Int. Conf. Plasma Physics and Controlled Nuclear Fusion
Research, Kyoto, Japan, (1986)

/LEE 1959/: Lee,L.L., Schiffer,J.P., Phys.Rev. 115, No.1 (1959) 160

/LEMMEL 1983/: Lemmel,H.D., IAEA-NDS-53 (1983)

/MANI 1963/: Mani,G.S., Forsyth,P.D., Perry,R.R., Nucl.Phys. 44 (1963) 625

/MANI 1966/: Mani,G.S., Dutt,G.C., Nucl.Phys. 78 (1966) 613

/MILEY 1974/: Miley,G., Towner,H., Ivich,N., U.Illinois Report COO-2218-17 (1974)

/MILEY 1981/: Miley,G.,Advanced Fuels and the Development of Fusion Power, in: Unconventional Approaches to Fusion (B.Brunelli, G.Leotta, edts.), Ettore Majorana International Science Series, Plenum Press 1982.

/MCNALLY 1979/: McNally,J.R.Jr., Rothe,K.E., Sharp,R.D., ORNL-TM-6914 (1979), (revised 1980)

/MCNALLY 1982/: McNally,J.R.r., Nuclear Technology/Fusion 2 (1982) 9

/MUMINOV 1980/: Muminov et al., At.Energija, Vol.49(2) (1980) 101

/NORBECK 1980/: Norbeck,E., Report Univ. of Iowa 80-32 (1980)

/OTT 1972/: Ott,W.R., Weller,H.R., Nucl.Phys.A 198 (1972) 505

/PERKINS 1984/: Perkins,S., Hansen,A., Howerton,R., UCRL-50400 Vol.26 (1984)

/RAMAVATARAM 1983/: Ramavataram,S., Z.Phys.A - Atoms and Nuclei 310 (1983) 87

/RAMIREZ 1972/: Ramirez,J.J., Blue,R.A., Weller,H.R., Phys.Rev.C 5, No.1 (1972) 17

/SEGEL 1981/: Segel,R.E., Bina,M.J., Phys.Rev. 124 (1961) 814

/SEGEL 1965/: Segel,R.E., Hanna,S.S., Allas,R.G., Phys.Rev. 139, No.4B (1965) 818

/SHUY 1979/: Shuy,G.W., Conn,R.W., in: Proc.Int.Conf. on Nuclear Cross Sections for Technology, U.Tennessee, Knoxville, TN, 22.-26.10.1979

/SYMONS 1963/: Symons,G.D., Treacy,P.B., Nucl.Phys. 46 (1963) 93

/SZABO 1972/: Szabo,J., Csikai,J., Varnagy,M., Nucl.Phys.A 195 (1972) 527

/TAUTFEST 1956/: Tautfest,G.W., Rubin,S., Phys.Rev. 103, 1 (1956) 196

/VAN DER ZWAN 1975/: Van der Zwan,L., Geiger,K.W., Nucl.Phys.A 246 (1975) 93

/WALKER 1949/: Walker,R.L., Phys.Rev. 76, 2 (1949) 244

/WIESCHER 1983/: Wiescher,M., et al., Phys.Rev.C 28, 4 (1983) 1431

REQUIREMENTS FOR CHARGED-PARTICLE REACTION CROSS-SECTIONS IN THE D-D, D-T, T-T AND D-^{3}He FUEL CYCLES*

N. JARMIE
Los Alamos National Laboratory,
Los Alamos, New Mexico,
United States of America

Abstract

This paper reviews the status of experimental data and data evaluations for charged-particle reactions of interest in fusion-reactor design. In particular, the ^{2}H(t,α)n, ^{2}H(d,p)^{3}H, ^{2}H(d,^{3}He)n, ^{3}H(t,α)nn and ^{3}He(d,p)^{4}He reactions at low energies are studied. Other secondary reactions are considered. The conclusion is that such cross sections are well known for the near and medium term, and that no crucial experimental lack exists. There is a serious lack of standard evaluations of these reactions, which should be in an internationally acceptable format and easily accessible. Support for generating such evaluations should be given serious consideration.

1. Introduction

As progress in the design and development of both magnetic and inertial-confinement fusion reactors takes place, the need for reliable and accurate cross section measurements of the basic fuel cycle nuclear reactions increases. A 1981 evaluation [1] of past work on the d + t reaction and of other nuclear reactions important for fusion energy indicated the possibility of large systematic errors in some of the experiments. Since that time several careful experiments have much improved the data sets. In addition, several widely used parametrizations of the cross sections and reactivities have been compared [2-5] and found to be discrepant-- sometimes seriously--especially at the lower energies.

The ^{2}H(t,α)n reaction is dominated by a J^π=3/2$^+$ resonance, causing the cross section to peak at a value of about 5 b near a deuteron bombarding energy of 107 keV. With a 17.6 MeV Q-value and such a high

cross section, this reaction will certainly dominate the energy production in the first magnetic- and inertial-confinement fusion reactors that will eventually provide sufficient energy for commercial use. These reactors are expected to operate in the temperature range kT=1-30 keV, which corresponds to laboratory bombarding energies that lie in the range of energies studied in this review. In a burning mixture of deuterium and tritium, the reactions ^{2}H(d,p)^{3}H, ^{2}H(d,^{3}He)n, and ^{3}H(t,α)nn will also be important. The reaction ^{3}He(d,p)^{4}He is of importance as it burns the ^{3}He coming from the d + d reaction in a DT plasma, and would also be of interest as the main energy producer in an advanced few-neutron reactor whose future has been stimulated by speculation that large amounts of ^{3}He may be available on the surface of the moon [6]. In the fuel-cycle reactions, both reactants and at least one resultant particle are charged allowing accurate measurements to be made perhaps more easily than in neutron experiments.

Because the most important data lie at a low energy where the cross section is dominated by the penetration of the Coulomb barrier and is steeply falling in value as the energy decreases, we shall display all the data in this review as the astrophysical S function [7,8], or S factor. This function factors out from the cross section in the incident channel the energy dependence of the Coulomb penetrability and wavelength of the bombarding particle, and consequently emphasizes the nuclear effects and makes more meaningful comparisons possible. Specifically, for S in keV-b:

$$\text{for d+t,} \quad S = 0.59962 \, \sigma \, E_d \exp(1.40411 \, E_d^{-1/2}), \quad (1)$$

$$\text{for d+d,} \quad S = 0.50000 \, \sigma \, E_d \exp(44.4021 \, E_d^{-1/2}), \quad (2)$$

$$\text{for t+t,} \quad S = 0.50000 \, \sigma \, E_t \exp(54.3378 \, E_t^{-1/2}), \quad (3)$$

$$\text{for } ^3\text{He+d,} \quad S = 1.00000 \, \sigma \, E_c \exp(68.7380 \, E_c^{-1/2}), \quad (4)$$

where E_d or E_t is the corresponding laboratory energy, E_c is the c.m. energy, (all energies are in keV), and σ (cross section) is in barns.

After commenting on the data requirements for fusion reactor design, I shall review the present status of data for the above reactions, their mathematical parametrizations and give suggestions for future experimental work and evaluations. Local data lists and parametrizations exist at numerous laboratories [9]. Some well-known previous evaluations of fuel-cycle reaction cross sections and reactivities include those of Greene [10], Duane [11], Miley [12], Peres [13], Slaughter [14], Kozlov [15], Stewart and Hale [16], and Hively [17].

Review topics at this conference given by R. Feldbacher, and G.M. Hale are also of interest concerning the subjects discussed in this review. Note that nuclear-reaction cross-section data should be used with caution below 10 keV where shielding by electrons in the particular atomic or plasma environment becomes important (see comments on page 2045 of Ref. [2]).

2. Fuel Cycle Data Requirements for Reactor Design

After questioning a number of people working on fusion reactor design, it became apparent that a concise statement would be impossible. The question "What uncertainties in the fuel-cycle reaction cross sections would begin to make a difference in your calculations?" brought a great variety of answers (ranging from 10% up to factors of 2 or more), reflecting the difficulties in the present state of plasma physics and reactor design. The situation is complicated also by the fact that an error in the reactivity could be compensated by a change in another parameter like a small change in the magnetic field. Considering all this, I submit the following statement as at least a fair approximation of the data requirements:

a. Up to now, cross sections known to 15-20% have been sufficient.

b. As experimental devices reach a state of significant burning or ignition, design calculations are calibrated and become more accurate. Then, 5-10% uncertainties would become highly desirable. Some devices are entering this region at the present time.

c. For the long term, 1-2 % uncertainties, at least for the main energy-producing reactions, would be needed for well engineered reactors.

Previous statements and studies of fuel-cycle data requirements include those of Cheng [18]; Gohar [19]; Head [20]; Haight and Larson et al. [21]; The 1986 Argonne Fusion-Data Advisory Meeting [22]; Cheng, Mathews, and Schultz [23]; and Larson and Haight [24].

3. The ^{2}H(t,α)n Reaction.

Experiments at the Los Alamos facility called LEFCS (Low Energy Fusion Cross Sections) measured [2-4] the total cross section from 8-80 keV deuteron bombarding energy with an absolute error of 1.4% for most of the points. This accurate work helped settle the discrepancies mentioned in Ref. [1]; an example is given in figure 1. Details and complete references are given in Ref. [2]. That paper also provides several
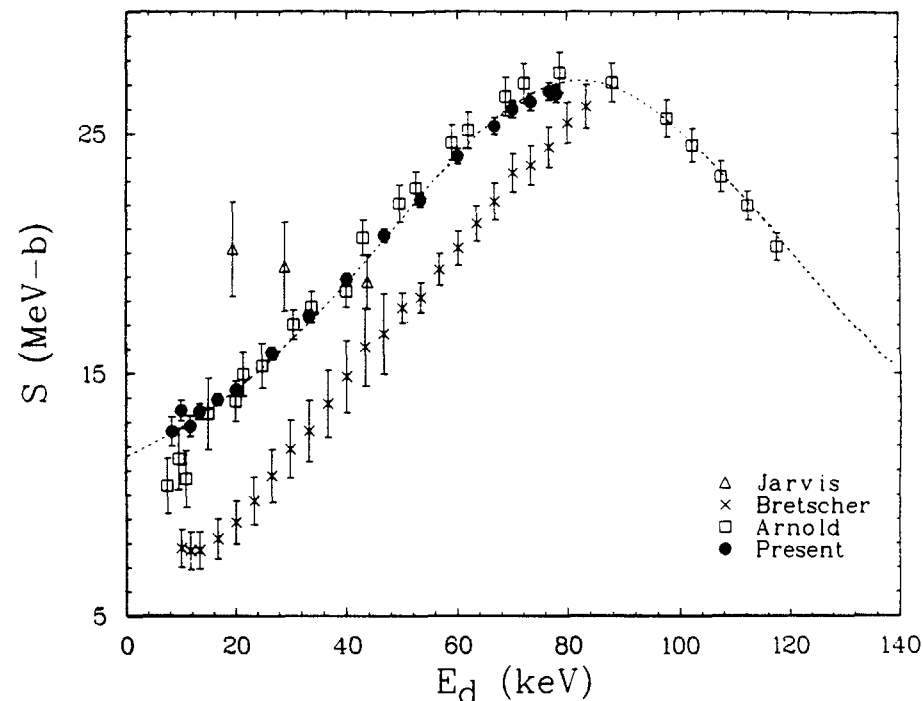
Fig. 1. The S function, [see Sec. I, Eq. (1)], vs equivalent deuteron bombarding energy for the D(t, α)n reaction. Shown are the Los Alamos data [2] and a selection of some of the previous data [46]. Note the suppressed zero. Total errors are shown. The curve is the result of a single level R-matrix fit to an edited data set [2].

parametrizations of the data. The authors calculate the parameters for a two-channel single-level R-matrix fit for their data and other selected experiments up to 250 keV (E_d). In addition they compute coefficients for a power-series polynomial fit to their cross section data and to the corresponding reactivity: $<\sigma v>$.

Los Alamos has recently added 8 more points [25] over the resonance (80 to 116 keV, E_d) with an absolute error of 1.6%, see figure 2. These data were taken by exchanging the beam and target particle, ^{3}H(d,α)n. Shown is a preliminary 2-level R-matrix fit as above including the new data , and a preliminary fit with an EDA R-matrix code [26] that uses a large set of data in all mass-5 channels up to 8 MeV. The new Los Alamos data with
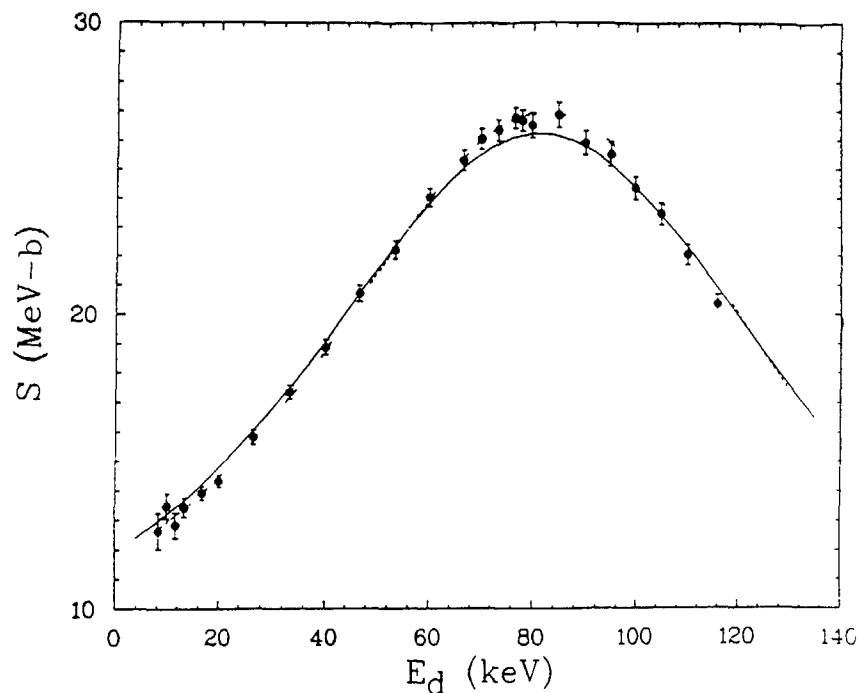
Fig. 2. The S function [Eq (1)] vs deuteron bombarding energy E_d for the ^{3}H(d α)n reaction   The eight highest energy points snow the newest Los Alamos data [25] and the remaining points are those of Ref [2], which has been measured with the same apparatus   The dashed curve is from a two-level two-channel R-matrix fit to a data base including the data shown and other data selected from the literature (see Ref 2) up to a deuteron energy of 250 keV   The solid curve is from a multilevel, multichannel R-matrix fit   [26 28]   using data up to a deuteron bombarding energy of 8 MeV

4. The ^{2}H(d,p)^{3}H and ^{2}H(d,^{3}He)n Reactions.

The Los Alamos LEFCS group has also made the most accurate absolute measurements [3,4] for these reactions in the range 20-117 keV laboratory bombarding energy   Previous data were not discrepant but lacked sufficient accuracy   The Los Alamos data (solid circles) are shown in Figure 3 and 4 in comparison to a representative set of data of other experiments [29]   The Los Alamos errors are shown as 3% but will be in the range 1 6 to 2 0% when some final small corrections are made   The lines are R-matrix fits from a unified mass-4   R-matrix analysis [26 27] that did not include the LEFCS results   Also shown are 26 representative points (crosses) from an important new experiment at Munster by Krauss Becker, Trautvetter, Rolfs and Brand [30] whose measurements have a larger energy range, 6 to 325 keV laboratory energy   Their data are in fairly good agreement with the LEFCS work (considering that the Munster absolute error is 6-8%, their data being roughly 5-10% lower)   Those interested in the d+d angular distributions and anisotropies should refer to the work of Theus, McGarry, and Beach [31] as well as Krauss et al [30] and Jarmie and Brown [3,4]

An important new experimental facility [32] at Bruyères- le-Châtel France, is beginning experiments at low energy which will include the study of the d+d reactions   Accurate cross sections from this effort will improve knowledge of the d+d data

Experimentally, the data for the d+d reactions are fairly well known for present needs   An additional accurate experiment [32] would be useful   A careful evaluation and parametrization including all the recent data does not exist   One would be tempted to use the polynomial fit in Krauss' paper raised in value by several percent to account for the absolute accuracy of the Los Alamos experiment   Polynomial fits will also appear in the final Los Alamos paper

final fits and parametrizations will be published soon   In addition, G Hale has now calculated his final EDA fit with all of the new LEFCS data [28] and has tabulated it in an ENDF-like MASS-storage file for a CRAY computer in a revision of Ref [27]

I conclude that the ^{2}H(t,α)n data are now accurate enough for the indefinite future and are unlikely to be improved   The only remaining question is how to make the best evaluated fits available to the international community in the most efficient way

5. The ^{3}H(t,α)nn Reaction.

Previous data for this reaction were both discrepant and inaccurate The experiment is a difficult one, using both a tritium target and beam and with the three-body reaction producing a spectrum of resultant particles instead of an isolated peak   The Los Alamos LEFCS group has made measurements [3,4] of the alpha spectrum in the range 30-115 keV laboratory energy, and when final corrections are made will give total
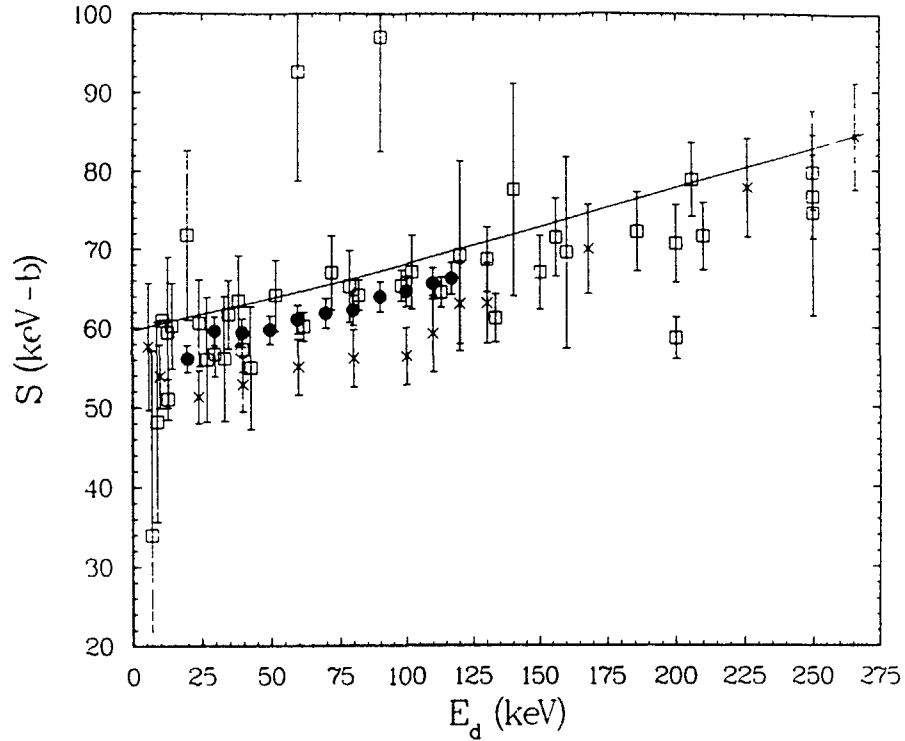
Fig. 3. The S function [Eq. (2)] for the $^2H(d,p)^3H$ reaction as a function of deuteron bombarding energy. Absolute errors are shown The solid circles are the Los Alamos data [3,4] shown with 3% errors (will be less than 2% with the final analysis). The crosses are the Münster data [30]. The squares are a representative selection of other data from other experiments [29]. The curve is from a unified, mass-4, R-Matrix analysis [26] that does not include the Los Alamos or Münster data.
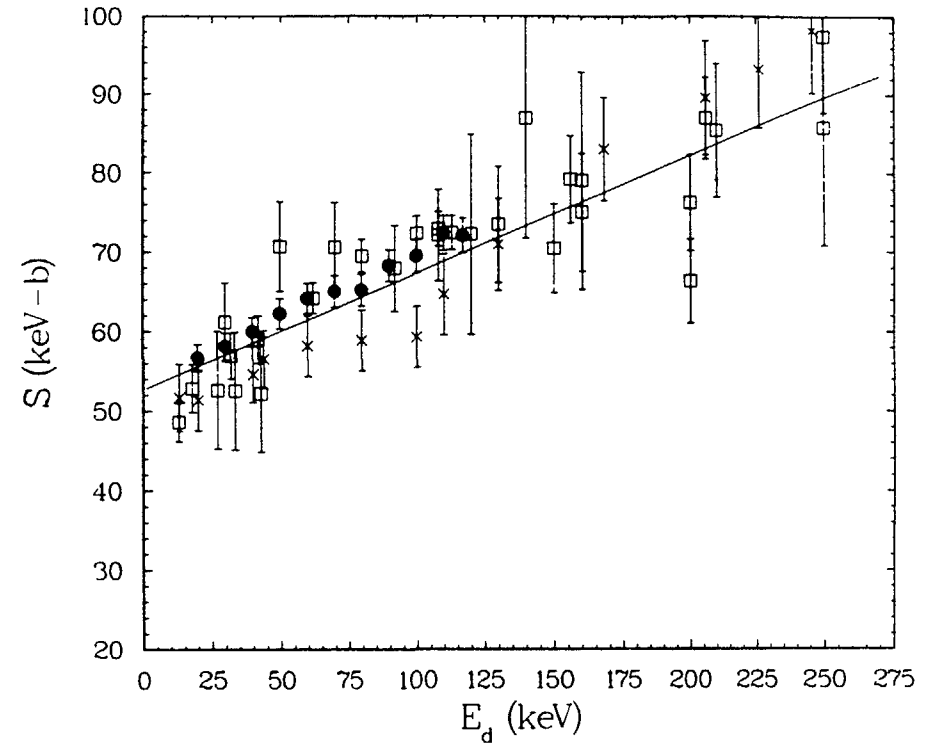
Fig. 4. The S function [Eq. (2)] for the $^2H(d,^3He)n$ reaction as a function of deuteron bombarding energy. Absolute errors are shown. The solid circles are the Los Alamos data (3,4) shown with 3% errors (will be less than 2% with the final analysis) The crosses are the Munster data [30]. The squares are a representative selection of other data from other experiments [29]. The curve is from a unified, mass-4, R-Matrix analysis [26] that does not include the Los Alamos or Münster data.

cross sections accurate to 4-5%, as shown in figure 5. The black curve is from a mass-6 R-matrix analysis [26,27] that does not include the LEFCS points.

The cross sections for the ^{3}H(t,α)nn reaction are now well known, with errors on the order of of 5%. Improvement will be difficult. An experiment measuring the neutron spectrum directly would be useful but would be very difficult. A data evaluation including the present data and in accessible form would be desirable. Hale's fit in figure 5 is a good approximation.

6. The ^{3}He(d,p)^{4}He Reaction.

One look at figure 6 should convince one that there has been trouble in this reaction's cross section experiments in the past [33-39]. The recent work of Möller and Besenbacher in 1980 [40] and Krauss et al. in 1986 [30] have improved the situation. Considering the relationship of the work of Krauss and Möller in this reaction and of Krauss [30], Arnold [33], and Los Alamos [3,4] in the d+d reactions, a "best" cross section line

Fig. 5. The integrated S function [Eq. (3)] for the ^{3}H(t, α)nn reaction vs triton bombarding energy. The solid circles are the preliminary Los Alamos data [3,4] shown with 5% absolute errors. The squares are the data of Ref. [47], triangles Ref. [48], and crosses Ref. [49]. The solid curve is an R-matrix analysis [26,27] that does not include the Los Alamos data. The dashed curve is from the compilation of Greene [10].

Fig. 6. The S function for the ^{3}He(d,p)^{4}He reaction [(Eq. (5)] vs c.m. energy. Absolute errors are shown. The curve is a polynomial fit to the Münster (Krauss) data [30], solid circles, below 130 keV. The remaining data are from Möller [40], Arnold [33], Kunz [34], Bonner [35], Carlton [36], Freier [37], Yarnell [38], and Dwarakanath [39]. Note that the S-function resonance peak is about 50 keV lower in c.m. energy than the peak position when plotted as that of the cross section, due mostly to the unfolding of the exponential penetrability.

would appear to be obtained by normalizing the Krauss fit upwards by 5% (a value less than their absolute error of 6-8%) Until a formal evaluation is done, I suggest that those desiring a parametrization for the total cross section for the ^{3}He(d,p)^{4}He reaction use the fitting function (equation 2) of Möller and Besenbacher [40] for c m. energies 80 keV and higher, and the polynomial fitting function of Krauss et al (in section 5 of Ref [30]) multiplied by 1 05 for c m energies of 100 keV and lower (users choice between 80 to 100 keV). Absolute cross section values thus chosen should be good to 5%, certainly less than 10%.

Such formulae may satisfy users in the near future Eventually, additional precision measurements on the order of 2% uncertainty would be desirable, especially in the region of the resonance. Additional accurate data from the new French effort [32], mentioned above, would be very welcome A careful evaluation, perhaps with a mass-5 R-matrix analysis would be highly desirable at this time and in the future

7. Other reactions.

Charged particle elastic scattering (or "slowing-down") cross sections in the few MeV energy region, such as ^{3}H(d,d)^{3}H, ^{3}H(α,α)^{3}H, and ^{2}H(α,α)^{2}H are needed to estimate energy losses of ions by collisions in ionized plasmas These cross sections can be very well estimated (to 2-4%) by energy-dependent R-matrix calculations (see Hale, Dodder, and DeVeaux [41]). This method works well because the cross sections are tied to measured cross sections at Van-de-Graaff energies on the high energy side, and to Coulomb cross sections on the low energy side The R-Matrix method is also useful for estimating other secondary reactions

High-energy gamma rays from capture processes may be important for diagnostic measurements [42] of fusion reactor systems. Reactions of interest include ^{3}H(d,γ)^{5}He, ^{2}H(d,γ)^{4}He, and ^{3}He(d,γ)^{5}Li . These cross sections, usually very small, have been measured in recent years to uncertainties of 5-10% [43-45]. Experiments to significantly improve the accuracy of these cross sections will be difficult, and will probably await a certain measure of success in using these reactions as a diagnostic.

Little is known about the ^{3}He(^{3}He,α)pp reaction at low energies [50,51] Its contribution to the power of a reacting d+^{3}He plasma is expected to be small because of the increased Coulomb barrier between the reactants. The Münster Group is planning a study [52]

8. Conclusions.

Experimental knowledge of charged particle cross sections for use in fusion reactor design appears to be good, certainly in the near to medium term Precision experiments for the ^{3}He(d,p)^{4}He reaction, and for various mass-6 reactions to help pin down the ^{3}H(t,α)nn reaction in an R-matrix analysis, should eventually be useful.

What are badly lacking are cross-section data evaluations for the various reactions which are considered to be the "standard", are easily available to anyone, and are in an internationally accepted format Support for generating such evaluations should be seriously considered.

9. Acknowledgments

REFERENCES

1 N Jarmie, Nucl Sci and Eng **78** (1981) 404

2 N Jarmie, R E Brown, and R A Hardekopf, Phys Rev C **29** (1984) 2031, erratum **33** (1986) 385

3 N Jarmie and R E Brown, Nucl Instr and Methods **B10/11** (1985) 405

4 R E Brown and N Jarmie, Radiation Effects **92** (1986) 45 (Santa Fe 1985, conference on Nuclear Data for Basic and Applied Science)

5 See, for example, page 15, item 9 of H W Hendel A C England D L Jassby, A A Mirin, and E B Nieschmidt, Report PPPL-2318 Princeton (1986)

6 L J Wittenberg, J F Santarius, and G L Kulcinski, Fusion Technology **10** (1986) 167

7 D D Clayton, *Principles of Stellar Evolution and Nucleosynthesis* (McGraw-Hill, New York, 1968)

8 C A Barnes, in *Advances in Nuclear Physics*, edited by M Baranger and E Vogt (Plenum, New York, 1971), Vol **4**, page 133

9   See, for example, page 228 of A H Futch, Jr , J P Holdren J Killeen and A A Mirin, Plasma Physics **14** (1972) 211

10   S L Greene Jr , UCRL-70522, Lawrence Radiation Lab (May 1967)

11   B H Duane, Report BNWL-1685 p 75 W C Wolkenauer Ed Battelle Northwest Laboratory (November 1972)

12   G H Miley, H H Towner, and N Ivich Report C00-2218-17 University of Illinois (1974)

13   A Peres, J Appl Phys **50**, (1979) 5569

14   D Slaughter, J Appl Phys **54** (I983) 1209

15   B N Kozlov, Atomnaya Énergiya **12** (1962) 238

16   L Stewart and G M Hale, Report LA-5828-MS, Los Alamos Nat Laboratory (Jan 1975)

17   L   M Hively, Nuclear Fusion **17** (1977) 873, and Nuclear Technology/Fusion **3**, (1983) 199

18   E   T Cheng,   Fusion   Technology   **8**   (1985) 1423   (San Francisco, Sixth Topical   Conference on the Technology of Fusion Energy) See also report GA-A17881

19   Y Gohar, Radiation Effects **92**, (1986) 15   (Santa Fe 1985 conference on Nuclear Data for Basic and Applied Science)

20   C R Head, Proc of the Advisory Group Meeting on Nuclear Data for Fusion-Reactor Technology, IAEA-TECDOC-223, p 1 IAEA Vienna (1979)

21   R C Haight, and D C Larson, and panel members, UCID-19930 Lawrence Livermore Nat Lab (October 1983)

22   Proc of the Fifth Coordination Meeting of the Office of Basic Energy Sciences Program to Meet High Priority Nuclear Data Needs of the office of Fusion Energy, Argonne (September I986) to be published

23   E T Cheng, D R Mathews, and K R Schultz, GA Technologies Report GA-A18152 UC-20 (1985),   and similar reports for previous years referenced therein

24   D C Larson and R C Haight, ORNL/TM-9335, Oak Ridge Nat Lab (October 1984)

25   R E Brown and N Jarmie, private communication

26   G   M Hale and D C Dodder, in Nuclear Cross Sections for Technology,   edited by J L   Fowler, C H Johnson, and C D Bowman (National Bureau of Standards, Washington D C , 1980) Special Publications 594, p 650

27   G   M Hale Los Alamos National Laboratory Memo T-2-L-3360 (1979), and also same memo number but "1981 revision"

28   G M Hale Los Alamos National Laboratory Memo T-2-M-1767 (1986)

29   See the references numbered "35-45" contained in Ref 1

30   A Krauss, H W Becker, H P Trautvetter   C Rolfs and K Brand private communication (Sept 1986),   Submitted to Nuclear Physics

31   R B Theus, W I McGarry, and L A Beach, Nucl Phys **80** (1966) 273

32   G Haouat, private communication (October 1986)

33   W R Arnold, J A Phillips, G A Sawyer, E J Stovall, Jr , and J L Tuck, Phys Rev **93** (1954) 483 , Los Alamos Scientific Laboratory Report LA-1479, 1953

34   W E Kunz, Phys Rev **97** (1955) 456

35   T W Bonner, J P Conner, and A B Lillie, Phys Rev **88** (1952) 473

36   R F Carlton, Thesis, University of Georgia (1970)

37   G Freier and H Holmgren, Phys Rev **93** (1954) 825

38   J L Yarnell, R H Lovberg, and W R Stratton, Phys Rev **90** (1953) 292

39   M R Dwarakanath, Thesis, California Inst of Technology (1969)

40   W Moller and F Besenbacher, Nucl Instr and Methods **168** (1980) 111   and W Moller, private communication, (Oct 1986)

41   G M Hale, D C Dodder, and J C DeVeaux, in Nuclear Science and Technology,   International Conference, Antwerp (1982) edited by K H Bockhoff (Reidel, Dordrecht 1983), p 326

42   F E Cecil, D M Cole, F J Wilkinson III, and S S Medley, Nucl Instr and Methods, **B10/11** (1985) 411

43   F E Cecil, and F J Wilkinson III, Phys Rev Lett **53** (1984) 767 F J Wilkinson III, and F E Cecil, Phys Rev C **31** (1985) 2036

44   G L Morgan, P W Lisowski, S A Wender, R E Brown, N Jarmie, J F Wilkerson, and D M Drake, Phys Rev C **33** (1986) 1224

45   F E Cecil, D M Cole, R Philbin, N Jarmie, and R E Brown,   Phys Rev C **32** (1985) 690

46   These experiments are cited as "Ref 7" in Reference 4   above

47   V I Serov, S N Abramovich, and L A Morkin, Sov J At Energy **42** (1977) 66,   National Nuclear Data Center, Brookhaven Natl , Data Base CSISRS(EXFOR) #A0007, 770825,   See also Yu V Strel'nikov, S N Abramovich, L A Morkin, and N D Yur'eva, Bull Acad Sci USSR Phys Sci (Isv) **35** (1971) 149

48   A M Govorov, Li Ka-Yeng, G M Osetinskii, V I Salatskii, and I V Sizov, Sov Phys JETP, **15** (1962) 266

49   H M Agnew et al , Phys Rev **84** (1951) 862

50   M R Dwarakanath, Phys Rev C **9** (1974) 805

51   F Ajzenberg-Selove, Nucl Phys **A413** (1984) 1

52   C Rolfs, private communication (November I986), the study will be from $E_{c\,m}$ = 17 9 to 342 5 keV

NUCLEAR DATA REQUIREMENTS FOR TRANSMUTATIONS,
GAS PRODUCTION AND ACTIVATION OF REACTOR WALL
AND STRUCTURAL MATERIALS*

F.M. MANN
Westinghouse Hanford Company,
Richland, Washington,
United States of America

---

* was presented at the meeting orally and main conclusions were included
into the report of Working Group I.

STATUS OF
EXPERIMENTAL AND THEORETICAL INVESTIGATIONS
OF MICROSCOPIC NUCLEAR DATA

(Session B)

Chairmen

H. LISKIEN
Commission of the European Communities

M. MEHTA
India

SYSTEMATICS OF 14 MeV NEUTRON INDUCED REACTION CROSS-SECTIONS

S.M. QAIM
Institut für Chemie 1 (Nuklearchemie),
Kernforschungsanlage Jülich GmbH,
Jülich, Federal Republic of Germany

Abstract

The relative contributions of 14 MeV neutron induced nuclear reaction cross sections for medium and heavy mass nuclei are outlined and some of the systematic trends observed in the data are reviewed. The systematics of the common reactions like (n,p), (n,α) and (n,2n) are well known; they are treated here only briefly. Special attention is paid to less common and rare reactions like (n,d), (n,n'p), (n,nα), (n,t) and (n,^{3}He) for which the data base has improved in recent years and analysis of systematic trends is now more reliable.

INTRODUCTION

The energetically possible nuclear reactions induced by 14 MeV neutrons include (n,γ), (n,n'γ), (n,2n), (n,p), (n,d), (n,t), (n,^{3}He), (n,α), (n,2p), (n,np), (n,nα) and, in the heaviest target mass nuclei, low-probability (n,3n) and nuclear fission processes. The relative contributions of the various reactions vary from one mass region to another: in the light mass region, for example, emission of charged particles is favoured, whereas in the heavy mass region, neutron emission is more dominant. Although in the lightest mass region the cross sections of various reactions are difficult to systematize and to predict, mainly due to strong nuclear structure effects, the magnitudes of various reaction cross sections for elements with A>40 can be roughly sketched out and are shown in Fig. 1 [1,2]. Evidently (n,p), (n,α), (n,n'γ) and

(n,2n) reactions are the strongest, followed by (n,d), (n,n'p), (n,n'α) and (n,γ) processes. The reactions (n,t), (n,^{3}He) and (n,2p) are rare.
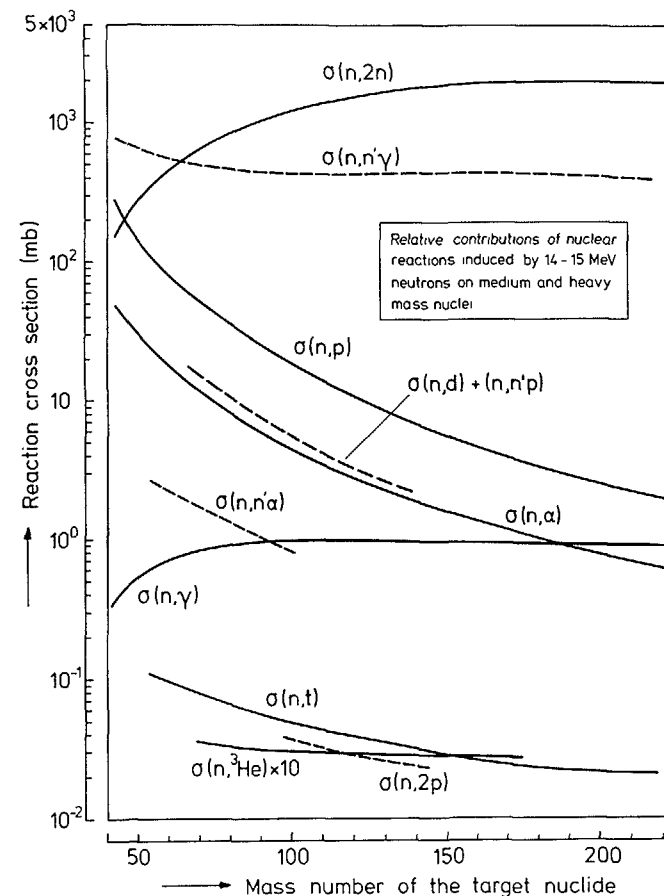
Fig. 1 Relative contributions of nuclear reactions induced by 14 MeV neutrons on medium and heavy mass nuclei [1,2].

SYSTEMATICS OF CROSS SECTIONS

Differential reaction cross-section data, such as angular and energy distributions of the emitted particles, lead to useful information on reaction mechanisms as well as nuclear structure. However, since each nucleus possesses its own fine structural details, a systematization of the differential data is extremely difficult and also quite uncertain. Analysis of systematic trends has therefore been attempted only in the case of integrated data where the individual effects are averaged out. In looking for the systematics the integrated cross sections are generally considered as a function of mass (A), charge (Z), neutron number (N), neutron excess (N-Z), or relative neutron excess ((N-Z)/A) of the target nucleus. It should, however, be pointed out that the reaction energies involved even in the same type of reaction (e.g. (n,p)) on various target nuclides in different mass regions are different. Even for one target element the cross section varies as one proceeds from the lightest to the heaviest mass isotope, evidently due to changing Q-value and reaction energy. For reactions where a large body of data is available as a function of energy, the data around 14 MeV were occasionally normalized to a constant reaction energy while developing the systematics [cf. 3]. In most of the other cases, however, this aspect was neglected and the trends observed are thus empirical. Nonetheless, such trends allow a quick prediction of unknown cross sections. In cases where experimental measurements are extremely tedious or where theory cannot be applied with certainty, the systematics, if used with caution, could provide useful information on the various competing processes.

We give below a brief survey of some of the systematic trends observed in various reaction cross sections. Wherever possible, integrated data obtained using all the techniques (purely physical, radiochemical, mass spectrometry etc.) were taken into account. For (n,3n) and (n,2p) processes only scanty data are available and no systematic trend has been reported. The other reactions are discussed below.

These reactions constitute the most well investigated nuclear processes at 14 MeV. Although some of the fine details of the reaction mechanisms, especially those relevant to the emission spectra, are still not fully understood, the systematic trends in integrated cross sections are fairly well established. Starting from the early works [cf. 3-9] the systematics were worked out well by 1973 [cf. 10-16]. It was found that the (n,p) and (n,α) reaction cross sections increase as a function of Z, reaching a maximum at about Z=16, and then decrease. The whole trend for each
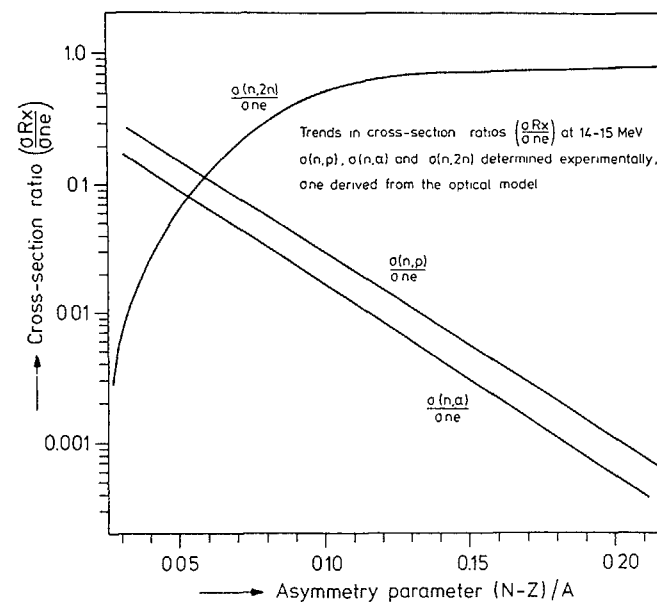
Fig. 2   Trends describing in broad terms for nuclei with A>30 the relative contributions of (n,p), (n,α) and (n,2n) reaction cross sections to the nonelastic cross section of the target nucleus at 14.5 MeV as a function of (N-Z)/A [17].

reaction is reminiscent of a giant excitation function. For medium and heavy mass nuclei both the (n,p) and (n,α) reaction cross sections show a strong dependence on (N-Z)/A. The (n,2n) cross section was also found to be strongly dependent on (N-Z)/A [cf. 11,15]. In all the three cases it was concluded that shell effects, if any, were negligible. A summary of the systematics of these three reactions was given in 1975 [cf. 1]; since then no major effort has been devoted in this direction. It is now possible to predict the unknown (n,2n), (n,p) and (n,α) reaction cross sections at 14 MeV with uncertainties of about 30 %.

In order to establish in broad terms the relative contributions of the three reactions under discussion, the ratios $\sigma(n,p)/\sigma_{ne}$, $\sigma(n,\alpha)/\sigma_{ne}$ and $\sigma(n,2n)/\sigma_{ne}$ were determined for nuclei with A>30, and the plots of those ratios against (N-Z)/A are reproduced as general trends in Fig. 2 [cf. 17]. Evidently, in the lighter mass region (A = 30 to 50) the (n,p) and (n,α) reactions contribute significantly but the respective contributions do not exceed 30 % and 20 % of the total nonelastic cross section. The (n,2n) reaction, on the other hand, is insignificant for nuclei with A<50. In the medium and heavy mass region, however, the (n,2n) contribution increases rapidly and for nuclei with A≥100 it accounts for >80 % of the nonelastic cross section.

(n,γ) and (n,n'γ) Reactions

The radiative capture cross sections obtained by γ-ray spectrum integration were plotted against A [cf. 1,18]. The values showed an increasing trend up to A=80 beyond which the cross section was found to be almost constant. Early activation results, on the other hand, were very discrepant. Measurements done after 1974, using improved methods, however, gave more consistent results and it is now believed that for most of the nuclei the (n,γ) cross section at 14 MeV is ≤1 mb. No new systematic trend has been analysed in recent years. Useful mechanistic information has been derived in the last few years via measurements of γ-ray spectra. A discussion of those studies, however, is beyond the scope of this review.

Due to the paucity of data no detailed systematic trend in the (n,n'γ) cross sections could be observed. A plot of the available data [cf. 16] against (N-Z)/A suggested [cf. 1] that after an initial increase the cross section becomes practically constant and remains so over the entire region of medium and heavy mass nuclei. The excitation of some isomeric states in the (n,n'γ) process is treated in a separate review by Vonach (cf. these Proceedings).

(n,d) and (n,n'p) Reactions

Considerable amount of work on these reactions in the medium and heavy mass regions has been done in recent years, especially at Julich using the radiochemical technique [cf. 19-21], and Livermore using charged particle detection [cf. 22-25]. The radiochemical data give a sum of [(n,d)+(n,n'p)+(n,pn)] processes and are shown in Fig. 3 as a function of (N-Z)/A [21]. The data
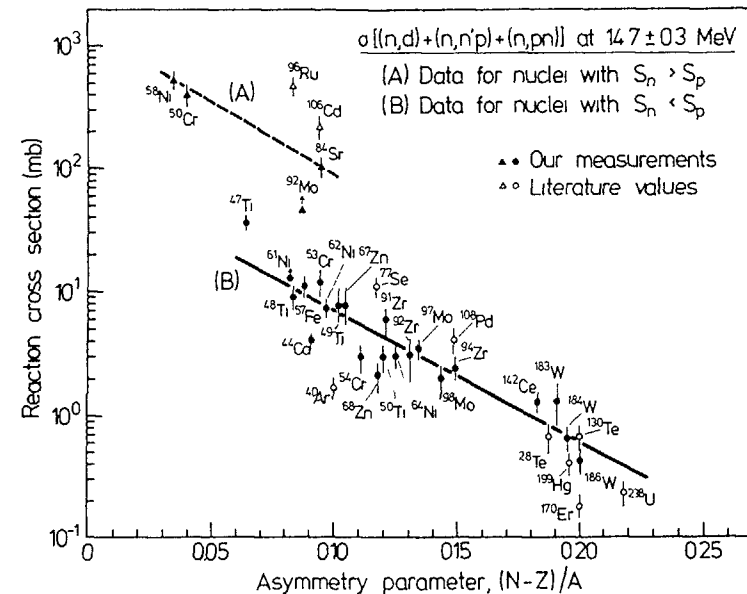
Fig. 3   Systematics of radiochemically determined [(n,d)+(n,n'p)+(n,pn)] reaction cross sections at 14 MeV [21].

fall distinctively on two curves: one for the lightest stable target nuclei, which are rather away from the stability line of the investigated elements, and the other for nuclei richer in neutrons. The curve for the lightest stable nuclei, for which the neutron separation energy (S_n) is higher than the proton separation energy (S_p), is as yet rather uncertain, but the descending trend is obvious. It is attributed to the predominance of the (n,n'p) process. The curve for nuclei richer in neutrons describes the general trend in [(n,d)+(n,n'p)+(n,pn)] cross sections.

The results on the (n,d) reaction reported from Livermore [cf. 22-25] are given in Fig. 4 and compared with the radiochemical data [19-21]. The trend for the (n,p) reaction based on the activation data is also depicted for reference. A comparison of the (n,p) and (n,d) reaction cross sections reveals that the first

chance p-emission is much more probable than d-emission. The (n,d) cross section, on the other hand, is practically constant over the entire investigated mass range. This is due to the predominance of direct interaction processes in d-emission.

It should be emphasized that the (n,n'p) reaction cross sections are of considerable significance in calculations on hydrogen formation in structural materials, but only for those target nuclei which have $S_n > S_p$. For neutron richer nuclei hydrogen generation is small and the main contributing reaction is the (n,p) process.

$(n, x\alpha)$ and $(n, n\alpha)$ Reactions

The $(n, x\alpha)$ cross sections obtained in recent years using the three common techniques, viz. charged particle detection, mass spectrometry and activation, are generally in agreement [cf. 26]. The recent total α-emission cross-section data for elements of

Fig. 4   Gross trends in (n,p), (n,d) and [(n,d)+(n,n'p)+(n,pn)] reaction cross sections at 14 MeV [21].
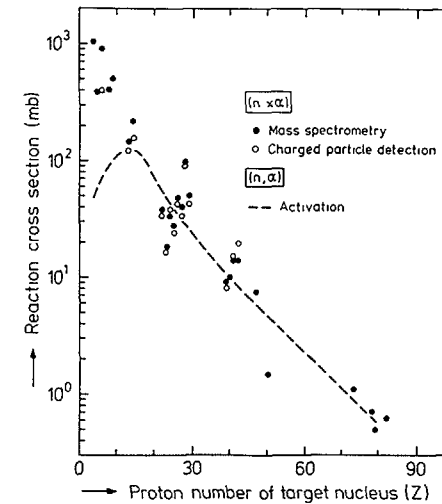
Fig. 5   Helium emission reaction cross sections at 14 MeV [cf. 22-25, 27-31] as a function of Z of the target nucleus. The curve describing the activation data relates to the pure (n,α) contribution [cf. 12].

natural isotopic composition obtained via integration of the emitted α-particle spectra [cf. 22-25,27,28] as well as mass spectrometry [cf. 29-31] are given in Fig. 5. The trend for the pure (n,α) reaction [cf. 12] based on activation measurements on individual isotopes of various elements is also shown for comparison. Obviously for very light nuclei (Z<10) the pure (n,α) contribution is small, the (n,2α) and multiparticle breakup processes leading to the emission of several α-particles being dominant. For nuclei with Z>10, however, a greater part of the measured (n,xα) cross section is furnished by the (n,α) reaction.

As far as the (n,nα) cross sections are concerned, the activation technique has some advantage since it yields data measured independent of the (n,α) cross section. The systematic trend observed in the data [26] is reproduced in Fig. 6. The contribution of the (n,nα) process generally amounts to between 10 and 15 % of the (n,α) cross section; in some cases, however, it is as low as 0.5 %. It is evident that besides (n,α) reaction the contribution of the (n,nα) process must be taken into account while estimating helium production in structural materials.

However, the role of the (n,nα) process in total helium production is not as important as of the (n,n'p) process in total hydrogen generation.

(n,t) Reaction

The (n,t) reaction has high cross section in the light mass region. In the medium and heavy mass regions first unambiguous and systematic studies were performed radiochemically at Jülich [cf. 32,33], followed by measurements at Debrecen [cf. 34,35] and elsewhere. An updated version of the trend originally reported from Jülich is given in Fig. 7. For this purpose the data given in a recent compilation [36] were used. The increasing trend for elements with Z = 13 to 20 is postulated to arise from the occurrence of statistical processes [cf. 37]; for all of the other nuclei, however, direct interactions appear to be dominant. The data for nuclei with Z>22 showed some dependence on (N-Z)/A

Fig. 6   Systematics of activation cross sections of (n,nα) reactions induced by 14 MeV neutrons [26].
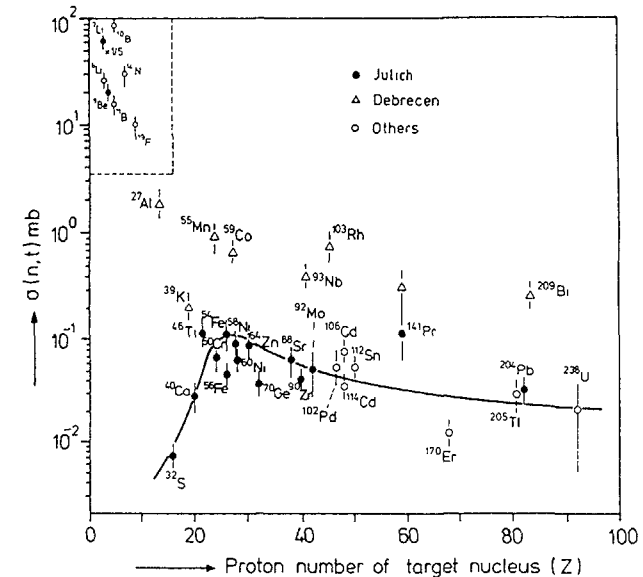
Fig. 7   Updated version of the systematics of (n,t) reaction cross sections at 14 MeV [cf. 32-35].

[32,33] and an updated version of the systematics is reproduced in Fig. 8 [cf. 38]. The data for even and odd mass nuclei show different trends due to differences in Q-values [cf. 35]. The slope for the odd-mass nuclei is steeper, so that in the heavy mass region the cross sections for even and odd mass nuclei do not differ strongly: this is due to almost similar Q-values for (n,t) reactions on all the investigated heavy mass nuclei. It should be pointed out that the odd-even effect is not observed at high incident neutron energies.

The (n,t) reaction is one of the most important nuclear processes to be considered in a DT fusion reactor since it will be used for tritium fuel breeding. Systematic studies cited above led to the conclusion that for tritium breeding only the lightest elements are of interest. For this purpose, of particular significance are the $^6Li(n,t)^4He$ and $^7Li(n,n't)^4He$ reactions. Except for some small uncertainties in the latter reaction, the 14 MeV data for these two major tritium breeding processes are well known [cf. 39].

$(n,^3He)$ Reaction

Systematic studies on this reaction were carried out almost exclusively by the radiochemical method, mainly at Jülich [cf. 40,41]. The results are shown in Fig. 9. The trend is somewhat

Fig. 8   Updated version of the systematics of (n,t) reaction cross sections at 14 MeV for nuclei with Z>22 [cf. 38]. The trend for even-mass nuclei was suggested by the Julich group and that for odd-mass nuclei by the Debrecen group.

Fig. 9   Systematics of $(n,^3He)$ reaction cross sections at 14 MeV for medium and heavy mass nuclei [40,41].

similar to that for (n,t) cross sections on even mass nuclei; in terms of absolute magnitude, however, the (n,^{3}He) cross section is by an order of magnitude smaller than the (n,t) cross section.

Very recently the ^{40}Ca(n,^{3}He)^{38}Ar reaction cross section was measured by integration of the emitted ^{3}He-spectrum, and some other (n,^{3}He) cross sections were derived from the data for inverse reactions [42]. Those data are much higher than the activation results shown in Fig. 9. The difference is attributed to the strongly varying Q-values, especially in view of the fact that the energies of the outgoing ^{3}He-particles are all below the Coulomb barrier. For resolving the finer details in the gross trend, more experimental data are needed.

SYSTEMATICS OF ISOMERIC CROSS-SECTION RATIOS

The cross sections for the formation of individual discrete states in the product nuclei are difficult to systematize since they are strongly dependent on the spin and parity of the state concerned. Some systematic studies on the formation of the first excited states of even-even target nuclei via the (n,n'γ) process have been reported [cf. 43]. These are discussed in another contribution [cf. Vonach, these Proceedings]. We limit ourselves here to a consideration of the isomeric cross-section ratios.

The isomeric cross-section ratios [σm/(σm+σg)] for (n,2n) reactions were systematically analysed in terms of spin cut-off parameter and moment of inertia of the nucleus [cf. 44], as well as the various statistical models [cf. 45]. The ratios for (n,p), (n,α) and (n,2n) reactions were also treated empirically by plotting them against the spin J_m of the metastable state [cf. 46]. It was found that all the experimental data could be encompassed within a broad band having a maximum at J_m value between 4 and 6. As far as the other reactions are concerned, the available information on the isomeric cross-section ratios is very scanty. Some measurements have been reported in the case of (n,t) reactions. The results are reproduced in Fig. 10 [cf. 38]. It appears that isomeric states with spin values between 3/2 and 3 are preferentially populated, transitions to states with spin
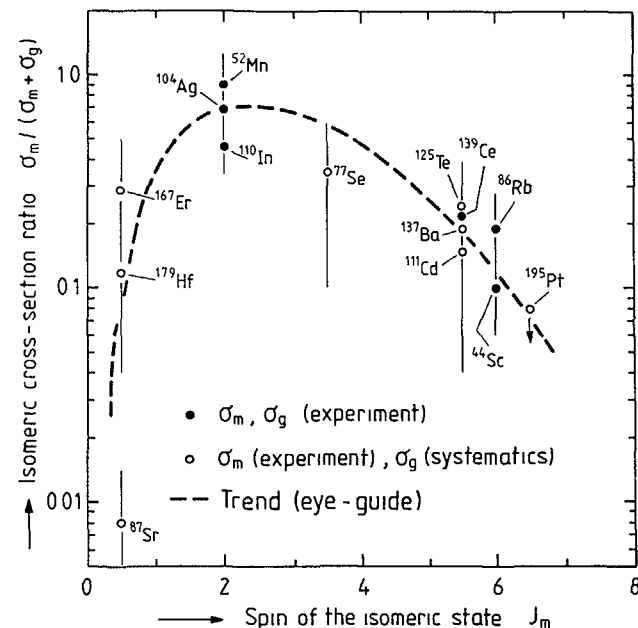
Fig. 10   Isomeric cross-section ratios in (n,t) reactions at 14 MeV on nuclides with Z$\geq$22 as a function of the spin of the isomeric state [38].

values $\leq$1 or $\geq$5 being very weak. This tendency differs from that observed for the common reactions described above. Evidently, for a detailed systematic analysis of isomeric cross-section ratios a considerable amount of further experimental data is required.

REFERENCES

[1] S.M. Qaim, in Proc. Conf. on Nuclear Cross Sections and Technology, Washington, D.C. (1975), NBS Special Publication 425 (1975) p. 664

[2] S.M. Qaim, in Handbook of Spectroscopy, Vol. III (CRC Press, Florida, 1981) p. 141

[3] J. Csikai and G. Peto, Phys. Lett. 20 (1966) 52

[4] D.W. Barr, C.I. Browne and J.S. Gilmore, Phys. Rev. 123 (1961) 859

[5] B.P. Bayhurst and R.J. Prestwood, J. Inorg. Nucl. Chem. 23 (1961) 173

[6] D.G. Gardner, Nucl. Phys. 29 (1962) 373

[7] A. Chatterjee, Nucl. Phys. 47 (1963) 511, idem 60 (1964) 273

[8] V.N. Levkovskii, JETP (Sov. Phys.) 18 (1964) 213

[9] M. Bormann, Nucl. Phys. 65 (1965) 257

[10] D.G. Gardner and S. Rosenblum, Nucl. Phys. A96 (1967) 121

[11] P. Hille, Nucl. Phys. A107 (1968) 49

[12] S.M. Qaim, Z. Naturforschung 25a (1970) 1977

[13] G. Eder, G. Winkler and P. Hille, Z. Phys. 253 (1972) 335

[14] A.K. Hankla and R.W. Fink, Nucl. Phys. A180 (1972) 157

[15] S.M. Qaim, Nucl. Phys. A185 (1972) 614

[16] J. Csikai, Atomic Energy Review 11 (1973) 415

[17] N.I. Molla and S.M. Qaim, Nucl. Phys. A283 (1977) 269

[18] F. Cvelbar, A. Hudoklin and M. Potokar, Nucl. Phys. A158 (1970) 251

[19] S.M. Qaim and G. Stocklin, in Proc. 8th Symp. on Fusion Technology, Noordwijkerhout (The Netherlands) June 1974 (EUR 5182 e, 1974) p. 939

[20] S.M. Qaim and N.I. Molla, in Proc. 9th Symp. on Fusion Technology, Garmisch Partenkirchen, June 1976 (Pergamon Press, Oxford, 1976) p. 589

[21] S.M. Qaim, Nucl. Phys. A382 (1982) 255

[22] S.M. Grimes, R.C. Haight and J.D. Anderson, Nucl. Sci. Eng. 62 (1977) 187

[23] S.M. Grimes, R.C. Haight and J.D. Anderson, Phys. Rev. C17 (1978) 508

[24] S.M. Grimes, R.C. Haight, K.R. Alvar, H.H. Barschall and R.R. Borchers, Phys. Rev. C19 (1979) 2127

[25] R.C. Haight, S.M. Grimes, R.G. Johnson and H.H. Barschall, Phys. Rev. C23 (1981) 700

[26] S.M. Qaim, Nucl. Phys. A458 (1986) 237

[27] A. Paulsen, H. Liskien, F. Arnotte and R. Widera, Nucl. Sci. Eng. 78 (1981) 377

[28] R. Fischer, G. Traxler, M. Uhl and H. Vonach, Phys. Rev. C30 (1984) 72; idem C34 (1986) 460

[29] H. Farrar IV and D.W. Kneff, Trans. Am. Nucl. Soc. 28 (1978) 197

[30] D.W. Kneff, B.M. Oliver, M.M. Nakata and H. Farrar IV, J. Nucl. Materials 103+104 (1981) 1451

[31] D.W. Kneff, B.M. Oliver, H. Farrar IV and L.R. Greenwood, Nucl. Sci. Eng. 92 (1986) 491

[32] S.M. Qaim and G. Stocklin, J. Inorg. Nucl. Chem. 35 (1973) 19

[33] S.M. Qaim and G. Stocklin, Nucl. Phys. A257 (1976) 233

[34] T. Biro, S. Sudar, Z. Miligy, Z. Dezso and J. Csikai, J. Inorg. Nucl. Chem. 37 (1975) 1583

[35] S. Sudar and J. Csikai, Nucl. Phys. A319 (1979) 157

[36] Z.T. Body and K. Mihàly, INDC(HUN)-22/L, IAEA, Vienna (1985)

[37] S.M. Qaim, H.V. Klapdor and H. Reiss, Phys. Rev. 22 (1980) 1371

[38] S.M. Qaim, Nucl. Phys. A438 (1985) 384

[39] S.M. Qaim and R. Wolfle, Nucl. Sci. Eng., in press

[40] S.M. Qaim, J. Inorg. Nucl. Chem. 36 (1974) 239; 36 (1974) 3886

[41] S.M. Qaim, Radiochimica Acta 25 (1978) 13

[42] D. Miljanic, M. Zadro and D. Rendic, Nucl. Phys. A419 (1984) 351

[43] W. Breunlich, G. Stengel and H. Vonach, Z. Naturforschung 26a (1971) 452

[44] J. Karolyi, J. Csikai and G. Peto, Nucl. Phys. A122 (1968) 234

[45] M. Guidetti and C. Oldano, Nucl. Phys. A152 (1970) 387

[46] I. Uray, T. Torok, P. Bornemisza-Pauspertl and L. Végh, Z. Phys. A287 (1978) 51

STATUS OF EXPERIMENTAL AND THEORETICAL GAMMA RAY EMISSION SPECTRA

P. OBLOŽINSKÝ
Institute of Physics,
Electro-Physical Research Centre,
Slovak Academy of Sciences,
Bratislava, Czechoslovakia

Abstract

Reviewed are recent developments in experimental and theoretical
γ ray emission spectra for fusion reactor technology. .e concent-
rate on $(n,x\gamma)$ reactions at $E_n \approx 0.1 - 20$ MeV, and on the progress
achieved after the previous IAEA Advisory Group Meeting held in
1978.

1. Introduction

Designers of fusion reactors need γ ray emission spectra ba-
sically for two reasons: γ ray heating and shielding calculations.
None of these problems seems crucial in the fusion reactor tech-
nology, and γ ray production data have been and still are in the
shadow of higher priority nuclear data such as tritium production,
neutron scattering and charged particle production. This circum-
stance can be traced also in the evaluated nuclear data libraries.
From major libraries practically only the ENDF/B4, ENDF/B5 [1,2]
and the Livermore ENDL [3] deal systematically with the γ ray pro-
duction data [4-6].

The present subject has been reviewed at the previous Advisory
group meeting in 1978 by F.G. Perey [7]. Most of the important de-
velopments discussed in his presentation should be contained in
the paper published in 1980 by Fu [8] dealing with the compound/pre-
compound model with conservation of angular momentum. We recog-
nize the importance of the problem and not incidentally address
it here again.

Neutron energies of interest for the fusion reactor technology
cover 9 orders of magnitude, from thermal energies up to about
20 MeV. A schematical picture of γ ray production cross section
as a function of the incident neutron energy is shown in fig.1.
In this review, however, we shall not discuss slow neutron radi-
ative capture (for this subject see, e.g., ref. 11). Rather, we
deal with fast neutrons, i.e., with $(n,x\gamma)$ reactions above the
threshold and fast neutron capture, and concentrate on recent ex-
perimental and theoretical developments in the γ ray emission
spectra.

As a warm-up we start with a brief overview of the γ ray pro-
duction data needed for the fusion reactor technology. This is
done in sect. 2. In sect. 3 we discuss experimental works. Apart
from major contributions from the Oak Ridge pulsed white neutron
source we shall emphasize also some less traditional measurements.
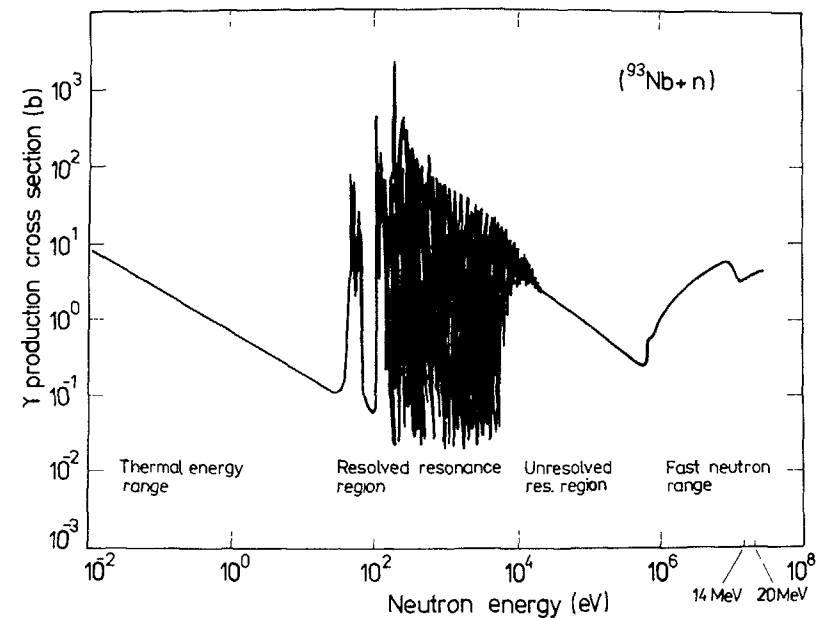
Fig.1. Schematical view of γ production cross sections over 9 or-
ders of magnitude of the incident neutron energy. The curve
is approximately valid for 93Nb+n. Based on data from
JENDL-2 (9) and from Morgan (10).

Theoretical developments as discussed in sect. 4 stress the importance of advanced theoretical tools for evaluation of γ ray spectra. Finally, a few concluding remarks is made in sect. 5.

2. Data needs

Probably the best list of current requests for neutron nuclear data still is the IAEA's WRENDA. The last issue of this world request list released in 1983 [12] includes 37 requests for γ emission data that are motivated by the fusion reactor technology and are summarized in tab.1. Some more recent requests should be found in a series of 1985-1986 papers [13-17].

Given in tab.1 are elements, neutron energy range, accuracy, priority, a type of requested γ emission data and a specifics of the motivation related to the fusion reactor technology. It is seen that a majority of requests covers the incident neutron energies from the thermal point up to 15 MeV, requested accuracy is generally 15% and priority is specified mostly as 2. A great deal of requests is limited to fast neutrons only. The majority of requests call for the total γ ray production cross sections as well as the γ ray spectral distributions. The motivation is generally related to calculations of nuclear γ ray heating and shielding.

Apart from the last two subjects reviewed in detail at the 1978 meeting by Seki [18] and Abdou [19], the motivation includes also some less frequent points. Among them are radiation damage and transport calculations that partly use particle production cross sections obtained from the accompanied γ emission data.

Another important issue is the energy balance of the evaluated nuclear data libraries. It has been stressed earlier by Bhat [20], Fu [5] and quite recently again by Gohar [15] that the γ emission data should be included into the evaluated libraries in order to check the energy balance. This point can be best illustrated on the kerma (the kinetic energy released in a material) factors as

TABLE 1. REQUEST LIST OF GAMMA EMISSION DATA FOR FUSION REACTOR TECHNOLOGY (Extracted from WRENDA [12])

Element	E_n (MeV)	Accuracy (%)	Priority	(n,γ) total	$d\sigma/dE_\gamma$	$d^2\sigma/dE_\gamma d\omega$	heating	shielding	other
Li-6	9-15	15	2	x	x		x	x	
Li-7	9-15	15	1	x	x		x	x	
Be-9	8-15	10	2		x				not specified
	3-15	15	2	x	x		x	x	
B-10	.7-15	20	2		x	x	x		
F-19	.5-15	15	2	x	x		x	x	
Na-23	.5-22	10	2	x					activation for FMIT
	22-40	20	2	x					activation for FMIT
Al-27	th-15	15	3	x			x		
Ti	th-15	15		x			x		
V	1keV-2	15	1	x			x		neutron absorption
	14	15	1	x			x		neutron absorption
	.3-15	15	1	x	x		x		
	th-15	10	2	x			x		
Cr	th-15	30	2	x					neutron economy calcul.
	15	15	2	x	x		x		
Fe	th-15	15	2	x			x		neutron economy calcul.
	th-15	15	2	x			x		
	1-15	10	2		x		x	x	
Ni	th-15	30	2	x					neutron economy calcul.
	th-15	10	2	x			x		
Cu	th-.6	15	2	x			x		resolve discrepancies
	15	15	2	x					neutronics calculations
	.5-15	15	2	x	x		x	x	
	th-15	15	2	x	x		x		
Zr	15	15	2	x			x	x	
Nb	1-15	20	2		x	x			radiation damage
	15	15	1	x			x	x	
	1eV-20	20	2	x					resolve discrepancies
Mo	10-15	15	1	x					heavy isotopes accumul.
	th-15	15	1	x			x	x	
	th-15	15	2	x	x		x		neutron balance
Ta	2eV-15	20	2	x	x			x	advanced shielding
Pb	2keV-.6	5	2	x					not specified
	th-15	15	2	x	x		x	x	
	th-15	15	2	x	x		x	x	
Bi	th-15	15	2	x	x		x	x	
Sum=37	18(th-15) 14(fast)			11	20	19	2	25	13
	23(15%)	28(priority 2)							9(n,γ)+5(n,xγ)

used, e.g., in nuclear heating calculations. The neutron kerma factor can be expressed as

$$K(E_n) = \mathcal{G}_{tot}\left(E_n + \sum_i \frac{\mathcal{G}_i}{\mathcal{G}_{tot}} Q_i + \sum_i \frac{\mathcal{G}_i}{\mathcal{G}_{tot}} \overline{E}_i^{dec} - \sum_{\lambda} \frac{\mathcal{G}_i}{\mathcal{G}_{tot}} \overline{E}_\lambda^{n'} - \sum_q \frac{\mathcal{G}_q}{\mathcal{G}_{tot}} \overline{E}_q^\gamma \right), \quad (1)$$

where $\mathcal{G}_{tot}$ is the total cross section. The terms in paranthesis reflect the energy brought into the system (the neutron incident energy E_n, the Q-values of reaction channels and the radioactive decay) and the energy taken out of the system (scattered neutrons and emitted γ rays). Most of the elements of interest for the fusion reactor technology in the ENDF/B5 library suffer from negative $K(E_n)$, violating the energy conservation [15].

Further points of interest with respect to the γ emission data are low energy γ rays ($E_\gamma \lesssim 0.3$ MeV) that are usually not measured but may be of importance for local heating [6,20], high energy γ rays ($E_\gamma \gtrsim 15$ MeV) coming from fast neutron capture and usually omitted in evaluations [21] as well as the data for high energy incident neutrons ($E_n \gtrsim 20$ MeV) needed for non-standard fusion facilities [22].

3. Experimental γ emission spectra

A bulk of the γ ray production data in $(n,x\gamma)$reactions of interest for the present application have been taken by NaI(Tl) spectrometers that are probably still most suitable for measuring full γ emission spectra. In several cases, however, measurements were done with NE 213 liquid scintillators, pair spectrometers and more recently also using BGO spectrometers. These devices have modest or even poor energy resolution, but account effectively for all γ rays of interest what is valuable. On the other hand, high resolution spectrometers, Ge(Li) and HPGe diodes, provide information only about production of distinct discrete γ lines. These data are directly of limited use for the present application, but they are of great interest for testing nuclear model codes for γ ray production. The coincident method based on NE 213-NaI(Tl)

or Ge(Li)-NaI(Tl) spectrometry also provide valuable γ emission data for code testing.

3.1. Systematic measurements

Systematic measurements of γ emission spectra were carried out at 14 MeV incident neutron energy in Los Alamos, Kurchatov Atomic Energy Institute at Moscow and partly also in the Ljubljana University. The most valuable set of data, however, is due to the Oak Ridge measurements in the neutron energy range $E_n \approx 0.1$--20 MeV.

Drake et al. [23] measured γ emission spectra at $E_n \approx 14$ MeV for 15 elements, and more recently Bezotosnyi et al.[24] reported γ spectra for even a more complete set of 27 elements. Though both the Los Alamos and the Kurchatov groups used rather similar experimental techniques, the discrepancies between their data are in several instances quite remarkable : a factor of 2 for Cu and a factor of 1.8 for Ta. This can be drawn from tab.2, where we compare the γ production cross sections, as integrated over the γ ray energies $E_\gamma = 0.5$--8.5 MeV or 0.5--8.0 MeV, of these two major data sets for 10 elements.

TABLE 2. COMPARISON OF GAMMA PRODUCTION CROSS-SECTIONS AT 14 MeV FROM TWO MAJOR DATA SETS
(after Bezotosnyi [24])

Element	$\mathcal{G}_{(n,x\gamma)}$(mb)	
	Drake [23]	Bezotosnyi [24]
Mg	1 400 (170)	1 620 (330)
Al	1 430 (170)	1 860 (310)
Si	1 550 (180)	1 855 (345)
Ti	3 040 (330)	3 920 (650)
Fe	3 160 (350)	4 160 (700)
Cu	2 820 (310)	5 740 (1220)
Mo	4 900 (545)	6 770 (1180)
Ta	4 980 (1000)	9 000 (1830)
U-235	15 380 (1850)	16 600 (2820)
Pu-239	16 330 (2360)	17 060 (2910)

The Ljubljana group have measured high energy parts of γ ray spectra, $E_\gamma \gtrsim 11.5$ MeV, for 28 elements at $E_n = 14$ MeV using a telescopic scintillation pair spectrometer. Their data are summarized in a report by Budnar et al.[25] . These results are of interest since they cover usually omitted γ ray energy range and supplement thus the above two sets of spectra.

An example of the complete γ ray emission spectrum at $E_n = 14$ MeV is given in fig. 2. Shown is $Si(n,x\gamma)$ as collected and evaluated by Hermsdorf [26] . This is probably the first work, where the evaluation of the γ ray spectrum covered the full γ ray energy range including high energy capture γ rays.

The Oak Ridge group measured the γ emission spectra with a large NaI(Tl) spectrometer using a pulsed white neutron source, based on the Oak Ridge linear accelerator, in the neutron energy range $E_n = 0.1-20$ MeV. Their results for 22 elements were collected in a 1977 paper by Dickens et al. [29] . A more recent summary of these measurements reported in 1980 by Larson [30] , see tab. 3, include 27 elements. In 17 instances these data were used in the ENDF/B5 evaluations.

TABLE 3. SUMMARY OF THE OAK RIDGE (n, xγ) MEASUREMENTS OVER THE NEUTRON ENERGY RANGE 0.1-20 MeV AND THE SPECTRAL ENERGY RANGE $0.3 < E\gamma < 10.5$ MeV (after Larson [30])

Element	90°	125°	Used in ENDF/B-V	ORNL Report
Li		X	N	TM-4538
C	X	X	Y	TM-3702
N	X	X	Y	ORNL-4864
O		X	N	ORNL-5575
F		X	Y	TM-4538
Na		X	Y	TM-6281
Mg	X	X	Y	TM-4544
Al	X	X	Y	TM-4232
Si	X	X	Y	TM-4389
Ca		X	Y	TM-4252
Ti		X	N	TM-6323
V		X	Y	TM-5299
Cr		X	Y	TM-5098
Mn		X	Y	TM-5531
Fe		X	Y	TM-5416
Ni		X	Y	TM-4379
Cu		X	Y	ORNL-4846
Zn		X	N	TM-4464
Nb	X		N	TM-4972
Mo		X	N	TM-5097
Ag		X	N	TM-5081
Sn		X	N	TM-4406
Ta	X	X	Y	TM-3702
W		X	Y	ORNL-4847
Au		X	N	TM-4973
Pb		X	Y	TM-4822
Th		X	N	TM-6758

28-Si(N,Xγ) CROSS SECTION (MBARN/MEV)

γ-RAY - SPECTRUM

$E_n = 14$ MEV

DICKENS
CVELBAR
H F MODEL
(n n γ)
(n γ)
γ EXCITON MODEL
(n γ)

ENERGY (MEV)

Fig.2.

Total γ ray spectrum for Si+n at 14 MeV. The experimental data were taken by NaI(Tl) (27) and by the pair spectrometer (25). The curves refer to the statistical model calculations, while the (n,γ) part is purely preequilibrium (28). After Hermsdorf (26).

One way of presenting the γ emission data in the whole neutron energy range of interest is to plot the γ ray production cross section as a function of E_n. This is done for Fe in fig. 3 [31]. This example indicates the existence of a similar problem already exposed in tab. 2 at E_n= 14 MeV: often, there are substantial discrepancies between various data sets. Of interest in the present case are also the evaluated ENDF/B4 and ENDF/B5 data that disagree above $E_n \gtrsim 12$ MeV practically with all measured cros sections.
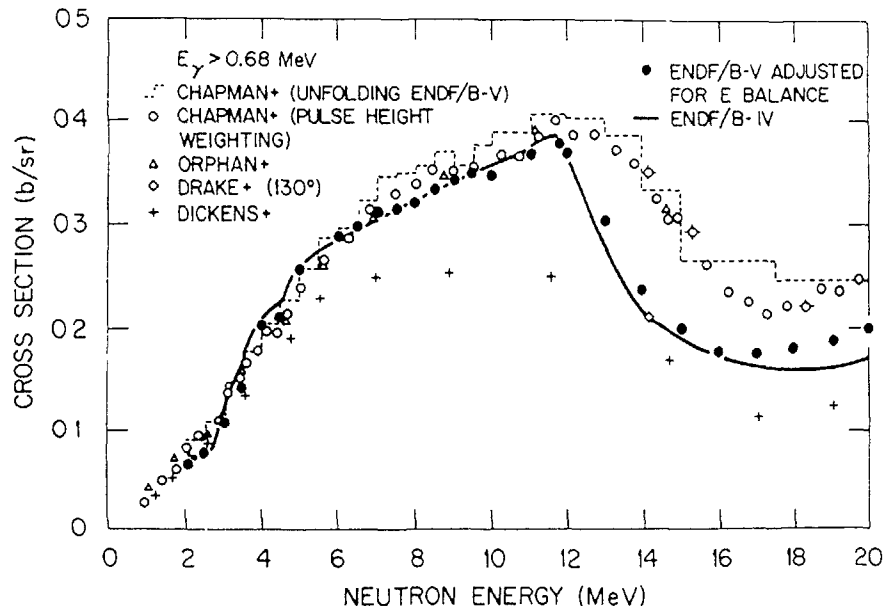
Fig.3.

Gamma ray production cross sections for Fe as a function of the incident neutron energy. The older Oak Ridge data of Dickens were remeasured in Oak Ridge by Chapman. Also shown are evaluated cross sections from ENDF/B4 and B5. After Fu (31).

3.2. Other measurements

Apart from the above works of basic importance for the present application, the Oak Ridge laboratory contributed also by measuring (n,xγ) spectra simultaneously with (n,xn) spectra for 5 elements (Li, Al, Ti, Cu and Nb) [30] using NE 213 spectrometer [32]. Shown in fig. 4 are the γ ray spectra for Cu(n,xγ) at 3 neutron energies. These data demonstrate one of the typical difficulties with many experimental γ ray spectra, namely, the absence of data in the low spectral energy region. In the present case the γ ray energy threshold is set at 1 MeV and lower energies can be accounted for only by model calculations [33].

A growing interest in employing BGO crystals in in-beam γ ray spectroscopy seen in recent years concerns also (n,xγ) reactions. These detectors are advantageous over the NaI(Tl) ones in view of their superior detection efficiency and better peak-to-Compton ratio. A system of five BGO crystals, ∅ 7.6cm x 7.6cm each, was developed by Wender et al. [35] to measure γ ray spectra and angular distributions at the Los Alamos spallation neutron source. So far, they observed γ rays from boron, carbon, calcium and lead. Shown in fig. 5 is production of the 4.44 MeV γ ray in $^{12}C(n,n'\gamma)$ as a function of the neutron energy in the range E_n= 4-100 MeV. In the energy range we are primarily interested in, $E_n \lesssim 15$ MeV, the above γ line represents practically the whole γ ray spectrum.

High resolution γ emission data as measured by Ge(Li) spectrometers provide important additional information to full γ ray emission spectra obtained by scintillation spectrometers. Ideally, one should like to know γ emission spectra specified according to isotope and reaction channel instead of a single full spectrum given by the sum of all channels for all isotopes present in a natural element. In practice, this is very hard to achieve experimentally and one should rather make use of nuclear model codes. High resolution data, i.e., production of discrete γ lines whose origin can often be uniquely identified even for a natural sample, are needed to test model calculations and to fix parameters used in these calculations. Another important justification
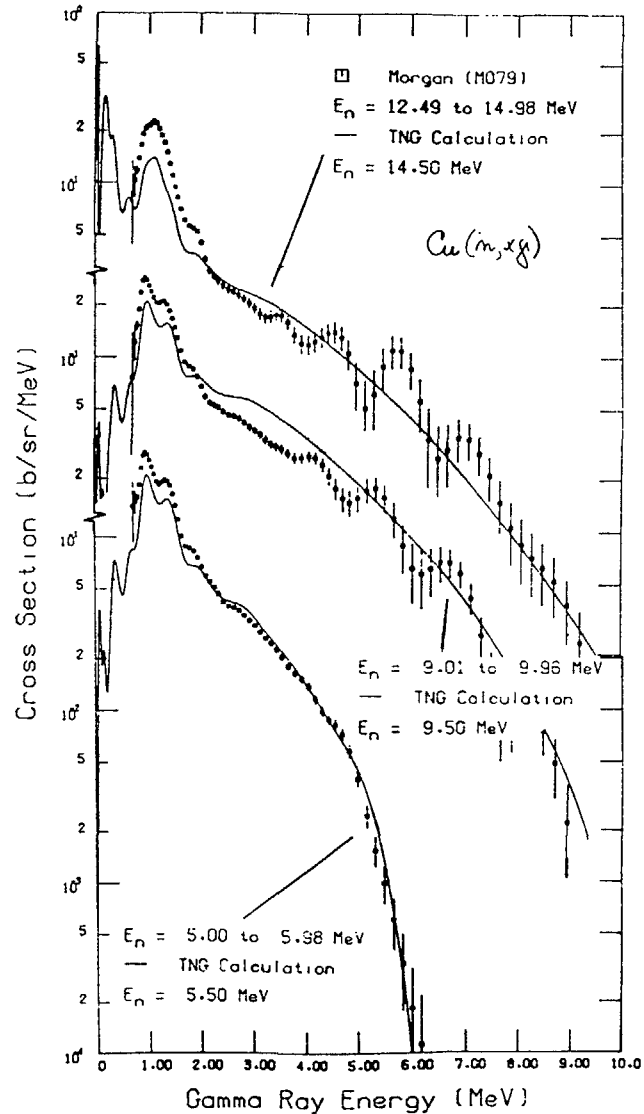
Fig.4. Gamma ray spectra for Cu(n,xγ) at 3 incident neutron energies measured with the NE 213 spectrometer by Morgan (34). Comparison is made with the statistical model calculations using the code TNG. After Hetrick (33).

^{12}C(n,n'γ=4.44 MeV)
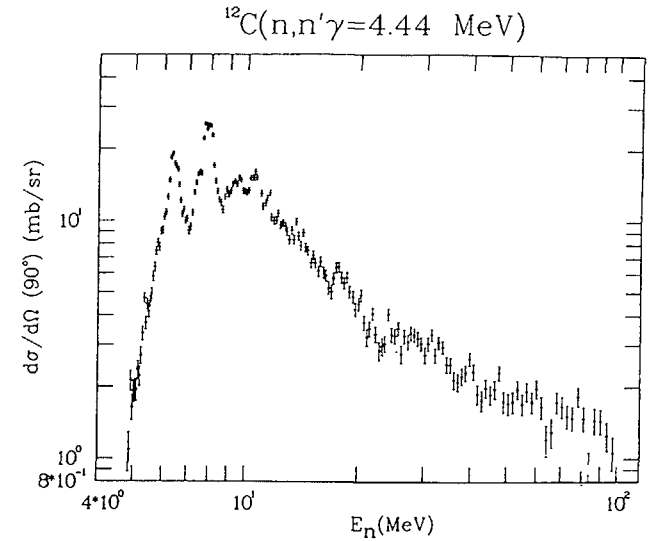
Fig.5. Production cross section of the 4.44 MeV γ ray in 12C(n,n'γ) as a function of the neutron energy in the range 4 - 100 MeV. Use was made of a BGO spectrometer and the LAMPF/WNR spallation neutron source. After Wender (35).
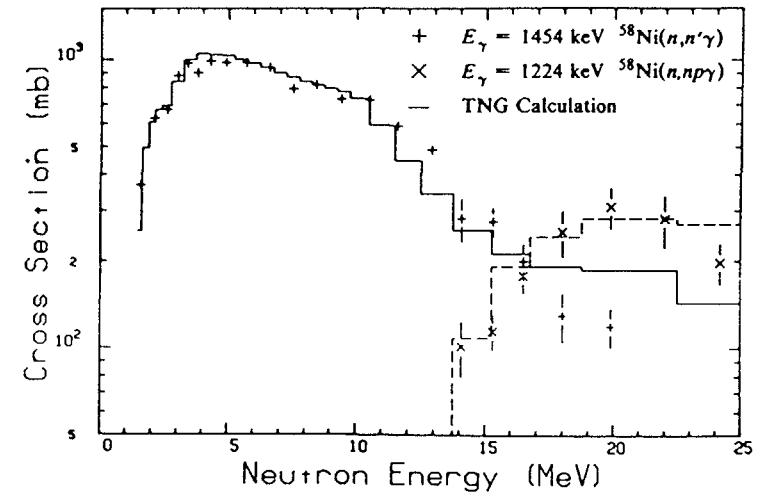
Fig.6. Excitation function for the 1454 keV γ ray from 58Ni(n,n'γ) and for the 1224 keV γ ray from 58Ni(n,npγ). Experimental data are compared with statistical model calculations using the code TNG. After Larson (41).

for these data is information they may bring on tertiary reacti-
on cross sections that are important in fusion reactor design
application but are difficult, if not impossible, to measure
directly.

Production of discrete γ rays in $(n,x\gamma)$ reactions from thres-
hold up to $E_n \lesssim 20$ MeV and their availability in the international
computerized data files have been reviewed recently in refs.[36,37]. Generally, the situation was found to be unsatisfactorial,
though data are more or less available at 14 MeV and measurements
exist for several elements and even isotopes over the whole neu-
tron energy range of interest. For the present application of
most interest are the latter data as measured in several recent
years at Oak Ridge. So far, Larson et al. [38-41] measured on ^{7}Li,
^{56,57}Fe, nat,^{58}Ni, nat,^{53}Cr and Cu. Shown in fig. 6 are the exci-

tation curves for 2 discrete γ rays observed after irradiating
^{58}Ni. Comparison with the statistical model calculations show a
quality of accord that can be achieved between experimental data
and advanced nuclear model codes.

Coincident measurements, such as n-γ using NE 213-NaI(Tl) and
γ-γ using Ge(Li)- NaI(Tl), provide more subtle γ emission data
than can be obtained by simple measuring with a single γ ray spec-
trometer. Coincident data are generally rare and only a very few
measurements were done at 14 MeV. For this purpose a multidetec-
tor arrangement was developed at Bratislava [42] and studied were
basic structural elements nat$_{Fe}$, nat,^{58,60}Ni and ^{52}Cr [43,44].
Shown in fig. 7 is a part of the coincident γ emission data, the
average γ ray multiplicities, as observed in ^{52}Cr$(n,x\gamma)$ reactions
after bombarding highly enriched ^{52}Cr sample with 14.6 MeV neu-
trons. The γ ray multiplicity represents a number of γ rays in a
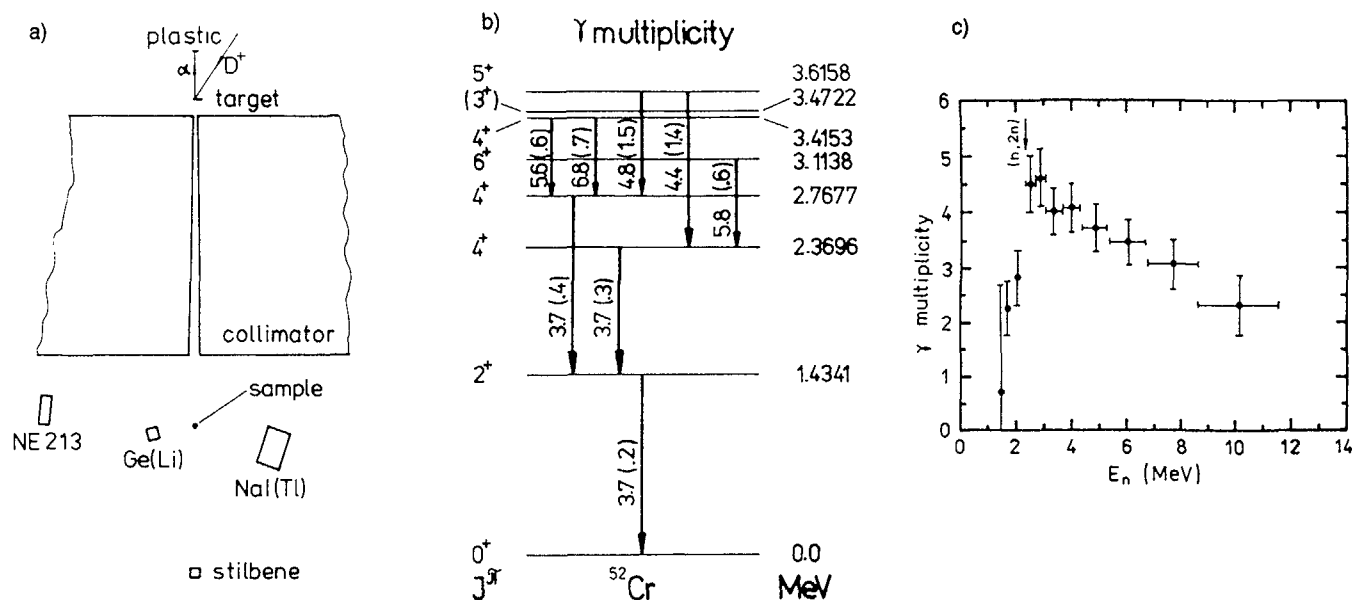
Fig.7. Arrangement for coincident measurements at 14.6 MeV and a part of results obtained for
52Cr(n,xγ). a) Experimental arrangement. b) Average γ ray multiplicities for 8 discrete
γ lines in 52Cr. Given in brackets are uncertainties. c) Average γ ray multiplicity as
a function of the energy of secondary neutrons. Arrow marks the (n,2n) threshold.
After Hlaváč and Obložinský (44).

cascade. Given are the average multiplicities specified either by a single discrete γ ray or by energy of secondary neutron that preceeds the emission of a γ cascade. Although these data do not occur directly on request lists for fusion reactor technology applications, they are of considerable interest especially for testing nuclear model codes dealing with γ ray emission.

3.3. Summary and outlook

Basic experimental data sets of γ emission spectra needed for fusion reactor technology are available both at 14 MeV and at the neutron energy range 0.1-20 MeV. These data are generally more than 10 years old and they are available on elemental rather than isotopic basis. There are cases, where substantial differencies exist between various data sets. Practically no measurements of double differential (angle-energy) γ production cross sections have been performed.

A new generation of experimental γ emission data often provide a more subtle information. These data, however, should be usually viewed rather in the context of nuclear model codes needed in the evaluation process than in terms of simple immediate use for the present application.

It seems that new systematic measurements of γ emission data using scintillation spectrometers should be expected in at least two laboratories. In the near future, the white neutron source at Los Alamos should provide high quality data for fusion energy applications [45,46], and at the Tokyo Institute of Technology a program was started of measurements of γ ray production data at neutron energies from the keV region to 14 MeV for technology applications [47].

4. Theoretical developments

Throughout the nuclear data community there is a growing recognition that calculational methods can and should be used in data evaluations as much as possible [48]. A key theoretical tool for analysis of fast neutron induced cross sections is the unified model of nuclear reactions. This model can be applied to all nuclei of interest except of very light ones, such as [6,7]Li, where the R-matrix approach should help to solve the problem. In several recent years, a considerable progress has been achieved in developing the unified model and in treating the γ ray emission. Given below is a brief account of these developments, and of the present status of nuclear model codes for calculations of γ ray emission spectra.

4.1. The unified model

The model. The unified model includes the Hauser-Feshbach statistical model of nuclear reactions and the preequilibrium exciton model extended to account for angular momentum conservation. Although several attempts in this direction were made already previously, a plausible solution to this problem was reported only recently [49-51].

Following Gruppelaar et al. [50,51] the cross section for a reaction (a,b) can be written in the unified model as

$$\frac{d\sigma}{d\varepsilon}(a,b) = \sum_{J\pi} \sigma_a^{J\pi} \frac{\sum_n W_b^{J\pi}(n,\varepsilon)\tau^{J\pi}(n)}{\sum_{n'} W_{tot}^{J\pi}(n')\tau^{J\pi}(n')} , \tag{2}$$

where $\sigma_a^{J\pi}$ is the compound nucleus formation cross section, $W_b^{J\pi}$ and $W_{tot}^{J\pi}$ stand for the emission rates and $\tau^{J\pi}(n)$ is the mean lifetime of the n-exciton level having quantum numbers $J\pi$. The mean lifetime can be evaluated using the Ansatz

$$\tau^{J\pi}(n) \cong \frac{\sigma_a^{J\pi}}{\sigma_a} \frac{W_{tot}(n)}{W_{tot}^{J\pi}(n)} \tau(n), \tag{3}$$

where $\tau(n)$ is obtained by solving the usual set of non-spin master equations.

Level densities. Uncertainty in the level density typically can represent the largest contribution to the overall uncertainty in a calculated cross section. This viewpoint is fairly recognized and a specialized IAEA meeting was held in 1983 to discuss many current problems of nuclear level densities [52]. In the unified model, two points are of special importance: (i) consistency between particle-hole level density and total level density [53,55], and (ii) spin cut-off factors for particle-hole level densities [54,55].

Probably the best results as regards the above two points have been reported in a recent paper by Fu [55]. The idea is to get a particle-hole level density $\varrho(p,h,U,J)$ that satisfies the consistency condition

$$\sum_{p,h} \varrho(p,h,U,J) = \varrho(U,J), \tag{4}$$

where $\varrho(U,J)$ is the total level density of the Gilbert-Cameron type. In view of eq. (4) one has to find out a proper particle-hole spin cut-off factors and to work out a method leading to the consistency between energy parts of the level densities. An example of the quality of Fu's results is shown in fig. 8. The particle-hole spin cut-off factors averaged over p-h agree well with the spin cut-off factors for the total level density, and the particle-hole level densities summed over p-h and J agree equally well with the energy part of the total level density.

Intranuclear transition rates. An important requisite of any preequilibrium model are intranuclear transition rates. The spin-dependent formulation of these rates for the preequilibrium exciton model have been given recently in ref. [56]. The intranuclear transition rate of a type n → n+2, for example, reads

$$W_{n,3}^{n+2} \equiv W_{n,3}^{\downarrow} = \frac{2\widetilde{x}}{\hbar} |M_n^{n+2}|^2 Y_n^{\downarrow} X_{n,3}^{\downarrow}, \tag{5}$$

where $Y_n^{\downarrow}$ represents the energy part of the density of accessible final states and $X_{nJ}^{\downarrow}$ keeps all spin dependence of the process.

105
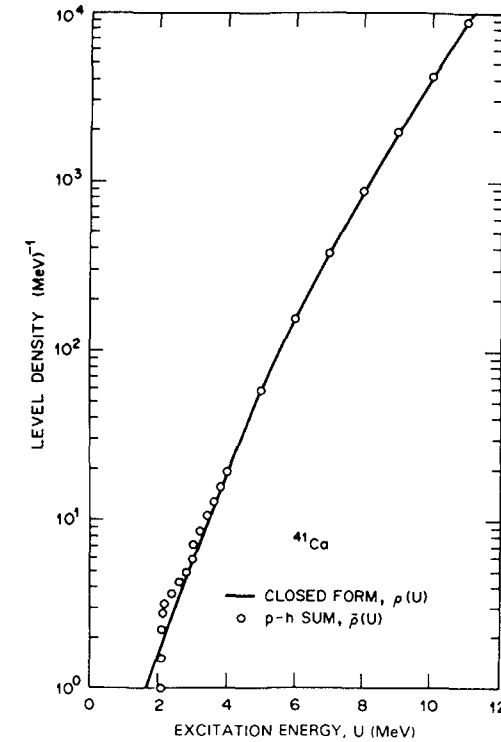
Fig.8. The particle-hole level density is summed over spins and p-h to compare with the closed-form formula for the total level density. After Fu (55).

The evaluation of X-functions is based on the technique developed by Feshbach et al.[57] extended to spin 1/2 particles in ref.[58].

It was suggested in ref.[56] that the non-spin part of the intranuclear transition matrix element can be expressed as

$$|M_n^{n+2}|^2 = \frac{n+1}{4\langle X_{3J}^{\downarrow}\rangle} \frac{K}{A^3E}, \tag{6}$$

where $\langle X_{3J}^{\downarrow}\rangle$ is averaged over all spins for n = 3, and the term K/A^3E corresponds to the usual parametrization of the matrix element in the non-spin formulation of the preequilibrium exciton model.

As an example of the angular momentum dependence of nucleon emission rates and intranuclear transition rates we show in fig. 9 the widths for ^{56}Fe+n at E_n= 14.6 MeV [56] . The widths, $\Gamma = \hbar W$, shown there for neutron emission and intranuclear transitions demonstrate weak dependence on the spin J. The dependence is indeed weak with the exception of the intranuclear transitions for n = 1. This supports the mean-lifetime Ansatz as given by eq.(3).
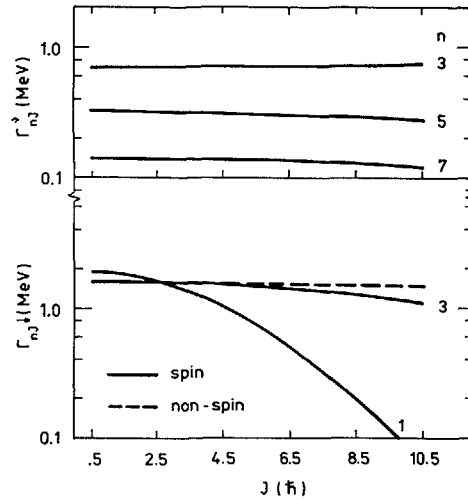
Fig.9. Preequilibrium neutron emission widths (above) and intranuclear transition widths n→n+2 (below) for 56-Fe+n at 14.6 MeV as functions of the angular momentum. After Obložinský (56).

4.2. Gamma ray emission

Preequilibrium γ rays. Important developments have been achieved very recently in solving the problem of preequilibrium γ ray emission. First, a plausible formulation of the preequilibrium γ ray emission was proposed by Akkermans and Gruppelaar [59] . It overcomes the inconsistency with equilibrium limit inherent in the ear-

lier formulation by .Běták and Dobeš [28] . Secondly, the full spin-dependent formulation of the preequilibrium γ ray emission rate was worked out by Obložinský [56] . This rate for the electric dipole γ rays, $\lambda = 1$, reads

$$W^{\gamma}_{m\mathfrak{I}}(EJ \xrightarrow{\mathcal{E}\lambda} \mathcal{U}S) = \frac{\mathcal{E}^2 \, \sigma^{abs}_{g.s.}(\mathcal{E})}{3\pi^2 \hbar^3 c^2} \, \frac{\rho(m-2,\mathcal{U},S)\, b^{m\mathfrak{I}}_{m-2S} + \rho(m,\mathcal{U},S)\, b^{m\mathfrak{I}}_{m\,S}}{\rho(m,E,\mathfrak{I})} \qquad (7)$$

where b-factors are the branching ratios for the inverse process, i.e., the γ ray absorption. The non-spin branching ratios are given as

$$b^{m}_{m-2} = \frac{g^2 \mathcal{E}}{g^2 \mathcal{E} + g(m-2)} \quad , \quad b^{m}_{m} = \frac{g\,m}{g^2 \mathcal{E} + g\,m} \quad , \qquad (8)$$

and the angular-momentum coupling terms of the type

$$\hat{\jmath}_1 \, \hat{\lambda} \, \hat{\jmath}_2 \, \hat{\mathfrak{I}} \begin{pmatrix} j_2 & \lambda & j_1 \\ \frac{1}{2} & 0 & -\frac{1}{2} \end{pmatrix}^2 \begin{Bmatrix} j_2 & j_3 & S \\ \mathfrak{I} & \lambda & j_1 \end{Bmatrix}^2 \quad , \qquad (9)$$

$\hat{\jmath} = 2j+1$, should be added to account for the angular momentum conservation.

Shown in fig. 10 are the preequilibrium γ ray emission rates, $\Gamma^{\gamma}_{n\mathfrak{I}} = \hbar W^{\gamma}_{n\mathfrak{I}}$, for ^{56}Fe(n,$\gamma$) at E_n= 14.6 MeV as functions of the angular momentum J. Seen is the dominance of the lowest n-exciton levels both in terms of the absolute γ emission intensity and importance of the angular momentum coupling.

The corresponding preequilibrium γ ray spectrum shown in fig. 10 accounts well for the fast neutron radiative capture. This represents 2 orders of magnitude improvement over the standard statistical model (cf. fig. 12). In the (n,nγ) and (n,2nγ) channels, however, where higher n-exciton levels dominate, the difference between the unified model and the standard statistical model should be much smaller or eventually quite negligable. The reason is the consistency of the preequilibrium γ ray emission rate of eq.(7) with the equilibrium limit. Thus, the unified model seems to have a unique capability to become a universal theoretical tool for analysis of full γ ray emission spectra.
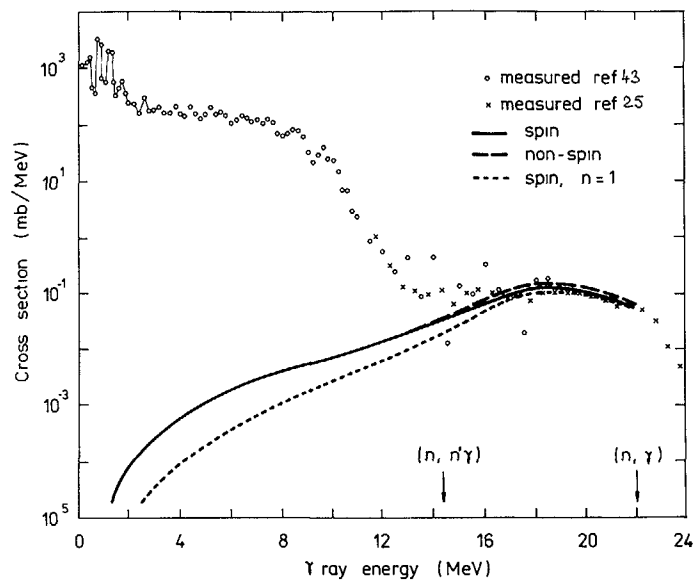
Fig.10. Preequilibrium γ ray spectra as calculated for 56Fe(n,γ) at En = 14.6 MeV are compared with measured cross sections. Arrows mark the end-point energies of γ rays. After Obložinský (56).
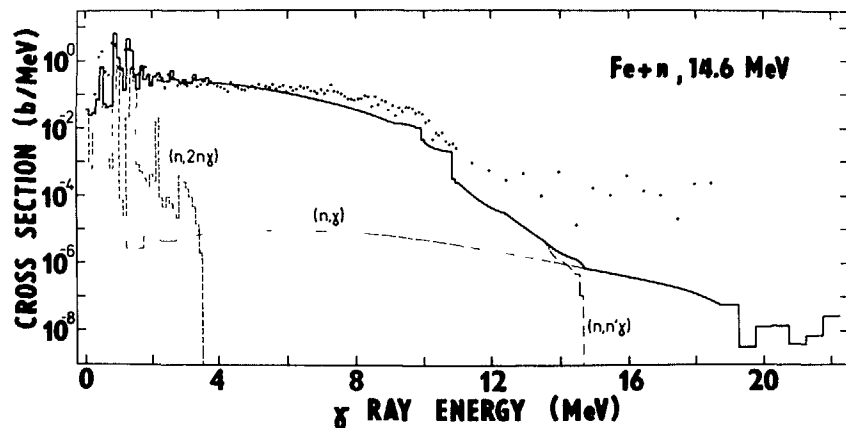
Fig.11. Gamma ray spectrum as calculated for 56Fe+n at En = 14.6 MeV by STAPRE is compared with the experimental data. Calculated components (n,2nγ), (n,n'γ) and (n,γ) are shown separately. After Hlaváč (43).

Gamma ray strength functions. One of the most important parameters that enters the calculations of γ ray emission spectra is the γ ray strength function. In the formulation of eq.(7) this entry goes via the photoabsorption cross section, σ^{abs}, which is proportional to the γ ray strength function. In recent years, detailed systematics for E1 and M1 gamma ray strength functions have been worked out by Gardners at Livermore [61,62]. Thanks to them the predictive capability of model calculations for γ ray emission spectra and γ ray production cross sections was greatly enhanced. In this respect the recent systematics of E1/M1 ratio of γ ray strength functions by Kopecky [63] is also of considerable interest.

4.3. Nuclear model codes

The present status of nuclear model codes, that can be used for calculations of γ emission spectra in (n,xγ) reactions, is summarized in tab. 4. Given is original status and recent modification (if any) for 8 codes: GROGI, STAPRE, GNASH, TNG, PENELOPE, EMPIRE, PEQGM and ALICE. Most of these codes is based on the statistical Hauser-Feshbach model adopted for subsequent emission of several particles (usually 2 is enough), some version of the preequilibrium exciton model, and a more or less complete treatment of γ emission cascades.

The complete tratment of γ cascades, which is of special importance for the present application, considers that the deexcitation process proceeds via transitions of the type continuum-continuum, continuum-discrete level and finally discrete level-discrete level. In several codes, however, discrete levels are not considered and the cascades are treated as if only statistical (continuum-continuum) transitions are present. This inevitably deteriorates low energy parts of the γ emission spectra.

GROGI is the early code developed by Grover and Gilat [64]. Their level densities make use of the yrast level concept, no preequilibrium decay is included. The code has been recently mo-

TABLE 4. NUCLEAR MODEL CODES FOR GAMMA EMISSION SPECTRA
Given are the original status and recent modifications (Refs [64-75])

Program	Authors	Affiliation	Year	Formalism	Comments
GROGI	Grover,Gilat Kitazawa	BNL,Upton TIT,Tokyo	1967 1983	multiple H-F γ cascade	yrast dens., no preeq.decay improved level densities
STAPRE	Uhl,Strohmaier	IRK,Wien	1976 1981	multiple H-F exciton full γ cascade	only equilibrium JX distrib.
GNASH	Young,Arthur Arthur,Kalbach	LASL,Los Alamos	1977 1986	multiple H-F exciton full γ cascade	close to STAPRE released JX conservation, of interest to high E_n
TNG	Fu Shibata,Fu	ORNL, Oak Ridge	1980 1986	multiple H-F exciton full γ cascade	unified concept, several evaluations for ENDF preeq.γ,consistent densities
PENELOPE	Fabbri, Reffo	ENEA,Bologna	1980 1985	multiple H-F exciton JX full γ cascade	unified concept preequilibrium γ included
EMPIRE	Herman	INR,Warsaw	1986	multiple H-F hybrid g.d. full γ cascade	no preequilibrium γ
PEQGM	Běták,Dobeš	IP SAS Bratislava	1983	evaporation exciton γ cascade	preequilibrium γ included
ALICE	Blann	LLNL,Livermore	1986	evaporation hybrid γ cascade	of interest to high E_n

multiple H-F = Hauser-Feshbach model adopted for multiple particle emission
evaporation = statistical model without JX conservation
γ cascade = included are statistical transitions only
full γ cascade = included are statistical as well as discrete transitions
exciton = preequilibrium exciton model
exciton JX = preequilibrium exciton model with JX conservation
hybrid = preequilibrium hybrid model (g.d. stands for geometry dependent)

dified by Kitazawa et al.[65] , who used it in analysis of a number of (n,xγ) spectra.

STAPRE [66] and GNASH [67] are more sophisticated codes that already consider the preequilibrium particle decay. They are quite similar conceptually, although STAPRE seems to be a bit more popular among users. In the recent modification of GNASH (ref. 68) the JX conservation was released in order to gain computational speed. This modification is of interest for incident neutrons with very high energies.

TNG by Fu [10] is probably the first code based on the unified concept. It seems, however, that the angular momentum conservation in the preequilibrium part is treated in an oversimplified way. This code has been used in several advanced evaluations of

γ ray emission spectra for the ENDF/B5 library [5] . Recent modification included preequilibrium γ rays and consistent level densities [69] .

PENELOPE by Fabbri and Reffo [70] is based on the unified model. The code seems to be superior for its possibilities to calculate tricky gated spectra and cross sections. It is,however, available only at the home laboratory at Bologna [71] . Recent modification included preequilibrium γ rays.

EMPIRE is the code developed by Herman et al. [72] very recently. It uses preequilibrium geometry dependent hybrid model rather than the exciton model, prequilibrium γ rays are not included.

Two last codes do not consider the angular momentum conservation. The PEQGM by Běták [73] is the extension of the earlier PREEQ

code [74] to multiparticle emission and γ ray emission. The well known ALICE has been recently extended to account for γ ray emission [75] and may be of interest for high energy incident neutrons.

Most of the γ ray emission spectra available at present in the evaluated neutron nuclear data libraries, such as ENDF and ENDL, are not backed by advanced nuclear model calculations [5,76]. Often, these evaluations are more than 10 years old. In more recent evaluations, however, theoretical calculations represent an important part of the evaluation procedure. Thus, for example, in a few recent years, STAPRE was used in the evaluation of the γ emission spectra for Si[26,27], TNG for Fe[31,78], GNASH for Au[79] and PE-NELOPE for Cr[80]. There are cases when theoretical data are clearly prefered in evaluations especially if experimental data are controversial (see, e.g., the Fe γ production data as shown in fig. 3). Theoretical calculations automatically account for the energy balance and can be easily extended, if necessary, to provide isotopic rather than elemental γ emission data.

5. Concluding remarks

We reviewed recent developments in experimental and theoretical γ emission spectra for fusion reactor technology. These data are basically needed for γ ray heating and shielding calculations. We concentrated on fast neutron induced reactions, i.e., (n,xγ) above threshold up to about 20 MeV including fast neutron capture, and did not discuss thermal and resonance capture.

Availability of (n,xγ) data in the evaluated nuclear data libraries is rather limited. Usually, these libraries keep no information on γ production except of low energy neutron (n,γ) data. As a recent example of this type we mention the Japanese JENDL-2 library released in 1984 [60,9]. The (n,xγ) data are systematically included only in the ENDF/B4 and the subsequent ENDF/B5 libraries as well as the Livermore ENDL library.

Most of the evaluated γ emission spectra from (n,xγ) reactions are at present not backed by the advanced nuclear model calculations. This often shows up as the violation of the energy balance as seen on negative kerma factors calculated from the evaluated cross sections. Gamma emission data should be included into the evaluated data files for energy balance checking. Ideally, the evaluations should be isotopic rather than elemental and channel-specific rather than non-elastic only.

In recent years a powerful theoretical tool has been developed for calculations of γ emission spectra in (n,xγ) reactions. It consists of the unified model of nuclear reactions including the pre-equilibrium γ ray emission with the angular momentum conservation as well as the full treatment of γ cascades. Little attention was devoted to calculations of angular distributions of emitted γ rays and this problem should be addressed.

In experiment, a good set of γ emission spectra is still needed at 14 MeV since significant differencies exist between available data sets. Furthermore, the γ emission spectra are based usually on a single 125° point which is multiplied by 4π to get angle-integrated γ production. Thus, it seems useful if angular distributions were measured at least at 14 MeV. High resolution as well as coincident γ emission data are needed to test nuclear model codes and to provide backing for isotopic and channel-specific γ emission data.

REFERENCES

1. ENDF/B4, US evaluated nuclear data file, summary documentation, compiled by D. Garber, Report BNL-17541 (ENDF-201, second edition, October 1975)

2. ENDF/B5, US evaluated nuclear data file, summary documentation, compiled by R. Kinsey, Report BNL-17541 (ENDF-201, third edition, July 1979)

3. Eds. D.E. Cullen and P.K. McLaughlin: ENDL-84, the Lawrence Livermore National Laboratory evaluated nuclear data library in the ENDF-V format, Report IAEA-NDS-11, rev. 4 (IAEA, Vienna 1985)

4. P.C. Young: Nuclear models and data for gamma-ray production, in Proc. Conf. on Nuclear Cross Sections and Technology, Wasington 1975 (NBS Special Publication 425) p. 149

5. C.Y. Fu: Evaluation of photon production data from neutron-induced reactions, in Proc. Workshop on Nuclear Data Evaluation Methods and Procedures (BNL, September 1980), Report BNL-NCS-51363 (1981) p. 753

6. S.T. Perkins, R.C. Haight and R.J. Howerton: A technique for calculation of continuum photon and conversion-electron production cross sections and spectra from neutron-induced reactions, Nucl. Sci. Eng. 57 (1975) 1

7. F.G. Perey: Neutron total, elastic and inelastic scattering and gamma-ray production data, review paper at the IAEA Advisory Group Meeting on Nuclear Data for Fusion Reactor Technology, Vienna, 11-15 December, 1978

8. C.Y. Fu: A consistent nuclear model for compound and precompound reactions with conservation of angular momentum, Report ORNL/TM-7042 (Oak Ridge 1980)

9. Eds. T. Asami and T. Narita: Graphs of evaluated neutron cross sections in JENDL-2, Report JAERI-M 84-052 (JAERI, 1984)

10. G.L. Morgan and F.G. Perey: Cross sections for Nb(n,xn) and Nb(n,xɣ) reactions between 1 and 20 MeV, Report ORNL/TM-5829 (Oak Ridge 1977)

11. Ed. R.E. Chrien: Neutron Radiative Capture (Pergamon Press, Oxford 1984)

12. Ed. V. Piksaikin: World request list for nuclear data, WRENDA 83/84, Report INDC SEC-88/URSF (IAEA, Vienna, November 1983)

13. O.N. Jarvis: Nuclear data needs for fusion reactors, European Appl. Res. Rept., Nucl. Sci. Technology 3 (1985) 127

14. E.T. Cheng: Nuclear data needs for fusion energy development, Fusion Technology 8 (1985) 1423

15. Y. Gohar: Nuclear data needs for fusion reactors, in the Proc. Inter. Conf. on Nuclear Data for Basic and Applied Science, Santa Fé 1985, Radiation Effects 92 (1986)

16. Y. Kanda: Review on nuclear data for fusion reactors, in the Proc. of Specialists' Meeting on Nuclear Data for Fusion Neutronics, eds. S. Igarasi and T. Asami, Report JAERI-M 86-029 (JAERI, Tokai 1986) p. 3

17. H. Maekawa et al.: Data requests for the JENDL-3, see ref. 12, Report JAERI-M 86-029 (JAERI, Tokai 1986) p. 192

18. Y. Seki: Review of nuclear heating in fusion reactors, in Nuclear Data for Fusion Reactor Technology, Proc. IAEA Advisory Group Meeting, Krakow 1978 (eds. A. Lorencz and D.W. Muir, Report IAEA-TECDOC-223, Vienna 1979) p. 31

19. M.A. Abdou: Nuclear data requirements for fusion reactor shielding, see ref. 18, Report IAEA-TECDOC-223 (Vienna 1979) p. 91

20. M.R. Bhat: Evaluated files of nuclear cross sections for fusion reactor calculations, see ref. 18, Report IAEA-TECDOC-223 (Vienna 1979) p. 153

21. G. Longo and F. Fabbri: Production of high energy photons in fast neutron radiative capture, in Proc. Inter. Conf. on Nuclear Data for Basic and Applied Science, Santa Fé 1985, Radiation Effects 92 (1986) 1205

22. Eds. M.R. Bhat and S. Pearlstein, Proc. of the Symposium on Neutron Cross-Sections from 10 to 50 MeV, Upton 1980 (Report BNL-NCS-51245, Brookhaven 1980) vols. 1,2

23. D.M. Drake, E.D. Arthur and M.G. Silbert: More 14-MeV neutron-induced gamma-ray production cross sections, Report LA-5983-MS (Los Alamos 1975)

24. V.M. Bezotosnyi, V.M. Gorbatschev, M.S. Svecov and L.M. Surov: Group and total gamma-ray production cross sections in inelastic scattering of 14 MeV neutrons on various nuclei, Atomnaya Energija 49 (1980) 239

25. M. Budnar, F. Cvelbar, E. Hodgson et al.: Prompt ɣ ray spectra and integrated cross sections for the radiative capture of 14 MeV neutrons for 28 natural targets in the mass region from 12 to 208, Report INDC(YU)-6/L (IAEA, Vienna 1979)

26. D. Hermsdorf: Description of the evaluated nuclear data file 2015 for silicon of the SOKRATOR library, Report INDC(GDR)-20/L (IAEA, Vienna 1982)

27. J.K. Dickens, T.A. Love and G.L. Morgan, Phys. Rev. C10(1974) 958

28. E. Běták and J. Dobeš: Gamma emission in the preequilibrium exciton model, Phys. Lett. 84B(1979)368

29. J.K. Dickens, G.L. Morgan, G.T. Chapman, T.A. Love, E. Newman and F.G. Perey: Cross sections for gamma-ray production by fast neutrons for 22 elements between Z = 3 and Z = 88, Nucl. Sci. Eng. 62(1977)515

30. D.C. Larson: ORELA measurements to meet fusion energy neutron cross section needs, in Proc. Symp. on Neutron Cross-Sections from 10 to 50 MeV, Upton 1980 (eds. M.R. Bhat and S. Pearlstein, Report BNL-NCS-51245, Brookhaven 1980) p. 277

31. C.Y. Fu: Summary of ENDF/B5 evaluations for carbon, calcium, iron, copper, and lead and ENDF/B5 revision 2 for calcium and iron, Report ORNL/TM-8283, ENDF-325 (Oak Ridge 1982)

32. G.L. Morgan, T.A. Love and F.G. Perey: An experimental system for providing data to test evaluated secondary neutron and gamma-ray production cross sections over the incident neutron energy range from 1 to 20 MeV, Nucl.Instr.Meth. 128(1975)125

33. D.M. Hetrick, C.Y. Fu and D.C. Larson: Calculated neutron-induced cross sections for 63,65-Cu from 1 to 20 MeV and comparisons with experiments, Report ORNL/TM-9083, ENDF-337 (Oak Ridge 1984)

34. G.L. Morgan: Cross sections for the Cu(n,xn) and Cu(n,xγ) reactions between 1 and 20 MeV, Report ORNL-5499 (Oak Ridge 1979)

35. S.A. Wender, G.F. Auchampaugh, J.F. Wilkerson, N.W. Hill, L.R. Nilsson and N.R. Roberson: A high-energy gamma-ray detector system for fast neutron-induced reactions, Report LA-UR-83-2243 (Los Alamos 1983)

36. P. Rose, T. Borrows and J. Tuli: An example of nuclear data services for geophysical applications, paper presented at the IAEA Consultants' Meeting on Nuclear Data for Applied Nuclear Geophysics, Vienna, April 7-9, 1986, to appear in Inter. J. Nucl. Geophys.

37. P. Obložinský and S. Hlaváč: Discrete γ ray production in (n,xγ) reactions for applied nuclear geophysics, invited talk at the IAEA Consultants' Meeting on Nuclear Data for Applied Nuclear Geophysics, Vienna, April 7-9, 1986, to appear in Inter. J. Nucl. Geophys.

38. D.C. Larson: High-resolution structural material (n,xγ) production cross sections for En from 0.2 to 40 MeV, in Reports to the DOE nuclear data committee, DOE/NDC-36/U(1985) p. 130

39. Z.W. Bell, J.K. Dickens, D.C. Larson and J.H. Todd: Neutron-induced gamma-ray production in 57-Fe for incident neutron energies between 0.16 and 21 MeV, Nucl.Sci.Eng. 84(1983)12

40. G.G. Slaughter and J.K. Dickens: Gamma-ray production due to neutron interactions with copper for neutron energies between 0.7 and 10.5 MeV, Nucl. Sci. Eng. 84(1983)395

41. D.C. Larson: High-resolution structural material (n,xγ) production cross sections for 0.2 < En < 40 MeV, Radiation Effects 92(1986)

42. S. Hlaváč and P. Obložinský: A multidetector setup for (n,xnγ) studies at 14 MeV, Nucl. Instr. Meth. 206(1983)127

43. S. Hlaváč and P. Obložinský: Gamma ray production cross sections and gamma ray multiplicities from Fe and Ni bombarded with 14.6 MeV neutrons, Report INDC(CSR)-5/GI(IAEA, Vienna 1983)

44. P. Obložinský and S. Hlaváč: Coincident in-beam measurements on 52-Cr bombarded with 14.6 MeV neutrons, in Report INDC(CSR)-6/GI (IAEA, Vienna 1986) p. 17

45. R.C. Haight, private communication (1986)

46. P.W. Lisowski, C.D. Bowman and S.A. Wender: Status of the WNR/PSR facilities, in Reports to the DOE nuclear data committee, DOE/NDC-38/U (Brookhaven 1986) p. 93

47. M. Igashira, H. Kitazawa and N. Yamamuro: A heavy shield for the gamma-ray detector used in fast neutron experiments, Nucl. Instr. Meth. A245(1986)432

48. M.A. Gardner: Calculational tools for the evaluation of nuclear cross-section and spectra data, Santa Fé 1985, Radiation Effects 92(1986)1481

49. G. Reffo and F. Fabri: Neutron capture in the frame of the unified exciton model, in Proc. Inter. Conf. on Nuclear Reaction Mechanisms, Varenna 1985 (ed. E. Gadioli, University Milano 1985) p. 63

50. H. Gruppelaar, J.M. Akkermans and Shi Xiangjun: A unified angular-momentum conserving model for precompound and compound emission, Report ECN-86-134 (Petten 1986)

51. Shi Xiangjun, H. Gruppelaar and J.M. Akkermans: Effects of angular-momentum conservation in unified pre-equilibrium and equilibrium reaction models, Report ECN-86-133 (Petten 1986) and submitted to Nucl. Phys. A

52. Ed. M.R. Bhat, Proceedings of the IAEA Advisory Group Meeting on Basic and Applied Problems of Nuclear Level Densities, Report BNL-NCS-51694 (Brookhaven 1983)

112

53. H. Gruppelaar: Level density in unified preequilibrium and equi-
librium models, see ref. 52, in Report BNL-NCS-51694 (Brookha-
ven 1983) p. 143

54. G. Reffo and M. Herman: Spin distribution of exciton levels
for spherical nuclei, Lett. Nuovo Cimento 34(1982)261

55. C.Y. Fu: Simplified spin cutoff factors for particle-hole le-
vel densities in precompound nuclear reaction theory, Nucl.
Sci. Eng. 92(1986)440

56. P. Obložinský: Preequilibrium 𝛾rays with angular momentum
coupling, Phys. Rev. C35(1987)407

57. H. Feshbach, A. Kerman and S. Koonin: The statistical theory
of multi-step compound and direct reactions, Ann. Phys.(N.Y.)
125(1980)429

58. M. Herman, A. Marcinkowski and K. Stankiewicz: Statistical and
multi-step compound emission in (n,2n) reactions, Nucl. Phys.
A430(1984)69, erratum Nucl. Phys. A435(1985)859

59. J.M. Akkermans and H. Gruppelaar: Analysis of continuum gamma-
ray emission in precompound-decay reactions, Phys. Lett. 157B
(1985)95

60. Ed. T. Nakagawa: Summary of JENDL-2 (Japanese Evaluated Nuc-
lear Data Library) general purpose file, Report JAERI-M 84-
103 (JAERI, Tokai 1984)

61. D.G. Gardner: Current status of fast neutron capture calcula-
tions, in Proc. NEANDC/NEA CRP Specialists' Meeting on Fast
Neutron Capture Cross Sections, Report ANL-83-4(Argonne 1983)
p. 67

62. D.G. Gardner: Methods for calculating neutron capture cross
sections and gamma-ray energy spectra, in Neutron Radiative
Capture, ed. R.E. Chrien (Pergamon, Oxford 1984) p. 62

63. J. Kopecky: Averaged neutron capture data and their applicati-
ons to nuclear structure and reaction mechanisms, in Capture
Gamma-Ray Spectroscopy and Related Topics-1984, ed. S. Raman
(American Institute of Physics, New York 1985) p. 318

64. J.R. Grover and J. Gilat, Phys. Rev. 157(1967)802

65. H.Kitazawa et al.: Calculation of gamma-ray production cross
sections at neutron energies of 1 - 20 MeV, Nucl. Sci. Tech.
20(1983)273

66. M. Uhl and B. Strohmaier: Program manual for STAPRE code, Re-
port N.E.A. Data Bank (Gif sur Yvette 1981)

67. P.G. Young and E.D. Arthur: GNASH, a preequilibrium-statistic-
al nuclear model code for calculation of cross sections and
emission spectra, Report LA-6947 (Los Alamos 1977)

68. E.D. Arthur and C. Kalbach-Walker: Improvements to the GNASH
nuclear model code, in Reports to the DOE Nuclear Data Commit-
tee, DOE-NDC-38/U (Brookhaven 1986) p. 100

69. K. Shibata and C.Y. Fu: Recent improvements of the TNG statis-
tical model code, Report ORNL/TM-10093 (Oak Ridge 1986)

70. F. Fabbri and G. Reffo: PENELOPE, a FORTRAN-IV code for multiple
particle and gamma-ray cascades up to 50 MeV, Bologna 1980,
unpublished

71. G. Reffo, private communication (1986)

72. M. Herman, A. Marcinkowski and K. Stankiewicz: EMPIRE, a code
based on the combined preequilibrium/compound nucleus model of
nuclear reactions, Comp. Phys. Comm. 33(1984)373

73. E. Běták and J. Dobeš: PEQGM, a preequilibrium computer code
with gamma emission and multiple particle emission included,
Report IP EPRC SAS, No. 43/83 (Bratislava 1983)

74. E. Běták: Program for spectra and cross-section calculations
within the preequilibrium model of nuclear reactions, Comp.
Phys. Comm. 9(1975)92, erratum 10(1975)71

75. M. Blann, G. Reffo and F. Fabbri: Calculation of 𝛾 ray casca-
des in code ALICE, presented at the IAEA CRP Meeting on Methods
of Calculating Fast Neutron Nuclear Data for Structural Mate-
rials, Bologna, October 7-10, 1986

76. R.J. Howerton, private communication (1986)

77. B. Bararragtscha, D. Hermsdorf and E. Paffrath: An approach
for a consistent description of gamma ray spectra from (n,x𝛾)
reactions induced by fast neutrons, J. Phys. G8(1982)272

78. C.Y. Fu and M. Hetrick: Update of ENDF/B5 mod-3: neutron-indu-
ced producing reaction cross sections and energy-angle correla-
tions, Report ORNL/TM-9964, ENDF-341 (Oak Ridge 1986)

79. P.G. Young and E.D. Arthur: Analysis of n + [197]Au cross secti-
ons for En = 0.01 - 20 MeV, in Capture Gamma-Ray Spectroscopy
and Related Topics, Knowville 1984, ed. S. Raman (AIP, New
York 1985) p. 530

80. A. Mengoni, F. Fabbri and G. Maino: Evaluation of gamma-ray
production cross sections and spectra for neutron induced re-
actions on chromium, Report ENEA RT/TIB/86 (Bologna 1986)

STATUS OF EXPERIMENTAL AND THEORETICAL
DOUBLE-DIFFERENTIAL NEUTRON EMISSION DATA

D. SEELIGER
Technical University Dresden,
Dresden, German Democratic Republic

Abstract

The present status of double-differential neutron emission cross section (DDNECS) data for fusion reactor applications is analyzed briefly. First, the request for and availability of DDNECS for fusion reactor purposes is considered. In the following sections, the status for continuous DDNECS at 14 MeV incident energy and below as well as for cross sections of isolated levels will be analyzed for selected nuclei. Finally, a few recommendations concerning the further work in this field are formulated.

---

1. <u>Request and availability of experimental DDNECS for fusion</u>
   <u>reactor purposes</u>

The knowledge of DDNECS at neutron incident energies up to 15 MeV is of principal importance for the neutron transport calculations in the first wall, blanket and shielding of a fusion or fusion-fission-hybrid reactor. Calculational predictions of tritium breeding, breeding of fissile materials, estimates of radiation effects in structural materials and superconductors a.o. directly depend on the quality of neutron transport calculations using the DDNECS data as a fundamental input information.

The table 1 shows typical fusion materials for which DDNECS are required.

Table 1

Fusion Materials for which DDNECS are requested

Component	Elements
Structure	Fe, Cr, Ni, V, Ti, Al, W, Mn, Si
Multiplier	Be, Pb, O
Breedor/Coolant	^{6}Li, ^{7}Li, F, H, O, Pb, He, Be, Al
Shield	Fe, H, O, W, Si, C, Ba, Ca
Hybrid Blanket	Th, U, Pu

Sometimes DDNECS have been requested for fusion reactor purposes also for N, Cu, Zr, Nb, Mo, Ta and Bi.

Following WRENDA 83/84 [1] the highest priority is desired for ^{6}Li, ^{7}Li and ^{16}O data - from 3 % to 15 % within 2...15 MeV incident energy range.

For the other candidates requests are characterized with priority 2 and the accuracy desired is typically 10 % (in some cases 5 % in others only 20 %).

No doubt, the most important DDNECS data for DT-fusion applications are the continuous neutron spectra at 14 MeV incidence energy.

The situation of this experiments was analyzed recently [2], showing, that a remarkable progress was made during the last decade.

At present new experimental programmes are underway at the University Osaka, the Technical University Dresden, the IRK Vienna and in other institutes [3-6]. Resulting from this effort, now for the most of fusion related elements data from at least two independent high-quality experiments are available. The level of agreement between different experiments, however, remains generally in the order of 15...20 % (Differences between experiments usually arise in the high-energy part of the spectra due-to procedures of elastic peak separation and limited resolution but also in the lowest part of the spectra due-to uncertainties of the proton recoil

energy bias.), whereas the quoted level of accuracy, generally, is
in the order of 10...15 %. For Li-isotopes and elements
like B, N, O, F, Ca, V, Mn, Ba a.o. the situation remains uncertain
due-to the limited number of experiments. Generally, the require-
ments for DDNECS data with the highest accuracy (from 3 % to 10 %)
are not met at present. DDNECS data for ^{232}Th and ^{238}U have to be
carefully analyzed taking into account the different reaction
channels contributing to the neutron emission including fission
neutron spectra.

2. DDNECS at 14 MeV for lead

Recently, an attempt was made to improve substantially the
situation for the multiplier material lead by a combination of
differential [7] and integral [8] experiments with calculations
by theoretical reaction models and transport codes.

In fig. 1 the angle-integrated emission spectrum from this experi-
ment is shown in comparison with recent experiments by IRK [4] ,
OSA [5] and the previous TUD-experiment [3] . Taking into
account statistical and systematic uncertainties of the data as
given by the authors, the four measurements are consistent. Compared
with the ENDF/B-IV evaluation the experimentally determined cross
sections are obviously larger. Remarkable more neutrons as evaluated
are observed in the energy range 1.5 MeV $\leq$ E $\leq$ 5 MeV. The deviation
is up to 30 % in the range 2 $\leq$ E $\leq$ 3.5 MeV.
In Fig. 2 the experimental data are theoretically interpreted as
superposition of three components: direct excitations of vibra-
tional modes calculated in DWBA approach, pre-equilibrium and com-
pound-nucleus neutron emission calculated with the Generalized
Exciton Model code AMAPRE and secondarily emitted neutrons of
(n, 2n) calculated with the statistical model code STAPRE. The agree-
ment of the calculated spectrum with the experimental is satisfac-

Fig. 1   Angle-integrated neutron emission cross sections for lead
from different measurements: o [7] , ◊ [3] , + [4] ,△ [6]
and ▽ [5] ; - compared with the ENDFB-IV evaluation ----;
solid line - new recommended experimental data.
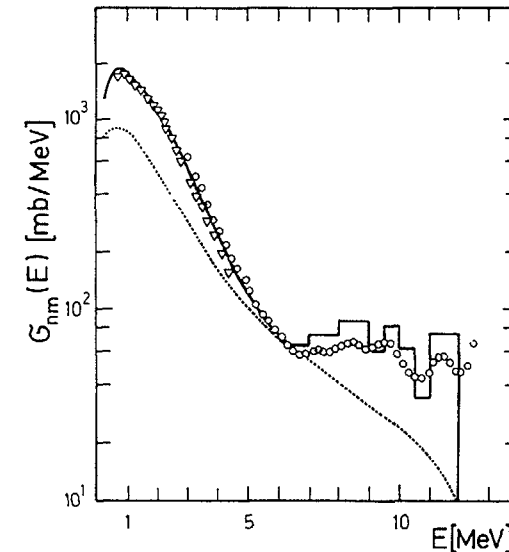
Fig. 2   Theoretical interpretation of the lead neutron emission
spectrum: experimental data - o [7] , ▽ [5] ; dotted line -
first emitted neutron spectrum by Generalized Exciton
Model with AMAPRE, full line - additionally direct
excitations by DWBA method and secondary neutrons included.

tory in the low-energy part. In the high-energy part the neutron
emission is overestimated. The direct component with the averaged
deformation parameters used would alone explain the neutron emission
for E > 8 MeV. But, reducing adequately the pre-equilibrium emission,
discrepancies appear in the middle part of the spectrum where only
the pre-equilibrium component is able sufficiently to describe the
experimental data.

Angular distributions of neutrons emitted from Pb with E = 3.5,
5.5 and 7.5 MeV are presented in Fig. 3. The experimental data
show with increasing E a pronounced forward scattering. In the
ENDF/B-IV evaluation these angular distributions are assumed to
be isotropic. In the measurements of Kammerdiener /9/ and of
Takahashi et al. /5/ the increase of the incidence neutron energy
E_0 by about 1.5 MeV going from backward to forward angles has the
tendency to overestimate the forward-peaking. The theoretically
obtained angular distributions describe the present experimental
data at E = 5.5 MeV satisfactory. At E = 3.5 MeV they deviate for
$\vartheta \leq 30°$ and at E = 7.5 MeV the sum of the calculated direct col-
lective excitations and of the pre-equilibrium emissions over-
estimates the neutron emission as discussed for the angle-inte-
grated spectrum.

The good consistency between all the experiments at the one side
and between data averaged over experimental points and theoretical
curves at the other side leads to the conclusion that now for lead
the DDNECS at 14 MeV are in a quite good shape. This conclusion,
additionaly, is supported by the results of the integral experi-
ments with lead spheres [8] .

Double-differential spectra at 90° and integral spectra for lead
could, therefore, be used as a reference for proving the methods
used in further DDNECS measurements. But, even in this case the
uncertainties achieved are between 5 % and 10 %, i.e. still some-
what higher than it is requested for fusion reactor calculations.
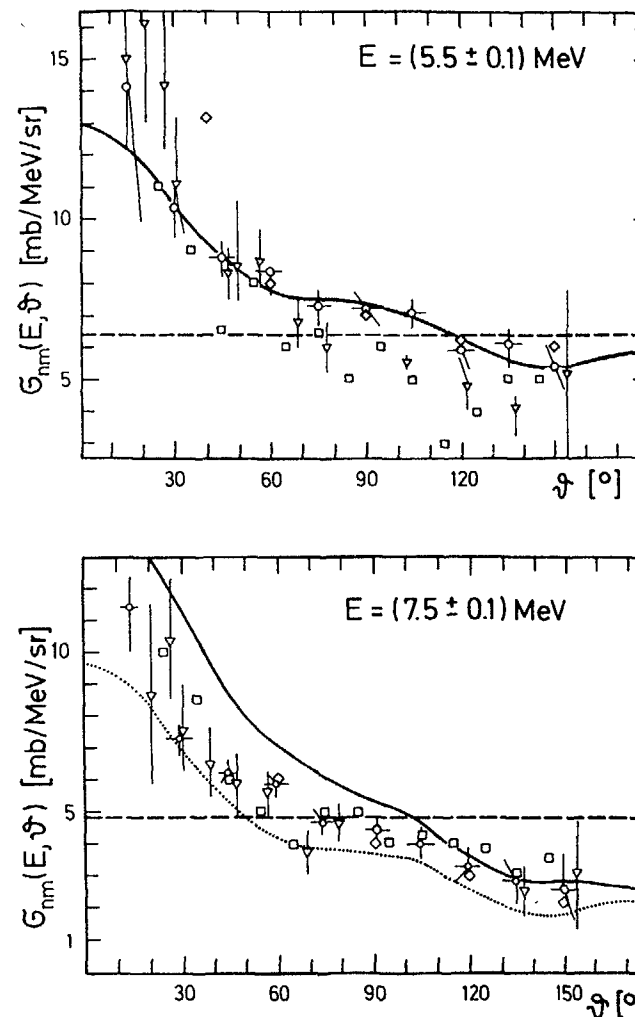
Fig. 3 Angular distributions of neutrons emitted from Pb + n in
the emission energy intervals inserted; experimental data -
o [7] , □ [9] , ◇ [3] and ▽ [5] ; evaluated data -
dashed line represents ENDF/B-IV; theoretical curves - full
line for pre-equilibrium plus equilibrium components,
dotted line - first neutron emission only.

3. <u>DDNECS below 14 MeV for niobium</u>

For fusion reactor calculations in the whole incident energy range
up to about 15 MeV DDNECS for the most important structural,
blanket and shielding materials are needed. For medium and heavy
nuclei continuous emission spectra occur above 5...6 MeV incident
energy. Below this energy level there was a lot of experimental
information obtained about the excitation of isolated levels by
inelastic scattering for fission reactor programmes. However,
between 7 and 14 MeV there is still a gap of experimental informa-
tion on DDNECS. The only exception is the nucleus ^{93}Nb (and to
less extend ^{56}Fe), for which experimental spectra are available at
seven incident energies between 5 MeV and 25 MeV [3,5,9,10-12] .
Furthermore, for ^{93}Nb + n an extensive inter-comparison of computer
codes was carried out by Gruppelaar and Nagel, recently [13] .
From this situation the following conclusion can be drawn for the
further work on nuclear data for fusion reactor applications:

- New measurements of DDNECS below 14 MeV hardly can give the
  full information needed. This time-consuming measurements can
  be carried out at tandem-accelerators only, using complicated
  spectroscopic technique as well as data routing methods. At
  present, only a few groups are working in this field.

- Therefore, most of the information on DDNECS needed for
  fusion reactor purposes must be obtained by theoretical inter-
  polation between experiments at 14...15 MeV and the region of
  a few MeV, where only isolated levels occur in the emission
  spectra.

- Though, niobium is not a first choice fusion material, due-to
  the experimental situation mentioned above, the case ^{93}Nb + n
  is a very suitable one for testing the applicability of
  different models and computer programmes for the interpolation
  along the energy scale (Of course, as an other important case
  ^{56}Fe + n should be considered also). At the other side, for
  14...15 MeV spectra the mass number dependence of different
  model predictions could be tested. In this way the most suitable
  theoretical approaches could be selected for the calculation of
  the main body of missing information on DDNECS.

Let me show a few results of such investigations for ^{93}Nb + n [14] .
At fig. 4. Experimental neutron emission spectra at 9.0 MeV,
12.3 MeV and 14.6 MeV are shown in comparison with theoretical
analyses including the exciton model plus Hauser-Feshbach calcula-
tions. In this way the highest part of the spectra cannot be des-
cribed very well due-to the presence of direct collective excita-
tions in (n n') reactions. The discrepancies between theory and
experiment become even higher at lower energies. This is shown
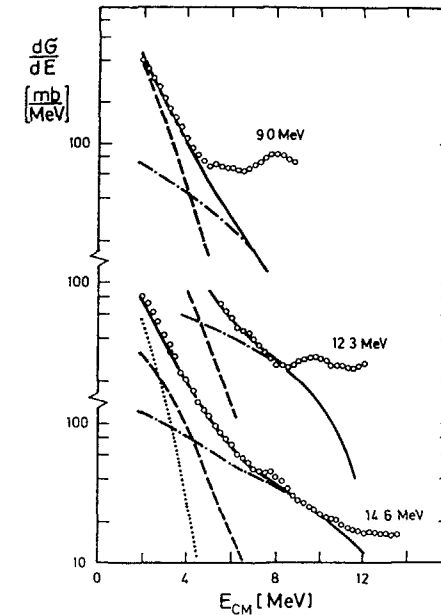
Fig. 4 Angle-integrated neutron emission cross sections for
niobium at 9.0 MeV, 12.3 MeV and 14.6 MeV incidence energy;
experiments are taken from [3,10] ; theoretical description
shows pre-equilibrium and equilibrium contribution calculated
with the exciton model and HF-Theory [14] .

clearly at fig. 5, where beyond the experimental points at 7 MeV
and 9 MeV are shown typical curves of pre-equilibrium contributions
with reasonable parameter variations (dotted and full lines) and
the difference between calculated equilibrium emission and experi-
ment (step function). Calculated pre-equilibrium spectra neither in
shape nor in the absolute height are able to explain the step
functions! If direct collective excitations calculated by the DWBA
method [15] are included the shape of neutron emission spectra
at 14 MeV can be explained - this is shown on fig. 6. But about the
same quality of agreement can be obtained, if instead of using the
DWBA-method phonon excitations are included into the generalized
exciton model [16] . These and other approaches should be compared
carefully over incident energy and target mass number for making

Fig. 6   Angle-integrated neutron emission cross section for niobium
          at about 14 MeV incidence energy; experiments: • - UCRL,
          1972 [9] , o - TUD, 1975 [3] , ■ - PEI, 1971; theory:
          dotted step function - averaged DWBA calculation [15] ;
          dashed line - HF-calculation; full step function - sum of
          both components; full line - calculation with a Generalized
          Exciton Model including phonon excitations [16] .

Fig. 5   Angle-integrated neutron emission cross sections for
          niobium at 7.0 MeV and 9.0 MeV [10] ; full and dotted lines
          represent exciton model calculations with reasonable
          parameter veriations and the step function is the difference
          between this calculations and experimental points [14] .

final conclusions. In the computer code and model intercomparison
by Gruppelaar and Nagel [13] the high energy part was not consi-
dered especially for this effect which becomes even more pronounced
at lower energies.

4. Status of fast neutron scattering on Li-isotopes

Several systematical measurements of neutron scattering cross
sections have been carried out in the last years on light
nuclei being of interest for neutronics and tritium breeding
in possible thermonuclear reactor designs. Of special interest

118 are the two lithium isotopes, since neutron interactions with
them produce tritium via the reactions $^6Li(n,t)^4He$ (Q= +4.784 MeV)
and $^7Li(n,t)n^4He$ (Q= -2.467 MeV). Accurate and systematic data of
neutron scattering cross sections for those elements are important
also for reliable calculations of the neutron transport in the
fusion reactor blanket.

The neutrons produced by ^6Li+n and ^7Li+n interactions are coming
from a variety of reactions as described in detail by Batchelor
and Towle[17]. The resulting emission spectra, which contain both
peaks and continuum, are complicated and require for cross section
determination an advanced level of experimental technique as well
as a careful data evaluation. In the works concerning neutron
interactions with ^6Li and ^7Li, mostly the elastic and inelastic
(Q= -2.185 MeV) scattering from ^6Li as well as the sum of the

elastic scattering and unresolved inelastic scattering to the
0.48 MeV excited state and the inelastic scattering (Q= -4.63 MeV)
from ^7Li have been measured. Thus, partial cross sections related
to these reaction channels are reasonably well known, but systematic
data for the inelastic scattering to other excited states or double-
differential cross sections of the continuum are practically not
published.

In the energy range below 14 MeV a number of experimental results
have been reported covering more or less completely this energy
region. But there are some differences which may be caused by the
different experimental techniques used.

In figs. 7 and 8 angle-integrated cross sections of the neutron
scattering on ^6Li and ^7Li are shown covering the incident energy
region between 6 and 14 MeV [17-30]. A comparison of differential
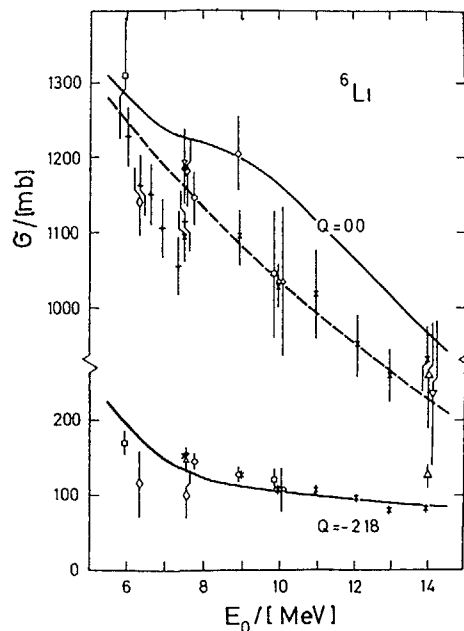
Fig. 7 Angle-integrated elastic and inelastic cross sections for
^6Li in the energy range between 6 MeV and 14 MeV [31].
Experimental data taken from refs. [17-30]. Solid line -
ENDF/B-IV, dashed line - ENDF/B-V.
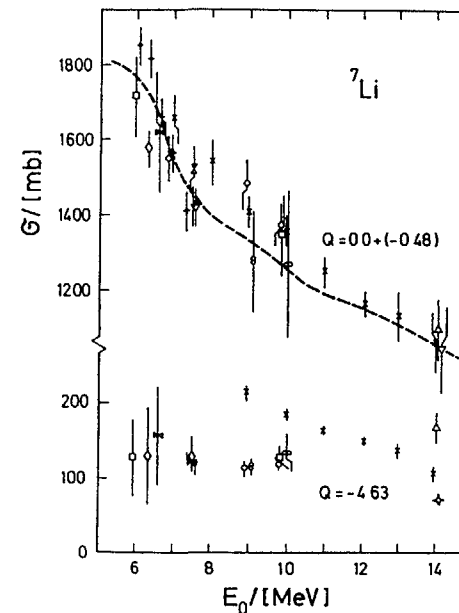
Fig. 8 The same as fig. 7 but for ^7Li.

data at bombarding neutron energies arround 14 MeV had been carried
out for the elastic scattering on ^{6}Li and ^{7}Li recently [30] .
A further comparison of differential data for ^{6}Li and ^{7}Li is
shown on figs.[7 - 11] in the energy range between 7 and 10 MeV [31].
From this figures the following conclusions can be drawn:
The elastic scattering data from ^{6}Li and ^{7}Li (here included the
first excited state at Q= -0.48 MeV) are in agreement within 10 %
or less with respect to an averaged value, which could be represented,
for instance, by evaluated excitation functions or averaged

Legendre polynomial fit curves. In the case of inelastic scattering
on ^{6}Li (Q= -2.18 MeV) errors and deviations of the experimental
data are higher, in some cases up to 50 %. But systematic deviations
are estimated to concern more the angle-integrated cross sections,
i.e. the normalization procedure, less the shape of angular distri-
butions. In the case of the ^{7}Li(n,n$_2$) channel the experimental
results are in a rather strong disagreement. The angle-integrated
cross sections differ up to a factor two, and the shape of angular
distributions is also quite different. In order to find reasons for
these deviations some possible error sources are recognized in the
following.

Fig. 9   Differential cross sections for ^{6}Li between 7.47 MeV and
7.75 MeV [31] .
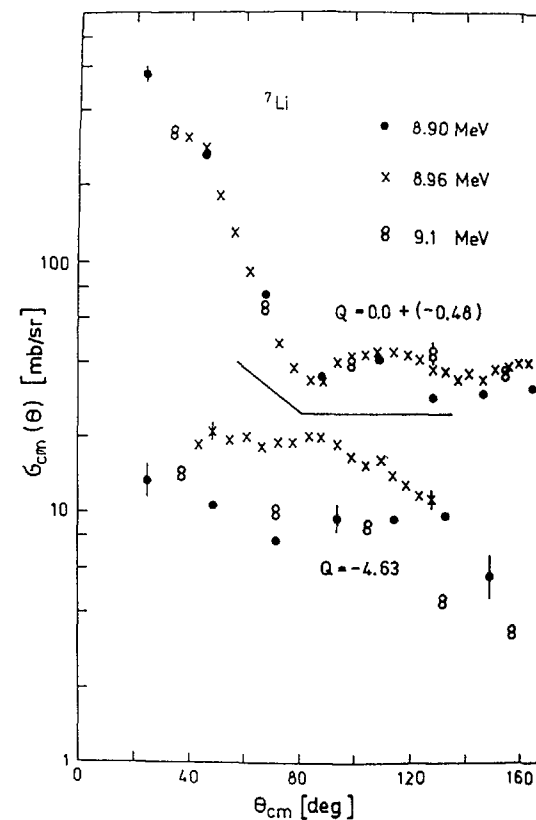
Fig. 10   Differential cross sections for ^{7}Li between 8.9 MeV and
9.1 MeV [31] .
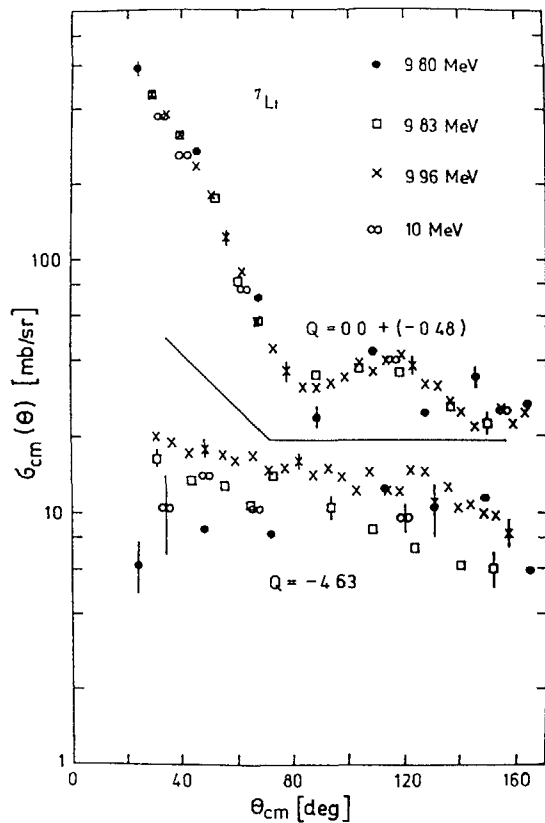
Fig. 11   The same as fig. 10 but around 10 MeV.

At first it should be mentioned the peak separation problem.
Another disturbing influence could be originated by the scattering
of non-monoenergetic neutron lines or groups from the source.
On figs. 12 and 13 the integral cross sections are compared.
The analysis of all data leads to the following conclusion:
In the bombarding energy range between 6 and 14 MeV, there is
a lot of experimental data for the elastic and the first excited
states inelastic neutron scattering on both the lithium isotopes.
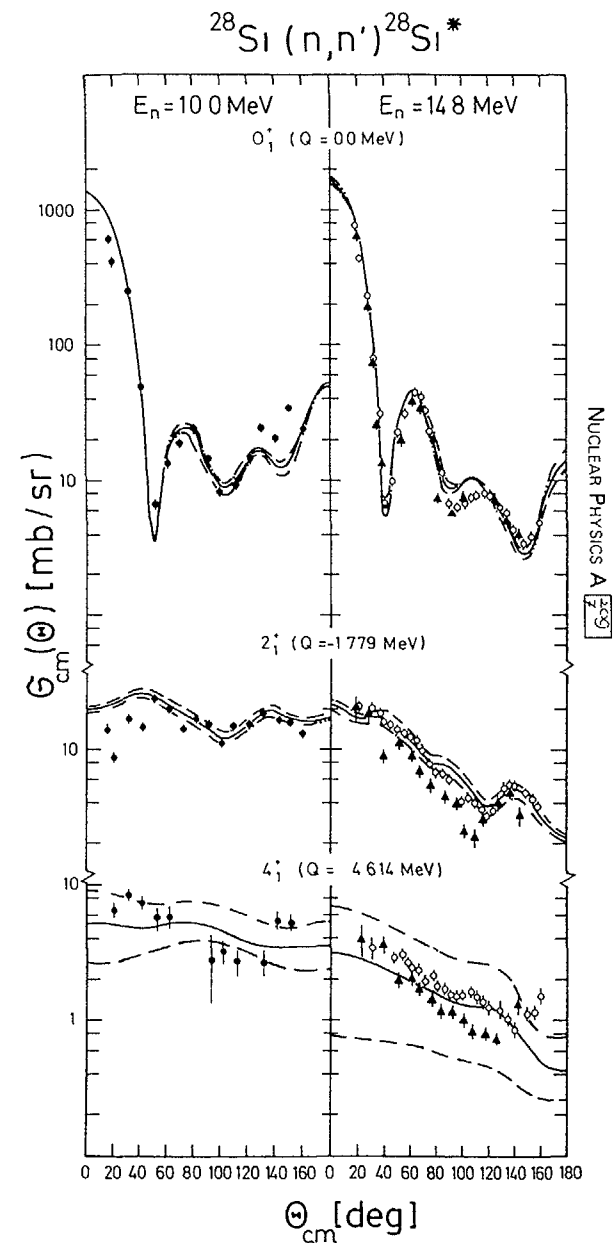
Fig. 12   Differential cross sections for ^{28}Si at 10 MeV and 14.8 MeV
and analysis in the frame of HF-plus CC-theory [34].
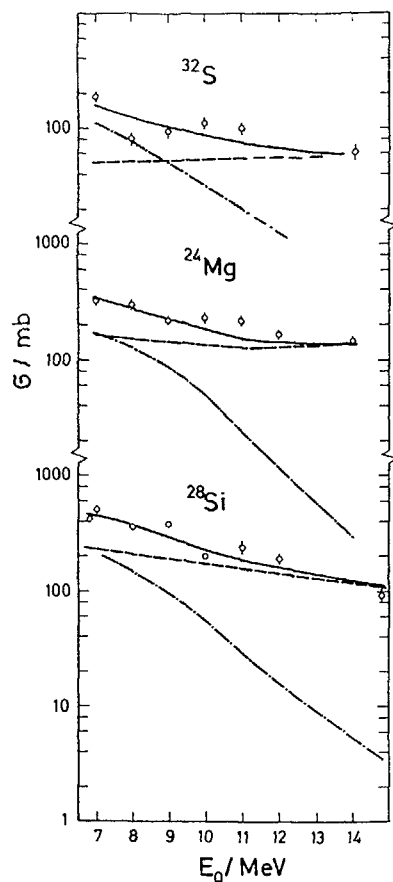
Fig. 13 Excitation functions of the first 2[+] levels for ^{24}Mg, ^{28}Si and ^{32}S in dependence from incident energy; theoretical curves represent direct (dashed line),compound (dash-dotted line) and the sum (full line).

The agreement of elastic differential as well as angle-integrated cross sections is in the order of 10 % or better. For the ^{6}Li(n,n$_1$) reaction channel the deviations are some-what greater, the reason for this seems to lie in the absolute normalization and peak separation problem.
The situation for the ^{7}Li(n,n$_2$) reaction channel is quite unclear up to now. The background relations (neutron continuum from the

investigated isotopes and scattered background) for the different experimental arrangements can be the reason for the deviations pointed out.

Special investigations in the frame of R-matrix theory are necessary for the lightest nuclei, which generally cannot be described by coupled-channels-method or Hauser-Feshbach-Theory.

5. Partial inelastic scattering cross sections for isolated levels

In high resolution tof-measurements of continuous DDNECS [5-7] the contribution of low lying isolated nuclear states is included in the spectra determined experimentally. As described in sec. 2. and 3., this contribution has to be accounted in the theoretical analysis, too. Therefore for fusion transport calculations no special experimental investigations are needed for the determination of partial inelastic scattering cross sections (Of course, their might be other physical reasons for measuring this quantities). This situation concerns generally medium and heavy nuclei. For light nuclei there is a very broad excitation energy region with well-isolated levels, but no or only a small continuous part of the spectra. In this cases a special experimental and theoretical investigation of partial inelastic scattering cross sections is desirable and in most cases of fusion related materials this is done already.

For nuclei with A $\gtrsim$ 12 in the incident energy range of interest (7...15 MeV) for the theoretical analysis the coupled channels method for direct elastic and inelastic excitations and the Hauser-Feshbach-Theory for compound contributions with well-established parameter sets [32] can be used for a calculation, practically free of fitting parameters.(Of course, this standard optical a.o. parameter sets are proved by many other experiments.)

As an example at the next two figures there are shown some experimental results for ^{24}Mg, ^{28}Si and ^{32}S together with 'a-priori' calculations with CC-method plus HF-theory, taken from refs. [33,34].

On fig. 14 differential cross sections for ^{28}Si elastic and inelastic scattering are shown together with the theoretical analysis [34] .
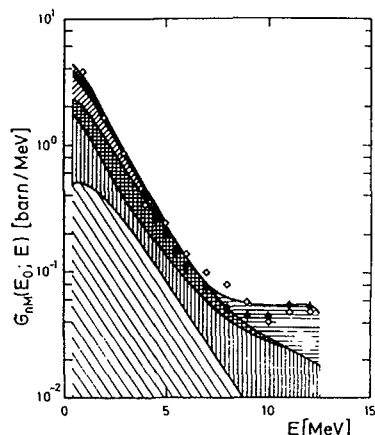
Fig. 14   Angle-integrated neutron emission cross section for ^{238}U
at 14 MeV incident energy: experiment - ● [36], ◊ [35] ;
theory - analysis of the different contributions to the
neutron spectra in the frame of the Complex Evaporation
Model [37] and the Generalized Exciton Model [16].

Fig. 13 gives integrated cross sections of the excitation of the first 2^+ levels for ^{24}Mg, ^{28}Si and ^{32}S depending on the incident energy. The dominance of direct excitation of this states at 14 MeV in evident.
Generally, for gg-nuclei in this region the status of investigations is much better than for ug- or gu-nuclei.

6. DDNECS for hybrid fuel elements

For neutron transport calculations in fusion-fission-hybrid blankets the DDNECS for fissile nuclei like ^{232}Th, ^{238}U and ^{239}Pu are needed in the whole neutron incident energy range up to 15 MeV. Neutron emission spectra for this nuclei contain significant contributions from (n n'),(n, 2n), (n, 3n), (n, f) and other reactions, therefore, a theoretical analysis of such spectra is rather complicated.

Fission neutron spectra are experimentally determined mainly for incident thermal neutrons. As yet, the theoretical predictions of fission neutron spectra in most cases is basing on the phenomenological Watt formula.

The experimental determination of the full neutron emission spectra at 14 MeV was carried out in several tof measurements [9,35] , but in this measurements it was very difficult to distinguish between elastic scattering an inelastic excitation of the very low lying rotational states. An averaged DWBA calculation for the direct one-step and two-step excitation was not published, as yet.

There are almost no experiments at incident energies between 6 MeV and 13 MeV neither for the full neutron emission spectra nor for fission neutron spectra.

Alltogether this means, that during the next years a substantial work has to be done in this field to fulfil requirements of hybrid blanket calculations.

At fig. 14 for example a new tof-measurement with good resolution of the DDNES for ^{238}U at 14 MeV incident energy is shown [36] together with the theoretical analysis. In this case the fission neutron spectra are calculated with the complex evaporation model [37] and the pre-fission neutron spectrum is calculated with a generalized exciton model approach including phonon excitations [16] .

REFERENCES

1   WRENDA 1983/84   INDC(SEC)-88/URS

2   D. Seeliger
    Measurements of Cross Sections and Spectra for Neutron
    Emitting Channels by Fast Neutron Spectroscopy
    Proc. 2nd RCM on Measurement and Analysis of 14 MeV
    Neutron Nuclear Data for Fission and Fusion Reactor
    Technology
    INDC(NDS)-173/GI and INT (85)-J, IAEA, Vienna, Sept. 1985,
    ed. M.K. Metha, p. 26-61

3   D. Hermsdorf et al., (TUD) ZfK-277U, 1975

4   A. Chalupka et al., IRK Vienna, ZfK-410 (1980) 25

5   A. Takahashi et al. OSA, OKTAVIAN-Report A-83-01, 1983

6   A. Takahashi et al. OSA, OKTAVIAN-Report A-87-01, 1987

7   T. Elfruth et al., TUD, INDC(GDR)-044/GI INT (86)-12

8   T. Elfruth et al. TUD, Atomenergie-Kerntechnik 49 (1987) 121

9   J.L. Kammerdiener, Thesis PhD UCRL-51232 (1972)

10 Adel-Fawzy, M., et al., EXFOR entry 32001 IAEA Vienna

11 Marcinkovski et al., Nucl. Sci. Eng. 83 (1983) 13

12 Simakov et al., Yad. Fiz. 37 (1983) 801

13 Gruppelaar, H., Nagel, P., NEANDC-204 "U", INDC (NEA) 6
    Newsletter Nr. 32, 1985

14 Mittag, S., Schmidt, D., Seeliger, D. to be publ.

15 Ignatyuk, A.V., Proc. IInd Int. Conf. Neutron Induced
    Reactions, Smolenice, 1979, p. 245

16 Kalka, H., private Communications

17 R. Batchelor and J.H. Towle, Nucl.Phys. 47, 385 (1963)

18 H. Förtsch, D. Schmidt, D. Seeliger, T. Streil, G.N. Lovchi-
    kova and A.M. Trufanov, Yad. Konst. 45, 7 (1982)

19 M. Adel-Fawzy, H. Förtsch, S. Mittag, D. Schmidt, D. Seeliger
    and T. Streil, EXFOR-32001

20 P.W. Lisowski, G.F. Auchampaugh, D.M. Drake, M. Drosg,
    G. Haouat, N.W. Hill and L. Nilsson, "Cross sections from
    neutron-induced, neutron producing reactions in ^{6}Li and ^{7}Li
    at 5.96 and 9.83 MeV", LA-8342, Los Alamos Scientific
    Laboratory (1980)

21 H.D. Knox, R.M. White and R.O. Lane, Nucl. Sci. Eng. 69,
    233 (1979)

22 M. Baba, N. Hayashi, T. Sakase, T. Iwasaki, S. Kamata and
    T. Momota, EXFOR-21630

23 H.H. Hogue, P.L. von Behren, D.W. Glasgow, S.G. Glendinning,
    P.W. Lisowski, C.E. Nelson, F.O. Purser, W. Tornow,
    C.R. Gould and L.W. Seagondollar, Nucl. Sci. Eng. 69 (1979);
    EXFOR-10707

24 J.C. Hopkins and D.M. Drake, Nucl. Phys. A 107, 139 (1968)

25 N.S. Biryukov, B.V. Zhuravlev, N.V. Kornilov, V.I. Popov,
    A.P. Rudenko, O.A. Salnikov and V.I. Trykova, Atomnaya
    Energiya 43, 176 (1977)

26 J.A. Cookson, D. Dandy and J.C. Hopkins, Nucl. Phys. A 91,
    273 (1967)

27 D.M. Drake, Annual report BNL-NCS-29426, Brookhaven National
    Laboratory, p. 72 (1981)

28 A.H. Armstrong, J. Gammel, L. Rosen and G.M. Frye Jr., Nucl.
    Phys. 52, 505 (1964)

29 M. Hyakutake, M. Sonoda, A. Katase, Y. Wakuta, M. Matoba,
    H. Tawara and I. Fujita, J. Nucl. Sci. Technol. 11, 407 (1974)

30 D. Miljanic, S. Blagus, V. Pecar and D. Rendic, Nucl. Phys.
    A 334, 189 (1980)

31 Schmidt, D., et al., Nucl. Sci. Eng. 96 (1987) 159

32 Obst, A.W., Weil, C., Phys. Rev. C 7 (1973) 1076
    Perey, C.M., Perey, F.G., Al. Nucl. Data Tables 17 (1976) 1
    Brandenberger, J.P., et al., Nucl. Phys. A 196 (1972) 65

33 Adel-Fawzy, M., et al., Nucl. Phys. A 440 (1985) 35

124 34   Seeliger, D., et al., Nucl. Phys. A 460 (1986) 265

35   Voignier et al., Report CEA-3503 (1968)
      Boschung et al., Helv. Phys. Acta 42 (1969) 225
      Salnikov et al., Preprint FEI-441, 1973
      Baryba et al., Preprint FEI-671, 1976
      Degtjarev et al., Yad. Fiz. 34 (1981) 299

36   Seidel, K., et al., TUD, 1987, to be publ.

37   Märten, H., Seeliger, D.,
      J. Phys. G: Nucl. Phys. 10 (1984) 349

R-MATRIX DESCRIPTION OF NEUTRON PRODUCTION FROM LIGHT CHARGED-PARTICLE REACTIONS*

G. HALE
Los Alamos National Laboratory,
Los Alamos, New Mexico,
United States of America

REPORT ON THE IAEA CO-ORDINATED RESEARCH PROGRAMME ON MEASUREMENT AND ANALYSIS OF 14 MeV NEUTRON NUCLEAR DATA NEEDED FOR FISSION AND FUSION REACTOR TECHNOLOGY

M.K. MEHTA*
Bhabha Atomic Research Centre,
Bombay, India

Abstract

The Nuclear Data Section of the IAEA implemented a Co-ordinated Research Programme (CRP) during the period 1982-85 on measurement and analysis of neutron nuclear data needed for fission and fusion reactor technology with the objectives of improving the status of 14 MeV neutron data and to bring about transfer of technology of fast neutron cross section measurements to a few laboratories in the developing countries. The paper describes the operational aspects of the CRP in general, the working, implementation and co-ordination of the programmes between the participating laboratories and summarises the conclusions, results and recommendations arising out of the full implementation of this programme. The results indicated that the status of 14 MeV neutron data is considerably improved with a need for more measurements for double differential neutron emission spectra, some specific activation measurement for products of isomeric States and certain long life activities.

I. INTRODUCTION

The Nuclear Data Section implemented a Co-ordinated Research Programme (CRP) during the period 1982-85 on measurement and analysis of 14 MeV neutron nuclear data needed for fission and fusion reactor technology. This co-ordinated research programme was aimed at two main objectives. The first one was to improve the status of the 14 MeV neutron data required for fission and fusion reactor technology. This was to be achieved through the participant laboratories who would carry out measurement and analysis of scattering and reaction cross sections and of secondary particle energy and angular distributions for 14 MeV neutrons available from neutron generators via the $^3H(d,n)^4He$ reaction. The measurements were to be made on elements and their isotopes which are the constituents of fission and fusion reactor structural, coolant, absorber, shielding, reprocessing and neutron flux/fluence monitoring materials.

----

* Staff member of the Nuclear Data Section of the IAEA from January 1983 to January 1986.

The second objectives was to bring about transfer of technology of fast neutron cross section measurements to a few laboratories in the developing countries. Capability to perform accurate and reliable nuclear measurements is fundamental to any infrastructure needed to implement any nuclear science and technology programme and a neutron cross section measurements programme would be one of the most effective ways to transfer the technology for such measurements. As this meeting is aimed at discussion on the status of the data - the first objective of the CRP. I shall emphasis that aspect more in the rest of my talk.

II. IMPLENTATION

1. Research Co-ordination Meetings:

The research work under such CRP's is supported and recognised through the awards of research contracts and agreements to principal scientific investigators of the participating laboratories from developing and developed countries respectively.

The co-ordination of the research work done under such programmes is generally carried out through holding periodical meetings - called the Research Co-ordination Meetings (RCM) - of the principal scientific investigators (or their nominees) from all the participant laboratories.

In the present case three RCM's were held during November 1983 here at Dresden, February 1985 at Chiang Mai, Thailand, and May 1986 at Dubrovnik, Yugoslavia, respectively.

The objectives of the first two RCM's were to review the status and progress of the measurement programme of each participating laboratory, to review and discuss the experimental and analysis techniques used, to intercompare the results of measurements already made and to discuss and decide on the programme of the following year for each laboratory.

The total number of participating laboratories were 13 (7 research contracts and 6 research agreements) at the time of the first RCM which increased to 16 (9 research contracts and 7 research agreements by the time the third and the final RCM was held at Dubrovnik in May 1986. The objectives of this final meeting were: to discuss and evaluated the final results of the measurement and analysis carried out by the participant laboratories, prepare final reports on all fast neutron cross sections measured under this CRP, review the status and remaining gaps in the need for such data and if necessary define the scope of a new CRP to fill these gaps. Summary reports of the three RCM's are published as IAEA documents

    (i)   INDC(NDS)-161/GI
    (ii) INDC(NDS)-172/GI
and (iii) INDC(NDS)-181/GI

2. Working Groups:

The work to be carried out under the CRP was divided into five categories and Working Groups (WG's) were formed from amongst the participants for each of the categories as follows:

(i) Working Group A Activation Measurement
Chairman - J. Csikai

(ii) Working Group B Charged particle emission cross section measurements
Chairman - H. Vonach

(iii) Working Group C1 Double differential neutron emission cross section measurements
Chairman - K. Seidel/D. Seeliger

(iv) Working Group C2 Prompt gamma ray measurments
Chairman - P. Oblozinsky

(v) Working Group D Nuclear reaction model calculations
Chairman - A. Marcinkowski

These WG's were then responsible for co-ordinating, intercomparing and evaluating the work performed under each category and to produce a final report incorporating all the results and recommended values. The chairmen of the WG's co-ordinated the work during the periods between the RCM's through correspondence with the other member os the WG's.

3. Concurrent International Symposia and Conferences:

A special feature of this CRP was that concurrent with each of the RCM's the host institutions organised either an international symposium or an international conference on topics directly related to the theme of CRP. The following symposia and conferences were held concurrently with each RCM .

(i) XIII International symposium on Nuclear Physics - Fast Neutron Reactions - organised by Technical University, Dresden at Gaussig, GDR, during 21-25 November 1983. Concurrent with the First RCM.

Total no. of participants: 51

(ii) International Symposium on Fast Neutrons in Science and Technology - organised by Chiang Mai University at Chiang Mai, Thailand, during 4-8 February 1985. Concurrent with the Second RCM.

Total no. of participants - 45

(iii) International Conference on Fast Neutron Physics - organised by Ruder Boskovic Institute at Dubrovnik, Yugoslavia, during 26-31 May 1986. Concurrent with the Third and Final RCM.

Total no. of participants - 65

These concurrent meetings with a wider participation contributed considerably to the scope of the CRP and its two main objectives and as a results number of relevant measurements, carried out at laboratories which were not formally participating in the CRP, could be incorporated and taken into consideration in planning and co-ordinating the research programme and final reports under the CRP. An outstanding example of such contribution is the work done at the Octavian Faculty of the Osaka University in Japan from where Dr. A. Takahashi was a regular participant at all the three RCM's mainly because of the concurrent symposia and conferences.

III. RESULTS

The numerical data produced as a result of this CRP are contained in the final reports of the five Working Groups prepared by the respective Chairmen based on the inputs from individual laboratories and the discussions during the RCM's. These reports also contain a critical appraisal of the work with a recommended set of data in a few important cases and general conclusions regarding the improvement in the status of 14 MeV data. These reports will be published by the IAEA in the TECDOC series and are expected to be useful to the scientific community as reference material.

Although the data were exhibited during the presentation of this paper at the AGM, to include all the numercial data in this proceedings would be wasteful as they would be available through the TECDOC publication. Only a few general remarks about the data are given below, the forthcoming TECDOC publication may be referred to for more details and the numerical values.

(a) More than hundred activation cross sections are reported under WG A. All the measurements are very relevant to the latest WRENDA list, filling many gaps and considerably improving the 14 MeV data status for those isotopes. However there is still need for (n, n'x) type of reaction cross section measurements especially at other energies.

(b) The report of WG B indicates that the status of data required for calculation of gas production in structural and blanket materials is now very good as a result of charged particle emission cross sections reported under this CRP. No important gaps remain in the availability of good quality data for this purpose.

(c) The report of WG C1 contains, in addition to the new data measured under this CRP, recommended sets of data on neutron emission spectrum from natural lead under 14 MeV neutron bombardment and differential cross sections for elastic and inelastic neutron scattering from carbon at 14 MeV bombarding energy. These recommended data wuld be useful as measurement reference standards to those new laboratories who are starting such work. The report points out that there are still many gaps in the double differential data needed for the fusion reactor technology and more work is necessary.

(d) The reports of the Working Groups C2 and D include appraisals of the work done under the CRP and reviews of current status and recommendation for further work.

IV. CONCLUSIONS AND RECOMMENDATIONS

In conclusion, I would like to quote the following excerpts from the sections on Conclusions and Recommendations contained in the document entitled summary Report of the third and final RCM of this CRP (INDC(NDS)-189/GI).

1. The two main objectives of the CRP were to improve the status of the 14 MeV neutron nuclear data required for fission and fusion reactor technology and to bring about transfer of technology of fast neutron cross section measurements to a few laboratories in the developing countries. Judging by the reports from individual laboratories and final reports of the five working groups the CRP has been very successful in fulfilling these objectives to a considerable extent.

   The cross sections measured under the CRP are very relevant to the WRENDA request list. A few of the data measured under the CRP have been evaluated and are already included in the evaluated data files of one of the nuclear data centres which is a part of the international nuclear data centres network.

2. The participants noted that as a result of this CRP large number of cross sections have been measured through activation techniques. However, there is still need for measurements of the cross sections for reactions of type (n,n'x) where x could be proton or alpha particles. Similarly there is need for cross section measurements for isomeric states production. These measurements could be made with activation technique but are a little more difficult. These cross sections are needed at 14 MeV as well as lower neutron bombarding energies.

3. Similarly as noted in the report of the Working Group C1 there are still large gaps in the data for double differential neutron emission cross sections. The data are needed both to understand the reaction mechanism and for applications in fusion reactor technology. The need is for data at 14 MeV as well as lower neutron energy.

4. The participants were of the unanimous opinion that the transfer of technology of high quality nuclear cross section measurements, one of the objectives of the current CRP, has been a very successful result of the CRP. However, the participating laboratories from the developing countries were just beginning to make such measurements now and need continued interaction with their peers from the advanced laboratories. A discontinuation of coordinated research programme at this stage will affect them adversely and will considerably slow down their progress towards generating highly trained manpower and establishing the core of the infrastructure required for an applied research programme in nuclear techniques.

EXCITATION OF ISOMERIC STATES IN (n,n') REACTIONS

H. VONACH
Institut für Radiumforschung und Kernphysik,
Österreichische Akademie der Wissenschaften,
Vienna, Austria

Abstract

The present status of our knowledge on activatiom cross-sections for metastable nuclear states by (n,n') reactions is reviewed and summarized. Though the emphasis is given to the cross-sections for 14 MeV neutrons, the neutron dependence of these cross-sections is also discussed briefly. Both the status of experimental data and the possibilities of theoretical calculations of (n,n') cross-sections are addressed and a new systematic of (n,n') cross-sections for isomer production at $E_n \sim 14$ MeV is presented. Some striking discrepancies between the existing measurements and theoretical expectations are identified and possibilities for improved measurements are discussed.

1. Introduction

While the status of 14 MeV cross-sections for (n,2n), (n,p) and (n,α) cross-sections and its systematic dependence on target mass, Q-values and relative neutron excess (N-Z)/A has been discussed extensively in the literature /1/, no such review and systematics exists for (n,n') cross-sections for formation of metastable states of the target nuclei. As these cross-sections may assume values up to about 25% of the total reaction cross-sections, they are important for a complete description of the interaction of 14 MeV neutrons with nuclei and the following review is intended to fill the discussed gap.

2. General properties of the (n,n') reactions, shape of (n,n') excitation functions

As metastable states with half-lives $>$ 1 sec are only observed for nuclei with A $\leq$ 77, we can restrict our discussion to heavy nuclei where the emission of charged particles is negligible. In this case the (n,n') reaction will be the dominant reaction channel and its cross-section almost equal to the total reaction cross-section until emission of a second neutron becomes energetically possible. Above the (n,2n) threshold this reactions quickly become dominant and the total (n,n') cross-section drops to about 20% of the nonelastic cross-section at E_n = 14 MeV (which is about 5-8 MeV above the (n,2n) threshold for most of the discussed nuclei). It's also important to note that there is a definite change in the mechanism of the (n,n') reaction as function of incident neutron energy. Below the (n,2n) threshold the (n,n') reaction proceeds almost completely by compound nucleus decay and is well described by the Hauser-Feshbach theory; at E_n = 14 MeV that is well above the (n,2n) threshold, the (n,n') reaction is mainly due to preequilibrium emission of neutrons from the composite system target + 14 MeV neutrons and has to be described by much more phenomenological theories like the exciton model.

The cross-section σ^m for production of metastable states by the (n,n') reaction is equal to the total (n,n') cross-section multiplied with the branching ratio $f^m = \sigma^m/(\sigma^g + \sigma^m)$ (σ_g = cross-section for formation of the ground-state by the (n,n'))

(1) $\qquad \sigma^m = \sigma(n,n') \cdot f^m$

The branching ratios f^m and f^g ($f^m + f^g = 1$) for population of the metastable state and the ground state depend essentially on the spin distribution initially formed by absorption of the incident neutrons, the modification of this spin

distribution in the process of deexcitation of the compound nucleus by neutron and subsequent gamma emission and on the spins of the two competing levels, the ground and metastable state, which are reached at the end of the γ-cascade. The initial spin distribution is determined to a large extent by the orbital angular momentum transferred by the incident neutron, which is roughly proportional to the square root of the neutron energy. Accordingly also the branching ratios f^m will depend somewhat on neutron energy. The f^m values will increase if the metastable state has a higher spin than the ground state and decrease in the opposite. This dependence, however, is rather weak and therefore the excitation functions $\sigma^m(E_n)$ are rather similar to the excitation functions for the total (n,n') cross-section as shown in fig. 1 both for a low and two high spin metastable states. The figure shows the characteristic shape of (n,n') cross-sections, the fast rize above the inelastic threshold, a plateau in the MeV range and a sharp decrease of the cross-section above (n,2n) threshold. In addition the figure shows the characteristic difference in the excitation of low and high spin isomers, the much slower initial rise of the cross-section with neutron energy in the case of high-spin isomers, which besomes even more pronounced for very high spin isomers like ^{199m}Hg.

3. Experimental information on cross-sections σ^m for formation of metastable states in (n,n') reactions

The existing information on σ^m values for 14 MeV neutrons is summarized in table 1. The table lists all metastable states of stable nuclei with half-lives above 1 sec and their characteristic properties and gives - when ever possible - recommended values for cross-sections at E_n = 14.7 MeV. In a number of cases the metastable state is not the lowest excited state and there are several excited levels (which all decay to the ground state) below the mestable state. In
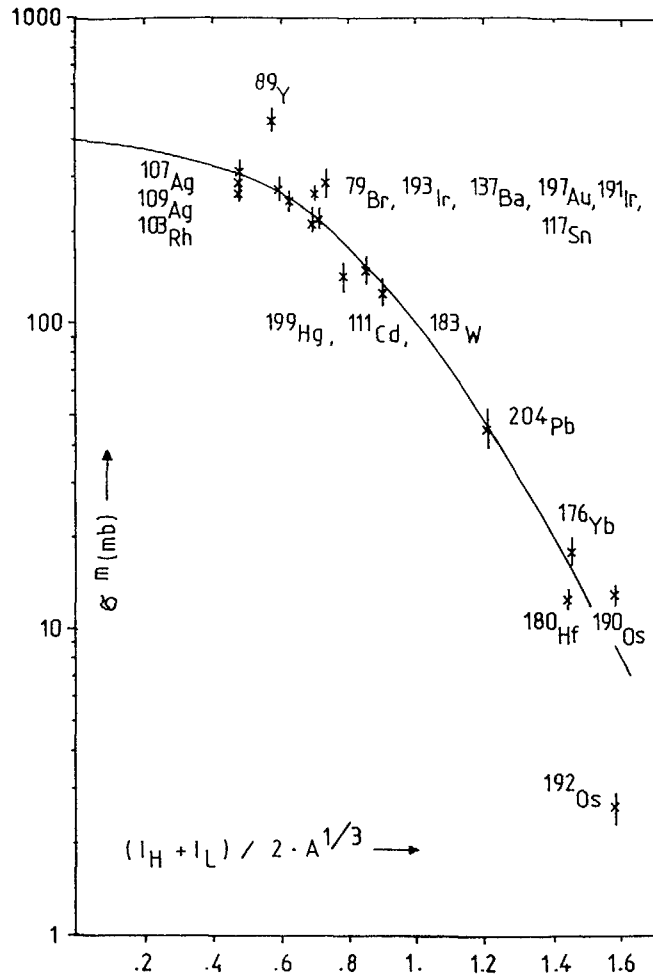
Fig. 1. Typical excitation functions for population of isomers in (n,n') reactions;
(a) high-spin isomers, x ^{103}Rh(n,n')^{103m}Rh, I_m = 7/2, I_g = 1/2 /2/, o ^{199}Hg(n,n')^{199m}Hg, I_m = 13/2, I_g = 1/2 (from ref. 3 and table 1);
(b) low-spin isomers, ^{115}In(n,n')^{115m}In, I_m = 1/2, I_g = 9/2 (from ENDF/B V dosimetry file)

Table 1: Cross-sections σ^m for formation of isomers in (n,n') reactions at E_n = 14.7 MeV

Target Nuclide	$T_{1/2}$	I_g	I_m	σ_m (mb)	Ref.	$Q_{n,2n}$ (MeV)
^{77}Se	17.5 s	1/2$^-$	7/2$^+$	--		- 7.4
^{79}Br	4.9 s	3/2$^-$	9/2$^+$	273. ± 20	4^a,5	- 10.7
^{83}Kr	1.83 h	9/2$^+$(7/2)	1/2$^-$	--		- 7.5
^{87}Sr	2.81 h	9/2$^+$	1/2$^-$	74. ± 10	6	- 8.4
^{89}Y	16 s	1/2$^-$	9/2$^+$	460. ± 40	2,7,8	- 11.5
^{93}Nb	13.6 a	9/2$^+$	1/2$^-$	36.5 ± 3	9	- 8.8
^{103}Rh	56.1 m	1/2$^-$	7/2$^+$	260. ± 15	2	- 9.3
^{107}Ag	44.3 s	1/2$^-$	7/2$^+$	304. ± 37	10	- 9.5
^{109}Ag	39.6 s	1/2$^-$	7/2$^+$	291. ± 35	10	- 9.2
^{111}Cd	49 m	1/2$^+$(5/2)	11/2$^-$	150. ± 15	6,7,11, 12	- 7.0
^{113}In	99.48 m	9/2$^+$	1/2$^-$	53.4 ± 2.1	13	- 9.4
^{115}In	4.5 h	9/2$^+$	1/2$^-$	53.1 ± 2.2	13	- 9.0
^{117}Sn	14.0 d	1/2$^+$(3/2)	11/2$^-$	284. ± 32	14	- 6.9
^{119}Sn	245 d	1/2$^+$(3/2)	11/2$^-$	--		- 6.5
^{123}Te	119.7 d	1/2$^+$(3/2)	11/2$^-$	--		- 6.9
^{125}Te	58 d	1/2$^+$(3/2)	11/2$^-$	--		- 6.6
^{129}Xe	8.89 d	1/2$^+$(3/2)	11/2$^-$	--		- 6.9
^{131}Xe	12.0 d	3/2$^+$	11/2$^-$	--		- 6.6
^{135}Ba	28.7 h	3/2$^+$	11/2$^-$	--		- 7.0
^{137}Ba	2.55 m	3/2$^+$	11/2$^-$	214. ± 15	12	- 6.9
^{167}Er	2.3 s	7/2$^+$	1/2$^-$	252. ± 18	5	- 6.4
^{176}Yb	12 s	0$^+$ (8)	(8)$^-$	18. ± 2	4,5 ^{a}	- 6.9
^{180}Hf	5.5 h	0$^+$ (8)	8$^-$	12. ± 1.	15 ^{a}	- 7.4
^{183}W	5.3 s	1/2$^-$(9/2)	(11/2)$^+$	127. ± 14	5	- 6.2
^{189}Os	6 h	3/2$^-$	9/2$^-$	--		- 5.9
^{190}Os	9.9 m	0$^+$ (8)	10$^-$	13. ± 1.	5,11,16, 17	- 7,8
^{192}Os	5.9 s	0$^+$ (8)	(10$^-$)	2.6 ± .3	5	- 7.6
^{191}Ir	4.88	3/2$^+$(5/2)	11/2$^-$	221. ± 22	5	- 8.1
^{193}Ir	11.9 d	3/2$^+$	11/2$^-$	248. ± 21	18	- 7.8
^{195}Pt	4.02 d	1/2$^-$(5/2)	13/2$^+$	--		- 6.1
^{197}Au	7.8 s	3/2$^+$(5/2)	11/2$^-$	268. ± 15	4 ^{a},19, 20	- 8,1
^{199}Hg	42.6 m	1/2$^-$(5/2)	13/2$^+$	142. ± 15	21 ^{b} 22 ^{b}	- 6.6
^{204}Pb	66.9 m	0$^+$(5$^+$)	9$^-$	55. ± 7	21,23	- 8.4
^{235}U	26 m	7/2$^-$	1/2$^+$	--		- 5.3

a) renormalized to present values of ^{27}Al(n,α) cross section
b) renormalized to present values of gamma emission probabilities of ^{199m}Hg decay

this case the table gives (in parenthesis) also the spin of that level below the metastable state which is closest in spin to the metastable state. The recommended cross-section values do contain some necessarily subjective judgements. For ^{113}In and ^{115}In it was decided to rely only on the precision measurement of Ryves et al. /13/ as this is much better in quality than all the numerous other measurements as will be discussed later; for the other reactions about one third of the papers were rejected because at least one of the given cross-sections was obviously wrong (for example exceeding the total (n,n') cross-section etc.) and some of the accepted results were renormalized in order to take into account the present values of standard cross-sections, e.g. Al(n,α) or γ-emission probabilities for the produced isomers (in case of ^{199}Hg). In those cases where several measurements are listed, the recommended cross-sections are weighted averages derived from all the mentioned results.

As obvious from table one, the experimental situation is still very unsatisfactory. For about one third of the isomers no cross-section measurements exist, for another third there is just one measurement and only in three cases (for ^{93}Nb, ^{113}In and ^{115}In) precise measurements with uncertainties below 5% have been performed. Actually the situation is even much worse than table 1 seems to indicate.

The uncertainties attached to the recommended cross-section values are based on the estimates of the respective authors. Unfortunately most of the authors including some very recent work have not considered one of the most important source of error, the impurity of the used 14 MeV neutron field.Every 14 MeV neutron field is contaminated by evaporation neutrons (E_n $\sim$ 0-4 MeV) which are produced by (n,n') and (n,2n) reactions in all materials in the vicinity of the neutron producing tritium target, especially in the target backing and in the activation samples themselves. Even in carefully designed low-mass target assemblies this contamination is of the order of 1% and in many conventionally used target

assemblies this contamination may well be of the order of 5%. This does not produce problems for the investigation of reactions with high threshold, like (n,2n) reactions, in the case of (n,n') reactions (see fig. 1) the cross-section at E_n $\sim$ 2 MeV is several (2-5) times higher than at 14 MeV. This means that a 5%-contribution of evaporation neutrons may produce a cross-section error of 10-25% and this really seems to be the case in many of the experiments as demonstrated in table 2, which summarizes the existing measurements in the excitation of ^{115m}In by 14 MeV neutrons. This isomer has a very convenient half-live of 4.5 hours and γ-energy of 335 keV and thus it is very easy to measure the ^{115}In activity quite accurately. Contrary to this expectation there is a large scatter in the results and - more important - almost all cross-sections values are considerably higher than the results of the precision measurement of Ryves et al. /13/ which can approximately be taken as the "true value". It seems almost certain that the main reason

Table 2:

Measurements of the ^{115}In(n,n')^{115m}In cross-section at E_n = 14-15 MeV

Authors	Ref.	Date of Publ.	E_n (MeV)	σ^m (mb)	Correction for low-energy neutrons applied
Nagel	/24/	1966	14.6	50. ± 7.8	yes
Rötzer	/25/	1968	14.70	83.5 ± 4.2	no
Minetti and Pasquarelli	/26/	1968	14.70	125. ± 10.	no
Barral et al.	/27/	1969	14.60	67. ± 7.	no
Barrall et al.	/28/	1969	14.80	69. ± 5.	no
Temperley and Barnes	/29/	1970	14.10	63. ± 3.	no
Decovski et al.	/30/	1970	14.52	83.8 ± 1.2	no
Paszit and Csikai	/31/	1972	14.70	63. ± 4.	no
Santry and Butler	/32/	1976	14.50	57.7 ± 2.3	no
Andersson et al.	/33/	1978	14.90	65. ± 4.	no
Garlea et al.	/34/	1983	14.75	78.6 ± 4.55	yes
Kudo et al.	/35/	1984	14.60	66.2 ± 2.3	no
Pepelnik et al.	/36/	1985	14.70	90.5 ± 4.5	no
Ryves et al.	/13/	1983	14.67	53.1 ± 2.	yes

for these high cross-section values is the contamination by lower energy neutrons with their high cross-section (see fig. 1) for the ^{115}In(n,n')^{115m}In reaction. It is thus to be expected that such effects are also present for most of the cross-sections listed in table 1 and that the true values may well be about 10-30% lower than given in the table. The sensitivity of the cross-section values to the presence of low-energy neutrons is largest for low-spin isomers and decreases considerably with increasing spin of the isomer as also apparent from fig. 1; thus it will probable not be important for the very high spin isomers ($I_m \geq 8$).

At energies other than 14 MeV - as usual - only very few measurements of σ_m values have been made. Rather complete excitation functions from threshold to 14 MeV do exist for the production of ^{103m}Rh /2/, ^{115m}In /37/, ^{113m}In /37/ and ^{204m}Pb /38/ (see fig. 1); considerable parts of the excitation function have been measured for production of ^{93m}Nb (see figs. 3 and 4) /2, 39, 40/ and ^{199m}Hg (see fig. 1) /3/ and in addition a number of point measurements at $E_n = 2.8$ MeV have been performed /41, 42/.

4. Sytematics of (n,n') cross-sections for population of isomers at $E_n = 14$ MeV

As the isomer production cross-section σ_m are a product of the total (n,n') cross-section $\sigma(n,n')$ and the specific branching ratio f^m in principle both factors could be responsible for the observed variations in cross-section (see table 1). Actually the $\sigma_{nn'}$ values are very similar for most cases. With the exception of ^{79}Br and ^{89}Y all the listed nuclei have (n,2n) Q-values smaller than -9.5 MeV and accordingly at $E_n = 14.5$ MeV the (n,2n) cross-section should amount about 80% of the total reaction cross-section and $\sigma_{nn'}$ is probably around 400 mb for most of the nuclei /1/ and the different σ^m values have to be attributed to variations of f^m and one expects a systematic behaviour on the

spin of the metastable state. Accordingly we will separately treat the low- and the high-spin isomers.

a) Low-spin isomers

There is the group of 5 spin 1/2$^-$ isomers above a spin 9/2$^+$ ground-state in a narrow mass-range A = 83-115 and an additional spin 1/2$^-$ isomer in ^{167}Er above a spin 7/2 ground-state. From any statistical model calculation using smoothly varying parameters, all five 1/2 isomers above 9/2 ground-state should be almost equal and that the ^{167}Er(n,n')^{167m} should be similar and probably somewhat smaller than the other ones. As table 3 shows this is the case with one exception, the cross-section for formation of ^{167m}Er. All other σ_m values are quite similar of the order of 50 mb, if one takes into account that the true cross-section for the formation of ^{87m}Sr is probably somewhat lower than the value of Table 3, as the same authors also derived a somewhat high ^{115}In cross-section (see table 2); the cross-section

Table 3: Cross-sections for formation of low-spin isomers in (n,n') reactions at $E_n = 14.7$ MeV

Target Nucleus	I_g	I_m	σ_m (mb)	Ref.	$Q_{n,2n}$ (MeV)
^{87}Sr	9/2	1/2	74 ± 10 *	6	- 8.4
^{93}Nb	9/2	1/2	36.5 ± 3	9	- 8.8
^{113}In	9/2	1/2	53.4 ± 2.1	13	- 9.5
^{115}In	9/2	1/2	53.1 ± 2.2	13	- 9.2
^{167}Er	7/2	1/2	252 ± 18	5	- 6.4

*) Cross-section probably about 20% too high as measurement of the ^{115}In(n,n')^{115m}In cross-sections by same authors are also too high (see table 2).

131

tion for formation of ^{167m}Er, however, is about 5 times larger. This is not explainable by the discussed effect of contamination by low energy neutrons, nor can any reasonably theoretical model explain this result. Thus a new measurement of this cross-section is highly desirable.

b) High-spin isomers

It can be expected that the branching ratio f^m depends mainly on the spins of the two competing levels (that is the spin I_{high} of the isomer and the spin I_{low} (which is either the ground state or the highest spin of all levels below the isomer also given in table 1) and the average angular momentum transferred to the target nucleus by the incident neutrons. At a fixed neutron energy this latter quantity is proportional to the nuclear radius and thus to $A^{1/3}$. Therefore in fig. 2 we have plotted σ_m values for all high-spin isomers versus the quantity $R = (I_H + I_L)/A^{1/3}$.

As the figure shows there is a remarkably smooth dependence of the measured cross-section on the chosen variable $R = (I_H + I_L)/2A^{1/3}$ and with exception of a few cases (^{89}Y, ^{190}Os and ^{192}Os) all measured values do not deviate more than 30% from a smooth curve drawn through the data. One of the exceptions - the high cross-section for the ^{89}Y(n,n')^{89m}Y reaction - can be easily understood; it is due to the fact that ^{89}Y has a much more negative Q-value for the (n,2n) reaction than all other nuclei listed in table 2. Thus at E_n = 14 MeV the total (n,n') cross-section for ^{89}Y is about a factor of 1.5 higher than the common value of ∿ 400 mb of all the other nuclei and accordingly also the isomer production cross-section exceeds the prediction of the systematics by about the same factor.

The other case, the large difference of the σ_m values for production of ^{190}Os and ^{192}Os is not easily understood. Both nuclei have isomers with the same quantum
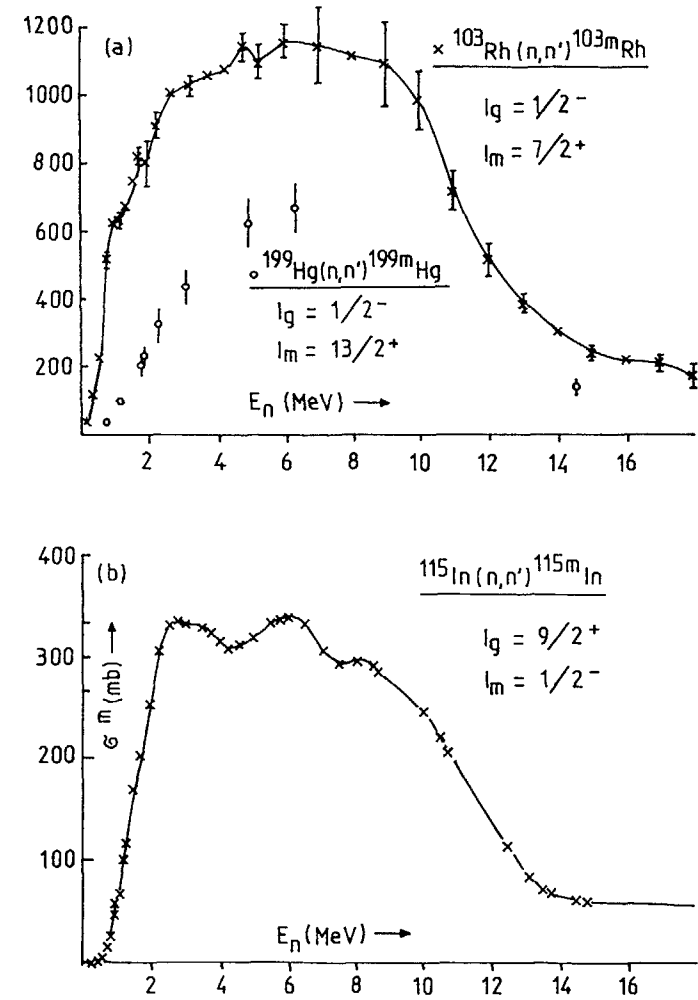
Fig. 2. Systematics of the cross-sections σ^m for formation of high-spin isomers in (n,n') reactions at E_n = 14.7 MeV (cross-sections from table 1)

number 8^- at similar excitation energy and thus any theoretical description using smoothly varying parameters will predict very similar cross-sections. Thus either the σ_m value of ^{192}Os is in error (the value for ^{190}Os is confirmed by several independent measurements) or the σ_m values for very high-spin isomers (where the cross-sections are only a few percent of the total (n,n') cross-section) are extremely sensitive to details of the nuclear level scheme. Apart from this question, the systematics shown in figure 2 seems to be able to predict unknown σ_m values with an accuracy of better ± 50% which is comparable to much more complicated nuclear model calculations. It has to be kept in mind, however, that most cross-sections given in the figure may be systematically somewhat too high for the reasons discussed in section 2. Thus in order to make really reliable estimates the data base of the systematic should be improved by more accurate new measurements (see section 6).

5. Calculation of cross-sections for isomer production in (n,n') reactions

As already mentioned σ_m values can be calculated by means of the statistical model of nuclear reactions. The problems associated with these calculations are somewhat different, however, for neutron energies above and below the (n,2n) threshold and thus these two cases will be treated separately.

a)   Neutron energy below (n,2n) threshold

Below the (n,2n) threshold inelastic neutron scattering is the dominant reaction channel for the compound nucleus decay. Accordingly it is possible to describe the population of the isomer quantitatively by the Hauser-Feshbach theory. For the application of this theory it is necessary to know the optical potentials

for the incident and outgoing neutrons, gamma strength functions and the spin dependence of the level density of the target nucleus (that is the spin cutoff-factor σ). Absolute values of the level densities and their energy dependence are also needed for such calculations but the results are very insensitive to their choice if the compound nucleus decay as in all our cases proceeds only via neutron emission.

In such cases the uncertainties in the mentioned quantities allow at present to calculate isomer production cross-sections with accuracies of $\sim$ ±20% except very near to threshold where details of the nuclear level scheme become very important. As an example figure 3 shows a calculation of the excitation function for ^{93}Nb(n,n')^{93m}Nb reaction done in 1980 /2/ when no experimental data existed and the results of measurements performed in the meantime /38, 39/. As the figure shows the experiments confirm the calcuations within their claimed accuracy, which was estimated from the uncertainties of the mentioned input parameters of the Hauser-Feshbach calculations /2/. Thus below the neutron binding energy calculated excitation cross-sections should be sufficiently accurate for many purposes.

b)   Neutron energies above the neutron binding energy

Above the neutron binding energy calculations of the σ^m values from (n,n') reactions become much more difficult. For example at E_n = 14 MeV the (n,n') process proceeds predominantly by means of precompound emission populating levels of the target nucleus below the neutron binding energy. Thus it is necessary to do a combined preequilibrium + equilibrium statistical model calculation which needs a much larger number of poorly known input parameters. Especially we need a parameters describing the fraction of precompound emission and we need some information of the spin distribution of the special nuclear states (e.g. few-particle-hole states
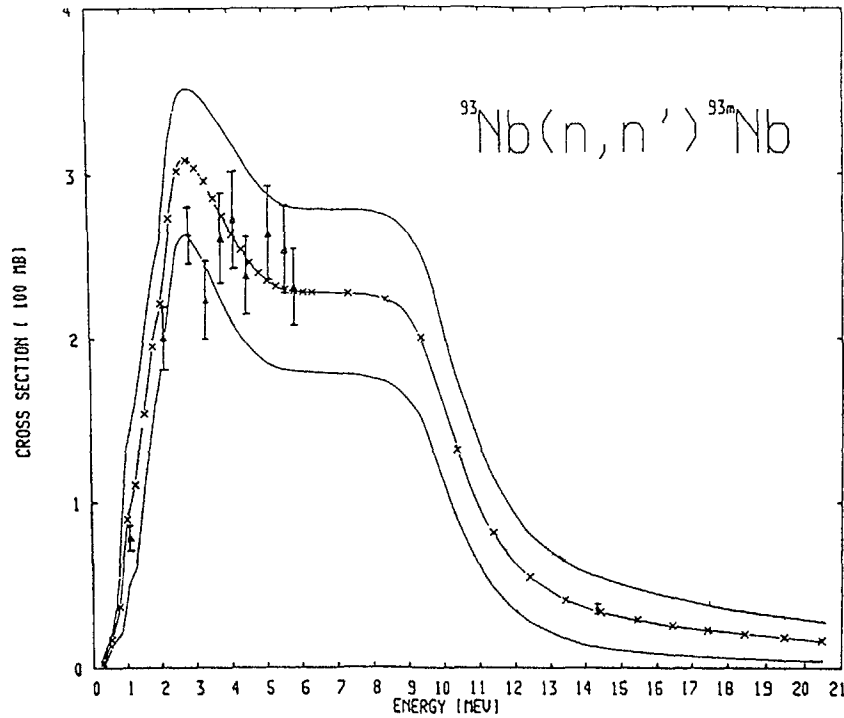
Fig. 3. Comparison of nuclear model calculations with
subsequent measurements for the reaction
^{93}Nb(n,n')^{93m}Nb: x-x statistical model calculati-
ons /2/, solid lines: estimated uncertainty limits
of the calculations /2/; measured cross-sections:
o ref. 9, Δ ref. 38, + ref. 39.

Fig. 4. Results of same calculations with the additional
constraint that any allowed variation of input
parameters must reproduce the measured 14 MeV
cross-section /9/ within the experimental error.
Meaning of symbols as in fig. 3.

in the exciton model) populated in precompound emissi-
on. These quantities have much larger uncertainties
than the input parameters for the Hauser-Feshbach
calculations described before. Therefore without any
experimental data it is not possible at present to do
such calculations to better than a factor of two as
apparent from fig. 3. If, however, the cross-section is
known at one energy, e.g. at 14 MeV, such calculation

can be done much more accurately. The requirements of
fitting this measured cross-sections imposes severe
constraints on the admissible combinations of parameter
variations with the result that the uncertainty of the
calculated cross-sections is drastically reduced for a
considerable energy range above and below the measured
cross-section values. As an example fig. 4 shows the
improvement in the accuracy of the calculated excitati-

on function for the $^{93}Nb(n,n')^{93m}Nb$ reaction obtained by the condition that the calculation should be in agreement with the precision measurement of ref. 9 at $^{192}Os(n,n')^{192m}Os$. The isomeric states in both nuclei have the same spin and parity (see table 1) and similar excitation energy. Thus any nuclear model calculation will predict the two cross-sections to be very similar whereas the measurements (see table 1) indicate a cross-section ratio of $\sim$ 5. At energies other than 14 MeV new measurements in the energy region from threshold to a few MeV above threshold will probably be most useful. Combination of such measurements, with accurate 14 MeV data and nuclear model calculations will probably allow to estimate the whole excitation functions up to about 20 MeV with reasonable accuracy.

Acknowledgements

REFERENCES

/1/ S. Qaim, Proc. Conf. Nucl. Cross-Sections and Technology, Washington 1975, NBS Special Publ. 425, p. 664

/2/ B. Strohmaier, S. Tagesen amd H. Vonach, Physics Data Nr. 13-2, Karlsruhe 1980

/3/ K. Sakuri et al., J. Nucl. Sci. and Technol. 19, 775 (1982)

/4/ P. Bornemisza-Pauspertl, P. Hille, Österr. Akad. Wiss., math.-naturwiss. Kl., Sitz-Abt. 2, 176, 227 (1968) Atomki (Atommag Kut. Intez.) Kozlem., 9, 227 (1967)

/5/ B. Anders, R. Pepelnik, H.-U. Fanger, Int. Conf. on Nuclear Data for Science and Technology, Antwerp, 6-10 Sept. 1982, p. 859

/6/ J.K. Temperley, Nucl. Sci. Eng. 32, 195 (1968)

/7/ E. Rurarz et al., Acta Phys. Pol. B2, 553 (1971)

/8/ K.G. Broadhead, D.E. Shanks, H.H. Heady, Phys. Rev. B139, 1525 (1965)

/9/ T.B. Ryves, P. Kolkowski, J. of Physics G7, 4, 529 (1981)

/10/ I. Wagner, M. Uhl, Anz. Österr. Akad. Wiss., math.-naturwiss. Kl., 108, 185 (1971)

/11/ M. Herman et al., Nucl. Phys. A297, 335 (1978)

/12/ R. Pepelnik, B. Anders, B.M. Bahal, Int. Conf. on Nucl. Data for Basic and Applied Science, Santa Fé, 13-17 May 1985

/13/ T.B. Ryves et al., J. of Physics G9, 1549 (1983)

/14/ P. Decowski et al., Prog. Rept. INR-1318, 8 (1971)

/15/ M. Hillman, E. Shikata, J. Inorg. Nucl. Chem. 31, 909 (1969)

/16/ P. Bornemisza-Pauspertl, P. Hille, Radiochim. Acta 27, 71 (1980)

/17/ W. Augustyniak et al., Prog. Rept. INDC(SEC)-42, 205 (1974)

/18/ B.P. Bayhurst et al., Phys. Rev. C12, 451 (1975)

/19/ M. Bormann et al., Prog. Rept. EANDC(E)-76, 51 (1967)

/20/ F. Özek, H. Özyol, A.Z. Ortaovali, Radiochem. and Radioanal. Letters 41, 87 (1979)

/21/ A.K. Hankla, R.W. Fink, J.H. Hamilton, Nucl. Phys. A180, 157 (1972)

/22/ J.K. Temperley, Phys. Rev. 178, 1904 (1969)

/23/ P. Decowski et al., Nucl. Phys. A204, 121 (1973)

/24/ W. Nagel, Physica 31, 1091 (1965)

/25/ H. Rötzer, Nucl. Phys. A109, 694 (1968)

/26/ B. Minetti, A. Pasquarelli, Z. Phys. 217, 83 (1968)

/27/ R.C. Barrall, J.A. Holmes, M. Silbergeld, Report AFWL-TR-68-134 (1969)

/28/ R.C. Barrall, M. Silbergeld, D.G. Gardner, Nucl. Phys. A138, 387 (1969)

/29/ J.K. Temperley, D.E. Barnes, Report BRL-1491 (1970)

/30/ P. Decowski et al., Prog. Rept. INR-1197, 18 (1970)

/31/ A. Pazsit, J. Csikai, Sov. J. Nucl. Phys. 15, 232 (1972)

/32/ D.C. Santry, J.P. Butler, Ca. J. Phys. 54, 757 (1976)

/33/ P. Andersson, S. Lundberg, G. Magnusson, Report LUNF-D6-3021 (1978)

/34/ I. Garlea et al., Report INDC(ROM)-15 (1983)

/35/ K. Kudo et al., Prog. Rept. NEANDC(J)-106/U, 1 (1984)

/36/ R. Pepelnik et al., Prog. Rept. NEANDC(E)-262U, 32 (1985)

/37/ D.L. Smith, J.W. Meadows, Nucl. Sci. Eng. 60, 319 (1976)

/38/ D.L. Smith, J.W. Meadows, Report ANL-NDM-37 (1977)

/39/ D.B. Gayther et al., Proc. Int. Conf. on Nucl. Data for Basic and Applied Science, Santa Fé 1985, Gordon and Breach, 1986

/40/ M. Wagner and G. Winkler, priv. Comm.

/41/ K.G. Broadhead, D.E. Shanks, Appl. Radiat. Isotop- 18, 279 (1967)

/42/ P. Bornemisza-Pauspertl, J. Karolyi, G. Peto, Atomki (Atommag Kut. Intez.) Kozlem. 10, (2), 112 (1968)

NEUTRON ANGULAR DISTRIBUTIONS FROM 7Li

H. LISKIEN
Central Bureau for Nuclear Measurements,
Joint Research Centre,
Commission of the European Communities,
Geel

Abstract

Status of knowledge of the angular distribution of emitted neutrons after the interaction of primary neutrons with the breeder material 7Li is presented. Experimental methods as well as nuclear model calculations of (double-) differential neutron emission cross sections are overviewed.

1. INTRODUCTION AND SCOPE

This contribution reports on the status of knowledge of the angular distribution of emitted neutrons after the interaction of primary neutrons with the breeder material 7Li. This knowledge is summarized in the following files (all in ENDF/B-5 format):

JEF-1	MAT # 4037 [1]
JENDL-2	MAT # 2032 [2]
JENDL-3	MAT # 0307 [3]
ENDF/B-5	MAT # 3007 [4]

There is also a recent Russian 7Li-evaluation [5]. Unfortunately this file could not be made available in time by NDS/IAEA for consideration. All these files do not contain uncertainty information concerning angular distributions. To get an idea about the accuracy one has to go back to the experimental input data or to compare different evaluations with each other. Only relative angular distributions will be regarded, that means that the uncertainty of the angle-integrated cross sections have to be added to obtain the uncertainty for absolute (double-) differential cross sections.

The total cross section of ^{7}Li can be conveniently subdivided in (see Fig. 1.1.):

(n,n_0) elastic scattering
(n,n'_1) inelastic (478 keV) scattering
(n,xt) tritium breeding
$(n,2n)$

where the small (n,2n)-cross section only contributes at higher energies. The discussion of neutron angular distributions will follow the above subdivision.
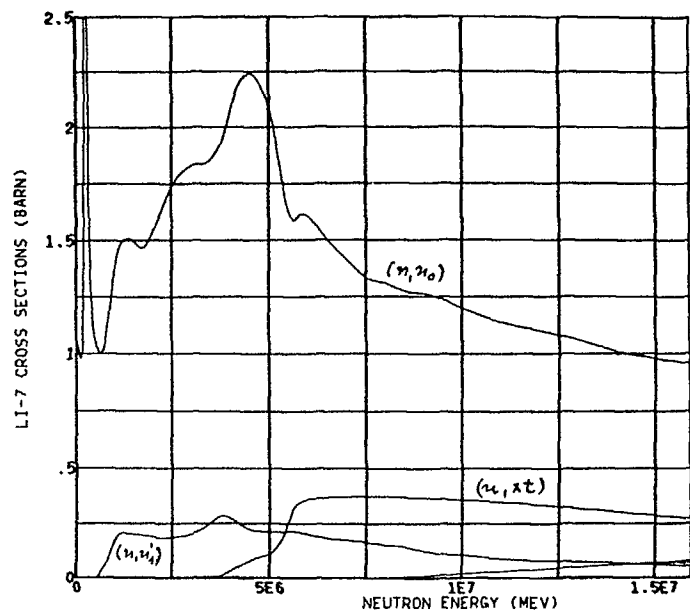
Fig. 1.1. A convenient subdivision of the total ^{7}Li cross section as function of neutron energy.

Improvement of the accuracy of the evaluated neutron angular distributions in the future will mainly be based on more and better experimental data. Therefore it is indicated to summarize the available techniques for such data determinations, especially as two new approaches have recently been implemented at CBNM Geel which both were applied to ^{7}Li. Conclusive statements for consideration of the working groups have been underlined throughout the text.

2. ELASTIC SCATTERING

Most of the angular distribution measurements were performed with an accelerator-based pulsed mono-energetic neutron source, such that the energy of the scattered or emitted neutron can be determined by time-of-flight. A typical set-up as used earlier at the Van de Graaff accelerator of CBNM Geel [6] is shown in Fig. 2.1. The cylindrical sample under investigation is mounted at 10 to 20 cm

1	Detector 1
2	Detector 2
3	Detector 3
4	Monitor
5	Paraffin
6	Lead
7	Shadow cone
8	Scatterer
9	Target can
10	Pick-up loop
11	Accelerator tube

Scale: |———50cm———|
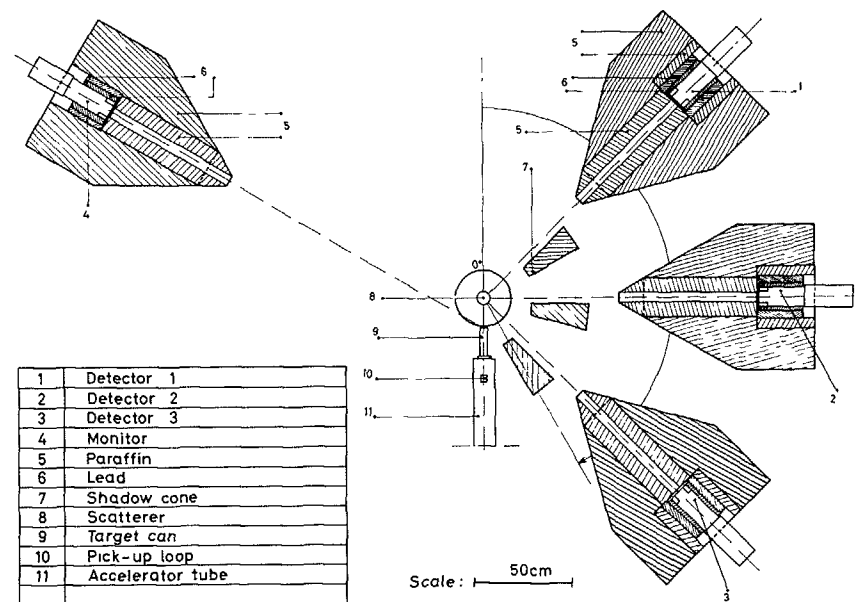
Fig. 2.1. Typical set-up to determine (double-) differential neutron emission cross sections using an accelerator-based pulsed mono-energetic neutron source [6].

from the neutron source in the direction of the ion beam and viewed by shielded neutron scintillation counters under various angles. Intensities are sufficient to use sample-detector distances between 1.5 and 3.0 m. In addition shadow cones are inserted between source and detectors. The geometry does not allow the observation of secondary neutrons at extreme forward and backward angles and also not at low energies due to the detection bias of the scintillation counters. Typical time-of-flight resolution is 2 to 3 ns. The relative detection efficiency has to be known. Absolute (double-) differential cross sections are obtained by

comparing with the hydrogen elastic scattering cross section using a polyethylene scatterer. Multiple scattering corrections for the sample are essential.

Experimental results from such ^{7}Li experiments at various primary neutron energies have been used by evaluators to predict the angular distribution of elastically scattered neutrons. At higher energies (> 5 MeV) the experiments are unable to separate the ground state transition from the transition to the first excited state at 478 keV. The corresponding corrections contribute to the uncertainty of the evaluated results. The evaluations assume isotropy below 200 keV (JEF-1), below 50 keV (JENDL-2) or below 10 keV (JENDL-3, ENDF/B-5). Evaluation results for three selected primary neutron energies are given in Fig.2.2.

Differences exceed often 20 % and this not only in the experimentally inaccessible region $|\cos\theta|\geq 0.9$ JENDL-2 and JENDL-3 elastic angular distributions are identical above 4 MeV. Above 14 MeV all four evaluations rely on optical model extrapolations which explains the large differences at 16 MeV and backward angles. Concerning angular distributions all the four discussed evaluations do not contain uncertainty information. The scatter of results may allow the conclusion that relative angular distributions of neutrons elastically scattered on ^{7}Li are generally known with about ± 15 % accuracy.

Fig. 2.2. Relative C.M. angular distribution from four evaluations for neutrons of 1,4 and 16 MeV elastically scattered on ^{7}Li

As outlined above most of the experimental information stems from mono-energetic source experiments. To cover the incident neutron energy range up to 16 MeV required for fusion technology applications, this is a very time consuming method and for that reason the existing experimental data base is limited. Recently an experiment has been set-up at CBNM Geel [7] which employs the white pulsed neutron source of GELINA (see Fig. 2.3.). Since the distance for the
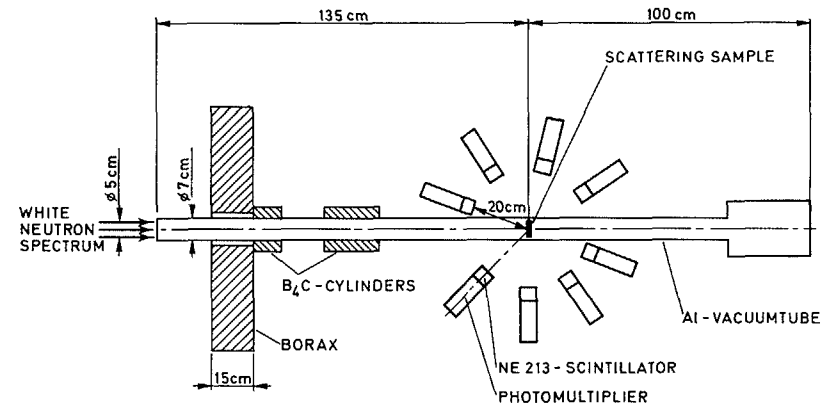
Fig. 2.3. Set-up to determine (double-) differential neutron emission cross sections using GELINA as an accelerator-based pulsed white neutron source [7], which is ≈ 60 m away. Primary neutron energies are determined by TOF, secondary neutron energies by pulse-height unfolding.

secondary neutrons (0.2 m) is negligible compared to the flight-path length of the incident primary neutrons (60 m), the primary neutron energy can be determined by time-of-flight. The secondary neutron energy is determined by unfolding the observed pulse-height distributions from the scintillation counters which needs the additional knowledge of the response functions for these detectors. Absolute (double-) differential cross sections are obtained by employing a ^{235}U(n,f) standard fission chamber as spectrum shape monitor and by comparing with the carbon elastic scattering cross section (below 2 MeV). Mainly due to the long source-sample distance the background conditions are much better than in the usual mono-energetic source experiments which allows the use of thin samples (transmission > 90 %) and reduces the multiple scattering corrections.

Fig. 2.4. shows a typical ^{7}Li result from this <u>new set-up which allows to</u> <u>determine (double-) differential emission cross sections simultaneously for all</u> <u>primary energies of interest.</u>
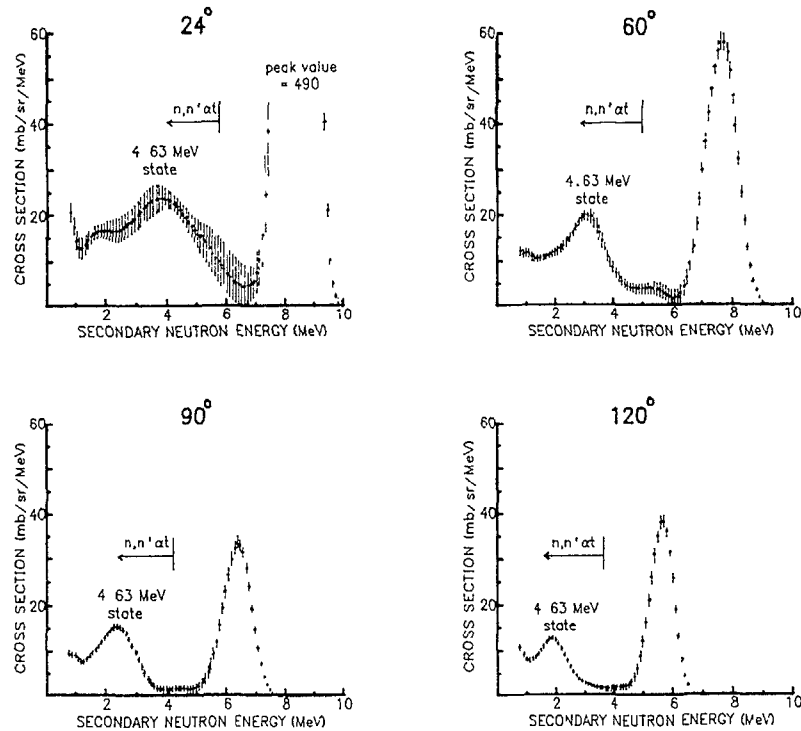
Fig. 2.4. Typical ^{7}Li result from the GELINA experiment for the primary neutron energy bin (8.55 ± 0.15) MeV.

3. INELASTIC (478 keV) SCATTERING

This inelastic line has been resolved from the elastic line only for primary neutron energies below ≈ 5 MeV [8,10]. In this range the angular distribution seems to be rather isotropic in the C.M. system as may be seen from Fig. 3.1. Knox et al. [11] have tried to separate the inelastic contribution also for their data at higher energies by performing a shape analysis of their observed lines. However, these results are extremely uncertain.

At Ohio University R-matrix calculations have been tried [12,13].
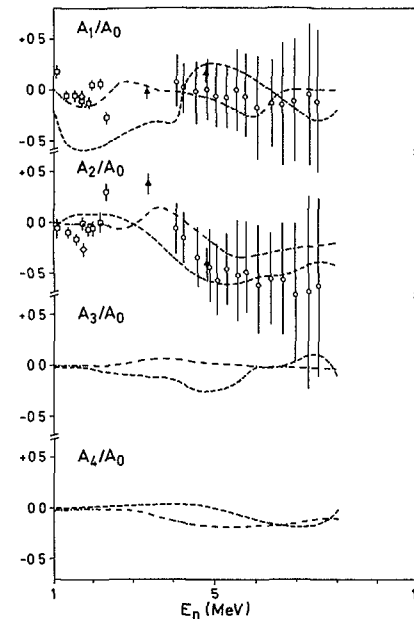
Fig. 3.1. Relative Legendre coefficients for ^{7}Li(n,n'$_1$). ref. 8, □ ref.9, $\triangle$ ref. 10, 0 ref. 11.The curves are from R-matrix calculations.- - - - ref.12, ------ref. 13.

However, depending on the assumptions made for the ^{8}Li level scheme, the results are quite different. The earlier work [12] (dashed-dotted line) is based on a cluster model while the dashed line refers to very recent shell model results [13].

A new experimental method to determine these neutron angular distributions has been developed recently at CBNM Geel [14]. Not the neutron angular distribution but the ^{7}Li* recoil angular distribution has been determined and this via the Doppler shift of the 478 keV γ-quanta. Both angular distributions correspond to each other because
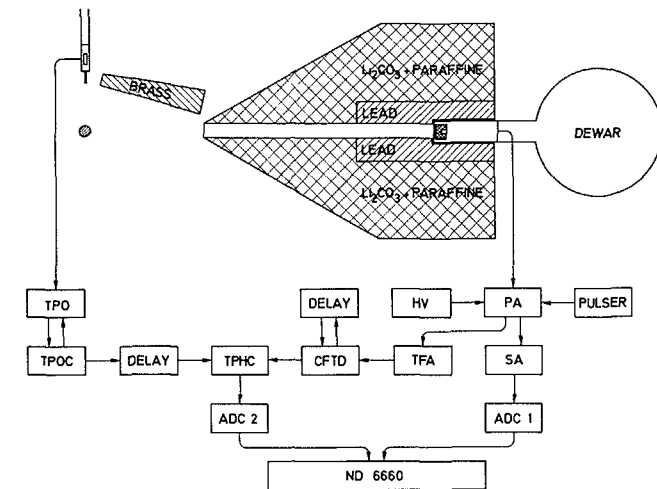
Fig. 3.2. Set-up to determine ^{7}Li(n,n'$_1$) angular distributions via the Doppler broadened γ-lines.
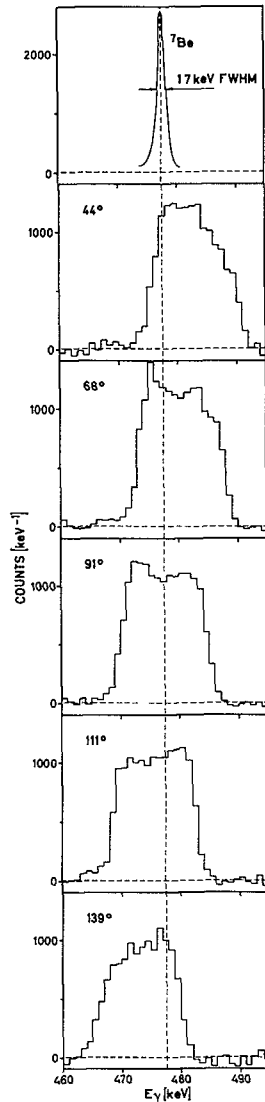
Fig.3.3. Doppler broadened 478 keV γ-lines. Position and shape change with observation angle. The fit does not use any other free parameter than the relative Legendre coefficients.

the γ-deexcitation of the excited recoil occurs very soon after the reaction. Due to the short half-life involved (73 fs) the energy loss of the recoil in the sample material(metallic lithium) can be treated as small correction. The experimental set-up is shown in Fig. 3.2. As an example the observed and analysed γ-spectra for five observation angles at $E_n \approx 8$ MeV are given in Fig. 3.3. The method can be regarded as complementary to the usual method described earlier (Section 2): with increasing primary neutron energy the resolution of the TOF-spectrometers decreases, while the Doppler-effect increases. This method was applied for neutron energies between 4 and 8.5 MeV [15]. There is excellent agreement in the 4-5 MeV range with the TOF results of Hopkins et al. [10]. Most of the evaluated ^{7}Li files [1-3] assume simply C.M. isotropy up to 20 MeV. The only exception is the ENDF/B-5 evaluation which uses up to 6 MeV the earlier R-matrix fit [12], above 8 MeV DWBA calculations [4] and a smooth connection between 6 and 8 MeV. We think that this can be improved because:

- there are new data in the 4 to 8 MeV region obtained by analyzing Doppler broadened γ-lines [15].
- the value of the R-matrix results is over-estimated as may be seen from the big differences resulting from different assumptions on the ^{8}Li level scheme.

It is suggested to describe the angular distribution of these inelastic neutrons by C.M. isotropy below 4 MeV, by DWBA results above 8 MeV and to use the experimental Geel results for the 4 to 8 MeV range.
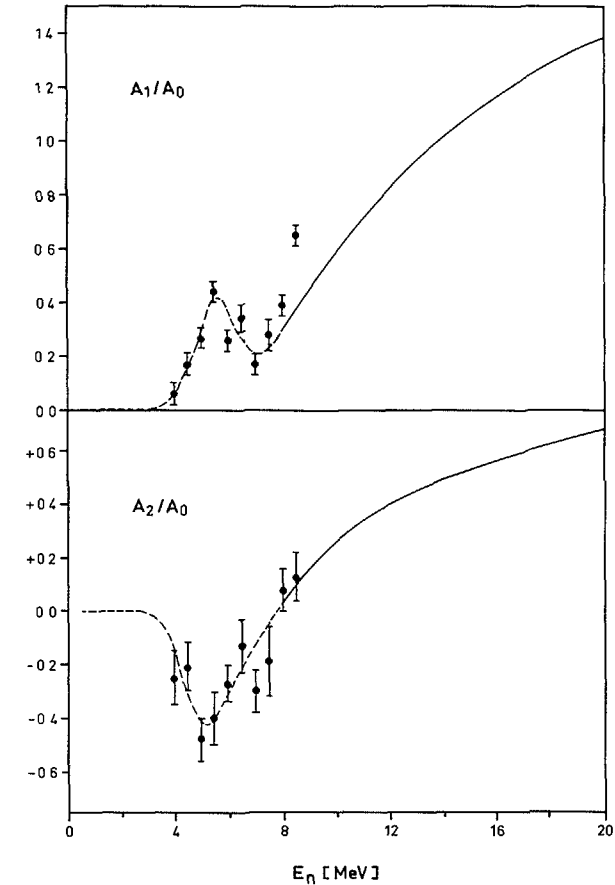
Fig. 3.4. Proposed relative Legendre coefficients for ^{7}Li(n,n'$_1$) when reduced to $l_{max} = 2$. Full line is from DWBA calculations (ref. 4), experimental points are from ref. 15.

The proposal is given graphically in Fig. 3.4. The restriction to $l_{max} = 2$ is not indicated by theory but simply by the quality of the experimental results [15] and has been applied for consistency reasons also to the DWBA results which in their original form extend to $l_{max} = 10$. Average differences due to this l-reduction stays below 3 % below 18 MeV which is certainly much smaller than the accuracy of the prediction.

4. NEUTRON EMISSION FROM TRITIUM BREEDING

Neutron emission combined with tritium production can occur via different modes where each mode will have its own neutron angular distribution pattern:

$$^7Li(n,n'_2)^7Li^* \rightarrow t + \alpha \qquad Q = -4.6 \text{ MeV}$$
$$^7Li(n,n'_3)^7Li^* \rightarrow t + \alpha \qquad Q = -6.7 \text{ MeV}$$
$$^7Li(n,n'tx) \qquad Q = -2.5 \text{ MeV}$$
$$^7Li(n,t)^5He \rightarrow n' + \alpha \qquad Q = -3.4 \text{ MeV}$$
$$^7Li(n,t)^5He^* \rightarrow n' + \alpha \qquad Q = -7.4 \text{ MeV}$$
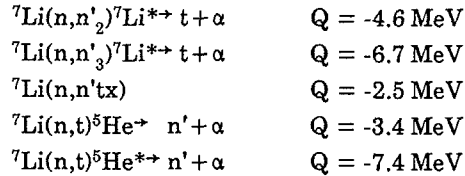
The first two branches are inelastic scattering with subsequent $^7Li^*$ decay (only the first excited state of ^7Li is particle-stable). The third branch is the three-body break-up while the last two branches are two-step reactions where the emitted neutron is stemming from the ^5He decay. What is generally called the neutron "continuum" is therefore a sum of five overlapping spectra which makes the separation very difficult.

Fig. 4.1. shows the velocity triangle. For convenience the velocities have been multiplied with $\sqrt{M/2}$ to form an energy-triangle. E_1 is then the laboratory energy, F_1 the C.M. energy and G_1 the square of the velocity of the C.M. system in the laboratory system multiplied by M/2. Starting from the energy-triangle(s) (Fig. 4.1.) we come to neutron energy ranges and double-differential cross sections as given in the following table. $R(x_1)$ are the needed C.M. angular distributions and $k = M_n/M_{5He}$.

$$x_i = \cos \vartheta_{CM}$$
$$y_i = \cos \vartheta_{LAB}$$
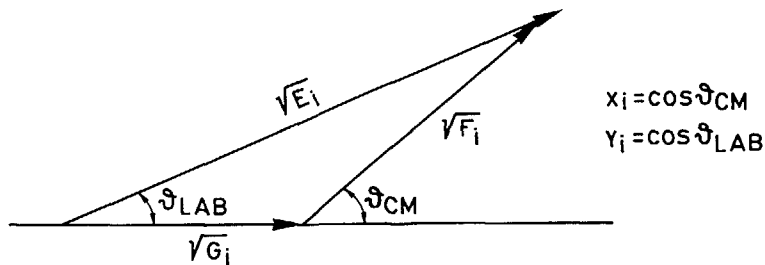
Fig. 4.1. The energy triangle.

Table 1

Mode	(Double-) Differential Cross Section	Secondary Energy Range
Scattering	$\dfrac{d^2\sigma}{dE_f d\Omega}(E,y_1) = \dfrac{\sigma \cdot R(x_1)}{4\sqrt{F_1 G_1}}$	$E_f = E^+$
Three-body Break-up	$\dfrac{d^2\sigma}{dE_f d\Omega}(E,y_1) = \dfrac{2\sigma}{n^2 \cdot F_1^2}\sqrt{E_1(F_1 - E_1 - G_1 + 2y_1\sqrt{E_1 G_1})}$	$0 \le E_f \le E^+$
Two-step	$\dfrac{d^2\sigma}{dE_f d\Omega}(E,y) = \dfrac{\sigma}{32n^2\sqrt{k} \cdot F_1 F_2 G_1} \displaystyle\int \dfrac{R_1(x_1) \cdot R_2(x_2) \cdot dE_1}{\sqrt{E_1} \cdot \sqrt{(1-y_1^2)(1-y_2^2)} - (y-y_1 y_2)^2}$	Zone I $\quad 0 \quad \le E_f \le E^{++}$ Zone II $\; E^{+-} \le E_f \le E^{++}$ Zone III $\; 0 \quad \le E_f \le E^{--}$ $E^{+-} \le E_f \le E^{++}$

Of course for scattering there is a complete angle-energy correlation. Only one angular distribution is needed and E_f is simply given by:

$$E^+ = \left[y_1 \cdot \sqrt{G_1} \pm \sqrt{F_1 - G_1(1 - y_1^2)} \right]^2$$

although the fact that both levels of interest here are broad has to be included. When scattering cross sections can be separated from the continuous parts then there is no need to complicate the matter by providing these data in form of double-differential cross sections. Even worse, doing so carries on the deficiencies of the experiment (finite energy resolution for neutron production and detection, finite detection solid angle) towards the evaluated file.

The three-body break-up double-differential cross sections here assume simply homogeneous filling of the phase-space (the different Q-value for three-body break-up leads of course to a different maximum energy E^+).

The two-step part agrees with the formula derived by Beynon [17] with the present more simple notation. The allowed energy ranges are given by the following bi-quadratic expression:

$$E^{\pm \pm} = k \cdot \left[y\sqrt{G_1} \pm \sqrt{\left(\sqrt{F_2/k} \pm \sqrt{F_1}\right)^2 - G_1\left(1 - y^2\right)} \right]^2$$

142
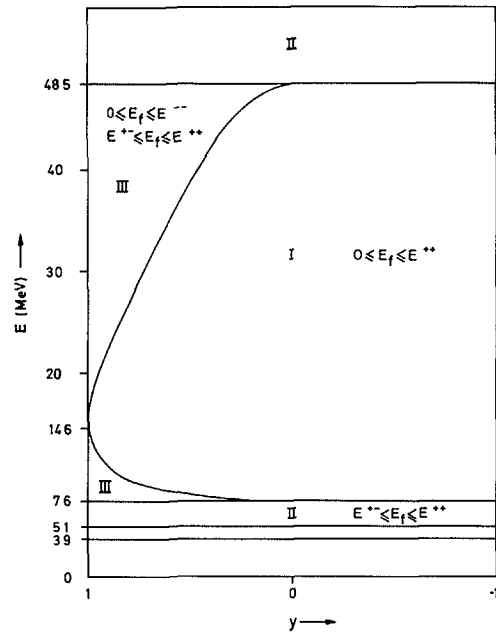
Fig. 4.2. Conditions which fix forbidden energy ranges in the two-step process.

Interesting enough the theory predicts a forbidden range between 0 and E^{+-} and between E^{--} and E^{+-} for conditions which are explained in Fig. 4.2. An angular distribution for each step is needed.

Fig. 4.3. gives the estimated size of the five contributions which sum up to the nowadays well-known tritium production cross section. This figure is based on earlier attempts by Oastler [18] and Bondarenko and Petrov [5]. The accuracy of this break-down should not be overestimated as may be seen from Fig. 4.4. which compares the estimated curve of the largest contribution (inelastic scattering via the 2nd state)
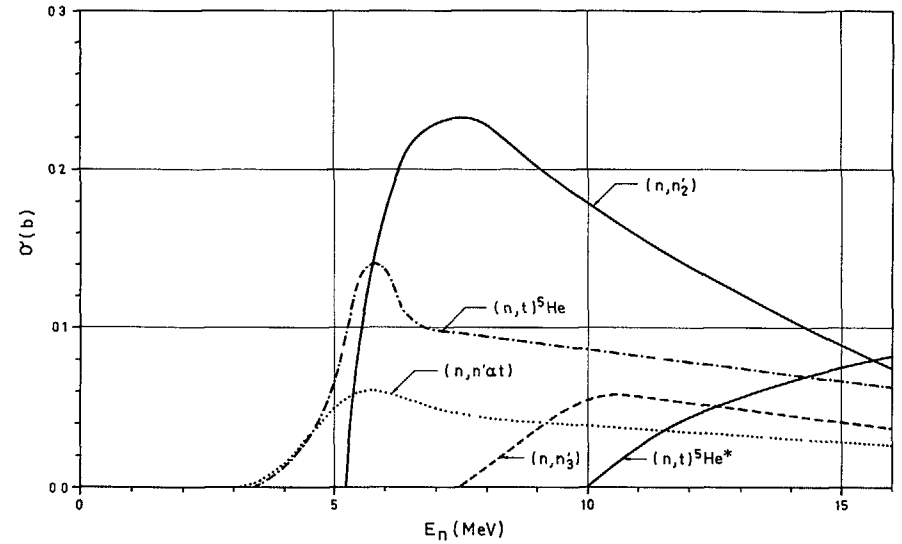
Fig. 4.3. Estimated size of the five continuum contributions.
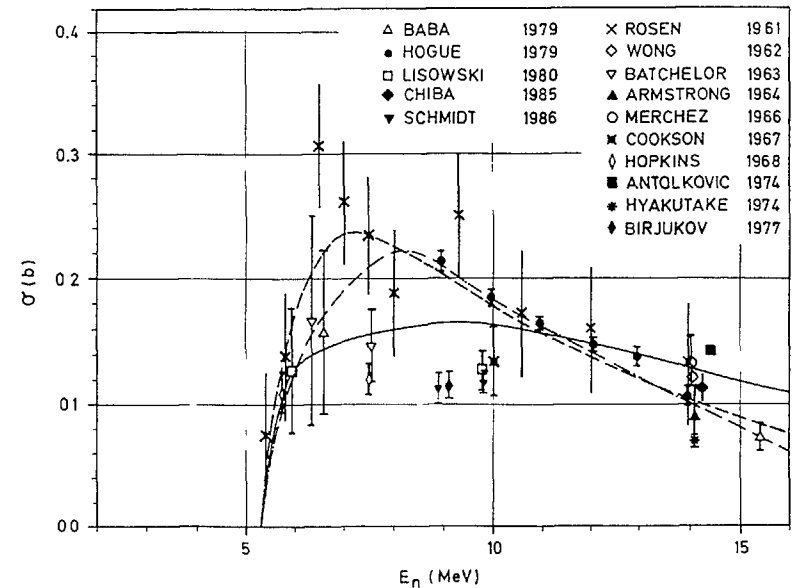
Fig. 4.4. Experimental and evaluated size of the $^7Li(n,n'_2)$ contribution.
---------- from Fig. 4.3; - - - - - JENDL-3; ———— ENDF/B-5.
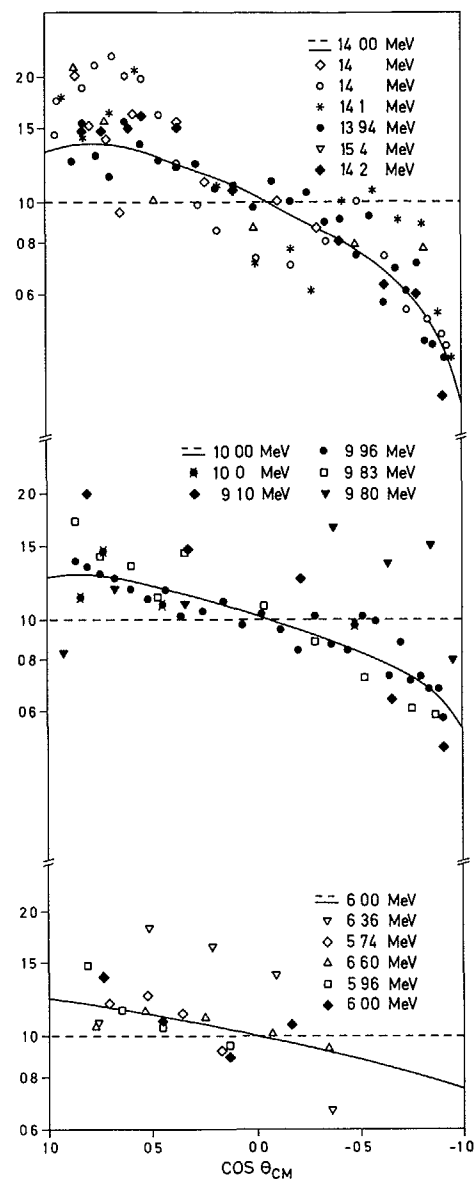
Fig. 4.5. Relative C.M. angular distribution for neutrons of 6, 10, and 14 MeV inelastically scattered on 7Li* (4.63). ------ JENDL-3; ———— ENDF/B-5

with experimental data. There is a big discrepancy around 8 to 10 MeV between the results of Hogue et al. [19] and others which reflects the difficulty to separate in the obtained spectra this line from other continuum contributions.

The corresponding angle-differential data for three energies are given in Fig. 4.5. Although these data have been normalised to represent relative angular distributions there is a scatter by at least ± 30 %. The different evaluated files reflect the degree of sophistication which has been used to represent the "continuum" (see Table 2).

Future evaluations should aim at separation of all inelastic contributions. The remaining part should be separated in three-body break-up and two-step reactions followed by parametrizations according to the formulae of Table 1. Such a procedure results in angle-energy correlations which are founded by physics. At the same time consistent double-differential neutron-, triton-, and α-particle-emission cross sections are produced.

Table 2

	Q = - 4.63 MeV	Other "continuum"
JENDL-2	not separated	isotropy
JEF-1	not separated	anisotropy
JENDL-3	separated, isotropy	anisotropy
ENDF/B-5	separated, anisotropy	anisotropy + pseudo level approach

REFERENCES

1) JEF Report 1, OECD/NEADB (1985).

2) K. Shibata,
Report JAERI-M-84-163, NEANDC(J)-104/U, INDC(JPN)-90/L (1984).

3) K. Shibata,
Report JAERI-M-84-204, NEANDC(J)-109/U, INDC(JPN)-95/L (1984).

4) P. Young, Private communication (1985).

5) I.M. Bondarenko and S.E. Petrov, Report INDC(CCP)-204/6 (1984).

6) M. Coppola and H.-H. Knitter, Z. Physik 232 (1970) 286.

7) E. Dekempeneer, H. Liskien, L. Mewissen and F. Poortmans,
Proc. Conf. on Fast Neutron Physics, Dubrovnik (1985) 227;
Proc. Intern. Conf. "Nuclear Data for Basic and Applied Science", St. Fé (1985) 133; Radiation Effects 92 (1986) 133.

8) R. Batchelor and J.H. Towle, Nucl. Phys. 47 (1963) 385.

9) H.-H. Knitter and M. Coppola, Report EUR 3903.e (1968).

10) J.C. Hopkins, D.M. Drake and H. Condé,
Nucl. Phys. A107 (1968) 139; Report LA-3765 (1967).

11) H.D. Knox, R.M. White and R.O. Lane, Nucl. Sc. Eng. 69 (1979) 223.

12) H.D. Knox and R.O. Lane, Nucl. Phys. A359 (1981) 131.

13) H.D. Knox,
Proc. Intern. Conf. "Nuclear Data for Basic and Applied Science", St. Fé (1985) 1007; Radiation Effects 95, (1986) 1.

144

14) H. Liskien,
Proc. Intern. Conf. "Nuclear Data for Basic and Applied Science", St. Fé (1985) 1277; Radiation Effects 95 (1986) 271.

15) H. Liskien and S. Bao,
Proc. Conf. on Fast Neutron Physics, Dubrovnik (1986) 275.

16) H. Liskien, Internal Report GE/R/VG/53/86 (1986).

17) T.D. Beynon and A.J. Oastler, Ann. Nucl. Energy 6 (1979) 537.

18) A.J. Oastler, Ph.D.-Thesis Univ. Birmingham (1977).

19) H.H. Hogue et al., Nucl. Sc. Eng. 69 (1979) 22;
Ph.D.-Thesis Duke University (1977).

STANDARD CROSS-SECTIONS FOR FUSION

H. CONDÉ
Gustaf Werner Institute,
Uppsala University,
Uppsala, Sweden

Abstract

The status of neutron cross section standards in the energy region 1 to 20 MeV is presented. Potential use of secondary reference cross sections and standard cross sections above 20 MeV is also discussed. Recommendations are given to improvements of the standard data base for fusion related cross section measurements.

1   Introduction

Standard cross sections for fusion related data measurements have not been discussed as a special issue before. One of the reasons for that depends on the fact that the existing neutron data files including the standards file cover the energy region up to 20 MeV. The neutron energy spectrum from a d-T plasma at 10-30 keV temperature is a couple of MeV wide and peaks at about 14 MeV. Thus, the standard cross sections for fusion related data measurements, which cover the energy region from 15-16 MeV down to thermal, can in most cases be found in the existing standard files.

The INDC/NEANDC Nuclear Standards File [1] has been agreed upon as the international standards file for nuclear data measurements. The large majority of the recommended numerical data for the standard cross sections is taken from ENDF/B-V, produced by the United States Cross Section Evaluation Working Group (CSEWG).

The next version (VI) of CSEWGs standards file is well underway. These standard evaluations are following a different process compared with that used for earlier versions of ENDF. The primary effort has been concentrated on a simultaneous evaluation using a generalized least squares program, R-matrix evaluations, and a procedure for combining the results of the evaluations. Preliminary results have been reported [2] which indicate a number of changes in the standard data compared to ENDF/B-V. A new version of the INDC/NEANDC standards file is planned following the release of the ENDF/B-VI standards.

Intermediate energy neutron sources have been proposed to study material damage effects of great importance for fusion reactor technology. To convert the results obtained at such a source to a d-T plasma source a large number of high energy cross sections (20-100 MeV)

have to be known. No standard cross sections have internationally been agreed upon for neutron data measurements in the intermediate energy range. A program has recently been started at the National Nuclear Data Center (NNDC) to improve selected medium energy nuclear data for applications. The activities include indexing the bibliography, compiling experimental data and coordinating the Medium Energy Nuclear Data Working Group in the establishment of data requirements and validation of nuclear analysis codes and nuclear data libraries via comparison with benchmark experiments. So far no standard cross sections have been discussed within this group.

Another topic, which is open for discussions, is that of secondary standards. An accurate known cross sections of a certain type of reaction opens the possibility of measuring the ratio of this cross section to the same reaction cross section in different materials and at different energies but also of measuring the ratio to cross sections for other reactions, which are experimentally determined with a similar technique as the reference. The impact of systematic uncertainties can in general be reduced in ratio measurements. Examples of reactions of importance for fusion reactor neutroniques are double differential elastic and inelastic scattering and other non-elastic cross sections as e.g. (n,x)-,(x-charged particle) (n,2n)- and (n,n'x)-reactions.

In the present review the status of the standards cross sections are discussed for measurements in the energy region above a few MeV. The discussion is hampered by the fact that the ENDF/B-VI standards file has not yet been released. Standard cross sections for the intermediate energy region are briefly discussed as also some secondary standard cross sections of potential use.

2 Neutron cross section standards in the energy region of 1-20 MeV

2.1 The H(n,n)H cross section

The hydrogen scattering cross section is at present the most accurately known of the standards. The ENDF/B-V evaluation was based on a phase-shift analysis by Hopkins and Breit [3] which indicated a degree of anisotropy and asymmetry about 90° in n-p scattering, even below 10 MeV, which is important in practical applications. The $\sigma(180°)/\sigma(90°)$ cross section ratio are approximately 1.023 at 7 MeV, 1.011 at 3 MeV and 1.004 at 1 MeV.

The Hopkins and Breit or the ENDF/B-V evaluation, which covers the neutron energy region between 100 keV and 30 MeV, has an estimated standard deviation in the total cross section of less than ±1 percent. High accuracy measurement of the hydrogen total cross section indicate that the ENDF/B-V evaluation is to high in the MeV region by fractional percentage amounts. The Hopkins and Breit analysis was based on energy-dependent phase-shift analysis by the Yale [4] and Livermore [5] groups. The agreement between the two analysis as represented by Hopkins and Breit up to 30 MeV is better that 2 percent for $\sigma(0)$ and within 1 percent for $\sigma(180)$. The values of $\sigma(180)-\sigma(0)$ from 1 to 30 MeV vary as much as 22 percent and indicate the uncertainty in the P-wave

phases, particularly $\delta(^1P_1)$, which determine the asymmetry in scattering at low energies.

More recent analysis of nucleon-nucleon scattering data has been made by Bohannon et al [6] and by Arndt et al [7]. The phase parameters obtained from the two analysis by Bohannon et al and Arndt et al at 25 MeV are in agreement but large uncertainties on the values of $\delta(^1P_1)$ of -5.18±0.47° (Bohannon) and -4.49±0.94° (Arndt) indicate that more differential scattering data are needed over a wide angular range. These values of $\delta(^1P_1)$ are also in reasonable agreement with those of -4.90±0.48° and -4.61±0.08° obtained from the Yale and Livermore analyses, respectively on which the Hopkins and Breit analysis is based.

A new evaluation by Dodder and Hale [2] has been accepted as the new hydrogen standard for ENDF/B-VI. This evaluation is a result of the analysis of n-p and p-p data using R-matrix formalism. In Figure 1 (from Ref [2]) the ENDF/B-VI evaluation and high accuracy total neutron cross section measurements are compared with ENDF/B-V. The new evaluation is in somewhat better agreement with measurements than the ENDF/B-V results.
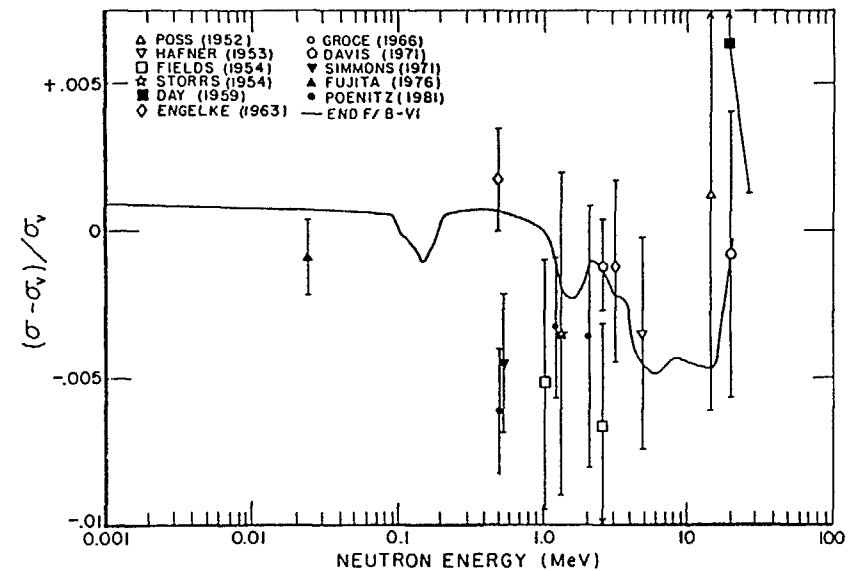
FIG.1. Comparison of high accuracy measurements of the hydrogen total neutron cross-section and the ENDF/B-VI evaluation with the ENDF/B-V evaluation (A.D. Carlson et al., Santa Fe (1985) p. 1429).

2.2 The C(n,n)C cross section

The C(n,n)C cross section is widely used as a scattering standard up to 2 MeV or below the sharp resonance at 2.087 MeV. The ENDF/B-V evaluation is taken from the R-matrix fits of Fu and Perey [8]. A slight uncertainty comes from the fact that scattering cross section on natural carbon (containing 1.11 % ^{13}C) is recommended as a standard while R-matrix evaluation refer to the $^{12}C(n,n)^{12}C$ cross section. There are two resonances in ^{13}C below 2 MeV, and each resonance will contribute about 0.2 % to the natural carbon cross sections. Therefore, the energy ranges from 0.13 to 0.18 MeV and from 1.72 to 1.78 MeV are not recommended as standards until sufficient evaluation is done for these resonances.

More recent works on the neutron total and scattering cross sections and R-matrix interpretation by Holt, Smith and Whalen [9] and Poenitz et al [10] verify the ENDF/B-V file to fractional percent accuracies (Fig 2).
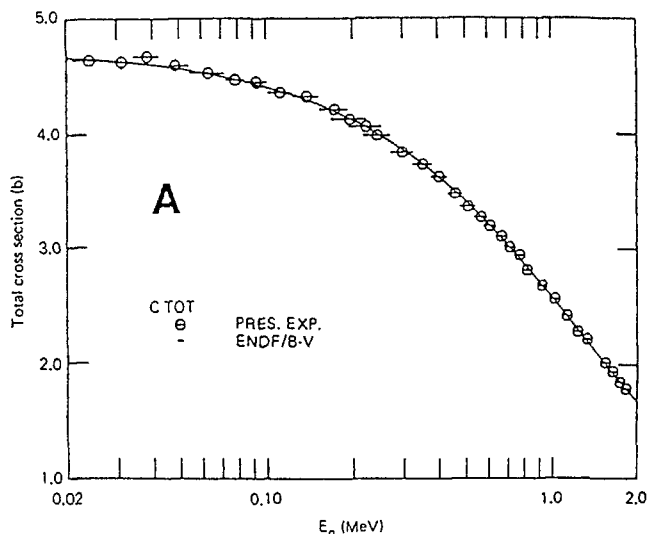
FIG.2. Comparison of the neutron total cross-sections of natural carbon measured by Poenitz et al. [10] with the corresponding values given in ENDF/B-V.

If care is taken to avoid resonance energies the n+C is a suitable scattering standard up to about 4.8 MeV {(n,n')-threshold}. In this energy region the total and elastic cross sections are essentially equivalent and known to accuracies of about 1 %.

The C(n,n)C could be a useful scattering standard also at higher energies above 5 MeV if the cross sections were well known at selected energies. Scattering cross sections at eight different energies between 6 and 14 MeV were recently measured by Böttger et al [11]. Large discrepancies were reported between the observed angular distributions and ENDF/B-V which is supported by a comparison of various experimental and evaluated data sets made for a Japanese evaluation [12].

Further measurements of the C(n,n)C cross section in the energy region 5-15 MeV are encourage.

2.3 The $^{27}Al(n,\alpha)^{24}Na$ cross section

The $^{27}Al(n,\alpha)^{24}Na$ cross section is widely used as a standard in dosimetry and activation measurements.

The evaluations by Hale, Stewart and Young [13] for ENDF/B-V and by Tagesen and Vonach [14], adopted for the INDC/NEANDC standard file, are in agreement within the given errors. Except for the low threshold region at about 8-9 MeV, the accuracy of the Tagesen-Vonach evaluation was claimed to be better than 5 %. In particular, an accuracy of about 0.5 % was claimed for the 14 MeV region.

In addition, an evaluation has been made by Kornilov et al [15]. Except for the low threshold region from 5.5 to 8.5 MeV the accuracy was well below 5 %. However, a structure was obtained for the cross section in the energy region from 6.5 to 8 MeV in discrepancy with Vonach and Tagesens evaluation (Fig 3).
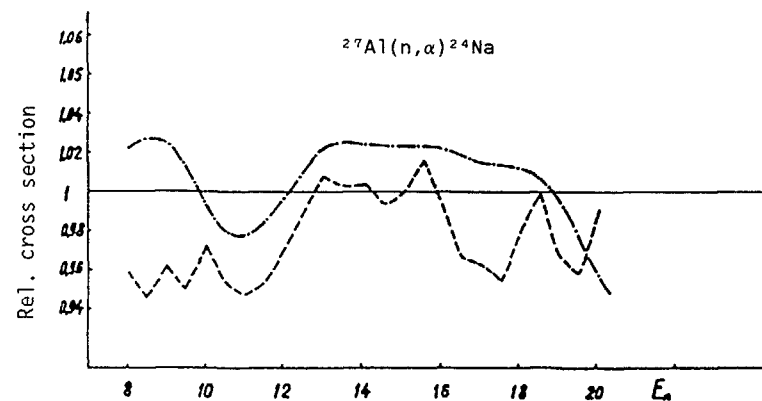
FIG.3. The ratios of the cross-sections recommended by S. Tagesen and H. Vonach [14] (- - - -) and in ENDF/B-V (·······) to the cross-section recommended by Kornilov et al. [15].

Vonach [16] has reported that new measurements are underway in the energy region 6-12 MeV followed by a new evaluation due for late 87.

2.4 ^{197}Au(n,γ) cross section

The ^{197}Au(n,γ) cross section is recommended as a standard in the energy region 0.2-3.5 MeV. Though, gold has excellent properties as a capture standard at low neutron energies since the material is near isotopic, easy to fabricate and has a simple decay scheme, it becomes more problematic to use above 1 MeV because of the small cross section and background problems. The experimental problems of high energy (n,γ) activation capture cross section measurements have been investigated and discussed by Andersson et al [17].

Furthermore, there seams to be a general concensus that the most recent measurements have cross sections lower that ENDF/B-V values for neutron energies between 1 and 3.5 MeV with uncertainties ranging from 4-8 %. At higher energies around 6-7 MeV the recent measurements give values considerably higher than the evaluation.
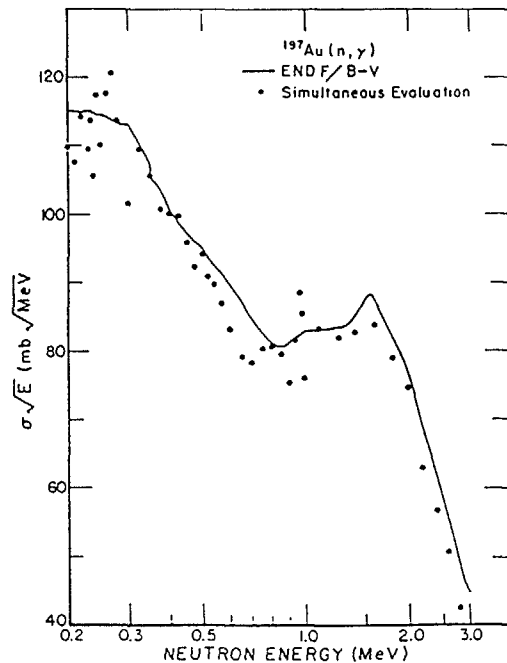
FIG.4. Preliminary results of the simultaneous evaluation of the Au(n,γ) cross-section for neutron energies from 0.2-3 MeV compared with the ENDF/B-V evaluation. The data are from the non-overlapping database analysis (A.D. Carlson et al., Santa Fe (1985) p. 1429).

Preliminary results from the simultaneous evaluation of the Au(n,γ) cross section for ENDF/B-VI do also support a lower cross section above 1 MeV [2] (Fig 4).

2.5 The ^{235}U fission cross section

The ^{235}U fission cross section is a recommended standard over the energy range 0.1 to 20 MeV. In WRENDA there are requests for measurements to an accuracy of ±1 percent over the whole energy range.

The uncertainties in the ENDF/B-V evaluations, which was adopted as the international standard, increase from 2.5 percent at 1 MeV to 6 at 20 MeV. The uncertainties in the ^{235}U fission cross-section suggested by the IAEA Consultants' Meeting at Smolenice in April 1983 (INDC(NDS)-146) also increase from 2-3 percent at 1 MeV to 6 percent at 20 MeV with the exception of the region around 14 MeV where the cross section was believed to be known to 1-2 %.

A number of accurate, and also absolute measurements of the ^{235}U fission cross section, have been made after the release of the ENDF/B-V evaluation (see e.g. Sowerby and Patrick [18]). The results of the new measurements are in general 2-3 % lower than the ENDF/B-V evaluation in the energy region below 4 MeV. Above 4 MeV accurate absolute measurements have been made at about 4.5, 14 and recently also at 18.8 MeV [19]. The results agree with ENDF/B-V within the stated uncertainties which in general are of the order of 2-3 percent.

Sowerby and Patrick discussed in their report to the Geel 1984 meeting [18] the contribution to the overall error in a fission cross section measurement from the fission counting, the assay of the amount of fissile material and the incident neutron flux determination. They concluded that the flux measurement was the biggest problem on the way to achieve 1 percent accuracy. The most promising method to measure the flux was the time correlated associated particle (TCAP) technique, which was recommended to be tested against a black neutron detector and/or the n-p scattering cross secti··n to prove that there are no unknown systematic errors in the method.

The observed fission rate has to be corrected for the angular distribution of the fragments. The correction is small when the fission fragments are collected over almost a 2π solid angle. If not the correction might be substantial and particular severe in the energy regions of second and third chance fission, where the anisotropy is not well known and changes rapidly.

The preliminary result of the simultaneous evaluation for ENDF/B-VI of the ^{235}U fission cross section (Fig 5) has been reported by Carlsson et al [2]. This evaluation is 1-2 % lower below 4 MeV and approximately the same above 4 MeV compared with ENDF/B-V.

2.6 The ^{238}U fission cross section

The ^{238}U fission cross section is a recommended standard from the threshold up to 20 MeV. However, the cross section shows fluctuation of
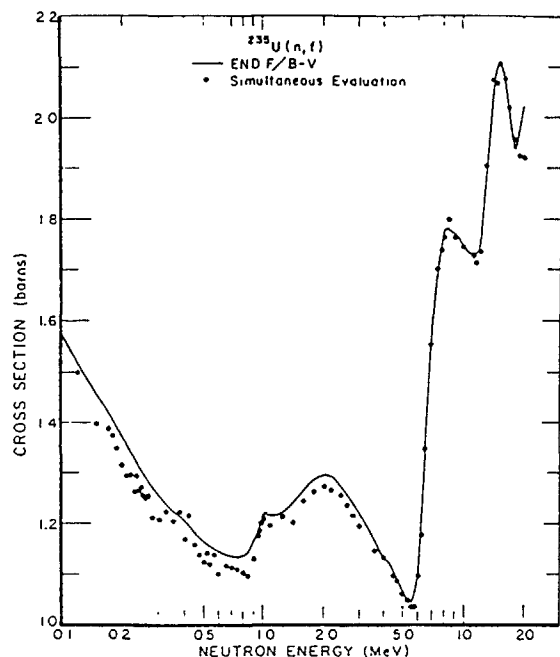
FIG.5. Preliminary results of the simultaneous evaluation of the ^{235}U(n,f) cross-section for neutron energies from 0.1–20 MeV compared with the ENDF/B-V evaluation. The data are from the non-overlapping database analysis (A.D. Carlson et al., Santa Fe (1985) p. 1429).

several percent, as remarked by A B Smith [20], well into the few MeV range and care should be taken to use the cross section as a standard in this energy range.

In the fission plateau areas from 2 to 6 MeV the ^{238}U fission cross section could be a useful standard if better known. The accuracy of the ENDF/B-V evaluation increases from about 2 percent at 2 MeV to 9 percent at 20 MeV. Recent measurements have improved the accuracy at 14 MeV to about 1 percent but still discrepancies exists up to 10 percent at 20 MeV [21].

2.7 Prompt fission neutron spectrum of ^{252}Cf

The neutrons from the spontaneous fission of ^{252}Cf can be used for energy calibration in the MeV region of neutron detectors if the shape of the neutron spectrum is well known.

Madland et al [22] reported an overall consensus between recent experiments and calculation of the spectrum from 1 to 10 MeV. Compared to a Maxwellian spectrum with T=1.42 MeV which was earlier accepted as a standard, there is a positive deviation reaching a maximum of 3 percent at about 3 MeV followed by a negative deviation increasing continuously with energy and becoming ~20 percent at 20 MeV. New evaluations are excepted both for the ENDF/B file (Madland-Nix calculated spectrum) and the INDC/NEANDC file (W Mannharts evaluation).

3 Secondary standards

In ratio cross section measurements systematic errors are reduced if the two measurements are made with the same experimental technique and the samples have a similar response to neutrons. Thus, a number of well determined reference cross sections (secondary standards), can be of great value for the experimentalists.

In particular, the large number of activation cross section measurements around 14 MeV have resulted in a set of well determined activation cross sections, which are commonly used as references. In a recent compilation and evaluation of 14-MeV neutron activation cross sections by Evain et al [23] it is concluded that the following reactions are the most commonly used references.

Reaction	Cross Section (mb) (at 14.7 MeV)	Uncertainty (%)
^{27}Al(n,α)^{24}Na	113.7	0.6
^{32}S (n,p)^{32}P	215	1.5
^{56}Fe(n,p)^{56}Mn	107.8	0.6
^{63}Cu(n,2n)^{62}Cu	537	1.2
^{65}Cu(n,2n)^{62}Cu	962	1.2

The cross sections and the uncertainties are taken from an evaluation by Ryves [24] in which he also gives the evaluated data for the reactions ^{93}Nb(n,2n)^{92m}Nb {451 mb, 1.6 %} and ^{197}Au(n,2n)^{186}Au {2160 mb, 1.6 %}.

The ^{56}Fe(n,p)^{56}Mn reaction has the advantage that natural Fe can be used taking into account the higher specific activity. The ^{56}Fe(n,p) cross section was measured by Kudo et al [25] between 14 and 19.9 MeV. The results were in agreement with measurements by Ryves et al [26] between 14 and 16 MeV but was 5-15 % higher above 16 MeV. The ENDF/B-V evaluation was systematically lower over the whole energy range.

The IAEA CRP on Measurement and Analysis of 14 MeV Neutron Nuclear Data Needed for Fusion Reactor Technology has recommended the use of the ^{27}Al(n,α), ^{56}Fe(n,p) and ^{238}U(n,f)-reaction as flux monitors in activation analysis.

In many flux measurements, e.g. in the international fluence rate intercomparison organized under the auspicies of CCEMRI/CIPM [27], the ^{115}In(n,n')^{115m}In-reaction has been used as a reference. The accuracy at 14 MeV was claimed to be 4.7 percent according to the evaluation by Evain et al [23].

Also for neutron spectrometry or double differential cross section measurements the IAEA CRP on 14 MeV Neutron Nuclear Data has recommended the use of DDCS for C, Fe, Nb and Pb as standards. They request a careful evaluation of these elements including the newest experimental data available to reach at least 5 percent accuracy. A comprehensive evaluated nuclear-data file for elemental niobium was prepared by A B Smith et al [27]. The file contains detailed information throughout the energy region of primary fusion interest, i.e. from 100 keV to 20 MeV. The estimated uncertainties in the elastic cross section were 3-5 percent up to 15 MeV and 7 percent at 15-20 MeV. Compilations of neutron emission measurements are in progress at TUD and LLL for Pb and C at 14 MeV [29].

Different reference cross sections have been used in γ-ray production cross section measurements. The gamma production cross sections for the 4.4 MeV and the 0.85 MeV γ-rays in C and Fe, respectively have been mentioned as suitable candidates but no one of the cross sections are known with enough accuracy (± 5 percent) over a wide enough energy range.

At 14 MeV several reaction cross sections are known with enough accuracy to be used as secondary standards. However, at energies aside of 14 MeV the cross section are in general not known well enough and more measurements to improve the accuracy over a wider energy range would be of interest.

4   Nuclear standard cross sections above 20 MeV

Neutron cross section standards in this energy region have not yet internationally been agreed upon.

Neutron cross sections above 20 MeV are of interest in fusion reactor research mainly because of several proposals of high energy neutron sources for radiation damage research. As examples can be mentioned the US 35 MeV (d+Li) source, FMIT, and the European 600 MeV spallation source EURAC.

The large number of reaction channels which opens up at high energies and the large number of materials involved makes it necessary to rely to a large extent on nuclear reaction models to calculate the cross sections. Experiments are mostly set up to test the reaction models. For radiation damage studies the gasproduction, displacement-per-atom (dpa) and transmutation reactions are of main importance.

Very few differential neutron cross sections have been measured as a whole and only the H(n,n)H cross section is relatively accurately known up to several hundred MeV. The total cross section measurement by Larsson [30] and the nucleon-nucleon phase shift analysis by Arndt [7] show agreement to better than 1 percent in the energy region 2-80 MeV.

Some candidates for reference cross sections in the energy region from 20 to 100 MeV can be mentioned beside the H(n.n)H cross section.

The fission cross section of ^{235}U could be a useful standard in connection with measurements using white neutron sources as it covers the full energy range from 0.1 MeV to the maximum energy. The same cross section for ^{238}U might be a better choice for monoenergetic intermediate neutron energy sources as it discriminates against slow neutrons. Plans have been reported from LANL to measure the ^{235}U(n,f) cross section up to at least 100 MeV.

Furthermore, the 90° excitation function for the 4.4 MeV γ-rays of the $^{12}C(n,n'\gamma)^{12}C$-reaction from threshold to 100 MeV has been measured by Wender and Auchampaugh [31]. However, the accuracy was fairly poor and a pronounced structure was observed which in combination limits the use of the cross section as a reference.

5   Conclusions

Standard cross sections are in general available up to 15 MeV with acceptable accuracies (<5 %) for fusion related neutron data measurements. Above this energy up to 20 MeV, which is the high energy limit in available data files, the situation is not quite statisfactory. Uncertainties are increasing to 10 % or more at 20 MeV.

Version VI of the ENDF/B standards file is in a final state of preparation. The accuracies of the standards, in particular of the ^{235}U fission cross section, are most probable to be improved compared to version V. The recommendation is to wait for the release of ENDF/B-VI standards before any descision are taken on further works.

Secondary reference cross sections exist with good accuracy at around 14 MeV. Evaluations of the most commonly used cross sections over a wide energy range are recommended followed by measurements to improve accuracy and fill in the gaps.

Above 20 MeV measurements could be of great value of the fission cross sections of ^{235}U and ^{238}U up to 100 MeV to backup the potential use of these cross sections as standards for intermediate energy neutron cross section measurements.

REFERENCES

1   Nuclear Data Standards for Nuclear Measurements, IAEA Technical Reports Series No 227, Vienna 1983

2   A D Carlsson, W P Poenitz, G M Hale and R W Peelle, Proc Nuclear Data for Basic and Applied Science, Santa Fe, May 13-17, 1985, p 1429

3   J C Hopkins and G Breit, Nuclear Data Tables A9 (1971) 137

4   R E Seamon, K A Friedman, G Breit, R D Haracz, J M Holt and A Prakash, Phys Rev 165 (1968) 1579

150

5   M H MacGregor, R A Arndt and R M Wright, Phys Rev <u>182</u> (1969) 1714

6   G E Bohannon, T Burt and P Signell, Phys Rev <u>C13</u> (1976) 1816

7   R A Arndt, R H Hackman and L D Roper, Phys Rev <u>C15</u> (1977) 1002

8   C Fu and F Perey, At Data Nucl Tables <u>22</u> (1978) 249

9   R Holt, A Smith and J Whalen, Argonne National Lab Report ANL/NDM-43 (1978)

10   W Poenitz and J F Whalen, Nucl Phys <u>A383</u> (1982) 224

11   H Bottger, H J Brede, H Klein, H Scholermann and B Siebert, Proc Nuclear Data for Basic and Applied Science, Santa Fe, May 13-17, 1985, p 1455

12   K Shibata, Report JAERI-M 83-221 (December 1983)

13   G M Hale, L Stewart and P Young, LA-8036-PR (1979)

14   S Tagesen and H Vonach, Physics Data 13-1, Fachinformations-zentrum, Karlsruhe (1981)

15   N V Kornilov, N S Rabotnov, S A Bachikov, E V Gay, A B Kagalenko and V I Trykova, IAEA AGM Nuclear Standard Reference Data, Geel, 1984, p 135

16   H Vonach, private communication

17   P Andersson, R Zorro and I Bergqvist, Proc Nuclear Data for Basic and Applied Science, Santa Fe, May 13-17, 1985, p 1459

18   M G Sowerby and B H Patrick, IAEA AGM Nuclear Standard Reference Data, Geel, 1984, p 151

19   C M Herback et al (INDC(GDR)-37) 1985

20   A B Smith, Nuclear Data Standard for Nuclear Measurements, IAEA Technical Reports Series No 227, p 53

21   Y Kanda, IAEA AGM Nuclear Standard Reference Data, Geel, 1984, p 191

22   D Madland, R Labauve and R Nix, Proc Nuclear Data for Basic and Applied Science, Santa Fe, May 13-17, 1985, p 1445

23   B P Evain, D L Smith and P Lucchese, Argonne National Laboratory Report, ANL/NDM-89 (1985)

24   T B Ryves, Prov Nuclear Standard Reference Data, November 1984, Geel, p 431

25   K Kudo, T Michikawa, T Kinoshita, Y Hino and Y Kawada, Proc Nuclear Standard Reference Data, November 1984, Geel, p 449

26   T B Ryves, P Kolkowski and U J Zieba, Meteorologia <u>14</u> (1978) 127

27   H Lieskien and V E Lewis, Proc Nuclear Standard Reference Data, November 1984, Geel, p 324

28   A B Smith, D L Smith and R J Howerton, ANL/NDM-88 (1985) and A B Smith, P T Guenther, W P Poenitz, D L Smith, J F Whalen and R J Howerton, Proc Nuclear Data for Basic and Applied Science, Santa Fe May 13-17, 1985, p 129

29   D Seeliger private communication (1986)

30   D C Larsson, Proc Symp on Neutron Cross-Sections from 10 to 50 MeV, BNL-NCS-51245, p 277

31   S Wender and G Auchampaugh, Reports to the DOE Nuclear Data committee

SYSTEMATICS OF EXCITATION FUNCTION
FOR (n, charged particle) REACTIONS

Zhixiang ZHAO, Delin ZHOU
Institute of Atomic Energy,
Beijing, China

Abstract

On the bases of evaporation model considering
the preequilibrium emission under some approximations,
the analytical expressions including two adjustable pa-
rameters have been derived for excitation functions of
(n, charged particle) reactions. Fitting these expres-
sions to the available measured data, these parameters
have been extracted and the systematic behaviours of the
parameters have been studied. More accurate predictions
than before could be obtained by using these expressions
and systematics parameters.

Introduction

Charged particle producing data of neutron induced reactions
are of great importance for design of fission and fusion reactor.
Unfortunately, experimental data especially measured excitation
functions are very scarce. The unmeasured energy regions and nuclei
may be complemented by model theory calculation and systematics
predictions. Generally, The latter is more efficient. All earlier
work on systematics of (n,q) cross sections (q=p,d,t, ^{3}He and α)
except Pearlstein's[1] and Krivan's[2] are carried out at $E_n=14.5$ MeV[3-8].

In the present work, we concerned that the neutron energy
region is up to about 20 MeV and that target mass region is 23 $\leqslant$ A
$\leqslant$ 197. Charged particle p,d,t, ^{3}He and α emitted in (n,q) reactions
are considered.

Formulae

Based on evaporation model considering preequilibrium emis-
sion, the analytical expressions of excitation function for (n,q)
reactions have been derived under some approximations. Some primary
approximations are as follows:

1. The preequilibrium emission only occurs at the state of
exciton number n=3.

2. There is only one competing reaction of (n,n').

3. The (n,qn) reaction is primary channel for secondary pa-
rticle emission and the neutron emission must follow if the rest
energy in compound nucleus system is enough for such emission
after the q emission.

4. Complex particle such as d,t, ^{3}He and α are regarded as
excitons which are prior formed in target nucleus with a probability
P_q. In this work, we took $P_\alpha=0.2$ [9] and $P_d,P_t,P_{3He} \ll 1$.

5. The penetration factor of rectangular-well potential

$$D_q(e_q)=\exp(-a_q(1-e_q/E_c^q)) \qquad (1)$$

here

$$a_q=0.63772(A_q)^{\frac{1}{2}}(1+A^{1/3})(E_c^q)^{\frac{1}{2}} \qquad (2)$$

are used to describe the effects of coulomb barrier. In eq.(1) and

eq.(2). The A and A_q are the mass number of target nucleus and emitted charged particle respectively. The e_q and E_c^q are kinetic energy of particle q and the generalized height of coulomb barrier respectively.

6. The energy level density of compound nucleus is taken in the form of constant temperature.

The details of the formulae deriving have been given in ref. 10. The ultimate expressions are given as follows:

$$\sigma_{n,q}(E_n)=C_q(B_1^q+\frac{\lambda_2}{L_n}\cdot\frac{B_2^q}{1+\Gamma_n/\Gamma_q})/(1+\lambda_2/L_n+L_q/L_n) \tag{3}$$

for p and α and

$$\sigma_{n,q}^t(E_n)=C_q(\frac{L_q/L_n}{\lambda_2/L_n}+\Gamma_q/\Gamma_n) \tag{4}$$

for d,t and ^{3}He, where

$$\lambda_2/L_n=0.035A(1+S_n/E_n)^3 \tag{5}$$

$$B_1^q=\begin{cases}\theta_q h(t_0^q,t_0^q,t_2^q;a_q) & E_n\leqslant -Q_{qn} \\ \theta_q(h(t_0^q,t_0^q,t_2^q;a_q)-\alpha h(t_0^q,t_1^q,t_2^q;a_q)) & E_n>-Q_{qn}\end{cases} \tag{6}$$

$$B_2^q=\begin{cases}1 & E_n\leqslant -Q_{qn} \\ 1-\alpha f_q(E_n+Q_{qn})/f_\infty^q & E_n>-Q_{qn}\end{cases} \tag{7}$$

$$L_q/L_n=\theta_q h(t_0^q,t_0^q,t_2^q;a_q) \tag{8}$$

$$\Gamma_n/\Gamma_q=u_q\beta\left\{1-(1+E_n/T)\exp(-E_n/T)\right\}f_\infty^q/f_q(E_n+Q_q) \tag{9}$$

$$h(z_0,z_1,z_2;a_q)=\frac{6}{z_2^3}\times$$

$$\times\begin{cases}\{z_0+2+(z_0z_1-z_0+2z_1-z_1^2-2)\exp(z_1)\}\exp(-a_q) & z_1\leqslant a_q \\ (z_0+2)\exp(-a_q)+a_qz_0-z_0-a_q^2+2a_q-2+z_0z_1^2/2-z_1^3/3-z_0a_q^2/2+a_q^3/3 & z_1>a_q\end{cases} \tag{10}$$

$$f_q(z)=\begin{cases}b_q^2\left\{1-(1-z/(Tb_q))\exp(z/(Tb_q))\right\}\exp(-a_q) & z\leqslant E_c^q \\ f_\infty^q-(1+z/T)\exp(-z/T) & z>E_c^q\end{cases} \tag{11}$$

$$f_\infty^q=b_q^2\left\{1-(1-E_c^q/(Tb_q))\exp(E_c^q/(Tb_q))\right\}\exp(-a_q)+(1+E_c^q/T)\exp(-E_c^q/T) \tag{12}$$

$$b_q=(a_qT/E_c^q-1)^{-1} \tag{13}$$

$$a_q=0.63772(A_q)^{\frac{1}{2}}(1+A^{1/3})(E_c^q)^{\frac{1}{2}} \tag{14}$$

$$T=\begin{cases}13A^{-\frac{1}{2}} & A\leqslant 165 \\ (0.0125A-1.0625)\times13A^{-\frac{1}{2}} & A>165\end{cases} \tag{15}$$

$$\begin{cases}t_0^q=(E_n+Q_q)a_q/E_c^q \\ t_1^q=(E_n+Q_{qn})a_q/E_c^q \\ t_2^q=E_na_q/E_c^q\end{cases} \tag{16}$$

α and β are two empirical parameters

$$\alpha=\begin{cases}1-A/130 & A\leqslant 130 \\ 0 & A>130\end{cases} \tag{17}$$

$$\beta=\begin{cases}1 & A\leqslant 128 \\ 1.740-0.0063A & A>128\end{cases} \tag{18}$$

The values of θ_q and u_q are given in table I.

Tab. I The values of θ_q and u_q

q	p	d	t	^{3}He	α
θ_q	1	6	9	9	1.6
u_q	1	1/3	1/3	1/3	2.5

In eq.(3) to eq.(18), E_n is the incident neutron energy; S_n

the neutron separation energy of compound nucleus system; T the

nuclear temperature of target, the meanings of A and A_q are as the

same as in eq.(2), Q_q and Q_{qn} are reaction energy for (n,q) and (n,

qn) respectively. The E_n, S_n, T, Q_q and Q_{qn} are all in unit of MeV.

For the emissions of d,t and ^{3}He, the process of secondary

particle emission have been omitted so that the sum of cross

sections

$$\sigma^t_{n,q} = \sigma_{n,q} + \sigma_{n,qn} + \sigma_{n,q2n} + \sigma_{n,qp} + \cdots \qquad (19)$$

are given as eq.(4).

In eq.(3) and eq.(4), there are two adjustable parameters C_q

and E^q_c. The E^q_c represents the generalized height of coulomb barrier

and C_q a constant proportional to maximum of $\sigma^t_{n,q}$ defined by eq.(19).

Systematics of Local Parameters C_q and E^q_c

For (n,p) and (n,α) reactions in mass region $23 \leqslant A \leqslant 197$ the mea-

sured excitation functions for about fifty nuclei have been collec-

ted in the light of ref. 11 and ref. 12. The least squares fits have

been carried out for available experimental data by using eq.(3) and

the fitting parameters (called local parameters) have been obtained.

Before fitting, Q_q and Q_{qn} have been calculated from ref. 13 and S_n

taken from ref. 10. The agreement between fitting curves and measured

data is satisfactory. These results demonstrated that the contribu-

tion of the preequilibrium emission must be taken into accout in the

formulae. For medium weight nuclei, the fraction of preequilibrium

is about 30-50% at E_n=20MeV (see fig.1).
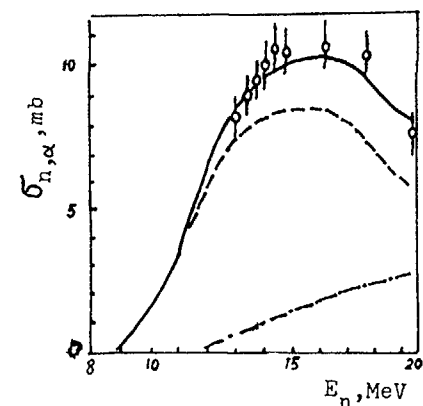
Fig.1 Excitation Function
of ^{92}Zr(n,α)^{89}Sr

- - - evaporation
- · - preequilibrium
——— evaporation +
preequilibrium

The local parameters C_q and E^q_c for (n,p) and (n,α) reactions

can be expressed as a simple functions of neutron number N and proton

number Z of target nucleus as following

$$\overline{E^p_c} = (-0.6+0.25Z-0.001Z^2-2\exp(-0.05(Z-28)^2))\exp(29.6\frac{N-Z}{A^{3/2}}), \text{MeV} \qquad (20)$$

$$\overline{E^\alpha_c} = -3.4+0.57Z-0.003Z^2-3\exp(-0.3(Z-28)^2), \text{MeV} \qquad (21)$$

$$\overline{C_p} = (1+A^{1/3})^2\exp(5.88-33.7\frac{N-Z}{A} -16.8A^{-2/3}), \text{mb} \qquad (22)$$

$$\overline{C_\alpha} = (1+A^{1/3})^2\exp(2.0-23.7\frac{N-Z}{A} +21.0A^{-2/3}), \text{mb} \qquad (23)$$

The parameters $\overline{C_q}$ and $\overline{E_c^q}$ calculated from above systematics
are called regional parameters. The comparisions between local and
regional parameters are given as fig.2 to fig.5. From fig.2 and
fig.3, one can find that the shell effects exists at Z=28 for E_c^q.
And it can be illustrated empirically with a normal function. It
is not evident for shell effect and odd-even effect of target nucleus
on parameter $\overline{C_q}$.
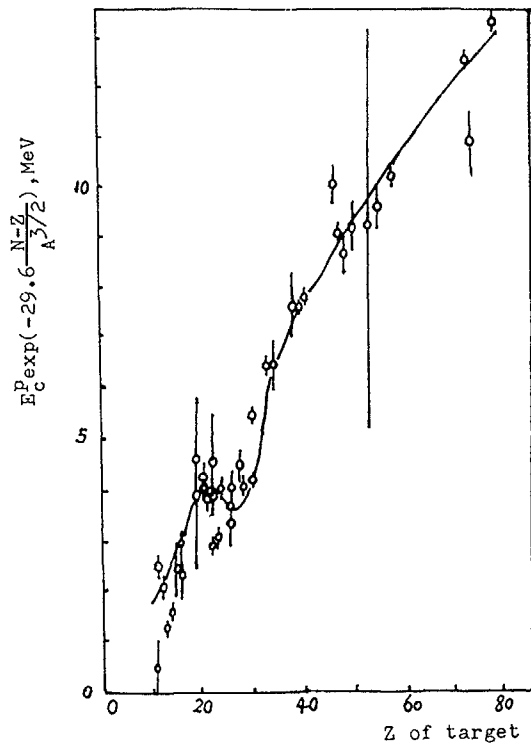
Fig.2 Systematics of E_c^p
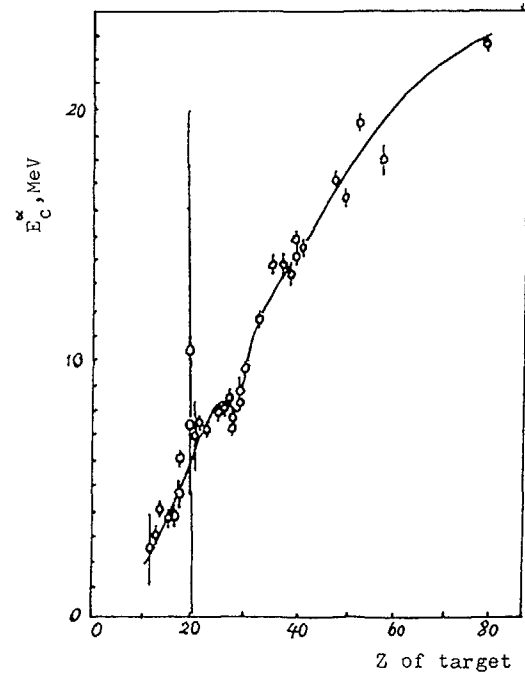
Fig.3 Systematics of E_c^α
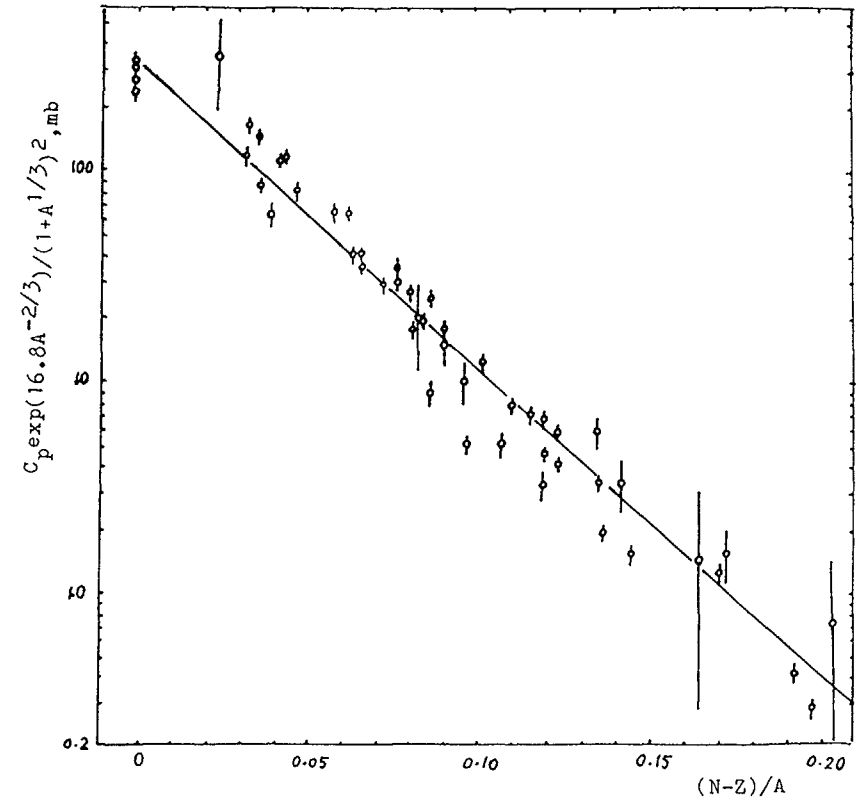
Fig.4 Systematics of C_p
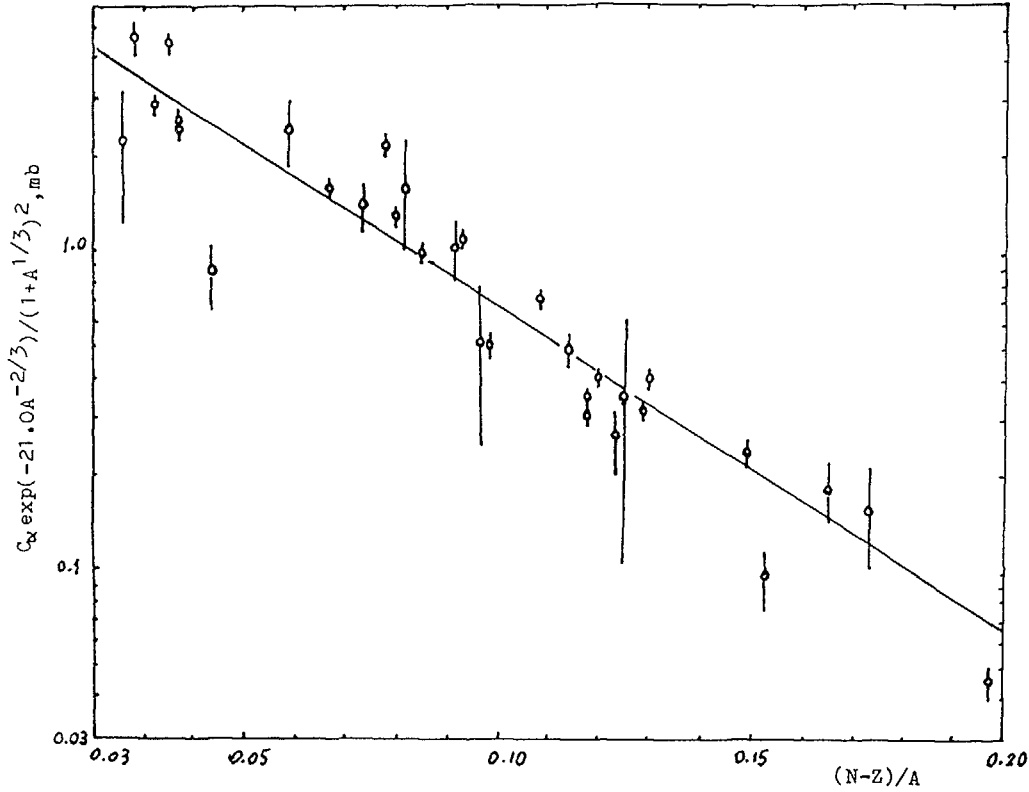
Fig.5 Systematics of C_α

The corvarance matrix $\bar{V}_q$ of regional parameters would be estimated in order to get the uncertainties of cross sections predicted with regional parameters. To combine the uncertainties such as negligence error, correlated error and uncertainties of the expression for excitation function and the systematics into $\bar{V}_q$, $\bar{V}_q$ was estimated by moment method [14]. Let

$$\bar{V}_q = \bar{P}_q \bar{M}_q \bar{P}_q \tag{24}$$

where

$$\bar{P}_q = \begin{pmatrix} \bar{C}_q & 0 \\ 0 & \bar{E}_c^q \end{pmatrix} \tag{25}$$

$$\bar{M}_q(1,1) = \frac{1}{m-1} \sum_{i=1}^{m} (t_i^q)^2 - \frac{1}{m(m-1)} (\sum_{i=1}^{m} t_1^q)^2 \tag{26}$$

$$\bar{M}_q(2,2) = \frac{1}{m-1} \sum_{i=1}^{m} (u_i^q)^2 - \frac{1}{m(m-1)} (\sum_{i=1}^{m} u_i^q)^2 \tag{27}$$

$$\bar{M}_q(1,2) = \bar{M}_q(2,1)$$

$$= \frac{1}{m-1} \sum_{i=1}^{m} t_i^q u_i^q - \frac{1}{m(m-1)} \sum_{i=1}^{m} t_i^q \sum_{i=1}^{m} u_i^q \tag{28}$$

and

$$t_i^q = (\hat{C}_q(N_i,Z_i) - \bar{C}_q(N_i,Z_i))/\bar{C}_q(N_i,Z_i) \tag{29}$$

$$u_i^q = (\hat{E}_c^q(N_i,Z_i) - \overline{E_c^q}(N_i,Z_i))/\overline{E_c^q}(N_i,Z_i) \tag{30}$$

It follows that

$$\bar{M}_p = \begin{pmatrix} 0.30^2 & 0.11(0.30)(0.25) \\ 0.11(0.30)(0.25) & 0.25^2 \end{pmatrix} \tag{31}$$

$$\bar{M}_\alpha = \begin{pmatrix} 0.31^2 & -0.24(0.31)(0.14) \\ -0.24(0.31)(0.14) & 0.14^2 \end{pmatrix} \tag{32}$$

For $(n,d),(n,t)$ and $(n,{}^3He)$ reactions, the fitting with two parameters C_q and E_c^q could not be carried out because of lack expe-

rimental data for excitation function. We had to replace E_c^d and E_c^t with $\overline{E_c^p}$ and to replace E_c^{3He} with $\overline{E_c^\alpha}$ so that there is one parameter C_q in eq.(4). Therefore, only one point cross section is needed to determine parameter C_q. Taking into accout the meaning of eq.(4) and status of experimental data for (n,d), (n,t) and (n,^{3}He) reactions, the following experimental data have been selected:

(n,d) reaction: data measured at LLL with magnetic quadrupole

   spectrometer in neutron energy E_n=14-15MeV[15].

(n,t) reaction: t emission cross sections measured at

   $\overline{E}_n$=22.5MeV[16].

(n,^{3}He) reaction: cross section measured by activation method

   at $\overline{E}_n$=22.5MeV[17].

Assuming the shapes of C_d, C_t and C_{3He} versus Z all are the same, the systematics for C_d, C_t and C_{3He} have been found as follows:

$$\overline{C}_d=23(1-0.052Z+0.00083Z^2),mb \qquad (33)$$

$$\overline{C}_t=5.81(1-0.052Z+0.00083Z^2),mb \qquad (34)$$

$$\overline{C}_{3He}=2.9(1-0.052Z+0.00083Z^2),mb \qquad (35)$$

By the moment method, the relative errors have been estimated:

$$\left\{ \begin{array}{l} \Delta\overline{C}_d/\ \overline{C}_d \cong 0.38 \\ \Delta\overline{C}_t/\ \overline{C}_t \cong 0.35 \\ \Delta\overline{C}_{3He}/\ \overline{C}_{3He} \cong 0.51 \end{array} \right. \qquad (36)$$

The comparision between local parameters and regional parameters are given in fig.6 to fig.8 for C_d,C_t and C_{3He} respectively.
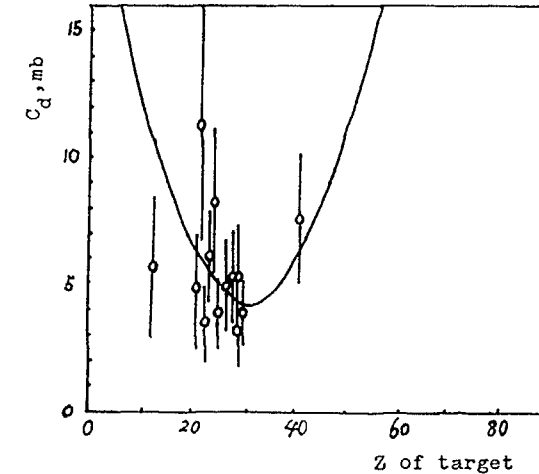
Fig.6 Systematics of C_d
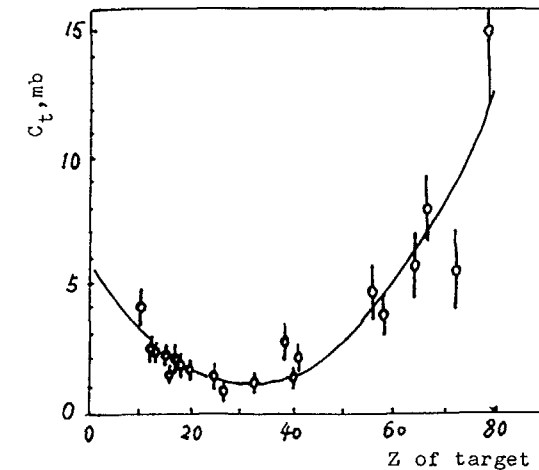
Fig.7 Systematics of C_t
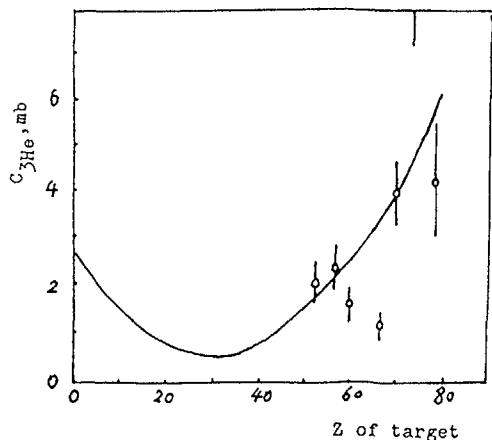
Fig.8 Systematics of C_{3He}

Discussion

With regional parameters, the excitation functions of (n,p) and (n,α) reactions have been calculated for about fifty nuclei in the region of $23 \leq A \leq 197$. The predicted cross sections are consistent with measured ones within errors calculated from $\bar{V}_q$. Several typical results are shown in fig.9 and fig.10. The excitation function of (n,t) reaction have also been predicted for several nuclei for which experimental data are available. The agreement between the predicted curves and the experimental data are satisfactory (see fig.11).
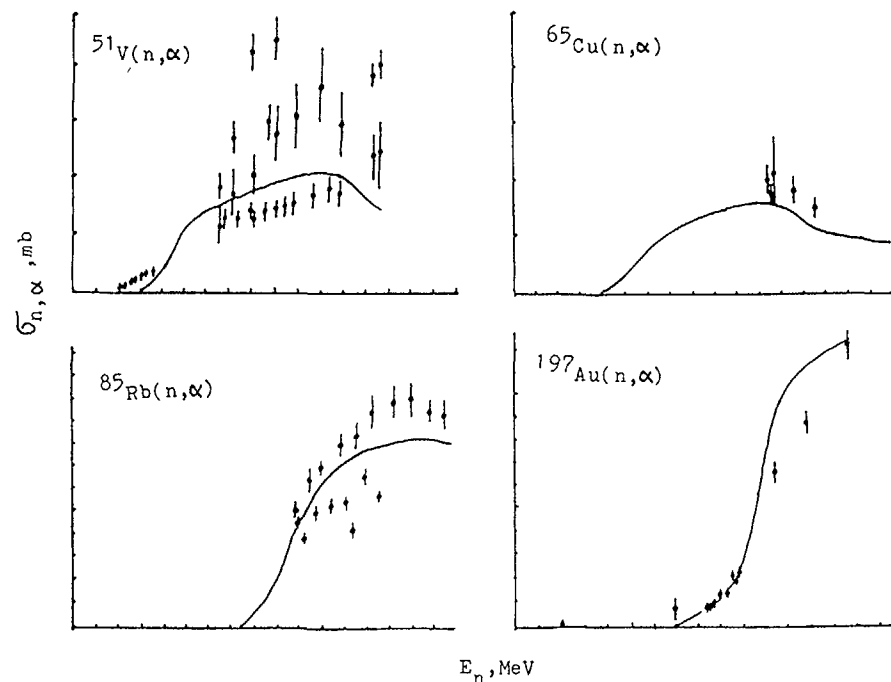
Fig.9 Excitation Functions of (n,p) Reaction

    o   experimental data

    —— predicted values by this systematics

Fig.10 Excitation Functions of (n,α) Reaction

    o   experimental data

    —— predicted values by this systematics

$\sigma_{n,t}$, mb

E_n, MeV

^{27}Al ^{32}S ^{55}Mn
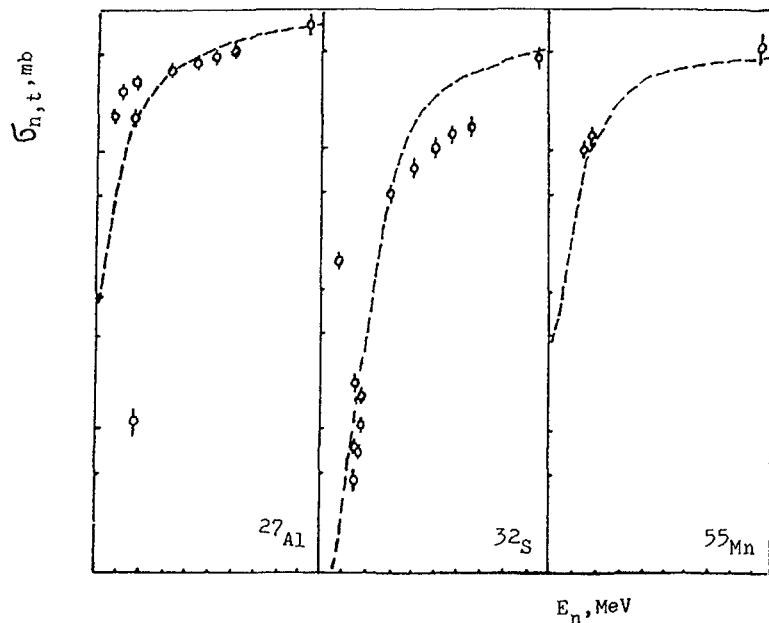
Fig.11 Excitation Functions of (n,t) Reaction

  o experimental data

  —— predicted values by this systematics

REFERENCES

1 S.Pearlstein, J.Nucl.Energy, 27,81,1973

  "Neutron Cross Section and Their Uncertainties Obtained From Nuclear Systematics", Proc. Conf. Nucl. Cross Sections and Tech., Wash., P.332,1975

2 V.Krivan et al., J.Inorg. Nucl. Chem., 34, 2093, 1972

3 V.N.Levkovskii et al., Soviet Physics-JETP, 4,291, 1957

4 I.Kumabe et al., NEANDC(J)-65/U, 45, 1978

5 G.Eder et al., Z.Physik, 253, 335, 1972

6 D.C.Gardner et al., Nucl. Phys., A96, 121, 1967

7 B.P.Bayhurst et al., J.Inorg. Nucl. Chem., 23, 173, 1961

8 S.M.Qaim et al., Nucl. Phys., A257, 233, 1976

9 A.Chevarier et al., Phys. Rev., C11, 886, 1975

10 Zhao Zhixiang, "Systematics of excitation function for (n, charged particle) reactions", Master thesis, Institute of Atomic Energy, Academia Sinica, China, 1985

11 S. F. Mughabghab, BNL-325, 3rd, 1973

12 CINDA77, CINDA82(1977-1982) and CINDA85

13 C.Michael Lederer et al., "Table of Isotopes", Sixth edition,1967

14 D.L.Smith et al., ANL/NDM-81,1983

15 S.M.Grimes et al., Phys. Rev., 17,508,1978

  R.C.Haight et al., BNL-NCS-51245, Vol.1,245,1980

16 S.M.Qaim et al., J.Inorg. Nucl. Chem., 36,3669, 1974

  Nucl. Phys., A257,233, 1976

17 S.M.Qaim et al., Nucl. Phys., A410,421,1983

18 S.M.Qaim et al., "Handbook of Spectroscopy", Vol.3,141, 1981

SYSTEMATICS OF (n,2n) AND (n,3n) CROSS-SECTIONS

Jin ZHANG, Delin ZHOU, Dunjiu CAI
Institute of Atomic Energy,
Beijing, China

Abstract

A body of new measurements of (n,2n) and (n,3n) reaction excitation function for the energy region up to 30 MeV has been fitted to the parameterized formulae with two adjustable parameters which based on the constant temperature evaporation model taking account of the preequilibrium contribution. The systematic behaviours of those parameters have been studied.

INTRODUCTION

The majority of the previous studies of the systematics of $\sigma_{n,2n}$ are performed on the neutron energy of ~ 14 MeV or on the energy dependence of the cross sections but limited to the lower energy region below the threshold of (n,3n). For example, in the work of Davey et al. [1], the cross sections below the threshold of (n,3n) were analyzed in terms of a constant temperature evaporation model and a level density formulation.

The present work attempt to establish the systematics of the behaviours of (n,2n) and (n,3n) excitation function based on a body of new measurements up to 30 MeV. Similar to Barr et al. [2] and Davey et al., the data have been fitted to the expressions that describe the constant temperature evaporation model taking the contribution of preequilibrium emission into account. It is expected that the improvements over the earlier work should be obtained and more accurate predictions may be provided.

FORMULAE FOR DATA FITTING

Obviously, to treat the measured $\sigma_{n,2n}$ for a wide energy region up to 30 MeV the competition of (n,3n) reaction and the contribution from preequilibrium emissions can not be ignored.

Empirically, the preequilibrium emission can only occur during the first neutron emission process. We have

$$\sigma_{ne} = (1-\delta)\sigma_{ne} + \delta\sigma_{ne} \tag{1}$$

$$\sigma_{n,2n} = \sigma_{n,2n}^{EQ} + \sigma_{n,2n}^{PE}$$

$$= (1-\delta)\sigma_{ne}\left(\frac{\sigma_{n,M}}{\sigma_{ne}}\right)_{EQ}\left(\frac{\sigma_{n,2n}}{\sigma_{n,M}}\right)_{EQ} + \delta\,\sigma_{ne}\left(\frac{\sigma_{n,M}}{\sigma_{ne}}\right)_{PE}\left(\frac{\sigma_{n,2n}}{\sigma_{n,M}}\right)_{PE} \tag{2}$$

$$\sigma_{n,M} = \sigma_{n,n'} + \sigma_{n,2n} + \sigma_{n,3n} + \cdots$$

Where δ denotes the fraction of preequilibrium stage and σ_{ne} is used instead of σ_c. $\sigma_{n,M}$ is the neutron emission cross section. Approximately

$$\left(\frac{\sigma_{n,M}}{\sigma_{ne}}\right)_{PE} \simeq \left(\frac{\sigma_{n,M}}{\sigma_{ne}}\right)_{EQ} \simeq \frac{\sigma_{n,M}}{\sigma_{ne}}$$

$$\sigma_{n,2n} \simeq \sigma_{ne}\frac{\sigma_{n,M}}{\sigma_{ne}}\left\{(1-\delta)\left[\left(\frac{\sigma_{n,2n}}{\sigma_{n,M}}\right)'_{EQ} - \left(\frac{\sigma_{n,3n}}{\sigma_{n,M}}\right)'_{EQ}\right] + \delta\left[\left(\frac{\sigma_{n,2n}}{\sigma_{n,M}}\right)'_{PE} - \left(\frac{\sigma_{n,3n}}{\sigma_{n,M}}\right)'_{PE}\right]\right\} \tag{3}$$

and

$$\sigma_{n,3n} \simeq \sigma_{ne}\frac{\sigma_{n,M}}{\sigma_{ne}}\left\{(1-\delta)\left[\left(\frac{\sigma_{n,3n}}{\sigma_{n,M}}\right)'_{EQ} - \left(\frac{\sigma_{n,4n}}{\sigma_{n,M}}\right)'_{EQ}\right] + \delta\left[\left(\frac{\sigma_{n,3n}}{\sigma_{n,M}}\right)'_{PE} - \left(\frac{\sigma_{n,4n}}{\sigma_{n,M}}\right)'_{PE}\right]\right\} \tag{4}$$

Using the constant temperature level density $\rho(E)\sim \exp(E/T)$ also $T(A-1)=T(A)$ and $T(A-2)=T(A)$ for equilibrium process, we have

$$\left(\frac{\sigma_{n,2n}}{\sigma_{n,M}}\right)'_{EQ} = 1 - (1+X_1)\,e^{-X_1} \tag{5}$$

$$\left(\frac{\sigma_{n,3n}}{\sigma_{n,M}}\right)'_{EQ} = 1 - \left(1+X_2+\tfrac{1}{2}X_2^2+\tfrac{1}{6}X_2^3\right)e^{-X_2} \tag{6}$$

$$\left(\frac{\sigma_{n,4n}}{\sigma_{n,M}}\right)'_{EQ} = 1 - \left(1+X_3+\tfrac{1}{2}X_3^2+\tfrac{1}{6}X_3^3+\tfrac{1}{24}X_3^4+\tfrac{1}{120}X_3^5\right)e^{-X_3} \tag{7}$$

$$X_i = \begin{cases} 0 & \text{for } E_n \leq B_i \\ \dfrac{E_n - B_i}{T} & \text{for } E_n > B_i \end{cases}$$

where B_1 B_2 and B_3 are the neutron separation energy of nucleus A, A-1 and A-2 respectively.

Following the formulae of the exciton model, the cross section of β type particle emission with the energy between $E_b \rightarrow E_b + \Delta E_b$ at the n exciton state is expressed as follows

$$\sigma_{(n,E_b)}^{PE}\,dE_b = \sigma_c\frac{1}{\lambda_{+2}(n)+L(n)}\left[\prod_{\substack{i=3 \\ \Delta i=2}}^{n-2}\frac{\lambda_{+2}(i)}{\lambda_{+2}(i)+L(i)}\right]\omega_\beta(n,\xi,E_b)dE_b$$

Here the backward transition λ_{-2} are neglected. From this expression, and under some approximations, we can get

$$\delta = \sum_{\substack{n=3 \\ \Delta n=2}}^{\bar{n}} \frac{L(n)/\lambda_{+2}(n)}{1 + L(n)/\lambda_{+2}(n)} \left\{ \prod_{\substack{i=3 \\ \Delta i=2}}^{n-2} \frac{1}{1 + L(i)/\lambda_{+2}(i)} \right\} \tag{8}$$

$$\left(\frac{\sigma_{n,2n}}{\sigma_{n,M}}\right)'_{PE} \cdot \delta = \sum_{\substack{n=3 \\ \Delta n=2}}^{\bar{n}} \frac{L(n)/\lambda_{+2}(n)}{1 + L(n)/\lambda_{+2}(n)} \left[\prod_{\substack{i=3 \\ \Delta i=2}}^{n-2} \frac{1}{1 + L(i)/\lambda_{+2}(i)} \right] \left[1 - n\left(\frac{B_i}{E_n}\right)^{n-1} + (n-1)\left(\frac{B_i}{E_n}\right)^{n} \right] \tag{9}$$

$$\frac{L(n)}{\lambda_{+2}(n)} = G \frac{(n+1)^2}{n} \left(\frac{E_n}{\varepsilon}\right)^{n} \times \begin{cases} 1 & \text{for } E_n \le V_c \\ [1 + (1 - \frac{V_c}{E_n})^{n}] & \text{for } E_n > V_c \end{cases} \tag{10}$$

$$G = \frac{81.4}{K \cdot A^{\frac{2}{3}}}$$

Where $\bar{n} = \sqrt{\frac{1.6}{\pi^2} A(E_n + B_0)}$, $\varepsilon = B_0 + E_n$, B_0 is the neutron separation energy of nucleus A+1. $V_c = 1.2Z/A^{1/3}$ is the coulomb barrier of A+1 nucleus on proton emission. And K(in MeV^3) is a well known parameter in exciton model.

Taking some approximations and considering $G \ll 1$, also $L(n)/\lambda_{+2}(n) \ll 1$, use $\exp[-L(n)/\lambda_{+2}(n)]$ instead of $1/[1+L(n)/\lambda_{+2}(n)]$ and ∞ instead of $\bar{n}$, the simplified expressions of the contribution of preequilibrium emission are obtained as follows

$$\delta \simeq \sum_{\substack{n=3 \\ \Delta n=2}}^{\infty} \left[1 - \exp\left(-\frac{L(n)}{\lambda_{+2}(n)}\right) \right] \exp\left[-\sum_{\substack{i=3 \\ \Delta i=2}}^{n-2} \frac{L(i)}{\lambda_{+2}(i)} \right]$$

$$= 1 - \exp\left\{ -G[F_1(x) + F_1(y)] \right\} \tag{11}$$

$$\left(\frac{\sigma_{n,2n}}{\sigma_{n,M}}\right)'_{PE} \delta = \delta - \delta^2 \left\{ \delta - (1-\delta) G\{F_1(x) + F_1(y)\} \right\} - (1-\delta) G \cdot \{F_2(x,\delta) + F_2(y,\delta)\} \tag{12}$$

$$F_1(\zeta) = \frac{\zeta^2}{(1-\zeta^2)^2} (5 - 3\zeta^2)$$

$$F_2(\zeta,\delta) = \frac{(\zeta\delta)^2}{(1-(\zeta\delta)^2)^3} \left\{ \zeta[15 - 10(\zeta\delta)^2 + 3(\zeta\delta)^4] - 2(\zeta\delta)[5 - (\zeta\delta)^2] \right\}$$

$$\zeta = x \text{ or } y$$

$$x = E_n/\varepsilon$$

$$y = \begin{cases} 0 & \text{for } E_n \le V_c \\ \dfrac{E_n - V_c}{E_n + B_0} & \text{for } E_n > V_c \end{cases}$$

$$g = \begin{cases} 1 & \text{for } E_n \le B_i \\ B_i/E_n & \text{for } E_n > B_i \end{cases}$$

Fig.1 shows the comparisons of the approximate calculation and the exact ones
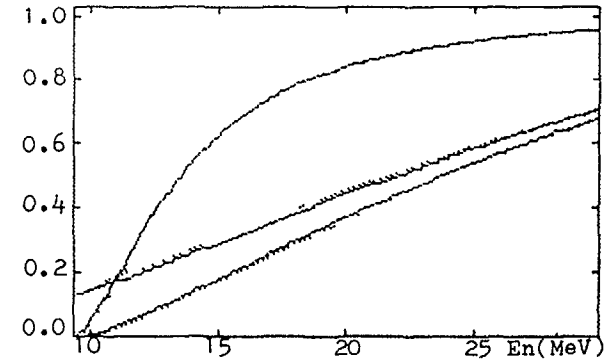
FIG.1 Dotted lines: exactly, Solid lines: approx.
From top to bottom: $\left(\frac{\sigma_{n,2n}}{\sigma_{n,M}}\right)_{PE}$, δ, $\left(\frac{\sigma_{n,2n}}{\sigma_{n,M}}\right)_{PE} \cdot \delta$

The expressions of $(\sigma_{n,3n}/\sigma_{n,M})_{PE} \cdot \delta$ and $(\sigma_{n,4n}/\sigma_{n,M})_{PE} \cdot \delta$ are similar to $(\sigma_{n,2n}/\sigma_{n,M})_{PE} \cdot \delta$ but multiplied by a factor.

$$\left(\frac{\sigma_{n,3n}}{\sigma_{n,M}}\right)'_{PE} \cdot \delta = \delta \cdot \left(\frac{\sigma_{n,2n}}{\sigma_{n,M}}\right)'_{PE} (B_1 \Rightarrow B_2) \cdot \left(\frac{\sigma_{n,3n}}{\sigma_{n,M}}\right)'_{EQ} / \left(\frac{\sigma_{n,2n}}{\sigma_{n,M}}\right)'_{EQ} (B_1 \Rightarrow B_2) \tag{13}$$

$$\left(\frac{\sigma_{n,4n}}{\sigma_{n,M}}\right)'_{PE} \cdot \delta = \delta \cdot \left(\frac{\sigma_{n,3n}}{\sigma_{n,M}}\right)'_{PE} (B_1 \Rightarrow B_3) \cdot \left(\frac{\sigma_{n,4n}}{\sigma_{n,M}}\right)'_{EQ} / \left(\frac{\sigma_{n,2n}}{\sigma_{n,M}}\right)'_{EQ} (B_1 \Rightarrow B_3) \tag{14}$$

RESULTS AND DISCUSSION

The measurements of $\sigma_{n,2n}$ and $\sigma_{n,3n}$ up to 30 MeV have been collected as complete as possible. They are 114 sets of $\sigma_{n,2n}$ for 71 nuclei within A=12-238 and 21 sets of $\sigma_{n,3n}$ for 15 nuclei within A=59-238 measured since 1975. For getting parameters T and

σn,M, the selected σn2n and σn3n data sets were fitted to equations (3)-(7) and (11)-(14) by means of the nonlinear least squares method. In these equations the empirical formulae for
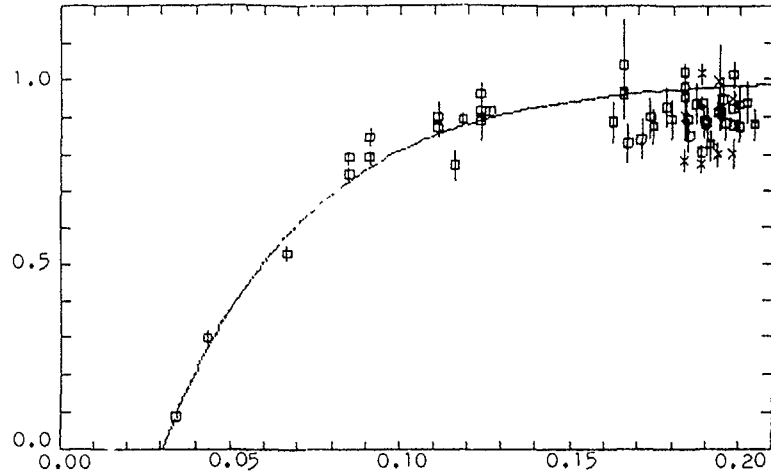

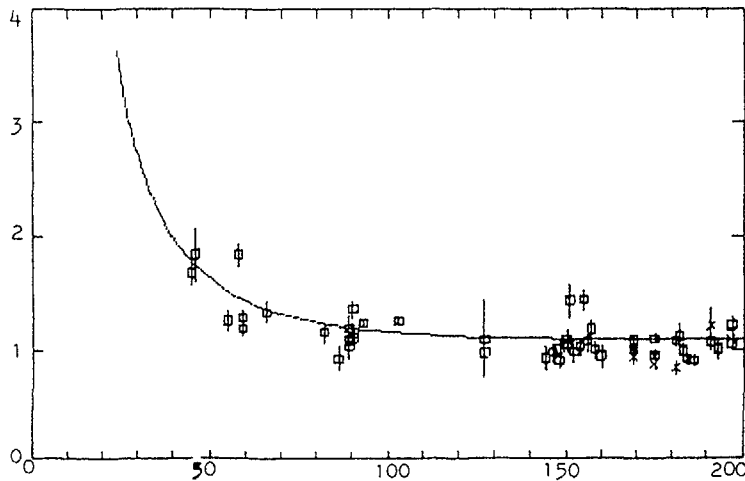FIG.2 $\quad \dfrac{\sigma_{n,M}}{\sigma_{ne}} \quad$ vs $\quad \dfrac{(N-Z)}{A}$

FIG.3   T(MeV) vs A

One provided by Davey et al. were used as follows

for $E_n \leq 14.2$ MeV

$$\sqrt{\frac{\sigma_{ne}}{\pi}} = \begin{cases} 0.196\, A^{1/3} & \text{for } A^{1/3} \leq 2.785 \\ 0.2317 + 0.1128\, A^{1/3} & \text{for } A^{1/3} > 2.785 \end{cases}$$

for $E_n > 14.2$ MeV

$$\sqrt{\frac{\sigma_{ne}}{\pi}} = \begin{cases} [0.196 - 0.00167\,(E_n - 14.2)]A^{1/3} & \text{for } A^{1/3} \leq A_o^{1/3} \\ 0.2317 - 0.2189 \cdot \ln\frac{E_n}{14.2} + 0.04777\,(\ln\frac{E_n}{14.2})^2 \\ \quad + (0.1128 + 0.03263\ln\frac{E_n}{14.2})\cdot A^{1/3} & \text{for } A^{1/3} > A_o^{1/3} \end{cases}$$

$$A_o^{1/3} = \frac{0.2317 - 0.2189\,\ln\frac{E_n}{14.2} + 0.04777\left(\ln\frac{E_n}{14.2}\right)^2}{0.0832 - 0.00167\,(E_n - 14.2) - 0.03263\,\ln\frac{E_n}{14.2}}$$

The fit mainly based on the data points in the energy range well above the threshold. The data near (n,2n) threshold did not be rejected, but the errors of these data have been enlarged.

69-Tm-169
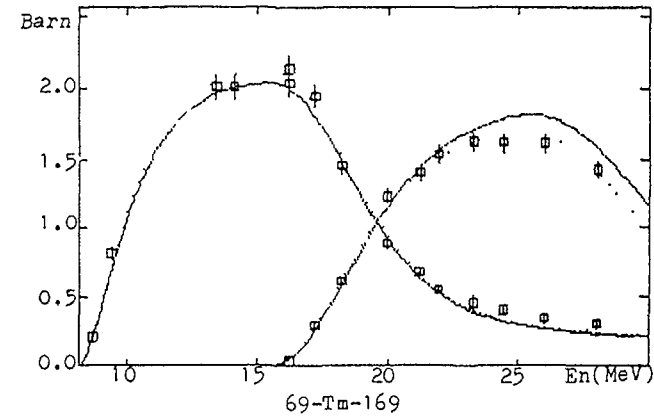
FIG.4 Calculations with parameters from:
... fitting; —— systematics

In the fitting process, parameter K has been adjusted and then fixed at k=207. i.e. $G=0.4/A^{1/3}$. So the systematics formulas for σn,m/σne and T can be expressed as

$$\frac{\sigma_{n,M}}{\sigma_{ne}} = 1 - 2.05\, \exp\left(-24\,\frac{N-Z}{A}\right) \tag{15}$$

$$\frac{1}{T} = 0.91\left[1 - (1 + 0.046A)\cdot\exp\left(-0.046A\right)\right] \tag{16}$$

The systematic behaviours of the parameters are shown in Fig.2-3.
A typical fitting and systematics prediction results for $\sigma_{n,2n}$
and $\sigma_{n,3n}$ are shown in Fig.4. The agreements of the systematics
prediction with experimental data for $\sigma_{n,2n}$ in mass region of
A=23 ~ 197 and $\sigma_{n,3n}$ of A=148 ~ 197 are satisfactory. In the mass
region of A < 23 for $\sigma_{n,2n}$ and A < 148 for $\sigma_{n,3n}$, the agreement
are not good enough. The deviations of T parameter from the exp-
ression (16) appearing in mass region of A=200 ~ 210 can be inter-
preted as the shell effects of nuclei.

REFERENCES

1. W. G. Davey, R. W. Goin & J. R. Ross, ANL-75-34(1975)
2. D. W. Barr, C. I. Browne & J. S. Gilmore, Phys. ReV.,123,
   859(1961).
3. Zhang Jin, Zhou Delin and Cai Dunjiu, Proc. Internat. Conf.
   on Nucl. Data for Basic and Applied Science, Santa Fe, New
   Mexico, 13-17 May 1985, P.1611

STATUS OF EXISTING LIBRARIES
FOR FUSION NEUTRONIC CALCULATIONS

(Session C)

Chairman

H. VONACH
Austria

USE OF NEUTRONIC DATA IN THE CALCULATIONS
OF HYBRID FUSION REACTOR BLANKET

D.V. MARKOVSKIJ, G.E. SHATALOV
I.V. Kurchatov Institute of Atomic Energy,
Moscow, Union of Soviet Socialist Republics

Abstract

A review of the integral and calculational methods for neutronic data testing, that were carried out in I.V. Kuchatov Institute of Atomic Energy for the hybrid fusion reactor design is presented.

INTRODUCTION

Data testing and improving for neutronic calculations of fusion reactors is still a timely and vast problem including multiple aspects and affecting the interests both of data supplier and consumer. At the present time a large amount of evaluated neutron data is accumulated and probably comparable with this are the lists of recommendations for obtaining more specific information. But the experience of the integral experiment calculation analyses tells us that merely rise of separate microscopic data accuracy does not always ensure satisfactory accuracy of the integral result in a calculation with a certain nuclid data. A natural criterion for the data quality is an integral experiment that enables the data supplier to get information about the advantages and disadvantages of a file and the consumer to specify the level of confidence in his calculation results.

Up to date a large number of integral experiments with 14-MeV neutron sources has been published [1-5] and it is

still growing. But it does not mean that the needs in experimental information for data testing and correction are fully satisfied, because many of these experiments fail to meet the requirements to the description completness and accuracy while the set of measured parameters is not always sufficient. Thus the data consumer is urged along with the calculation analysis of published data to undertake additional experimental studies in accordance with the pursued reactor concept.

This report represents a short review, from a data consumer standpoint, of calculation and experimental studies on neutronic data testing that were carried out in I.V.Kurchatov Institute of Atomic Energy in 1984-85 within the frame of OTR hybrid fusion reactor [6] design effort. The purpose of this activity was to verify the adequacy and needs for correction of some neutronic data responsible for the accuracy of the hybrid reactor blanket/shield neutronic characteristics prediction and finally to select the best available data versions.

Below the calculation technique, neutronic data and blanket concept are briefly described. The studies of the model parameters sensitivity to data and some data testing in integral experiments are reviewed and some remarks on the ways, that seem reasonable to us, towards improving the neutronic data employed in fusion reactor calculations are given.

Calculation method

The engineering calculations of a fusion reactor neutronics are usually carried out in two stages: determination of the detailed space-energy neutron distribution (neutron transport) and obtaining neutron flux linear functionals, that is

tritium and fissile fuel breeding reaction rates, power densi-
ty, activation and radiation damage distributions. Consequent-
ly the demand for neutronic calculation data comprises both
the need for the evaluated neutron transport data files and
those providing the reaction cross sections for the functionals
calculation.

In this study the neutron transport and functional calcu-
lations have been carried out with BLANK code complex [7] in
one and three-dimensional modifications. In the one-dimensional
option either a combination of Monte Carlo method within 0.1-
14 MeV range and numerical calculation in P_1 approximation be-
low 0.1 MeV or Monte Carlo method for both energy ranges are
used. For the energy range above 0.1 MeV the data are prepared
with NEDAM code [8] from the evaluated data files practically
without any simplifications. Below 0.1 MeV a 21 group constant
system of P_1 approximation [9] is used that has been success-
fully approbated in fission reactor calculations. In the three-
dimensional BLANK code option based on the same constant sys-
tems the neutron transport equation is solved with Monte Carlo
method through the entier energy range.

The working constant library for E > 0.1 MeV has been ba-
sed upon the evaluated data files from ENDL, UKNDL, ENDF/B-IV
and SOCRATOR libraries [33].

For the functional calculations BLANK code is equiped
with the corresponding microconstant libraries. For the ener-
gy release calculation the gamma-sources from ENDL library and
kerma-factors from [11,12] are used. Disagreements in these da-
ta result sometimes in violations of collision energy balance

up to 20% and even higher. The main sources of the activati-
on and gas production cross sections are the files from ENDL-
75, UKNDL and ENDF/B-IV libraries. For the radiation damage
calculations Doran's data [13] have been used and data from
DAMSIG-81 library are being adapted now.

Calculation model

The accepted in the USSR design concept of a hybrid reac-
tor [6,14,15] is based on uranium fuel cycle. The neutron ba-
lance in such a reactor substantially depends on U-235 and
Pu-239 concentrations. The increase of these concentrations
causes the fission rate and blanket power rise but it degra-
des the Pu-239 production per power unit. And what is more,
these isotopes can be "burnt" in a simpler and more efficient
way in thermal neutron fission reactors. So the concept of hy-
brid reactors employed mainly as plutonium breeders for fissi-
on reactors seems the most benefitial [16]. Obviously in this
case natural or depleted uranium should be used in the blanket.
An example of one-dimensional calculation model of the hybri-
de reactor uranium blanket/shield is presented in Fig.1. It
incorporates the stainless steel first wall (0.7 cm), uranium
(24.7 cm) and lithium (35 cm) zones, iron/water shield (110cm)
and magnetic coil zone. The uranium zone contains 27.5% of
natural uranium and provides the plutonium production coeffi-
cient $K_{Pu} = 1.1$. The lithium zone consists of $Li_{17}Pb_{83}$ eute-
ctic and calcium hydride moderator layers, here tritium bre-
ding ratio $K_t = 1.17$. The coil shield consists of alternated
layers of stainless steel, borated steel (0.6 Wt.% of boron
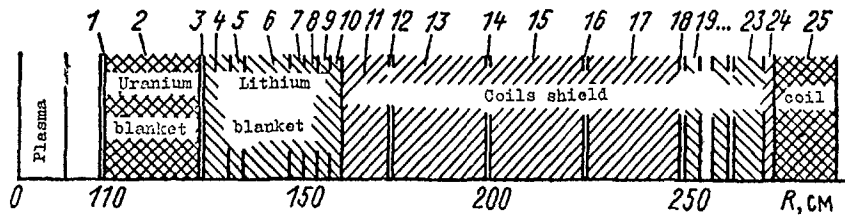content) and water. Such a blanket concept is justified for

Fig.1. One-dimensional calculation model of fusion reactor
blanket/shield. Zone composition (volumetric): 1,3,
11, 13, 15, 17, 24 - stainless steel (100%); 2 - ura-
nium (27.5%), iron (23.0%); 4.6 - iron (4.3%), $Li_{17}Pb_{83}$
(79.0%); 5, 7, 9 - iron (5.3%), eutectic (46.8%), cal-
cium hydride (48.6%). 8,10 - iron (2.0%), eutectic
(98%); 12,14, 16, 18, 20, 22 - water (100%); 19, 21,
23 - borated steel (100%); 25 - steel (50%), copper
(50%). a - plasma, b - uranium blanket, c - lithium
blanket, d - shield, e - coil.

1 MW/m^2 neutron load to the first wall. At the permissible ne-
utron load rise above 5 MW/m^2 the blanket concept with thorium
can become more benefical [32] .

The key functionals in neutronic calculations are the to-
tal neutron source and its major components that is plutonium
production coefficient, tritium breeding ratio, total energy
release in the blanket and shield and also the fast neutron
(E > 0.1 MeV) flux at the shield outer surface.

Sensitivity to data

To evaluate the impact of the blanket neutronic parame-
ters uncertainty due to nuclear data uncertainty one needs the
data sensitivity coefficients. In [17] the relative sensitivity

of K_{pu}, K_T and fast neutron (E > 0.1 MeV) flux energy dependen-
cies to the cross section variations have been studied for the
blanket model presented in Fig.1. The abosrption, Σ_a, elastic,
Σ_{el} and inelastic, Σ_{in} scattering cross sections have been
varied, the fission and total cross sections for U-238, Pb,
Li-6, Li-7, Fe as well as $\Sigma_{n\gamma}$ for U-238 and $\Sigma_{n\alpha}$ for Li-6. The
sensitivity functions were calculated with ZAKAT code [18] that
realized a method based on linear perturbation theory. In this
code the solutions of the direct and adjoint transport equa-
tions obtained with ROZ-11 code [19] and 49-groups BND-49 con-
stants [20] were used as the input data. Some results are
shown in Fig.2,3. K_{Pu}, K_T and φ_f sensitivity to the absorption
cross section has been shown to be low for all the nuclides
except U-238 and Li-6. E.g. for iron the K_{Pu} and K_T sensitives
did not exceed 0.05 which can be seen from Fig.2. K_T and K_{Pu}
sensitivities to Σ_a^v were approximately constant in 4.65 keV -
1 MeV energy range and somewhat higher than for iron. Within
the energy range above 0.25 MeV resonance the Li-6 (n,α) T
reaction cross section is small that results in a low K_T and
K_{Pu} sensitivities to the absorption on lithium. Neutrons in the
range of the resonance add about 5% to K_T while the major con-
tribution is done by low energy neutrons. The sensitivities to
the elastic and inelastic scattering cross sections of U-238
and Fe are shown in Fig.3. The K_T and K_{Pu} sensitivities to the
elastic cross sections are not high but the hard neutron spec-
trum of the source results in a high functional sensitivities
to the inelastic scattering cross section variations of urani-
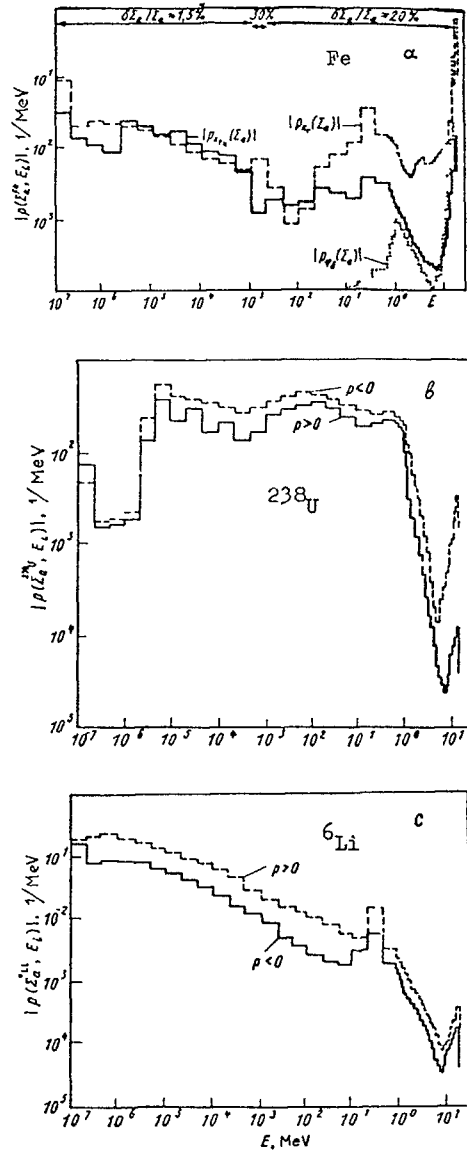um, lead and, to a smaller degree, iron. The uncertainties of

Fig.2. Energy dependence of $K_{Pu}(\underline{\quad})$, $K_T(---)$, $\varphi_f(\cdots)$ relative sensitivity to absorption cross section variations a - Fe, b - U-238, c - Li-6.
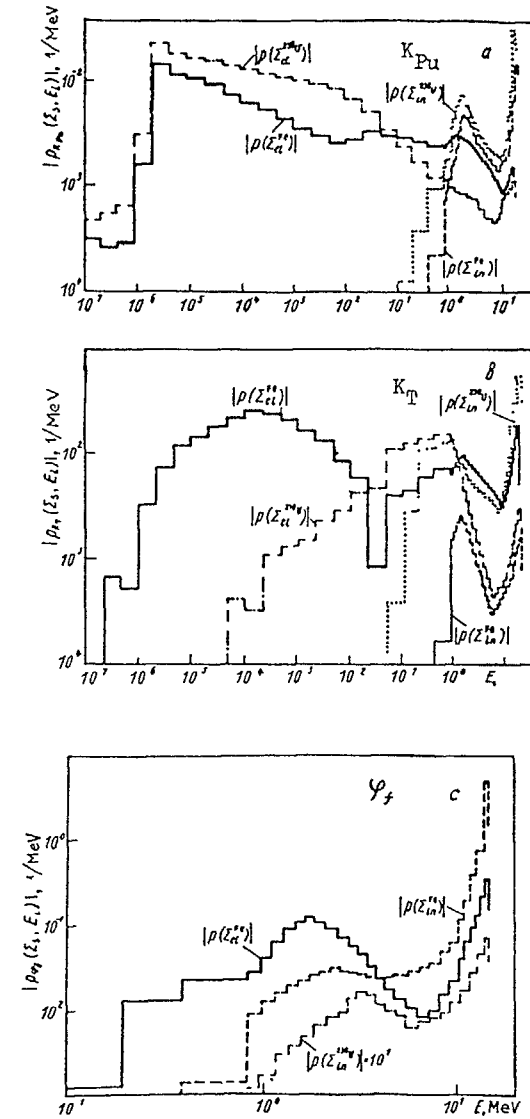
Fig.3. Energy dependence of $K_{Pu}(a)$, $K_T(b)$, $\varphi_f(6)$ relative sensitivity to elastic/inelastic scattering cross section variations of U-238, Fe.

these cross sections contribute mostly to the K_T, K_{Pu} and calculation errors.

The sensitivities of K_T, fission rate, n_f, and fission source, Q_f, to the secondary neutron spectrum hardness have been studied in [21] . Calculations were performed with a modified BLANK code version [7] . The functional variations were obtained via the correlated sampling method with the use of the same neutron trajectories set both for the reference and perturbed system where the scattering nucleus properties change was taken into account by using a weight coefficient. The employed constants within 0.1 - 14 MeV range were prepared with NEDAM code [8] on the basis of ENDL evaluated data files. The pertubed secondary neutron spectrum was obtained by compression and renormalization of the reference spectrum with 20% temperature decrease. The calculated dependencies of sensitivity to neutron spectrum for the reactions U-238 (n,2n), U-238 (n,n') Cont and Fe (n,n')Cont on the neutron energy before collision are given in Fig.4. The fission rate and fission source sensitivities to U-238(n,2n) reaction spectrum have an abrupt rise at the neutron collision energy above 11 MeV that corresponds to the neutron spectrum shape in the uranium zone. The inelastically scattered neutrons related to the U-238 continuum excitation give the major contribution to the functionals at the collision energy within 2-6 MeV range whereas the addition from the neutrons with energy above 14 MeV does not exceed 15-20%. The sensitivity to the neutron spectrum of Fe (n,n')Cont reaction is to one third conditioned by 14.1 MeV neutron interaction with the first wall. At lower energies the
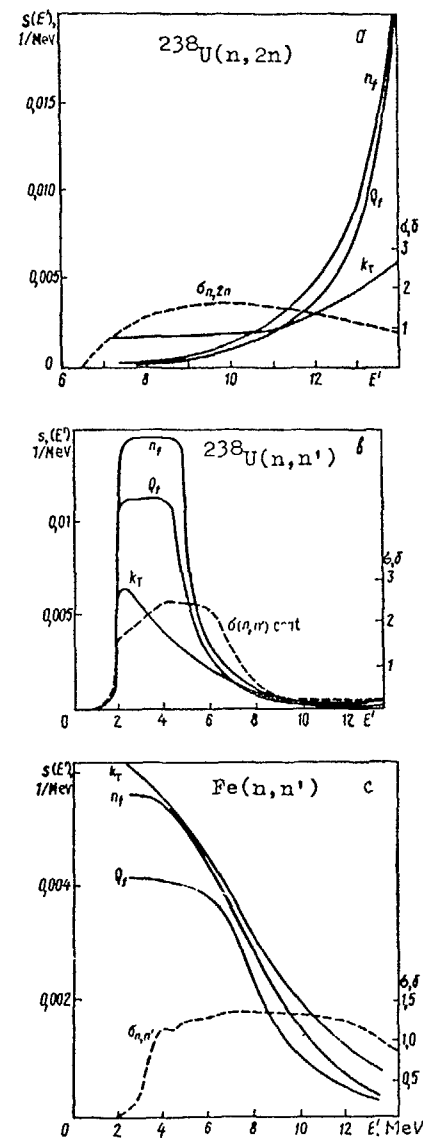
Fig.4. Differential sensitivity to neutron spectra of the reactions: a - U-238(n,2n), b - U-238(n,n')Cont, c - Fe(n,n')Cont.

sensitivity increases following the spectrum shape within the uranium zone. The functional sensitivity to U-238(n,3n) and Fe(n,2n) reaction spectra is considerably lower due to smaller cross sections of these reactions and lower energy of the secondary neutrons.

The calculated sensitivity coefficients show that in a hybrid reactor the major impact on the main functionals results from U-238(n,2n),U-238(n,n') and Fe(n,n') reaction cross sections and spectra of secondary neutrons the latter being able to make a substantial contribution to the fission rate on U-238 and, consequently, to the neutron multiplication. The functional uncertainties due to 15-20% spectra uncertainty are evaluated at 3-4% for the fission rate and 2-2.5% for tritium breeding.

Thus the major attention should be paid to the problem of testing the materials breeding properties and neutron spectra in inelastic interactions.

Measuring of neutron leakage from spherical shells made of U-238, Th-232, Be and Pb

There is a number of hybrid reactor designs where uranium, thorium, berillium and lead are considered as neutron multiplies. Uranium and thorium are also the fertile materials for Pu-239 and U-233 production in the hybrid fusion reactor blankets.

At the multiplier thickness of 1-2 neutron mean free paths at 14 MeV (such thicknesses are usually considered in blanket designs) the neutron leakage is the most adequate characteristic of multiplication effect. In [2] the neutron leakages normalized to one 14-MeV neutron of the source have been measured on spherical shells of different thickness made of U-232, Be and Pb. The experimental data were compared with corresponding calculation results obtained with BLANK code [7] with the use of ENDL (1975) version constants for uranium, thorium and lead and UKNDL constants for berillium. The leakage measuring has been done via "boron tank" technique [22] . The investigated spherical assemlies were placed in the center of a large tank having form of a spherical layer filled with boric acid solution in water. The "boron tank" had 1320 mm outer and 400 mm inner diameters. The inner diameter surface of the tank surrounding the cavity werein the assemblies were located had been lined with 1 mm Cd layer to prevent thermal neutrons backstreaming to the assemblies. Boron - 10 concentration in water was $7.95 \cdot 10^{19} cm^{-3}$, the boron acid being enriched with B-10 up to 88.6%. The assemblies dimensions and compositions are presented in Table I.

As the neutron source NG-150M neutron generator has been used with a modified generator tube. 28.5 mm diameter TiT target of the neutron generator was located in the assembly center. The detailed description of the experimental facility and measuring technique has been presented in [4] . The counting rate distribution of KNT-10 boron counter was measured over the "boron tank" radius and azimuthal angle, to the deuteron beam direction. The normalization to one 14-MeV neutron was done by counting the associated alpha-particles from T(d,n) reaction.

TABLE 1. DIMENSIONS AND COMPOSITIONS OF ASSEMBLIES

Element	Nuclear concentration x 10^{24}, cm^{-3}	Multiplier layer thickness, cm	R_{in} cm	R_{out} cm
U	U-238 4.76 10^{-2}	1	10	11
	U-235 1.91 10^{-4}	2	10	12
		8	4	12
Th	2.930 10^{-2}	3	3	6
		7	6	13
		10	3	13
Be	1.236 10^{-2}	1.5	3	4.5
		5	6	11
		8	3	11
Pb	3.300 10^{-2}	3	9	12
		9	3	12

$$N_s = \frac{N - \mathcal{E}_{14MeV} \cdot T}{\mathcal{E}_{c_f}} , \tag{1}$$

$$M = T + N_s , \tag{2}$$

where M is the total neutron leakage from the assembly; N is the integral of KNT-10 count rate over the "boron tank" volume with the investigated assembly and central 14-MeV neutron source; T is 14 - MeV neutron streaming; $\mathcal{E}_{14MeV}$ is the integral of KNT-10 count rate over the "boron tank" volume with 14-MeV neutron source and without spherical shells; $\mathcal{E}_{c_f}$ is the integral of KNT-10 count rate over the "boron tank" volume with C_f-252 neutron source; N_s is the secondary neutrons leakage. T values for each assembly were established in additional experiments with measuring the activity of F-19 (n,2n) threshold detectors located at 1 m distance from the target with or without the spherical shell.

It was found in [2,4,23] that due to high energy threshold of the neutron multiplication reactions the presence of borated water around the assemblies had no effect on the neutron leakage from them. The effect of U-235 fission in uranium assemblies on the neutrons scattered from water has been proved negligible either because of Cd screen.

Thus the calculated leakage can be considered adequate to one measured with the "boron tank" technique. Table 2 represents the experimental and calculated values of the total neutron leakage from the assemblies, the secondary neutron leakage and neutron streaming, T . The experimental data errors are given with 68% confidence probability. The Monte Carlo statistic calculation error did not exceed 1%.

The neutron leakage spectrum is a superposition of 14-MeV source and secondary neutron spectrum. The major part of the inelastic scattering secondary neutrons belongs to 0.01-6 MeV energy interval. The number of neutrons absorbed by boron in this interval has been shown in [23] to be independent of the neutron energy, thus the integral of KNT-10 count rate over the "boron tank" volume does not depend on the neutron energy within this interval either.

The neutron leakage from the assembly was determined by formulae

It is seen from Table 2 that the neutron leakages from U and Be shells are satisfactorily reproduced by calculations with BLANK code. The leakage from lead shells exceed the calculated one by 5.5%. For Th shells the experimental data are higher than the calculated one, the difference being larger with greater spherical shell thickness and amounting to 11% at the thickness of 10 cm. The lead neutron multiplication underestimating in calculations with BLANK code does not contradict to the results of [24,5]. The most probable cause of the experimental and calculated leakage descrepancy is the fact that the (n,2n) reaction cross section for lead at 14 MeV is larger than that adopted in ENDL-75 library. The conclusion about the experimental leakage from thorium shells exceeding the calculated levels is correlated with the results of another experiment [25] for which the calculation with BLANK code and ENDL data underestimated the neutron leakage within 0.8-15 MeV range by 8.4%.

TABLE 2. EXPERIMENTAL AND CALCULATED NEUTRON LEAKAGES FROM THE ASSEMBLIES, NUMBERS OF SECONDARY NEUTRONS IN THE LEAKAGES, NEUTRON STREAMING, T

Material	Multiplication zone thickness, cm	T exper.	T BLANK	M exper.	M BLANK	N_s exper.	N_s BLANK
U	1	$0,830 \pm 0.011$	0.840	1.331 ± 0.054	1.308	0.501 ± 0.053	0.468
	2	0.720 ± 0.010	0.712	1.569 ± 0.059	1.601	0.849 ± 0.058	0.889
	8	0.301 ± 0.004	0.303	2.667 ± 0.072	2.681	2.366 ± 0.072	2.378
Th	3	0.725 ± 0.009	0.724	1.352 ± 0.038	1.292	0.627 ± 0.037	0.568
	7	0.500 ± 0.007	0.505	1.633 ± 0.043	1.521	1.233 ± 0.042	1.016
	10	0.388 ± 0.006	0.391	1.823 ± 0.052	1.642	1.435 ± 0.052	1.251
Be	1.5	0.832 ± 0.011	0.824	1.143 ± 0.039	1.120	0.311 ± 0.037	0.296
	5	0.622 ± 0.009	0.603	1.364 ± 0.040	1.363	0.753 ± 0.039	0.760
	8	0.456 ± 0.007	0.463	1.530 ± 0.043	1.524	1.074 ± 0.042	1.061
Ps	3	0.739 ± 0.009	0.749	1.259 ± 0.041	1.193	0.520 ± 0.040	0.444
	9	0.440 ± 0.006	0.447	1.530 ± 0.044	1.449	1.090 ± 0.044	1.002

An integral experiment with shield assembly

One of shielding compositions including steel, lead and polyethylen layers has been studied on an assembly [5] schematically presented in Fig.5. A neutron generator mounted on a vehicle is placed in a cell. The assembly is mounted on a concrete block. Due to its large transversal dimensions (~10 free paths of the source neutrons) and "physical" extention by the concrete of the block and walls it can be considered as physically infinite in the transversal directions when carrying out measurements along the central axis. The assembly composition incorporates four materials: steel, lead, lead/polyethylen/polystyrene mixture and borated polyethylen. The composition and layer thickness data are summarized in Table 3. By means of activation detectors the following reaction rates were measured: Cu-63 (n,2n)Cu-62, Cu-65(n,2n)Cu-64, Al-27(n,α)Na-24, Fe-56(n,p)Mn-56, Al-27(n,p)Mg-27, Pb-204(n,n')Pb-204m, In-115(n,n')In-115m. The relative distribution of Th-232(n,f) reaction rate was measured with solid state nuclear track detectors.

▨ – steel   ▨ – PSSB-2   ▨ – concrete

▧ – lead   ▨ – PeH-B

Fig.5. Shield assembly location in the door opening of a
cell.1 – NG target; 2 – monitoring channel counter,
3 – shield assembly, 4 – spectrometer sensor, 5 –
concrete block, 6 – vehicle.

a – steel, b – lead, c – PSSB-2, d – PeH-B, e – concrete.

TABLE 3. SHIELD ASSEMBLY COMPOSITION

Material	Thickness, mm	Density, g/cm^3		Ingredients, %(w)	
1	2	3		4	
Steel 3	20.0±0.2	7.85		Iron	– 99.8
				Carbon	– 0.14 ÷ 0.22
Lead	100±0.2	11.34		Lead	– 99.98
PSSB-2	82.7 ± 0.2	4.05	0.05	Lead	– 81 ± 4
				Polyethylen(CH)	– 11.2
				Polystyrene-(CH$_2$)	– 2.8
PEh-B	325±0.5	0.945	0.005	Polyethylen(CH)	– 97
				Boron	
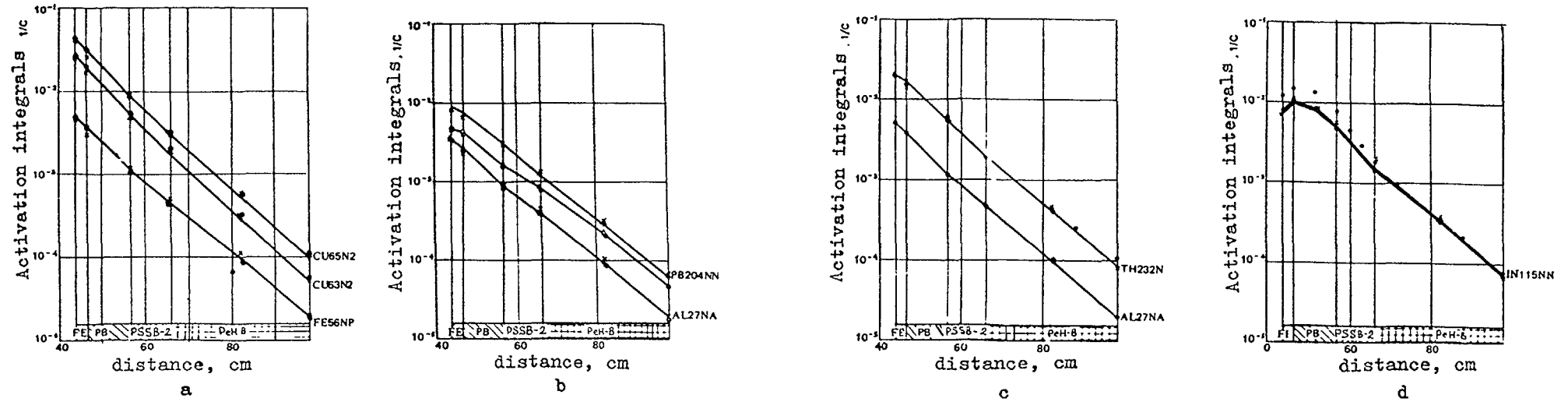
Fig.6. Activation integrals distribution along the assem-

bly axis. The experimental data are normalized to

one source neutron with the reference value of the

calculated activation integral for Cu-63(n,2n)cu-62

reaction at position 1. a – calculation with RADUGA

code (+), experiment (⊙), calculation with BLANK co-

de (x); b – calculation with RADUGA code (Δ,+), ex-

periment (⊙), calculation with BLANK code (x),

c – calculation with RADUGA code (+), experiment (⊙),

calculation with BLANK code (x); d – calculation with

RADUGA code (+, Δ) experiment (⊙), calculation with

BLANK code (x).

1 – activation integrals, s^{-1}, 2 – distance, cm.

Inside and beyond the assembly the neutron spectra have been measured with a stilbene counter. All the measuring results were normalized to the relative neutron generator output.

The neutron flux space distribution was calculated with BLANK [7] and RADUGA [26] codes. Both of them employed constants obtained from ENDL files treatment. RADUGA code is intended to solve the integro-differential transport equation by the method of characteristics [27] in r-z geometry. In the calculations with three-dimensional version of BLANK code in xyz geometry the neutron flux at the detector locations was obtained via a local estimate. The cross sections for the activation detectors were taken from [28] . Calculations were carried out for $150 \cdot 10^3$ neutron histories. At the primary neutron flux attenuation by a factor of 10^3 the accuracy of the activation reaction rates on the assembly back surface was ~20%.

A comparison between the experimental activation rates along the assembly axis and those calculated with BLANK and RADUGA codes is presented in Fig.6. The distributions have been normalized by equalizing the calculated and experimental activation integrals for Cu-63(n,2n) reaction at the front side of the assembly. For the major part of detectors which were efficient in the hard spectrum the distributions agreed to within the error. The only exceptions were the activities of Pb-204(n,n') and In-115(n,n') detectors. The disagreement in Pb-204(n,n') activities is explained by the inaccuracy of the reaction cross sections description in [29] within 12-15 MeV range. The calculation with cross sections from [30] for this energy range has eliminated the disagreement. The most consi-

derable disagreement near the front wall of the assembly was connected with In-115(n,n') activity. It has substantially exceeded the background level that, according to experimental data, was below 10%. Besides this, one can see that the disagreement did not decrease across the assembly thickness but had a maximum within the lead layer. It can be assumed to result from the uncertainty of the employed data on cross sections and neutron spectra of Pb(n,2n) reaction, since the indium activation depends on the spectrum maximum position with respect to In-115(n,n') reaction threshold. Obtained results on the whole show that the spectrum of neutron leakage from the investigated shield is determined mainly by the leading group of the source neutrons. The distribution of the latter across the assembly thickness is described correctly by the use codes coupled with the working constants libraries based on ENDL files.

Conclusion

Suggestions on creating a library or a library set of neutronic data for fusion reactor blanket/shield calculations were made already at the previous IAEA Advisory Group Meeting on nuclear data for fusion reactor technology in 1978 [2] . The initiative in complication under IAEA auspices INDL/F library [10] is the first practical step in this direction. But such an activity can be fruitfull if only the library is continuously modified with the latest versions tested in integral experiments and if it includes, besides the neutron transport data, the cross sections for the flux functionals calculation. And on the contrary the restricted access to modern versions of evalua-

ted data is an obstacle on the way to wide cooperation in this field, resulting in double efforts and uncertain formulation of data needs.

The major part of requirements to neutron data improvement, as they were identified at the previous meeting [2] , is still-valid [31] . The same can be said about the suggestions that the experimental activity on data testing for fusion reactor calculations would be better coordinated from the viewpoint of unified requirements to integral experiments and calculations and the evaluated data presentation first of all of those needed for neutron flux functionals calculation) would be convinient for wide application in calculations.

The main data uncertainty in neutron transport calculations is connected with the secondary neutron spectra in inelastic collisions and the secondary neutrons anisotropy with respect to the direct processes in materials exposed to the hard neutron spectrum, that is multipliers (U-238, Pb), structural materials (iron, stainless steel) and lithium containing ones. In some cases precising of (n, 2n) reaction and neutron capture (with $E > 1$ MeV) cross sections are needed, e.g. for lead. Creation of data library kerma-factors and gamma-sources for energy release calculations with 5-10% accuracy of energy balance is another important issue. The requirements to accuracy of activation, gas production and radiation damage cross sections are more soft and accuracy 10-20% seems acceptable for today. The question about the data adequacy to these requirements should be answered in principle by integral expe-

riments that probably involve the development of suitable measuring techniques.

REFERENCES

I. D.V.Markovskii, G.E.Shatalov. Neutron Data for Hybrid Reactor Calculations. Proceedings of the Advisory Group Meeting on Nuclear Data for Fusion Reactor Technology. IAEA-TECDOC-223, P.111, IAEA, Vienna (1979).

2. V.A.Zagryadskij et al. Measurements of neutron leakage from spherical shells of U-238, Th-232, Be with central 14-MeV neutron source. Preprint IAE-4222/8, 1985.

3. V.M.Novikov et al. An integral experiment on U-238 spherical shell with 14-MeV neutron source. Preprint IAE-3919/8, 1984.

4. V.M.Novikov et al. 14-MeV neutron multiplication measurements on spherical shells of lead and bismuth by total absorption method. Preprint IAE-4197/8, 1986.

5. A.M.Bogomolov et al. Investigation of 14-MeV neutron transport in a fusion reactor shield assembly. Preprint IAE-4030/8, 1984.

6. V.V.Orlov, A.A.Rakitin, G.E.Shatalov. Experimental fusion reactor (OTR). The fusion reactor first wall issues and neutronic studies. Proc. CMEA member countries expert meeting, April 26-29 1983, Sukhumi. Moscow, TsNIIAtominform 1984.

7. S.V.Marin, D.V.Markovskij, G.E.Shatalov. BLANK code of one dimensional neutron distribution calculation with a fast

neutron source. Voprosy atomnoj nauki i tekhniki. Ser.Fizika i tekhnika yadernykh reaktorov. Iss. 9(22), P.26-31 Moscow, NIKIEhT, 1981.

8. L.N.Zakharov, D.V.Markovskij, A.D.Frank-Kamenetskij, G.E.Shatalov. NEDAM Code for neutron microconstants preparing for Monte Carlo calculations on the basis of evaluated data files. Preprint IAE-2994, 1978.

9. G.E.Shatalov. DENSTY code for microconstents preparing. Voprosy atomnoj nauki i tekhniki. Ser. Fizika i tekhnika yadernykh reaktorov. Iss. 8(21), P.39-41. Moscow, NIKIEhT, 1981.

10. V.G.Pronyaev, D.E.Cullen, P.K.McHaughlin. Evaluated Neutron Reaction Data Library for INTOR Fusion Neutronics Calculations (1983 version). IAEA-NDS-57.

11. J.J.Ritts, M.Solomito, D.Steiner. ORNL-TM-2564.

12. M.A.Aldou, C.W.Maynard, UW-FDM 66.

13. D.G.Doran, N.J.Graves. HEDL-SA 1058.

14. V.V.Kotov, G.E.Shatalov. In: Proc. of a US-USSR Symp. on Fusion-Fission Reactors. Livermore 13-16 July, 1976, P.129.

15. B.D.Gornostaev, et al. Experimental power fission fuel breeder. Fission-Fusion. Proc. 2-d Soviet-American Seminar, Marth 14 - April 1, 1977. Moscow, Atomizdat, 1978, P. 94-121.

16. I.N.Golovin, B.N.Kolbasov, V.V.Orlov, V.I.Pistunovich, G.E.Shatalov. The problem of nuclear fuel and hybrid reactors. Preprint IAE-2931, 1977.

17. A.I.Ilushkin, I.I.Linge, et al. Investigation of neutron cross section uncertainties impact on fusion reactor blanket/shield characteristics. Atomnaya Energiya, V.56, iss. 1, January 1984.

18. V.V.Bolyatko, et al. In: Numeric solution of transport equation in one-dimensional problems, Moscow, Inst. Applied Math. Acad.Sci., USSR, 1981, P.202.

19. T.A.Germogenova, et al. Ibid, P.222.

20. M.Yu.Vyrskij, et al. Atomnaya Ehnergiya, 1982, V.53, iss. 2, P.113.

21. D.V.Markovskij, G.E.Shatalov. Sensitivity of hybrid reactor characteristics to the secondary neutron spectra. Atomnaya Ehnergiya, V.49, iss.2, P.79-83, 1980.

22. R.D.Vasil'ev. Osnovy metrologii nejtronnogo izlucheniya. Atomizdat, Moscow, 1972.

23. V.A.Zagryadskij, et al. The total absorption method in measurements of 14-MeV neutron multiplication. Preprint IAE-4171/8, 1985.

24. V.D.Aleksandrov, et al. Experimental study of neutron spectrum in lead with 14-MeV neutron source. Atomnaya Ehnergiya, v.52, iss.6, 1982.

25. L.Hansen et al. Neutron and Gamma-Ray Spectra from ^{232}Th, ^{235}U, ^{238}U and ^{239}Pu after Bombardment with 14-MeV neutrons. Nucl. Sci. Eng., V.72, N 1, P.35 (1979).

26. L.P.Bass,T.A.Germogenova. A single-rate RADUGA code.Preprint No.117. M.V.Keldysh Inst.Appl.Math.,Acad.Sc.USSR,1973.

27. T.A.Germogenova, L.P.Bass. On the solution of transport equation by the method of characteristics. In: Voprosy fiziki zashchity reaktorov. M., iss.3, 1968.

28. A.A.Lapenas. Group cross section library for threshold reactions (BGS-1).In:Metrologiya nejtronnykh izmerenij na yaderno-fizicheskikh ustanovkakh. Proc.Conf., V.1, M., 1976.

29. I.Heertje, L.Delvenne. Cross section for the reactions $^{204}Pb(n,n')^{2o4m}Pb$ and $^{206}Pb(n,3n)^{204}Pb$. Physica 30, 1964, P. 1604-1611.

30. P.Decowsci. Cross sections for the (n,n') and (n,2n) reactions on ^{113}In and ^{204}Pb. Nuclear Physics, 1973, A204, P.121-128.

31. Y.Gohar. Nuclear Data Needs for Fusion Reactors. International Conference on Nuclear Data for Basic and Applied Science. Santa Fe, New Mexico. May 13-17, 1985.

32. V.V.Deriglasov, N.E.Polikhovskaya, G.E.Shatalov. On Feasibility of Direct Enrichment of Fission Reactor Fuel Elements in a Fusion Reactor Blanket. Technical Committee on fusion reactor design and technology. Yalta, 26 May-6 June, 1986.

33. V.E.Kolesov, N.N.Nikolaev. Recommended nuclear data library format for reactor calculations. Yadernye konstanty, iss.8, part 4. M., TsNIIAtominform, 1972, P.3.

STRUCTURE OF WORKING CONSTANTS FOR NEUTRONIC CALCULATIONS OF FUSION REACTOR BLANKETS AND SHIELDS BY THE MONTE CARLO METHOD ON THE BASIS OF THE EVALUATED DATA FILES

A.A. BORISOV, D.V. MARKOVSKIJ, G.E. SHATALOV
I.V. Kurchatov Institute of Atomic Energy,
Moscow, Union of Soviet Socialist Republics

Abstract

General remarks on using of nuclear data in ENDF/B-6 format for the neutronic calculations of fusion reactor blanket and shield by Monte-Carlo method are presented.

A detailed information on cross-sections, anisotropy os scattering and on secondary-neutron spectra is necessary for calculating fusion reactors, shields, fast neutron source experiments etc. The working constants used for calculating such models by the Monte Carlo method with the BLANK-code (1) are oriented to the most complete account of parameters in the processes of interaction between neutrons and a material in a fast spectrum range (E<0.1MeV) given in the evaluated data files. In this case, their structure considerably differs from that adopted in the calculations of fission reactors. The main pecularities are as follows (2):

1. A number of groups is rather high. Therefore the problem of an intergroup spectrum option is of minor importance;

2. Different energy group scales are used for a total cross-section and for partial cross-sections, and only the group scales, where the total cross-sections are given, should be general for all the elements;

3. The data of elastic scattering anisotropy are given in the form usual for the Monte-Carlo method, i.e. as the partition of an indicatrix into N equiprobable ranges, where $N=2^P$;

4. The energy distribution data of (n,n), (n,2n), (n,3n) secondary neutrons are represented by the same laws as in the initial file, not as the transition matrices in the usual group constants.

5. Elastic transitions are described by the known kinetic formulae;

6. Angular distributions of secondary neutrons in inelastic reactions, except the scattering to a single level, are considered to be isotropic in the laboratory coordinate system.

In the calculations with such constants the position of a neutron is fixed on both discrete (group) and continuous energy scales.

Recently a new approach to the data of inelastic reactions has been formed. This approach has been induced, on the one hand, by the necessity of taking the account of direct processes and energy-angle correlations in the secondary neutron distributions and, on the other hand, by a tendency of evaluators to simplify the structure of data, using the reactions with the parameters close to those measured in the experiment.

At the Vienna meeting of experts in 1984 (3) it was proposed to introduce the MTIO-reaction describing all the primary neutrons in inelastic interactions, except the scattering to discrete levels, and thus to separate the parameters of the first neutron from those of consecutive ones. In this case, a possibility of verifying the primary neutron spectra directly in spectroscopic measurements (say, by the time-of-flight technique) emerges.

Another approach (4,5) proposed to use a more compact data format, in which only the processes of elastic scattering and those of inelastic scattering to discrete levels were singled out, other processes were combined in the MTIOO-reaction, which was characterized by a number of secondary neutrons, $\nu(E)$, by their energy and angle distributions given in the MF-6 file.

At present some versions of the code for programming working constants and for the collision module in the BLANK-code, which allow the evaluated data representation in the form mentioned above, have been developed within the frames of the BLANK-code set. At insufficient experience in the utilization of these codes and in the analyses of calculated results has not allow yet to judge of the advantages and disadvantages of this new approach to the data. However, one can make some general remarks concerning the analysis of their structure from the view-point of the data user.

1. The energy-angle distribution format, MF-6 (6), provides a set of secondary energies and the anisotropy expansion coefficients for each neutron energy before collision. Such a format is convenient for representing the parameters of scattering to continuum (in the second part of Section), and it is inconvenient for representing the parameters to discrete levels because of a difficulty in identification of a level by the secondary energy in interpolating angular parameters between the incident energy values. It can be avoided, presetting the reaction energy instead of the secondary energy. There is no necessity to preset the secondary energy in this case, as it is unambiguously calculated on the basis of an initial energy, scattering angle and on that of the reaction energy.

2. The exception of the partial reaction cross-sections, which form the MTIO or MTIOO-reaction cross-sections, from the neutron transport calculations in an explicit form prevents the calculation of these reaction rates directly from the collision analysis. The cross-sections of these reactions should be preset in the corresponding section of the data file to make it possible to evaluate the reaction rates with the calculated neutron fluxes.

3. The use of the composite spectra of secondary neutrons does not allow the account of correlation between the parameters of the first neutron and consecutive ones and thus excludes the energy balance maintenance at a single collision.

4. The inclusion of a fission reaction into a composite reaction, MTIOO, complicated the fission source interation by the neutron generation method in calculations of the systems with fission material. It is expedient not to include a fission reaction into the MTIOO-reaction by this reason.

REFERENCES

1. S.V. Marin, D.V. Markovskij, G.E. Shatalov
   "Code for the calculation of energy-space distribution of neutrons in one-dimensional geometry" Preprint IAE-3044, 1978 (in Russian).

2. D.V. Markovskij, A.D. Frank-Kamenetskij, G.E. Shatalov, L.N. Zahavov
   "Energetical modul FORTUN for Monte Carlo calculations with microconstants make of evaluated nuclear data files" Voprosy atomnoj nauki i tehniki. Ser. Fizika i tehnica yad. reactovov. Vol. 8, 21, 1984.

3. O. Schwerer, H.D. Lemmel, Report INDC(NDS)-156, 1984.

4. Collection of working papers of IAEA-Specialists' Meeting, Vienna, 2-4 April, 1984.

5. H. Gruppelaar, Report ECN-83-194, 1984.

6. R.E. Mac Farlane et al. LA-VR-84-1026, 1984.

STATUS OF THE UK ACTIVATION CROSS-SECTION LIBRARY FOR FUSION

R.A. FORREST
Nuclear Physics Division,
Atomic Energy Research Establishment,
Harwell, Didcot, Oxfordshire,
United Kingdom

Abstract

The UK is improving its fusion library (UKCTRIIIA) for activation and this involves increasing both the number of isotopes and reactions The treatment of isomer formation is recognized as a major deficiency that requires more effort The systematics used in the calculation of unmeasured cross sections have been reassessed and improved formulae are given here A sensitivity analysis is planned to identify reactions that will need a more thorough treatment A major use of these data is in the design of new alloys with low activity after irradiation, some results are given and it is stressed that the calculations will require validation A list of areas of future work is given

1 Introduction

The UK is pursuing an active programme of research into fusion, which includes work at Culham and participation in JET Work on future reactor design, including details of structural materials, walls and blankets, requires detailed information on the behaviour of a wide range of materials in an intense flux of high energy neutrons This information is embodied in data libraries and for the UK the existing fusion activation library is UKCTRIIIA

This paper gives some general background on the activation problem in fusion reactors, describes the evolution of the present library and the work that is proceeding to improve it Details of collaboration with other groups in the UK and in Europe and some results of this collaboration are given A summary of problems that require additional work by the international community in the support of this programme is included

2 Background to fusion activation and transmutation

There are many differences between the material properties that are important for fusion and for the well-defined fission systems In the latter much of the highly stressed structural material can be located outside the core, and the core components, the fuel and

cladding, can be replaced readily The cladding contains activated material produced by the neutron flux, but this is minor in comparison with the highly active fission products that become incorporated in the cladding from the fuel The main structural materials outside the core are transmuted and activated to a much smaller extent This is of consequence at decommissioning, but no routine replacement is required The situation is very different in a fusion reactor because the structure will be highly stressed and in a position of peak flux Radiation damage will therefore limit the useful lifetime of a first wall structure to a few years

The reason for the more demanding radiation environment in fusion as compared to fission reactors is the higher flux at high energies (14 5 MeV) The total flux however, in a fast fission reactor is greater than in a comparable power fusion reactor The high energy neutrons mean that many more nuclear reactions are feasible and important in the activation of fusion materials

Although damage calculations of both atom displacements and gas production are very important in the choice of materials, this paper concentrates on activation and transmutation The details will depend on the type of fusion system (e g magnetic or inertial confinement) to be used and here Tokamaks will be considered

The main ways in which activation will affect the design of a reactor are

1. Safety in the event of an accident. The release of volatile tritium is probably of more importance than release of activation products which are structurally confined and so melting of the material and subsequent aerosol or vapour transport is necessary before they are released to the environment

2. Safety during routine operation. Activation products of the reactor cover gas and coolant can be released during operation, however, these do not appear to be as important as escapes of tritium

3. Dose levels during maintenance. As in the case of fission, routine maintenance is the main cause of operator dose Short lived activation products in addition to the longer lived ones will determine the cooling time and type of maintenance possible

4. Waste management: recycling or ultimate disposal. This is considered in more detail in section 2 4

It is important for the long term public acceptance of fusion, that all the above areas are shown to be of much less trouble than in the case of fission[1] The specific parts of the reactor in which activation is important are

1 Activity in the first wall and blanket
2 Activity in the shielding and magnets
3 Activation of gases in the reactor building

These are considered in more detail below

2.1 First wall and blanket

The lifetime of the first wall is restricted to a few years given the upper limit of the thermal loading of about 20 MWym^{-2} and the estimated neutron wall loading ($\sim$4 MWm^{-2}) This will lead to substantial amounts of material from the Li based blanket and structural alloys having to be processed

2 2 Shielding

The shielding has to reduce radiation levels at the fence to low limits (typically 50 μSvy^{-1}) This should last the life of the reactor and represents a decommissioning problem (typically 13,000 tonnes of iron and 2,200 tonnes of copper will be removed from the reactor)

2.3 Gases

Typical products from the interaction of neutrons with atmospheric gases are (half lives in brackets) ^{16}N (7s), ^{13}N (10 m), ^{41}Ar (1 83h) and ^{14}C (5570y) The first two decay rapidly and by restricting the number of air changes, the discharged amounts are small The remaining two appear to be controllable with current approaches

The use of standard materials gives an initial estimate for the production of activity Materials with different nuclear properties can then be introduced to reduce activity to meet required levels There are two main possible approaches to reducing activation

1. **Element selection** where elements with high activation products are replaced by more suitable ones, and impurities are carefully controlled
2. **Isotope tailoring** where isotopic separation is used to remove a particular isotope which is responsible for high activity

For the foreseeable future 2 is unlikely to be seriously considered due to the very high cost and this paper will therefore concentrate on 1 The highest priority is the production of low activity alloys to replace stainless steel

2.4 Waste Management

Most ($\sim$98%) of radioactivity from activation products will be generated in the first wall and blanket, this is termed the *primary waste* If stainless steel were used then the volumes and masses of highly active waste at shutdown would be comparable to that arising from fission systems ($\sim$1 C1W(th)$^{-1}$), but the absence of long lived fission products and actinides will reduce the fusion activity, relative to fission, after 100 years by about 4 orders of magnitude

If the primary waste were disposed of after initial cooling then in the long term (a fusion economy) this could lead to the disappearance of a valuable reserve of materials and give a disposal problem To avoid this there must be some recycling This can be done remotely or with a 'hands-on' approach For the latter and conventional materials a waiting time of approximately 1,000 years might be needed to produce a dose of 25 μSvh^{-1}

The disposal regulations in the UK consider four categories of radioactive waste[2] (there is no special category for fusion generated waste as yet)

1 **Heat generating waste :–** sufficiently highly active that the temperature may rise significantly as a result of radioactive decay
2 **Intermediate waste :–** can be safely stored, but mostly too active for present disposal routes
3 **Low level waste :–** can be safely disposed of by shallow land burial or dispersion to the environment

4 **Ordinary waste :–** no special precautions are required if the activity < 0 37 Bqg^{-1}

Jarvis[2] shows that only for a structural material composed of Mg, V or Cr would it be possible to classify it as ordinary waste after 300 years Even minor impurities mean that *any* structural material will be unable to be classified as ordinary Even low level disposal may be impossible to achieve, and purpose built repositories will probably be required

3 Low activation materials

Jarvis[3] considered 39 elements in a flux from the Culham Conceptual Thermonuclear Reactor Mark II, and calculated maximum concentrations permitted as constituents of structural material on the assumption that it is necessary to reprocess the materials within 100 years The details are summarized in Table 1

This work is continuing and recently some preliminary calculations have been carried out by replacing gaps in UKCTRIIIA by calculations made with THRES-F These are reported by Giancarli[4] and some details are given in Table 2

In addition to work on individual isotopes, information on specific alloys is reported A summary of the work of Hancox et al[5] is given below

Austenitic and martensitic steels have been developed as typical 'low-activation' materials in which Ni is replaced by Mn and N in the austenitic steel and Mo is replaced by W in the martensitic steel Recycling of these components could be possible with surface γ dose rates of $\sim$10 mSvh^{-1} Conventional steels do not fall below this figure for several hundred years For comparison, low-activation steels reach this figure within a few decades with ^{54}Mn and ^{60}Co being the dominant radionuclides

Presence of Ni and Co impurities cause increased dose rate, but the presence of Ag, Tb and Nb at the ppm level give the long lived γ emitters An important part of the work is to see how much the conclusions of such studies depend on the accuracy of the data in the library

4 The history of the UK library

Details of UKCTRIII were published in 1979 The library was compiled by Jarvis and was based on the LASL library DLC–33C/Montage 400[6] However, the latter only includes reactions leading to unstable product nuclides and it was therefore necessary to generate many data sets by using variants of the code THRESH based on the work of Pearlstein[7] This library (UKCTRIII) was used by Jarvis for studies of activation and transmutation of fusion reactor structures and coolant materials

The library was updated in 1980[8] by merging UKCTRIII with the library DLC–69/ACTL[9] (after processing to a suitable group structure) This has the advantage that data generated by models have already been normalized to the Livermore Evaluated Nuclear Data Library UKCTRIIIA contains data for 1,477 reactions on about 300 nuclides The cross sections are given in 100 group form (GAM-II) Nuclides in isomeric states as targets were omitted and the product isomer data was also removed and isomer

ratio information for the relevant reactions was input separately. An improved version of THRESH (THRESH2) was used to generate cross sections.

In 1981 Gruppelaar inspected UKCTRIIIA and normalised many of the reactions using recent systematics and data compilations. Isomers were treated more consistently by introducing branching ratios (however, many of these were arbitrarily set to 0.5). This version of the library is referred to as UKCTRIIIAR2.

Some of the recognized deficiencies of the library are listed, and in the next section the strategy for improvement is given.

1 The number of isotopes and reactions is too small.
2 The treatment of isomers is inconsistent.
3 THRESH calculations are used in the absence of data.
4 The data and systematics used for normalisations are rather old.

Table 1 Percentage of element permitted in first wall or blanket materials so as not to exceed chosen threshold levels after cooling for 100 years. (Taken from reference 3)

Element	% permitted in first wall (no chemical separation)		% permitted in first wall (after chemical separation)		% permitted in blanket (no chemical separation)	
	Criterion Activity	Dose-rate	Criterion Activity	Dose-rate	Criterion Activity	Dose-rate
Li	1	100	100	100	10^{-1}	100
Be	1	100	100	100	1	100
B	1	100	100	100	10^{-1}	100
C	100	100	100	100	100	100
N	5×10^{-2}	100	100	100	5×10^{-2}	100
O	50	100	100	100	50	100
F	50	100	100	100	50	100
Na	100	10	100	100	100	100
Mg	100	100	100	100	100	100
Al	10	3×10^{-3}	10	3×10^{-3}	10	3×10^{-3}
Si	100	20	100	100	100	100
P	100	100	100	100	100	100
S	100	100	100	100	100	100
Cl	3	100	20	100	3	100
Ar	10^{-3}	100	10^{-3}	100	10^{-3}	100
K	3×10^{-3}	40	100	(100)	3×10^{-3}	100
Ca	10^{-1}	5	15	100	4×10^{-1}	100
Sc	1	3×10^{-2}	100	10	10	10
Ti	10	2×10^{-1}	100	100	100	30
V	100	100	100	100	100	100
Cr	100	100	100	100	100	100
Mn	30	100	100	100	100	100
Fe	20	100	100	100	30	100
Co	100	10^{-1}	100	10^{-1}	100	10
Ni	10^{-2}	1	10^{-2}	100	5×10^{-3}	1
Cu	10^{-3}	1	100	100	10^{-3}	100
Zn	10^{-2}	5	100	100	10^{-2}	100
Y	100	100	100	100	100	100
Zr	2	3×10^{-1}	5	100	2	30
Nb	5×10^{-3}	10^{-4}	5×10^{-3}	10^{-4}	10^{-3}	10^{-4}
Mo	3×10^{-2}	10^{-2}	5×10^{-2}	100	10^{-2}	10^{-1}
Ag	10^{-3}	10^{-6}	10^{-3}	10^{-6}	3×10^{-4}	10^{-5}
Cd	3×10^{-1}	10^{-3}	100	100	6×10^{-1}	3×10^{-2}
In	100	1	100	100	100	100
Sn	10^{-2}	1	10^{-2}	100	10^{-2}	7
Ta	100	100	100	100	100	100
W	100	100	100	100	100	100
Tl	100	100	100	100	100	100
Pb	50	100	100	100	100	100

Activity criterion – 8 6 10^{-6} CikW(th)$^{-1}$
Dose-rate criterion – 25 μSvh^{-1}

Table 2 Number of ppm (by weight) permitted for troublesome impurity elements. (Taken from reference 4)

ELEMENT	First wall flux neutron wall load: 5 MW m^{-2}		Rear blanket flux neutron wall load: 5 MW m^{-2}	
	100 y surface dose criterion	250 y surface dose criterion	100 y surface dose criterion	250 y surface dose criterion
35-Br	$2.8 \cdot 10^{4}(2.8\%)$	$2.8 \cdot 10^{4}(2.8\%)$	$5.53 \cdot 10^{5}(55.3\%)$	$5.53 \cdot 10^{5}(55.3\%)$
36-Kr	96.9	3440.	238.	6650.
37-Rb	$1.31 \cdot 10^{4}(1.3\%)$	no limit	$8.22 \cdot 10^{4}(8.22\%)$	no limit
38-Sr	1310.	no limit	$1.46 \cdot 10^{4}(1.46\%)$	no limit
44-Ru	$1.52 \cdot 10^{4}(1.5\%)$	$1.52 \cdot 10^{4}(1.5\%)$	$1.80 \cdot 10^{5}(18\%)$	$1.80 \cdot 10^{5}(18\%)$
45-Rh	$8.80 \cdot 10^{5}(88\%)$	no limit	no limit	no limit
46-Pd	6.08	13.8	371.	845.
54-Xe	9.26	295.	24.5	767.
55-Cs	20.8	$4.16 \cdot 10^{5}(41.6\%)$	346.	no limit
56-Ba	16.1	828.	164.	$1.18 \cdot 10^{4}(1.18\%)$
57-La	$2.12 \cdot 10^{5}(21.2\%)$	no limit	no limit	no limit
58-Ce	$1.95 \cdot 10^{5}(19.5\%)$	no limit	no limit	no limit
60-Nd	61.3	6980.	238.	$8.31 \cdot 10^{4}(8.31\%)$
62-Sm	5.77	772.	22.9	8220.
63-Eu	$4.73 \cdot 10^{-3}$	0.56	$6.05 \cdot 10^{-3}$	2.15
64-Gd	19.1	$1.63 \cdot 10^{4}(1.63\%)$	75.3	$3.02 \cdot 10^{5}(30.2\%)$
65-Tb	$5.04 \cdot 10^{-3}$	0.01	0.04	0.08
66-Dy	7.06	14.12	197.	393.
67-Ho	0.03	0.033	0.044	0.05
68-Er	31.7	34.6	393.	429.
69-Tm	64.8	70.6	566.	617.
75-Re	$1.17 \cdot 10^{4}(1.17\%)$	$1.17 \cdot 10^{4}(1.17\%)$	$1.20 \cdot 10^{4}(1.2\%)$	$1.20 \cdot 10^{4}(1.2\%)$
77-Ir	0.025	0.039	0.17	0.27
78-Pt	79.9	123.	3490.	5360.
83-Bi	0.11	1.32	5.09	16.9

Dose-rate criterion – 25 μSvh^{-1}

5 Programme of improvement

5.1 General strategy

The general strategy has been as follows

1 To produce an enlarged library that will still contain large amounts of THRESH generated and possibly poorly normalised results

2 To use this *interim* library with a sensitivity code to identify a small fraction of reactions that are of major importance

3 To focus improvements on these reactions by the use of improved calculation codes and more detailed evaluations.

4 To continue a series of iterations of this procedure in parallel with overall increases in accuracy by the use of improved systematics and recent normalisation data

5.2 The calculational methods

In order to carry out this programme a series of computer codes are necessary These include the calculation codes (in order of increasing complexity) THRESH, CADE and GNASH, the codes for processing data into various group formats (e g NJOY) and a code for sensitivity analysis (a version of FISPIN) In addition a series of revised systematics for some neutron induced reactions has been prepared These will be described in more detail and where the work has been done in collaboration with other organizations this is also given

5.2 1 THRESH

A new version of THRESH specifically designed for fusion applications has been prepared by Giancarli (Culham) and Gruppelaar (ECN Petten)[10] This is known as THRES-F It includes improved systematics and facilities for producing cross sections in multigroup (GAM-II) form This enables data sets to be generated quickly for inclusion in the data library A further version of this code using the most recent systematics and a graphics output (useful for quick inspection of data trends) has been prepared at Harwell A major disadvantage with all versions of THRESH is that no values for the (n,γ) reaction are given

5.2 2 CADE

A more physical, but still approximate, approach to calculating cross sections is to use the Weisskopf–Ewing theory This has the additional advantage that (n,γ) reactions are included, although not very well at low energy A code covering this was prepared at Harwell by Wilmore[11] This has the disadvantage of requiring a fair amount of input data and is not therefore suitable for the mass production of cross sections The operation of the code has been considerably simplified in collaboration with Oxford University (Hodgson), and a version of CADE containing this user-friendly input and pre-equilibrium calculations has been prepared by Ait-Tahar[12] An early version has been implemented on the Harwell CRAY computer and with the continuing work on simplifying and speeding up the calculational method, this will be a good way of generating more accurate results where required

5.2 3 GNASH

The detailed Hauser–Feshbach code, GNASH, developed at Los Alamos[13] has been implemented on the CRAY at Harwell by Muir[14] This is capable of accurate calculations, but requires a considerable amount of effort to prepare suitable input data Therefore the code could only be used for a small number of very important nuclides

5.3 Systematics

A reassessment of the systematics for the reactions (n,p), (n,α) and (n,d) at 14 7 MeV and (n,t) and (n,h) (h=³He) at 14 6 MeV has been carried out recently at Harwell Details are available in a report[15], and the work is summarized here

Data on these reactions covering work up to about 1980 are based on the compilations by Cuzzocrea et al[16], Qaim[17], Bychkov et al[18] and Body and Mihaly[19] Literature searches gave more data covering work up to 1985 Simple evaluations (no renormalisation of data to allow for changes in standard cross sections, half lives or decay schemes) were generally undertaken The existing systematics were fitted to the data by the method of weighted least squares and the parameters in the existing formulae recalculated New systematics for all the reactions (except (n,h)) have been derived with smaller values of χ^2 per degree of freedom A further improvement on the existing systematics is an estimate of the error to be expected if the systematic is used to predict an unknown cross section This information is important as error estimates will be required for sensitivity analysis of the data library to determine the most important reactions

The covariance matrix of the parameters, which can be estimated by the fitting subroutines, can be used to calculate the error in any predicted cross section This method however has the following disadvantages A formula containing p parameters has a covariance matrix containing p^2 terms and requires a separate complicated calculation to propagate the errors through to each cross section For these reasons a simplified approach, using the *error factor* φ was adopted For the (n,p) data it has been shown that the two methods are in very good agreement

The ratio $\sigma(expt)/\sigma(calc)$ plotted against A is a good way to show the fit of an equation to data These plots suggest that $r = \log_{10}(\sigma(expt)/\sigma(calc))$ is approximately normally distributed about 0 The spread of this distribution is related to the error expected in fitting and so the standard deviation about an assumed mean of 0 (Δ_0) is found, and the error factor calculated as shown in equation (1)

$$\varphi = 10^{\Delta_0} \tag{1}$$

The 1–standard deviation limits on the calculated cross section (σ_{calc}) using this simplified approach are therefore $\sigma_{calc}\varphi$ and σ_{calc}/φ This approach requires only one calculation to give φ which can then be directly applied to any predicted cross section For the reactions considered there is no significant variation in the spread of r values with A, and it is therefore sufficient to use one value of φ for all A

The new systematics for each of the reactions are summarized below In addition some details of the most successful existing systematic are given for comparison The selection of nuclides with incorrect data is discussed in more detail in the report These nuclides are candidates for priority measurement

The (n,p) data library covers 150 nuclides. A plot of the data against s, where $s = (N-Z)/A$, A = mass number, Z = atomic number and N = neutron number, is given in Figure 1. The present formula for the cross section (mb) is shown in equation (2)

$$\sigma_{np} = 7.567(A^{1/3}+1)^2\exp(-28.80s-59.24s^2+0.2365A^{1/2}) \qquad (2)$$

and uses 4 parameters to give a small χ^2 of 3.92. A histogram showing numbers of nuclides with various values of F^2 ($F = (\sigma(calc) - \sigma(expt))/error$) is given in Figure 2. When using the formula to predict unknown cross sections an error factor of 1.50 is employed. The existing formula by Kumabe and Fukuda[20] uses 8 parameters and gives a χ^2 of 4.42. The measured data for the nuclides ^{40}Ca, ^{45}Sc, ^{64}Ni, ^{100}Ru, ^{115}In, ^{112}Sn, ^{165}Ho, ^{208}Pb and ^{209}Bi are probably incorrect as they are poorly fitted by equation (2).

The (n,α) data library covers 114 nuclides. The present formula for the cross section (mb) is shown in equation (3)

$$\sigma_{n\alpha} = \begin{cases} 10.82(A^{1/3}+1)^2\exp(-9.402s-127.3s^2-0.00717A), & Z \leq 50 \\ 129.4(A^{1/3}+1)^2\exp(-42.45s-0.00212A), & Z > 50 \end{cases} \qquad (3)$$

and uses 8 parameters to give a χ^2 of 4.99. Figure 3 shows the fit in the form of the ratio $\sigma(expt)/\sigma(calc)$ plotted against A. When using the formula to predict unknown cross sections an error factor of 1.58 is employed. The existing formula by Kumabe and Fukuda[20] uses 8 parameters and gives a χ^2 of 6.16. The measured data for the nuclides ^{64}Ni, ^{89}Y, ^{114}Cd, ^{118}Sn and ^{197}Au are probably incorrect.

The (n,d) data library covers 35 nuclides. The present formula gives the sum of $\sigma(n,d)+\sigma(n,np)+\sigma(n,pn)$ in units of mb, that is obtained from activation measurements and it is shown in equation (4),

$$\sigma_{nd} = 900.9(A^{1/3}+1)^2 \, (1-0.4828 \tanh(\xi+1)) \exp(-52.3s-135.7/A) \qquad (4)$$

it uses 4 parameters to give a χ^2 of 9.38. The variable ξ is the difference between the proton and neutron separation energies (MeV). This type of equation is able to give the two groups of points found experimentally. When using the formula to predict unknown cross sections an error factor of 2.03 is employed. The existing formula by Qaim[21] uses 3 parameters and gives a χ^2 of 36.07. The data are limited for this reaction, consequentially the systematics are poorer than for the previous cases. The measured data for the nuclides ^{77}Se, ^{96}Ru and ^{183}W are probably incorrect.

The (n,t) data library covers 25 nuclides and the data is shown in Figure 4. The present formula for the cross section (μb) is shown in equation (5)

$$\sigma_{nt} = \begin{cases} 1.516(A^{1/3}+1)^2\exp(-24.35s+0.2670A^{1/2}), & A \text{ even} \\ 4402.1 \exp(-20.509s), & A \text{ odd} \end{cases} \qquad (5)$$

and uses 5 parameters to give a χ^2 of 3.4. When using the formula to predict unknown cross sections an error factor of 1.64 is employed. When more data are available for odd A, the standard type of 2-parameter equation will probably give better results than the present one. The existing formula by Qaim and Stocklin[22] uses 4 parameters and gives a χ^2 of 3.64. The measured data for the nuclides ^{88}Sr, ^{103}Rh and ^{205}Tl are probably incorrect.
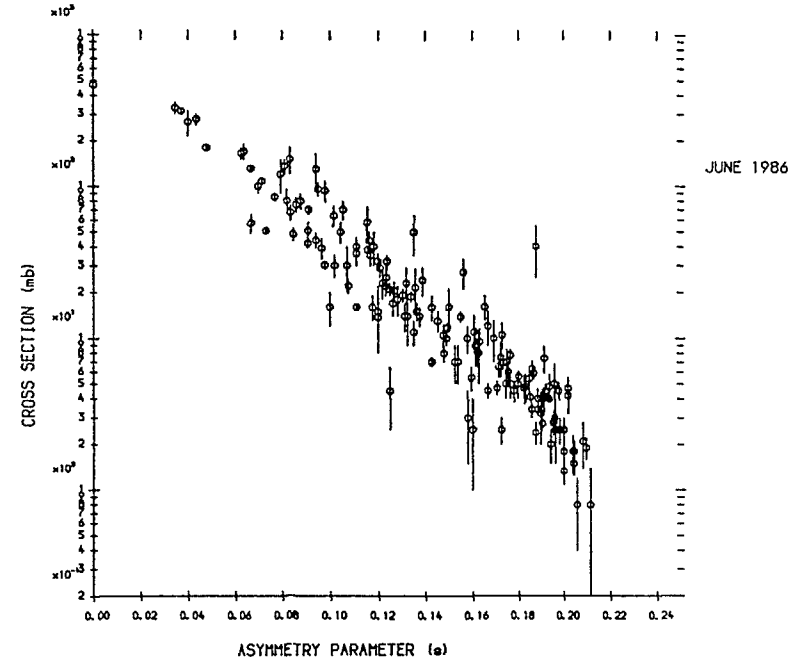
Figure 1 The (n,p) data plotted against s.
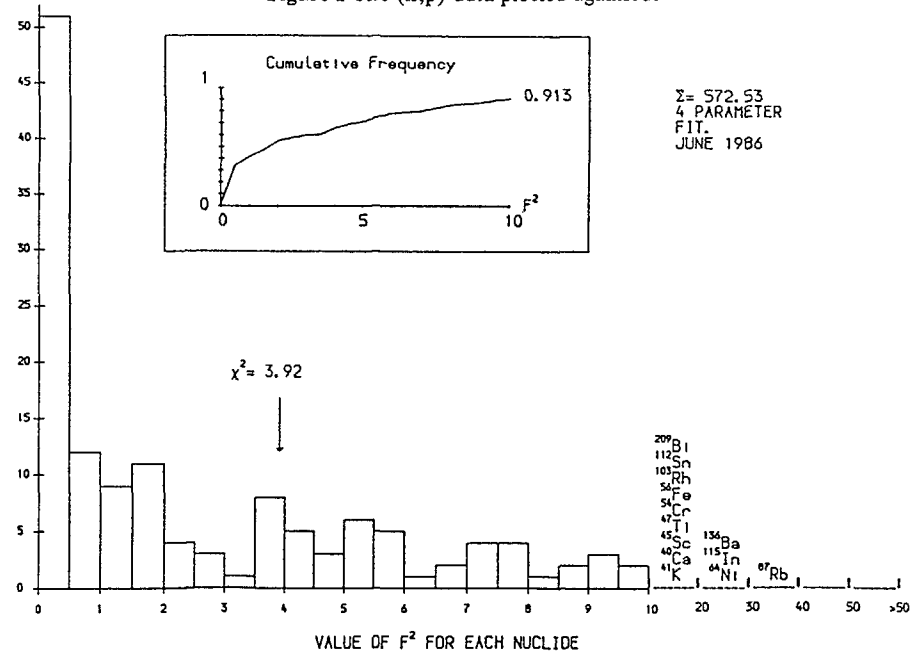
Figure 2 Histogram showing the fit of equation (2) to the (n,p) data.
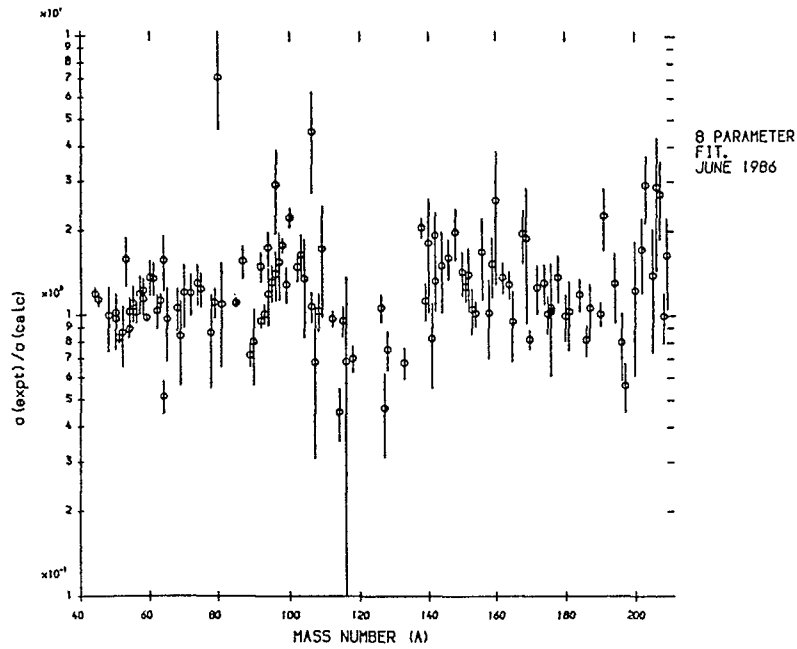
Figure 3 The fit of equation (3) to the (n,α) data.
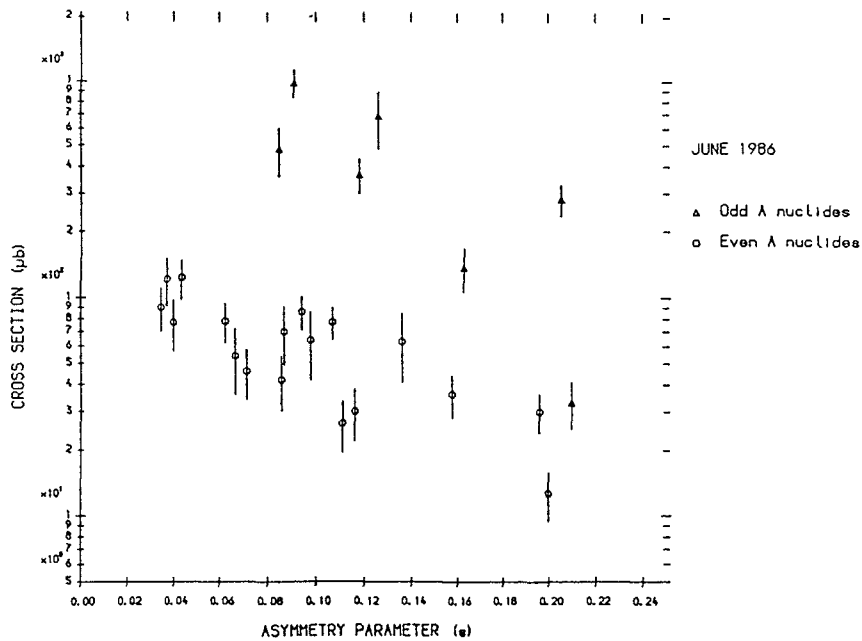
Figure 4 The (n,t) data plotted against s.

The (n,h) data library covers only 13 nuclides, because partial or disputed data have not been used for fitting. Figure 5 shows the data plotted against s, and no good trend is obvious. The present formula for the cross section (μb) is shown in equation (6)

$$\sigma_{nh} = 0.1357(A^{1/3}+1)^2\exp(-3.00s) \qquad (6)$$

and uses 2 parameters. This is of the same form as the previous formula by Qaim[23], but it is not a good representation of the data. This is partly due to renormalisation of some of the monitor reactions with more recent data. The small χ^2 of 3.92 is largely due to the very high experimental errors. When using the formula to predict unknown cross sections an error factor of 1.86 is employed.
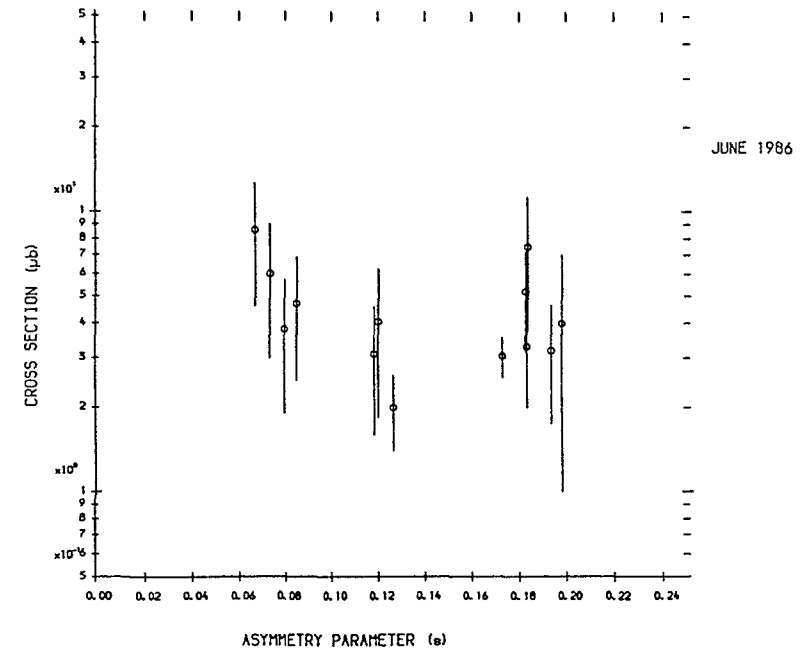
Figure 5 The (n,h) data plotted against s.

5.4 Sensitivity analysis

Using an interim library based extensively on THRESH calculations and systematics, it is possible to calculate the sensitivity of the amounts of each nuclide after an irradiation in a fusion flux to the values of the cross sections. Using these sensitivities and suitable estimates of errors in the cross sections the most important reactions for producing troublesome activation products can be identified. These reactions will be studied in more detail and where appropriate more accurate calculations of cross sections (using CADE) or better evaluations will be made. This procedure will be iterated until a satisfactory library is obtained.

It is intended that the inventory code to be used for calculations of fusion transmutation and activation will be FISPIN[24]. Some reasons for the change from ORIGEN[25] are given below:

1 FISPIN is a UKAEA originated code and considerable effort is spent (under the fission programme) keeping the code and data libraries up to date.
2 A sensitivity version of FISPIN was written several years ago. This should be easier to update than writing a version for ORIGEN.

Work at Imperial College (Goddard) is continuing on various aspects of activation of fusion materials. The existing FISPIN3 sensitivity version has been rewritten and incorporated into FISPIN6 by Khursheed and is being presently tested with UKCTRIIIA.

6 The interim library

Informal agreement between Harwell and ECN Petten has been reached on collaboration to produce an improved fusion library. Gruppelaar (ECN) has made considerable progress in producing an improved library, following a request from JRC Ispra (Ponti).

This is based on the REAC library (version 2) produced at Hanford by Mann et al[26]. It contains pointwise data for more than 6,000 reactions and over 300 isotopes. It is based on recent sources and extends up to 40 MeV in energy. Many of the calculations are still based on THRESH, and many are unnormalized to data or systematics. There appears to be an overestimation of the contribution of isomeric states in some cases.

The programme carried out by Gruppelaar et al[27] includes:

1 A renormalization of all THRESH cross sections at 14.5 MeV using systematics.
2 Automatic setting of the branching ratio to 0.5 for all isomers; these are replaced by experimental values where these are available.
3 Addition of 45 missing reactions e.g. $^{11}B(n,d)$, $^{54}Fe(n,2n)^{53}Fe^m$ and $^{125}Sn(n,\gamma)$, and the addition of reactions for 37 additional stable nuclides.
4 Data are missing in many cases where $t_{1/2} > 1$ day. These were generated using THRES-F for 184 nuclides.
5 Renormalisations to data have been largely based on the compilation by Qaim[17].
6 The systematics include a new formula for (n,t) for odd mass nuclei and a method of splitting $\sigma(n,d)+\sigma(n,np)$ into its components — this is useful for gas production calculations, but is not required for activation.
7 Conversion of the pointwise REAC file to a 100 group (GAM-II) structure.

The library (GREAC-ECN) has been supplied to Harwell and it will be used as the input for the sensitivity analysis and further modifications.

6.1 Use of GREAC for activation calculations

Although this library has only recently become available some preliminary calculations have been done at Ispra by Ponti (private communication). These indicate that the increase in number of reactions covered by GREAC compared to UKCTRIIIA leads to some very different conclusions about the levels of isotopes that can be used in a fusion reactor if the resulting activated waste is to be capable of recycling or shallow land burial. These include Ti, Co, Sn, Sb, Hf, Ta and W.

7 Isomer ratios

One area that requires considerable further work to improve the libraries is the treatment of isomer ratios. All the neutron induced reactions can lead to nuclei in metastable states in addition to ground states. If the isomer is sufficiently long lived then the possibility exists for further reactions. Isomers with half lives of several tens of years and high energy γ emissions can themselves cause activation problems. Data on branching ratios at 14.5 MeV are limited and where they exist, are often discrepant especially for the (n,charged particle) reactions. Some work has been carried out searching for a formula which could give reasonable estimates when data or detailed calculation are not available. Uray et al[28] show that data for (n,2n), (n,p) and (n,α) follow a parabolic trend for $\log_{10}(\sigma^m/\sigma^g)$ when plotted against J^m (spin of the isomeric state) and Figure 6 is taken from their paper. A similar trend was given by Qaim and Stocklin[22] for $\log_{10}(\sigma^m/(\sigma^m + \sigma^g))$ for production of isomers in the (n,t) reaction.
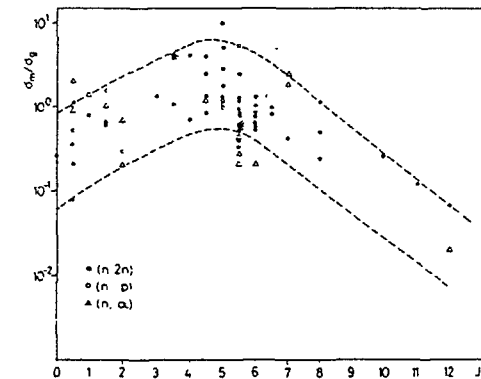
Figure 6 Systematics of the isomer ratio as published by Uray et al[28].

Data collected at Harwell to produce the systematics described above have been used as a database to search for correlations. Figure 7 shows a plot of σ^m/σ^g against J^m and no good correlation is obvious given the large spread in data and the errors. As would be expected physically the two points at high spin are low, and the best prescription is given by equation (7).

$$\sigma^m/\sigma^g = \begin{cases} 1 & , J^m \leqslant 7 \\ 10^{-2}, & J^m > 7 \end{cases} \tag{7}$$

A further search for systematics is planned for the (n,2n) and other reactions

A further class of reactions that need to be added to GREAC are those for which the target nuclei are isomers If they are not present, many of the chains of reactions important in determining the overall activation will not be calculated correctly These reactions should not present a major problem, as in most cases the ground state cross section can be used
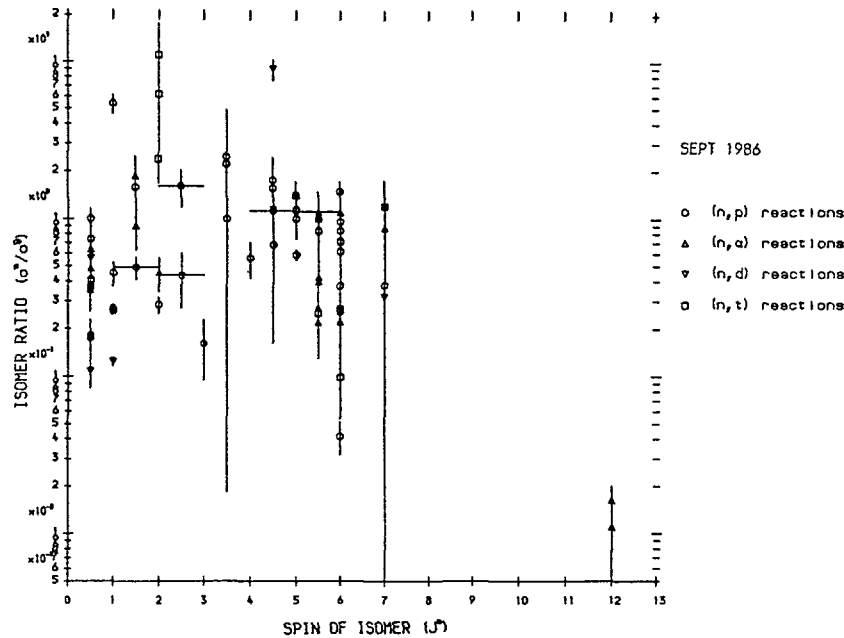
Figure 7 Isomer ratio plotted against the spin of the isomer

8   An example of current interest

Using the library UKCTRIIIA Jarvis[3] predicted that there is no restriction in the amount of Ta or W that can be used and that Hf is restricted to about 10% This refers to the elements being used in an alloy and then after irradiation either being recycled or disposed in shallow land burial Culham are currently considering various alloys which contain Ta or W Similar calculations have been carried out by Ponti (private communication) using the library GREAC and the conclusions are very different There are stringent limits on the amounts of each of the three elements mentioned above

Inspection of the library shows that the default branching ratio of 0 5 has been used for the formation of an isomer in the reaction ^{179}Hf(n,2n) This is however extremely unlikely as the 31 year isomer has a spin of 16 or 17 Calculations by Giancarli (private communication) indicate that even with a branching ratio of 5 10^{-3} a problem on the tolerable amounts of these elements still exists

The reactions (n,γ), (n,n'γ), (n,2n), (n,3n), (n,α), (n,n'α), (n,d), (n,h), (n,t) and (n,p) are all important in producing the ^{178m}Hf(31y) isomer

Figure 8 Details[29] of nuclides involved in the formation of an isomeric state of ^{178}Hf

Mention has already been made that no reactions with isomers as targets are as yet included in GREAC Figure 8 shows some details of the isotopes involved in the formation of ^{178m}Hf(31y) and it is obvious that these have to be included if the calculation is to be done correctly. There are, for example, many possibilities for the formation of ^{179m}Hf(25d) which can then undergo (n,2n).

Data for the branching ratios for these reaction at these energies appear to be unavailable, and with such high spins involved it is uncertain whether GNASH would be capable of giving an answer of sufficient accuracy Measurements will also be difficult with the long half-lives the isomers typically have This points out again the need for a reliable empirical formula for isomer ratio, especially for high spins Until the library is substantially improved in these two respects, conclusions of calculations based on it should be treated with caution

9 A measurement programme

The library that will be available shortly should be a guide in the selection of materials for the construction of planned fusion reactors However, it must be remembered that the library will only be partly based on experimental measurements It is therefore imperative that at some stage experiments be carried out in a realistic flux ($\sim 10^{14}$ n cm^{-2}s^{-1}) for a sufficiently long time (months) to validate the predictions of the library

At this stage it is only planned to include neutron induced reactions in the library However, charged particles will be present as products of reactions and these may in particular cases cause further reactions Photon induced reactions have also been neglected, although as the most likely reaction would be (γ,n), which is much smaller than the corresponding (n,2n), reaction this omission is probably justified

There are few real alternatives to carrying out such an experiment in a fusion reactor, as alternative sources give too small a flux which is not capable of reproducing the chains of reactions which have a time scale due to the lifetimes of the intermediates It may be possible to use the facility at JET for such irradiations once tritium is introduced into the plasma

Since the decision not to proceed with the Fusion Materials Irradiation Test Facility (FMITF) at Hanford there are no plans for a neutron source of high flux and fluence Although the arguments for this type of facility on grounds of materials testing (damage) may not have have been strong enough, the need to test materials for low activity is crucial if fusion technology is to convince a sceptical public of its ability to operate with extremely low environmental impact

In addition to the testing of materials prior to their eventual use, it is also important that thought be given to testing certain reactions that are used in the library Although this would require high energy neutrons with a reasonably intense flux, these experiments are feasible with some existing sources Two types of measurement are considered in more detail below

9.1 Check of systematics

In developing the systematic formulae it is noticeable that there are some data points that lie very far away from the trend Often these represent old or poor quality measurements, and it is important that some of these be remeasured If the data are incorrect and the majority of the outliers can be removed then the confidence that can be placed on the formulae for predicting unknown cross sections increases dramatically If the data are confirmed then it may be possible to determine some *physical* reason, such as shell structure, to explain this and so help in modifying the formulae in other similar cases

9 2 Isomer ratios

High quality measurements on a set of well chosen nuclides would give a data set with low errors that could be useful in spotting correlations It is the rather poor quality of many of the existing data that that has hampered such a search Calculations of extremely high

spin isomers (e g $J^m = 16$) are difficult because of lack of information on the high lying levels and the consequent use of approximate level density formulae This will mean that much of the isomer information used in the library will have to come from some systematic and efforts to make this as representative as possible should be given high priority

10 Summary of additional studies required

In this section the areas in which new information is required are summarized

1 The role of 'rare reactions' such as α–induced reactions should be clarified It is of no use embarking on an expensive programme of isotope tailoring if a rare reaction on the dominant isotope will still produce activity

2 The branching ratios for the production of long-lived isomers must be dealt with thoroughly in the data libraries

3 The treatment of nuclides with two isomeric states must be improved

4 A systematic search for very high spin isomers should be conducted This might use the techniques of heavy ion collisions

5 Some of the activation data are discrepant amongst themselves and these reactions could be usefully remeasured with modern equipment

6 A new evaluation of the activation data for all reactions would be very timely

7 The data for outliers in the various systematics must be remeasured (some candidates are given in section 5 3) so as to improve the confidence with which the formulae can be applied

8 Thought must be given to the eventual validation of the data libraries by the testing of materials in a high-flux high-fluence source

11 Summary and conclusions

The importance of activation of fusion materials is summarized The possibility of producing low-activation alloys means that calculations based on data libraries must be capable of covering a very wide range of isotopes and reactions Differences in conclusions resulting from the use of GREAC rather than UKCTRIIIA stress that the calculations are only as good as the data in the library

The evolution of the present UK data library and the present efforts to improve it are discussed A major problem is the importance of realistically including information on the probability of forming long-lived isomers Much of the present information is no more than a guess The library will have to contain very many calculated cross sections and a sensitivity analysis will identify reactions that require treatment with a more detailed theory

Low-activation materials may be dominated by impurity elements, measurements will have to confirm that after irradiation the alloy has low enough activity and that the level agrees with calculations Various types of experimental programmes are discussed and it is stressed that a high flux source will be essential at some stage to validate the data libraries

References

1 Jarvis O N , 'Transmutation and activation of fusion reactor wall and structural materials', **AERE – R9298**, 1979

2 Jarvis O N , 'Low-activity materials reuse and disposal', **AERE – R10860**, 1983

3 Jarvis O N , 'Selection of low-activity elements for inclusion in structural materials for fusion reactors', **AERE – R10496**, 1982

4 Giancarli L , *J Nucl Materials* **139**, 1, 1986

5 Hancox R , Mitchell B and Butterworth G J , 'Radiological implications of low-activation steels as structural materials in fusion reactors', **IAEA – CN–47/H–I–5**, 1986

6 'DLC–33C/Montage 400 100–Group neutron activation cross-section data for fusion reactor structure and coolant materials' RISC Data Library Collection, Oak Ridge National Laboratory, Radiation Shielding Information Centre, Oak Ridge, Tennessee U S A

7 Pearlstein S , *J Nucl Energy* **27**, 81, 1973

8 Jarvis O N , 'Description of the transmutation and activation data library UKCTRIIIA', **AERE – R9661(Rev)**, 1980

9 Gardner M A and Howerton R J , 'ACTL Evaluated neutron activation cross-section library – evaluation techniques and reaction index' **UCRL–50400 (vol.18)** Lawrence Livermore Laboratory (1978) Available from the Radiation Shielding Information Centre, Oak Ridge, under package name DLC–69/ACTL

10 Giancarli L and Gruppelaar H , *Culham Report* **CLM-R 261**, 1985

11 Wilmore D , 'CADE – A computer program for the calculation of nuclear cross-sections from the Weisskopf–Ewing theory', **AERE – R11515**, 1984

12 Ait–Tahar S , 'Weisskopf–Ewing and pre-equilibrium calculations of nuclear reaction cross-sections', MSc Thesis, Oxford, 1986

13 Young P G and Authur E D , 'GNASH A pre equilibrium statistical nuclear-model code for calculation of cross sections and emission spectra', Los Alamos Scientific Laboratory Report **LA–6947**, 1977

14 Muir D W , 'Implementation of GNASH and auxiliary codes on the Harwell CRAY–1', **AERE – R11877**, 1985

15 Forrest R A , 'Systematics of neutron-induced threshold reactions with charged products at about 14 5 MeV', **AERE – R12419**, (in course of publication), 1986

16 Cuzzocrea P , Perillo E and Notarrigo S , *Nuovo Cim* **4A**, 251, 1971

17 Qaim S M , *Handbook of Spectroscopy Vol 1*, CRC Press Inc, Florida, 141, 1981

18 Bychkov V M , Manokhin V N , Pashchenko A B and Plyaskin V I , *INDC(CCP)* **146/LJ**, 1, 1980

19 Body Z T and Mihaly K , *INDC(HUN)* **22/L**, 1, 1985

20 Kumabe I and Fukuda K , *NEANDC(J)* **65/U**, 45, 1978

21 Qaim S M , *Nucl Phys* **A382**, 255, 1982

22 Qaim S M and Stocklin G , *Nucl Phys* **A257**, 233, 1976

23 Qaim S M , *Radiochim Acta* **25**, 13, 1978

24 Burstall R F , 'FISPIN – A computer code for nuclide inventory calculations', **ND –R–328(R)**, 1979

25 Bell M J , 'ORIGEN – The ORNL isotope generation and depletion code', **ORNL – 4628**, 1973

26 Mann F M , Lessor D E and Pintler J S , *Nuclear Data for Basic and Applied Science, Santa Fe*, 207, 1986

27 Gruppelaar H *et al*, 'Cooperation between ECN Petten and JRC Ispra on the improvement and extension of activation data for fusion reactor technology', (in course of publication), 1986

28 Uray I , Torok I , Bornemisza-Pauspertl P and Vegh L , *Z Physik* **A287**, 51, 1978

29 Tuli J K , *Nuclear Wallet Cards*, National Nuclear Data Center, Brookhaven National Laboratory, 1985

STATUS OF THE EUROPEAN FUSION FILE

H. GRUPPELAAR
Netherlands Energy Research Foundation,
Petten, Netherlands

Abstract

The European Fusion File (EFF) is a nuclear-data file for application in
fusion-reactor blanket design calculations, in particular for neutron-
transport calculations of the Next European Torus (NET). This paper gives
a status report on the EFF-project.

---

1. INTRODUCTION

The EFF-project is part of the European Fusion Technology Programme of the
European Community (EC). The following laboratories are contractors in the
EFF-project: CEA (Saclay), ECN (Petten), ENEA (Bologna) and KfK
(Karlsruhe). Moreover, JRC (Ispra) and CBNM (Geel) are involved as EC in-
stitutes. The project is conducted by the NET-team at Garching and by
EC-Brussels. The file maintenance and management is performed at ECN
(Petten). Other European laboratories are also involved: SCK/CEN (Mol)
with an experimental programme performed at CBNM, the UK laboratories at
Harwell, Birmingham and Culham (JET), ENEA (Frascati), IKE (Stuttgart),
KfA (Jülich) and EIR (Würenlingen). Furthermore, technical support is re-
ceived from the NEA Data Bank at Gif-sur-Yvette.

Early 1986 a first version of the file (EFF-1) has been distributed to EC
laboratories [1,2]. Since a large part of the data file consists of eva-
luations taken from the Joint Evaluated File (JEF-1) the same distribution
policy as for JEF-1 (NEA Data Bank member countries) is followed. JEF-1 is
primarily directed towards fission reactors [3] and therefore some of the
nuclear data at high energies (above 10 MeV) may be less accurate. The
demands for fusion-reactor applications [4] are not entirely fulfilled by
the present, JEF-1 data library. In particular, there is no emphasis in
the JEF-project on the introduction of double-differential neutron-
emission cross sections in the high-energy range. This requires a new for-
mat for the storage of these data that is different from the currently
adopted format of JEF-1 (ENDF-V). For the above reasons the EFF-project
was initiated, concentrating on the specific demands for neutron-transport
calculations of fusion-reactor blankets. However, it was decided to keep
EFF as close as possible to the JEF data file and to take advantage of its
developments.

Although a very large body of nuclear data is required for blanket engi-
neering of fusion reactors, the first phase of the EFF-project is directed
mainly towards the tritium-breeding problem. This means that there is
emphasis on the tritium-production reactions $^6Li(n,\alpha)T$ and $^7Li(n,n'\alpha)T$, on

the neutron multiplication (Be,Pb) and on the parasitic absorption. A good
knowledge of the neutron-emission cross sections and their energy-angle
distributions is very important for the neutron multipliers and structural
materials. These double-differential cross sections are not very well re-
presented in the existing files. For ceramic blankets the cross sections
of Al and Si need to be considered. Most of these problems have been
addressed in the first stage of the project, cf. Sect. 2.

The main use of the EFF-1 file will be the application in neutron and
gamma-ray transport calculations to study the tritium breeding and the
radiation shielding (e.g. of superconducting magnets). Therefore, it was
decided to derive a multi-group constant file similar to the VITAMIN-C and
-E data libraries [5,6], currently used in many neutronics and photonics
calculations in fusion-reactor technology. The name of the EFF-1 based
group constant set is GEFF-1 and its status is described in Sect. 3.

Work for a second version of the EFF-file is in progress. The plans for
EFF-2 are described in Sect. 4. A new project is the development of a
supplementary European Activation File (EAF).

2. PRESENT STATUS OF EFF-1

Early 1986 the first version of EFF has been distributed. It consists of a
file with the 26 materials as mentioned in Table 1. The format of EFF-1 is
ENDF-V, with the addition of file MF6 of ENDF-VI [7] for reaction types
$MT = 10$, 16, 17 and 91. Furthermore, gas-production cross sections
($MT = 203$-207) and the neutron-disappearance cross sections (MT101) have
been added. The file contains 17 evaluations that are different from
ENDF/B-IV, which is still frequently used for neutronics calculations. The
largest part of the EFF-1 library has been taken from the Joint Evaluated
File (JEF-1). Below an updated summary (cf. Ref. [2]) is given of work
made for EFF-1.

2.1. Lithium (tritium-production cross sections)

For ^6Li and ^7Li recent evaluations from Los Alamos National Laboratory
have been adopted. The ^6Li evaluation was taken from ENDF/B-V. The impor-
tant (n,t) cross section is considered as a standard for this material.

For ^7Li a recent evaluation was provided to us thanks to a special arran-
gement with Dr. Ph.G. Young [8]. Its tritium-production cross section
clearly differs from that of ENDF/B-IV as is shown in Fig. 1. The adopted
evaluation agrees with that of Goel et al. [9] made for KEDAK. A compari-
son of recent evaluations and experimental data is given in Figs. 1a and
1b. In the last-mentioned figure very recent data of Takahashi et al. [10]
and Smith et al. [11] are displayed, together with revised data of Swinhoe
[12], that are higher than before [13], but still low as compared with
most other data. The EFF evaluation is slightly higher than the recent
JENDL-3 evaluation of Shibata [14]. Some further reduction of the (n,n't)
cross section of EFF-1 may be necessary (see curve of Goel et al.).
The carefully evaluated gas-production file of ^7Li [8] has been merged
to the EFF-1 data file (MT = 203-207).

Table 1
Contents of EFF-1 library

Material	Source	Comment
H	JEF-1	
D	JEF-1	
T	JEF-1	
Li-6	ENDF/B-V	
Li-7	LANL	Young [8]
Be-9	LANL	Young and Stewart [17]
B-10	JEF-1	
B-11	JEF-1	
C	JEF-1	
O	JEF-1	
Al	ENEA	revised ENDF/B-IV
Si	ENEA	revised ENDF/B-IV
Ti	JEF-1	
V	JEF-1	
Cr	JEF-1	Reich-Moore
Mn	JEF-1	
Fe	JEF-1	Reich-Moore
Ni	JEF-1	Reich-Moore
Cu	JEF-1	
Zr	JEF-1	
Nb	JEF-1	
Mo	JEF-1	
Ba-isotopes	JEF-1	
W-isotopes	JEF-1	
Pb	ECN	revised ENDF/B-IV
Bi	JEF-1	

There is a large implication for tritium breeding if the more recent (EFF) evaluation is used as compared to ENDF/B-IV or similar evaluations. In a recent paper by Stepanek et al. [15] on calculations for the LOTUS experiment the tritium-production rates in the hardest part of the spectrum were 12% lower when calculated with the recent EFF-1 (or ENDF/B-V) calculations. Further work on ^{7}Li is in progress, see Sect. 4.

2.2. Ceramic blanket materials (Al and Si)

In view of their importance in ceramic breeder materials a revision of the ENDF/B-IV evaluations for Al and Si has been performed at ENEA-Bologna [16]. For Si the low-energy range (upto 1.9 MeV) was completely re-evaluated, using new experimentally determined resolved-resonance data. The new curves for $\sigma_{n\gamma}$ and σ_{el} are quite different from those of ENDF/B-IV. At higher energies the (n,p), (n,d) and (n,α) cross sections were revised. Large modifications were needed for these cross sections to update the EFF-1 evaluation with the available experimental information. Similar improvements

1a)

1b)
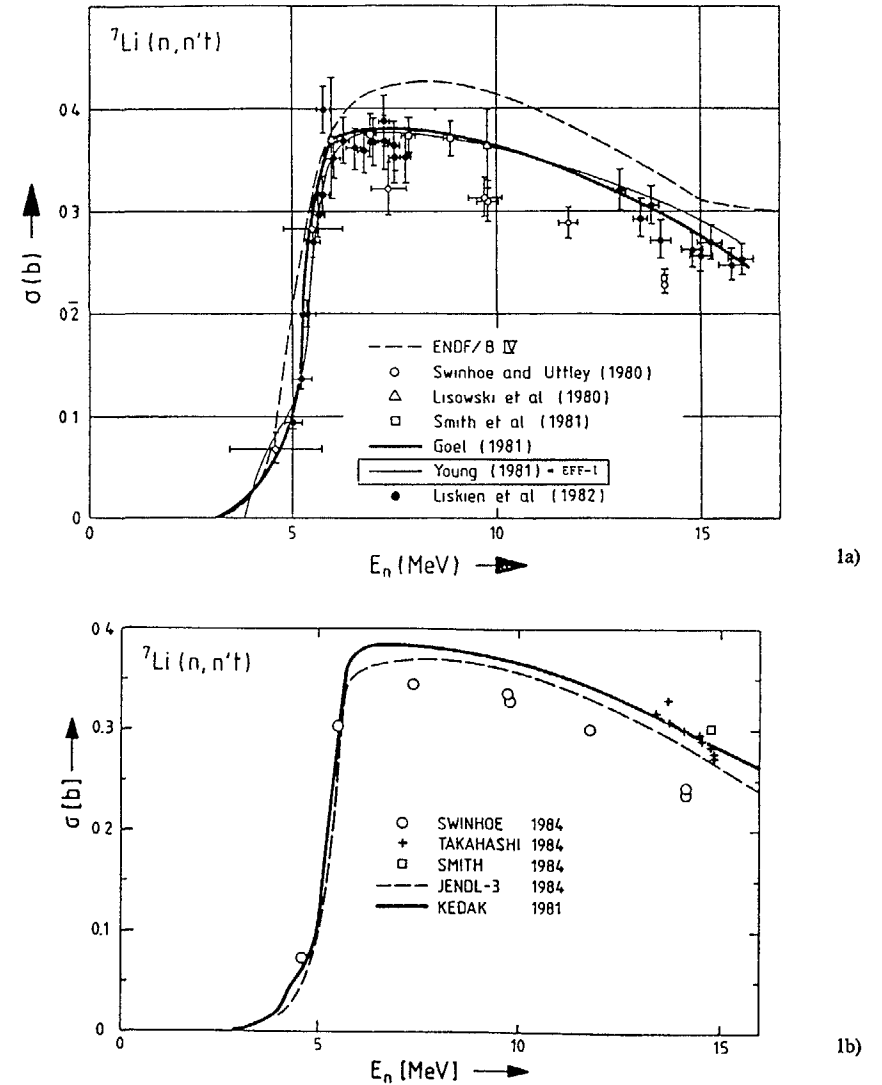
Fig. 1. Three evaluated curves and experimental data of the tritium-production cross section ^{7}Li(n,n't) as a function of incident energy. In Fig. 1a the experimental data upto 1982 are given. The solid curve has been revised by Goel et al. [9]. In Fig. 1b the most recent data have been plotted, together with the recent JENDL-3 evaluation [14]. The curve of Young [8] has been adopted in EFF-1.

were made for Al, both in the resolved-resonance range and at higher energies. Important revisions were made for the (n,p), (n,d), (n,t) and (n,2n) reactions, based upon recent experimental data and nuclear models, including the precompound model. As an example of these revisions the ^{27}Al(n,p) reaction cross sections of ENDF/B-IV and EFF-1 (ENEA) are shown in Fig. 2. Further work on Al is made at ENEA to support the investigations of a mixed LiAlO$_2$ and Be blanket, cf. Sect. 4.
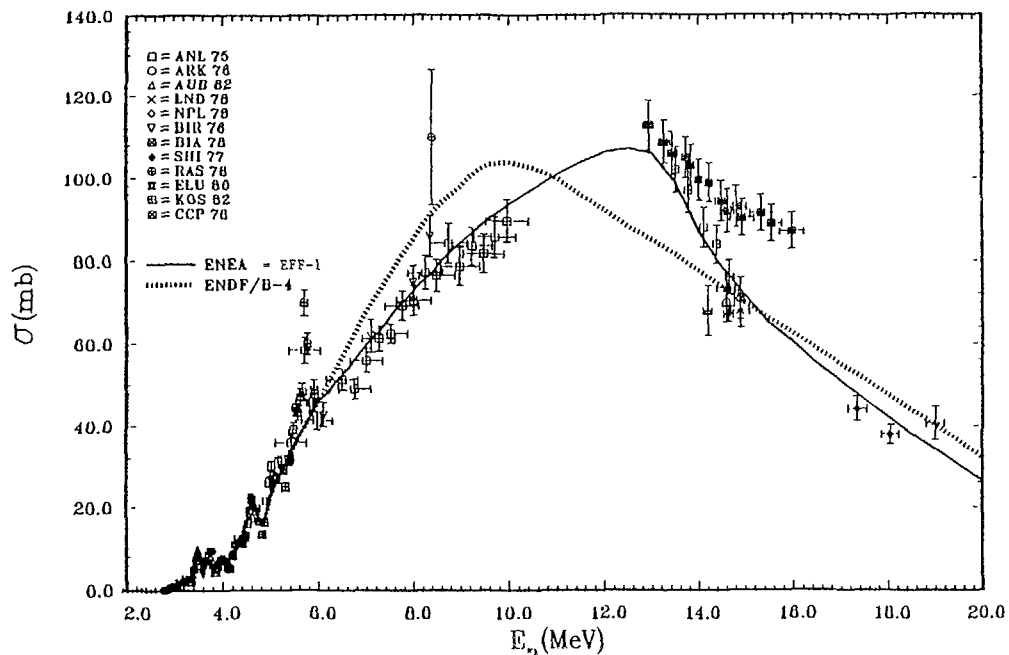
Fig. 2. Revision of the evaluated ^{27}Al(n,p) cross section, based upon recent data and model calculations. The full curve, evaluated at ENEA [16] has been adopted in EFF-1.

2.3. Berylium neutron multiplier material

For neutron multipliers in fusion reactors the (n,2n) cross section is the most important quantity. However, not only the angle- and energy-integrated cross sections are of interest, also their energy distributions and angular distributions are important. Since these distributions are coupled, the present description in the ENDF-V format by means of seperate files (MF = 4 and 5) is not adequate. Therefore in future evaluations the new format for MF6 should be used to store these data. This has been done in EFF-1 so far only for lead (see Sect. 2.4).

For ^{9}Be we have obtained a recent evaluation through collaboration with Dr. P.G. Young et al. [17] in which a different approach is used, based upon
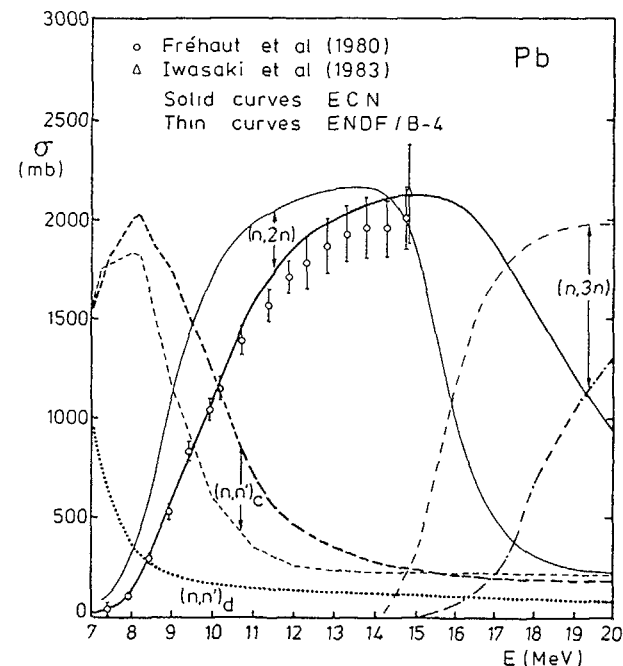
Fig. 3. Revisions of inelastic scattering, (n,2n)- and (n,3n) cross sections for Pb at energies from 7 to 20 MeV. The solid curves (EFF-evaluation) are compared with the ENDF/B-IV evaluation [19]. The experimental data are of Fréhaut et al. [20] and Iwasaki et al. [25].

the fact that in the ENDF-V format the description of coupled angle- and energy distributions is entirely correct for inelastic scattering to discrete levels (MT = 51-90). For continuum inelastic scattering this description can be generalized by means of a "pseudo-level representation" [18], adopting bins of excitation energy. This has been used in ENDF/B-V and EFF-1 for various materials (^{6}Li, ^{7}Li, ^{10}B, ^{16}O, ^{27}Al). In the ^{9}Be evaluation of Los Alamos the (n,2n) reaction is supposed to proceed through (n,n')-reactions which are binned in excitation energy into MT = 51 to 83 (MF = 3,4). An LR-flag, normally adopted to indicate further break-up, is used to signal the processing code that a second neutron is emitted and that accordingly the neutronproduction cross section should be multiplied by 2. The calculation of the double-differential neutron cross sections is exactly the same as for discrete-level excitation, except for this factor of 2. The application of this method is straightforward for ^{9}Be, because there is no inelastic scattering without emission of a second neutron. The user has to be aware that in this evaluation the (n,2n)-data are stored in MT = 4, 51-83 rather than in MT = 16 that is absent.

It is clear that the above description for ^{9}Be is somewhat ad-hoc. However, the above modelling reproduces the available angular distribution

Pb (n,xn)
E=14.5 MeV

secondary
n-emission

dσ/dE (mb/MeV)

f_1

f_2

E (MeV) →
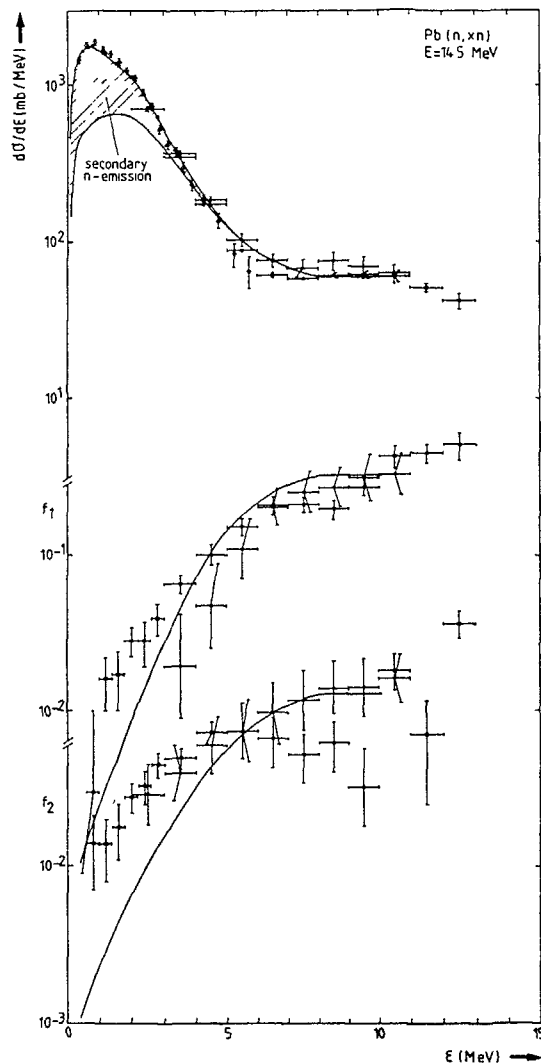
Fig. 4. Continuous energy spectrum and angular-distribution coefficients of the neutron-emission cross section of Pb at about 14.5 MeV. The solid curve represents the EFF evaluation, based upon GRAPE model calculations [21] upto an emission energy of about 7 MeV. At higher energies, upto about 10 MeV the results of model calculations (dashed curve) are below the evaluated curve, to account for structure effects in the data. Above 10 MeV the inelastic scattering is described by the DWBA method (discrete-level excitation). The experimental data are given in Refs. [22] (●), [23] (◇) and [24] (■). The angular-distribution coefficients are reduced first- and second-order Legendre coefficients (relative to dσ/dε), calculated with GRAPE [21]. Please note that the calculated curve still has to be converted from c.m. to lab. system, cf. Fig. 6.

data quite well and therefore it is recommended as an improvement over the ENDF/B-V evaluation. Further work in ⁹Be is in progress, see Sect. 4.

2.4. Lead neutron multiplier material

The ENDF/B-IV lead evaluation [19] has been revised with respect to the continuum part of the inelastic scattering and the (n,2n) and (n,3n) reactions. This work was performed at ECN, Petten. The sum of the cross sections for the above-mentioned reactions was not altered, but the division between (n,n'), (n,2n), (n,3n) has become quite different as is shown in Fig. 3 . These results are based upon model calculations and recent experimental data. The (n,2n) data of Fréhaut et al. [20] show that the ENDF/B-IV evaluation for this cross section is too high upto about 14 MeV. This was confirmed by model calculations with the exciton-model code GRYPHON [21], recently developed at ECN. At about 14.5 MeV the calculated ratio σ(n,2n) to σ(n,n') is sensitive to the shape of the total neutron-emission spectrum that has been measured by a few authors [22-24], see Fig. 4. In the precompound-model this shape is determined by the values of the average transition matrix $<M^2>$ occurring in the internal transition rates. In GRYPHON this quantity is related to the mean free path, which can be adjusted with a multiplier k [21]. It occurrred that for k = 1.5 a reasonable good fit was obtained with the data of [22] upto about 6 MeV; at higher emission energies the structure effects in the experimental data make such a comparison difficult, see upper part of Fig. 4. These calculations lead to the revised (n,2n) cross sections, shown in Fig. 3, which are about one standard deviation above the data of Fréhaut et al. [20]. The evaluated neutron-emission spectrum is given in Fig. 4. It is in agreement with data of Refs. [22-24], except near 6 MeV, where the IRK [23] and Osaka results [24] are somewhat lower.

Our estimate of the (n,2n) cross section 14.5 MeV is about 2.1 b, in agreement with the estimate of Iwasaki et al. [25], but lower than the values suggested by Takahashi [26] based upon integral data. At energies near the threshold the evaluation follows the data of Fréhaut et al. [20]. The above-mentioned revision for lead also contains the energy-angle distributions for the neutron-emission cross sections (n,n'), (n,2n) and (n,3n). In addition such data are given for the newly defined continuum-particle emission (MT10), which in the absence of charged-particle emission is equal to the continuum-neutron emission. In the ENDF/B-IV evaluation the energy distribution of continuum emission was already somewhat adjusted to account for precompound effects. The present revision is mainly based upon model calculations; only at the highest-energy end, referring to the range of excitation energies from 4.4 to about 6 MeV, a manual correction was needed to account for direct-coherent effects in the data (discrete-elastic scattering is given upto 4.4 MeV), cf. Fig. 4.

The energy spectra are also in reasonably good agreement with the data measured at 7.5, 10 and 12 MeV [27]. In the ENDF/B-IV evaluation the continuum angular distributions were assumed to be isotropic. The present revision contains anisotropic angular distributions calculated by the GRYPHON code for all continuum reactions. Some results for the total neutron-emission cross section at about 14.5 MeV are given in Figs. 4 and 5. The new double-differential cross sections at forward angles (Fig. 5a) are appreciably higher than the ENDF/B-IV data and are quite close to the Osaka results [24]. At emission energies near 1 to 2 MeV the comparison be-

5a)

5b)
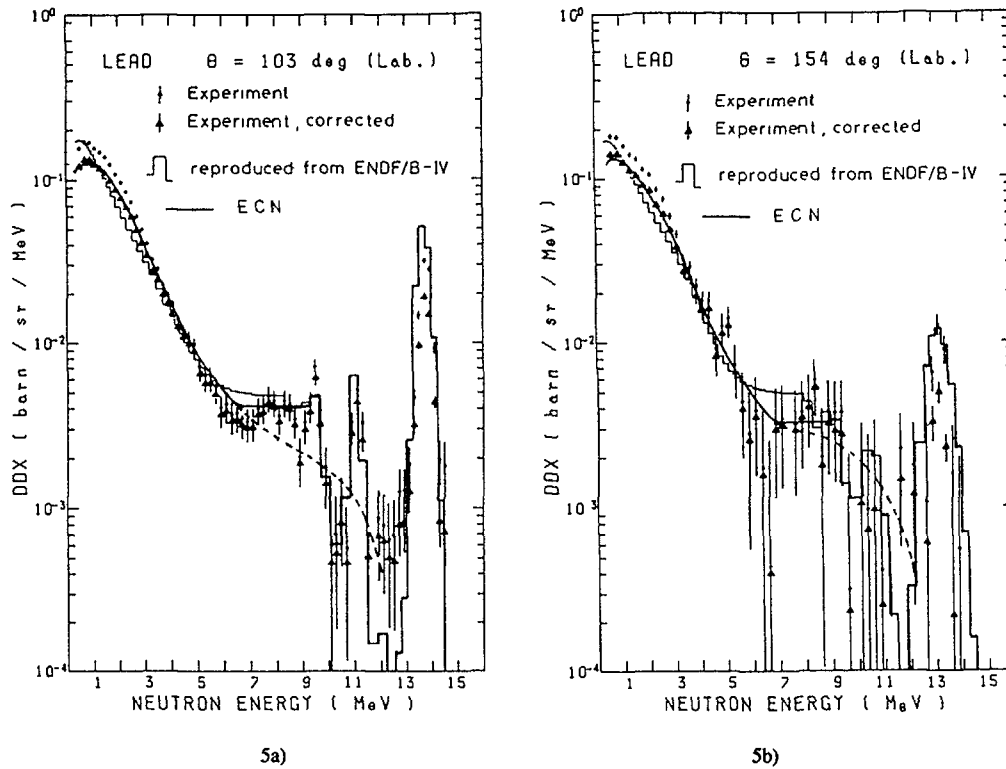
Fig. 5. Double-differential neutron emission cross section of Pb at about 14.5 MeV at forward angles (Fig. 5a) and at backward angles (Fig. 5b). These figures have been reproduced from the work of Takahashi et al. [24], with the addition of the pre-liminary EFF-evaluation (solid curve). The evaluated data should be compared with the corrected experimental points (triangles). The histograms represent the ENDF/B-IV evaluation. The new evaluation is in much better agreement with the data at forward angles that ENDF/B-IV, due to the introduction of anisotropy calculated with the precompound-model code GRAPE [21]. Please note that the calculated curve still has to be converted from c.m. to lab. system, cf. Fig. 6.

tween measured and calculated data is difficult, because the experimental data need corrections, e.g. for multiple-scattering in the target (triangles) and for the conversion to the c.m. system, see below.

On the file Legendre coefficients f_k (E → E') are given for k = 1 to 4. As an example the reduced coefficients f_1 and f_2 are given in Fig. 4. Thus, for these data the usual (uncoupled) representation in files MF4 and MF5 is replaced by coupled energy-angle distributions in file MF6. This new representation is needed because the almost-isotropic angular distributions at low outgoing energies differ from the forward-peaked distributions at high emission energies. This is shown clearly in Fig. 6, where the average cosine of the scattering angle μ (E → E'), proportional to the ratio of f_1 and f_0, has been plotted as a function of E' at E = 15 MeV. The full line represents the evaluated data in the center-of-mass system. The dashed curve represents the same quantity after a transformation to the laboratory system performed with the help of the code GROUPXS [28], cf. Sect. 3.3. The data points were evaluated from experimental measurements of Takahasi et al. [24].

E' (eV)
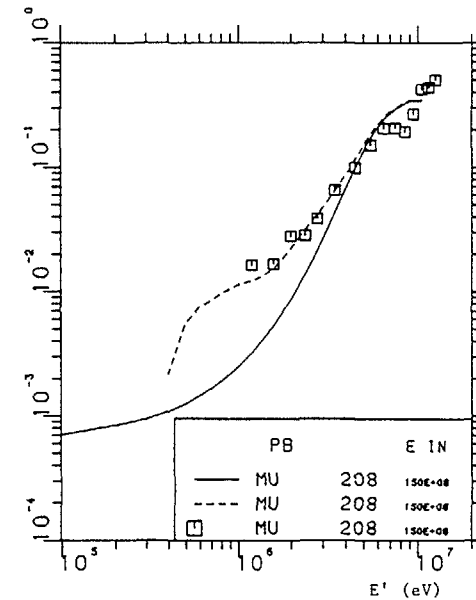
Fig. 6. Transformation of average value of the cosine of the scattering angle from the center-of-mass system (full curve) to the laboratory system (dashed curve) as a function of emission energy. The incident energy of the Pb(n,x) reaction considered is 15 MeV. The data points were evaluated from the experimental results of Takahashi et al. [24].

2.5. Structural materials

For the structural materials, such as the components of stainless steel, the JEF-1 evaluations have been adopted. These are in general of better quality than ENDF/B-IV, at least in the resolved-resonance range, where the cross sections are represented by Reich-Moore parameters. At high energies revisions are needed, in particular for the description of double-differential cross sections, using direct and precompound models, cf. Sect. 4.

2.6. Gas-production cross sections

The evaluations given in Table 1 have been supplemented with gas-production data by adding all production cross sections for each charged particle into reaction types MT = 203-207. Although these data are, in fact, redundant; their retrieval from the original file was not always trivial. Checks are still needed to compare the collected gas-production data with those of other data files.

3. FILE HANDLING, PROCESSING AND GEFF-1

The aim of the EFF-1 project is not only to create a basic nuclear data file, but also to make this file available to the actual user. Therefore, assistance is provided within the EC to obtain derived data, useful in applications. First of all we mention that there are two versions of EFF-1: one with resolved-resonance parameters as far as available and one with point-wise given data. The latter file is most complete and also contains some "redundant" cross sections that were requested by the users: neutron-disappearance cross sections, gas-production cross sections and the continuum particle-production cross sections (new quantity, MT = 10). Furthermore, various file-handling options are available with the file and new software has been developed to calculate group transfer matrices of data represented in the MF6 format of ENDF-VI. Finally, a complete multi-group library has been made under the name GEFF-1. Below these developments are discussed in some detail.

3.1. File handling

For file handling of EFF-1 the existing ENDF-V and the recently developed ENDF-VI utility routines are available. For the file handling of file MF6 [7] we have developed at ECN a code (NELIS) for lumping MF6 files. This code is useful for creating a natural-element data file starting from isotopic evaluations or for lumping various reaction types of one material (e.g. to obtain MT10). Furthermore, we have various options in our GROUPXS code [28], e.g. to convert MF6 Legendre coefficients from c.m. to lab. (cf. Sect. 3.2), to convert Legendre coefficients to an angular representation, or to convert MF6 into MF4 and MF5. This last-mentioned option is not recommended, because the coupling between energy and angle is lost after converting to an energy-integrated angular distribution (MF4) and an angle-integrated energy-distribution (MF5). Still, we have made a version of the EFF-1 lead evaluation in this representation, because it can be readily processed by installed processing codes. The possibility to obtain an MF6 file in the laboratory system in an angular representation may be of interest to users of Monte-Carlo codes.

3.2. Processing into multi-group transfer matrices

The main tool for calculating multi-group constants from the EFF-1 file is the NJOY-code [29] or its French version THEMIS. However, this code should at present be supplemented with the GROUPXS code for the processing of continuum reactions. A full description of this code is given elsewhere [28]. Here we only mention that GROUPXS treats all possible continuum reactions for all possible particles, provided that the angular distribution is represented by Legendre coefficients. There are some other restrictions [28] for the EFF-1 data file in order to facilitate the computation of transfer matrices by GROUPXS.

The most interesting part of the code is the c.m. to lab. conversion that should be executed first. After this conversion we have for each incident energy E and outgoing particle and for each emission energy E'_{lab} the Legendre coefficients $f_k(E \rightarrow E'_{lab})$ for $k = 0$ to k_{max}, where k_{lab} is usually larger than the maximum-order of Legendre coefficients in the c.m. system. As an example we refer to Fig. 6 that was already shortly discussed in Sect. 2.4. We may add here that the effect shown for lead was calculated by assuming the same transformation laws for the first and second emitted neutrons. To be more precise: the second neutrons emitted in the (n,2n) process were assumed to be isotropic in the center-of-mass system, but not so in the laboratory system, where a forward peaking was calculated in exactly the same way as for the first-emitted neutrons. This approximation was thought to be more realistic than the evidently wrong assumption of isotropy in the laboratory system for secondary emitted particles. However, there may be some uncertainty in the results at low outgoing energies (the region near 1 MeV in Fig. 6). Further study on this topic is in progress [53].

The c.m. to lab conversion part of the code has been tested thoroughly by intercomparisons with a routine made by Bersillon [30] and with a code based upon an analytical method by Shi Xiangjun et al. [31]. In the last-mentioned paper an exact expression is also given for the transformation of isotropic angular distributions from the center-of-mass to the laboratory system. The following problems were considered: (a) uniform energy distribution, (b) linearly-increasing energy distribution, (c) analytical evaporation spectrum.

In these cases various target masses were assumed. Furthermore, both isotropic and simple anisotropic distributions were considered. The results of all these tests were quite satisfactory, although it became clear that in case (c) a very fine energy mesh (in emission energy) is needed for accurate results. No problems were encountered if an analytical expression for the evaporation peak was inserted in the codes. The above tests increased our confidence in the adopted transformation method applied in GROUPXS [28]. However, it was found necessary to change the interpolation method used for the emission energies from linear to logarithmic in the calculations for lead, shown in Fig. 6.

After the c.m. to lab. conversion the group-to-group transfer matrices for continuum reactions are calculated by GROUPXS. These have to be added to those calculated for the elastic and discrete inelastic scattering (NJOY) in order to obtain the total scattering matrices, used in transport calculations. This has been done at ECN-Petten for lead.

At Karlsruhe the GROUPXS code has been extended with an option to calculate group constants and transfer matrices in a tabulated angular representation. There are also plans to include the c.m. to lab. conversion in this new option. The background of this work is to avoid the Legendre-polynomial representation in the lab. system and perhaps also in the c.m. system, in order to avoid the well-known problems of this representation (e.g. negative cross sections, very large order) for very anisotropic distributions. We note that these problems may become severe for elastic rather than for inelastic scattering.

3.3. The GEFF-1 file

Although there are many different ways to utilize the basic EFF-1 data, it was thought to be useful to have one set of reference group constants derived from EFF-1 for P_N-type of calculations. Therefore, a first version of the GEFF-1 data file has been produced from EFF-1 by ENEA-Bologna, CEA-Saclay, NEA-Data Bank, IKE-Stuttgart and ECN-Petten. The editing of the file has been performed at the NEA-Data Bank and at ECN-Petten. The starting point of the file was the VITAMIN-J library with auxilliary material provided by Dr. E. Sartori (NDB). The VITAMIN-J library is based upon JEF-1. It has a 175 neutron group structure that can be condensed to the VITAMIN-C and -E [5,6] and many other standard group structures.

At present the GEFF-1 library contains three parts. The first part of the GEFF-1 file contains the neutron cross sections (P_5) at 300 and 800 K. The identification numbers are ordered according to increasing Z, A, first for infinite dilution than bulk shielding. The second part of GEFF-1 contains photon-production cross sections at the same temperatures. The identification numbers correspond to those of the neutron data. Some data are still missing, because of photon data lacking in EFF-1. The last part of GEFF-1 contains γ-ray interaction data. These data are the same for all isotopes of the same element. All data have been stored in compressed FIDO (coded) format in exactly the same way as for the VITAMIN-J library.

The library has been distributed to a few laboratories within the EC for further testing and for benchmark calculations. Extensions of the library will be made to include all reaction cross sections, gas production data and kerma factors. Some work in this direction has been performed at ENEA-Bologna [52] and at KfK-Karlsruhe.

4. PROGRESS ON EFF-2

The first version EFF-1 already means a large improvement compared to ·' presently available ENDF/B-IV data file. However, further updating is required, in particular for high-energy cross sections of the structural materials. A survey of possible improvements is given in Sect. 4.2, whereas in Sect. 4.3 the plans for a fusion activation file are discussed. The required improvements are closely related to recent developments in nuclear-model codes, in particular, the precompound exciton model.

4.1. Nuclear-model codes and evaluation techniques

For the evaluation of nuclear cross sections at energies above the re-solved-resonance range the basic theoretical tools are the optical model

and the statistical model. For the purpose of a fusion nuclear-data file a deformed optical model may be required and coupled-channel calculations to predict the scattering cross sections to the ground state and direct-excited states. In some cases an equivalent spherical optical model, fitting the total and elastic scattering cross sections, could be used if supplemented with DWBA calculations to fit the direct components of inelastic scattering cross sections to low-lying states. The last-mentioned approach has been followed in many existing evaluations for the structural materials. Updates are perhaps not of very high-priority except that for EFF-2 we would like to have evaluations for the separate isotopes, rather than for the natural element.

The main reason for updating the existing evaluations in EFF-2 is to improve the cross sections at high-energies that are calculated by means of the statistical model. One would like to recalculate these cross sections with the improved versions of these models that include precompound effects both in the energy spectra and in the angular distributions. During the past decade significant progress has been made in these models and further developments are under way. A recent review of these developments has been made by Gruppelaar et al. [32]. Two directions are followed in literature. One is a further sophistication of the semi-classical exci-ton-model approach and the other the application of quantum-mechanical theories of multi-step direct and multi-step compound theory. There is a very strong interaction between these two lines of development. Many problems are in common, the most central of these is the description of particle-hole level densities.

For the purpose of updating the EFF data library the semi-classical approach is followed at present. The differences between the various nuclear-model codes based upon the exciton model were studied in an international model and code intercomparison performed under auspicies of the NEA Data Bank [33]. This exercise undoubtedly has stimulated the further improvement of these evaluation tools. Four important developments are:

a) The description of angular distributions based upon the fast-particle method of Mantzouranis et al. [34], modified with the exact Kikuchi-Kawai double-differential cross section for (at least) the first collission [35,36]. This method correctly explains the important forward angular distribution, but needs a simple empirical corrrection for the symmetric second-order coefficient, as included in GRAPE [21].

b) The inclusion of explicit angular-momentum conservation into the model, often indicated by a "unification" of the Hauser-Feshbach and exciton models. The unified models show similarity with the quantum-mechanical multi-step compound theory, however, no division between multi-step compound and multi-step direct is made. Spin effects turn out to be moderate [37].

c) The improvement of the level-density description of particle-hole components, guided by results of microscopic level-density calculations, see e.g. Ref. [38].

d) The inclusion of pre-compound γ-ray emission into the model. Here the method of Běták [39], modified by Akkermans and Gruppelaar [40] provides a simple and effective way to include direct, semi-direct and further pre-compound γ-ray emission into a statistical model. Recently, spin effects have been introduced in this description [41].

e) The description of complex-particle emission using a cluster method as proposed by Iwamoto et al. [41].

The EFF-evaluators at Bologna, Karlsruhe and Petten have made contributions to most of the above-mentioned developments, which are needed to make further progress in the evaluations. These model-code improvements take a substantial part of the evaluators' time.

Another time-consuming part of the evaluation is the compilation of all results on a file in the correct format. For EFF-1 some experience has been gained by adopting the MF6 format of ENDF-VI for lead. For EFF-2 this format will be used for all new evaluations. A particular challenge will be to adopt the new format for the light elements and to see whether the results of Beynon and Oastler [42] can be modelled into this format.

4.2. Plans for EFF-2

The programme for EFF-2 is supplementary to that of JEF-2. The priorities are determined by the users and therefore the programme given below is only indicative. The format of EFF-2 will probably be ENDF-VI, however with some restrictions to keep the processing simple. On the other hand, some new quantities, defined for "derived" files will be introduced, as discussed before.

The main goal for EFF-2 is to introduce evaluated MF6 files for double-differential neutron-emission cross sections of important fusion-reactor materials. If possible, MF6 files will be given for other emitted particles as well. Of equal priority is the simultaneous revision of photon-production data. It is recommended [4] to consider the energy balance in the evaluation process in order to obtain consistent data files from which reliable kerma factors can be calculated. The application of the most-recent model codes for isotopic evaluations automatically guarantees the required consistency conditions.

4.2.1. Tritium production and double-differential neutron emission in lithium

For the ⁶Li(n,t) cross section the forthcoming ENDF/B-VI standard evaluation will be adopted. The tritium production in ⁷Li is determined by inelastic neutron scattering to states above the first level. Some reduction of the ⁷Li(n,n't) cross section of EFF-1 may be necessary, cf. the data in Fig. 1.

The angular distribution of neutrons emitted to the first-excited state (MT=51, MF=4) can be improved by introducing the new data of Liskien et al. [43] into the file. A partial evaluation has been provided to us by Liskien. At higher energies a pseudo-level description is followed at present in EFF-1. A more basic treatment is given by Beynon and Oastler [42] who separate in their treatment the following different processes:

$$
\left.
\begin{array}{l}
{}^7\mathrm{Li} + \mathrm{n} \rightarrow {}^8\mathrm{Li}^*, \\
{}^8\mathrm{Li}^* \rightarrow {}^5\mathrm{He(g.s.)} + \mathrm{t} - 3.42 \ \mathrm{MeV}, \\
{}^5\mathrm{He(g.s.)} \rightarrow \alpha + \mathrm{n'} + 0.96 \ \mathrm{MeV},
\end{array}
\right\} \quad (1)
$$

$$
\left.
\begin{array}{l}
{}^7\mathrm{Li} + \mathrm{n} \rightarrow {}^8\mathrm{Li}^*, \\
{}^8\mathrm{Li}^* \rightarrow {}^7\mathrm{Li}^* + \mathrm{n'}, \\
{}^7\mathrm{Li}^* \rightarrow \alpha + \mathrm{t},
\end{array}
\right\} \quad (2)
$$

$$
{}^7\mathrm{Li} + \mathrm{n} \rightarrow \alpha + \mathrm{t} + \mathrm{n'} - 2.46 \ \mathrm{MeV}, \quad (3)
$$
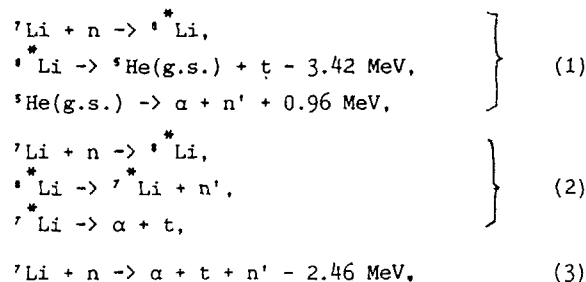
Reactions (1) and (2) occur through sequentially two-body events after the formation of a compound state. There is a complication in process (1) due to finite lifetime of ⁵He (ground-state decay). This has been considered in Ref. [42]. The direct 3-body process (3) can be treated using phase-space correlations. Beynon and Oastler have modelled the above expressions and have obtained double-differential data in the laboratory system. These results could be improved by introducing new experimental data, e.g. the forthcoming double-differential neutron-emission data of DeKempeneer et al. [44], measured at CBNM. Finally, there will be a considerable effort to introduce these data on a file (MF6). Probably the data should be represented using a fine angular-energy grid, rather than by means of Legendre polynomials. The work on ⁷Li is a cooperation between laboratories within the EC and Los Alamos.

4.2.2. Neutron multipliers

For Be similar remarks as for Li could be made with respect to the modelling of the ⁹Be(n,2n)2α reaction. Work at Birmingham [42] is in progress to model the seven possible reaction mechanisms. It will be a challenge to include this information on a file in the MF6 format (angular-energy tabulated, laboratory system).

For lead the developments will be followed and if necessary adjustments will be made. This may also depend upon experience with the EFF-1 evaluation with respect to the analysis of integral experiments.

For Zr some work has been performed at ECN and the NEA Data Bank in the resonance-range in connection with JEF-2. Revisions are needed at high energy.

4.2.3. Ceramic blanket materials

Further work on Al is made at ENEA-Bologna with emphasis on double-differential neutron-emission cross sections and photon-production data using the PENELOPE code [45]. Recently a precompound γ-ray emission option [40] has been included into this code system [38].

4.2.4. Structural materials

In the JEF-2 programme the low-energy range of these evaluation will be considered. Supplementary work at higher energies will be performed at ENEA-Bologna, KfK-Karlsruhe and ECN-Petten. If possible the new evaluations will be made for each of the isotopes of the structural materials Fe, Cr and Ni. Some initial work has been made at Petten on the Ni-isotopes. For ⁵⁸Ni and ⁶⁰Ni the optical model parameters of Guss et al. [46] were selected. Preliminary calculations have been performed with the GRAPE code system [21] that has been coupled to GNASH [47]. The results show that like for lead the calculated high-energy end of the spectrum needs to be supplemented with a direct-coherent contribution [48] in order to fit the data [24]. Calculations with the GRAPE-GNASH system are in progress to obtain double-differential particle emission cross sections and photon-production data.

4.3. European Activation File for fusion

There are plans to create a separate European Activation File (EAF) for fusion technology that is consistent with EFF, but contains far more reactions. A starting point for this activity is the work performed at

ECN-Petten under contract with JRC-Ispra and the work for the national UK programme. A status report on the UK activities, covering also part of the Petten-Ispra work, is given by Forrest [49] at this meeting. For future improvements the modified REAC-ECN data file, based upon the original REAC file of Mann et al. [50], will be used. This file will be made consistent with EFF-1 as far as possible. Continuous updating is needed. It is of high priority to include new systematics of 14.5 MeV neutron cross sec-

tions and isomeric ratios. A graph with experimental values of the isomeric ratios for (n,2n)-reactions has been prepared by Kopecky [51] at Petten, see Fig. 7. This graph suggests that there is a systematic behaviour of the isomeric ratio as a function of the spin of the isomeric state. A set of updating routines has been prepared to perform automatic revisions, e.g with new systematics [49]. The final goal is to obtain fast codes that reproduce the data by using simple global input parameters. The GRAPE code [21] could perhaps be used for such calculations after some modifications. For very important reactions special evaluations may be required (cooperation ECN, KfK, ENEA). The EAF file will be converted to a 175 neutron group structure, consistent with GEFF.
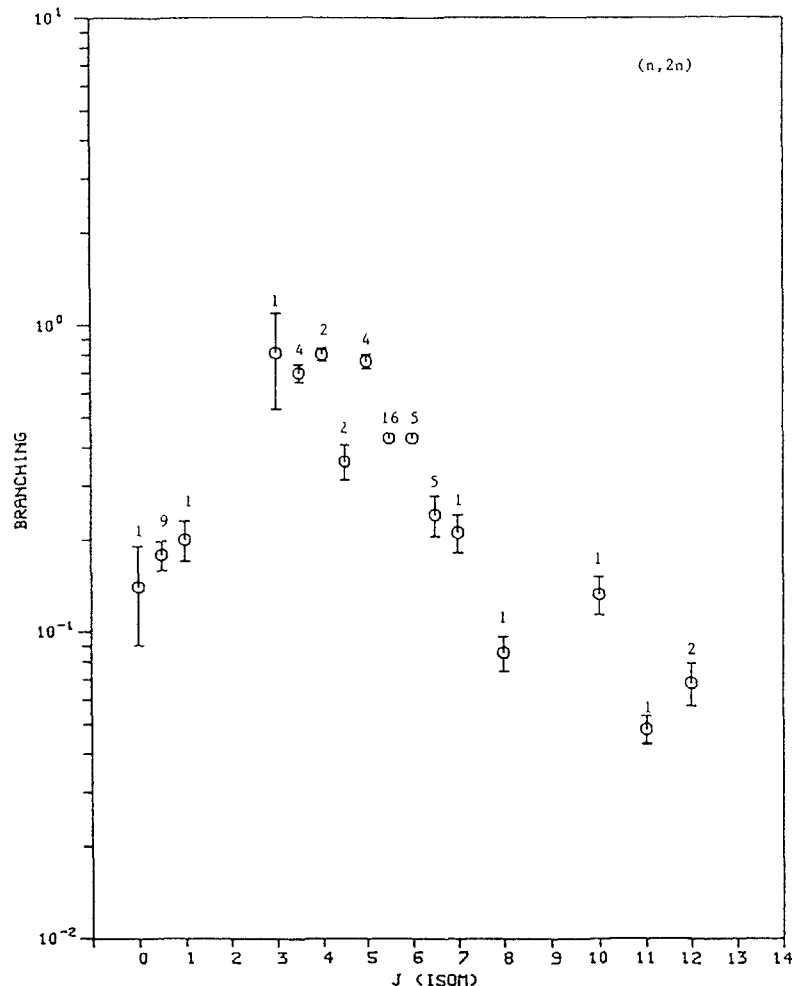
5. CONCLUSION

At present there is a first European Fusion File and an organised team of evaluators, experimentalists and users working on the project to create a second version of the file. EFF-1 already means a large improvement compared to the presently available ENDF/B-IV data file (Sect. 2). It also contains for one important material (lead) double-differential continuum cross sections in the new MF6 format of ENDF-VI.

The next step is to further improve the situation with respect to double-differential cross sections. Some of this work has been delayed, because of the very important need to process these data (Sect. 3). Now, since GEFF-1 is available, all emphasis is given to improve the data for EFF-2 (Sect. 4). In particular, there are plans to revise the double-differential cross sections for ^{7}Li, Be, Al, Fe, Cr and Ni. In the case of ^{7}Li the inelastic-scattering data for the first-excited state, recently measured by Liskien [43] will be used. The forthcoming measurement results of the CEN/Mol and CBNM/Geel cooperation [44] will be used in an evaluation according to the methods given by Beynon and Oastler [42]. Similar work is needed for Be, even if no new data are available at present. For Al, Fe, Cr and Ni the addition of MF6, like performed already for Pb, is urgent. In these revisions it is aimed to update the photon-production cross sections as well. For the activation cross sections the existing programme will be further extended to form a "European Activation File" (EAF).

Fig 7 Experimental values of isomeric ratios $\sigma_m/(\sigma_g+\sigma_m)$ for the (n,2n) reaction at 14.5 MeV as a function of the spin of the isomeric state. The data points represent weighted averages, the number of measurements are indicated on top of each data point [51]

REFERENCES

[1] H. Gruppelaar, Europe sets up its own fusion file, Nuclear Europe VI, no. 2, February 1986, p. 40.
[2] H. Gruppelaar, Present status of the European Fusion File, Proc. Int. Seminar on Nuclear Data Cross Section Libraries and Their Application in Nuclear Technology, Bonn, 1-2 October 198, p. 288 (Kerntechnische Gesellschaft E.V.).
[3] J.L. Rowlands and N. Tubbs, The Joint Evaluated File: A New Nuclear Data Library for Reactor Calculations, Int. Conf. on Nuclear Data for Basic and Applied Science, May 1985, Santa Fe, NM.

[4] Y. Gohar, Nuclear Data Needs for Fusion Reactors, Int. Conf. on Nuclear Data for Basic and Applied Science, May 1985, Santa Fe, NM.; see also review papers presented by various authors at this meeting.

[5] R.W. Roussin et al., VITAMIN-C: the CTR Processed Multigroup Cross-Section Library for Neutronics Studies, ORNL/RSIC-37 (1980).

[6] C.R. Weisbin et al., VITAMIN-E: An ENDF/B-V Multigroup Cross Section Library for LMFBR Core and Shield, LWR shield, Dosimetry and Fusion Blanket Technology, ORNL-5505 (1979).

[7] R.E. MacFarlane, L. Stewart, G.M. Hale and C.L. Dunford, Preliminary Proposals for Extending the ENDF Format to Allow Incident Charged Particles and Energy-Angle Correlation for Emitted Particles, IAEA Consultants Meeting on Format for the Exchange of Evaluated Neutron Nuclear Data, Vienna April 1984 and preprints of a new version of the ENDF-format manual received from NNDC, Brookhaven National Laboratory, 1986.

[8] P.G. Young, Trans. Am. Nucl. Soc. 39 (1981), p. 272 and private communication (1985).

[9] B. Goel, B. Krieg, E. Stein, private communication (1985).

[10] A. Takahashi et al., 13th Symposium on Fusion Technology (SOFT), Varese, Sept. 1984, and private communication.

[11] D.L. Smith et al., Cross Section Measurement for the ⁷Li(n,n't)⁴He Reaction at 14.74 MeV, ANL/NDM-87 (1984).

[12] M.T. Swinhoe, private communication, 1984.

[13] M.T. Swinhoe and C.A. Uttley, AERE-R-9929 (1980).

[14] K. Shibata, Evolution of Neutron Nuclear Data of ⁷Li for JENDL-3, JAERI-M-84-204, NEANDC(J)109/U (1984); see also Proc. Int. Conf. on Nuclear Data for Basic and Applied Science, May 1985, Santa Fe, NM.

[15] J. Stepanek et al., Analysis of the LBM experiments at LOTUS, private communication (1986).

[16] V. Benzi et al., private communication (1985).

[17] P.G. Young and L. Stewart, Evaluated data for n+⁹Be reactions, LA-7932-MS (1979), and private communication (1985).

[18] L. Stewart, P.G. Young, Evaluated data for CTR applications, Trans. Am. Nucl. Soc. 23 (1976), p. 22.

[19] C.Y. Fu and F.G. Perey, An evaluation of neutron and gamma-ray production cross sections for lead, At. and Nucl. Data Tables 16 (1975), p. 409.

[20] J. Fréhaut, A. Bertin, R. Bois and J. Jary, Status of (n,2n) Cross Section Measurements at Bruyeres-le-Chatel, Symp. on Neutron Cross Section from 10 to 50 MeV, Brookhaven, May 1980, BNL-NCS-51245 (1980), p. 399.

[21] H. Gruppelaar and J.M. Akkermans, The GRAPE Code System for the Calculation of Precompound and Compound Nuclear Reactions - GRYPHON Code Description and Manual -, ECN-164 (1985); the code is available from NEA Data Bank.

[22] D. Hermsdorf, A. Meister, S. Sassonoff, D. Seeliger, K. Seidel and F. Shahin, ZfK Rossendorf bei Dresden, ZfK-277, 1975.

[23] H. Vonach, A. Chalupka, F. Wenninger and G. Staffel, Measurement of the Angle-Integrated Secondary Neutron Spectra from Interaction of 14 MeV Neutrons with Medium and Heavy Nuclei, Symp. on Neutron Cross Sections from 10 to 50 MeV, Brookhaven, May 1980, BNL-NCS-51245 (1980), p. 343.

[24] A. Takahashi et al., Double Differential Neutron Emission Cross Sections, Numerical Tables and Figures (1983), OKTAVIAN Rept. A-83-01, Osaka University (1983).

[25] S. Iwasaki et al., Measurement and Analysis of Neutron Emission Spectra for Pb(n,xn) reaction between 14 and 20 MeV, Int. Conf. on Nuclear Data for Basic and Applied Science, May 1985, Santa Fe, NM.

[26] A. Takahashi, Integral Measurements and Analysis of Nuclear Data Pertaining to Fusion Reactors, Int. Conf. on Nuclear Data for Basic and Applied Science, Ma 1985, Santa Fe, NM, and references quoted thereine.

[27] A. Beyerle et al., Double Differential Neutron Scattering Cross Sections for Fe, Cu, Ni and Pb between 8 and 12 MeV, Int. Conf. on Nuclear Cross Sections for Technology, Knoxville, 1979, NBS-SP-594 (1980), p. 139.

[28] H. Gruppelaar, Processing of double-differential cross sections in the new ENDF-VI format - GROUPXS code description and users' manual - ECN-182· (1986).

[29] R.E. MacFarlane, D.W. Muir and R.M. Boicourt, The NJOY Nuclear Processing System, Vol. 1: User's Manual, LA-9303-M Los Alamos Laboratory (1982).

[30] O. Bersillon, private communication (1986), CEA, Bruyère-le-Châtel.

[31] Shi Xiangjun, H. Gruppelaar, J.M. Akkermans and Zhang Jingshang, Transformation formulas for Legendre coefficients of double-differential cross sections, presented at the IAEA CRP meeting on Methods for the Calculation of Fast Neutron Nuclear Data for Structural Materials, Bologna, Italy, 7-10 October 1986.

[32] H. Gruppelaar, P. Nagel and P.E. Hodgson, Pre-equilibrium processes in nuclear reaction theory: the state of the art and beyond, Riv. Nuovo Cim. 9 (1986), p. 1 (no. 7).

[33] H. Gruppelaar and P. Nagel (editors), International nuclear model and code comparison on pre-equilibrium effects, NEA Data Bank Newsletter 32 (September 1985), NEANDC-204 "U", INDC(NEA)6.

[34] G. Mantzouranis, D. Agassi and H.A. Weidenmüller, Phys. Lett. 57B (1975), p. 220.

[35] C. Costa, H. Gruppelaar and J.M. Akkermans, Phys. Rev. C28 (1983), p. 587.

[36] M. Blann, W. Scobel and E. Plechaty, Phys. Rev. C30 (1984), p. 1493.

[37] Shi Xiangjun, H. Gruppelaar and J.M. Akkermans, Effects of angular-momentum conservation in unified pre-equilibrium and equilibrium reaction models, subm. to Nucl. Phys. A.

[38] G. Reffo, CRP meeting on Methods for the calculation of fast neutron nuclear data for structural materials, Bologna, October 1986.

[39] E. Běták and J. Dobes, Phys. Lett. 76B (1979), p. 253.

[40] J.M. Akkermans and H. Gruppelaar, Phys. Lett. 157B (1985), p.95.

[41] A. Iwamoto and K. Harada, Phys. Rev. C26 (1982), p. 1821.

[42] T.D. Beynon and A.J. Oastler, Annals of Nucl. Energy 6 (1979), p. 537 and private communication (1985).

[43] H. Liskein, Angular distribution for ⁷Li(n,n')⁷Li* (478) by Analyzing Doppler-Broadened γ-lines, Int. Conf. on Nuclear Data for Basic and Applied Science, May 1985, Sante Fe, NM.; see also this meeting.

[44] E. DeKempeneer, H. Liskien, L. Mewissen and F. Poortmans, Double-Differential Neutron-Emission Cross Section for the

^{7}Li(n,nx) Reaction between 1.6-16 MeV, Int. Conf. on Nuclear Data for Basic and Applied Science, May 1985, Santa Fe, NM.

[45] G. Reffo, private communication (1986).

[46] P.P. Guss et al., Nucl. Phys. A438 (1985), p. 187.

[47] P.G. Young and E. Arthur, GNASH, A pre-equilibrium statistical model code for the calculation of cross sections and emission spectra, LA-6947 (1977) and private communication (1985).

[48] A.V. Ignatyuk, Role of the direct and pre-equilibrium processes in the description of threshold reaction excitation functions, CRP-meeting on Methods for the calculation of fast neutron nuclear data for structural materials, Bologna, October 1986.

[49] R.A. Forrest, Status of the UK activation cross section library for fusion, this meeting.

[50] F.M. Mann et al., REAC Nuclear Data Libraries, Proc. Int. Conf. on Nuclear Data for Basic and Applied Science, May 1985, Santa Fe, N.M. and private communication (1985); see also the review paper of F. Mann at this meeting.

[51] J. Kopecky, private communication (1986), Netherlands Energy Research Foundation ECN, Petten, The Netherlands.

[52] E. Cuccoli and G.C. Panini, private communication, October 1986, ENEA, Bologna.

[53] H. Gruppelaar and J.M. Akkermans, to be published.

STATUS OF FUSION-RELATED EVALUATED NUCLEAR DATA IN JAPAN

Y. KANDA
Department of Energy Conversion Engineering,
Kyushu University,
Kasuga, Japan

Abstract

Fusion-related evaluated nuclear data are included in Japanese Evaluated Nuclear Data Library version 3 (JENDL-3) which is progressing. The JENDL-3PR1 and -3PR2 data which are the preliminary versions of the fusion-related data for JENDL-3 are products of cooperation between evaluators and experimenters in Japan. High activities on both the differential and integral experiments in this field stimulate and encourage to improve the evaluated nuclear data. Angular and energy distributions of secondary neutrons are mainly interested in because they are essential nuclear data in the fusion blanket calculation. They are less accurate in existing evaluated files. The procedures of the evaluation for the JENDL-3PR2 data are briefly described. Another emphasized theme in JENDL-3 concerning on the fusion-related nuclear data is the compilation of gamma-ray production cross sections. A plan of their evaluation is presented. The tritium production and activation cross sections are also discussed.

1. Introduction

In a program of a fusion reactor development, evaluated nuclear data play a very important role. Fusion reactors can not be expected as a high-energy-gain facility and must be planned to generate large power as possible. Tritium breeding in a blanket is an absolute necessity for the reactor operation. Structural materials used in fusion reactors must be selected taking account of their life-times and their induced activities under heavy fast-neutron irradiation. The results of these studies determine whether a fusion reactor is industrially possible or not. The evaluated nuclear data are applied to calculate power densities, tritium breeding ratios, displacement of atoms, He production rates, and induced activities. Any evaluated nuclear data file which has been available is not so accurate to answer sufficiently the demand from users. Main defects of the existing files are in the neutron energy region higher than several MeV. They must be improved especially in the fusion-oriented nuclear data files.

This report describes the plan, progressive state, and method of the evaluation for the fusion-related nuclear data in Japan. Concerning on these issues, we discussed at the Specialists' Meeting on the Nuclear Data for Fusion Neutronics held at Tokai Research Establishment of Japan Atomic Energy Research Institute (JAERI) on 23-25 July 1985 [1] (hereafter, referred as Tokai meeting). The activities on the evaluated nuclear data for fusion reactors in Japan were wholly presented at the meeting. Some of them were also presented at the International Conference on Nuclear Data for Basic and Applied Sciences held at Santa Fe on 13-17 May 1985 [2]. Detailed description can be found in the papers presented in the meeting and conference.

2. Fusion-related Nuclear Data in JENDL-3

Nuclear data evaluations in Japan have been continued since about 1960 and an evaluated data file compiled as JENDL (Japanese Evaluated Nuclear Data Library). We have two versions JENDL-1 [3]compiled in 1979 and JENDL-2 [4, 5] completed in April 1983. at present. The third version JENDL-3 is progressing and planned to complete in March 1987. One of the main points of JENDL-3 is presentation of evaluated nuclear data valid for fusion reactor studies. We have not a project in Japan to compile a special file of the nuclear data for fusion reactors.

The number of nuclides to be compiled in JENDL-3 is 158 including 57 nuclides not available in JENDL-2. A list of fusion-related nuclides to be stored in JENDL-3 is shown in Table 1. They are selected referring literatures on the studies of a D-T fusion reactor development.

One of the main themes in the Tokai meeting is discussion on JENDL-3PR1 and -3PR2 (JENDL-3, Preliminary version 1 and 2). It has been pointed out that some fusion-relating data in JENDL-2 are not so valid especially in the neutron energies higher than 5 MeV and they must be revised. In particular, the secondary neutron spectra (so-called Double Differential Cross Section Cross Section, DDX) deduced from the JENDL-2 data did not agreed with experiments. Motivation to prepare JENDL-3PR1 prior to completion of JENDL-3 was an answering to the urged requests from the analysts of the Japan-US cooperative experiments in simulated fusion blanket assemblies using the JAERI Fusion Neutronics Source (FNS) [6] and the University jointed programs on fusion experiments using the Osaka University 14 MeV intense Neutron Source (OKTAVIAN) [7] and other facilities. The JENDL-3PR1 compiled in December 1983 have the evaluated data for eight nuclides, ^6Li, ^7Li, ^9Be, ^{12}C, ^{16}O, Cr, Fe and Ni. The data for ^6Li, ^7Li, ^9Be and ^{12}C were wholly reevaluated apart from JENDL-2. The ^{16}O data were newly evaluated for this file. The data relating to DDX for Cr, Fe and Ni in JENDL-2 were revised.

Comparison of JENDL-3PR1 with the current experiments demands partly revising of the version. In JENDL-3PR2 compiled in March 1985, a part of the data for ^6Li, ^7Li and ^{12}C in JENDL-3PR1 are replaced by the new evaluation. Comments on the new version by comparing with the recent experiments have been giving to the evaluators. Those will be referred in the final evaluation for JENDL-3.

The JENDL is compiled by adopting the ENDF/B format. The ENDF/B-IV format was applied to JENDL-1 and JENDL-2. JENDL-3PR1 and JENDL-3PR2 were compiled in the ENDF/B-V format. Although JENDL-3 will be also compiled in the ENDF/B-V format, the possibility of adopting the ENDF/B-VI format is now investigating [8].

In the ENDF/B format, the data of energy-angular distribution of secondary neutrons, DDX can be stored in the file-6 in ENDF/B format. This file is not compatible with the file-4 which is for the angular distributions of secondary neutrons. It is not fixed yet whether the file-6 is adopted in JENDL-3 or not.

There are some types of nuclear data which must be evaluated in fusion-oriented data files with emphasis. They are summarized as following,
   (1) Angular distributions and energy spectra of emitted neutrons,
   (2) Tritium production cross sections,
   (3) Gamma-ray production cross sections, and
   (4) Activation cross sections.
These cross sections take priority of the other ones in JENDL-3. Therefore, the evaluators, experimenters, and planners take a great interest in the studies to attain considerable accuracy for them. Especially, DDX is a matter of primary concern. In order to compare both the evaluated and measured data, two code were developed. They are the FAIR-DDX [9] and DDXPLOT [10] codes. The former produces DDX from JENDL with taking account of resolution in the experimental system and the latter plots it with the experimental data. They are powerful tools for the fusion-related data evaluation.

3. Angular Distributions and Energy Spectra of Emitted Neutrons

Angular distributions and energy spectra of emitted neutrons are included in existing evaluated nuclear data files. Nevertheless, most parts of them seem to be not almost accurate sufficient for applying them to fusion reactor calculation. In comparing integral experiments of blanket-mocked-up assemblies with the calculation using existing evaluated nuclear data files, it is realized that some data in the files should be substantially revised. The early evaluated nuclear data files

were prepared for fission reactor calculation in which neutron data above 10 MeV did not play an important role. In a fusion reactor, 14 MeV neutrons are generated in plasma and then travel into a blanket where they are scattered and absorbed by structural and breeding materials. Generally speaking, some differential cross sections relating to these processes have been roughly evaluated in the early files. A typical example is that most of angular distribution for inelastically scattered neutrons are assumed simply to be isotropic. These nuclear data have a little effect in the fission reactor calculation, since a major part of a fission neutron distributes in few MeV region and geometrical condition of a fission reactor is acceptable of the simple assumption. In fusion reactors, however, the energy of source neutrons is 14 MeV at which the angular distribution of inelastically-scattered neutrons are predominantly anisotropic. Calculated result in geometrical condition like a fusion reactor is sensitive to change of the neutron angular distribution. Evaluated energy spectra of secondary neutrons emitted in scattering and reactions are important with similar reasons. In these senses, the role of nuclear data and simulating experiments is different for thermal reactors, fast breeding reactors and fusion reactors [11].

Nuclear data stored in an evaluated data file are usually applied in neutron transport calculation for reactors as group constants which are produced by processing them with the special computer codes. If steps of procedures of the secondary neutron data from the measurement to the production of group constants are followed as shown in Fig.1, it can be understood that their angular and energy distribution measured with a differential experiment (DDX) are an essential quantity for the neutron transport calculation. This was emphasized at the previous meeting on the IAEA Nuclear Data for Fusion Reactors [12,13]. Takahashi [14-18] suggested it also, programmed the NITRAN code which used DDX in neutron transportation calculation as the basic data for the secondary neutrons, and have measured DDX of many nuclides at 14 MeV.

The DDX is also very useful to investigate drawbacks of the evaluated data for the secondary neutrons. They are at an intermediate position between the differential and integral data. The differential experiment is defined as the measurement with a sample whose size is less than a mean free path of concerning neutrons. In the integral one, the sample size is larger than the mean free path. The former is usually utilized to obtain the angular distribution and energy spectrum of the secondary neutron from (n,n), (n,n') and (n,2n) by unfolding the measured neutron spectrum at fixed angles against the incident neutron. The existing evaluated data files are separately compiled the quantities for an individual reaction. Therefore, DDX must be reproduced from the individual evaluated neutron data when the transport calculation is performed. In this scenario, DDX is a starting point and also a goal (Fig.1).
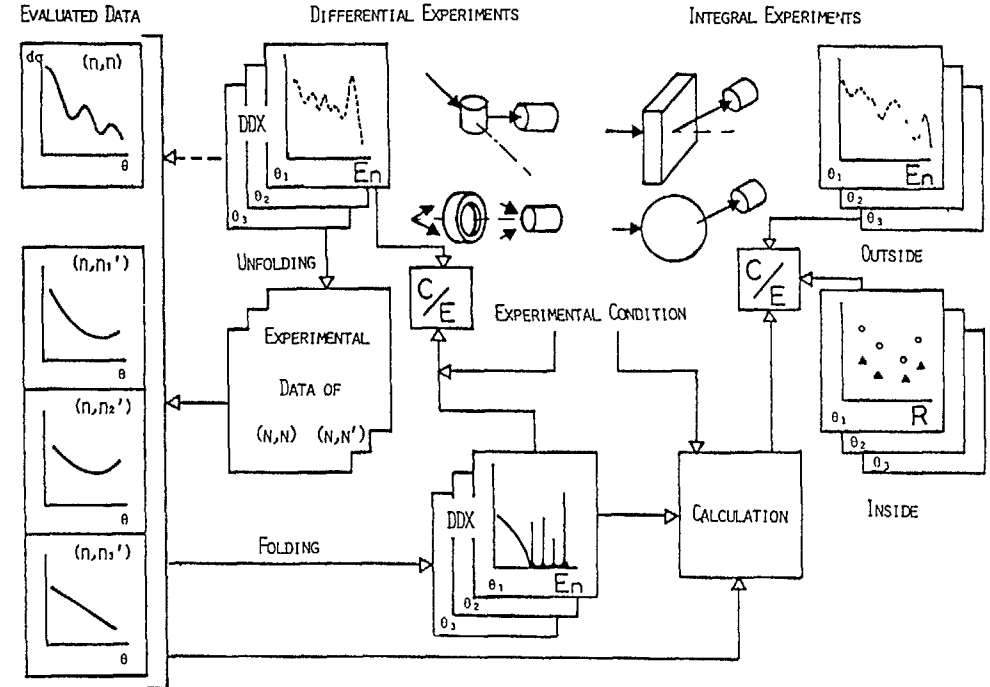
Fig.1 Data Processing and Comparing

There is a few kind of integral experiment[19], measurements of leakage neutron spectra from a sample and of neutron reaction rates in a sample. The sample thickness of the integral experiments conducted at present are few times of the mean free path of the 14 MeV neutron. The neutrons inside and outside the sample keep the effect of a collision. Comparison of the experiments with the calculations using the evaluated nuclear data are very effective to discuss the validity of the evaluation.

Activities of both the differential and integral experiments stimulate and encourage the studies on evaluations of fusion-related nuclear data. Mutual exchange of information between the evaluators and experimenters has made revising and improving the evaluated nuclear data.

The examples of the evaluation are presented in the following subsections.
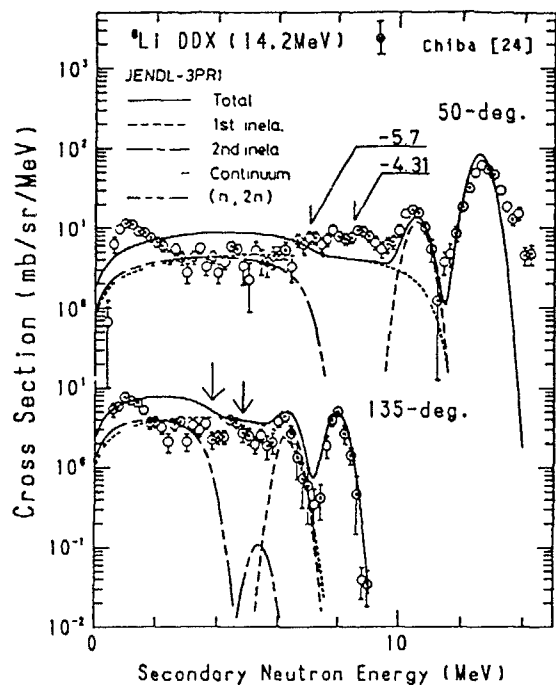
Fig.2-1 DDX of ^{6}Li.
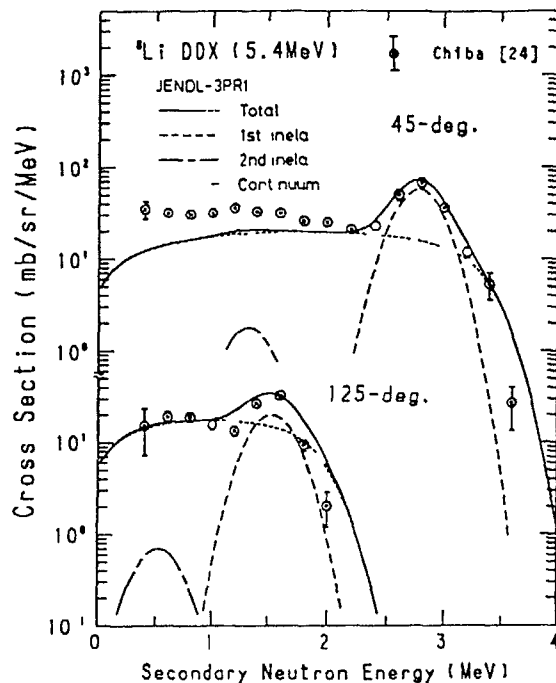
Fig.2-2 DDX of ^{6}Li.
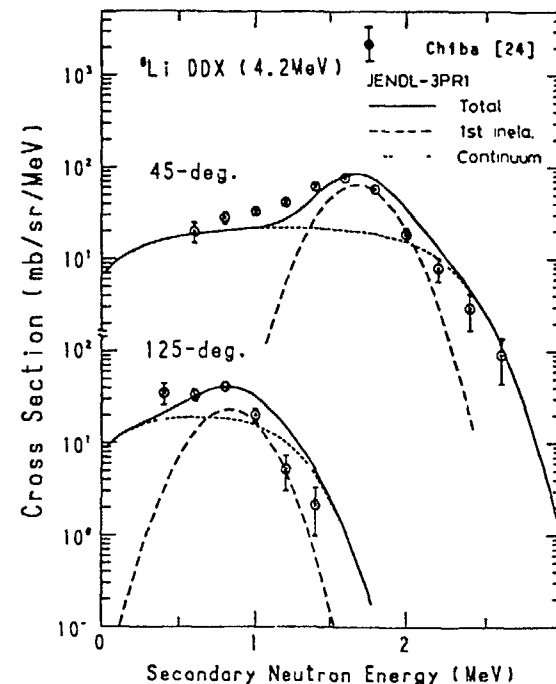
Fig.2-3 DDX of ^{6}Li.

3.1 Evaluation of Li Data

Both the data of ^{6}Li and ^{7}Li in JENDL-3PR1 [20] were evaluated by Shibata[21, 22]. The total, elastic scattering and (n,α) reaction cross sections of ^{6}Li were calculated with the R-matrix theory below 1 MeV and evaluated on the basis of the experimental data above 1 MeV. The ^{7}Li(n,n') and ^{7}Li(n,n't)α cross sections were evaluated from the current experiments. The JENDL-3PR1 data had been used for analyses of integral experiments [19, 23] and compared with newly-measured differential data [24-27]. In Figs.2, 3 and 4, the JENDL-3PR1 data are compared with experiments. They commonly pointed out a few problems.

1) Some higher levels not considered in the JENDL-3PR1 evaluation should be taken account as discrete levels.
2) The elastic scattering cross section of ^{7}Li is overestimated as much as 10% at high energies.

3) The energy spectra of the continuum neutrons emitted from the ^{6}Li(n,n'd)α, ^{7}Li(n,n't)α and ^{6,7}Li(n,2n) reactions are not reasonable.
4) The cross section of the ^{6}Li(n,2n) reaction is overestimated.

To improve these defects, the revision of the evaluated data of JENDL-3PR1 for ^{6}Li and ^{7}Li was performed by Chiba[28]. The newly evaluated data are included in JENDL-3PR2. In the following paragraphs, the procedures of this version are briefly presented according to Chiba's description.

Two excited levels of each nuclide, 4.31 and 5.71 MeV for ^{6}Li, and 6.68 and 7.47 MeV for ^{7}Li, not considered in JENDL-3PR1 were additionally taken into account in the evaluation of inelastic scattering cross sections, because the data of JENDL-3PR1 did not reproduce the DDX experiments at the energy region of the secondary neutron spectra responsible for these excited levels, as seen in Figs.2, 3 and 4. The excitation functions and

204
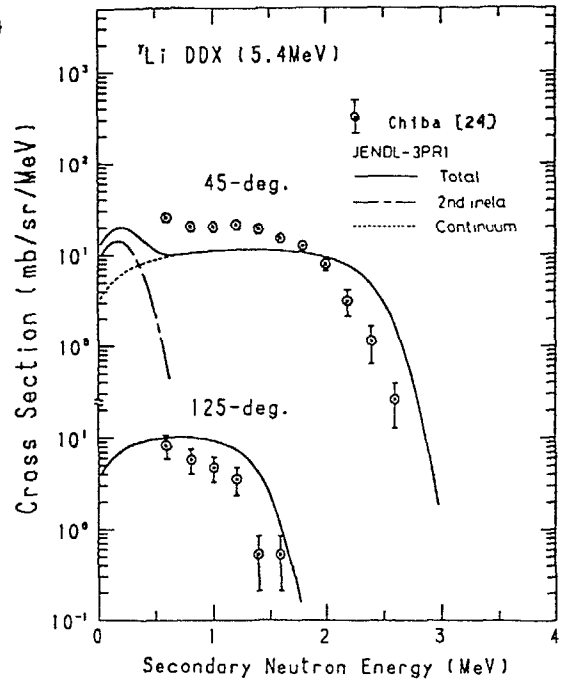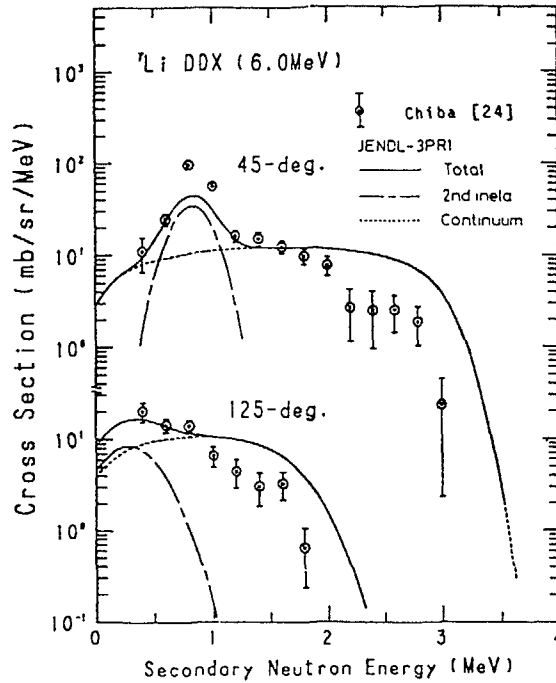
Fig.3-1 DDX of ⁷Li.

Fig.3-2 DDX of ⁷Li.
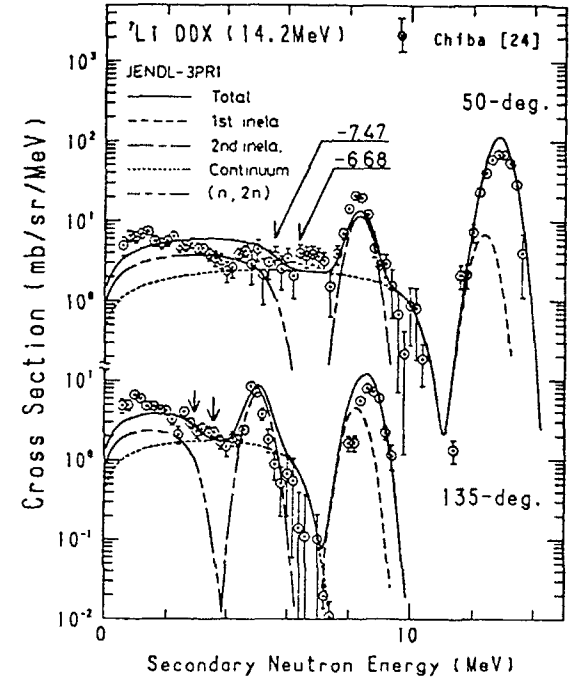
Fig.3-3 DDX of ⁷Li.
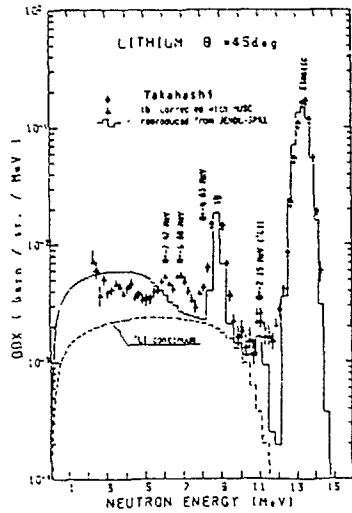
Fig.4-1 DDX of natural lithium
at 45 deg, compared
with JENDL-3PRI.
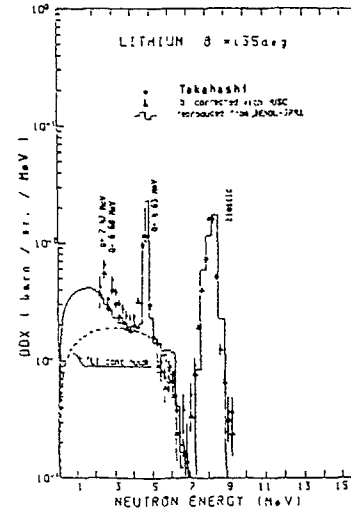
Fig.4-2 DDX of natural lithium
at 135 deg, compared
with JENDL-3PRI.

angular distributions of the secondary neutron from these levels were calculated with the coupled-channel optical model using the ECIS code [29] and the parameters presented by Chiba [24]. The calculated excitation functions of these levels were normalized to the experimental data measured at Tohoku [24] and Osaka [16-18] Universities. The 7.47-MeV level of ^7Li which was not included in the calculation with ECIS was assumed to have the same excitation function as that of the 6.68 MeV level.

The angular distribution for the 5.71-MeV level of ^6Li was assumed to be isotropic in the center-of-mass system. For the first level (0.478 MeV) of ^7Li, the angular distributions were calculated with the R-matrix theory adopting the parameters of Knox and Lane [30] below 10 MeV. Above 10 MeV, the coupled-channel calculation was performed. For the second level (4.63 MeV), the R-matrix theory was used below 8 MeV. The experimental

data of Hogue et al. [31] were adopted in the energy range between 8 and 14 MeV. Above 14 MeV, the coupled-channel calculation was adopted. The angular distribution for the 7.47 MeV level was assumed to be isotropic in the center-of-mass system.

The angular distribution data above 14 MeV of the elastically scattered neutrons were replaced with the calculated values in the new version. The elastic scattering cross section of ^7Li was reduced by 5% at 14 MeV. This reduction caused decrease of the total cross section by 3.5% at this energy.

The angular distributions of the elastically and inelastically scattered neutrons from ^7Li around 14 MeV were presented in Figs.5 and 6. Fig.7 shows the total cross section of ^7Li between 10 and 20 MeV.
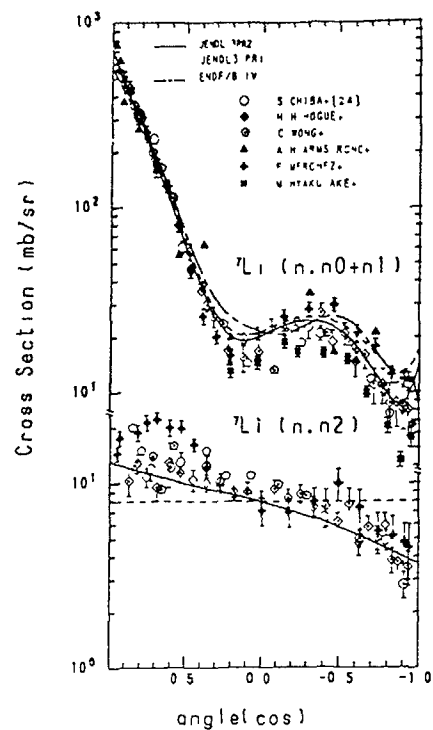
Fig.5 Angular distribution elastic and inelastic cross sections of ^7Li.
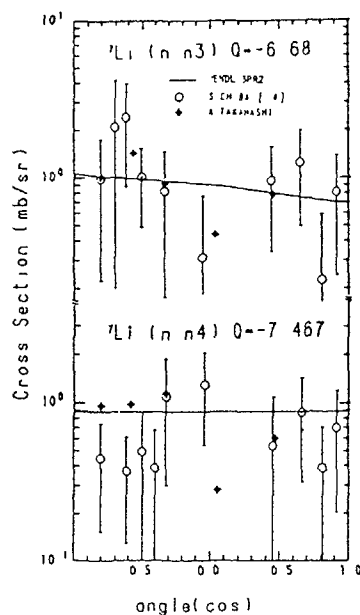
Fig.6 Differential inelastic scattering cross-sections of ^7Li around 14 MeV.
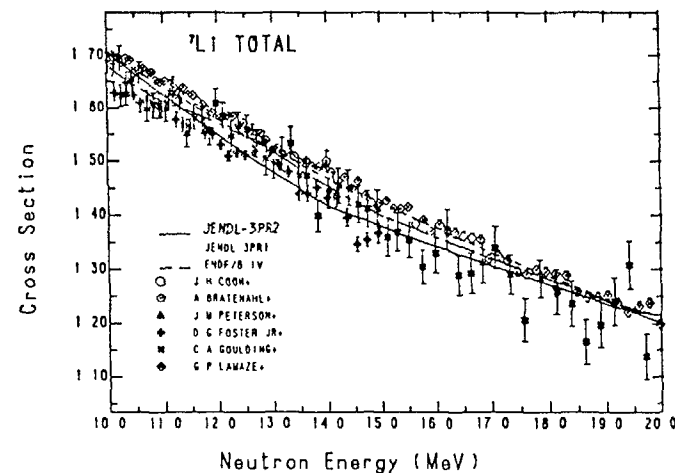
Fig.7 Total cross section of ^7Li.

The energy-angle distributions of the continuum neutrons were evaluated with the model of Holland [32].

In JENDL-3PR2 evaluation, pseudo levels were used. The excitation energies of the pseudo levels were given by 0.5 MeV intervals. The results are shown in Figs.8 and 9. [28] Sum of the cross sections of these levels were normalized to the $^6Li(n,n'd)\alpha$ and $^7Li(n,n't)\alpha$ reaction cross sections. For the angular distributions of the pseudo levels of ^7Li, the data of the continuum neutrons measured by Chiba [24, 25] were adopted. For ^6Li, they were assumed as isotropic in the center-of-mass system.
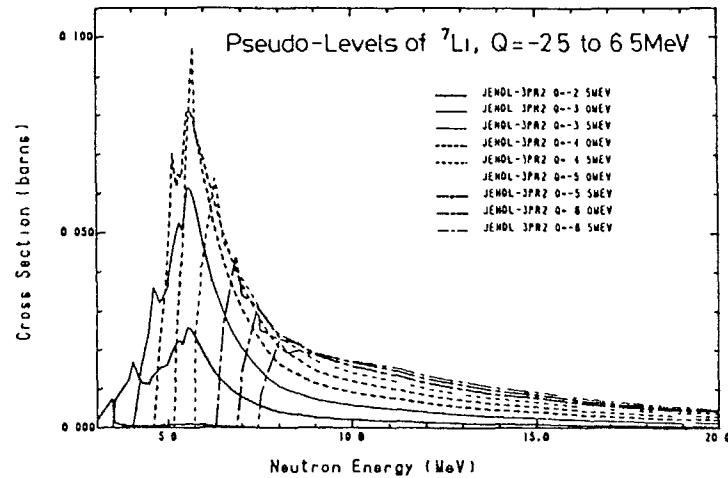
Fig.8 Inelastic cross sections for pseudo-levels for ^7Li (Q=-2.5 to -6.5MeV).

The energy distributions of the secondary neutrons from the $^{6,7}Li(n,2n)$ reactions were evaluated by the conventional evaporation model. For the evaporation temperatures, the data of Chiba [24] were adopted. The angular distributions of neutrons emitted from these reactions were also replaced by the data in Ref.[24]. In addition to these modifications, the $^6Li(n,2n)$ reaction cross section were reduced by 20% in the whole energy range so as to reproduce the experimental data [24, 33, 34]. Fig.10 shows the $^6Li(n,2n)$ reaction cross section.

The DDX of ^6Li and ^7Li are shown in Figs.11 and 12, respectively, comparing with the other evaluated data.
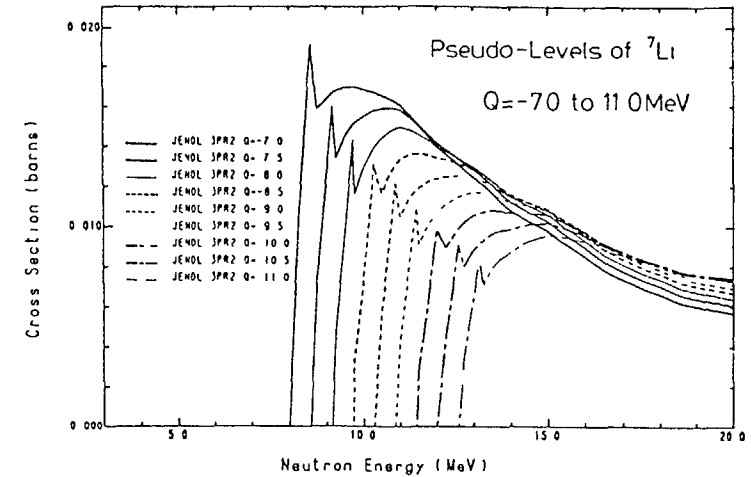
Fig.9 Inelastic cross sections for pseudo-levels for ^7Li (Q=-7.0 to -11.0MeV).
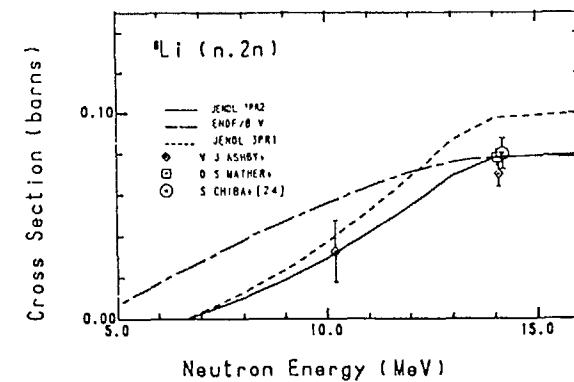
Fig.10 (n,2n) cross section for ^6Li.
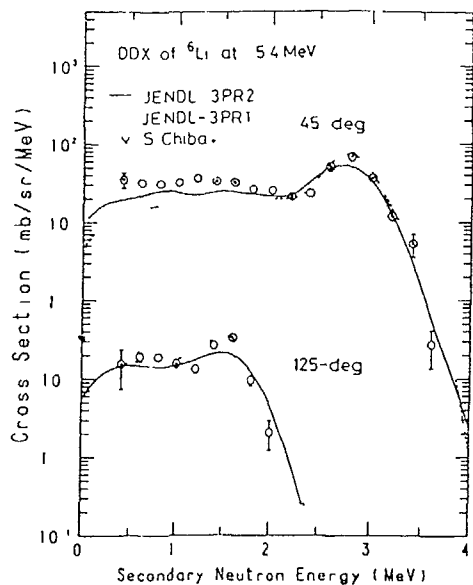
Fig.11-1 Comparison of evaluated data
files for ^6Li
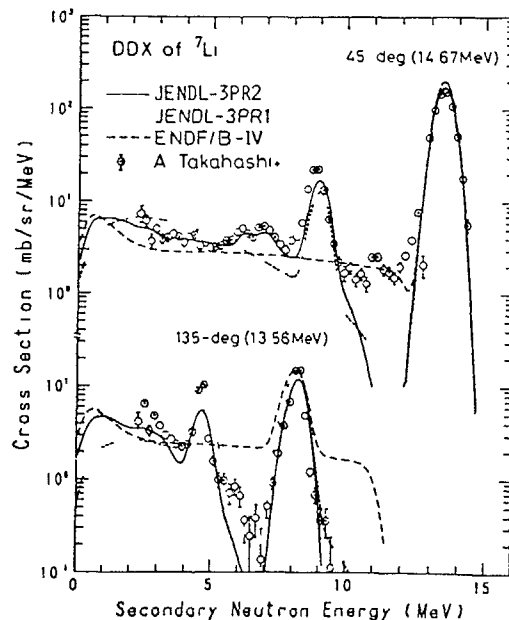
Fig.11-2 Comparison of evaluated data
files for ^6Li
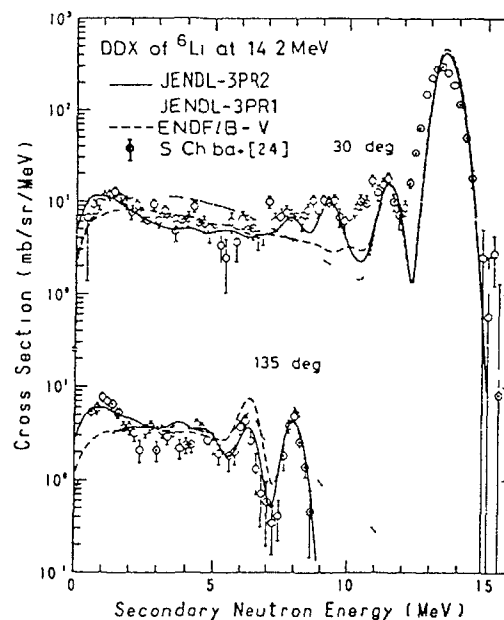
Fig.12-1 Comparison of evaluated data
files for ^7Li
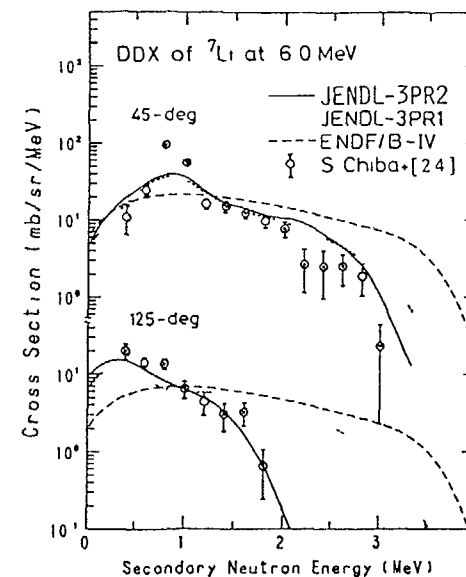
Fig.12-2 Comparison of evaluated data
files for ^7Li

The author is afraid to emphasize too much that the fusion-related neutron data have been evaluated predominantly depending on the DDX experiments. As seen in Fig. 1 and discussed in the head of this section, the DDX data are primary ones in the measurement of secondary neutrons. In a way of neutron data processing, they are unfolded to obtain partial cross sections which are physical quantities and can be compared directly with nuclear reaction model calculations. The partial cross sections should be compiled in the ideal nuclear data file. At present, however, experimental uncertainties are so large that the processes of unfoling and folding result in larger errors of nuclear data for neutronic calculation. It is better to use the DDX experiments as a reference for evaluation. There is another reason. The experiments on secondary neutrons, even the differential and integral experiments, are essentialy similar. There is no decisive quantity in fusion reactors as the effective neutron multiplication factor k_{eff} in fission reactors. The DDX data are used to check the evaluation.

Although the evaluation of the DDX data are discussing, it is difficult to compare the data measured in different

laboratories because of different experimental conditions. The most difficulty is that measuring angle is different. Interporation of the DDX data is diffcult. Therefore, the DDX must be evaluated by applying nuclear reaction model calculation.

3.2 Evaluation of Structural Materials

The data of structural materials, Cr, Fe and Ni in JENDL-3PR1 and -3PR2 were evaluated by Kikuchi et al. [35, 20]. Their data in JENDL-2 are insufficient for fusion neutronics calculation. Nuclear reaction model used in JENDL-2 evaluation was the spherical optical and statistical models without considering the direct and pre-equilibrium processes. These resulted in that the low-lying levels were much underestimated and secondary neutron spectra were too soft comparing with the measurement of DDX. Typical examples are shown in Figs.13, 14 and 15. To improve it, the two processes were taken into account for the inelastic scattering and (n,2n) reaction cross sections as well as their angular and energy distribution of
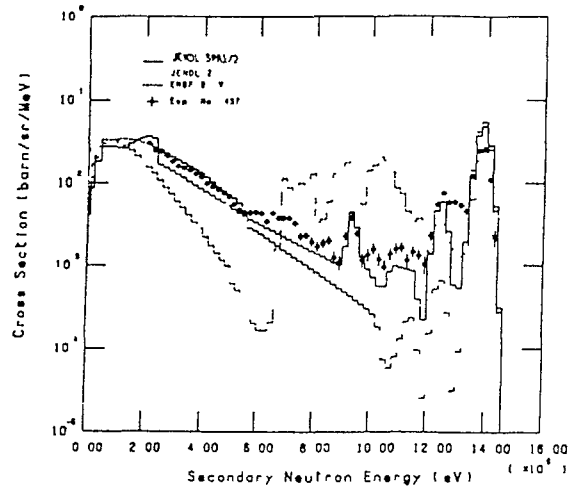
Fig.13 Comparison between DDX files of
Nat. Cr (80 deg.)
Double differential cross-section
of natural Cr at 80 degrees.
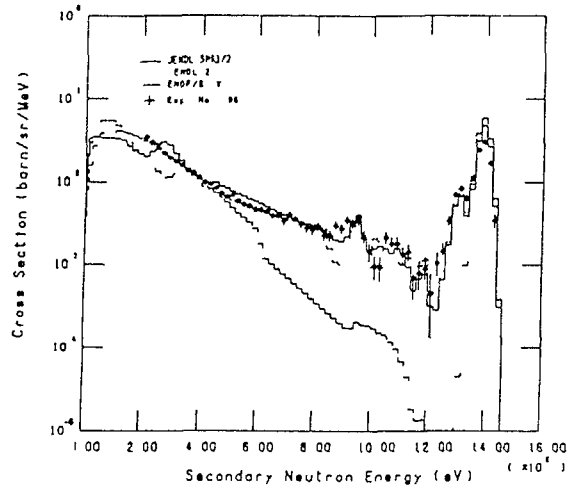
Fig.14 Comparison between DDX files of
Nat. Fe (80 deg.)
Double differential cross-section
of natural Fe at 80 degrees.
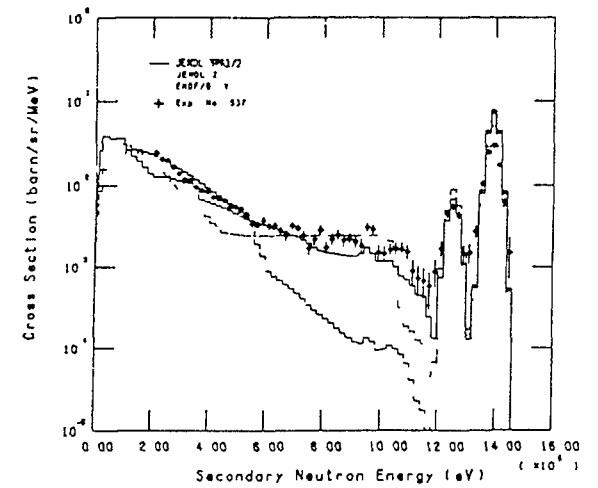
Fig.15 Comparison between DDX files of
Nat. Ni (80 deg.)
Double differential cross-section
of natural Ni at 80 degrees.

secondary neutrons. The compound process component in the
early evaluation was not modified and the direct and pre-
equilibrium components were added to it by adjusting the
elastic scattering cross section so as to keep the total cross
section unchanged. The additional components were calculated
for the major isotopes in natural, namely ^{52}Cr, ^{56}Fe and ^{58}Ni,
and they were assumed equally for minor isotopes to evaluate
the data for natural elements.

To calculate the direct process component, the coupled
channel optical model were applied by using the ECIS code [29].
Levels to be coupled are a 1-phonon quadrupole vibrational level
(2^+), three 2-phonon quadrupole vibrational levels $(0^+, 2^+, 4^+)$
and a 1-phonon octupole vibrational level (3^+). The optical
potential parameters were obtained so as to reproduce the
experimental total cross section above a few MeV.

The pre-equilibrium effects were calculated by GNASH code
[36]. The pre-equilibrium normalization constant in GNASH were
found to be reasonable after parameter searching and were
adopted.

A part of the results is shown in Figs.16-20 [37]. The DDX
data estimated from the evaluated values by FAIR-DDX [9] are
compared with the experiments by Takahashi et al. [16-18] in
Figs.13-15, additionally showing the data of JENDL-2 and ENDF/B-
IV. Generally speaking, JENDL-3PR1 underestimates slightly the

inelastic scattering and (n,2n) reaction cross sections and
overestimates the elastic scattering cross section.

The data in JENDL-3PR1 of ^9Be and ^{12}C were evaluated by
Shibata [38, 39]. Those of ^{16}O in JENDL-3PR1 are revising for
JENDL-3. The experiments relating to these data were reported in
Refs.[40, 41].

4. Cross section of $^7Li(n,n t)\alpha$ near 14 MeV

The $^7Li(n,n't)\alpha$ reaction is one of the tritium production
reactions and its cross section has been interested in by
experimenters and evaluators. The data of JENDL-3PR1 are
evaluated adopting the experiments available at the time [22].
Recently, the new measurements near 14 MeV are conducted. The
old experiment of Maekawa et al. [42] was not used in the JENDL-
3PR1 evaluation but agreed with the evaluation. It was a point
to confirm the evaluation in Shibata's work [22]. The new data
of Maekawa et al. [43], however, are about 7% larger than the old
one and agree with the data of Chiba et al. [24] and Takahashi et
al. [44]. The recent measurement of the fission-spectrum
averaged cross section of this reaction by Iguchi [45] pointed
out that the data of JENDL-3PR1 and -3PR2 were low. The
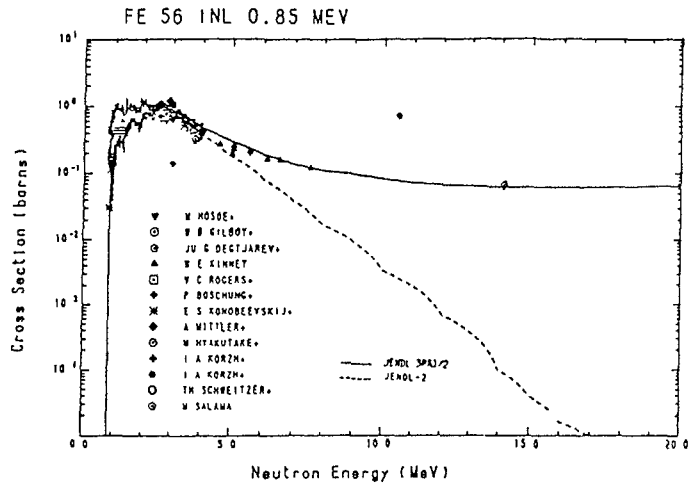evaluators and experimenters are discussing on these results.

FE 56 INL 0.85 MEV

Cross Section (barns)

Neutron Energy (MeV)

W HOSOE+
V W GILBOT+
JU G DEGTJAREV+
W E KINNET
Y C ROGERS+
P BOSCHUNG+
E S KONOBEEVSKIJ+
A MITTLER+
W MIYAKUTAKE+
I A KORZH+
I A KORZH+
TH SCHWEITZER+
W SALAMA

JENDL 3PR3/2
JENDL-2

Fig.16 Inelastic scattering cross-section of ^{56}Fe to 0.847 MeV level (2+).

FE 56 INL 2.96 MEV

Cross Section (barns)

Neutron Energy (MeV)

JENDL 3PR3/2
JENDL-2
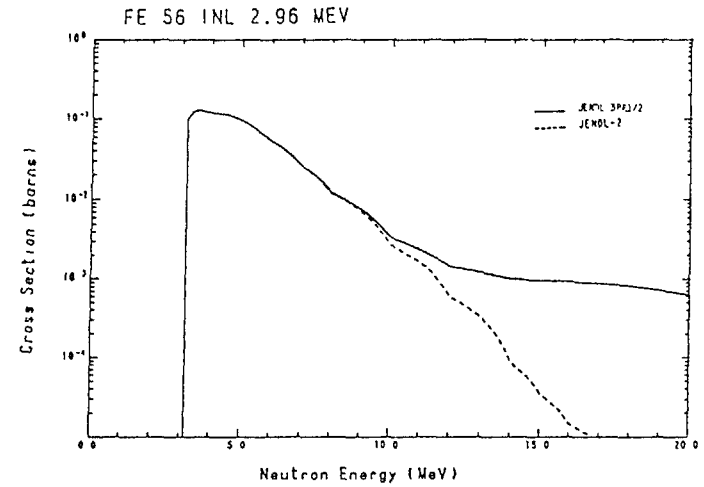
Fig.18 Inelastic scattering cross-section of ^{56}Fe to 2.96 MeV level (2+: non-collective).

FE 56 INL 4.51 MEV

Cross Section (barns)

Neutron Energy (MeV)

JENDL 3PR3/2
JENDL-2
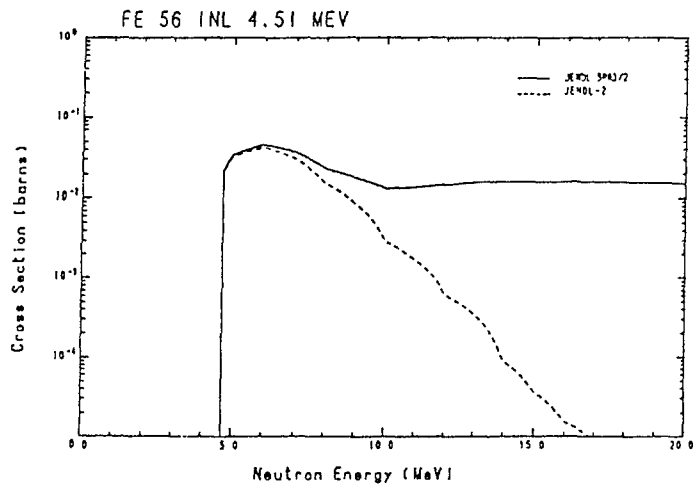
Fig.17 Inelastic scattering cross-section of ^{56}Fe to 4.51 MeV level (3-).

FE 56 INL CONTINIUM

Cross Section (barns)

Neutron Energy (MeV)

JENDL 3PR3/2
JENDL-2
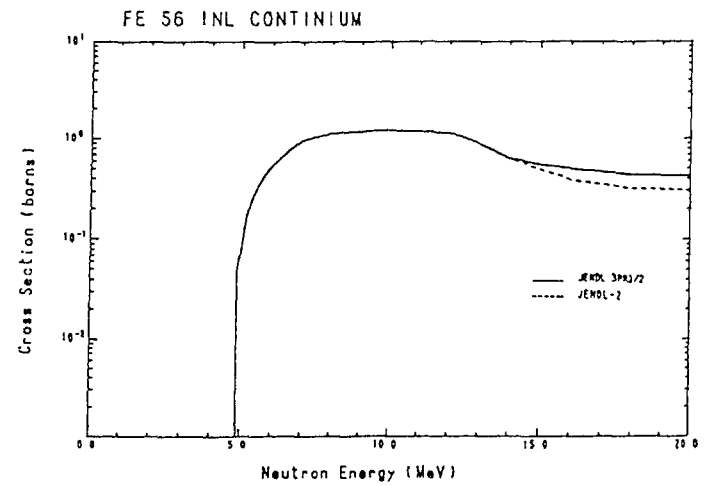
Fig.19 Inelastic scattering cross-section to continuum levels.

209

ANGULAR DISTRIBUTION FE-56(N,N') 0.847 MEV   ENERGY 5.05(MeV) - 14.10(MeV) system CMS

INCIDENT ENERGY 7.55(MeV)

INCIDENT ENERGY 14.10(MeV)

INCIDENT ENERGY 5.05(MeV)

INCIDENT ENERGY 8.56(MeV)
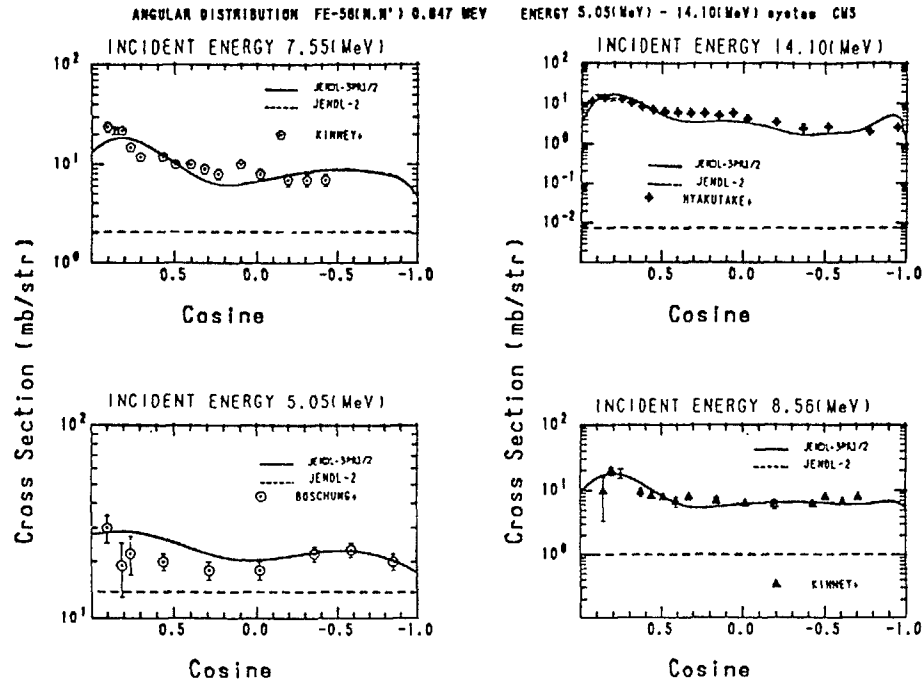
Fig.20 Angular distribution of ^{56}Fe inelastic scattering to 0.847 MeV level.

5. Gamma-ray production cross sections

It has been pointed out that an amount of the energy deposited by neutron-induced secondary gamma-rays is calculated approximately at 80% in the total energy deposited in a blanket. Therefore, evaluated gamma-ray production cross sections are strongly demanded by fusion reactor designers. The nuclides planned to evaluate the gamma-ray production cross sections in JENDL-3 are marked in Table 1.

Available experimental data of these cross sections are not so enough to evaluate the cross sections from experiments that the calculation by using nuclear reaction models is mainly applied to the evaluation. The parameters in the formulae are estimated from available experiments relating to those cross section. Ambiguity of the calculation models and uncertainty of the experiments are so large that it is troublesome and difficult to evaluate them in high accuracy. However, it is a policy in the JENDL-3 to evaluate the gamma-ray production cross section for many nuclides as possible as.

TABLE 1. Fusion-related Nuclides to be stored in JENDL-3

Atomic Number	Nuclides
1	^{1}H, ^{2}H
2	^{3}He, ^{4}He a)
3	*^{6}Li, *^{7}Li b)
4	*^{9}Be
5	^{10}B, ^{11}B
6	*^{12}C
7	*^{14}N
8	*^{16}O
9	^{19}F
11	*^{23}Na
13	*^{27}Al
14	*Si, ^{28}Si, ^{29}Si, ^{30}Si
19	K, ^{39}K, ^{40}K, ^{41}K
20	*Ca, ^{40}Ca, ^{42}Ca, ^{43}Ca, ^{44}Ca, ^{46}Ca, ^{48}Ca
22	*Ti, ^{40}Ti, ^{47}Ti, ^{48}Ti, ^{49}Ti, ^{50}Ti
23	^{51}V
24	*Cr, ^{50}Cr, ^{52}Cr, ^{53}Cr, ^{54}Cr
25	^{55}Mn
26	*Fe, ^{54}Fe, ^{56}Fe, ^{57}Fe, ^{58}Fe
27	^{59}Co
28	*Ni, ^{58}Ni, (^{59}Ni)c), ^{60}Ni, ^{61}Ni, ^{62}Ni, ^{64}Ni
29	*Cu, ^{63}Cu, ^{65}Cu
30	Zr
41	*^{93}Nb, (^{94}Nb)
42	*Mo, ^{92}Mo, ^{94}Mo, ^{95}Mo, ^{96}Mo, ^{97}Mo, ^{98}Mo, ^{100}Mo
74	*W, ^{180}W, ^{182}W, ^{183}W, ^{184}W, ^{186}W
82	*Pb, ^{204}Pb, ^{206}Pb, ^{207}Pb, ^{209}Pb
83	*^{209}Bi

a) " ": Nuclides to be compiled newly in JENDL-3.

b) " * ": Nuclides including evaluated gamma-ray production cross section.

c) "( )": Unstable Nuclide.

In order to assure energy conservation and consistency
between particle-emitted and gamma-ray production cross sections
in a reaction process, the gamma-ray cross section associated
with every kind of reaction are individually calculated. Total
values are obtained by summing up them. The computer code used
commonly is GNASH. A gamma-ray transition probability is
estimated by the Brink-Axel type strength function with the pygmy
resonance whose validity is discussed by Igashira et al. [46].

An example for Ni at approximately 15 MeV of the neutron
energy is shown in Fig.26 [47]. The peak near 1.5 MeV in the
figure coresponding to the gamma-rays emitted in transition of
the first excited state to the ground state of the Ni nuclide can
not be reproduced even if the direct process in (n,n') is taking
into account. The underestimation may be caused by lack of
enhanced transitions from higher excitation states to the first
excited state in the calculation. They can not estimate in this
method because knowledges of the spin and parity on the high
excited states. The underestimation appears in the energy range
higher than about 7 MeV.

Fig.22 Calculated and measured DDX data at 14 MeV.
The measurement was performed at Osaka
University (14).

Fig.21 Calculated and measured DDX data at 7 MeV.
The measurement was performed at Tohoku
University (16). The measured elastic
scattering peak is not shown in this figure.
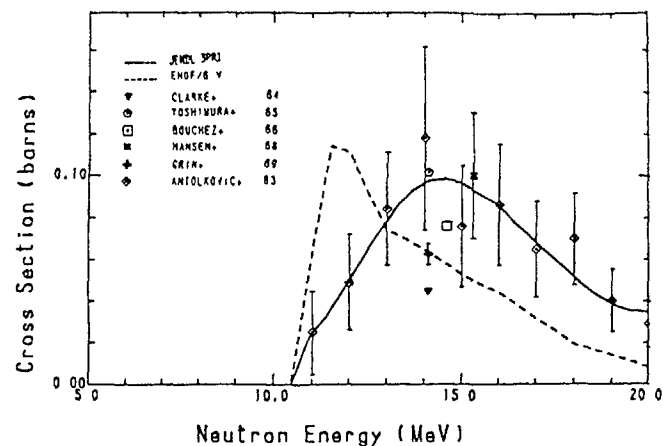
Fig.23 Measured and evaluated (n,n₃) cross-sections.
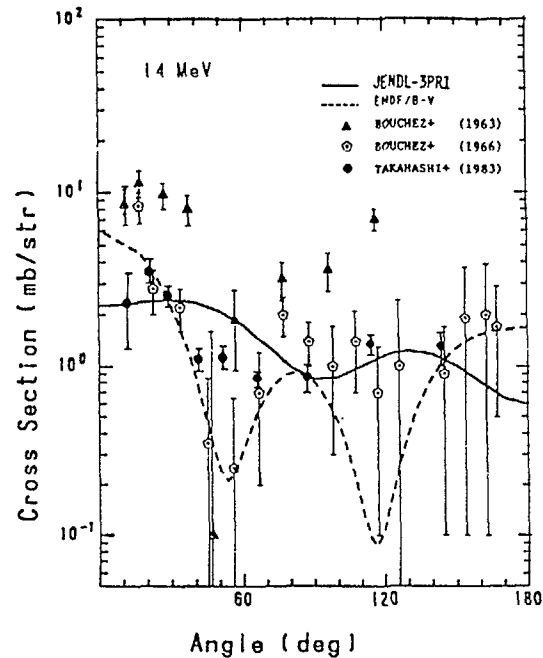
Fig.24 Measured and evaluated angular distributions for the (n, n₂) reaction at 14 MeV.
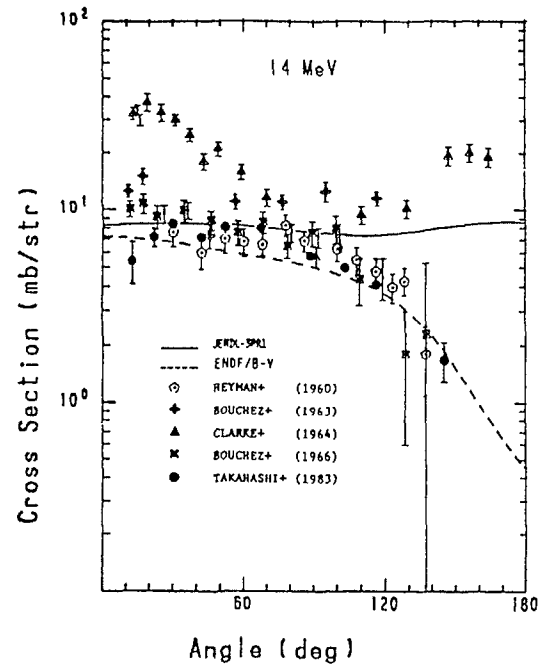
Fig.25 Measured and evaluated angular distributions for the (n, n₃) reaction at 14 MeV.
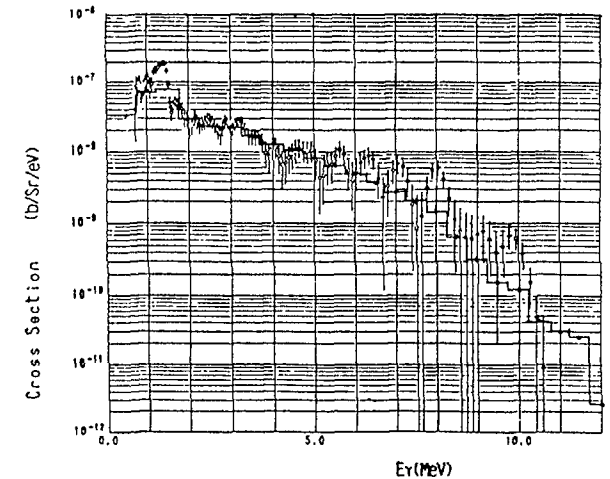
Fig.26 Gamma ray production cross-section of Ni.

6. Activation cross sections by fast neutrons

One of the difficulties in fusion reactor development is neutron-induced activities in blanket structural materials. Activation cross sections for many nuclides at 14 MeV have been measured in great quantities comparing with other kinds of cross section. Majority of the reaction cross sections relating to induced activities have been evaluated by adopting the measurements at 14 MeV. Therefore, estimation of neutron-induced activities at 14 MeV in materials candidated for fusion reactors is possible to some degree. A computer code THIDA [48] was developed to calculate the activity in fast neutron fields. The comparison of measurements by FNS with calculation by the THIDA code under the experimental condition predicted that a few reaction cross section must be revised. In order to investigate the evaluated activation cross sections, experiments were conducted at the laboratories in Japan [49-56]. These results will be applied to the evaluation of JENDL-3.

7. Concluding Remarks

In this report, the status of fusion-related evaluated nuclear data is reviewed with emphasis on the evaluation of the secondary-emitted neutron cross sections in JENDL-3PR2.

It is confirmed that the application of the nuclear reaction model calculaton is very useful in the evaluation near 14 MeV. This is valuable since the number of available experimental data is limited because of difficulties with experiments in this neutron energy region.

The DDX data are valuable for the evaluation of the cross sections and angular distributions for the elastic and inelastic scattering and (n,2n) reaction. The integral experimants are usable to test the evaluated nuclear data. The results and comments from the test are fed back to increase accuracies in the evaluation.

REFERENCES

[1] IGARASHI, S., ASAMI, T (Ed.), Proc. of Specialists' Meeting
     on Nuclear Data for Fusion Neutronics,. JAERI-M 86-029 (1986),

[2] YOUNG, P. G., et al. (Ed.), Nuclear Data for Basic and
     Applied Science, Proc. of the Int. Conf. Nucl. Data for Basic
     and Applied Science, Santa Fe, May 13-17, 1985, A Special
     Issue of Radiation Effects (Gordon an Breach Science Pub.
     1986)

[3] IGARASHI, S., et al. (Ed.), "Japanese Evaluated Nuclear Data
     Library, Version-1, JENDL-1", JAERI-1261 (1976)

[4] NAKAGAWA, T. (Ed.), "Summary of JENDL-2 General Purpose
     File", JAERI-M 84-103 (1984)

[5] ASAMI, T. NARITA, T. (Ed.), "Graphs of Evaluated Neutron
     Cross Section in JENDL-2", JAERI-M 84-052 (1984)

[6] NAKAMURA T., et al., "Fusion Neutronics Source (FNS), "Proc.
     Third Symp. on Accelerator Science and Technology, Osaka
     Univ., Japan, Aug. 27-29, pp55-56 (1980).

[7] SUMITA K., et al., "Neutron Source and Its Utilization for
     Fusion Studies (OKTAVIAN Program), "Proc. 12th Symp. Fusion
     Technology, Julich, Sep. 13-17, 1982, Vol.1, pp675-680
     (1982).

[8] NAKAGAWA, T., "On the Format of JENDL", Proc. of
     Specialists' Meeting on Nuclear Data for Fusion Neutronics",
     JAERI-M 86-029, pp41-51 (1986)

[9] MINAMI, K., YAMANO, N., "FAIR-DDX: A code for Production of
     Double Differential Cross Section Library" JAERI-M 84-022
     (1984) (In Japanese)

[10] IGUCHI, T., YAMANO, N., "DDXPLOT: A Program to Plot the
     Energy Angle Double-Differential Cross Sections", JAERI-M

[11] KANDA Y., "Review on Nuclear Data for Fusion Reactors,"
     Proc. of specialists' Meeting on Nuclear Data for Fusion
     Neutronics, JAERI-M 86-029, pp3-14 (1986)

[12] LORENQ, A., MUIR, D. W. (Ed.), "Nuclear Data for Fusion
     Reactor Technology", Proc. Advisory Group Meeting on
     Nuclear Data for Fusion Reactor Technology, Vienna, 11-15
     Dec. 1978, IAEA-TECDOC-223 (1979)

[13] SEKI, Y. (Private Communication, 1979)

[14] TAKAHASHI, A., RUSCH D., "Fast Rigorous Numerical Method
     for the Solution of the Anisotropic Neutron Transport
     Problem and the NITRAN System for Fusion Neutronics
     Application. Part I and II." KfK 2832/I and II (1979).

[15] TAKAHASHI, A., et al., "Neutron Transport Calculations by
     Using Double-Differential Cross Sections." J. Nucl. Sci.
     Technol., 19 [4] 276-288 (1982).

[16] TAKAHASHI, A., et al., "Measurement of Double Differential
     Neutron Emission Cross Sections with 14 MeV Source for D,
     Li, Be, C, O, Si, Cr, Fe, Ni, Mo, Cu, Nb and Pb." Proc.
     Int. Conf. Nucl. Data for Science & Technology. Antwerp.
     Sep 6-7, 1982, pp360-367.

[17] TAKAHASHI, A., et al., "Double Differential Neutron Emission
     Cross Section, Numerical Table & figures(1983)," OKTAVIAN
     Report A-83-01. Osaka University (1983).

[18] TAKAHASI, A., et al., "Measurements of Double Differential
     Neutron Emission Cross Sections for Fusion Reactor
     Candidate Elements." J. Nucl. Sci. Technol., 21 [8] 577-598
     (1984).

[19] The invited papers presented at this meeting by SUMITA and
     MAEKAWA.

[20] SHIBATA, K., KIKUCHI, Y., "Evaluation of Nuclear Data for
     Fusion Neutrons" Proc. Int. Conf. Nuclear Data for Basic
     and Applied Science, May 13-17, 1985, Santa Fe, pp1585-1588
     (1986)

[21] SHIBATA, K., "Evaluation of Neutron Nuclear Data of ^{6}Li for
     JENDL-3," JAERI-M 84-198 (1984)

[22] SHIBATA, K., "Evaluation of Neutron Nuclear Data of ^{7}Li for
     JENDL-3," JAERI-M 84-204 (1984)

[23] SUGIYAMA, K., et al., "Neutronic Experiments in a 120 cm
     Lithium Sphere, Proc 13th Symp. Conf. on Fusion Technology,
     Varese, Italy, Sept. 24-28, 1984

[24] CHIBA, et al., J. Nucl. Sci. Technol., 22 [10] pp771-787
     (1985)

[25] CHIBA, et al., "Interaction of Fast Neutrons with ^{6,7}Li,"
     Proc. Int. Conf. Nucl. Data for Basic and Applied Science,
     Santafe, May 13-17, 1985 Vol.1 pp227-230 (1986)

[26] TAKAHASHI, A., "Double Differential Neutron Emission Cross
     Sections at 14 MeV Measured at OKTAVIAN", Proc. of
     specialists' Meeting on Nuclear Data for fusion Neutronics,
     JAERI-M 86-029, pp99-118 (1986)

[27] BABA,M., "Measurements of Double-Differential Neutron
     Emission Cross Sections at Tohoku University", ibid. pp119-
     140

[28] CHIBA, S., "Revision of the Neutron Nuclear Data of
     Lithium", Proc. of Specialists' Meeting on Nuclear Data for
     Fusion Neutronics, JAERI-M 86-029, pp32-40 (1986)

[29] RAYNAL, J., "Optical Model and Coupled Channel Calculations
     in Nuclear Physics", IAEA SME-9/8, IAEA (1970)

[30] KNOX, H. D., LANE, R. O., Nucl. Phys., A359, 131 (1981)

[31] HOGUE, H. H., et al., Nucl. Sci. Eng., 69, 22 (1979)

[32] HOLLAND, R.E., et al., Phys. Rev., C19, 529 (1979)

[33] ASHBY, V. J., et al., Phys. Rev., 129, 1771 (1963

214

[34] MATAHER, D. S., PAIN, L.F., "Measurement of (n,2n) and (n,3n) Cross Sections at 14 MeV Incident Energy", AWRE-O47/69, (1969)

[35] KIKUCHI, Y., et al., J. Nucl. Sci. Technol., 22, pp503 (1985)

[36] YOUNG, P. G., Arthur, E.D., "GNASH: A preequilibrium Statistical Nuclear Code for Calculation of cross Section and Emission Spectra", LA-6947 (1977)

[37] KIKUCHI et al., Private communication (1984)

[38] SHIBATA, K., "Evaluation of Neutron Nuclear Data of ^{9}Be for JENDL-3", JAERI-M 84-226 (1984)

[39] SHIBATA, K., "Evaluation of Neutron Nuclear Data for ^{12}C", JAERI-M 83-221 (1983)

[40] IWASAKI S., "Measurement and Analysis of Neutron Emission Spectra for Pb(n,2n) Reaction Between 14 and 20 MeV," Proc. Int. Conf. Nucl. Data for Basic & Applied Science, Santa Fe, May 13-17, 1985, Vol.1 pp191-194

[41] BABA, M., et al., "Scattering of 14.1-MeV Neutrons from ^{10}B, ^{11}B, C, N, O, F and Si," ibid., Vol.1 pp223-226

[42] MAEKAWA, H., et al., "Measurements of Tritium Production-Rate Distribution in Simulated Blanket Assemblies at the FNS", JAERI-M 83-196 (1983)

[43] MAEKAWA, H., et al., "Measurement of ^{7}Li(n,n'α)^3 Cross Section Between 13.3 and 14.9 MeV" JAERI-M 86-125, PP130-132 (1986)

[44] TAKAHASHI, A., et al., (Private Communication) Osaka University

[45] IGUCHI, T., NAKAZAWA, M. "Measurement of the Fission Spectrum averaged Cross Section of ^{7}Li(n,nα) T Reaction," Proc. Fall Meeting of Atomic Energy Soc. of Japan, A49 (1968) (In Japanese)

[46] IGASHIRA, M., et al., Nucl. Phys. A457 pp301-316 (1986)

[47] IIJIMA, . (Private Communication)

[48] SEKI Y., et al., "THIDA-2 An advanced Code System for Calculation of Transmutation. Activation. Decay Heat and Dose Rate," JAERI 1301 (1986).

[49] YAMAMOTO, J., et al., "Numerical Tables and Graphs of Leakage Neutron Spectra from Typical of Shielding Materials with D-T Neutron Source," OKTAVIAN Report A-83-05, Osaka University (1983).

[50] YAMAMOTO J., et al., "Numerical Tables and Graphs of Leakage Neutron Spectra from Slabs of Typical shielding Materials with D-T Neutron Source, " OKTAVIAN Report A-83-05, Osaka University (1983)

[51] TAKAHASHI, A., et al., "Measurements of Tritium Breeding Ratios in Lithium slabs Using Rotating Neutron Source," Proc. of 13th Symp. Conf. on Fusion Technology, Verease, Italy, Sep. 24-28, 1984, Vol.II pp1325-1330, Pergamon Press

[52] IKEDA, Y., et al., "Measurement of High Threshold Activation Cross Sections for 13.5 to 15.0 MeV Neutrons." JAERI-M 85-116, pp106-111 (1985): Proc. Int. Conf. Nucl. Data for Basic and Applied Science, Santa Fe U.S.A., May 13-17 1985, Vol.1 pp175-178

[53] KAWADE, K., et al., Technol., 22 [10] 851-852 (1985)

[54] IKEDA, Y., et al., "Activation Cross Section Measurement of Zr and Cr for 14 MeV Neutrons," JAERI-M 86-125, PP127-129 (1986)

[55] KONNO, C., et al., "Measurements of Activation Cross Sections --- Short-Lived Nuclides --- ," ibid., pp133-135 (1986)

[56] OISHI, K., et al., "Experiments and Analysis of Induced Activities in Concrete Irradiated by 14 MeV Neutorn," Seventh Topical Meeting on the Technology of Fusion Energy, Reno, Nevada, June 15-19, 1986

STATUS OF INTEGRAL EXPERIMENTS
AND BENCHMARK TESTS

(Session D)

Chairman

D.V. MARKOVSKIJ
Union of Soviet Socialist Republics

COMPARATIVE STUDY OF TRITIUM BREEDING CALCULATIONS USING JEF-1 AND ENDF/B-V BASED NUCLEAR DATA LIBRARIES*

E.T. CHENG
GA Technologies Inc.,
San Diego, California,
United States of America

S. PELLONI
Swiss Federal Institute for Reactor Research,
Würenlingen, Switzerland

Abstract

A preliminary comparative neutronics study showed that there are large discrepancies in the $^6Li(n,\alpha)T$ and $^7Li(n,n'\alpha)T$ reaction rates calculated for top-ranking fusion blanket concepts with the JEF-1 and ENDF/B-V-based nuclear data libraries. Detailed analysis is necessary and data testing integral experiments should be employed to identify the deficiencies in these nuclear data evaluations.

RECENT JOINT DEVELOPMENTS IN CROSS-SECTION UNCERTAINTY ANALYSIS AT LOS ALAMOS AND EIR

J.W. DAVIDSON, D.J. DUDZIAK, D.W. MUIR
Los Alamos National Laboratory,
Los Alamos, New Mexico,
United States of America

J. STEPANEK, C.E. HIGGS
Swiss Federal Institute for Reactor Research,
Würenlingen, Switzerland

Abstract

Recent development and future plans for the SENSIBL code along with associated covariance data and cross section libraries are described.

1 Introduction

Since the last IAEA meeting on this topic, the pace of sensitivity and uncertainty analysis studies has slackened relative to those of the 1970s. The paucity of published studies, at least in the U.S.A., has not reflected a diminished interest in or importance of uncertainty analysis. Rather, it is a natural result of the indefinite postponement of plans for a next-generation fusion device burning DT and for a fusion materials irradiation test facility. Without a specific project as a successor to the TFTR, nuclear systems have been of secondary interest in the fusion program. However, recent emphasis on developing an integral experiment capability in support of fusion reactor blanket/shield analysis has led to renewed uncertainty analysis requirements. As for previous fusion reactor studies[1,2,3], a two-dimensional computational capability is required for improved accuracy of the analysis. This same capability will also be required for emerging fusion reactor design studies (e.g., the ETF in the U.S.A. and the NET in Western Europe).

The review of sensitivity and uncertainty methods, codes, and applications presented by one of the authors[4] at the 1978 IAEA meeting will not be updated here. A subsequent review[5] of the status of nuclear data (including covariances), sensitivity and uncertainty methods, and transport methods and codes is still reasonably timely in most respects. In the present paper we will restrict the discussion to recent developments and future plans for the SENSIBL code (the successor to the SENSIT[6] and SENSIT-2D[7] codes), along with associated covariance data and cross-section libraries.

While the original impetus to SENSIT-2D development was the Fusion Engineering Device (FED) project, renewed interest in developing and applying the code has come from ongoing fusion nucleonic integral experiments in Japan and Switzerland. Experiments at the Fusion

* presented in Fusion Technology (1986).

Neutron Source (FNS) facility at JAERI are being analyzed in a cooperative U.S./Japanese effort. A second major program of fusion nucleonics integral experiments is being conducted at the LOTUS facility in Lausanne, Switzerland. There the Lithium Breeding Module (LBM) constructed for the U.S. Electric Power Research Institute is being used by the Swiss Federal Polytechnic School (EPFL) for a series of tritium breeding experiments. An active analysis effort at EPFL, EIR and Los Alamos is underway to compare experimental data with computations using state-of-the-art nucleonic codes and cross-section data. In particular, an intensive joint effort by Los Alamos and EIR is being pursued in uncertainty analysis of the calculated tritium breeding data. These joint efforts are under the umbrella of an agreement of cooperation in fusion reactor nucleonics between EIR and Los Alamos[8,9]. Since 1982 several joint efforts under the agreement have been undertaken, including continued development of cross-section processing (the NJOY code[10]), sensitivity and uncertainty methods (the SENSIBL code), and transport methods (the TRISM code[11]). Some of the Los Alamos effort, especially the development of the COVFILS-2 multigroup covariance library[12], has also been in support of the U.S./Japan cooperation concerning integral experiments at the FNS. Perhaps it is of interest to note in passing that the development of covariance libraries and a two-dimensional sensitivity and uncertainty analysis code is responsive to recommendations of the IAEA Working Group on Neutron Transport and Gamma-ray Production[13].

Briefly, since the 1978 IAEA meeting there has been significant progress in providing both covariance data and multidimensional sensitivity and uncertainty analysis codes. Covariance data are much more prevalent in ENDF/B-V than in earlier evaluated data files, and several multigroup covariance libraries have been produced. Multidimensional sensitivity calculations have been performed by several researchers[2,3,14], using both multigroup deterministic and Monte Carlo transport methods. However, these data and codes are still under development and only now are extensive applications to analyses of integral experiment being undertaken. Perhaps by the next meeting in this series we will have a reservoir of experience and hence intuition regarding the uncertainties in fusion reactor design parameters caused by nuclear data uncertainties.

2 Calculational Methods

The calculational methods used for fusion blanket analysis at EIR and Los Alamos are basically identical and are shown in Figure 1. TRISM is a computer program for solving the two-dimensional neutral particle transport equation in rectangular (X,Y) and cylindrical (R,Z) geometries within a general domain having curved or other nonorthogonal boundaries. The spatial discretization is accomplished using triangular finite elements and discontinuous linear trial functions. TRISM is a follow-on version of TRIDENT-CTR[15] that includes deterministic streaming capabilities[16]. The use of this deterministic streaming option is useful in mitigating the inaccuracies due to the "ray effect" which plague calculations for fusion systems with large internal void regions. The use of triangles in R,Z geometry allows a user to accurately follow curved or irregularly shaped boundaries and material interfaces of toroidal and other fusion system shapes. TRISM maintains all of the capabilities of TRIDENT-CTR but incorporates a completely new user-friendly free-field input format similar to that of ONEDANT[17] and TWODANT[18]. In addition, several new input and edit options have been added. MIXIT[19] is the code for second-step homogenizations and group-ordered library production.

SENSIBL is an improved and accelerated version of SENSIT-2D, which was an extension of the one-dimensional sensitivity code SENSIT[6]. SENSIBL has the capability for cross-section
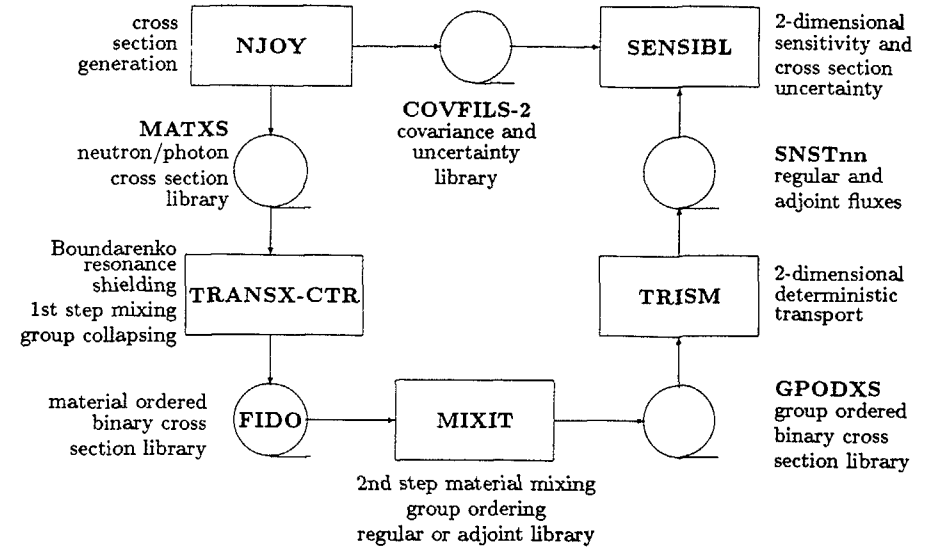
Figure 1: Calculational Scheme

sensitivity and uncertainty analysis, secondary-energy-distribution (SED) sensitivity and uncertainty analysis, and design sensitivity analysis. The algorithms used are based on first-order generalized perturbation theory. The code allows X,Y or R,Z geometry options and accepts group-dependent quadrature sets. It is intended for use with the two-dimensional, multigroup, discrete-ordinates transport code TRISM. The triangular mesh used by TRISM allows unique modelling capabilities which are applicable to fusion reactor configurations, and thus SENSIBL can also analyze these configurations. The forward and adjoint angular fluxes generated by TRISM are required input to SENSIBL. Because the number of angular fluxes can be voluminous, a sophisticated data management scheme was necessary for the code to keep the execution time and memory requirements within reasonable limits. As discussed in the following sections, SENSIBL incorporates a number of recently implemented improvements in SENSIT-2D, intended both to maintain consistency with COVFILS-2 and to add new calculational capabilities.

3 Cross-Section Data Libraries

The general-purpose MATXS8 coupled 187-neutron/24-photon group library, based on ENDF/B-V evaluations, is used as the basic library for transport calculations at Los Alamos. This multigroup library contains 31 isotopes and was produced in October 1983 using the NJOY system. It also contains Los Alamos evaluations for ^{7}Li, ^{182}W, ^{183}W, ^{184}W, and ^{186}W, as well as the ENDF/B-V.2 version of Fe(nat). The temperature is 300 K and a thermal + 1/E + fission +

fusion weighting spectrum is used. For all isotopes heating data (kerma), and for most important isotopes radiation-damage-energy production data, are available.

In the framework of the common Los Alamos/EIR analysis of the LBM experiments at the LOTUS facility[20,21,22], a new multigroup library was constructed at EIR from JEF-1 and the European Fusion File (EFF) using the same 187-neutron group structure. For photon production and interaction cross sections, the Los Alamos 48-group structure was selected. The pointwise neutron and photon files (PENDF) based on JEF-1 evaluations were produced using the June 1983 version of the NJOY system[10,23,24]. This neutron library was generated by obtaining ^{9}Be and ^{7}Li from a preliminary version of EFF developed presently under the leadership of Euratom. Those basic pointwise neutron files were reconstucted for temperatures from 296 to 3000 K, but only 296 K is included in the present groupwise library.

The multigroup library includes vectors for all reaction types, matrices for reactions producing neutrons (including fission), and data pertaining to fission yields of prompt and delayed neutrons. Furthermore, different kinds of gamma-ray production matrices, dosimetry and activation cross sections, as well as heating and damage data, were also processed. The CLAW weighting spectrum (cf. Ref. [24]) was used and a P_5 order of scattering was included. The most important resonances were shielded using the Bondarenko method. The library presently contains the 83 isotopes listed in Ref. [19].

COVFILS-2[12,27] is a library of multigroup neutron cross sections, scattering matrices, and covariances (uncertainties and their correlations). The 14 materials included in the first version of COVFILS-2 are ^{1}H, ^{6}Li, ^{7}Li, ^{9}Be, C(nat), ^{14}N, ^{16}O, ^{23}Na, ^{27}Al, Si(nat), Cr(nat), Fe(nat), Ni(nat), and Pb(nat). COVFILS-2 was produced using various modules of the NJOY nuclear data processing system[10,25]. It is largely based on data evaluations from ENDF/B-V, although some minor corrections and improvements are incorporated. In cases where the covariance evaluation is missing (as in the case of Be) or judged to be inadequate, private Los Alamos evaluations[26] are employed. The 74-group structure[12] was chosen for compatibility with the 187-group MATXS8.

4 Recent Developments

The theoretical foundations of cross-section sensitivity and uncertainty analysis are well documented in the literature (cf. Ref. [4] and other works cited there). For reference during the discussions below, we list here the principal expressions resulting from classical perturbation theory. For our subsequent development, we view the relative covariances (in COVFILS-2, for example) as microscopic cross-section covariances. handling possible spatial variations of the nuclide density within the calculation of the sensitivity of responses to changes in these microscopic data.

Given a set of multigroup microscopic cross-section data, σ_{xm}^g, we are interested in an expression for the standard deviation ΔI of a response I. Examples for I include kerma, displacements per atom (dpa), activation rates, or tritium breeding. The definition of I includes a specification of the spatial region over which the response is to be integrated (the "detector" region). Using the concepts of sensitivity profiles and covariance data, one has a straightforward way to evaluate the uncertainty in I caused by cross-section uncertainties; i.e.,

$$\left[\frac{\Delta I}{I}\right]^2 = \sum_{all\ xmg} \sum_{all\ x'm'g'} P_{xm}^g P_{x'm'}^{g'} \frac{cov(\sigma_{xm}^g, \sigma_{x'm'}^{g'})}{\sigma_{xm}^g \sigma_{x'm'}^{g'}} \tag{1}$$

In this expression σ_{xm}^g represents the interaction cross section for reactions of type x in material m in energy group g, $cov(\sigma_{xm}^g, \sigma_{x'm'}^{g'})$ is the covariance matrix for the indicated multigroup cross sections, and P_{xm}^g is the relative sensitivity profile of response I for cross section σ_{xm}^g, as defined by

$$P_{xm}^g = \frac{\partial I/I}{\partial \sigma_{xm}^g/\sigma_{xm}^g} \tag{2}$$

The relative sensitivity profile clearly can be interpreted as the fractional change in the response per fractional cross-section change. Note that in Eq. (1) the first two factors in each term of the summation (the product of sensitivity profile components) is strictly problem dependent, while the third factor involves only cross sections and their covariances and is hence problem independent.

In 1981 the ENDF/B-V 30-group covariance library COVFILS (cf. Ref. [28]) was produced. It contains multigroup cross sections and covariances for individual absorption and scattering reactions, but does not include group-to-group scattering matrices. In 1984 the COVFILS-2 library became available. This major new 74-group library contains not only cross sections and covariances, but also actual $P_0 - P_3$ scattering matrices for all scattering reactions present in the library, so as to ensure consistency between the library covariances and the scattering matrices used to calculate the corresponding, sensitivity profiles in SENSIBL. The addition of this new matrix data required substantial modifications to SENSIBL, as described below. As a result of both the voluminous covariance data now available and the presence of the large scattering matrices, COVFILS-2 is a rather large file. In order to make its storage and data transfer more manageable, the file was written in a very condensed format called BOXER[27] that compresses the 7.2 million data elements (which would occupy approximately one million card images in uncondensed form) onto about 40 thousand card images. A set of subroutines called COVARD2 was incorporated into SENSIBL in order to retrieve data in BOXER format. Also, a modification to COVFILS-2 was recently made to expand the special index at the beginning of the file. Details of this modification are discussed below in the section describing the incorporation into SENSIBL of the direct term.

One consequence of the detailed covariance data increasingly becoming available for individual scattering levels is that the SED sensitivity capability is rapidly becoming obsolescent. However, both SED and the corresponding angular distribution sensitivity capabilities are maintained in the new code. Miscellaneous changes since the original SENSIT-2D code include adaptation to CRAY computers (on both the CTSS and COS operating systems), improved efficiency of data transfer, improved architecture, and linkage to the TRISM code. The latter capability now allows performing sensitivity and uncertainty analyses on systems with large void streaming regions, which previously could not be accomplished conveniently with deterministic transport codes. Hence, the sensitivity and uncertainty analysis capability is being kept abreast with the state of the art of both deterministic transport methods and covariance libraries. Additional user-oriented improvements were made to the input and output formats. Most significant of these was the preparation of summary tables in the output listing, an addition made imperative by the sheer mass of covariance data for many materials and cross-section types, as well as the increasingly detailed nucleonic models possible with deterministic transport codes.

We now turn back to the sensitivity profile given by Eq. (2). The sensitivity profile for the response I can be expressed as

$$P_{xm}^g = \frac{1}{I}\left\{ R_{xm}^g\ \varphi_m^g - \sigma_{xm}^g\ \chi_m^g + \sum_{\ell=0}^{LMAX} \sum_{g'=g}^{IGM} \sigma_{xm\ell}^{g \to g'}\ \psi_{m\ell}^{gg'} \right\}, \tag{3}$$

The integral of the response over the volume of the "detector" (which may be the entire system) is

$$I = \sum_{\imath\,\epsilon\,det} V_\imath \sum_{all\,g} \phi_{0\imath}^{0g} \sum_{all\,xm} N_{m\imath}\, R_{xm}^g, \qquad (4)$$

where $V_\imath$ is the volume of spatial interval $\imath$, $\phi_{0\imath}^{0g}$ is the scalar flux in group g in interval $\imath$, and $N_{m\imath}$ is the local atomic density of material m in interval $\imath$. The quantity R_{xm}^g appearing in Eqs. (3) and (4) is the "response function," a response-weighted microscopic cross section. If the response of interest is the number of nuclear reactions of type x, then R_{xm}^g is just the microscopic cross section for that reaction. However, if the response of interest is the total nuclear heating, for example, then R_{xm}^g is the partial kerma factor (in units of eV-barns) for reaction x in material m in group g. Other complex responses, such as dpa and total helium production, can also be accommodated using suitable definitions of R_{xm}^g.

The quantities φ_m^g, χ_m^g, and $\psi_{m\ell}^{gg'}$ appearing in Eq. (3) are atom density-weighted, spatial integrals of the flux defined in Eqs. (5), (6), and (7), respectively. The quantity φ_m^g is defined as

$$\varphi_m^g = \sum_{\imath\,\epsilon\,det} N_{m\imath}\, V_\imath\, \phi_{0\imath}^{0g}\,. \qquad (5)$$

In Equation (3), σ_{xm}^g is the microscopic cross section for reaction x in material m and in group g, $\sigma_{xm\ell}^{g\rightarrow g'}$ is the ℓth Legendre moment of the scattering cross section for energy transfers from group g to group g' for a particular reaction type x in material m. In this same equation, χ_m^g is the numerical integral of the product of forward and adjoint angular fluxes over all angles and all spatial intervals, LMAX is the order of scattering, and MM is the number of angular directions:

$$\chi_m^g = 4\pi \sum_{all\,\imath} N_{m\imath}\, V_\imath \sum_{n=1}^{MM} \Phi_{n\imath}^g\, \Phi_{n\imath}^{*g}\, w_n = \sum_{\ell=0}^{LMAX} \psi_{\ell m}^{gg}. \qquad (6)$$

$\Phi_{n\imath}^g$ and $\Phi_{n\imath}^{*g}$ are discrete-ordinates representations of forward and adjoint angular fluxes, respectively, for group g, spatial mesh point $\imath$ and discrete direction n. $\psi_{m\ell}^{gg'}$ is the density-weighted spatial integral of the product of the spherical harmonics expansion for forward and adjoint angular fluxes for material m,

$$\psi_{\ell m}^{gg'} = 4\pi \sum_{all\,\imath} N_{m\imath}\, V_\imath\, (2\ell+1) \sum_{k=0}^{\ell} \phi_{\ell\imath}^{kg}\, \phi_{\ell\imath}^{*kg'}. \qquad (7)$$

Direct Term

The first term in the brackets of Eq. (3) is the direct term. Note that this term non-zero only if reaction x in material m contributes to the detector response function, so that both R_{xm}^g and φ_m^g are non-zero.

Incorporating the direct term into the sensitivity profile calculated by SENSIBL is straightforward, because zone-averaged fluxes such as φ_m^g are readily available from other calculations. The code was modified to accept, as input for each detector zone, the information needed to define the detector response function (and source for the adjoint flux calculation); namely, the material number MAT_d, the reaction number MT_d, and the corresponding material density.

In most cases the value of MT_d corresponds to the MT number of a single reaction in the COVFILS-2 library. Some complexity is introduced by the need to calculate sensitivities for complex reactions which have direct contributions from several different reactions in the library. An example is the $(n, n't)$ reaction in ^{7}Li, $MT_d = 33$. In terms of reaction MTs explicitly present in the library, this reaction is the sum of reaction MTs 853 through 858. An additional problem in ^{7}Li is that reaction numbers in the 851-870 range are used in ENDF/B to specify evaluator-defined groups or "lumps" of reactions[12]. In this case, the MT number alone does not determine whether or not a given reaction contributes to tritium production, for example. Therefore, the COVFILS-2 index was modified to include a list of important detector reactions (MT_d) to which the library MT makes a direct contribution. Logic was also added to SENSIBL to check, when computing the sensitivity for MAT/MT, whether this MT contributes to MT_d. If it does, the cross-section vector from COVFILS-2 is used to calculate the direct term. A diagnostic print was also included in SENSIBL to compare the sum of the cross sections found in this manner (for example, MT 853 through 858) to the input value for the detector response function ($MT_d = 33$).

Indirect Term

The second and the third terms of Eq. (3) comprise the indirect term. These terms are called the "loss" term and the "gain" term, respectively. Note that the indirect term receives contributions only from intervals in which the density $N_{m\imath}$ is non-zero. The indirect term may be derived from the expression for the forward difference approximation, Eq. (36) in Ref. [29] or Eq. (17) in Ref. [30] or Eq. (26) in Ref. [31], considering a two-dimensional geometry and expansion of the scattering into Legendre polynomial series and the flux angular expansions into the series of spherical harmonics.

The quantities χ_m^g and $\psi_{m\ell}^{gg'}$ in Eqs. (6) and (7) each result from performing a material-density-weighted sum over all spatial intervals. In SENSIT-2D the density term $N_{m\imath}$ was, in effect, brought outside these sums. This meant that, in a single computer run, sensitivity profiles, and hence uncertainties, could only be calculated for a single zone (domain of constant $N_{m\imath}$). To study a complex system having many zones, it was necessary to make multiple runs and then quadratically sum the uncertainties from the different runs. This procedure was time consuming and was only approximately valid, as it omitted the contribution to the total uncertainty from cross-zone correlation terms. In SENSIBL, this restriction has been lifted, and a more accurate region-summed total uncertainty is now calculated in a single computer run. With these modifications made, practical SENSIBL calculations were performed, using input fluxes from TRISM calculations of the LOTUS-facility LBM experiment.

In this process another major gain was made. Not only could we include the cross-zone effect, but the calculational time was also significantly reduced. The 11-zone LBM calculation performed in a single run required only as much time as that required previously for each separate one-zone run.

5   Formulation for the Direct Term for Complex Responses

For covariance analysis[32] of complex responses (such as kerma, dpa or helium production, for example) it is necessary to decompose the complex responses into contributions from individual reactions. These "partial" responses are not directly measurable quantities, but they provide the connection between the total response and the ENDF/B covariances, which are provided for individual reaction cross sections.

We recall from the previous section that σ_{xm}^g is the microscopic cross section (in barns) for reaction x in material m in group g. In the case of complex responses, these reactions will contribute the response I with an effect-weighted cross section R_{xm}^g that differs from σ_{xm}^g. The ratio of the two cross sections we denote by E_{xm}^g, so that

$$R_{xm}^g = \sigma_{xm}^g \cdot E_{xm}^g. \tag{8}$$

E_{xm}^g is thus the effectiveness of these particular nuclear reactions in producing the response I. Later in this section particular examples are discussed which may help clarify these points.

Combining Eqs. (4) and (8), we have

$$I = \sum_{i \,\epsilon\, det} V_i \sum_{all\; g} \phi_{0i}^{0g} \sum_{all\; m} N_{mi} \sum_{all\; x} \sigma_{xm}^g\, E_{xm}^g. \tag{9}$$

The cross sections σ are uncertain, and they influence the integral I in Eq. (9) both directly and through their indirect effect on the fluxes ϕ. The quantities E also are nuclear data. are uncertain, and influence I. However, the current ENDF files do not specify the covariances of charged-particle emission spectra, for example. Thus, for the present, we treat the E-parameters as constants. We return to this point at the end of this section.

Direct Term for Complex Reactions

The direct contribution to the sensitivity profile is, from Eqs. (2) and (9)

$$
\begin{aligned}
P_{xm}^g(\text{direct}) &= \frac{\sigma_{xm}^g}{I} \frac{\partial I}{\partial \sigma_{xm}^g}\Big|_{direct} \\
&= \frac{\sigma_{xm}^g}{I} \frac{\partial I}{\partial \sigma_{xm}^g}\Big|_{(\phi_{0i}^{0g}, E_{xm}^g)\; constant}.
\end{aligned} \tag{10}
$$

From Eq. (5) and (9),

$$\frac{\partial I}{\partial \sigma_{xm}^g}\Big|_{(\phi_{0i}^{0g}, E_{xm}^g)\; constant} = \sum_{i \,\epsilon\, det} V_i\, \phi_{0i}^{0g}\, N_{mi}\, E_{xm}^g = \varphi_m^g\, E_{xm}^g. \tag{11}$$

Combining Eqs. (10) and (11),

$$P_{xm}^g(\text{direct}) = \frac{\sigma_{xm}^g}{I} E_{xm}^g\, \varphi_m^g, \tag{12}$$

or

$$P_{xm}^g(\text{direct}) = \frac{R_{xm}^g}{I}\varphi_m^g. \tag{13}$$

Simple Reaction Rates

In order to illustrate the concepts of "response functions" and "effectiveness," we now consider some specific examples of integral responses. As our first example, we consider a "simple" response, namely, the total number of n,γ events in a specified region. From Eq. (5), we see that φ_m^g will be non-zero only for materials which are present in at least some intervals i of the detector region. Considering only these contributing materials, the effectiveness E_{xm}^g will be unity (for all groups) if x is the reaction index of the n,γ reaction and zero if x is any other reaction. Thus, R_{xm}^g will be equal to σ_{xm}^g or zero, depending on x.

Nuclear Heating

In the case of nuclear heating, the response cross section R_{xm}^g is just the partial kerma due to reaction x in material m in group g. The effectiveness E_{xm}^g is, in this case, the average net charged-particle energy deposited per reaction.

Displacements Per Atom

In the case of dpa, the effectiveness E_{xm}^g is the average number of atoms displaced from their normal lattice positions (due mainly to interactions of the primary recoil nucleus with the lattice) per reaction of type x in material m in group g. Methods for calculating both partial kerma factors and partial dpa-production cross sections are discussed in Ref. [22].

Helium Production

The reason that helium production differs from ordinary reaction rates is that a "multiplicity" is involved. In ENDF/B-V ^{12}C, for example, all inelastic levels above the first one decay via 3α emission. Thus,

$$\sigma(n, x\alpha)\big|_{^{12}C} = \sigma_{107} + 3\cdot(\sigma_{52} + \ldots + \sigma_{91}) \tag{14}$$

The multiplicity, then, is 1.0 for MT107 and 3.0 for reactions MT52 through MT91. In this case the effectiveness E_{xm}^g is just the multiplicity. The multiplicities for helium production are normally energy-independent integers, although there are exceptions. In ^{7}Li (ENDF/B-V.2) for example, covariances are given for the total $(n, 2n)$ reaction in MT851. This cross section is the sum of the $(n, 2n)$ and $(n, 2n\alpha d)$ reactions. The helium yield per "reaction" here is clearly energy-dependent. As in the case of kerma and dpa, NJOY can provide the separate cross sections for $(n, 2n\alpha d)$ and for MT851, and the group-dependent helium-production multiplicities (E_{xm}^g) can be obtained by division.

It is worth noting that total helium-production cross sections, H_m^g summed over all reactions, are provided directly in ENDF/B-V on Tape 533, along with "integral" covariances, such as

$$\text{cov}(H_m^g, H_m^{g'}) \tag{15}$$

These cross sections and covariances are suitable for thin foil reactor-dosimetry purposes, but they are not very useful for the analysis of fusion-reactor integral experiments, where the dosimetry foil and the transport medium are often made of the same material. When covariance information is presented in "integral" form, as in Eq. (15), the correlation between the individual helium-producing reactions and the reactions important to neutron transport is lost. On the other hand, combining sensitivities and covariances for separate reactions, using Eq. (1), preserves this correlation information.

Mechanics

To perform an uncertainty analysis of a complex reaction, it is clear from Eq. (3) that one needs access to the response cross section R_{xm}^g (or to the E_{xm}^g) for each COVFILS-2 reaction for the materials of interest. Because this information is not present on COVFILS-2, it must be supplied in the user input to SENSIBL. In the case of kerma or dpa, it would be convenient to supply the actual cross sections R_{xm}^g, thereby eliminating the need for a "hand" calculation of E_{xm}^g. For helium production, a mixed strategy is needed. For most reactions in most materials,

an energy - independent integer multiplier would be sufficient for constructing R^g_{xm} from σ^g_{xm}, as in the ^{12}C example above. For ^{7}Li, on the other hand, one would like to enter the $(n, 2n\alpha d)$ cross section (R^g_{xm}) from input, just as in the case of kerma. The capability to input a general, energy - dependent multiplier does not seem necessary.

E-parameter Covariances

Our final remarks concern a possible future generalization of this approach. Up to this point, we have considered only cross-section covariances, as are presently contained in COVFILS-2. It may be possible at a later date to add covariances of the effectiveness parameters, E^g_{xm}. If and when this occurs, it will become of interest to calculate the relative sensitivity to these E-parameters, as well as cross sections. Luckily, this will not complicate the coding of SENSIBL very much at all. Examination of Eq. (9) reveals that the direct effect of a fractional change in E^g_{xm} is numerically *equal* to the direct effect of changing σ^g_{xm}.

Since the E-parameters do not effect the neutron flux, there is no indirect term, and the relative sensitivity is obtained immediately from Eq. (13). Only a very few lines of code would be affected in adding an E-parameter sensitivity capability to SENSIBL.

6 Future Plans for SENSIBL

Plans for future work under the Los Alamos/EIR Cooperative Agreement include several tasks related to sensitivity and uncertainty analysis. Of immediate importance is the devising of a simple test case for SENSIBL code verification. Because of the lack of any detailed confirming calculations of uncertainty analyses employing the COVFILS-2 data, there is no experience to date upon which to base "intuitive" judgements on the reasonableness of results. Efforts are now underway to create an exceptionally simple covariance library and a corresponding two-material (^{1}H and ^{6}Li), two-region nucleonic model which would facilitate hand calculations for comparison purposes.

A study is also being conducted of the feasibility of putting multigroup covariance data into future MATXS libraries. One motivation for this study is the requirement to perform sensitivity studies for systems in which temperature dependence and self shielding of the cross sections is required. Both are presently available from the MATXS libraries via the TRANSX-CTR code[33], but not from the COVFILS-2 library. Provision of a MATXS library with the covariance multigroup data incorporated would permit a more automated approach to the sensitivity and uncertainty analysis of complex responses than is presently possible.

A group collapse routine for the 74-group COVFILS-2 library could be added to TRANSX-CTR at the same time. A collapse capability would allow sensitivity and uncertainty analyses making direct use of transport calculations in, for example, the Los Alamos 30-group structure, which has been employed in some recent analyses of the Japanese FNS blanket experiments.

Another feature expected to be incorporated into SENSIBL in the near future is a one-dimensional option, where the linkage would be to standard flux file output from the ONEDANT code[17]. Thus, one code would serve both one- and two-dimensional requirements.

Also investigated will be the use of CCCC standard interface files[34], such as the ONEDANT and TWODANT files NDXSRF, ZNATDN, and GEODST for nuclide densities, subzone nuclide atomic densities, and geometry description, respectively. TRISM employs a CCCC-like interface file (CCCC standard files are not defined for the TRISM banded, triangular mesh) called GEOMTY for geometry description while CCCC-like versions of NDXSRF and ZNATDN will require further development. These could lead to considerable simplification of SENSIBL input.

References

[1] M.J. Embrechts, "Two-Dimensional Cross-Section Sensitivity and Uncertainty Analysis for Fusion Reactor Blankets," Los Alamos National Laboratory report LA-9232-T (1982).

[2] M. J. Embrechts, W. T. Urban and Donald J. Dudziak, "Two-Dimensional Cross-section and SED Uncertainty Analysis for the Fusion Engineering Device (FED)," Proceedings of the Intl. Conf. Nuclear Data for Science and Technology, Antwerp, Belgium, 6-10 September 1982.

[3] Mark J. Embrechts, D. J. Dudziak and W. T. Urban, "Development of the Two-Dimensional Cross-section Sensitivity and Uncertainty Analysis Code SENSIT-2D with Applications to the FED," Proceedings of the 5th Am. Nucl. Soc. Topical Meeting on the Technology of Fusion Energy, Knoxville, Tenn., 26-28 April 1983.

[4] Donald J. Dudziak, "Cross-section Sensitivity and Uncertainty Analysis for Fusion Reactors (A Review)," Proceedings of the IAEA Advisory Group Meeting on Nuclear Data for Fusion Reactor Technology, Vienna, Austria, 11-15 December 1978 (IAEA-TEC-DOC-223).

[5] Donald J. Dudziak and Phillip G. Young, "Review of New Developments in Fusion Reactor Nucleonics," Proceedings of the 4th Am. Nucl. Soc. Topical Meeting on the Technology of Controlled Nuclear Fusion, King of Prussia, Penn., 14-17 October 1980.

[6] S.A.W. Gerstl, "SENSIT: A Cross-Section and Design Sensitivity and Uncertainity Analysis Code," Los Alamos Scientific Laboratory report LA-8498-MS (1981).

[7] M. J. Embrechts, "SENSIT-2D: A Two-Dimensional Cross- Section Sensitivity and Uncertainty Analysis Code," Los Alamos National Laboratory report LA-9515-MS (1982).

[8] D.J. Dudziak and J. Stepanek, "Status Report: LANL-EIR Co-operative Work in the Field of Nucleonics and Particle Transport in Fusion Reactors," for the period 1 January 1983 to 30 June 1984, EIR Bericht Nr. 542 and Los Alamos National Laboratory report LA-UR-84-3962 (1984).

[9] D.J. Dudziak and J. Stepanek, "Status Report: LANL-EIR Co-operative Work in the Field of Nucleonics and Particle Transport in Fusion Reactors," for the period 1 July 1984 to 30 June 1986 (to be published).

[10] R. E. MacFarlane, D. W. Muir and R. M. Boicourt, "The NJOY Nuclear Data Processing System, Vol. I: User's Manual," Los Alamos National Laboratory report LA-9303-M (1982).

[11] J. W. Davidson, B. A. Clark, D. R. Marr, T. J. Seed, J. Stepanek and C. E. Higgs, " TRISM: A Two-Dimensional Finite-Element Discrete-Ordinates Transport Code," Los Alamos National Laboratory report (draft, 1986).

[12] D. W. Muir, "COVFILS-2: Neutron Data and Covariances for Sensitivity and Uncertainty Analysis," *Fus. Techn.* 10 (3), Part 2B, 1461 (November 1986).

[13] Report of Working Group on Neutron Transport and Gamma-Ray Production, (D. J. Dudziak, Editor), Proceedings of the IAEA Advisory Group Meeting on Nuclear Data for Fusion Reactor Technology, ibid.

[14] Y. Seki. R. T. Santoro, E. M. Oblow and J. L. Lucius, "Comparison of One- and Two-Dimensional Cross-Section Sensitivity Calculations for a Fusion Reactor Shielding Experiment," technical note, *Nuc. Sci. Eng.* 73, 87 (1980).

[15] T. J. Seed, "TRIDENT-CTR: A Two-Dimensional Transport Code for CTR Applications." Proceedings of the Third Topical Meeting on the Technology of Controlled Nuclear Fusion, 9-11 May 1978, Santa Fe, NM, Vol. I, p. 844. Also available as Los Alamos Scientific Laboratory report LA-UR-78-1228 (1978).

[16] B.A. Clark, "The Development and Application of the Discrete Ordinates-Transfer Matrix Hybrid Method for Deterministic Streaming Calculations," Los Alamos National Laboratory report LA-9357-T (1982).

[17] R.D. O'Dell, F.W. Brinkley Jr., and D.R. Marr. "Users Manual for ONEDANT: A Code Package for One-Dimensional, Diffusion-Accelerated, Neutral Particle Transport," Los Alamos National Laboratory report LA-9184-M (1982).

[18] R.E. Alcouffe, F.W. Brinkley Jr., D.R. Marr and R.D. O'Dell, "User's Guide for TWODANT: A Code Package for Two-Dimensional, Diffusion-Accelerated, Neutral Particle Transport," Los Alamos National Laboratory report LA-10049-M (March 1984).

[19] F.W. Brinkley Jr., "MIXIT," Los Alamos Scientific Laboratory internal memo (1980).

[20] J. Stepanek, J.W. Davidson, D.J. Dudziak, C.E. Higgs and S. Pelloni, "Analysis of the LBM Experiments at LOTUS," *Fus. Techn.* 10 (3), Part 2B, 940 (November 1986).

[21] "TFTR Lithium Blanket Module Program. Final Design Report, LBM Neutronics Analysis," GA-A17467, Vol. V (1983).

[22] P.-A. Haldy, A. Kumar, C. Schraoui, S. Azam, D.V.S. Ramakrishnamand, and J.-P. Schneeberger, "Experimental Program at the LOTUS Facility," *Fus. Techn.* 10 (3), Part 2B, 931 (November 1986).

[23] R.E. MacFarlane, D.W. Muir, R.M. Boicourt, "The NJOY Nuclear Data Processing System, Volume II: The NJOY, RECONR, BROADR, HEATR, and THERMR Modules," Los Alamos National Laboratory report LA-9303-M Vol. II (ENDF-324) (1982).

[24] R.E. MacFarlane and D.W. Muir, "The NJOY Nuclear Data Processing System, Volume III: The GROUPR, GAMINR, and the MODER Modules," Los Alamos National Laboratory report LA-9303-M, Vol. III (ENDF-324) (to be published in 1987).

[25] D.W. Muir and R.E. MacFarlane. "The NJOY Nuclear Data Processing System, Volume IV: The ERRORR and COVR Modules," Los Alamos National Laboratory report LA-9303-M, Vol. IV (ENDF-324) (December 1985).

[26] P.G. Young and L. Stewart. "Evaluated Data for $n+{}^9$Be Reactions," Los Alamos Scientific Laboratory report LA-7932-MS (ENDF-283) (1979).

[27] D.W. Muir, "The COVFILS-2 Library of Neutron Cross Section and Covariances for Sensitivity and Uncertainity Analysis." pp. 38-42 in Los Alamos National Laboratory report LA-10288-PR (1984).

[28] D.W. Muir and R.J. Labauve, "COVFILS: A 30-Group Covariance Library Based on ENDF/B-V," Los Alamos National Laboratory report LA-9733-MS (ENDF-306) (1981).

[29] S.A.W. Gerstl, "The Application of Perturbation Methods to Shield and Blanket Design Sensitivity Analyses," Argonne National Laboratory Report AP/CTR/TM-25 or FRA-TM-67 (October 1974).

[30] D.E. Bartine, E.M. Oblow and F.R. Mynatt, "Radiation Transport Cross Section Analysis – A General Approach Illustrated for a Thermonuclear Source in Air," *Nucl. Sci. Eng.* 55, 147 (1974).

[31] S.A.W. Gerstl and W.M. Stacey Jr., " A Class of Second-Order Approximate Formulations of Deep Penetration Radiation Transport Problems," *Nucl. Sci. Eng.* 51, 339, (1973).

[32] D.W. Muir, "The Direct Term for Simple Reaction Rates and for Complex Responses," Los Alamos National Laboratory memorandum T-2-M-1779 (1986).

[33] R.E. MacFarlane, "TRANSX-CTR: A Code for Interfacing MATXS Cross-Section Libraries to Nuclear Transport Codes for Fusion System Analysis," LA-9862-MS (1984).

[34] R.D. O'Dell, "Standard Interface Files and Procedures for Reactor Physics Codes, Version IV," Los Alamos National Laboratory report LA-6941-MS (1977).

LiF BENCHMARK EXPERIMENTS AND DATA ANALYSIS

M.C. SCOTT
Department of Physics,
University of Birmingham,
Birmingham, United Kingdom

Abstract

Two sets of fusion reactor breeder-blanket integral experiments based on lithium fluoride are reviewed, namely those at the University of Birmingham and at the Tokyo Institute of Technology. The measurement procedures are outlined and the results obtained discussed, both in general terms and with respect to possible data adjustment and evaluation. Finally, some general comments are made on the utility and limitations of such measurements.

1. INTRODUCTION

In order to predict both the neutron and thermal-hydraulic behaviour of fission and fusion reactors an extensive range of neutron-nuclear data is required. There are two componants to this problem, the first being the range of materials used in their construction, and the second the large energy range over which neutron data is required, from MeV down to meV. The high cost of providing the necessary differential data is such that ways of identifying elements, energy regions, or reaction types where the data is uncertain can be extremely valuable in reducing both the cost and time scale involved in improving analytical procedures.

The integral experiment, where neutrons interact in assemblies large enough to subject then to a large number of collisions, has grown out of this requirement. Although frequently geometrically, or elementally, simple - in order to try and reduce uncertainties in interpretation - they may be analysed using the same computational codes and data sets as the larger structures under study, and hence comparison of theory and experiment can provide an overall check of computational procedures, or a basis for data adjustment.

However, although the principle is an attractive one, in practice such experiments may be of limited value, for a number of reasons. The first is that, unless the relationship between the data concerned and the parameters of interest are the same, or very similar, for the integral assembly and the structure under study (eg. a fission reactor core or a fusion reactor breeder blanket) then any data evaluation or adjustment based on it may concentrate on the wrong energy regions. In other words, the sensitivity profiles of the two systems for the reactions of interest need to be as closely matched as possible for the integral experiments to be of maximum utility (Bartino et al 1974 and Oblow et al, 1973).

A second possible reason why such experiments may be difficult to interpret lies in the problem of identifying and measuring integral parameters of interest. In fission reactors the fission rate itself is an easily identified parameter which can be readily measured using activation procedures to a few percent or better. In fusion reactors, on the other hand, the tritium breeding rate from $^7Li(n,n'\alpha)^3H$ and $^6Li(n,\alpha)^3H$ reactions is of similar importance, yet measurement is much more difficult because the only active reaction product is tritium, which has a long half life (12.3 y) and emits only very low energy (18 keV) beta particles. Thus, irradiation fluences have to be very high to get acceptable statistical precision in samples of lithium compounds throughout a large integral assembly. In addition, since the measurement is of an integral quantity, the interpretation of differences between measurement and prediction may be ambiguous.

One parameter which is frequently measured is the neutron spectrum. Here the difficulty lies in the nature of the measurement itself: the responses of all neutron spectrometers suitable for making measurements within an assembly, ie, of measuring the scaler flux, are complex, and relating the measured signals to the neutron spectrum - the unfolding process - is one which poses difficulties, not least because of the nature of the spectrum involved with D-T neutron sources.

In this paper we shall examine one set of integral fusion reactor breeder blanket experiments only, namely those involving the use of LiF as the lithium compound. Lithium fluoride is one constituent of FLIBE (LiF Be F$_2$) which was one of the materials proposed in the early days of fusion reactor interest as a combined tritium breeding medium and coolant. Although it subsequently lost favour to materials like lithium-lead eutectic, the fact that it is non-metallic can offer significant advantages, and some interest is reviving in its potential. Measurements on LiF assemblies have been conducted at only two centres, as far as the author is aware, namely at the Tokyo Institute of Technology and at the Department of Physics, University of Birmingham.

2. THE EXPERIMENTAL PROGRAMMES

2.1 At the University of Birmingham

(a) The integral assemblies

Three different experimental assemblies have been investigated in detail since this programme started in 1973. The first was intended to look at LiF alone in a simple, ie. spherically symmetric, geometry, and consisted of a spherical annulus of LiF with inner and outer diameters of 0.51 and 1.25m respectively (Perkins 1979, Perkins et al 1981). The tritium target was located at the centre of the sphere and the neutron yield was monitored using the associated particle technique (Evans et al 1979). Thin stainless steel re-entrant tubes allowed neutron spectra to be measured at different angles with respect to the incident deuterium beam direction and at any radius (Fig. 1) The space not occupied by the detectors was filled with LiF powder. A specially constructed vibro-compacting rig was used to ensure the uniformity of the LiF powder
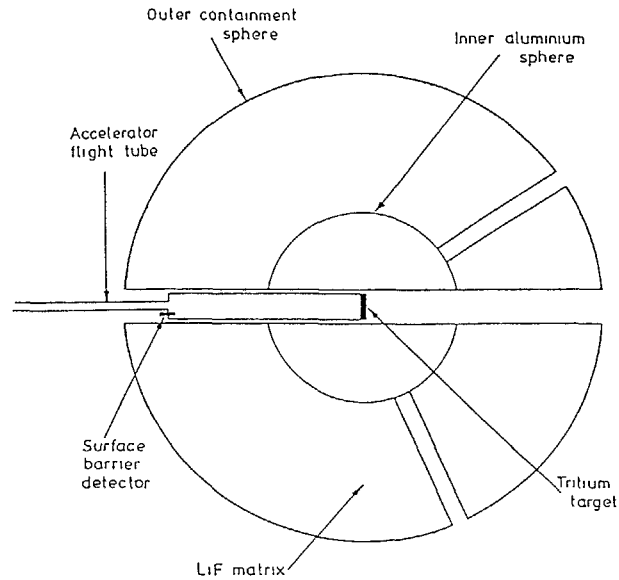
FIG 1

Cross section of the first Birmingham spherical LiF assembly.

FIG 2

Schematic diagram of the Birmingham slab assembly.

in the sphere, and the packing density was checked using a gamma ray transmission technique. The Dynamitron accelerator used was run with 750 keV D_3^+ ions, which produced three 250 keV deuterons on striking the tritium target.

In order to allow an investigation into the effect of beryllium multiplying/spectral softening regions this assembly was then modified by Koohi-Fayegh (1980) to allow spherical beryllium shells to be put round the target, and the inner diameter was increased, to 0.625 m. In both cases the LiF used was slightly depleted in ^{6}Li (5%), about 800 kg of material being used. In addition to making measurements on combined beryllium-LiF assemblies, transmission measurements were also made on spherical beryllium shells of different thicknesses.

The use of spherical assemblies had two disadvantages. The first was the that with 250 keV deuterons (the lowest energy possible on the Dynamitron accelerator) the neutrons are neither monoenergetic nor isotropic, requiring the development of special techniques to allow comparison to be made between 1-dimensional S_n code calculations and measurement. The second was the practical difficulty of incorporating different combinations of first wall materials, spectral softeners and

225

outer reflectors. Since the problem of interpretation using 1-dimensional S_n codes could best be circumvented by using a Monte Carlo code, the obvious step was to go from a spherical assembly to one of slabs, which then allowed greater experimental flexibility, as well as reducing the amount of each material required. The assembly was therefore rebuilt as six 1.0 × 1.0 × 0.15 m aluminium clad slabs (Fig. 2), the neutron source being external (Naylor, 1986).

In all cases the assemblies were placed on a gridded floor at the centre of a low scatter cell of dimensions 8.5 × 7.8 × 8.0m high. The effect of room return neutrons was determined by calculation, using both ANISN (Naylor, 1986) and MORSE (Malsbury, 1986) on a spherical concrete shell with a central D-T source. The main room returns were of low energy (< 1 keV), and the effect at all measurement points except at the back of the assembly was negligible, because of the shielding provided by the assembly itself.

(b) Measurement Procedures

In order to make neutron spectrum measurements from 14 MeV down to 1 MeV or so a special 1.5 cc cylindrical NE213 spectrometer was developed.

(Perkins and Scott, 1979), attached directly to a small (1.25 cm diameter) photomultiplier tube and surrounded by thin stainless steel encapsulation. The anisotrophy of response and perturbation produced by this detector was investigated by Underwood (1979a,b) and found to produce effects which were small compared to other measurement uncertainties (<0.5%). Unfolding the neutron spectra was originally accomplished using a differential unfolding code after the alpha particles from the $^{12}C(n,\alpha)$ and $^{12}C(n,3\alpha)$ reactions had been stripped off the two parameter response surface (pulse shape and pulse height), leaving only the proton recoil response (Perkins and Scott, 1979). However, in subsequent work the matrix unfolding code FERDOR was used, with response functions calculated using O5S but with the ^{12}C (n,3α) reaction modelled in more detail, to give better agreement between measured and predicted response functions (Koohi-Fayegh, 1980 and Scott et al, 1980).

To extend the neutron energy range down to 40 keV or so, proton recoil gas-proportional counters were also used in the first absolute measurement series (Evans, 1978), and considerable effort went into their calibration (Brierley, 1977, Brierley et al 1982). However, although some measurements were reported (Perkins et al 1981) the problem encountered was that the production of charged particles by (n,p) and (n,α) reactions is the stainless-steel walls of the counters produced significant perturbation of the detector response function (Petler and Scott, 1985), introducing uncertainties in the differential unfolding technique used, SPEC4 (Benjamin et al 1968).

Although the subsequent development of a lead-lined proton recoil counter reduced the perturbation produced by charged particles from the detector walls significantly (Sajo-Bohus, 1985) no further integral spectrum measurements in this energy range have yet been attempted.

In addition to neutron spectrum measurements, the slab assembly was also used to make direct measurements of tritium production from the ^6Li and ^7Li reactions (Naylor, 1986). For this purpose, compressed pellets of LiOH were used, of either natural lithium or 99.9% ^7Li. Each pellet weighed ~ 1g and was enclosed in a case of the same material, to compensate for tritium loss from the surface (Swinhoe, 1979). One of each assembly of pellet and case was sealed in an aluminium container for the measurement. Early trials indicated that tritium diffusing through the LiF assembly was strongly absorbed by the pellets, the absorbed tritium signal exceeding that of tritium produced in the pellet. The aluminium containers were therefore constructed with interference fitting lids, and assembled by immersing the outer can in liquid nitrogen, to provide a tight fit at room temperature. The efficiency of this seal was tested by exposing the container to tritium gas, no uptake in the enclosed LiOH pellets being observed.

Tritium assay of the irradiated pellets was performed by liquid scintillation counting, using the technique developed by Dierckx, 1973, as described by Swinhoe, 1979. Measurements were made at the centre of each of the six slabs, along the axis defined by the incident deuteron beam, both on the bare assembly and on one with a 15.5 cm thick graphite reflector at the rear.

Because high beam currents were required, a special high yield rotating target assembly was used in conjunction with a 150 kV linear accelerator, on which associated particle monitoring was not possible. For this reason, a ^{238}U fission chamber was used to monitor the target yield, having been calibrated absolutely using the associated particle technique. A correction of 16% was made for the additional fast neutron flux at the monitor reflected from the integral assemblies.

As indicated earlier, getting sufficient activity in such pellets, particularly at the back of the assembly, requires very long irradiation times – typically several days at beam currents of the order of mA. Consequently, attempts were made to find a way of monitoring spectral changes more simply, not to substitute for more accurate methods but as an adjunct to them, particularly in complex geometries, where modelling may be difficult. Ideally, one wants to use reactions having the same cross sections shapes as ^6Li and ^7Li for tritium production, ie. ones having matched sensitivities to spectral changes. Such reactions are, of course, not available. However, if one identified the main characteristics of the two reactions – that ^6Li has a high thermal cross section with a 1/v behaviour, and ^7Li has a reaction threshold of 2.82 MeV – then the ^{235}U and ^{232}Th fission cross sections bear some resemblances to them. It was therefore felt that the $^{235}U/^{232}Th$ reaction rate ratio could form the basis for an integral evaluation of computational procedures, not least because the cross sections are generally well known. The main disadvantage of ^{235}U is, however, that the fission cross section increases in the MeV region, because of second chance fission, so that it has a greater relative response to the higher energy neutrons than ^6Li does. In this respect, a BF$_3$ (or ^3He) counter would be a better choice in future work.

In order to explore these ideas, $^{235}U/^{232}Th$ reaction rate ratios were measured down the axis of several different assemblies.

2.2   At the Tokyo Institute of Technology

(a) The integral assemblies

The integral assemblies used were constructed from unclad ceramic blocks of LiF each measuring 10 × 10 × 2.5 cm, with normal lithium isotopic composition (7.593% ^6Li). Detectors were housed in 3 cm diameter holes, sandwiched between cylindrical plugs of LiF ceramic to minimise voids. The bare integral assembly consisted of 500 blocks, making a cube 0.5 × 0.5 × 0.5 m (Lee et al 1985, Sekimoto et al, 1985). Measurements were made with an external D-T source at the mid-point of the front face, at distances of 16.4, 26.4 and 31.4 cm from the front face along the central axis.

In order to investigate the influence of having a graphite reflector, the same ceramic blocks were reconfigured to make an assembly 0.5 × 0.5 × 0.4m, having a 20 cm graphite reflector on all sides except the front (0.5 × 0.5m) face (Sekimoto and Lee, 1986); the arrangement is shown in Fig. 3. For both assemblies the neutron source used was a Phillips PW-5320 generator producing 110 keV deuterons onto a tritium
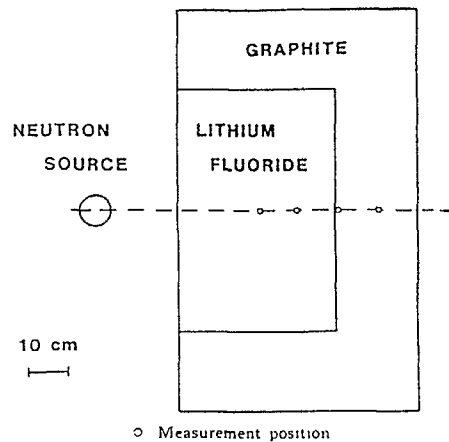
FIG 3

Experimental layout of the Tokyo graphite reflected LiF
assembly.

target, from which the neutron yield was measured to be almost isotropic,
and the assemblies were mounted on a 5 mm thick iron plate either 1.10 m
or 1.50 m above the floor. The walls and ceiling were all 3m or more from
the target (Sekimoto et al, 1984) and the effect of room returns was
determined by using a 50 cm^2 × 50 cm long iron shadow-bar between the
neutron source and the detector. The room return background was found to
be 25% at 1 light unit (∼ 2 MeV neutrons) and 0.6% at 6 light units
(∼ 10 MeV), the neutron energy equivalents given being estimated assuming
the detector used to have a similar light output curve to the Birmingham
one.

(b) Measurement Procedures

In order to measure neutron spectra in their assemblies the Tokyo
group developed a special 2.5 cc spherical NE213 scintillator cell
attached to a 0.9 cm diameter, 1 m long light guide of polymethylmet -
acrylate via a specially shaped light coupler, the whole assembly being
encapsulated in thin stainless steel (Sekimoto et al, 1981). A spherical
cell was chosen in order to minimise any anisotropy of the response
function, which was shown to be small (Sekimoto et al 1984). Like the
Birmingham group, pulse shape discrimination was used in conjunction with
a two parameter data acquisition system in order to separate neutron and
gamma induced events off-line before unfolding.

The perturbation produced by the detector and its light guide in a
0.1 m diameter sphere of graphite was examined using the one-dimensional
transport code ANISN in the forward and adjoint modes in conjunction with
the GICX40 cross section data set (Sekimoto et al, 1982). The conclusion

drawn was that the main perturbation was produced by the void around the
detector and by its stainless steel encapsulation: the perturbations
caused by the scintillator and light guide were similar, and less than 3%
between 2 and 15 MeV, whereas the total perturbation varied from -10%, at
7 MeV, to + 6%, at 14 MeV.

The accelerator used incorporated a sealed tritium source, so that
associated particle monitoring could not be used. Consequently,
measurement of the neutron source intensity at the surface of the assembly
was accomplished using the same miniature scintillator as was used for the
spectrum measurements; such a technique reduces normalisation
uncertainties, because the efficiency of the detector used was the same
for both the spectrum measurement and the source yield determination
(Sekimoto et al, 1985). A BF_3 long counter was used to provide the
inter-normalisation between different runs.

The matrix unfolding code FERDOR was used to determine the neutron
spectra from the measured detector responses, the detector response
functions being generated using the O5S Monte Carlo program in conjunction
with the ENDF/B-IV cross section set with the carbon data modified (Lee et
al, 1985). It was noted, however, that FERDOR frequently yields
oscillatory solutions, the amplitude of which increases at lower energies;
this behaviour is exacerbated by the fact that the neutron spectrum is
dominated by the 14 MeV peak at all measurement positions. Two approaches
were used to try and minimise this. One was to use a Gaussian smoothing
width determined from FORIST (Johnson, 1980), whilst the other was to
develop a new code which operated on the logarithm of the detector
response (Sekimoto, 1984). This latter approach had the effect of
contraining the solution to provide positive fluxes only, unlike FERDOR,
which has no such constraints.

3. COMPARISON OF MEASUREMENTS AND PREDICTION

3.1 On the Birmingham assemblies

(a) LiF sphere

Neutron spectrum measurements between 0.5 and 16 MeV were made at 0
and 75° to the incident deuteron direction, and at five positions. These
measurements are given in detail in Perkins, 1979, and summarised in
Perkins et al, 1981, which also discusses possible sources of systematic
error: the overall systematic error in normalisation of the flux per
source neutron arising from source yield uncertainties was estimated to be
± 5%.

The predicted spectrum in the assembly was obtained using a P_7S_{16}
ANISN calculation in conjunction with the ENDF/B-IV data set with 0.5 MeV
group widths above 10 MeV. However, because of the variation of neutron
source energy with angle, it was necessary to determine the effective
source energy. Comparing ANISN with Monte Carlo calculations using MORSE
with the same data set showed that the appropriate source energy to use
was that of the neutrons emitted at the measurement angle (Underwood
1978).

Examples of the comparison between measurement and calculation are shown in Figs 4 to 6, and Fig 6 also shows the differences obtained in unfolding using a differential code and FERDOR. We see from all these results that the source peak is modelled extremely well down to 10 MeV or so. However, below this energy the FERDOR unfolded spectrum is consistantly below the calculated one. We also note that the 14 MeV peak is at least an order of magnitude greater than the flux at lower energies.
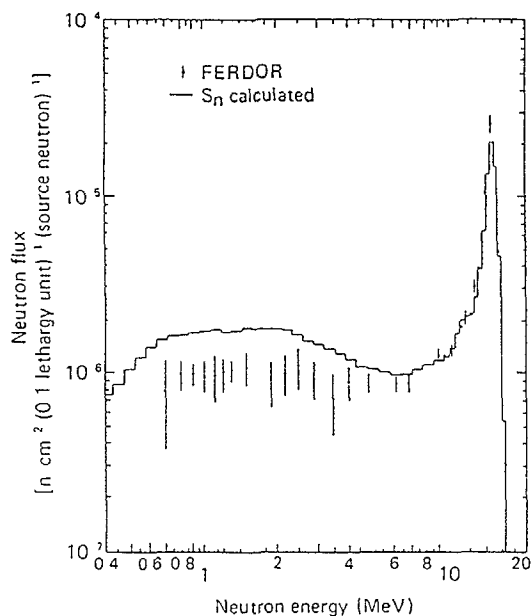

FIG 4

Scintillation counter measurement of the neutron spectrum at 0 deg and r = 44.7 cm in the Birmingham LiF sphere.

As an example of the proton recoil measurements, the results obtained by Brierley (1977) in a 1.25 m diameter sphere of LiF are shown in Figs 7 and 8, for measurement positions 27 and 37 cm from a central D-T neutron source. This source was obtained using 3rd harmonic (2.2 MeV) deuterons on the Nuffield Cyclotron in conjunction with an aluminium degrador foil, to reduce the deuteron energy and hence source anisotropy and energy spread. Three different detectors were used to cover the energy range, and the measured spectra were normalised to the predicted ones via the average fluxes in the regions from 303 to 365 keV, 0.8 to 1.0 MeV and 1.0 to 1.5 MeV. (This assembly has not been discussed earlier because it was only used for one set of measurements and absolute flux normalisation per source neutron was very difficult). From the comparison with ANISN
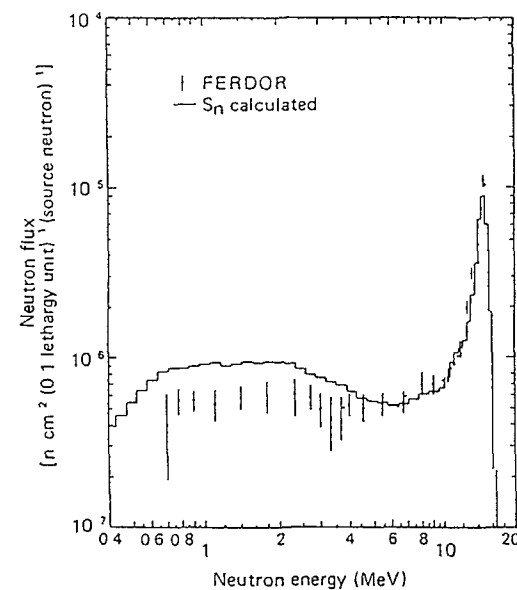
FIG 5

Scintillation counter measurement of the neutron spectrum at 0 deg and r = 54.8 cm in the Birmingham LiF sphere.
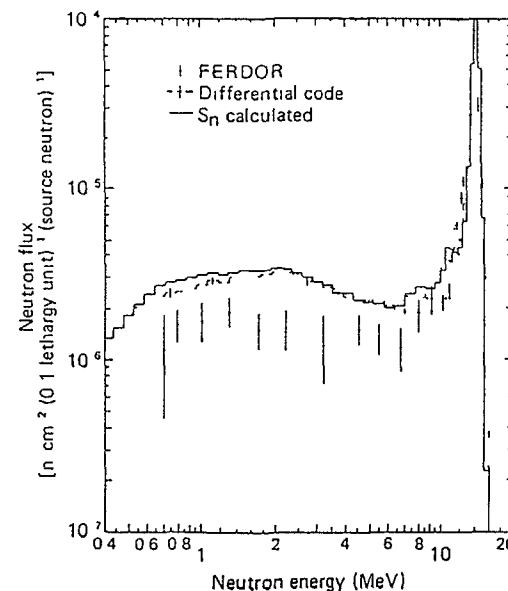
FIG 6

Scintillation counter measurement of the neutron spectrum at 75 deg and r = 66.4 cm in the Birmingham LiF sphere.

**** Hydrogen-argon counter
---- 10 Atm hydrogen counter
.... 2.5 Atm hydrogen counter
—— Calculated neutron flux (ANISN)
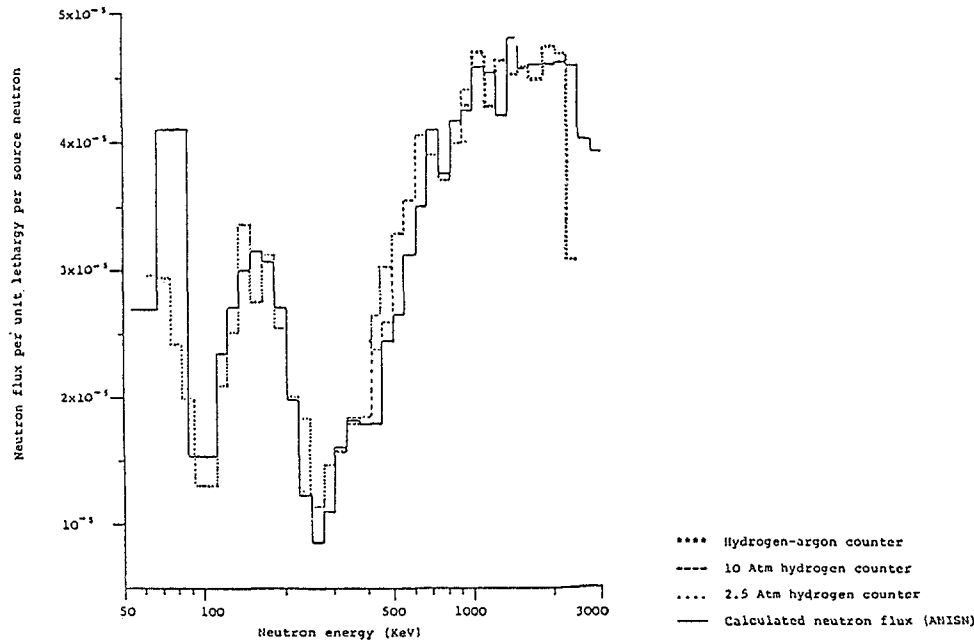
FIG.7.

Neutron spectrum at 27 cm in a LiF sphere.

xxxx Hydrogen-argon counter
---- 10 Atm hydrogen counter
.... 2.5 Atm hydrogen counter
—— Calculated neutron spectrum (ANISN)
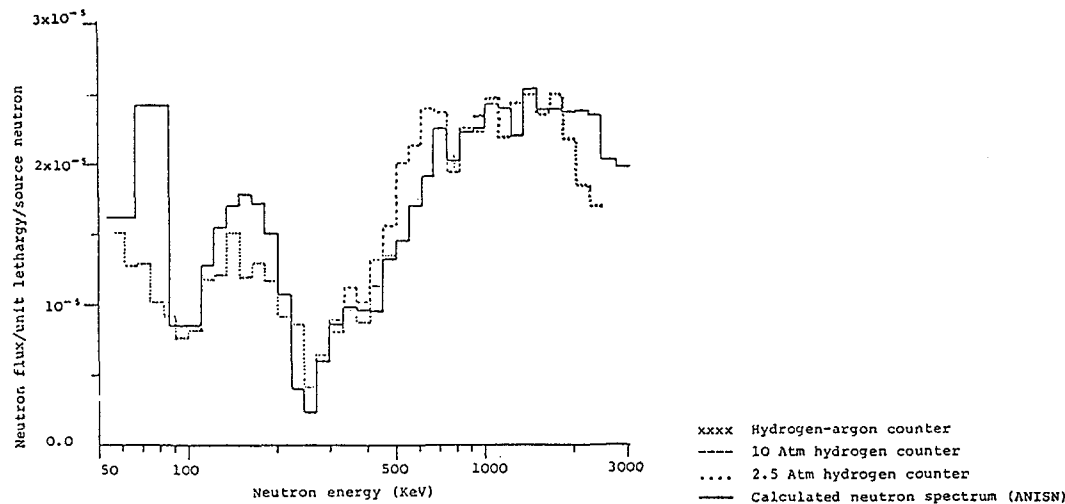
FIG.8.

Neutron spectrum at 37 cm in a LiF sphere.

calculations it can be seen that the positions of the fluorine resonance, at 110 keV, and of the lithium-6 resonance, at 250 keV, are well predicted, as is the general shape, although there are some systematic differences, particularly between 300 and 700 keV in the 37 cm measurements.

(b) **Measurements involving Be**

In Figs 9, 10 are shown the results of absolute transmission measurements (unfolded using FERDOR) on spherical beryllium shells of 2.54 and 9.65 cm thick respectively, where they are compared, to $P_5 S_{16}$ ANISN calculations using the ENDF/BIV data set (Koohi-Fayegh, 1980). We note that in each case the 14 MeV peak is again well modelled, but that the measured peak is broader on the low energy side. The flux dip at 3 MeV due to the Be resonance is clearly seen, but the measured fluxes between 10 and 3 MeV are significantly lower than those predicted.
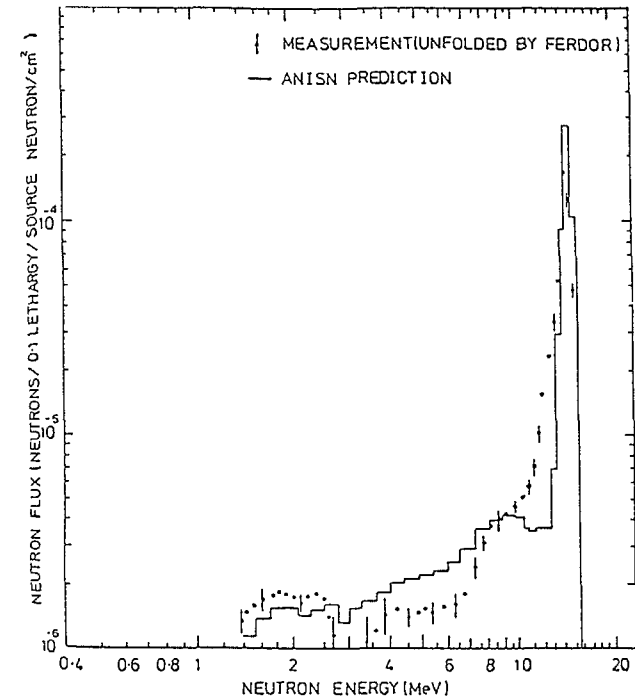
FIG.9.

Transmission Spectrum of 2.54 cm Be Shell.
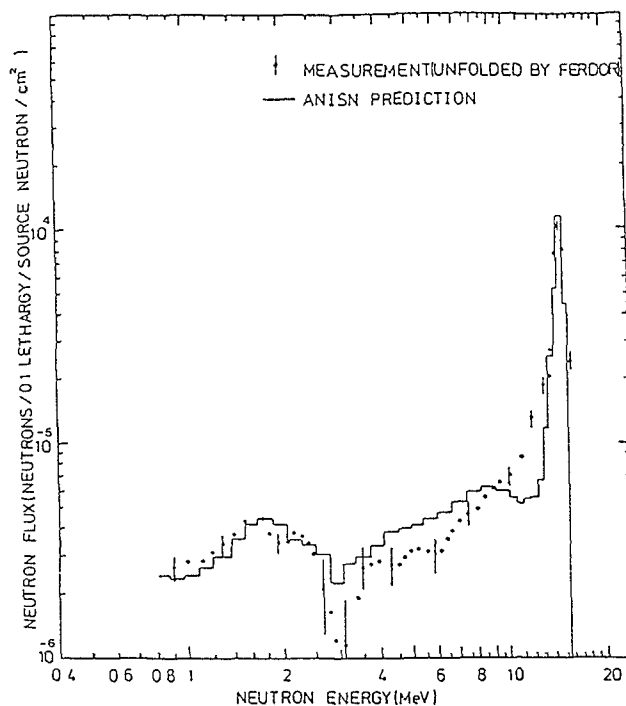
FIG 10

Transmission Spectrum of 9.65 cm Be Shell.
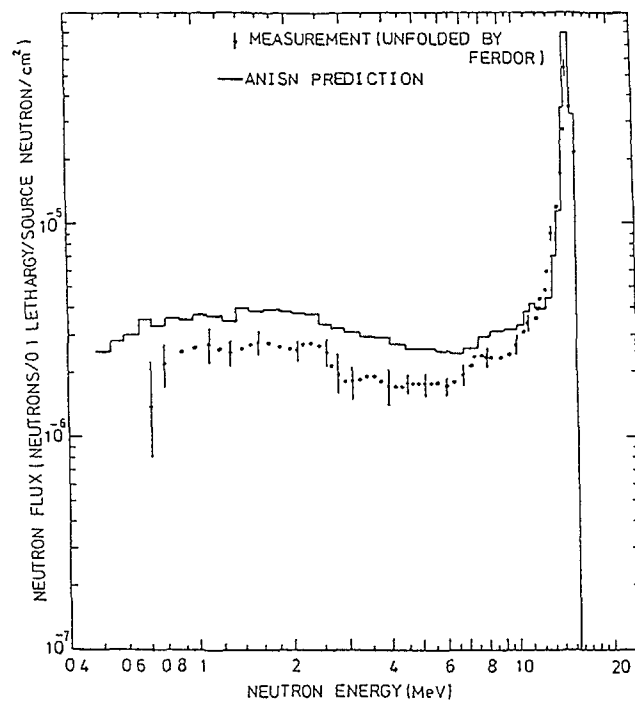
FIG 11

Neutron Flux in the Birmingham spherical assembly at
($r = 31.5cm$, $\Theta = \overset{\circ}{0}$) for $t = 2.54$ cm Be
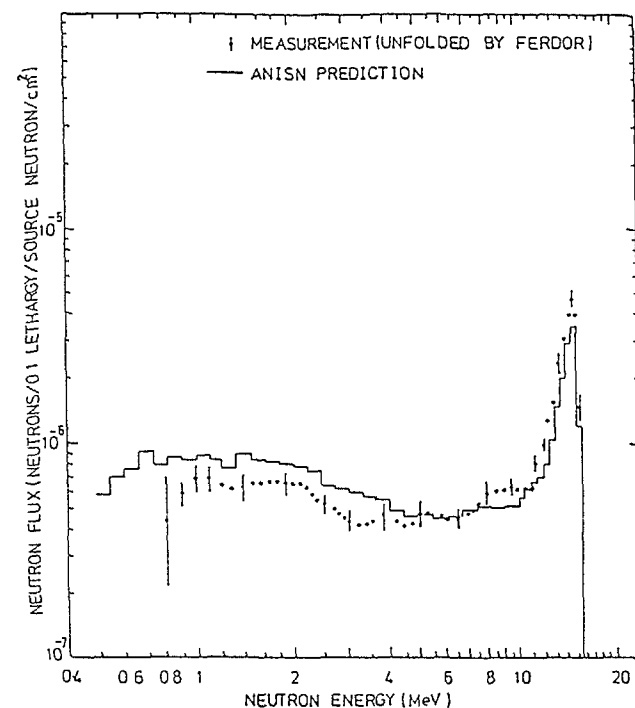
FIG 12

Neutron Flux in the Birmingham spherical assembly at
($r = 55.3cm$, $\Theta = \overset{\circ}{0}$) for $t = 9.65$ cm Be

Two measurements in the LiF assembly with Be shells round the target are shown in Figs 11 and 12; measurements at other angles and positions show similar trends, namely better agreement between measurement and theory at larger radii, but with the measured flux below 4 MeV consistantly lower than that predicted. As expected, the source peak amplitude reduces, and the width increases, as the thickness of beryllium is increased, and the flux below 10 MeV increases.

(c) Measurements in the LiF slab assembly

The main measurements performed on the slab assembly have been of tritium production, although some fission rate ratio determinations have also been made. The results of the two sets of tritium measurements are shown in Figs 13, 14 for the bare and graphite reflected assemblies respectively. In each case the calculated tritium disintegration rates were found using MORSE. In all cases both the experimental and computational uncertainties increased significantly towards the back of the assembly. Looking at the results for the ^{7}Li pellets first, we see

that both show similar characteristics, namely that the measured disintegration rates are significantly lower (by ~ 30-40%) than the calculated ones nearest the source, but that the differences reduce significantly towards the back of the assembly until there is agreement within the errors concerned. In other words, the gradient of the measured and calculated tritium production curves are different.

In the case of the natural lithium pellets, the contribution from the ^{6}Li(n,α)T reaction near the front of the assembly will be small compared to that from the ^{7}Li(n,n'α)T reaction. We see, therefore, that the natural lithium pellet results are consistant with those from ^{7}Li at the front. At the back of the reflected assembly the measured and calculated tritium production rates both rise, due to the moderating properties of the graphite reflector is enhancing the ^{6}Li(n,α)T reaction rate. However, we note that the measured ^{7}Li disintegration rate also increases near the reflector, an unexpected result, and one which was neither predicted nor explained.
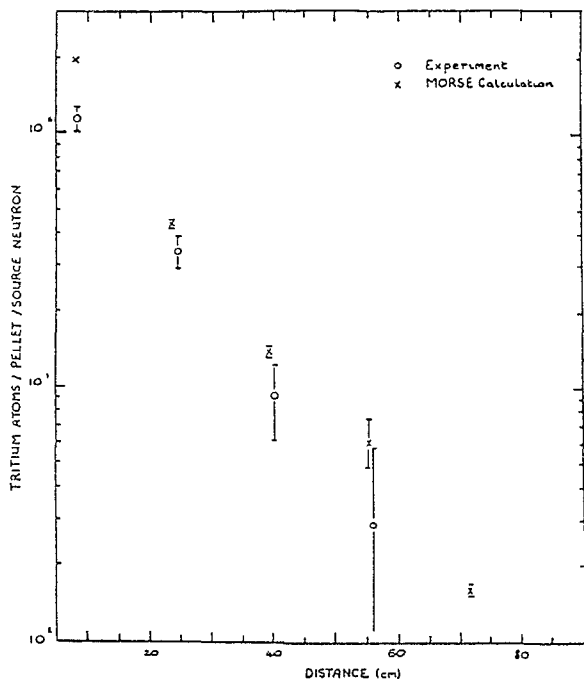
FIG 13a

Comparison of measured and calculated tritium production in
enriched ^{7}Li pellets in the Birmingham bare lithium fluoride
assembly.
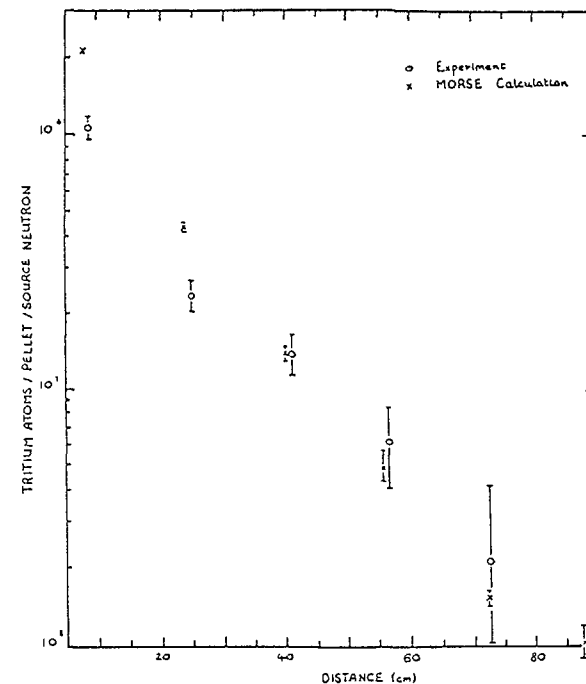
FIG 13b

Comparison of measured and calculated tritium production in
enriched ^{7}Li pellets in the Birmingham graphite reflected lithium
fluoride assembly.

Because of their simplicity, ^{235}U/^{232}Th fission rate ratio
measurements were made on a wider range of assemblies than were the
tritium production ones. In addition to the bare and graphite reflected
systems they were also made on the LiF slabs with (a) a 4.1 cm thick
beryllium hemisphere 15.7 cm diameter round the front of the D–T target,
and (b) with a 1.25 cm thick iron plate covering the front surface of the
assembly. The results of these measurements (made 10 cm off axis) are
shown in Fig 15, noting that the actual value of the ratios are arbitrary,
since they depend on the characteristics of the counters concerned. As
expected, the softening of the spectrum at all depths arising from the
iron results in an increase in the ^{235}U/^{232}Th ratio at all of the measured
positions; the results using beryllium are similar but slightly lower than
those for iron. The ratios for the bare and graphite reflected assemblies
are identical for the front 40 cm or so, when the softening from the
graphite increases the ratio until, at the back of the assembly (88 cm),
the ratio is doubled. In all cases the ratio increases by about an order
of magnitude from front to back of the assembly, making it a very
sensitive index of spectral shape.

231

3.2 Measurements on the Tokyo assemblies

(a) Bare LiF assembly

Measurements in this programme were compared with Monte Carlo
predictions using the MORSE–CG program in conjunction with the GICXFNS
group cross section set based on the ENDFB–IV and B–V data sets. In order
to reduce the variances associated with the use of a point detector
estimator the technique of Carter and Cashwell, 1975, was employed, using
a 2 cm radius sphere round the measurement point; the effect of different
sphere sizes on the variance and accuracy formed part of the study. The
results of two measurements, at 16.4 and 31.4 cm into the pile, are shown
in Figs 16 and 17. From these we see that the measured spectra show much
larger oscillations than were observed by the Birmingham group at all
energies. On the other hand, however, the general shape agreement appears
to be better overall, ie. the calculated spectra fall between the upper
and lower bounds of the measured ones. The authors note (Lee et al 1985)
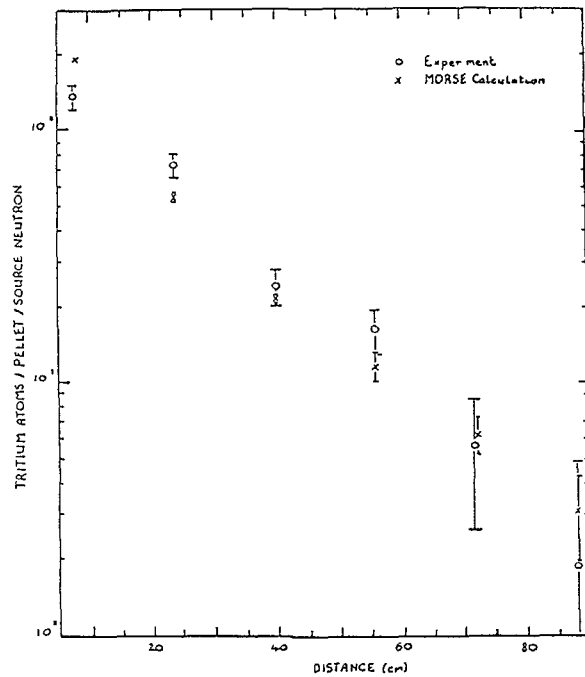that there is a ghost peak at 15 MeV which arises from the unfolding

FIG 14a

Comparison of measured and calculated tritium production in natural lithium pellets in the Birmingham bare lithium fluoride assembly.
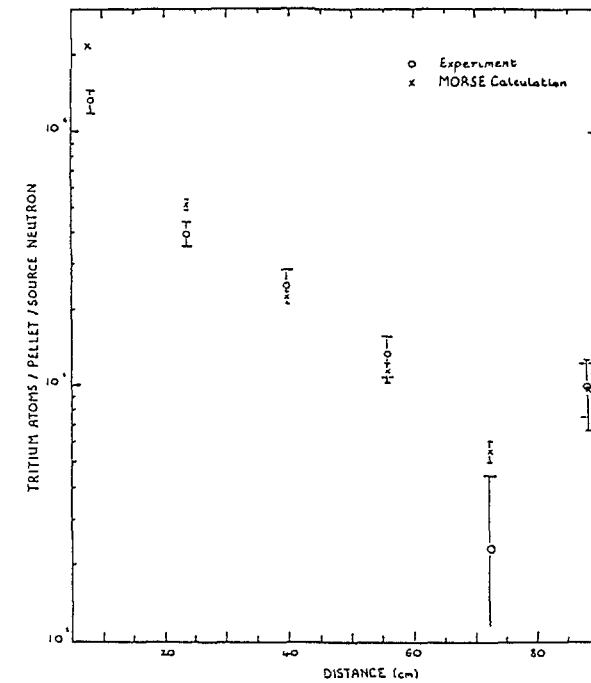

FIG 14b

Comparison of measured and calculated tritium production in natural lithium pellets in the Birmingham graphite reflected lithium fluoride assembly.

process, and that there are disagreements in the 14 MeV peak region of between 18 and 30%, the calculated spectra being the lower of the two. In contrast, the differences in the Birmingham results varied with measurement angle, but showed no systemmatic trend (Perkins, 1979). They also note that their results do not reproduce those at Birmingham, where the calculated fluxes below 10 MeV were consistantly higher than those measured using FERDOR, although using a differential unfolding code gave substantially better agreement in the Birmingham measurements (see Fig 6).

(b) Graphite reflected assembly

The results of measurements just inside the LiF (d = 21.4 cm) and near the centre of the graphite (d = 51.4 cm) are shown in Figs 18 and 19 (Sekimoto and Lee, 1986) where they are compared to MORSE calculations. The authors note (i) that the measured fluxes below 4 MeV are consistantly higher than calculation, particularly in the graphite, (ii) that the calculated flux below the source peak is systematically lower than that measured and (iii) structure corresponding to resonances in the carbon

cross section can be seen around 3, 6 and 8 MeV in the graphite measurements.

4. DATA ADJUSTMENT BASED ON INTEGRAL MEASUREMENTS

Clearly, evaluation of lithium cross section data can best be accomplished using lithium metal assemblies, and several such measurements have been made, notably at Julich (Herzing et al, 1976) and Karlsruhe (Frischer et al, 1978). In the latter case, a difference between measured and calculated tritium production rates was seen as consistant with the $^7Li(n,n'\alpha)T$ cross sections measured by Swinhoe and Uttley, 1979 at Harwell, which were significantly lower than the evaluated ones. However, in the case of LiF, data evaluation for lithium is obviously confounded by the known uncertainties in the fluorine scattering cross sections.

As far as this author is aware, only one attempt has been made to make data adjustments based on LiF assemblies, notably by Malsbury, 1986, when he studied the tritium production experiments of Naylor, 1986, in great
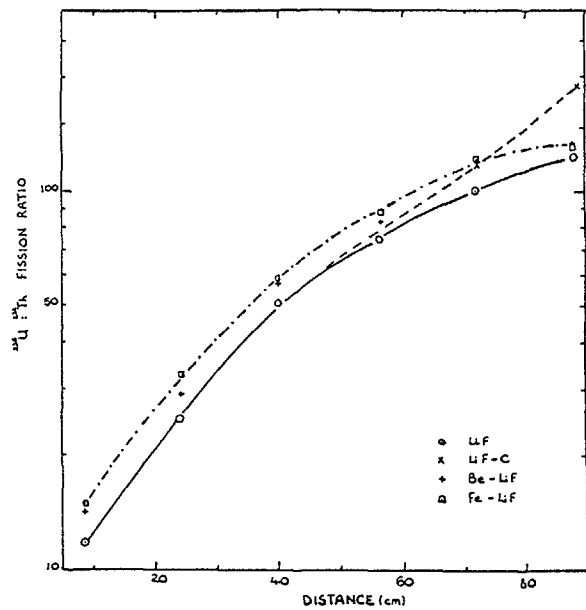
FIG.15.

Measured ^{235}U: ^{232}Th fission rate ratio distributions for various slab assembly configurations (Birmingham).

FIG.17.

Measured and calculated spectra at a distance of 31.4 cm from the front surface of the bare Tokyo LiF assembly.
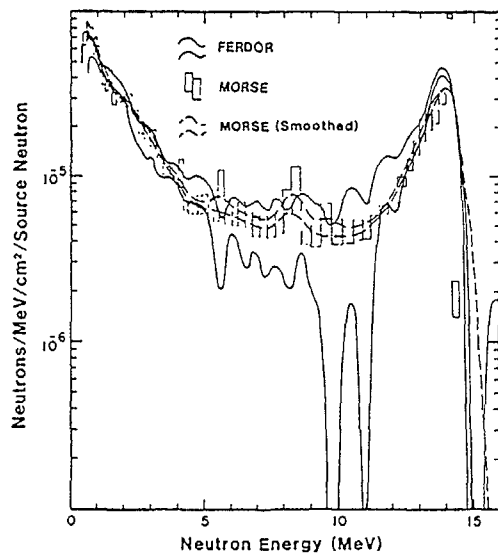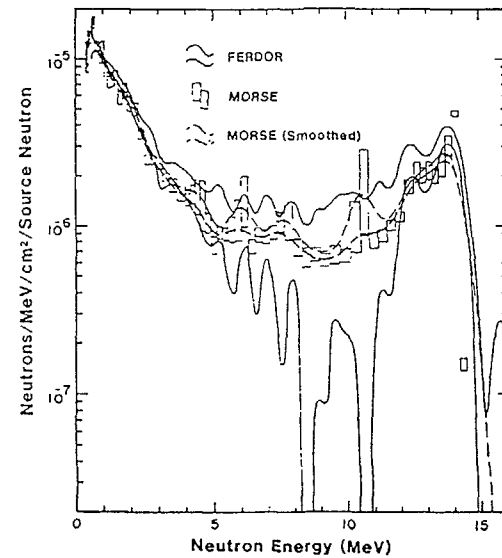

FIG.16.

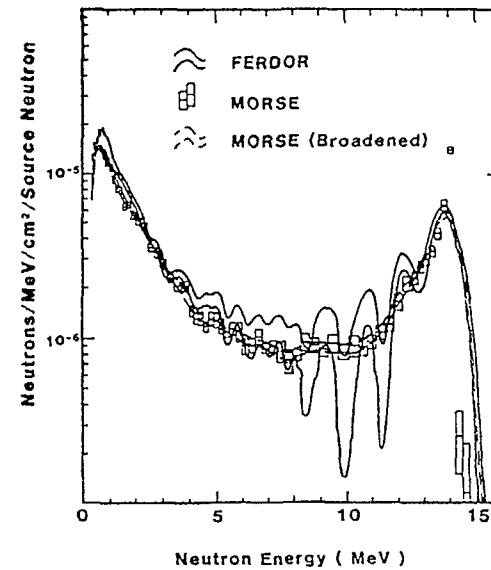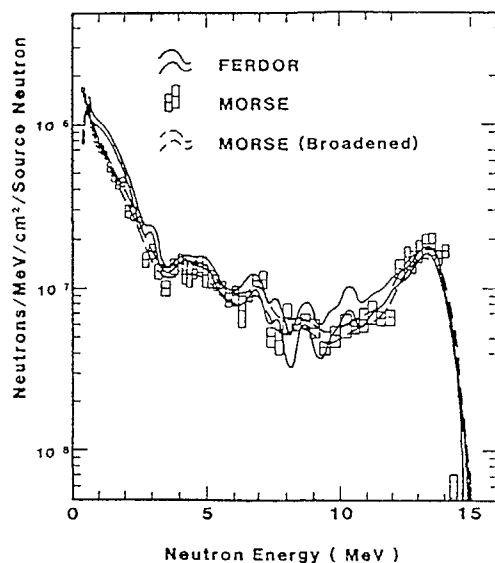Measured and calculated spectra at a distance of 16.4 cm from the front surface of the bare Tokyo LiF assembly.

FIG.18.

Measured and calculated spectra at distance d = 21.4 cm from the front surface of the Tokyo reflected LiF assembly.

FIG 19

Measured and calculated spectra at distance d = 51.4 cm
from the front surface of the Tokyo reflected LiF assembly.

detail. Because of the discrepancies between measurement and calculation
near the source, which we have already noted, he first concentrated on
modelling the experiment, in order to see if some hitherto unaccounted for
factor could explain the observed discrepancies. His study included
looking at source anisotropy, spectra and yields, D-D build up in the
target, the effect of aluminium encapsulation of the LiOH pellet and of
the stainless steel guide tubes, of uncertainties arising from the LiF
filler plug encapsulation and the effects of gaps between the LiF blocks
caused by slight bowing of the aluminium containers. However, although
these studies gave rise to small corrections in the measured tritium
yeilds, no significant systematic, and unaccounted for, source of
measurement error was revealed. The calculations performed by Naylor were
also broadly confirmed.

Since the differences between measurement and calculation could not be
attributed to measurement error, Malsbury therefore tried data adjustment
to obtain agreement. However, no plausible adjustment of the ^{7}Li(n,n'α)T
cross section data could be found to account for the differences involved.
Furthermore, using a specially developed correlated-tracking Monte Carlo
sensitivity code, he was able to show that the fluorine component of LiF
accounted for a greater fraction of the lithium reaction rate sensitivity
to total and scattering cross sections than did the ^{7}Li. For this reason,

measurements in LiF cannot be used to evaluate the lithium cross-sections
alone. This was, of course, obvious at the outset of the measurement
series; nevertheless, it should, perhaps, be stressed that one therefore
has to look to pure lithium experiments for the lithium evaluation, and
treat these as complementary to experiments in LiF, which can then be used
to evaluate the fluorine cross section data. Clearly, both types of
experiment are necessary if FLIBE is to be considered as a breeder blanket
material.

5. GENERAL OBSERVATIONS

As we have seen, data evaluation based on measurement and calculation
of neutron spectra depends critically on the ability to unfold the
detector response. Although this is a reasonably well established
technique in fission reactor studies, fusion reactors pose two particular
problems. The first is that the spectra have significant components above
the thresholds for the ^{12}C(n,α) and ^{12}C(n,3α) reactions and that both the
reaction mechanisms and alpha particle light curves need to be well known
in order to predict response functions. The current state of this data is
such that adjustment is normally required to get agreement between
measurement and prediction.

The second factor, which we have already noted, is that most spectra
in fusion breeder blanket assemblies are dominated by the 14 MeV peak.
Small errors in the response functions around 14 MeV may therefore be
reflected in large systematic errors in the flux at lower energies, which
is often more than one order of magnitude less. In this respect, the need
to establish adequate, and representative, test procedures for neutron
spectrometry should be an important feature of future work. Unfolding
monoenergetic spectra, or those from radioisotope sources, does not
provide a representative test for fusion reactor spectra; perhaps some
standard measurement set-up (eg the spectrum from a D-T source in a water
sphere) could form the basis for an international intercomparison?

Finally, it is suggested that data evaluation based on integral
assemblies ought to involve a range of different measurements, both
differential (eg. spectrum measurements) and integral (eg. reaction rates
in threshold foils). One would then treat the whole ensemble of
measurements as the basis for data evaluation and/or adjustment, rather
than any single one. Treating measurements in pure lithium and in LiF
assemblies together would be a natural extension of this procedure.

REFERENCES

Bartine D.E, Alsmiller R.G. (Jr), Oblow E.M. Mynatt F.R. (1974) Nucl. Sc.
Eng. 53, 304-318.

Benjamin P.W, Kemshall C.D, Redfearn J (1968) Nucl. Instr. Meth, 59,
77-85.

Brierley I.R. (1977) Ph.D thesis, University of Birmingham, "The calibration of recoil proton proportional spectrometers and the measurement of neutron slowing down spectra in a lithium fluoride assembly".

Brierley I.R, Bore A, Evans N, Scott M.C. (1982) Nucl Instr. Meth. 192, 439-446.

Carter L.L, Cashwell E.D. (1975), TID-26607.

Dierckx R. (1973) Nucl. Instr. Meth. 107, 397-398.

Evans N. (1978) Ph.D. thesis, University of Birmingham", The measurement of absolute neutron spectra in lithium fluoride from 40 keV - 2.5 MeV".

Evans N, Brierley I.R, Scott M.C. (1979) Nucl. Instr. Meth. 160, 465-470.

Frischer U, Kappler R, Rusch D. (1978) Nucl. Instr. Meth. 153, 563-570.

Herzing R, Kuypers L, Cloth P, Filges D, Hecker R, Kirch N. (1976) Nucl. Sc. Eng 60 169-175.

Johnson R.H. (1980) Nucl. Sc. Eng. 73, 93-97.

Koohi-Fayegh R. (1980) Ph.D. thesis, University of Birmingham, "Neutron spectrum measurement in a beryllium-lithium fluoride assembly using an NE213 scintillator".

Lee D, Sekimoto H, Yamamuro N. (1985) J. Nucl. Sc. & Tech 22, 28-37.

Naylor D.A. (1986) Ph.D. thesis, University of Birmingham "Tritium production by lithium in integral fusion reactor blanket assemblies".

Oblow E.M, Bartine D.E, Mynatt F.R. (1973) Oak Ridge National Laboratory Report ORNL-TM-4110.

Perkins L.J. (1979) Ph.D. thesis, University of Birmingham, "The design and development of a miniature fast neutron scintillation spectrometer and its application to the fusion neutronics of a lithium fluoride benchmark experiment".

Perkins L.J, Evans N, Koohi-Fayegh R, Scott M.C, Underwood B.Y. (1981) Nucl. Sc. Eng 78, 30-43.

Perkins L.J, Scott M.C. (1979) Nucl. Instr. Meth. 166, 451-464.

Petler J.S, Scott M.C. (1985) Nucl. Instr. Meth. 228, 425-431.

Sajo-Bohus L. (1985) Ph.D. thesis, University of Birmingham, "Development of a fast neutron proportional counter with a low wall response".

Scott M.C, Koohi-Fayegh R, Evans N, Perkins L.J, Taylor N.P. (1980), NEA Specialists Meeting on Nuclear Data and Benchmarks for Reactor Shielding, Paris, Oct. 1980.

Sekimoto H. (1984) Nucl. Instr. Meth. 228, 129-132.

Sekimoto H, Hojo K, Hojo T, Oishi K. (1985) Nucl. Instr. & Meth in Physics Res. A234, 148-151.

Sekimoto H, Lee D. (1986) J. Nucl. Sc & Tech 23, 381-386.

Sekimoto H, Lee D.W, Hojo T, Oishi K, Noura T, Ohtsuka M, Yamamuro Y. (1985) J. Nucl. Materials 133, 134, 882-886.

Sekimoto H, Ohtsuka M, Yamamuro N. (1981) Nucl. Instr. Meth. 189, 469-476.

Sekimoto H, Oishi K, Hojo K, Hojo T. (1984) Nucl. Instr. Meth. 227, 146-149.

Swinhoe M. (1979) Ph.D. thesis, University of Birmingham "An absolute measurement of the $^7Li(n,n't)^4He$ reaction cross-section between 5.0 and 14.0 MeV by tritium arraying".

Swinhoe M.T, Uttley C.A. (1979) Proc. Conf. Nucl. Cross Sections and Technology NBS-SP594 p 246.

Underwood B.Y. (1978) University of Birmingham Internal Report 78-06, "Investigation of the D-T neutron source anisotropy and its effect on scalar fluxes in an LiF integral benchmark experiment".

Underwood B.Y. (1979a) Nucl. Instr. Meth. 165, 523-530.

Underwood B.Y. (1979b) Nucl. Instr. Meth. 164, 247-254.

**NEUTRON MULTIPLICATION OF LEAD
AT 14 MeV NEUTRON INCIDENT ENERGIES***

T. ELFRUTH, D. SEELIGER, K. SEIDEL,
G. STREUBEL, S. UNHOLZER
Technical University Dresden,
Dresden, German Democratic Republic

D. ALBERT, W. HANSEN, K. NOAK,
C. REICHE, W. VOGEL
Zentralinstitut für Kernforschung,
Rossendorf, German Democratic Republic

D.V. MARKOVSKIJ, G.E. SHATALOV
I.V. Kurchatov Institute of Atomic Energy,
Moscow, Union of Soviet Socialist Republics

Abstract

    Neutron leakage spectra were measured with time-of-flight and with
proton recoil spectroscopy and activation and fission rates were
determined for a lead sphere of 4.1 mean-free path shell thickness fed in
its centre with 14-MeV neutrons. The results are compared with
calculations based on recent data files and are discussed in connection
with previous lead benchmarks. About 10% more neutrons are observed than
predicted by calculations.

**NEUTRONIC INTEGRAL BENCHMARK EXPERIMENTS ON
DDX FOR FUSION REACTOR DESIGN BY OKTAVIAN***

K. SUMITA
Department of Nuclear Engineering,
Osaka University,
Osaka, Japan

Abstract

    To investigate adequacy and accuracy of measured data and evaluated DDX
data file, several Integral Benchmark Experiments have been done for
Spherical and Slab Assemblies etc. of Fusion Materials on Tritium Breeding
Ratio and Neutron Transmission by OKTAVIAN. The results indicate necessity
of further elaborate experimental works in this field, for reliable
neutronic design, e.g., TBR in Fusion Reactor Blanket.

    Appendices show our lates measurements of DDX for several nuclides at a
fixed neutron energy. (14.1MeV) and studies on DDX for PKA in radiation
damage analysis.

BLANKET BENCHMARK EXPERIMENTS
AND THEIR ANALYSES AT FNS

H. MAEKAWA, T. NAKAMURA
Japan Atomic Energy Research Institute,
Tokai-mura, Naka-gun, Ibaraki-ken,
Japan

Abstract

Since the FNS, an intense 14 MeV neutron source for fusion neutronics studies, was completed in April 1981, many types of experiments have been done. Integral experiments were performed on cylindrical assemblies with 60-cm thick Li_2O, 60-cm thick graphite and 40-cm thick Li_2O followed by 20-cm thick graphite. Various reaction rates such as tritium production rate and neutron spectra were measured in these experiments. The time-of-flight experiments were conducted to measure angle-dependent neutron spectra leaking from Li_2O, graphite, Li-metal and Be-metal slab assemblies. These experiments were numerically analyzed by making use of DOT3.5, MORSE-DD and MCNP with various cross section sets based on JENDL-3PR1, -3PR2, ENDF/B-IV and -V. Another type of experiments called "Blanket Engineering-Oriented Benchmark Experiment" has been carried out as the JAERI-U.S.DOE Collaborative Program. Measured parameters such as tritium production rates and neutron spectra were analyzed by both parties.

I. Introduction

To design a controlled thermonuclear reactor blanket, it is necessary to know exactly the behavior of neutrons in the blanket. The methods and data used to analyze the neutronics in the blanket should be examined by comparing the calculated results with experiments. Lithium-oxide (Li_2O) has been proposed by JAERI's designers as a solid state tritium breeding material [1]. Integral experiment on a Li_2O blanket assembly was carried out using the PNS-A neutron source [2]. After the construction of a powerful neutron source named as the Fusion Neutronics Source (FNS) [3-4], benchmark experiments, especially, the measurements of tritium production-rate (TPR) distribution in the simulated Li_2O blanket assemblies are strongly requested to confirm the proper tritium breeding ratio. Two types of benchmark experiments have been performed at FNS. One is the clean benchmark experiment and the other is the fusion blanket engineering-oriented benchmark experiment.

Most suitable experiments for the verfication of methods and data are clean benchmark experiments on a simple geometry with simple material compositions. Two series of clean benchmark experiments, integral experiments on cylindrical assemblies and measurements of angle-dependent leakage spectra from slab assemblies, have been carried out at FNS. It is easy to make the two-dimensional model for the analyses of both series.

The breeding blankets in many conceptual designs, however, have rather complex configurations. It is not so simple to estimate the accuracies of neutronic parameters in a composite system by superposing the data obtained only in individual simple benchmark experiments. In the Fusion Blanket Engineering-Oriented Benchmark Experiment program at FNS, simplified models of some composite configurations of solid blanket are deliberately chosen, experimental data are obtained in a parametric way, then, the comparisons are made with the predicted values from different origins to assess the overall accuracies of the nuclear calculations, and to clarify the issues associated with the complex structure [5].

The JAERI proposed this program as one of the joint planning activities between JAERI and U.S.DOE on fusion reactor engineering. A collaboration for joint experiments and analyses started in 1984 with the use of resource available in both partries. The phase-I of the experimental program has been completed recently [6].

II. Outline of the FNS Facility

The Fusion Neutronics Source (FNS) is a high intensity 14 MeV neutron source installed for the purpose of studying the neutronics on D-T fusion reactor blanket and shielding. It provides following three functions to meet the experimental requirements.

a) High intensity DC point source.
b) DC point source with large variation of neutron yield rate .
c) Pulsed neutron source ranging from nS to μS.

The FNS is basically a combination of a 400 keV deuteron ion accelerator of high intensity DC and pulsed beam, and tritium metal target assemblies which have large cooling ability.

The accelerator was constructed from following equipments.

a) A cascaded trasformer type high voltage power supply that is capable of delivering up to 80 mA at 450 kV.
b) A 25 kVA motor-generator type auxiliary power supply for terminal. (Now this power supply is replaced by an insulated transformer of 40 kVA.)
c) A high voltage terminal deck that contains two Duoplasmatron ion sources (GIC 740 A & 820), 90° analyzing magnets, terminal lenses, pre-acceleration pulsing components, vacuum systems etc.
d) An accelerator tube designed to be as short as practicable to avoid beam spread due to space charge effect in the tube.
e) Two beam transport lines (0° & 80°) that include vacuum systems, Q lenses, steering devices, post-acceleration pulsing systems, insertable Faraday cups, beam profile monitor etc.
f) A control desk and a rear console that has a diagrammatical display for operation and interlocks.

The FNS accelerator system was completed in April 1981 at Tokai-site of JAERI. The data of performance test are shown Tables 2.1 and 2.2 with designed values. Figure 2.1 shows a layout of the accelerator system of FNS facility.

Each beam line leads to a separate target room surrounded by a thick concrete
shield: a 15 m × 15 m large target room (#1) for 80° beam line and a small 5 m ×
5 m target room (#2) for 0° beam line. The clean benchmark, i.e., integral and
time-of-flight experiments have been performed at the #1 target room. The
Phase-I experiments of JAERI-U.S.DOE Collaborative Program have been carried out
at the #2 target room and at the Experimental Port between the two target rooms.

Table 2.1 Results of DC beam test.

Beam-line	Ion source	Beam current at the target		
		Rated value	Measured value	
			Ammeter	Calorimeter
0 degree	740A	20 mA	23.4 mA	22.0 mA
80 degree	740A	10 mA	10.7 mA	11.0 mA
80 degree	820	3 mA	3.18 mA	3.21 mA

Table 2.2 Results of pulsed beam test.

Mode	Pulse width		Peak current		On/Off ratio	
	Rated	Measured	Rated	Measured	Rated	Measured
Bunch	2 ns	1.55 ns	25 mA	45.4 mA	10^5	4.1×10^5
Sweep (min. width)	30 ns	22 ns	3 mA	3.0 mA	10^4	1.9×10^5
(>50 ns)	50 ns ~8 μs	Same as rated values	3 mA	3.0 ~3.4 mA	10^4	6.1×10^5
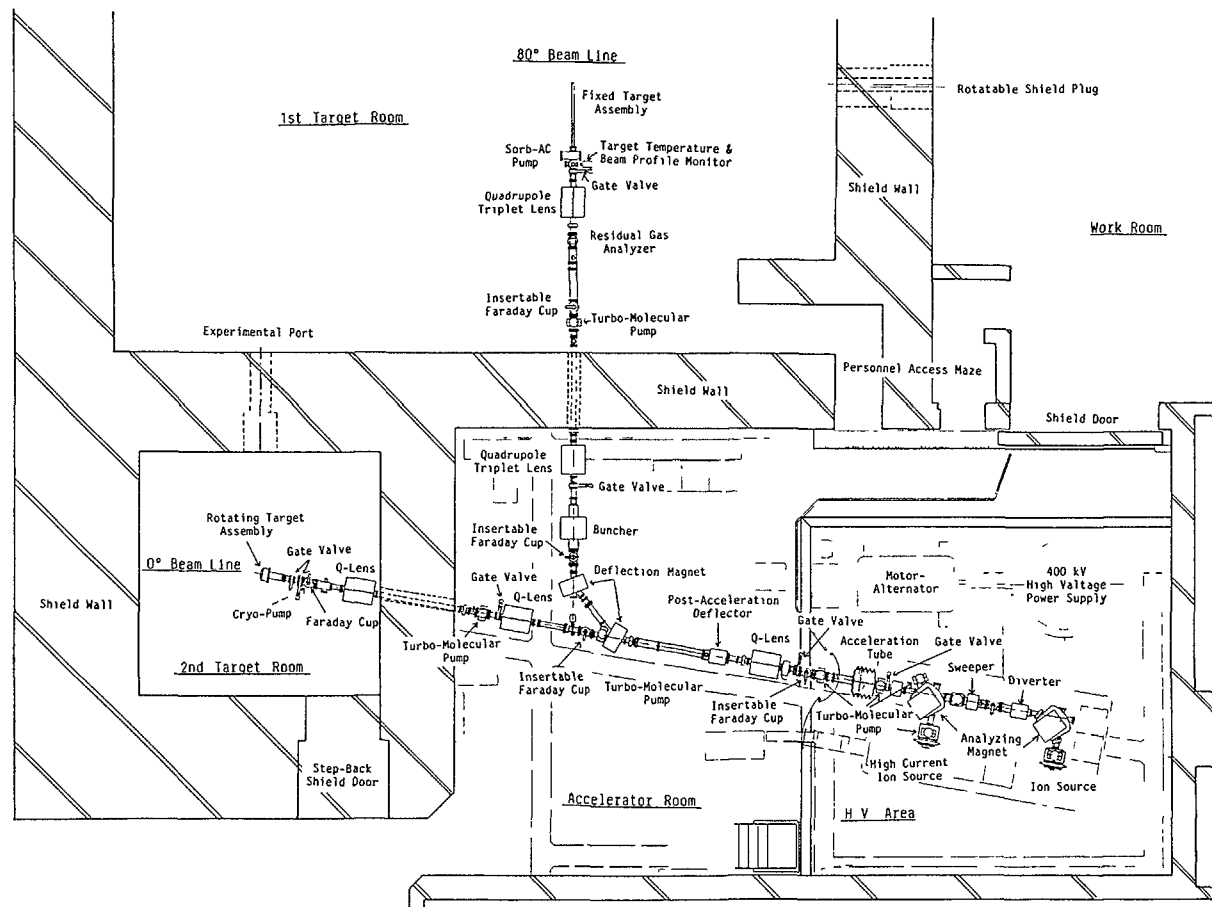
Fig. 2.1   Layout of 400 keV deuteron accelerator (FNS) system.

III. Integral Experiments and Analyses on Li$_2$O, Graphite and Li$_2$O-C
Cylindrical Assemblies

1. Experiments

The integral experiments have been carried out on the following three assemblies:

(1) 60-cm thick Li$_2$O cylindrical slab assembly (Li$_2$O assembly)
(2) 60-cm thick graphite cylindrical slab assembly (C assembly)
(3) 40-cm thick Li$_2$O cylindrical slab assembly followed by 20-cm thick graplhite reflector (Li$_2$O-C assembly).

Sectional views of the Li$_2$O-C assembly are shown in Fig. 3.1. Lithium-oxide and/or graphite block were stacked to form a cylinder in the same manner for the three assemblies. The effective diameter was 63 cm. In the cases of Li$_2$O and Li$_2$O-C, an experimental channel —— a set of sheath and drawer made of type 304 stainless steel —— was placed at the center of assembly. Special-sized blocks, some of which had experimental hole, were loaded in the drawer in order to set detectors and samples. while in the case of graphite assembly, a set of sheath and drawer was made of the same type graphite as the blocks. The D-T neutron target was located at 20 cm from the front surface of the assembly on the central axis.
Measuring quantities and their methods are summarized in Table 3.1. Neutron yields were determined by means of the associated α-particle detection method [7]. Source characteristics —— angular distribution and spectra —— of the target used, were measured by time-of-flight method, the foil activation method and an NE213 spectrameter [8]. They were analyzed by Monte Carlo calculations [9]. Good agreements between the experiments and calculations were obtained for the energy spectra and the angular distributions of foil activation. Experimental reports including digital data with errors will be presented in JAERI-M publications [10-12].
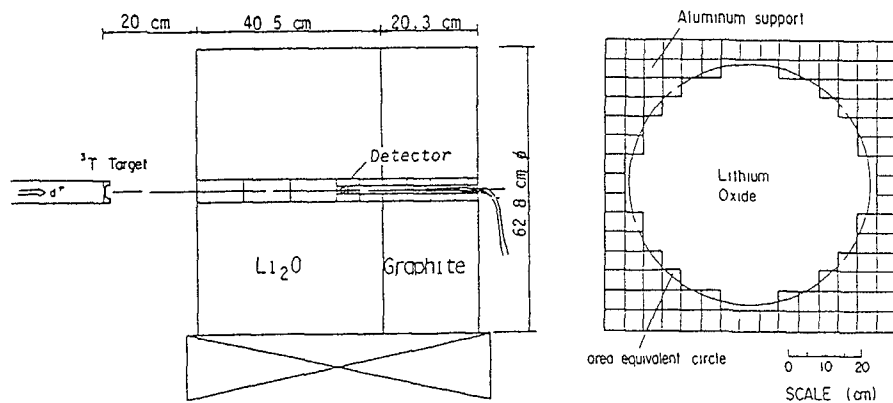
Fig. 3.1 Cross sectional views of experimental arrangement

Table 3.1 Measured quantities and their methods for integral experiments.

(1) Tritium production rates of ^{6}Li and ^{7}Li
   • Liquid scintillation method with ^{6}Li$_2$O and ^{7}Li$_2$O pellets
   • ^{6}Li and ^{7}Li glass scintillators
(2) Fission rates
   • Micro-fission chambers (mfc) (^{235}U, ^{238}U, ^{237}Np, ^{232}Th)
   • Solid-state track detectors (SSTD) with ^{235}U, ^{238}U, and ^{232}Th foils
(3) Reaction rates
   • Foil activation method
      -- with Al, In, and Ni foils for Li$_2$O assembly
      -- with Al, Au, In, Nb, Ni, and Zr foils for C assembly
      -- with Al, Au, Co, Fe, In, Mn, Na, Nb, Ni, Sc, Ti, Zn, and Zr foils for Li$_2$O-C assembly
(4) Response of PIN diodes
(5) Response of TLDs (measured in Li$_2$O and C assemblies)
   • TLD-600, -700, -100 ------- LiF
   • UD-110S ------------------ CaSO$_4$
   • Mg$_2$SiO$_4$, Sr$_2$SiO$_4$, Ba$_2$SiO$_4$
(6) In-system neutron spectra
   • Small sphere NE213 spectrometer

2. Analyses

In the present analyses the DOT3.5 code [13] was used with the P$_5$-S$_{16}$ approximation. The cross-section sets used were obtained from the nuclear data files of JENDL-3PR1 [14], JENDL-3PR2 [15], ENDF/B-IV, and ENDF/B-V (only for carbon data) using the processing code PROF-GROUCH-G/B [16]. These features are shown in Table 3.2 along with the cross section sets used in the pre-experimental analyses. As the weighting function, a Maxwellian distribution was used for the thermal group (125th group) and 1/E distribution was used for the other groups in the JENGIX and ENDGIX sets. A flat distribution was assumed in the JACKAS set [17] for 1 ~ 124 groups.

Table 3.2 Cross-section sets for DOT3.5.

Name	Group No.	Process Code	Weight	File
GICXFNS[*1]	135	NJOY	Flat[*2]	ENDF/B-IV
GICXFNS1	135	NJOY	Flat[*2]	ENDF/B-IV
GICXJ3	125	NJOY	Flat[*2]	J-3PR1[*5]
JENGIX	125	P-G-G/B[*3]	1/E and Maxwell	J-3PR1 & 2[*5]
JACKAS	125	P-G-G/B[*3]	Flat and Maxwell	J-3PR1 & 2[*5]
ENDGIX[*4]	125	P-G-G/B[*3]	1/E and Maxwell	ENDF/B-IV
GICX40	42	NJOY	1/E[*2]	ENDF/B-IV

*1 C   ENDF/B-V, ^{7}Li(n,n'α)^{3}T   Young's evaluation.
*2 The thermal group constants were calculated by SRAC code.
*3 PROF-GROUCH-G/B.
*4 Data of carbon in ENDF/B-V are include.
*5 JENDL-3PR1 and JENDL-3PR2.

The source neutron spectrum calculated by a Monte Carlo method [9] was adopted in the analysis of the integral experiments. The GRTUNCL code was used to calculate the first collision source for the succeeding DOT calculations.

3. Results and Discussions

The ratios of calculated-to-experimental values (C/E) for the tritium production rate (TPR) of ^{6}Li in the Li$_2$O assembly are shown in Fig. 3.2. The experimental values have been corrected for self-shielding and room-return effects. In the cases of 1/E weighting function, the calculation based on JENDL-3PR1 predicted the experimental values very well. The calculated value based on JENDL-3PR2 was a little higher than that based on JENDL-3PR1. On the other hand, the result obtained with ENDF/B-IV overestimated the experiment due largely to the incorrect ^{7}Li(n,n'α)^{3}T cross section in this data file.

The C/E values for TPR of ^{7}Li in the Li$_2$O assembly are shown in Fig. 3.3. The results calculated with both JENDL files agree well with those of the experiment within the experimental error and the accuracy of ^{7}Li(n,n'α)^{3}T cross section. It is clearly observed that those with ENDF/B-IV overestimated the experiment by about 20 %. The result using the spectrum calculated with ENDF/B-IV and ^{7}Li(n,n'α)^{3}T cross section in JENDL was close to that using JENDL itself. Therefore, the difference in the ^{7}Li cross section has little effect on the neutron spectrum in the higher energy region.

As a typical example of high-energy threshold reactions, the C/E values for the ^{27}Al(n,α)^{24}Na reaction are shown in Fig. 3.4. Results calculated using the cross-section set generated with the flat weighting function were smaller than that using the 1/E by up to 3 %. In the case of ^{58}Ni(n,2n)^{57}Ni, the calculation for the flat suggests that the D-T source neutron spectrum should be used for the weighting function in the higher-energy region.

The tendency of the C/E curve of ^{238}U(n,f) is similar to that of ^{27}Al(n,α)^{24}Na, though the measuring method for them were quite different and the data were obtained independently. The same tendencies are found in the cases of the C and Li$_2$O-C assemblies. The distributions of C/E value for energy-integrated neutron spectra also show the same tendency. It can be concluded that the experimental data are consistent to each other.

In the case of ^{235}U(n,f) which has a strong sensitivity to low energy neutrons, it becomes clear that the calculated result depends on the weighting function. The C/E values for ^{235}U(n,f) in Li$_2$O-C assemblies are shown in Fig. 3.5. It is clearly seen that the differences between the two cross-section sets are more than 15 % in the graphite regions. The differences in the Li$_2$O assembly are small in the case of ^{6}Li(n,α)^{3}T. Because the neutron population in the energy range below 250 keV is very small in this assembly, the following observations can be made from the present analysis:

(1) The calculated results using the JENDL-3PR1 and JENDL-3PR2 data sets agree well with the measured tritium production rates of both ^{6}Li and ^{7}Li.

(2) The difference of group structure affects on the high-threshold reaction rate.

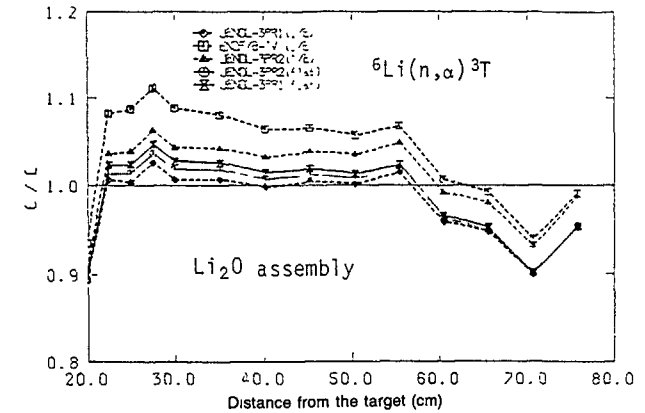(3) The impact of the difference in the weighting spectrum is small except some special cases such as ^{235}U(n,f).

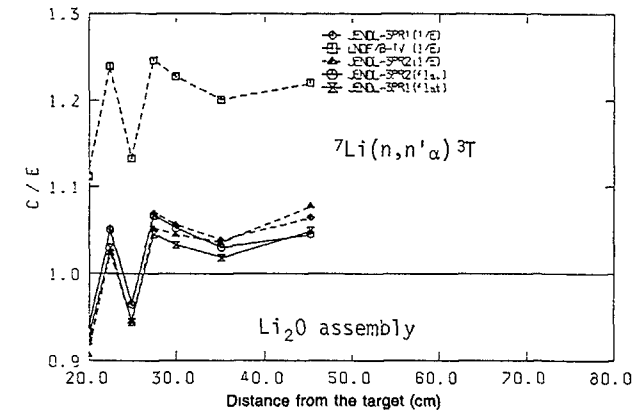Fig. 3.2 Comparison of C/E values for TPR of ^{6}Li in Li$_2$O assembly.

Fig. 3.3 Comparison of C/E values for TPR of ^{7}Li in Li$_2$O assembly

The calculation is expected to give good values when it is made with a cross-section set using the weighting function of a D-T neutron source spectrum in a higher-energy region, a Maxwellian distribution in a thermal region, and typical fusion reactor blanket spectrum in the region between them.
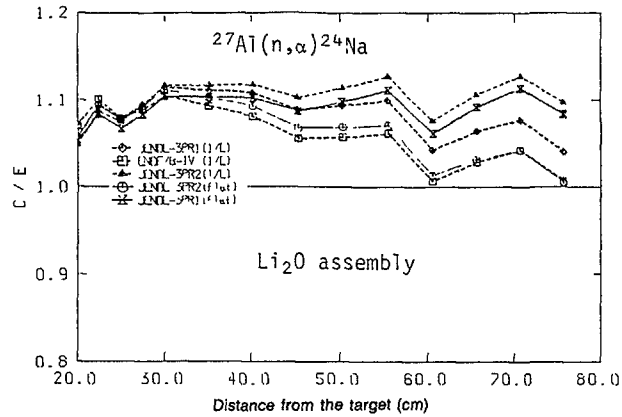
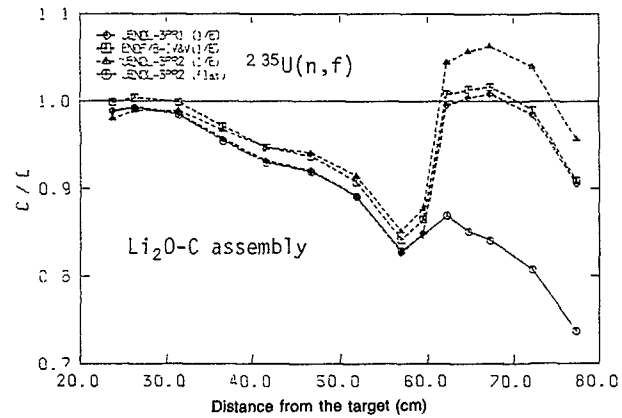Fig. 3.4 Comparison of C/E values for reaction rate in Li_2O assembly.

Fig. 3.5 Comparison of C/E values for fission rate in Li_2O-C assembly.

IV. Angle-Dependent Leakage Spectra from Li_2O, Li-Metal, Graphite and
     Beryllium Slab Assemblies

1. Experiment

Angle-dependent neutron leakage spectra from slab assemblies of candidate materials for fusion reactor were measured accurately by time-of-flight method. The thickness and material of slab assemblies are as follows:

Lithium-Oxide (Li_2O) : 5, 20, 40 cm
Graphite (C)   : 5, 20, 40 cm
Lithium (Li)   : 10, 30 cm
Beryllium (Be)   : 5, 15 cm

The blocks of Li_2O/graphite/Li-metal/Be-metal were stacked to form a pancake cylinder in a frame composed by stacking thin-walled aluminum square tubes of the same outer size as the blocks. The blocks of Li_2O and graphite were the same as that used in the integral experiments. The Li-blocks were covered with 1 mm-thick SS304. The equivalent diameter was 63 cm, except for Li, while the size of Li slab assemblies was 60 cm x 60 cm. The measured angles were 0, 12.2, 24.9, 41.8 and 66.8 degree. The experimental arrangement is shown in Fig. 4.1. The collimator was composed of two cylindrical sleeves, made of steel and paraffin containing powder of B_2O_3 (30 w/o), and the opening was 50 mm in diameter. The detector shield was made of the paraffin containing powder of Li_2CO_3 (20 w/o). The detector-collimator system was moved around the target. The collimator axis was aligned precisely to the rear-surface center of assembly corresponding to each measured angle and thickness of assembly by rotating the upper deck. The neutron detector was a 50.8 mm dia. x 50.8 mm NE213 liquid scintillator. The experimental technique is reported in Ref. [18].
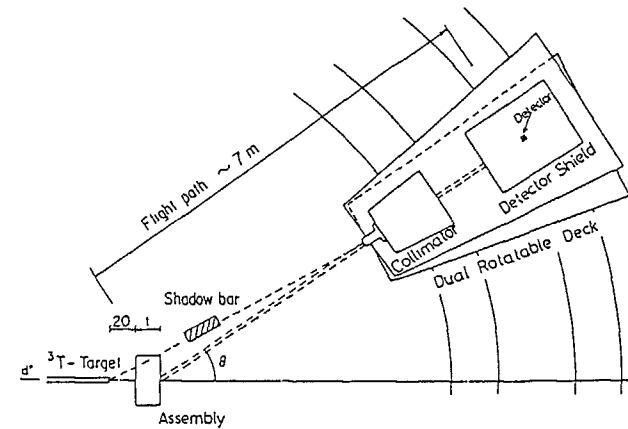

Fig. 4.1 Layout of time-of-flight experiment.

241

2. Analysis

The measured spectra were anlyzed by DOT3.5 [13], MORSE-DD [19] and MCNP [20]. They are summarized in Table 4.1. The measured spectra from the target without the assembly were used as the input for the calculations. The first collision source and P_5-S_{16} approximation were applied to the DOT3.5 calculations. The previous results for the leakage spectra from Li_2O slabs which were analyzed by DOT3.5 with GICXFNS cross section set [21], BERMUDA-2DN [22] with a DDX-type cross section set and MCNP with RMCCslaa (ENDF/B-V), were reported in Refs. [23-24].

Table 4.1 Transport codes and cross section sets for analysis

Code	C. S. Set	File	Process code	Remarks
DOT3.5	JACKAS	JENDL-3PR1&2	PROF-GROUCH	(n,2n), continuum isotropic
	ENFKAS	ENDF/B-IV&V	-G/B	E-flat weight
MORSE-DD	DDXLIB1	ENDF/B-IV	PROF-DD	(n,2n), continuum isotropic
	DDXLIB2	JENDL-3PR1		(n,2n), continuum anisotropic
	DDXLIB3	JENDL-3PR1		
		ENDF/B-IV		
MCNP	DBMCCS2	ENDF/B-V	built-in	Be slabs only
	BMCCS2	LASL-SUB	NJOY	Graphite and Be slabs
	———	JENDL-3PR1		

3. Results and Discussions

Figures 4.2 and 4.3 show the measured spectrum for the Li_2O slab of thickness 5.06 cm and 24.9 deg along with the calculated spectra by DOT3.5 with JENDL-3PR1 and ENDF/B-IV, and with JENDL-3PR1 and JENDL-3PR2, respectively [25]. The results with the three nuclear data files are almost the same except near the peak at $\sim$ 9 MeV. The peak corresponds to the first level (Q = -4.63 MeV) of inelastic scattering for ^7Li. It is clearly seen that the spectrum calculated with JENDL-3PR2 substantially improves the accuracy and is almost satisfactory in the region corresponding to the first level. The same tendencies are seen in the other thickness and angles. On the other viewpoint, the ratios of calculated to measured values (C/E) of energy-integrated fluxes are shown in Fig. 4.4 as the function of the thickness of slab and leaking angle. The nuclear data used in Fig. 4.4 were ENDF/B-IV. The C/E comparison in differential form indicates that the discrepancy depends on the thickness and angle, and is 50 $\sim$ 60 % at the maximum for JENDL-3PR1 and ENDF/B-IV. Though the agreement improves in the case of JENDL3PR2, the re-evaluation is recommended for the data of angular and energy distributions of seconary neutrons.
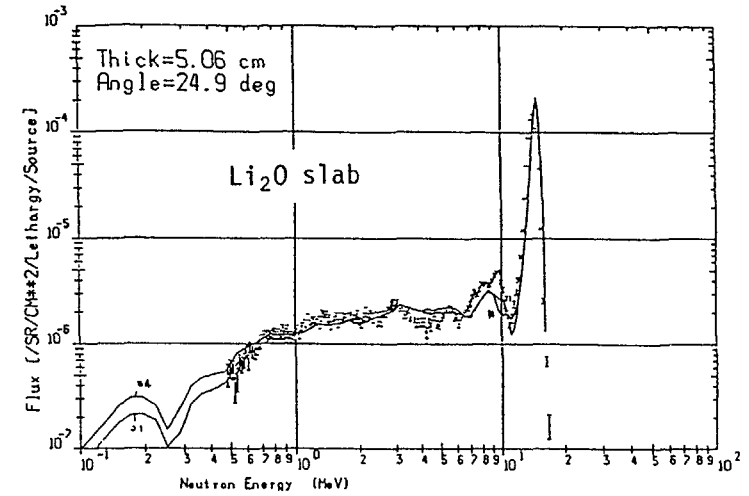

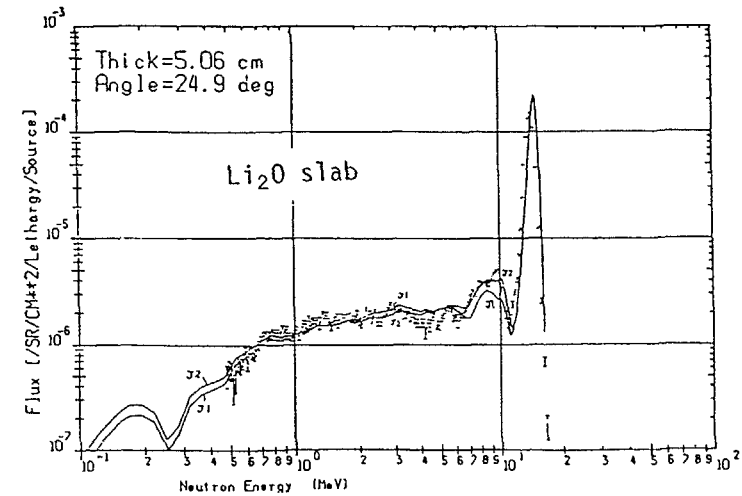Fig. 4.2 Leakage spectrum from Li_2O slab.
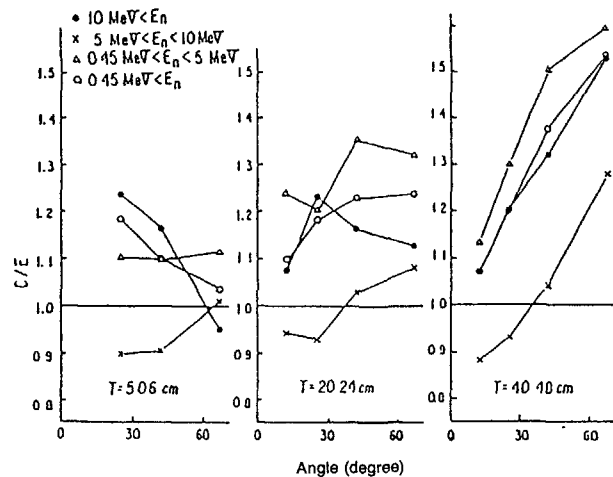

Fig. 4.3 Leakage spectrum from Li_2O slab.

Fig. 4.4 C/E comparison of integrated fluxes
(Li$_2$O assembly)

Fig. 4.5 Leakage spectrum from graphite slab.

For the graphite slabs, experimental results for 5.06-cm thickness and 24.9-deg angle are shown in Figs. 4.5 and 4.6 along with the calculated ones by DOT3.5 for ENDF/B-IV and ENDF/B-V, and JENDL-3PR1 and JENDL-3PR2, respectively. In the case of ENDF/B-IV, there exists only the peak corresponding to the first level of inelastic scattering for ^{12}C due to the lack of data for other levels. Even though the spectra calculated by the other three nuclear data files show the peaks which correspond to the first, second, and third levels, the values of these peaks are slightly different from the experiments. Comparisons of C/E values are shown in Figs. 4.7 and 4.8 for JENDL-3PR1 and ENDF/B- V, respectively. The C/E corresponding to the 3rd level is strongly dependent on the angle. The data of 2nd and 3rd levels in JENDL-3PR2 have been revised from JENDL-3PR1. The agreement for JENDL-3PR2 is much better than that for JENDL-3PR1 and is almost same as that for ENDF/B-V. Minor change is still needed for the data of angular and energy distributions of secondary neutrons in JENDL-3PR2 and ENDF/B-V.

The calculated and measured leakage spectra from the beryllium slab are shown in Fig. 4.9 for 5 cm-thick and 24.9-deg [26]. The calculated spectrum based on JENDL-3PR1 underestimates the measured one above 2 MeV, while the agreement is well in the region between 0.3 and 2 MeV. In the case of ENDF/B-V, the agreement is fairly well except for around 1 MeV. It can be concluded that the calculated spectrum based on any file does not reproduce the measured leakage spectrum for all energy region. Re-evaluations should be necessary for the JENDL-3PR1, ENDF/B-V and LANL files.

The analysis for Li-metal slabs is in progress. The result will be reproted elsewhere.
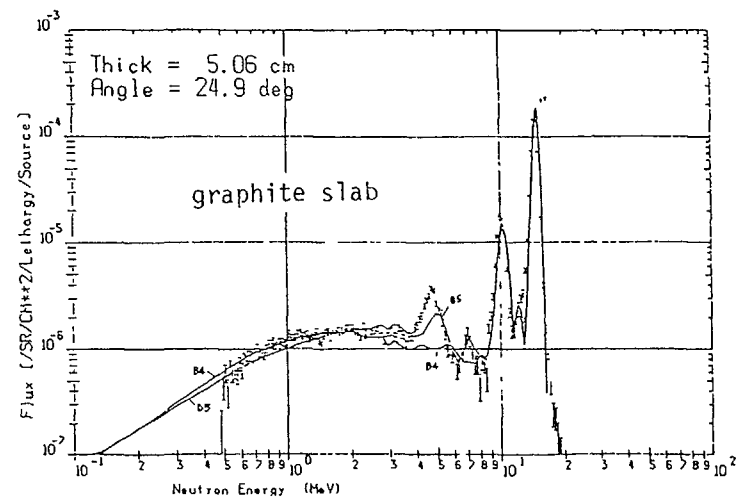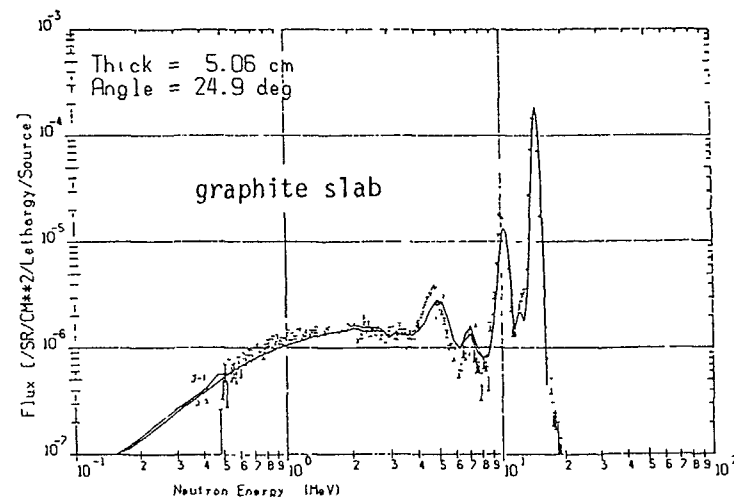

Fig. 4.6 Leakage spectrum from graphite slab.

CAL. · DOT3.5, JENDL-3PR1
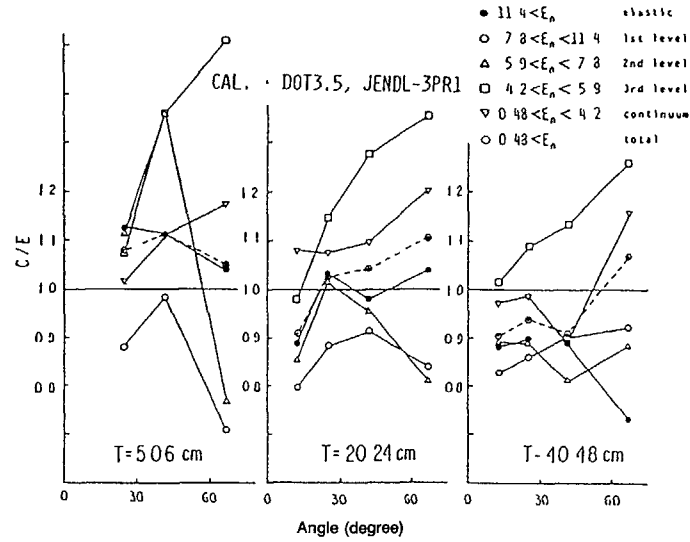
Fig. 4.7 C/E comparison of integrated fluxes.
(graphite slab, JENDL-3PR1)
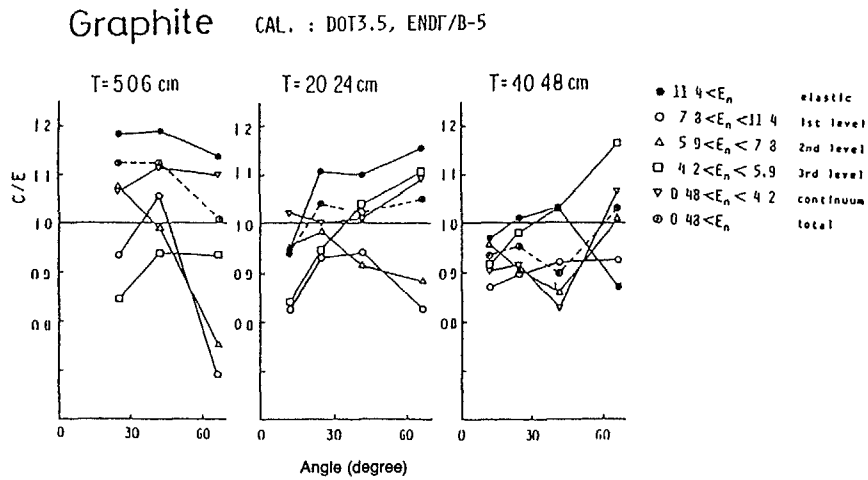
Graphite   CAL. : DOT3.5, ENDF/B-5

Fig. 4.8 C/E comparison of integrated fluxes.
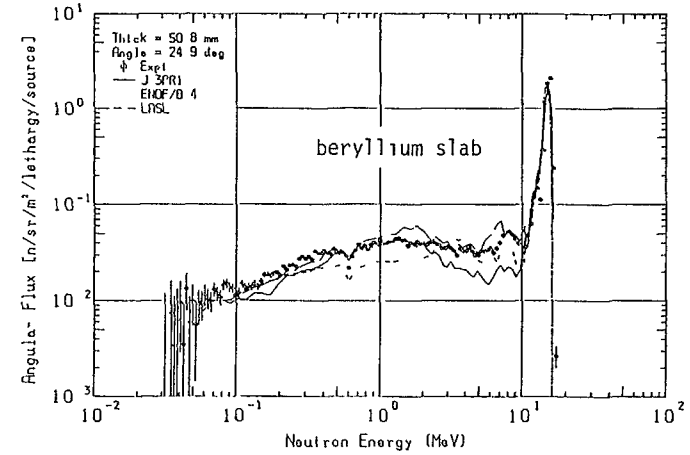(graphite slab, ENDF/B-V)

Fig. 4.9 Leakage spectrum from beryllium slab.

V. Status of the Fusion Blanket Engineering-oriented Benchmark Experiment

1. Experimental Arrangement

In the Phase-I experiment the target room #2 of the FNS is incorporated in the experimental arrangement assuming it corresponds to the plasma chamber of a fusion reactor, with its thick concrete shielding wall to a blanket zone. A portion of the enclosure is substituted by a test module of breeding blanket as shown in Fig. 5.1. The rotating neutron target (RNT) of the FNS locates at the center of the cavity simulating the neutron producing plasma. The mixed field of direct and room wall-reflected components is assumend to correspond that for a fusion blanket.

The module is composed by assembling blocks of rectangular prism. The breeding material used in the present experiment is just the same that used in the clean benchmark experiments. Figure 5.2 shows the loading pattern. The size of the module is 63 cm in equivalent diameter and 61 cm in length, which allows full-size simulation of radial configuration in a breeding blanket. The block structure allows easy modifications of the system by adding zones in front, rear or inside the breeder region. An example for a heterogeneous configuration is shown in Fig. 5.3.

2. Experimental Systems

Three experimental series have been conducted on different configurations of the module :

a) reference system,
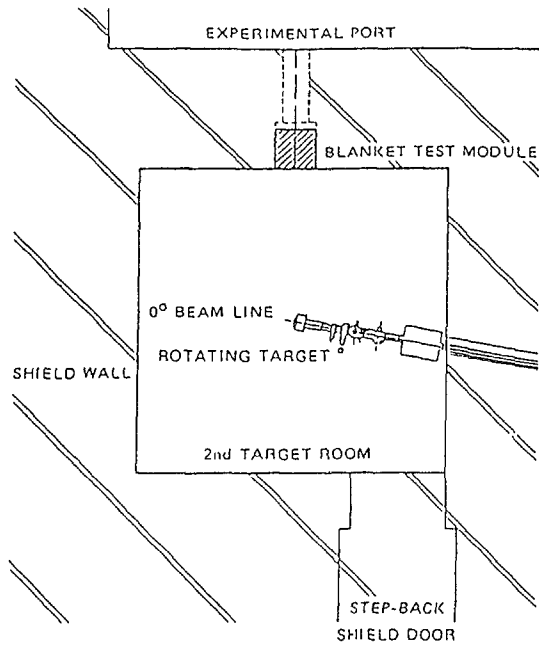b) first-walled system,
c) beryllium neutron multiplier system.

Fig. 5.1 Layout of Phase-I experiment.

: Tamper (fixed part)
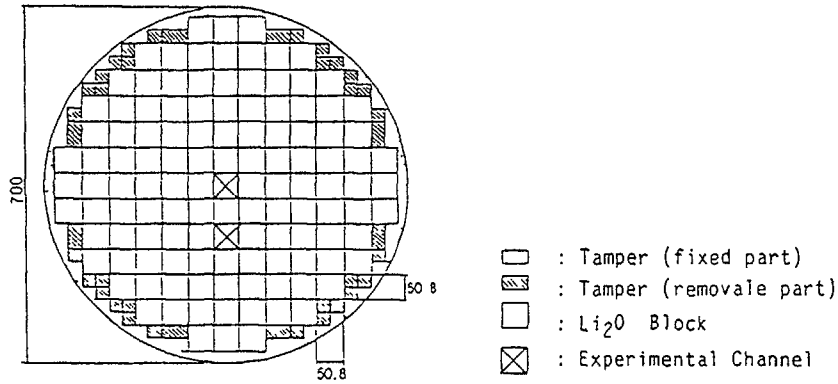: Tamper (removale part)
: Li$_2$O Block
: Experimental Channel

Fig. 5.2 Loading pattern of reference
assembly in the experimental port.
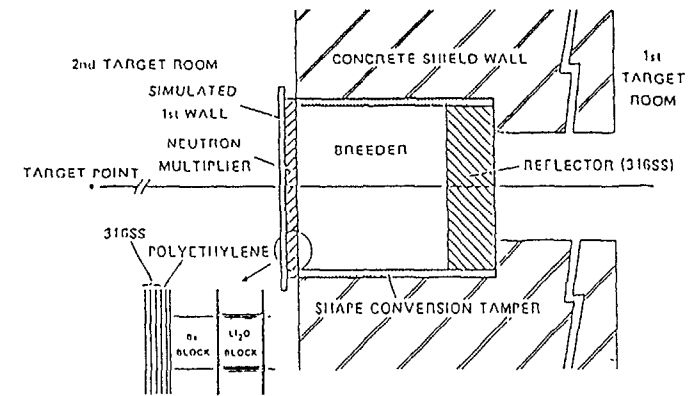
Fig. 5.3 Schematic drawing of candidate
experimental configurations.

First Wall Experiments   Be Neutron Multiplier Experiments
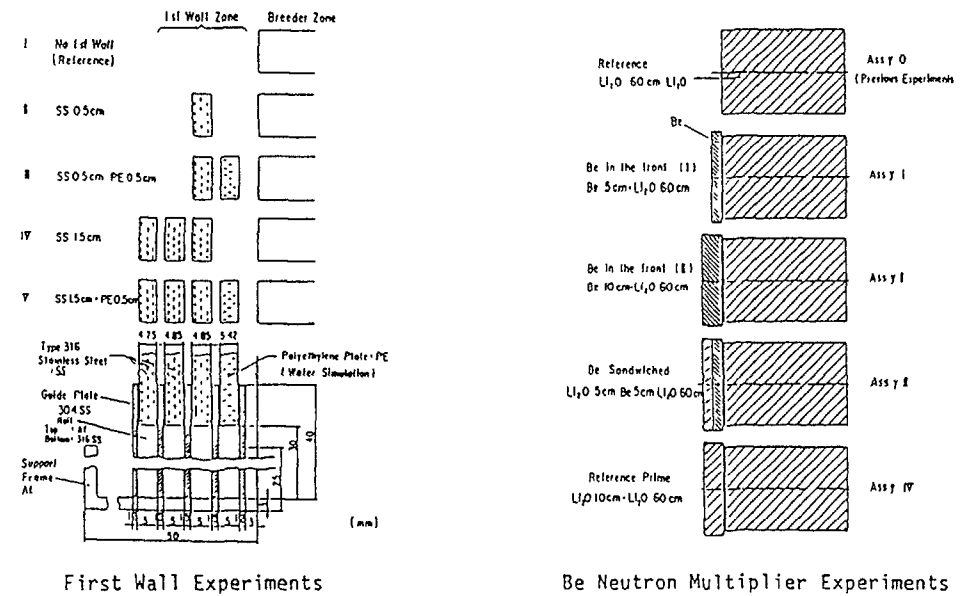
Fig. 5.4 Configurations of experimental assemblies.

Their configuration are summarized in Fig. 5.4 and Table 5.1.

The reference system is a single-region breeder that is made up by assembling Li_2O blocks. Since the system has the simplest composition it is used as the base in estimating the effects that are introduced by adding or inserting the regions of other materials.

Table 5.1 Test assemblies in Phase-I experiment.

• Reference System
   Single-region Li_2O breeder
      60cm Li_2O

• First Walled System
   No first wall   /60cm Li_2O*
   0.5cm SS[+]   /60cm Li_2O
   0.5cm SS/0.5cm PE[++] /60cm Li_2O
   1.5cm SS   /60cm Li_2O
   1.5cm SS/0.5cm PE   /60cm Li_2O

• Be Neutron Multiplier System
   5cm Be   /60cm Li_2O
   10cm Be   /60cm Li_2O
   5cm Li_2O/5cm Be/60cm Li_2O**
   10cm Li_2O /60cm Li_2O

---

   *: Identical with reference system
   **: Be sandwiched system
   +: Type 316 stainless steel
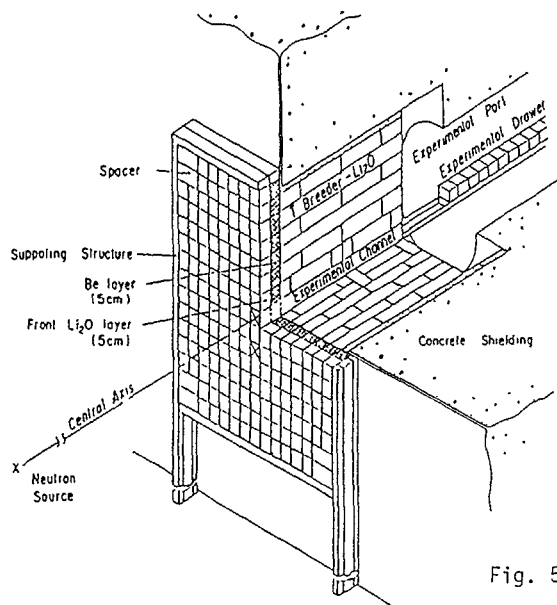   ++: Polyethylene as simulant of water

Fig. 5.5 Beryllium sandwiched assembly.

The first-walled system has a simulated wall layer that is placed on the front surface of the reference system.

In the Be neutron multiplier system, a Be layer is added to the reference system to examine the impact of the neutron multiplying material on the TPR value and its distribution. As an example of the loading, an illustration is shown in Fig. 5.5 for the Be sandwiched system.

3. Measured Parameters and Methods Applied

    1) Neutron Source

The neutron source and field characterization is an important part in this program [27]. Measurements were carried out on neutron yield, angular distribution and neutron spectra for the direct component from the RNT. The spatial distribution and spectrum were measured at the surface plane of the test module.

    2) Experimental Systems

Main efforts have been directed to the measurements of the TPR and neutron spectrum. These parameters were measured along the central axis of the test module. Two types of experimental approach have been undertaken:

    a) on-line method by radiation counters,
    b) irradiation method by counting the activities accumulated in small
       samples inserted in the experimental system [28].

The on-line method utilizes small-sized scintillation detectors which are suitable for parametric survey for the TPR in different configurations [29]. Since the method has high detection efficiency, it is applicable at low neutron fluence with reasonablly short measuring time. The on-line method was applied to all of the assemblies.

The irradiation method is adopted for the direct measurement of tritium produced in the Li containing samples in the modules on absolute basis. Another feature of this method is the smaller perturbation to the neutron field compared with the counter method. As it requires intense and long neutron exposure, this method was adopted in selected cases: the reference and Be-sandwiched systems.

The measured items and the methods applied are summarized in Table 5.2. On the TPR measurement of irradiation type approach, two methods were developed, each separately at JAERI [30] and Argonne National Laboratory (ANL) [31] for Li-containing sample and liquid scintillation counting technique. These two methods were applied in parallel to make a cross-check on the accuracies of measured values.

4. Calculational Methods and Cross Section

The analyses of the experiment were conducted both at JAERI and U.S.DOE-UCLA using different methods and data with common input conditions on the neutron source, room and experimental systems [32]. Both deterministic and Monte Carlo methods were applied in the analyses. The cross section libraries adopted in the JAERI analyses are based on recently evaluated JENDL-3PR1/2 file, while the U.S. used those from ENDF/B-V along with, in some cases, the latest evaluations for Be and ^7Li carried out at LANL for comparison. The calculational methods, nuclear data and cross section libraries used in the analyses are summarized in Table 5.3.

Table 5.2 Measured items and methods
applied.

TRITIUM PRODUCTION RATES

On-line Type (JAERI)
  T6 : Paired Li Glass Scintillation Counters
  T7 : Micro Spherical NE213 Spectrometer
       - Indirect method -

Irradiation Type
  T6
  T7 : Li₂O Pellet/Liq. Scint.* (JAERI)
  TN : Li Metal Foil/Liq. Scint. (U.S.)

NEUTRON SPECTRUM

On-line Type
  Fast Neutron : NE213 Spectrometer
     0.5MeV < E < 15MeV (JAERI)
  Slow Neutron : Proton Recoil Spectrometer**
     5keV < E < 2MeV (U.S.)

Irradiation Type (JAERI)
  Activation Foils : Al, Au, Co, In, Nb, Ni
  Spectral Indeces   Ti, Zn, Zr

----

*   Liquid Scintillation Counting Method
** Input Source Spectrum to the Test Module

Table 5.3 Calculational method, nuclear
data and cross section libraries.

	JAERI	U.S.
• Discrete ordinates (2-D, r-z model)	DOT3.5 + GRTUNCL JENDL-3PR1&2 JACKAS (P5, 125G)	DOT4.3 + GRTUNCL ENDF/B-V* MATXS6 (P5, 80G)
• Monte Carlo	MORSE-DD JENDL-3PR1 DDL/J3P1 (125G)	MCNP ENDF/B-V* BMCCS3 (continuous energy/ Angle)

*: Young's evaluation for ⁷Li(n,n'αt) was used.
   Latest and Previous evaluation for Be were
   compared.

5. Results and Discussion

1) Neutron source characteristics

The neutron spectrum at the front center of the experimental opening is shown in Fig. 5.6 as a representative of measured various quantities on neutron sourse characteristics; high energy range was measured by JAERI with NE213 spectrometer and low energy side by U.S.DOE-ANL with proton-recoil proportional counters. They showed a good fitting in the overlapping range on absolute comparison. Source characteristics was also estimated numerically by Monte Calro methods in which rigorous configurations of the RNT and room were represented. Reasonablly good agreement between measured and calculated shapes was obtained assuring the Monte Carlo results be appropriate as the input source for the analysis for the system.
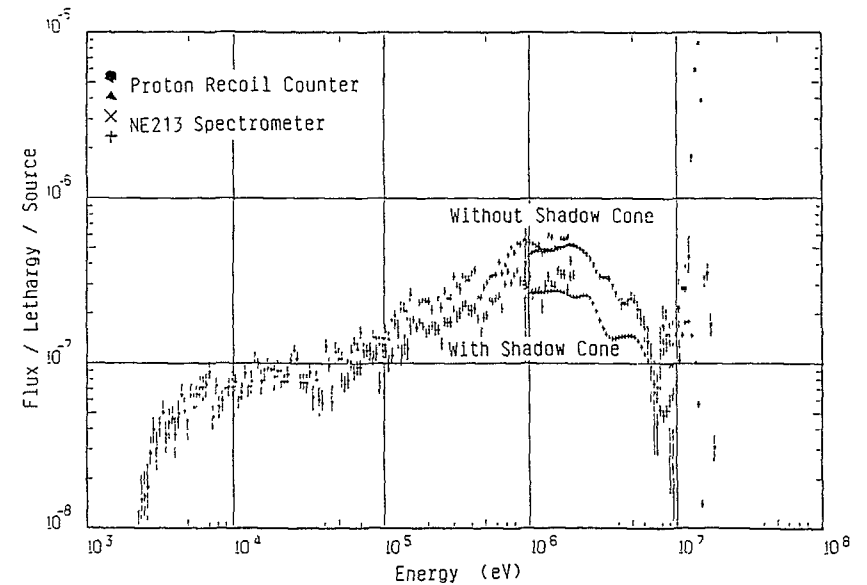

Fig. 5.6 Measured neutron spectra with and without the shadow cone at the entrance of experimental port without the assembly.

2) Reference system

The TPR distributions both from ⁶Li and ⁷LI are shown in Fig. 5.7 [5]. Agreement was obtained between JAERI and U.S.DOE-ANL results within the experimental errors showing the reliability of the measured values. In Fig. 5.8 are shown the calculated to measured value ratios of TPR from ⁶Li for different calculations [32]. There are differences among the calculated values even in this simple system. In the region deeper than 5-10 cm from the frontface, the C/E values are fairly constant ranging in 1.03 - 1.30; the Monte Carlo
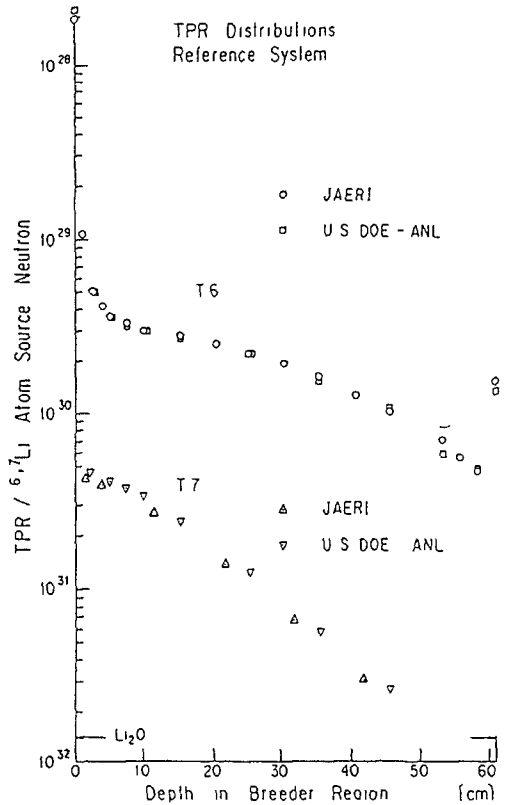
Fig 5 7 Measured tritium production rate
(TPR) in the reference system

Fig 5.8 Calculated to measured value of
tritium production rate for ^{6}Li
in the reference system.
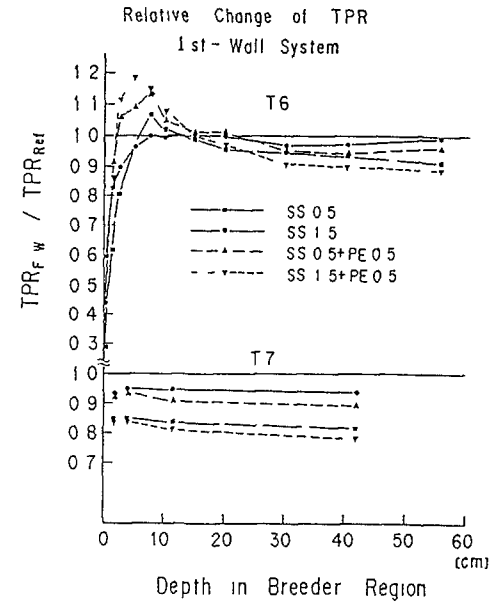
Fig 5 9 Relative change in TPRs for
first walled systems

calculations give better results. The deviations are even more in the front
region. Hence it is necessary to examine the calculational methods and modelling
before making comment on the nuclear data used. As for the C/E values for TPR
from ^{7}Li, there is a systematic difference of 12 ∿ 18 % between JAERI and U S.,
which is attributed to the difference in ^{7}Li$(n,n'\alpha)^3$T cross section data.

3) First wall system

The effect of first wall was studied by measuring TPR distributions with
on-line methods systematically. The results are given in Fig. 5.9 as the ratio
of with the first wall to without the first wall. The relative change is well
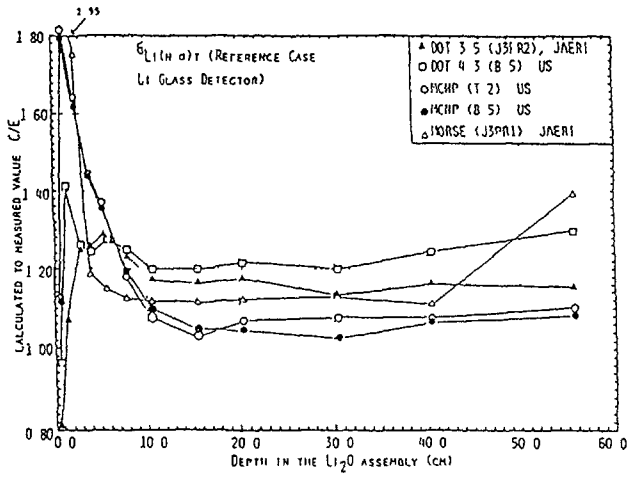reproduced in the S_N calculation.

4) Beryllium multiplier system

Figure 5.10 shows the the ratios of TPR from ^{6}Li in the Be systems to the
reference system both for measured and calculated values at JAERI [27]. There is
observed increase of TPR value behind the Be region in each case due to both
neutron multiplication and slowing down in the zone. It is noted that the
calculations underestimate TPR in this region in any case, it suggests that
nuclear data on Be in JENDL-3PR1 ought to be reexamined. The analyses on the Be-
sandwitched system showed wide scattering in the C/E values from one to the
others inside and at the boundaries of Be region. It is partly because both
calculation and experiment are very sensitive to spatial deviation as the
spectrum changes in a great extent around here. Much care should be taken in the
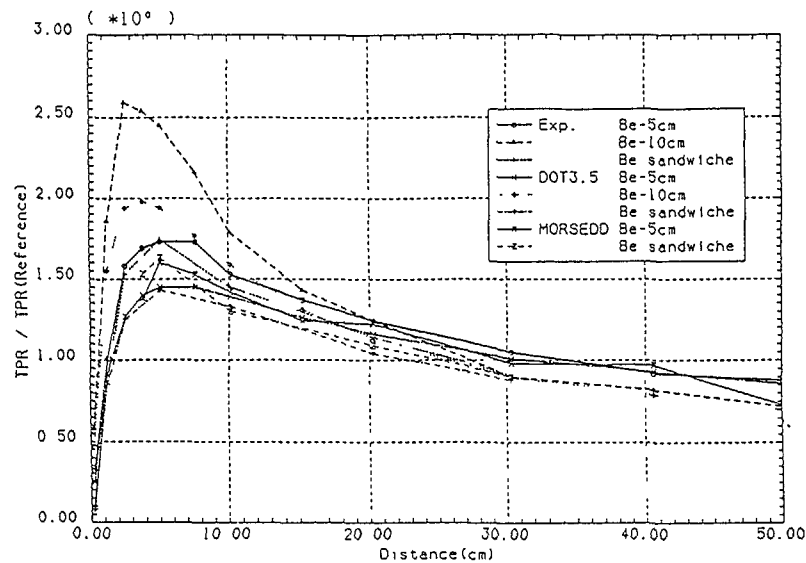calculation modelling.

Fig. 5.10 Ratios of [6]Li TPR in the beryllium experiments
to the reference system.

6. Concluding Remarks

A series of integral experiments were conducted in the Phase-I program, a new experimental approach. Tritium production rate and neutron spectrum profiles obtained here in a systematic way and with high precision are appropriate to examine the overall accuracies of methods and data in the calculations of composite systems as was explained in the preceding section for some examples.

REFERENCES

[1] SAKO K., et al., "Conceptual Design of a Gas-Cooled Tokamak Reactor," Proc. Symp. Fusion Reactor Design Problems, CONF-740131, pp27-49, IAEA (1982); JAERI-M 5502 (1973).

[2] MAEKAWA H., et al., "Absolute Fission-Rate Distribution in Graphite-Reflected Lithium Oxide Blanket Assembly," J. Nucl. Sci. Technol., 16 [5] 377-379 (1979).

[3] NAKAMURA T., et al., "Fusion Neutronics Source (FNS)," Proc. Third Sym. on Accelerator Science and Technology, Osaka Univ., Osaka, Japan, Aug. 27-29, pp55-56 (1980).

[4] NAKAMURA T., et al., Present Status of the Fusion Neutronics Source (FNS)," Proc. 4th Symp. on Accelerator Sci. & Techno., RIKEN, Saitama, Nov. 24-26, 1982,pp155-156.

[5] NAKAMURA T., ABDOU M. A., "Summary of Recent Results from the JAERI/U.S. Fusion Neutronics Phase-I Experiments," Seventh Topical Meeting on the Technology of Fusion Energy, Reno, Nevada, June 15-19, 1986.

[6] NAKAMURA T., "Fusion Blanket Engineering Benchmark Experiment," JAERI-M 86-029 pp183-191 (1986).

[7] MAEKAWA H., et al., "Neutron Yield Monitors for the Fusion Neutronics Source (FNS) --- For 80° Beam Line ---," JAERI-M 83-219 (1983).

[8] OYAMA Y., et al., "Development of a Spherical NE213 Spectrometer wth 14 mm Diameter," JAERI-M 84-124 (1984) (in Japanese); To be published in Nucl. Instr. Meth.

[9] SEKI Y., et al., "Monte Carlo Calculations of Source Characteristics of FNS Water Cooled Type Tritium Target," J. Nucl. Sci. Technol., 20 [8] 686-693 (1983).

[10] MAEKAWA H., et al., "Blanket Benchmark Experiments on a 60 cm-thick Lithium-Oxide Cylindrical Assembly," To be published in JAERI-M Report.

[11] MAEKAWA H., et al., "Benchmark Experiments on a 60 cm-thick Graphite Cylindrical Assembly," To be published in JAERI-M Report.

[12] MAEKAWA H., et al., "Fusion Benchmark Experiments on a 40 cm-thick Lithium-Oxide and 20 cm-thick Graphite Cylindrical Assembly," To be published in JAERI-M Report.

[13] RHOADES W. A., MYNATT F. R., "The DOT-III Two Dimensional Discrete Ordinates Transport Code," ORNL/TM-4280 (1973).

[14] SHIBATA K., KIKUCHI Y., "Evaluation of Nuclear Data for Fusion Neutronics," Proc. Int. Conf. on Nucl. Data for Basic & Applied Sci., Santa Fe, May 13-17, 1985, Vol. 2, 1585-1588.

[15] CHIBA S., et al., "Interaction of Fast Neutrons with [6,7]Li," ibid. Vol. 1, 227-230.

[16] HASEGAWA A., "Development of Processing Module for File 6: Energy-angular Distribution Data of END/F-V Format," JAERI-M 86-125 pp12-14 (1986); "PROF-GROUCH-G/B Code System," To be published in JAERI report.

[17] KOSAKO K., et al., "Neutron Cross Section Sets of 125-group for Fusion Neutronic Calculations," JAERI-M 86-125 pp157-159 (1986).

[18] OYAMA Y., MAEKAWA H., "Spectral Measurement of Angular Neutron Flux on the Restricted Surface of Slab Assemblies by the Time-of-Flight Method," Nucl. Instr. Meth. A245, 173-181 (1986).

[19] NAKAGAWA M., MORI T., "MORSE-DD : A Monte Carlo Code Using Multi-Group Double Differential Form Cross Sections," JAERI-M 84-126 (1984).

250

[20] Los Alamos Radiation Transport Group (X-6), "MCNP - A General Monte Carlo
Code for Neutron and Photon Transport," LA-7396-M, Revised (1981).

[21] SEKI Y., et al., "Calculation of Absolute Fission-Rate Distributions
Measured in Graphite-Reflected Lithium Oxide Blanket Assembly," JAERI-M
83-061 (1983).

[22] SUZUKI T., HASEGAWA A., MORI T., ISE T., "BERMUDA-2DN . A Two-Dimensional
Neutron Transport Code," Proc. of 6th Int. Conf. on Radiation Shielding,
May 16-29, 1983, Tokyo, Japan, Vol. I, 246-258.

[23] OYAMA Y., YAMAGUCHI S., MAEKAWA H., "Analysis of Time-of-Flight Experiment
on Lithium-Oxide Assemblies by a Two-Dimensional Transport Code DOT3.5,"
JAERI-M 85-031 (1985).

[24] SHIN K., OYAMA Y., ABDOU M., "Analysis of a 14-MeV Neutron Scattering
Experiment with Li_2O," Proc. Int. Conf. Nuclear Data for Basic & Applied
Science, Santa Fe, May 13-17, 1985, Vol. 1 pp239-243.

[25] YAMAGUCHI S., et al., "Analysis of the Time-of-Flight Experiment on
Lithium-Oxide and Graphite Assemblies Using JENDL-3PR1," JAERI-M 85-116,
pp132-134 (1985).

[26] OYAMA Y., MAEKAWA H., "Neutron Angular Flux from Berrylium Slab Assemb-
lies," Proc. Fall Mtg. of Atomic Energy Soc. of Japan, A36 (1986), To be
submitted to Nucl. Sci. Eng.

[27] OYAMA Y., et al., "Neutron Field Characteristics in Concrete Cavity Having
DT Neutron Source," Seventh Topical Meeting on the Technology of Fusion
Energy, Reno, Nevada, June 15-19, 1986.

[28] MAEKAWA H., et al., "Measured Neutron Parameters for Phase-I Experiments at
the FNS," ibid.

[29] YAMAGUCHI S., NAKAMURA T., "Tritium Production Measurements by the
Lithium-Glass Scintillation Method," ibid.

[30] TSUDA K., et al., "A Method for Tritium Production-Rate Measurement with
Sintered Li_2O Pellets and its Application to a 60 cm-thick Li_2O Slab
Assembly," JAERI-M 84-138 pp88-90 (1984).

[31] BENNETT E. F., et al., "Experimental Techniques and Measurement Accura-
cies," Sixth Topical Meeting on the Technology of Fusion Energy, San
Francisco, March 3-7, 1985, Fusion Technology 8 [1] 1535-1541 (1985).

[32] YOUSSEF M. Z., et al., "Analysis of Intercomparison for Phase-I Experiments
at FNS," Seventh Topical Meeting on the Technology of Fusion Energy, Reno,
Nevada, June 15-19 1986.

LIST OF PARTICIPANTS

BOETTGER, R.

Physikalisch Technische
  Bundesanstalt
Abteilung 6
Bundesallee 100
D-3300 Braunschweig, FRG

BORISOV, A.A.

Institut Atomnoi Energii
  I.V. Kurchatova
Ploshchad I.V. Kurchatova
Moscow D-182, 123182, USSR

CARO, R.

Junta de Energía Nuclear
Avda. Complutense 22
28040 Madrid, Spain

CHENG, E.T.

GA Technologies Inc.
P.O. Box 85608
San Diego, CA 92138, USA

CHRISTOV, V.

Institute of Nuclear Research
  and Nuclear Energy
Bulgarian Academy of Sciences
72 Lenin Blvd
1184 Sofia, Bulgaria

CONDE, H.

Gustav Werner Institute
Uppsala University
P.O. Box 531
S-751 21 Uppsala, Sweden

DOS SANTOS, R.

Nuclear Information Center
Comissao Nacional de Energia
  Nuclear (CNEN)
C.P. 11049
01000 Sao Paulo - SP, Brazil

FELDBACHER, R.

Technical University
Peterstrasse 16
A-8010 Graz, Austria

FORREST, R.

Atomic Energy Research
  Establishment (AERE)
Harwell, Didcot, Oxon. OX11 ORA
United Kingdom

GRUPPELAAR, H.

Netherlands Energy Research
  Foundation (ECN)
P.O.B. 1, 3 Westerduinweg
NL-1755 ZG Petten
The Netherlands

GOULO, V.
(Scientific Secretary)

IAEA Nuclear Data Section
Wagramerstrasse 5, P.O. Box 100
A-1400 Vienna, Austria

HALE, G.

Los Alamos National Laboratory
T-2 Nuclear Data
MS-243
Los Alamos, NM 87545, USA

ILIEVA, K.

Institute of Nuclear Research
  and Nuclear Energy
Bulgarian Academy of Sciences
72 Lenin Blvd
1184 Sofia, Bulgaria

JARMIE, N.

Los Alamos National Laboratory
Los Alamos, NM 87545, USA

JONES, R.

Atomic Energy of Canada Ltd.
Chalk River Nuclear Laboratories
Chalk River, Ontaria KOJ 1JO
Canada

KANDA, Y.

Department of Energy Conversion
  Engineering
Kyushu University
33 Sakamoto, Kasuga
Kasuga-shi 816, Japan

LISKIEN, H.

Central Bureau of Nuclear
  Measurements
Steenweg naar Retie
B-2440 Geel, Belgium

MAEKAWA, H.

Japan Atomic Energy Research
  Institute (JAERI)
FNS, Division of Reactor
  Engineering
Tokai-Mura, Naka-Gun
Ibaraki-ken 319-11, Japan

MANN, F.M.

Hanford Engineering Development
  Laboratory
P.O. Box 1970
Richland, Washington 99352, USA

MARKOVSKIJ, D.V.

Institut Atomnoi Energii
  I.V. Kurchatova
Ploshchad I.V. Kurchatova
Moscow D-182, 123182, USSR

MEHTA, M.K.

Bhabha Atomic Research Centre
Trombay, Bombay 400 085
India

OBLOZINSKY, P.   Electro-Physical Research Centre
                 Department of Nuclear Physics
                 Institute of Physics of the Slovak
                   Academy of Sciences
                 Fyzikalny Ustav SAV
                 CS-842 28 Bratislava, Czechoslovakia

PELLONI, S.   Swiss Federal Institute for
                   Reactor Research
                 5303 Wuerenlingen, Switzerland

QAIM, S.M.   Institut f. Chemie 1
                 Kernforschungsanlage Juelich GmbH
                 Postfach 1913
                 D-5170 Juelich 1, FRG

RADO, V.   ENEA Fusion Department
                 Via Enrico Fermi 27
                 I-00044 Frascati, Italy

REFFO, G.   Centro di Calcolo
                 ENEA Research Center "E. Clementel"
                 Via Mazzini 2
                 I-40138 Bologna, Italy

SCHMIDT, J.J.   IAEA Nuclear Data Section
                 Wagramerstrasse 5, P.O. Box 100
                 A-1400 Vienna, Austria

SCOTT, M.C.   Department of Physics
                 Birmingham University
                 P.O. Box 363
                 Birmingham B15 2TT, UK

SEELIGER, D.   Technische Universitaet Dresden
(Local Organizer) Sektion Physik
                 Mommsenstrasse 13
                 DDR-8027 Dresden, GDR

SEIDEL, K.   Technische Universitaet Dresden
                 Sektion Physik
                 Mommsenstrasse 13
                 DDR-8027 Dresden, GDR

SUMITA, K.   Department of Nuclear Engineering
                 Osaka University
                 2-1 Yamadaoka, Suita-shi
                 Osaka 565, Japan

VONACH, H.K.   Institut für Radiumforschung
                   und Kernphysik
                 Boltzmanngasse 3
                 A-1090 Vienna, Austria

ZHAO Zhixiang   Institute of Atomic Energy
                 P.O. Box 275 (41)
                 Beijing, People's Rep. of China